MOLECULAR AND CELLULAR CROSSTALK ON NEURONAL FUNCTIONALITY AND REGULATION, FROM DEVELOPMENT TO PATHOLOGY

EDITED BY: Inmaculada Segura and Joaquim Egea

PUBLISHED IN: Frontiers in Molecular Neuroscience

frontiers Research Topics

Frontiers eBook Copyright Statement

The copyright in the text of individual articles in this eBook is the property of their respective authors or their respective institutions or funders. The copyright in graphics and images within each article may be subject to copyright of other parties. In both cases this is subject to a license granted to Frontiers.

The compilation of articles constituting this eBook is the property of Frontiers.

Each article within this eBook, and the eBook itself, are published under the most recent version of the Creative Commons CC-BY licence. The version current at the date of publication of this eBook is CC-BY 4.0. If the CC-BY licence is updated, the licence granted by Frontiers is automatically updated to the new version.

When exercising any right under the CC-BY licence, Frontiers must be attributed as the original publisher of the article or eBook, as applicable.

Authors have the responsibility of ensuring that any graphics or other materials which are the property of others may be included in the CC-BY licence, but this should be checked before relying on the CC-BY licence to reproduce those materials. Any copyright notices relating to those materials must be complied with.

Copyright and source acknowledgement notices may not be removed and must be displayed in any copy, derivative work or partial copy which includes the elements in question.

All copyright, and all rights therein, are protected by national and international copyright laws. The above represents a summary only. For further information please read Frontiers' Conditions for Website Use and Copyright Statement, and the applicable CC-BY licence.

ISSN 1664-8714
ISBN 978-2-88976-636-9
DOI 10.3389/978-2-88976-636-9

About Frontiers

Frontiers is more than just an open-access publisher of scholarly articles: it is a pioneering approach to the world of academia, radically improving the way scholarly research is managed. The grand vision of Frontiers is a world where all people have an equal opportunity to seek, share and generate knowledge. Frontiers provides immediate and permanent online open access to all its publications, but this alone is not enough to realize our grand goals.

Frontiers Journal Series

The Frontiers Journal Series is a multi-tier and interdisciplinary set of open-access, online journals, promising a paradigm shift from the current review, selection and dissemination processes in academic publishing. All Frontiers journals are driven by researchers for researchers; therefore, they constitute a service to the scholarly community. At the same time, the Frontiers Journal Series operates on a revolutionary invention, the tiered publishing system, initially addressing specific communities of scholars, and gradually climbing up to broader public understanding, thus serving the interests of the lay society, too.

Dedication to Quality

Each Frontiers article is a landmark of the highest quality, thanks to genuinely collaborative interactions between authors and review editors, who include some of the world's best academicians. Research must be certified by peers before entering a stream of knowledge that may eventually reach the public - and shape society; therefore, Frontiers only applies the most rigorous and unbiased reviews.
Frontiers revolutionizes research publishing by freely delivering the most outstanding research, evaluated with no bias from both the academic and social point of view. By applying the most advanced information technologies, Frontiers is catapulting scholarly publishing into a new generation.

What are Frontiers Research Topics?

Frontiers Research Topics are very popular trademarks of the Frontiers Journals Series: they are collections of at least ten articles, all centered on a particular subject. With their unique mix of varied contributions from Original Research to Review Articles, Frontiers Research Topics unify the most influential researchers, the latest key findings and historical advances in a hot research area! Find out more on how to host your own Frontiers Research Topic or contribute to one as an author by contacting the Frontiers Editorial Office: frontiersin.org/about/contact

MOLECULAR AND CELLULAR CROSSTALK ON NEURONAL FUNCTIONALITY AND REGULATION, FROM DEVELOPMENT TO PATHOLOGY

Topic Editors:
Inmaculada Segura, Ludwig Maximilian University of Munich, Germany
Joaquim Egea, Biomedical Research Institute of Lleida, Spain

Citation: Segura, I., Egea, J., eds. (2022). Molecular and Cellular Crosstalk on Neuronal Functionality and Regulation, From Development to Pathology. Lausanne: Frontiers Media SA. doi: 10.3389/978-2-88976-636-9

Table of Contents

05 ***Editorial: Molecular and Cellular Crosstalk on Neuronal Functionality and Regulation, From Development to Pathology***
Inmaculada Segura and Joaquim Egea

08 ***Artemin Is Upregulated by TrkB Agonist and Protects the Immature Retina Against Hypoxic-Ischemic Injury by Suppressing Neuroinflammation and Astrogliosis***
Hsiu-Mei Huang, Chao-Ching Huang, Linda Yi-Chieh Poon and Ying-Chao Chang

21 ***Neuromodulation and Behavioral Flexibility in Larval Zebrafish: From Neurotransmitters to Circuits***
Laura Corradi and Alessandro Filosa

36 ***From Junk to Function: LncRNAs in CNS Health and Disease***
Rafaela Policarpo, Annerieke Sierksma, Bart De Strooper and Constantin d'Ydewalle

56 ***Held Up in Traffic—Defects in the Trafficking Machinery in Charcot-Marie-Tooth Disease***
Ronja Markworth, Mathias Bähr and Katja Burk

77 ***Expression of FLRT2 in Postnatal Central Nervous System Development and After Spinal Cord Injury***
Juntan Li, Yo Shinoda, Shuhei Ogawa, Shunsuke Ikegaya, Shuo Li, Yukihiro Matsuyama, Kohji Sato and Satoru Yamagishi

89 ***The Fine Art of Writing a Message: RNA Metabolism in the Shaping and Remodeling of the Nervous System***
María Landínez-Macías and Olivier Urwyler

117 ***Refinement of Active and Passive Membrane Properties of Layer V Pyramidal Neurons in Rat Primary Motor Cortex During Postnatal Development***
Patricia Perez-García, Ricardo Pardillo-Díaz, Noelia Geribaldi-Doldán, Ricardo Gómez-Oliva, Samuel Domínguez-García, Carmen Castro, Pedro Nunez-Abades and Livia Carrascal

131 ***With the Permission of Microtubules: An Updated Overview on Microtubule Function During Axon Pathfinding***
Carlos Sánchez-Huertas and Eloísa Herrera

156 ***FLRT3 Marks Direction-Selective Retinal Ganglion Cells That Project to the Medial Terminal Nucleus***
Tobias Ruff, Christian Peters, Akihiro Matsumoto, Stephan J. Ihle, Pilar Alcalá Morales, Louise Gaitanos, Keisuke Yonehara, Daniel del Toro and Rüdiger Klein

170 ***Structural and Functional Aspects of the Neurodevelopmental Gene* NR2F1*: From Animal Models to Human Pathology***
Chiara Tocco, Michele Bertacchi and Michèle Studer

199 ***GLP-1 Suppresses Feeding Behaviors and Modulates Neuronal Electrophysiological Properties in Multiple Brain Regions***
Xin-Yi Chen, Lei Chen, Wu Yang and An-Mu Xie

208 ***Biosensors for Studying Neuronal Proteostasis***
Irina Dudanova

217 ***Sevoflurane-Induced Apoptosis in the Mouse Cerebral Cortex Follows Similar Characteristics of Physiological Apoptosis***
Qi Wang, Yuan Li, Hong Tan and Yingwei Wang

227 ***Behavioral and Molecular Responses to Exogenous Cannabinoids During Pentylenetetrazol-Induced Convulsions in Male and Female Rats***
Antonella Zirotti Rosenberg, Maxs Méndez-Ruette, Mario Gorziglia, Benjamín Alzerreca, Javiera Cabello, Sofía Kaufmann, Lukas Rambousek, Andrés Iturriaga Jofré, Ursula Wyneken and Carlos A. Lafourcade

frontiers | Frontiers in Molecular Neuroscience

EDITORIAL
published: 30 June 2022
doi: 10.3389/fnmol.2022.966423

Editorial: Molecular and Cellular Crosstalk on Neuronal Functionality and Regulation, From Development to Pathology

Inmaculada Segura[1,2]* *and Joaquim Egea*[3,4,5]*

[1] Max Planck Institute for Biological Intelligence (in Foundation), Planegg, Germany, [2] Department of Cellular Physiology, Biomedical Center Munich, Ludwig Maximilian University, Planegg, Germany, [3] Departament de Ciències Mèdiques Bàsiques, Universitat de Lleida, Lleida, Spain, [4] Biomedical Research Institute of Lleida (IRBLLEIDA), Lleida, Spain, [5] Serra Húnter Programme, Generalitat de Catalunya, Barcelona, Spain

Keywords: neuronal development, neuromodulation, neuronal maturation, regulation–physiological, connectivity

OPEN ACCESS

Edited and reviewed by:
Jean-Marc Taymans, Institut National de la Santé et de la Recherche Médicale (INSERM), France

***Correspondence:**
Inmaculada Segura
inmaculada.segura@bi.mpg.de
Joaquim Egea
joaquim.egea@udl.cat

Specialty section:
This article was submitted to Molecular Signalling and Pathways, a section of the journal Frontiers in Molecular Neuroscience

Received: *10 June 2022*
Accepted: *16 June 2022*
Published: *30 June 2022*

Citation:
Segura I and Egea J (2022) Editorial: Molecular and Cellular Crosstalk on Neuronal Functionality and Regulation, From Development to Pathology. Front. Mol. Neurosci. 15:966423. doi: 10.3389/fnmol.2022.966423

Editorial on the Research Topic

Molecular and Cellular Crosstalk on Neuronal Functionality and Regulation, From Development to Pathology

The development and functions of the nervous system are precisely guided and controlled by the crosstalk of molecular and cellular processes that are often revealed during pathological conditions, as defective molecular signaling and cellular interactions lie behind their cause or course. This Research Topic combines several reviews and original research articles highlighting the relevance of some of these processes, studied in different model systems, to broaden our understanding of the function of the nervous system.

Proteins and RNAs are key players of the cellular systems. Protein homeostasis, i.e., proteostasis, controls the quality and the appropriated amount of functional proteins within the cell (Giandomenico et al., 2022). Defective proteostasis has been linked to several disorders, including neurodegenerative diseases or behavior alterations. Therefore, as reviewed by Dudanova, the development of biosensors to assess protein quality is a promising approach to understand pathological mechanisms and to test possible therapies in the aforementioned conditions.

Among the proteins, the transcription factors play a central role during development due to their capacity to control gene expression. These genetic programs underlie several important processes, such as cellular proliferation, migration, or differentiation, which are essential, for instance, during nervous system development and function (Jain and Zipursky, 2022). The review by Tocco et al. summarizes the molecular and neurodevelopmental defects observed in a recently described neurodevelopmental monogenic syndrome, the Bosch-Boonstra-Schaaf Optic Atrophy Syndrome (BBSOAS). BBSOAS is characterized by the haploinsufficiency of the transcription regulator NR2F1 (previously known as COUP-TFI), which results in intellectual disability, visual impairment, epilepsy and autistic traits.

In the case of the RNAs, it has become evident in the recent years that RNAs display complex biological activities, e.g., messenger RNAs (mRNAs) are more than mere "photocopies" of the DNA to be translated into proteins or long non-coding RNAs (Lnc-RNAs) are not just junk biomolecules (Aprea and Calegari, 2015; Sonneveld et al., 2020). The reviews by Landínez-Macías and Urwyler and by Policarpo et al. summarize recent insights in either mRNA metabolism, with special emphasis on the RNA-binding protein Musashi, or in Lnc-RNAs, respectively, during neuronal development and function, from neural stem cell maintenance to synapse specification and wiring. They also explore their link to neurological diseases.

Neurons are very polarized cells whose dendrites and axons excess in length the size of the somas. Regulation of cytoskeleton dynamics plays a key function in polarity, size and connectivity which are essential for proper neuronal function in integrated circuits (Schelski and Bradke, 2017). As reviewed by Sánchez-Huertas and Herrera, the regulation of microtubule assembly, stability and its interaction with the actin network are processes particularly important at the growth cone of the developing axons, supporting axonal pathfinding and proper connectivity. But microtubules also play an important function as "railways" for motor proteins supporting the bidirectional trafficking of vesicles and organelles along the axons (Cason and Holzbaur, 2022). The review by Markworth et al. summarizes the trafficking defects that have been identified as the cause of the Charcot-Marie-Tooth disease, a neurodegenerative disease of the peripheral nervous system that cause axonal degeneration and neuronal loss.

Neurons are integrated in functional circuits that are mainly developed during embryonal and larval/infant stages and consolidated and refined during the adulthood. In that context, the study of small animals such as fish or rodents are of great value for the understanding of neuron connectivity. The work by Perez-García et al. demonstrates how the majority of the electrophysiological properties of the main effector neurons in the rat motor cortex, the layer V pyramidal neurons, are refined postnatally and are not defined until adulthood's onset. Another important postnatal refining process of neuronal circuits is that non-integrated cells are eliminated by physiological apoptosis (Wong and Marín, 2019). The work by Wang et al. warns about the use of the anesthetic sevoflurane, widely used in pediatrics, as it enhances this physiological apoptotic wave in the somatosensory cortex in mice. In the adulthood, neuromodulatory circuits allow adaptation of the behavior of the animals to their ever-changing needs, as for example during feeding behavior. The main neuromodulatory circuits are conserved among species. The review by Corradi and Filosa highlights the use of the translucent larva of the zebrafish, which facilitates *in vivo* imaging, in combination with appropriate behavioral tests and transgenesis to decipher the mechanisms of circuitry connection and behavioral modulation. In mammals, feeding behavior is regulated by neurotransmitters and neuropeptides. The review by Chen et al. focuses on the mechanisms of the glucagon-like peptide-1 (GLP-1) to regulate food uptake and the activation of its receptor (GLP-1R) in several brain regions.

An alternative and accessible model system for the study of the central nervous system (CNS) is the retina. This internal layer of the eye is originated from the diencephalon and remains connected to the brain by the optic nerve, that projects to different brain areas. These projection areas include the thalamus and other accessory nuclei. Among them, the inputs to the medial terminal nucleus (MTN) in the ventral midbrain are necessary for reflex eye movements and retinal image stabilization during vision (Yonehara et al., 2009). Within the retina, photoreceptors, bipolar neurons, and retinal ganglion cells (RGCs, forming the optic nerve) are hierarchically organized in structural layers that are well-vascularized. The work by Huang et al. describes the neuroprotective effect of 7,8-dihydroxyflavone (DHF) in the immature retina of P7 rats against hypoxic-ischemic injury, a major cause of acquired visual impairment in children from developing countries. DHF acts as a synthetic TrkB agonist independent of BDNF that activates Artemin upregulation and reduces gliosis in the insulted immature retina. In this Research Topic, the work by Ruff et al. uses a new inducible genetic FLRT3-CreERT2 knock-in mouse to identify a new subpopulation of RGCs with direction selective properties. These RGCs express the transmembrane protein FLRT3 and their axons specifically project to the MTN. FLRTs are multifunctional transmembrane proteins with important functions during nervous system development (Peregrina and Del Toro, 2020). One additional member of the FLRT family, the FLRT2, is analyzed in the work by Li et al. FLRT2 expression is followed during both, normal brain and spinal cord postnatal development and adulthood and during spinal cord injury. This work suggests that FLRT2 might be necessary for the formation of the glial component of the injury scar at the lesion region.

Finally, in the search for therapeutic approaches to treat neuronal dysfunctions, the work by Zirotti Rosenberg et al. analyses the effect of the synthetic exogenous cannabinoid WIN 55212-2 on behavioral convulsions induced by pentylenetetrazol (PTZ) in young rats, comparing the response of males and females. Studying sex as a biological variable is of great interest nowadays as it will help to reduce the gap in the knowledge of the health between genders.

AUTHOR CONTRIBUTIONS

All authors listed have made a substantial, direct, and intellectual contribution to the work and approved it for publication.

ACKNOWLEDGMENTS

We are grateful to all authors and reviewers that contributed to this Research Topic. IS acknowledges to the Max Planck Society for support. JE acknowledges IRBLLEIDA and the University of Lleida for support and the Ministerio de Economia y Competitividad of Spain for funding (PGC2018-101910-B-I00).

REFERENCES

Aprea, J., and Calegari, F. (2015). Long non-coding RNAs in corticogenesis: deciphering the non-coding code of the brain. *EMBO J.* 34, 2865–2884. doi: 10.15252/embj.201592655

Cason, S. E., and Holzbaur, E. L. F. (2022). Selective motor activation in organelle transport along axons. *Nat. Rev. Mol. Cell Biol.* doi: 10.1038/s41580-022-00491-w. [Epub ahead of print].

Giandomenico, S. L., Alvarez-Castelao, B., and Schuman, E. M. (2022). Proteostatic regulation in neuronal compartments. *Trends Neurosci.* 45, 41–52. doi: 10.1016/j.tins.2021.08.002

Jain, S., and Zipursky, S. L. (2022). Temporal control of neuronal wiring. *Semin. Cell Dev. Biol.* doi: 10.1016/j.semcdb.2022.05.012. [Epub ahead of print].

Peregrina, C., and Del Toro, D. (2020). FLRTing neurons in cortical migration during cerebral cortex development. *Front. Cell Dev. Biol.* 8, 578506. doi: 10.3389/fcell.2020.578506

Schelski, M., and Bradke, F. (2017). Neuronal polarization: from spatiotemporal signaling to cytoskeletal dynamics. *Mol. Cell Neurosci.* 84, 11–28. doi: 10.1016/j.mcn.2017.03.008

Sonneveld, S., Verhagen, B. M. P., and Tanenbaum, M. E. (2020). Heterogeneity in mRNA translation. *Trends Cell Biol.* 30, 606–618. doi: 10.1016/j.tcb.2020.04.008

Wong, F. K., and Marín, O. (2019). Developmental cell death in the cerebral cortex. *Annu. Rev. Cell Dev. Biol.* 35, 523–542. doi: 10.1146/annurev-cellbio-100818-125204

Yonehara, K., Ishikane, H., Sakuta, H., Shintani, T., Nakamura-Yonehara, K., Kamiji, N. L., et al. (2009). Identification of retinal ganglion cells and their projections involved in central transmission of information about upward and downward image motion. *PLoS ONE.* 4, e4320. doi: 10.1371/journal.pone.0004320

Conflict of Interest: The authors declare that the research was conducted in the absence of any commercial or financial relationships that could be construed as a potential conflict of interest.

Publisher's Note: All claims expressed in this article are solely those of the authors and do not necessarily represent those of their affiliated organizations, or those of the publisher, the editors and the reviewers. Any product that may be evaluated in this article, or claim that may be made by its manufacturer, is not guaranteed or endorsed by the publisher.

Copyright © 2022 Segura and Egea. This is an open-access article distributed under the terms of the Creative Commons Attribution License (CC BY). The use, distribution or reproduction in other forums is permitted, provided the original author(s) and the copyright owner(s) are credited and that the original publication in this journal is cited, in accordance with accepted academic practice. No use, distribution or reproduction is permitted which does not comply with these terms.

frontiers in Molecular Neuroscience

ORIGINAL RESEARCH
published: 12 April 2021
doi: 10.3389/fnmol.2021.645000

Artemin Is Upregulated by TrkB Agonist and Protects the Immature Retina Against Hypoxic-Ischemic Injury by Suppressing Neuroinflammation and Astrogliosis

*Hsiu-Mei Huang[1], Chao-Ching Huang[2], Linda Yi-Chieh Poon[1] and Ying-Chao Chang[3]**

[1] Department of Ophthalmology, Kaohsiung Chang Gung Memorial Hospital, Chang Gung University College of Medicine, Kaohsiung City, Taiwan, [2] Department of Pediatrics, National Cheng Kung University Hospital, Tainan, Taiwan, [3] Department of Pediatrics, Kaohsiung Chang Gung Memorial Hospital, Chang Gung University College of Medicine, Kaohsiung City, Taiwan

Hypoxic-ischemia (HI) is a major cause of acquired visual impairment in children from developed countries. Previous studies have shown that systemic administration of 7,8-dihydroxyavone (DHF), a selective tropomyosin receptor kinase B (TrkB) agonist, provides long-term neuroprotection against HI injury in an immature retina. However, the target genes and the mechanisms of the neuroprotective effects of TrkB signaling are not known. In the present study, we induced an HI retinal injury through unilateral common carotid artery ligation followed by 8% oxygen for 2 h in P7 rat pups. DHF was administered intraperitoneally 2 h before and 18 h after the HI injury. A polymerase chain reaction (PCR) array was used to identify the target genes upregulated after the DHF treatment, which was then confirmed with quantitative real-time reverse transcriptase PCR and a western blot. Effects of the downstream mediator of DHF were assessed using an intravitreal injection of neutralizing antibody 4 h after DHF administration (24 h after HI). Meanwhile, the target protein was injected into the vitreous 24 h after HI to validate its protective effect when exogenously supplemented. We found that systemic DHF treatment after HI significantly increased the expression of the artemin (*ARTN*) gene and protein at P8 and P10, respectively. The neuroprotective effects of DHF were inhibited after the ARTN protein blockade, with an increase in neuroinflammation and astrogliosis. ARTN treatment showed long-term protection against HI injury at both the histopathological and functional levels. The neuroprotective effects of ARTN were related to a decrease in microglial activation at P17 and attenuation of astrogliosis at P29. ARTN enhances phosphorylation of RET, ERK, and JNK, but not AKT or p38 in the immature retina. Altogether, these results suggest that the neuroprotective effect of a TrkB agonist is partially exerted through a mechanism that involves ARTN because the protective effect is ameliorated by ARTN sequestration. ARTN treatment after HI injury protects the immature retina by attenuating late neuroinflammation and astrogliosis in the immature retina relating to the ARTN/RET/JNK/ERK signaling pathway. ARTN may be a strategy by which to provide long-term protection in the immature retina against HI injury.

Keywords: Artemin (ARTN), astrogliosis, c-Jun N-terminal kinase (JNK), extracellular signal-regulated kinase (ERK), hypoxic-ischemia injury, immature retina, neuroinflammation

OPEN ACCESS

Edited by:
Inmaculada Segura, Ludwig Maximilian University of Munich, Germany

Reviewed by:
Madhuvika Murugan, New Jersey Institute of Technology, United States
Rossella Russo, University of Calabria, Italy

***Correspondence:**
Ying-Chao Chang
ycchao@cgmh.org.tw

Received: *22 December 2020*
Accepted: *17 March 2021*
Published: *12 April 2021*

Citation:
Huang H-M, Huang C-C, Poon LY-C and Chang Y-C (2021) Artemin Is Upregulated by TrkB Agonist and Protects the Immature Retina Against Hypoxic-Ischemic Injury by Suppressing Neuroinflammation and Astrogliosis. Front. Mol. Neurosci. 14:645000. doi: 10.3389/fnmol.2021.645000

INTRODUCTION

With advances in perinatal care, the survival rates of infants with hypoxic-ischemic encephalopathy have increased (Lee et al., 2013). Up to 60% of infants who survive have severe disabilities, including intellectual disability, epilepsy, and cerebral palsy (Pierrat et al., 2005); however, hypoxic-ischemia (HI) is also a major cause of acquired visual impairment in children from developed countries (Tinelli et al., 2020). Although cortical visual dysfunction is an important cause of visual impairment, our previous studies demonstrated that the immature retina is also susceptible to HI injury (Huang et al., 2012, 2015). Compared with adult rodents, HI has been shown to cause more rapid and extensive damage of the retina at both the histopathological and functional levels in rat pups, involving prominent neuroinflammation with astrogliosis and caspase-dependent apoptotic neuronal death (Huang et al., 2012, 2015).

The neuroprotective role of brain-derived neurotrophic factor (BDNF) in the retina has been extensively tested over the past two decades (Afarid et al., 2016). Through the activation of tropomyosin receptor kinase B (TrkB), BDNF leads to increased neurogenesis, neuronal survival, and differentiation (Harada et al., 2011). However, the use of BDNF as a treatment for retinal degeneration has not been successful due to the challenges related to sustaining adequate therapeutic levels (Daly et al., 2018). The use of BDNF mimetics has thus been investigated as an alternative treatment against neuronal injury (Jang et al., 2010). In a previous study, we showed that in rat pups, the systemic administration of 7,8-dihydroxy-avone (DHF), a selective TrkB agonist, provided long-term protection against retinal HI injury at both the histological and functional levels and was related to both decreased astrogliosis and increased neurogenesis (Huang et al., 2018). To elucidate the subsequent gene expression involved in the TrkB-mediated neuroprotection, we used a quantitative real-time polymerase chain reaction (qRT-PCR) array and found that *artemin* was selectively upregulated after DHF treatment in the immature retina with an HI injury (see section "Results").

Artemin (ARTN) is a member of the glial cell line-derived neurotrophic factor (GDNF) family of ligands (GFLs, including GDNF, neurturin, ARTN, and persephin), which form ternary complexes with the GDNF family receptor (GFRα). Assembling of the GFL-GFRα-RET (tyrosine kinase receptor) complex triggers the dimerization of RET, leading to autophosphorylation of specific tyrosine residues in its intracellular domain and subsequent activation of different intracellular signal cascades. These include AKT, ERK, JNK, P38, and Src, which are involved in the regulation of cell survival, neurite outgrowth, and synaptic plasticity (Wong et al., 2015; Nencini et al., 2018). Previous studies have demonstrated the neuroprotective effects of GDNF against HI brain damage in neonatal rats (Ikeda et al., 2000). However, our array data showed significantly elevated *ARTN* mRNA instead of *GDNF* in DHF-treated HI retinas (see section "Results"). In the eye, ARTN is primarily expressed in the retina, and provides neuroprotection in cases of retinal degeneration or after axotomy (Hauck et al., 2006; Omodaka et al., 2014). Accumulating evidence indicates that ARTN plays a critical role in the adaptability of cancer cell populations to hostile challenges such as chemotherapeutics and ionizing radiation (Ding et al., 2014). The adaptive response involves hypoxia-induced ARTN, which promotes the epithelial-mesenchymal transition and decreased apoptosis (Hezam et al., 2018). However, it remains to be determined whether ARTN can rescue immature retina after HI injury, as well as the mechanisms involved.

Abbreviations: ARTN, artemin; ARTN Ab, ARTN-neutralizing antibody; BDNF, brain-derived neurotrophic factor; DHF, 7,8-dihydroxyavone; DAPI, 4',6−diamidino-2-phenylindole; ERG, electroretinography; ERK, extracellular signal-regulated kinase; GDNF, glial cell line-derived neurotrophic factor; GFAP, anti-glial fibrillary acidic protein; GFLs, GDNF family of ligands; GFRα, GDNF family receptor; HI, Hypoxic-ischemia; hr, hour; INL, inner nuclear layer; IOD, integrated optical density; i.p., intraperitoneally; IPL, inner plexiform layer; i.v.i, intravitreal injection; JNK, c-Jun N-terminal kinase; NFL, nerve fiber layer; ONL, outer nuclear layer; P, postnatal; RGC, retinal ganglion cell; TrkB, tropomyosin receptor kinase B.

MATERIALS AND METHODS

Animals

This study was approved by the Animal Care Committee and the Ethics committee of Chang Gung Memorial Hospital in Kaohsiung. Ten to twelve Sprague-Dawley rat pups per dam were used and housed with a 12/12 h light/dark schedule in a temperature- and humidity-controlled colony room. The pups were housed with their dams until weaning at postnatal (P) day 21 and then housed in groups of 4–5 per cage.

Hypoxic-Ischemia Eye Injury

At P7, the animals were anesthetized with 2.5% halothane (balance, room air), and the right common carotid artery was surgically exposed and permanently ligated. After surgery, the pups were returned to the dam for 1 h, then placed in air-tight containers through which humidified 3 L/min 8% oxygen (balance, nitrogen) was maintained for 2 h (Huang et al., 2012). The sham controls underwent anesthesia and surgical exposure but did not receive artery ligation and were not placed in a hypoxic chamber.

Systemic DHF Treatment

Two hours before and 18 h after the induction of HI, the rat pups were injected intraperitoneally with either DHF (5 mg/kg; Tokyo Chemical Industry Co., Tokyo, Japan) or dimethyl sulfoxide (DMSO; 10%; Sigma-Aldrich Corp., St. Louis, MO, United States).

PCR Array

The Rat Neurogenesis RT^2 Profiler ^{TM} PCR Array (Qiagen, Catalog # PARN-404Z, MD, United States), which consisted of primers for 84 genes related to neurogenesis and neural stem cells was used for the gene expression analysis. The rats treated with either DHF or DMSO were sacrificed, and total RNA was prepared from the retinas at P10 and immediately frozen at −70°C. Aliquots of 1 μg RNA per retina were reverse-transcribed using a RT^2 First Strand Kit (Qiagen). The complementary DNA (cDNA) was mixed with SYBR Green (Qiagen) into

the array plates, and cycling was performed according to the manufacturer's protocol. The data obtained from the array were normalized using multiple housekeeping genes and analyzed by comparing $2^{-\Delta Ct}$ of the normalized data. Fold changes were calculated relative to the retinal extracts from HI animals treated with DHF and DMSO. The results were confirmed using a quantitative real-time reverse transcriptase polymerase chain reaction analysis on the individual samples for genes that showed the strongest upregulation and downregulation.

Quantitative Real-Time Reverse Transcriptase Polymerase Chain Reaction

Retinas were dissected and ground with a mortar and pestle in liquid nitrogen under RNase-free conditions. Total RNA was extracted using TRIzol reagent (Invitrogen, Carlsbad, CA, United States). Aliquots of 5 μg total RNA were reverse-transcribed to cDNA using SuperScript III Reverse Transcriptase (Invitrogen). The cDNA was amplified by PCR using the following gene-specific primers: *ARTN*, 5′-CAGAGCCTGGAAAGATGACC-3′ (forward) and 5′-AGAGCTGGGATCCATGAACA-3′ (reverse); and glyceraldehyde 3-phos-phate dehydrogenase (*GAPDH*), 5′-TCTTGTGCAGTGCCAGCCTC-3′ (forward) and 5′-GTCACAAGAGAAGGCAGCCCTGG-3′ (reverse). The template was amplified at 95°C for 5 min, followed by 45 cycles of PCR at 95°C for 10 s, 60°C for 20 s, and 72°C for 20 s using the LightCycler® 480 SYBR Green I Master (Roche, Indianapolis, IN, United States) and LightCycler® 480 instrument (Roche) for analyzing the *ARTN* and *GAPDH*. The C_t assigned as the beginning of the logarithmic amplification was computed using the equipment's software program (Roche). The relative expression level was defined as $2^{-\Delta Ct}$, where $\Delta C_t = C_{ttargetgene} - C_{t\ \beta\ -actin}$. The fold changes in mRNA expression were defined as $2^{-\Delta\Delta Ct}$, where $\Delta\Delta C_t = \Delta C_{ttreatment} - \Delta C_{t\ vehicle}$.

Investigation of the Effects of Artemin

An evaluation of whether the protective effect of DHF comes from upregulating endogenous ARTN, intravitreal injection of either the ARTN-neutralizing antibody (ARTN Ab, 1 μg; R&D systems, Minneapolis, MN, United States) (DeBerry et al., 2015), or phosphate buffered saline (PBS) was performed at post-HI 24 h, which was 6 h after the DHF treatment. To assess the effect of exogenous ARTN in HI injured retinas, either ARTN (1 μg, Peprotech, Rocky Hill, NJ, United States) (Omodaka et al., 2014) or H_2O was administered by intravitreal injection at post-HI 24 h. The animals received intraperitoneal injection of 5-bromo-2′-deoxyuridine (BrdU; 100 mg/kg; Sigma-Aldrich Corp.) for three consecutive days from P8 to P10 for the purpose of identifying cell proliferation.

Functional Evaluation of the Retina Using Electroretinography

At P22 and P29, full-field scotopic flash electroretinograms (ERGs) (RETIport ERG; Roland Consult, Brandenburg, Germany), were recorded from both eyes of the rat pups, as previously described (Huang et al., 2012). Briefly, the pupils were topically dilated with 1% Tropicamide (Mydriacyl, Alcon, Puurs, Belgium) and 1% cyclopentolate (Cyclogyl, Alcon, Puurs, Belgium), then the eyes were dark-adapted for 1 h before performing ERG. The animals were sedated using intramuscular injections of a mixture of Rompun (10 mg/kg; Bayer Korea, Seoul, South Korea) and Zoletil-50 (25 mg/kg; Virbac, Carros, France); then, a standard white flash on a dark background scotopic 0-dB ERG was recorded. The stimulus luminance was 3 cds/m^2 with a duration of 10 ms. Responses from 20 identical flashes applied at 10-s intervals were averaged (Huang et al., 2015).

Histological Assessment of Retinal Injury

Paraffin sections of the retina were dewaxed, hydrated through graded concentrations of alcohol, and placed in phosphate-buffered saline. Cryosections were prepared after fixation in 4% paraformaldehyde and dehydration in a sucrose gradient. Eye blocks were cut at 10 μm. Two sections per retina were randomly selected for hematoxylin and eosin staining. Images were acquired using a light microscope (Nikon, Tokyo, Japan). Retinal damage was quantified within central retinal areas (100–200 μm from the optic disk), as described in our prior study (Huang et al., 2012) by assigning different grades: grade 0, preserved retinal ganglion cell (RGC) and all retinal layers comparable to the sham control; grade 1, moderate decrease in RGC counts and thickness of the inner plexiform layer (IPL); grade 2, complete loss of RGCs and IPL (**Supplementary Figure 1**).

Immunohistochemical Staining

After antigen unmasking and blocking of nonspecific sites, the sections were incubated overnight at 4°C with primary antibodies against ARTN (1:10; R&D systems), phosphorylated (p)RET (1:10; Abcam, Cambridge, United Kingdom), ED1 (1:100; Biosource, Camarillo, CA, United States), antiglial fibrillary acidic protein (GFAP; 1:200; Millipore, Temecula, CA, United States), and BrdU (1:100; Novocastra, Newcastle upon Tyne, United Kingdom) and then subsequently incubated with secondary antibodies for 60 min at room temperature. The immunoreactivity of ARTN was evaluated at a 200× magnification by calculating the integrated optical density (IOD) with ImagePro Plus 6.0 software (Huang et al., 2018). The number of $ED1^+$ and $Brdu^+$ cells were counted in an area of 400 × 100 μm at 200× magnification. The ameboid $ED1^+$ cells were defined as reactive microglial cells. GFAP immunoreactivity was quantified by assigning different grades: grade 1, immunoreactivity in the nerve fiber layer (NFL) and around vessels; grade 2, immunoreactivity in the NFL in an outward tentacle-like pattern, extending toward the inner nuclear layer (INL); grade 3, showing occasional and grade 4, showing extensive GFAP immunoreactivity extending from the NFL to the outer nuclear layer (ONL; Huang et al., 2018).

Western Blot Analysis

Retinas were homogenized, and 40 μg samples were resolved using a 10% sodium dodecyl sulfate polyacrylamide gel electrophoresis, after which they were blotted to nitrocellulose membranes. Membranes were blocked with 5% non-fat dry milk,

incubated with primary antibodies and horseradish-conjugated secondary antibodies, and the signal was visualized with enhanced chemiluminescence. The following primary antibodies were used: anti-ERK (1:10,000; Cell Signaling Technology, Danvers, MA,United States), anti-pERK (1:2000; Millipore), anti- c-Jun N-terminal kinase (JNK, 1:2,000; Cell Signaling Technology), anti-pJNK (1:1,000; Cell Signaling Technology), anti-p38 (1:5,000; Abcam), anti-pp38 (1:10,000; Abcam), anti-Akt (1:10,000; Cell Signaling Technology), and anti-pAkt (1:1,000; Cell Signaling Technology). After the densitometric analysis, data were normalized against GAPDH (Millipore), and the ratio of protein expression in the treated eyes to the sham controls was calculated.

Statistics

Statistical analyses were performed using a 1-way ANOVA or a Kruskal–Wallis test using GraphPad Prism 4 software (GraphPad, San Diego, CA, United States). Data were presented as mean ± standard error, and p values of <0.05 were considered statistically significant.

RESULTS

Systemic DHF Treatment Increases the Expression of ARTN After HI Injury in Immature Retinas

Previously we showed that systemic DHF treatment was able to protect the immature retina against HI injury (Huang et al., 2018). To identify the mediators for the HI protective effects of DHF treatment in the immature retina, a PCR array was performed at P10, and it was found that the expression of ARTN gene in the DHF-treated HI group was 2 times higher than that in the DMSO-treated HI group. In contrast, other neurotrophic factors, including glial cell line-derived neurotrophic factor (GDNF) and BDNF, were not significantly elevated in the DHF-treated HI group (**Supplementary Table**). Using a RT-PCR, we confirmed that the ARTN mRNA levels in the DHF-treated HI group were significantly higher than those in the DMSO-treated HI group and the sham controls 24 h after HI (**Figure 1A**). The immunohistochemical stain showed that ARTN protein was expressed in the RGC, IPL, and INL of the sham controls and the DHF-treated HI group at P8 but was decreased in the DMSO-treated HI group (**Figure 1B** and **Supplementary Figure 2**). The ARTN immunoreactivity was significantly lower in the INL of the DMSO-treated HI group compared to the DHF-treated HI group and the sham group at P10 ($p < 0.05$; **Figure 1C**).

Intravitreal Injection of ARTN-Neutralizing Antibody Blocks the Long-Term Neuroprotection of DHF Against HI at Both the Functional and Histopathological Levels

After HI injury, endogenous ARTN was sequestered using intravitreal injections of artemin-neutralizing antibody (ARTN Ab) to determine whether the neuroprotective effects of DHF in the immature retina were mediated by artemin (**Figure 2A**). ERG performed at P22 and P29 showed that the a-wave (associated with rod photoreceptor activity) and b-wave (Müller glial and bipolar cells activity) amplitudes in the DHF-PBS group were relatively preserved, while in the DMSO-treated group and the DHF-ARTN Ab group, the amplitudes of the a-wave and b-wave were markedly decreased (**Figure 2B**). Group data showed that the b-wave amplitude in the DHF-ARTN Ab group was significantly lower ($p < 0.05$) than that in the DHF-PBS group but was similar to that in the DMSO-treated group (**Figure 2B**). There were no significant among-group differences in the a-wave amplitudes of the DHF-PBS, DHF-ARTN Ab, and DMSO-treated HI groups (data not shown).

Compatible with the functional alterations, there was almost a complete loss of the inner retinal layers, including the RGC, IPL, and INL, in addition to a partial loss of the outer retina layers, including the outer plexiform layer (OPL) and the ONL in the DMSO-treated HI group at P16 and P29 (**Figure 2C**). Although in general thinner than the controls, the retinal layers in the DHF-PBS group were relatively preserved after HI. In contrast, the DHF-ARTN Ab group showed severe inner retinal damages after HI, especially at P29. Semiquantitative data showed that there were no significant between-group differences in the severity of retinal damage in the DMSO-, DHF-PBS- and DHF-ARTN Ab-treated HI groups at P16. However, at P29, the DMSO- and the DHF-ARTN Ab-treated HI groups showed significantly more severe retinal damage than the DHF-PBS group ($p < 0.05$; **Figure 2C**). There were no significant between-group differences in the DMSO- and DHF-ARTN Ab-treated HI groups. These data suggest that the neuroprotective effects of DHF are largely mediated by ARTN and that ARTN was involved in the long-term neuroprotective effects of DHF against HI retinal injury.

Blockade of ARTN Abolishes the Neuroprotection of DHF Through an Increase in Neuroinflammation and Astrogliosis

In our previous study, we also showed that the long-term neuroprotective effects of DHF were related to increased neurogenesis and decreased astrogliosis (Huang et al., 2018). In the current study, immunohistochemical staining showed that at P17, both the DHF-PBS and DHF-ARTN Ab groups had significantly increased $Brdu^+$ cells in the inner retina as compared to in the DMSO-treated HI groups ($p < 0.05$; **Figure 3A** and **Supplementary Figure 3A**), suggesting that DHF promotes cell proliferation in the inner retina, but its treatment effects are not affected by the blockade ARTN protein.

The GFAP immunoreactivity, indicating the presence of astrogliosis, in the DHF-PBS group was significantly lower than that in the DMSO-treated HI group at P29. However, the DHF-ARTN Ab group had extensive GFAP immunostaining throughout all of the retinal layers, similar to the DMSO-treated HI group, which was higher than the DHF-PBS group ($p < 0.05$; **Figure 3B** and **Supplementary Figure 3B**).

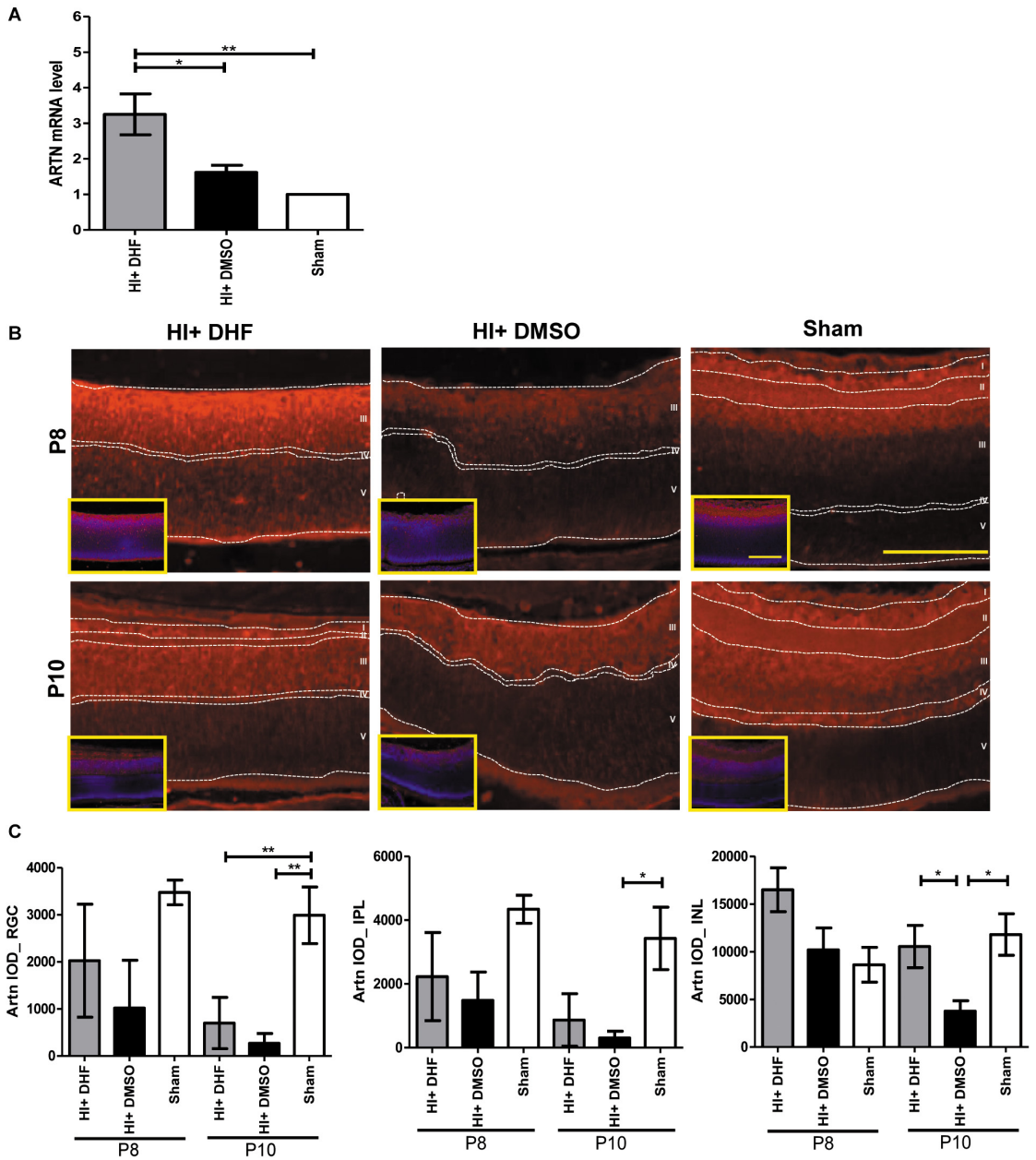

FIGURE 1 | Systemic TrkB agonist- DHF increases ARTN expression in the HI Injured immature retina. **(A)** At P8, the ARTN mRNA level significantly increased in the DHF-treated HI group as compared with the DMSO-treated HI and sham control groups. **(B)** The immunohistochemical stain showed that ARTN protein was expressed in the retina ganglia cells (RGC, layer I), inner plexiform layer (IPL, layer II) and the upper part of inner nuclear layer (INL, layer III) of the sham controls at P8. The ARTN protein expression further extended to outer plexiform layer (OPL, layer IV) in sham controls at P10. There was almost complete loss of layers I and II but preserved layers IV and V (outer nuclear layer, ONL) in both HI groups at P8. The DMSO-treated HI group had decreased ARTN immunostaining in layer III at P8 and P10. In contrast, the DHF-treated HI group had relatively preserved ARTN protein expression in the whole layer III at P8 and P10. The insets showed the nuclear counterstaining with DAPI (blue). **(C)** The group data showed that there was significant difference in the ARTN immunoreactivity of the RGC layer between the sham controls and both the HI group at P10. The DHF-treated HI group had significantly increased ARTN protein expression in the INL than the DMSO-treated HI group at P10. There was no significant difference of ARTN immunoreactivity in the INL between the sham controls and the DHF-treated HI group. Scale bars = 100 μm in figures and insets; n = 4 to 10 per group in each time point, power = 0.8, $^{*}p < 0.05$, $^{**}p < 0.01$.

At P17, reactive microglial cells, or active ED1^{+} cells, were present in the inner retina of all of the groups other than the control. However, the number of ED1^{+} cells was similar between the DMSO-treated and the DHF-ARTN Ab HI groups and was significantly higher than the number in the DHF-PBS group ($p < 0.05$; **Figure 3C** and **Supplementary Figure 3C**). These data suggest that the neuroprotective mechanisms of DHF mediated by ARTN

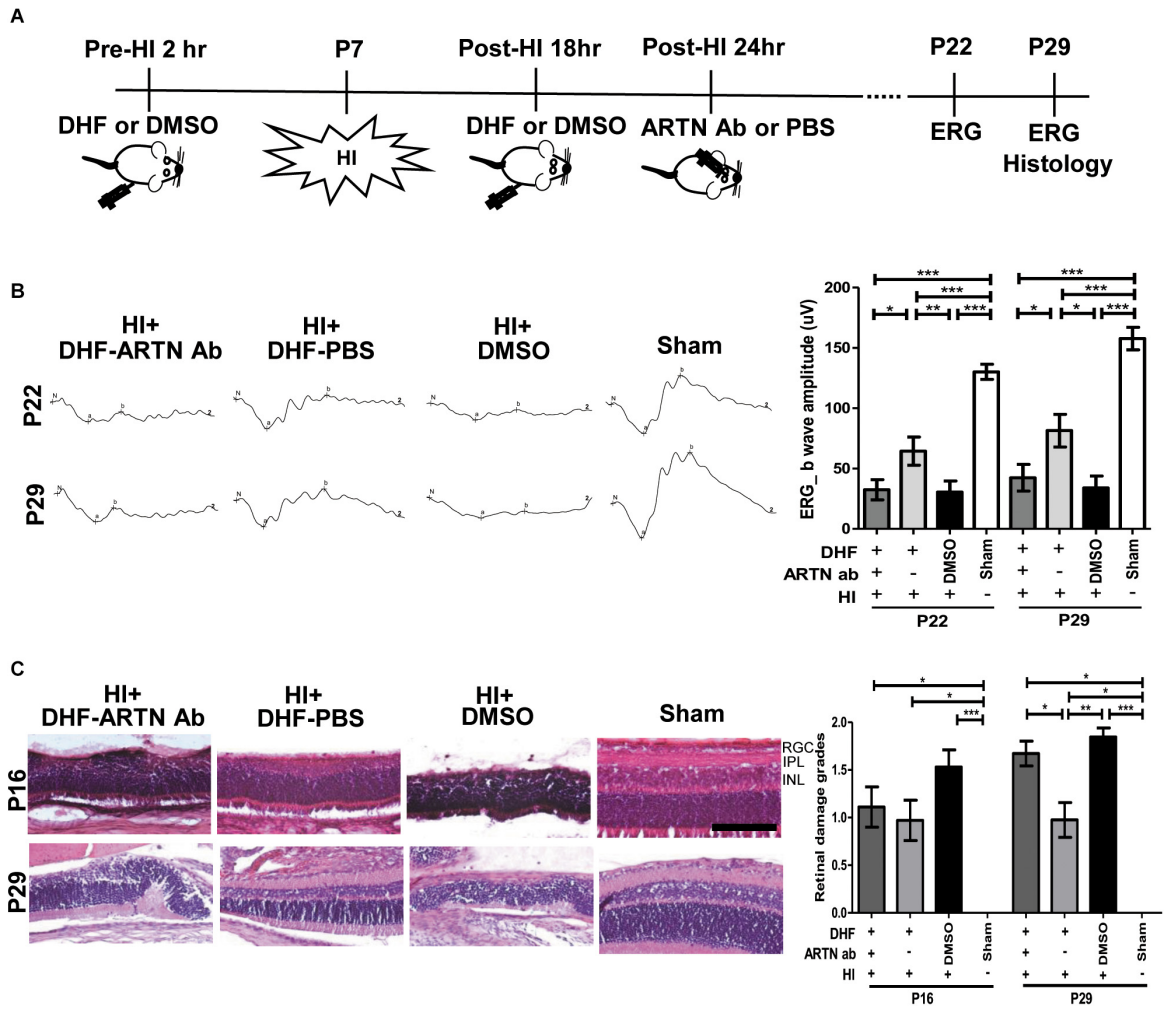

FIGURE 2 | Intravitreal injection of ARTN Antibody inhibits the functional and histological protection of systemic DHF in the HI-injured retinas. **(A)** Two hours before and 18 h after the HI, either DHF or DMSO was injected peritoneally. ARTN-Antibody (Ab) or PBS was injected intravitreally at post-HI 24 h. ERG or/and histology was performed at P22 and P29. **(B)** The retinal function evaluated using ERG demonstrated markedly depressed b-wave amplitudes in the HI injured groups at P22 and P29 as compared with the sham controls. The group data showed that the b-wave amplitude in the DHF-PBS group was significantly higher than that in the DHF-ARTN Ab and DMSO-treated groups after HI at P22 and P29. **(C)** Representative retinal histologic sections showed that the number of RGCs and the thickness of IPL and INL decreased after HI at P16 and P29. The group data showed that the grades of retinal damage were significantly higher in the HI groups than in the sham controls at P16 and P29. There were no significant differences between the DHF-PBS, DMSO, and DHF-ARTN Ab groups after HI injury at P16. As compared with the DHF-PBS group, the DMSO and DHF-ARTN Ab groups exhibited increased retinal damage grades at P29. Scale bars: 100 μm; n = 4–13 per group in each time point, power = 0.8, $^{*}p < 0.05$, $^{**}p < 0.01$, $^{***}p < 0.001$.

involves modulation of astrogliosis and neuroinflammation, but not cell proliferation.

Intravitreal Injection of ARTN Provides Long-Term Protection Against HI Injury at the Histopathological and Functional Levels in Immature Retinas

To verify whether ARTN provides protection against HI injury, the rat pups received intravitreal injections of either ARTN or H_2O 24 h after HI injury. The ERG at P22 and P29 showed that the a-wave and b-wave in the ARTN-treated HI group were relatively preserved, with b-wave amplitudes that were significantly higher than those in the H_2O-treated HI group (both $p < 0.05$; **Figure 4A**). In line with the functional alterations, despite the presence of damaged inner retinal layers in the ARTN-treated HI group, the damage still occurred to a lesser degree than that in the H_2O-treated HI group and was statistically significant at both P16 and P29 (both $p < 0.05$; **Figure 4B**).

ARTN Treatment Protects the Immature Retina Against HI Injury by Inhibiting Late Neuroinflammation and Astrogliosis

Immunohistochemical staining showed that at P17, the number of proliferating or Brdu^{+} cells were not significantly

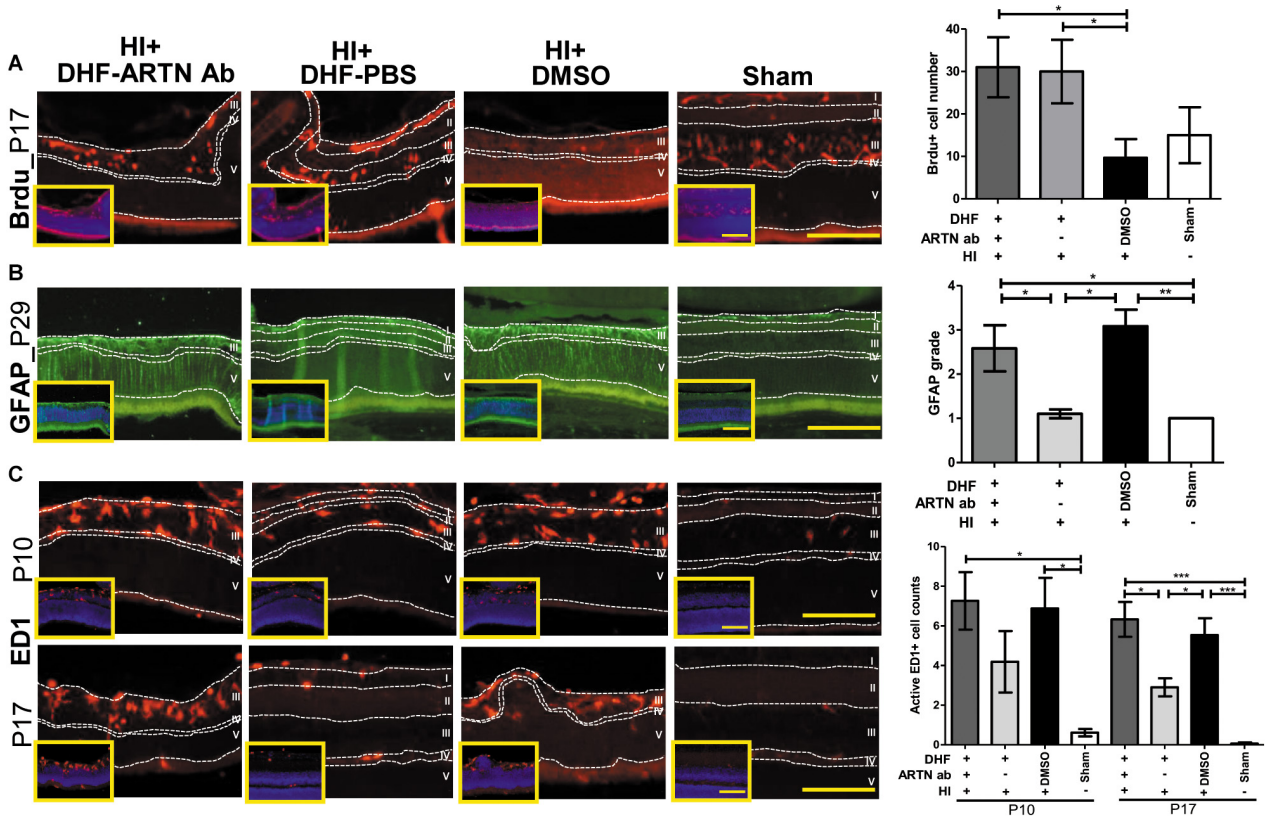

FIGURE 3 | ARTN Antibody blocks the protective effect of systemic DHF treatment in HI-injured retinas by increasing neuroinflammation. **(A)** At P17, he Brdu$^+$ cells localized in the retina ganglia cells (RGC, layer I), inner plexiform layer (IPL, layer II), and inner nuclear layer (INL, layer III) in sham controls. There was almost complete loss of layers I and II but preserved layers IV (outer plexiform layer, OPL) and V (outer nuclear layer, ONL) in DMSO- and DHF-ARTN Ab-treated HI groups in the representative figures. The DMSO-treated HI group had few Brdu$^+$ cells in the layer III. The total Brdu$^+$ cells was significantly lower in the DMSO-treated HI group as compared to in the DHF-PBS and DHF- ARTN Ab groups after HI. There was no significant difference in the DHF-PBS- and DHF- ARTN Ab-treated HI groups. **(B)** At P29, GFAP immunostaining was extensive throughout all retinal layers in the DMSO-treated and DHF-ARTN Ab groups after HI. The grades of GFAP immunoreactivity were significantly higher in the DMSO-treated and DHF-ARTN Ab groups than in the DHF-PBS and sham control groups. **(C)** The ameboid microglial cells (active ED1$^+$ cells) localized in the layers I, II and III after HI at P10. The DMSO- and DHF- ARTN Ab-treated HI groups had prominent ameboid microglial cells mainly in layer III as the layers I and II were lost. The microglial cells were less active in the DHF-PBS-treated HI groups at P17. But the DMSO- and DHF-ARTN Ab-treated HI groups still had prominent ameboid microglial cells in layer III of retina. The group data showed that the active ED1$^+$ cell counts were markedly increased in the DMSO- and DHF-ARTN Ab-treated HI groups as compared with the sham controls at P10 and P17. The DHF-PBS group exhibited significantly decreased active ED1$^+$ cells than the DMSO and DHF-ARTN Ab groups at P17. There was no significant difference between the DMSO- and DHF-ARTN Ab-treated HI groups at P10 and P17. The insets showed the nuclear counterstaining with DAPI (blue). Scale bars: 100 μm in main figures and insets; n = 4–11 per group in each time point, power = 0.8, $^*p < 0.05$, $^{**}p < 0.01$, $^{***}p < 0.001$.

different between the ARTN- and H_2O-treated HI groups (**Figure 5A** and **Supplementary Figure 4A**). However, GFAP immunostaining at P29 demonstrated that ARTN treatment significantly decreased astrogliosis after HI ($p < 0.05$; **Figure 5B** and **Supplementary Figure 4B**). Both the ARTN- and H_2O-treated HI groups showed significantly greater neuroinflammation, with increased active ED1$^+$ cells, as compared to the sham controls at P10 ($p < 0.001$; **Figure 5C** and **Supplementary Figure 4C**). However, at P17, the number of active ED1$^+$ cells in the ARTN-treated HI group was significantly decreased compared to the H_2O-treated HI group ($p < 0.05$; **Figure 5C** and **Supplementary Figure 4C**), which was similar to the sham controls. These data suggest that ARTN protects the immature retina by decreasing astrogliosis and late neuroinflammation after HI.

ARTN Treatment After HI Injury Enhances RET, ERK, and JNK Phosphorylation in Immature Retinas

The ARTN-treated HI group had prominent ARTN immunostaining in the RGC and INL at P10, which indicates that ARTN continued to be expressed in the inner retina two days after the treatment. There were significant differences between the ARTN-treated HI group and the H_2O-treated HI group and the sham controls ($p < 0.01$; **Figure 6A** and **Supplementary Figure 5A**). Immunostaining showed that the ARTN treatment after HI induces significantly increased RET phosphorylation (pRET) immunoreactivity in the RGC, IPL, and OPL ($p < 0.05$; **Figure 6B** and **Supplementary Figure 5B**).

To investigate the downstream signaling pathways of ARTN/RET, western blots were performed at P10. There were

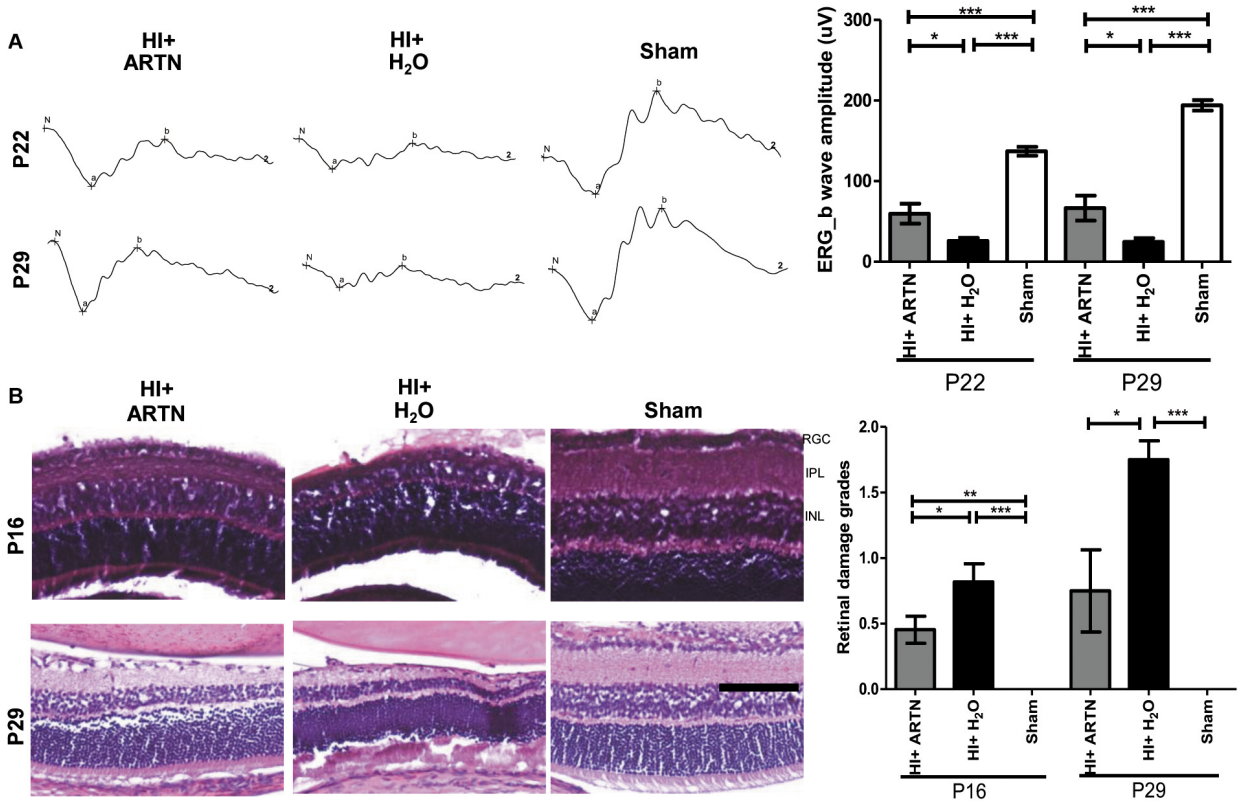

FIGURE 4 | Intravitreal injection of ARTN protects immature retinas against HI injury in both functional and histological levels. **(A)** At P22 and P29, the b-wave amplitudes of ERG were significantly decreased in the HI injured groups, as compared with the sham controls. The b-wave amplitude was significantly higher in the ARTN-treated as compared to in the H_2O-treated group after HI. **(B)** Representative retinal histologic sections showed that the number of RGCs and the thickness of IPL and INL decreased after HI. The group data showed that the retinal damage grades were markedly higher in the H_2O-treated HI group than the ARTN-treated HI group at P16 and P29. Scale bars: 100 μm; n = 6–16 per group in each time point, power = 0.8, $^{*}p < 0.05$, $^{**}p < 0.01$, $^{***}p < 0.001$.

no significant differences in the total and phosphorylated p38 or AKT between the ARTN- and H_2O-treated HI groups at P10 (**Figures 6C,D**). However, the ARTN-treated group exhibited significantly increased phosphorylation of ERK and JNK as compared to the H_2O -treated HI group (both $p < 0.05$; **Figures 6E,F**). There were no significant differences in the total ERK and JNK expression between the ARTN- and H_2O-treated HI groups.

DISCUSSION

The present study is the first to demonstrate that systemic treatment with DHF upregulates the expression of ARTN after HI injury in the immature retina. The higher expression of ARTN in the inner retina, which is more vulnerable to HI injury in an immature retina, may be one of the factors responsible for its neuroprotection. Surprisingly, the TrkB agonist triggers indirect neuroprotection through a mechanism that involves ARTN because the protection is ameliorated with ARTN sequestration. This result is consistent with our findings indicating that ARTN treatment after HI injury protects the immature retina by attenuating late neuroinflammation and astrogliosis. The ARTN/RET/JNK/ERK signaling pathway appears to be involved in the ARTN-mediated neuroprotection. We suggest that ARTN may represent a promising therapy for restoring retinal function after HI injury in neonates.

ARTN is an important mediator of various physiological and pathophysiological functions, including the development and maintenance of various neuronal populations, neurite outgrowth, and nerve regeneration (Wong et al., 2015). ARTN has been used in a clinical trial as a treatment for depression based on its neuroplasticity effects (Di Cesare Mannelli et al., 2011). There is increasing evidence that ARTN plays an important role in the adaptation of cancer cell populations to challenges that are not conducive to survival. The adaptive response involves hypoxia-induced ARTN promotion of epithelial-mesenchymal transition and decreased apoptosis (Ding et al., 2014; Hezam et al., 2018). Recent evidence suggests that ARTN plays a bi-directional role in the modulation of neuropathic pain and inflammation (Ikeda-Miyagawa et al., 2015). ARTN is increased by inflammation and mediates nociceptive signaling in both humans and animals (Thornton et al., 2013; Ikeda-Miyagawa et al., 2015; Nencini et al., 2018). Anti-ARTN Ab treatment has been shown to inhibit ARTN/RET/ERK activation and block capsaicin-induced calcitonin gene-related

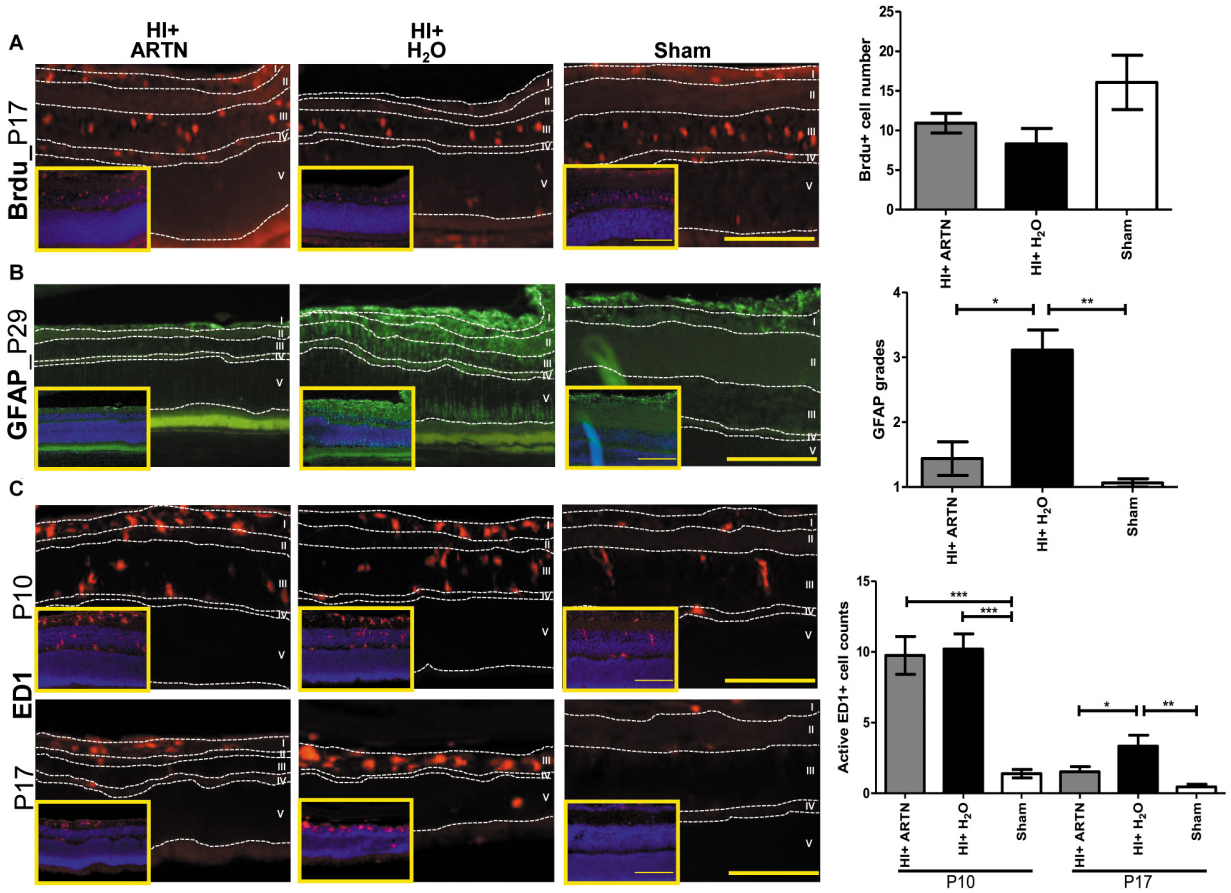

FIGURE 5 | Intravitreal injection of ARTN does not increase cell proliferation but decreases neuroinflammation and astrogliosis. **(A)** The representative figures showed that the Brdu$^+$ cells are mainly localized in the retinal ganglia cells (RGC, layer I) and inner nuclear layer (INL, layer III) at P17. There were no significant between-group differences in the Brdu$^+$ cell counts in the ARTN- and H_2O-treated HI groups. **(B)** At P29, the H_2O-treated HI group had marked GFAP immunostaining extending the whole retina. The GFAP immunostaining were significantly lower in the ARTN-treated HI group as compared to in the H_2O-treated HI group by the semiquantitative analysis. There was no significant difference between the ARTN-treated HI group and sham controls. **(C)** Active ED1$^+$ cells mainly localized in the layers I, II (inner plexiform layer, IPL) and III, but not in the outer plexiform layer (OPL, layer IV) and outer nuclear layer (layer V), after HI at P10. There were persistent prominently ameboid microglial cells in the layer III of the H_2O-treated HI groups at P17. The cell counts were significantly increased in the ARTIN-treated and H_2O-treated HI groups than sham controls at P10. The ARTN-treated HI group had markedly decreased active ED1$^+$ cells, as compared with the H_2O-treated HI group at P17. The insets showed the nuclear counterstaining with DAPI (blue). Scale bars: 100 μm in main figures and insets; n = 5–16 per group in each time point, power = 0.8, $^*p < 0.05$, $^{**}p < 0.01$, $^{***}p < 0.001$.

peptide secretion *in vitro* (Jeong et al., 2008). Conversely, a phase 2 clinical trial showed evidence of pain relief by ARTN in patients with lumbosacral radiculopathy (Backonja et al., 2017). Although the exact mechanisms underlying the regulation of inflammation by ARTN require further investigation, the findings of this study provide novel evidence suggesting that ARTN may protect the immature retina via its anti-inflammation action, likely through RET/JNK/ERK signaling pathway.

Post-ischemic neuroinflammation in the immature central nervous system is a key pathophysiological factor in the development of HI-related injury (Borjini et al., 2019). It is highly likely that this secondary inflammation augments damage in the early phase of evolving cell death (Hagberg et al., 2015). The downstream mediators of inflammation-induced injuries include induction of immune mediators, reactive oxygen and nitrogen species, excitotoxicity, mitochondrial impairment, and reduced vascular integrity (Hagberg et al., 2015). Microglial infiltration and astrogliosis has shown to potentially persist up to 21 days or 2 months after HI insult in animal and human studies, respectively (Galinsky et al., 2017; Galinsky et al., 2018). We also found that microglial activation in the inner retina from 6 h post-HI reached a peak level on P9, decreased from P14, and persisted to P33 in neonates. In contrast, the retinal Müller glial cells was shown to undergo reactive astrogliosis throughout all the ipsilateral retina layers from P21 to P60 after HI (Huang et al., 2012). Our data showed that ARTN treatment significantly attenuated microglial activation at P17 but not at P10. It seems that ARTN plays an important role in modulating late inflammation after HI injury. ARTN was also found to significantly decrease late astrogliosis at P29. While the mechanisms need to be further investigated, these

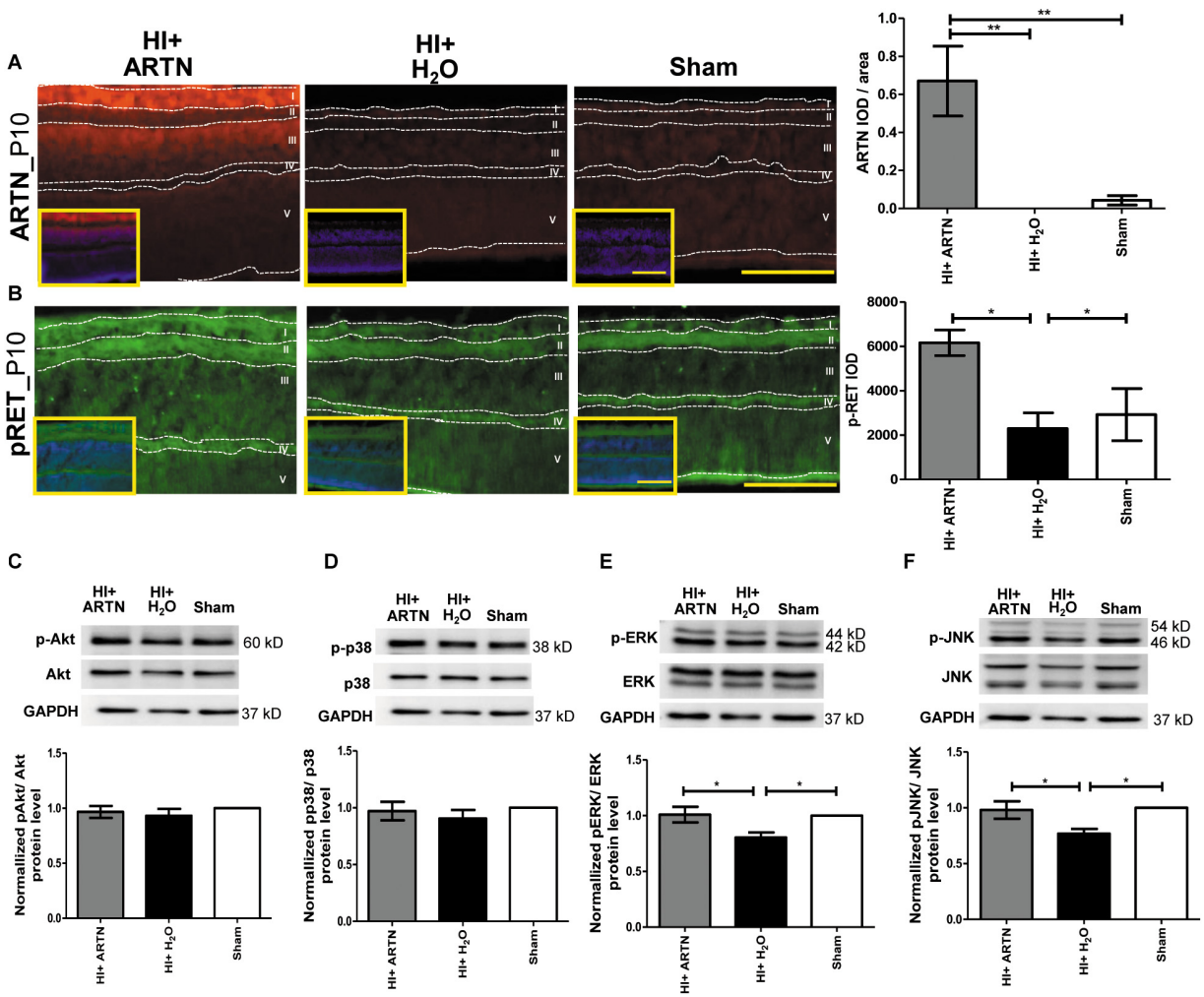

FIGURE 6 | Post-treatment with ARTN enhances RET, ERK, and JNK phosphorylation in the immature retina after HI injury. **(A)** At P10, the ARTN immunostaining was prominent in the retinal ganglia cells (RGC, layer I) and inner nuclear layer (INL, layer III) of the ARTN-treated HI group. The group data showed that the immunoreactivity of ARTN was significantly higher in the ARTN-treated HI group than in the H_2O-treated HI group and the sham controls. **(B)** Alt P10, the immunostaining of phosphorylated RET (pRET) localized in the layers I, II (inner plexiform layer, IPL), and IV (outer plexiform layer, OPL). The group data showed that the H_2O-treated HI group had significantly decreased pRET immunostaining as compared with the ARTN-treated HI groups and the sham controls. At P10, the western blot analysis showed there were no significant differences in the **(C)** phosphorylated (p) Akt or **(D)** pp38 among the ARTN-treated HI group, H_2O-treated HI group, and sham controls. The ARTN-treated HI group had a higher expression of **(E)** pERK and **(F)** pJNK than the H_2O-treated HI group. Nuclear counterstaining with DAPI (blue) was shown in the inset; layer V: outer nuclear layer (ONL); Scale bars: 100 μm in main figures and insets; n = 4–7 per group in each time point, power = 0.8, $^{*}p < 0.05$, $^{**}p < 0.01$.

data imply that supplementing or enhancing levels of ARTN make it possible to block the secondary or chronic inflammation caused by microglia and retinal Müller glial cells activation, which may be a viable therapeutic target leading to improvements in neurodevelopmental outcomes after HI injury.

The BDNF/TrkB signaling pathways and their requirements in the neuroprotection and neuron development processes are well-established, but little is known about how ARTN, one of the GFLs, induces retinal protection. BDNF protects injured RGCs both *in vitro* and *in vivo*, acting directly on the RGCs that express TrkB (Afarid et al., 2016). Conversely, it has been demonstrated that GFLs do not enhance the survival of RGCs *in vitro*, despite the fact that they enhance RGC survival *in vivo* (Koeberle and Ball, 2002). These results suggest that GFLs do not act directly on RGCs to increase cell survival *in vivo*. However, they reduces glutamate-mediated excitotoxicity in axotomized RGCs related to increasing the expression of the glutamate/aspartate transporter-1 in retinal Müller glial cells and astrocytes (Harada et al., 2011). Previous findings are, in general, consistent with the findings of the present study, in which it was found that increased ARTN levels, either induced by DHF treatment or exogenously supplemented by intravitreal administration, protect the immature retina against HI injury by ameliorating the activation of microglia and astrocytes, but this increase does not promote cell regeneration.

Recent evidence suggests that neurotrophic rescue of retinal neurons can be indirect, mediated by the interaction of other neurotrophic factors with glial cells, which in turn release secondary factors acting directly on neurons (Hauck et al., 2006). BDNF has no direct effect on isolated photoreceptor cells. Thus, it may protect photoreceptors, at least partly, through retinal Müller glial cells. BDNF-treated cultured retinal Müller glial cells was found to express BDNF, GDNF, and basic fibroblast growth factor (bFGF), in turn protecting RGCs against glutamate toxicity (Harada et al., 2011). Retinal Müller glial cells responded to Neurotrophin-3 or nerve growth factor (NGF), respectively, by increasing or decreasing their production of bFGF, which in turn resulted in either the protection or increased apoptosis of photoreceptor cells (Harada et al., 2015). We previously demonstrated that systemic DHF treatment does not prevent early neuronal apoptosis, but rather enhances the proliferation of retinal Müller glial cells and bipolar cells, thereby restoring retinal function after HI injury in rat pups (Huang et al., 2018). The present study further shows that the blockade of endogenous ARTN protein abolishes the long-term neuroprotective effects of DHF through increasing late neuroinflammation and astrogliosis. These data suggest that TrkB signaling involves not only RGCs but also retinal Müller glial cells, astrocytes, and microglia leading to neuroprotection. Therefore, a promising neuroprotective strategy may involve not only promoting neuronal survival but also may involve the cross-talks of neurotrophic factors with which the microglia, retinal Müller glial cells, and inner retinal neurons communicate during HI retinal injury.

We found that ARTN post-treatment activates both ERK and JNK signaling pathways in the immature retina during HI injury. The GFLs and GFR communications in the retina activate distinct signaling cascades, including ERK, JNK, and AKT, but with different time courses that are often involved in complex cross-talk on multiple levels (Hauck et al., 2006). These signaling pathways are involved in various cellular processes, including cell proliferation, differentiation, senescence, and apoptosis. The coordination between these pathways determines a cell's fate. Our previous data showed that ERK activation is pivotal for the long-term neuroprotective effects of DHF treatment. ERK signaling mediates the effects of TrkB on retinal neuron proliferation and transdifferentiation (Huang et al., 2018). Conversely, JNK contributes to the apoptotic response of neuronal cells, and JNK-dependent apoptosis can be suppressed by the activation of ERK (Clark, 2018). However, recent studies indicate that periostin, an adhesion molecule, enhances the migration and differentiation of mesenchymal stem cells via the JNK signaling pathway under inflammatory conditions (Tang et al., 2017). Although the exact mechanism underlying the neuroprotection of ARTN needs further clarification, the findings of this study indicate that the intracellular signaling dynamics between ERK and JNK may play a role in the inflammatory process in HI retinal injury.

The advent of therapeutic hypothermia for neonatal HI injury made it possible to intervene and alter the course of this disease with improved rates of infant survival (Higgins et al., 2011). However, 40% of infants with severe HI injury still suffer from significant neurologic disability (Shankaran, 2015). The combination of perinatal infection and HI insult causes greater brain injury and poorer response to therapeutic hypothermia (Osredkar et al., 2014). These concerns highlight the need for adding alternative therapeutic strategies, especially those targeting neuroinflammation, beyond hypothermia therapy for HI injury. Our data suggest that ARTN is a promising candidate since it provides long-term protection to the immature retina against HI injury by ameliorating late neuroinflammation.

DATA AVAILABILITY STATEMENT

The original contributions presented in the study are included in the article/**Supplementary Material**, further inquiries can be directed to the corresponding author/s.

ETHICS STATEMENT

The animal study was reviewed and approved by Animal Care Committee and the Ethics Committee of Chang Gung Memorial Hospital in Kaohsiung.

AUTHOR CONTRIBUTIONS

H-MH designed the research, planned and performed the experiments, analyzed the data, and drafted the manuscript. C-CH designed a part of the research and collaborated in performing the experiments. LY-CP analyzed the data and revised the manuscript. Y-CC designed the research project, analyzed the data, and revised the manuscript. All authors read and approved the final manuscript.

FUNDING

This work was supported by a grant from the Ministry of Science and Technology (Grant 106-2314-B-182A-047; Taipei, Taiwan).

SUPPLEMENTARY MATERIAL

The Supplementary Material for this article can be found online at: https://www.frontiersin.org/articles/10.3389/fnmol.2021.645000/full#supplementary-material

Supplementary Figure 1 | Grading of retinal damage. Grade 0, preserved RGCs and all retinal layers comparable to sham control; grade 1, moderate decreases in the RGC counts and thicknesses of the IPL; grade 2, complete loss of RGCs and IPL. Scale bars: 100 μm.

Supplementary Figure 2 | Systemic TrkB agonist- DHF increases ARTN expression in the HI Injured immature retina. In the DHF-treated HI and sham control groups, double staining of ARTN (red) and DAPI (blue) showed the immunoreactivity of ARTN was prominent in the RGC, IPL, and INL at P8, and the expression decreased at P10. Scale bars: 100 μm.

Supplementary Figure 3 | ARTN Antibody blocks the protective effect of systemic DHF in HI-injured retinas by increasing neuroinflammation. Nuclear

counterstaining with DAPI (blue) showed **(A)** most of the Brdu$^+$ cells (red) localized in the RGCs, IPL, and INL at P17; **(B)** GFAP immunostaining (green) was quite strong and extensive throughout all retinal layers in the DMSO-treated and DHF-ARTN Ab groups after HI at P29; **(C)** active ED1$^+$ cells (red) localized in the RGC, IPL, and INL after HI at P10 and P17. Scale bars: 100 μm.

Supplementary Figure 4 | Intravitreal injection of ARTN does not increase cell proliferation but decreases neuroinflammation and astrogliosis. Nuclear counterstaining with DAPI (blue) showed **(A)** most of the Brdu$^+$ cells (red) are localized in the RGC and INL at P17; **(B)** the GFAP immunostaining (green) was quite strong and extensive throughout all retinal layers in the H_2O-treated group as compared to in the ARTN-treated group at P29; **(C)** active ED1$^+$ cells (red) localized in the IPL and INL after HI at P10 and P17. Scale bars: 100 μm.

Supplementary Figure 5 | Post-treatment with ARTN enhances RET phosphorylation in the immature retina after HI injury. Nuclear counterstaining with DAPI (blue) showed **(A)** the ARTN immunostaining (red) was prominent in the RGC and INL of the ARTN-treated HI group at P10; **(B)** the immunostaining of phosphorylated RET (pRET, green) localized in the RGC, IPL, and OPL at P10. Scale bars: 100 μm.

REFERENCES

Afarid, M., Torabi-Nami, M., and Zare, B. (2016). Neuroprotective and restorative effects of the brain-derived neurotrophic factor in retinal diseases. *J. Neurol. Sci.* 363, 43–50. doi: 10.1016/j.jns.2016.02.024

Backonja, M., Williams, L., Miao, X., Katz, N., and Chen, C. (2017). Safety and efficacy of neublastin in painful lumbosacral radiculopathy: a randomized, double-blinded, placebo-controlled phase 2 trial using Bayesian adaptive design (the SPRINT trial). *Pain* 158, 1802–1812. doi: 10.1097/j.pain.0000000000000983

Borjini, N., Sivilia, S., Giuliani, A., Fernandez, M., Giardino, L., Facchinetti, F., et al. (2019). Potential biomarkers for neuroinflammation and neurodegeneration at short and long term after neonatal hypoxic-ischemic insult in rat. *J. Neuroinflammation* 16:194.

Clark, A. (2018). Psychiatric diagnoses and informed consent. *J. Clin. Ethics* 29, 93–99.

Daly, C., Ward, R., Reynolds, A. L., Galvin, O., Collery, R. F., and Kennedy, B. N. (2018). Brain-Derived neurotrophic factor as a treatment option for retinal degeneration. *Adv. Exp. Med. Biol.* 1074, 465–471. doi: 10.1007/978-3-319-75402-4_57

DeBerry, J. J., Saloman, J. L., Dragoo, B. K., Albers, K. M., and Davis, B. M. (2015). Artemin immunotherapy is effective in preventing and reversing cystitis-induced bladder hyperalgesia via TRPA1 regulation. *J. Pain* 16, 628–636. doi: 10.1016/j.jpain.2015.03.014

Di Cesare Mannelli, L., Vivoli, E., Salvicchi, A., Schiavone, N., Koverech, A., Messano, M., et al. (2011). Antidepressant-like effect of artemin in mice: a mechanism for acetyl-L-carnitine activity on depression. *Psychopharmacology (Berl).* 218, 347–356. doi: 10.1007/s00213-011-2326-0

Ding, K., Banerjee, A., Tan, S., Zhao, J., Zhuang, Q., Li, R., et al. (2014). Artemin, a member of the glial cell line-derived neurotrophic factor family of ligands, is HER2-regulated and mediates acquired trastuzumab resistance by promoting cancer stem cell-like behavior in mammary carcinoma cells. *J. Biol. Chem.* 289, 16057–16071. doi: 10.1074/jbc.m113.529552

Galinsky, R., Draghi, V., Wassink, G., Davidson, J. O., Drury, P. P., Lear, C. A., et al. (2017). Magnesium sulfate reduces EEG activity but is not neuroprotective after asphyxia in preterm fetal sheep. *J. Cereb. Blood Flow Metab.* 37, 1362–1373. doi: 10.1177/0271678x16655548

Galinsky, R., Lear, C. A., Dean, J. M., Wassink, G., Dhillon, S. K., Fraser, M., et al. (2018). Complex interactions between hypoxia-ischemia and inflammation in preterm brain injury. *Dev. Med. Child Neurol.* 60, 126–133. doi: 10.1111/dmcn.13629

Hagberg, H., Mallard, C., Ferriero, D. M., Vannucci, S. J., Levison, S. W., Vexler, Z. S., et al. (2015). The role of inflammation in perinatal brain injury. *Nat. Rev. Neurol.* 11, 192–208.

Harada, C., Azuchi, Y., Noro, T., Guo, X., Kimura, A., Namekata, K., et al. (2015). TrkB signaling in retinal glia stimulates neuroprotection after optic nerve injury. *Am. J. Pathol.* 185, 3238–3247. doi: 10.1016/j.ajpath.2015.08.005

Harada, C., Guo, X., Namekata, K., Kimura, A., Nakamura, K., Tanaka, K., et al. (2011). Glia- and neuron-specific functions of TrkB signalling during retinal degeneration and regeneration. *Nat. Commun.* 2:189.

Hauck, S. M., Kinkl, N., Deeg, C. A., Swiatek-De Lange, M., Schoffmann, S., and Ueffing, M. (2006). GDNF family ligands trigger indirect neuroprotective signaling in retinal glial cells. *Mol. Cell. Biol.* 26, 2746–2757. doi: 10.1128/mcb.26.7.2746-2757.2006

Hezam, K., Jiang, J., Sun, F., Zhang, X., and Zhang, J. (2018). Artemin promotes oncogenicity, metastasis and drug resistance in cancer cells. *Rev. Neurosci.* 29, 93–98. doi: 10.1515/revneuro-2017-0029

Higgins, R. D., Raju, T., Edwards, A. D., Azzopardi, D. V., Bose, C. L., Clark, R. H., et al. (2011). Hypothermia and other treatment options for neonatal encephalopathy: an executive summary of the Eunice Kennedy Shriver NICHD workshop. *J. Pediatr.* 159:e851.

Huang, H. M., Huang, C. C., Hung, P. L., and Chang, Y. C. (2012). Hypoxic–ischemic retinal injury in rat pups. *Pediatr. Res.* 72, 224–231. doi: 10.1038/pr.2012.74

Huang, H. M., Huang, C. C., Tsai, M. H., Poon, Y. C., and Chang, Y. C. (2018). Systemic 7,8-dihydroxyflavone treatment protects immature retinas against hypoxic-ischemic injury via müller glia regeneration and MAPK/ERK activation. *Invest. Ophthalmol. Vis. Sci.* 59:3124. doi: 10.1167/iovs.18-23792

Huang, H. M., Huang, C. C., Wang, F. S., Hung, P. L., and Chang, Y. C. (2015). Activating the Wnt/β-catenin pathway did not protect immature retina from hypoxic-ischemic injury. *Invest. Ophthalmol. Vis. Sci.* 56:4300. doi: 10.1167/iovs.14-16176

Ikeda, T., Xia, X. Y., Xia, Y. X., Ikenoue, T., Han, B., and Choi, B. H. (2000). Glial cell line-derived neurotrophic factor protects against ischemia/hypoxia-induced brain injury in neonatal rat. *Acta Neuropathol.* 100, 161–167. doi: 10.1007/s004019900162

Ikeda-Miyagawa, Y., Kobayashi, K., Yamanaka, H., Okubo, M., Wang, S., Dai, Y., et al. (2015). Peripherally increased artemin is a key regulator of TRPA1/V1 expression in primary afferent neurons. *Mol. Pain* 11:8.

Jang, S. W., Liu, X., Yepes, M., Shepherd, K. R., Miller, G. W., Liu, Y., et al. (2010). A selective TrkB agonist with potent neurotrophic activities by 7,8-dihydroxyflavone. *Proc. Natl. Acad. Sci. U.S.A.* 107, 2687–2692. doi: 10.1073/pnas.0913572107

Jeong, D. G., Park, W. K., and Park, S. (2008). Artemin activates axonal growth via SFK and ERK-dependent signalling pathways in mature dorsal root ganglia neurons. *Cell Biochem. Funct.* 26, 210–220. doi: 10.1002/cbf.1436

Koeberle, P. D., and Ball, A. K. (2002). Neurturin enhances the survival of axotomized retinal ganglion cells *in vivo*: combined effects with glial cell line-derived neurotrophic factor and brain-derived neurotrophic factor. *Neuroscience* 110, 555–567. doi: 10.1016/s0306-4522(01)00557-7

Lee, A. C., Kozuki, N., Blencowe, H., Vos, T., Bahalim, A., Darmstadt, G. L., et al. (2013). Intrapartum-related neonatal encephalopathy incidence and impairment at regional and global levels for 2010 with trends from 1990. *Pediatr. Res.* 74(Suppl. 1), 50–72. doi: 10.1038/pr.2013.206

Nencini, S., Ringuet, M., Kim, D. H., Greenhill, C., and Ivanusic, J. J. (2018). GDNF, neurturin, and artemin activate and sensitize bone afferent neurons and contribute to inflammatory bone pain. *J. Neurosci.* 38, 4899–4911. doi: 10.1523/jneurosci.0421-18.2018

Omodaka, K., Kurimoto, T., Nakamura, O., Sato, K., Yasuda, M., Tanaka, Y., et al. (2014). Artemin augments survival and axon regeneration in axotomized retinal ganglion cells. *J. Neurosci. Res.* 92, 1637–1646. doi: 10.1002/jnr.23449

Osredkar, D., Thoresen, M., Maes, E., Flatebo, T., Elstad, M., and Sabir, H. (2014). Hypothermia is not neuroprotective after infection-sensitized neonatal hypoxic-ischemic brain injury. *Resuscitation* 85, 567–572. doi: 10.1016/j.resuscitation.2013.12.006

Pierrat, V., Haouari, N., Liska, A., Thomas, D., Subtil, D., Truffert, P., et al. (2005). Prevalence, causes, and outcome at 2 years of age of newborn encephalopathy: population based study. *Arch. Dis. Child. Fetal Neonatal Ed.* 90, F257–F261.

Shankaran, S. (2015). Therapeutic hypothermia for neonatal encephalopathy. *Curr. Opin. Pediatr.* 27, 152–157. doi: 10.1097/mop.0000000000000199

Tang, Y., Liu, L., Wang, P., Chen, D., Wu, Z., and Tang, C. (2017). Periostin promotes migration and osteogenic differentiation of human periodontal

ligament mesenchymal stem cells via the Jun amino-terminal kinases (JNK) pathway under inflammatory conditions. *Cell Prolif.* 50:e12369. doi: 10.1111/cpr.12369

Thornton, P., Hatcher, J. P., Robinson, I., Sargent, B., Franzen, B., Martino, G., et al. (2013). Artemin-GFRalpha3 interactions partially contribute to acute inflammatory hypersensitivity. *Neurosci. Lett.* 545, 23–28. doi: 10.1016/j.neulet.2013.04.007

Tinelli, F., Guzzetta, A., Purpura, G., Pasquariello, R., Cioni, G., and Fiori, S. (2020). Structural brain damage and visual disorders in children with cerebral palsy due to periventricular leukomalacia. *Neuroimage Clin.* 28:102430. doi: 10.1016/j.nicl.2020.102430

Wong, L. E., Gibson, M. E., Arnold, H. M., Pepinsky, B., and Frank, E. (2015). Artemin promotes functional long-distance axonal regeneration to the brainstem after dorsal root crush. *Proc. Natl. Acad. Sci. U.S.A.* 112, 6170–6175. doi: 10.1073/pnas.1502057112

Conflict of Interest: The authors declare that the research was conducted in the absence of any commercial or financial relationships that could be construed as a potential conflict of interest.

Copyright © 2021 Huang, Huang, Poon and Chang. This is an open-access article distributed under the terms of the Creative Commons Attribution License (CC BY). The use, distribution or reproduction in other forums is permitted, provided the original author(s) and the copyright owner(s) are credited and that the original publication in this journal is cited, in accordance with accepted academic practice. No use, distribution or reproduction is permitted which does not comply with these terms.

frontiers in Molecular Neuroscience

REVIEW
published: 15 July 2021
doi: 10.3389/fnmol.2021.718951

Neuromodulation and Behavioral Flexibility in Larval Zebrafish: From Neurotransmitters to Circuits

*Laura Corradi and Alessandro Filosa**

Max-Delbrück-Center for Molecular Medicine in the Helmholtz Association (MDC), Berlin, Germany

Animals adapt their behaviors to their ever-changing needs. Internal states, such as hunger, fear, stress, and arousal are important behavioral modulators controlling the way an organism perceives sensory stimuli and reacts to them. The translucent zebrafish larva is an ideal model organism for studying neuronal circuits regulating brain states, owning to the possibility of easy imaging and manipulating activity of genetically identified neurons while the animal performs stereotyped and well-characterized behaviors. The main neuromodulatory circuits present in mammals can also be found in the larval zebrafish brain, with the advantage that they contain small numbers of neurons. Importantly, imaging and behavioral techniques can be combined with methods for generating targeted genetic modifications to reveal the molecular underpinnings mediating the functions of such circuits. In this review we discuss how studying the larval zebrafish brain has contributed to advance our understanding of circuits and molecular mechanisms regulating neuromodulation and behavioral flexibility.

Keywords: zebrafish, neuromodulation, behavior, neuronal circuits, flexibility, foraging, escape (avoidance), arousal

OPEN ACCESS

Edited by:
Inmaculada Segura, Ludwig Maximilian University of Munich, Germany

Reviewed by:
Filippo Del Bene, Institut National de la Santé et de la Recherche Médicale (INSERM), France
Joao Carlos Marques, Harvard University, United States

***Correspondence:**
Alessandro Filosa
alessandro.filosa@mdc-berlin.de

Specialty section:
This article was submitted to Methods and Model Organisms, a section of the journal Frontiers in Molecular Neuroscience

Received: *01 June 2021*
Accepted: *25 June 2021*
Published: *15 July 2021*

Citation:
Corradi L and Filosa A (2021) Neuromodulation and Behavioral Flexibility in Larval Zebrafish: From Neurotransmitters to Circuits. Front. Mol. Neurosci. 14:718951. doi: 10.3389/fnmol.2021.718951

INTRODUCTION

Animals live in dynamic environments, wherein to survive and thrive they need to adapt their behaviors on the basis of information from the external world acquired through sensory systems, and internal states coding for their physiological needs. For example, foraging behavior is regulated by internal factors such as hunger, and external variables including the availability of food and presence of potential threats (Lima and Dill, 1990; Mobbs et al., 2018). Studies conducted in invertebrates and vertebrates have identified several neuromodulatory circuits and molecular mechanisms responsible for regulating the way an animal integrates internal states and external stimuli to make flexible behavioral adjustments (Bargmann, 2012; Lee and Dan, 2012; Marder, 2012; Kennedy et al., 2014; Kim S. M. et al., 2017).

Here we will summarize recent discoveries that are giving us fresh insights into the mechanisms mediating neuromodulation in zebrafish larvae. The young zebrafish brain is a useful model system to identify neuronal circuits mediating neuromodulation and to characterize the effects of manipulations of their activity on downstream neurons and consequent behavioral alterations. Transgenesis methods allow the generation of fish lines labeling specific populations of neuromodulatory neurons (Kawakami et al., 2010; Förster et al., 2017). Optogenetic, chemogenetic, and targeted mutagenesis techniques allow altering their activity to test their role in sensory processing and generation of motor outputs (Curado et al., 2008; Baier and Scott, 2009; Friedrich et al., 2010; Wyart and Del Bene, 2011; Li et al., 2016; Dal Maschio et al., 2017; Vanwalleghem et al., 2018). Moreover, methods for imaging and analyzing activity of a large number of neurons are

lowering the barrier for discovering new neuromodulatory circuits (Ahrens et al., 2012; Freeman et al., 2014; Keller and Ahrens, 2015; Randlett et al., 2015; Lovett-Barron et al., 2017; Mu et al., 2020). Finally, zebrafish larvae perform several well-characterized behaviors (Budick and O'Malley, 2000; Orger and de Polavieja, 2017), some of which, such as hunting and threat avoidance, are modulated by internal states (De Marco et al., 2014, 2016; Filosa et al., 2016; Lovett-Barron et al., 2017). The behavioral repertoire of older zebrafish is wider, including for example territoriality, social, and reproductive behavior (Orger and de Polavieja, 2017), but their larger and optically-opaque brains constitute an obstacle for optical interrogation of neuronal circuits involved in neuromodulation. We will review mostly research performed in up to 2 weeks old larvae, when the applicability of powerful methods for optical interrogation of circuits is optimal. We will also discuss some findings related to learning in juvenile (up to 4 weeks old) zebrafish.

The large majority of neuromodulatory systems present in mammals can also be found in larval zebrafish, with the advantage of being composed of small amounts of neurons (often less than one hundred). A comprehensive description of neuromodulatory circuits present in zebrafish is beyond the scope of this review, and we suggest the interested reader to consult very detailed studies published before (Kaslin and Panula, 2001; Rink and Wullimann, 2002; McLean and Fetcho, 2004; Kastenhuber et al., 2010; Filippi et al., 2010; Panula et al., 2010; Tay et al., 2011; Semenova et al., 2014; Herget and Ryu, 2015). We will instead introduce several examples of neuromodulators in relation to their actions on specific neuronal circuits and behaviors. Since the main tasks of a young zebrafish are searching for food and avoid becoming food for predators, this review will mainly focus on mechanisms modulating foraging and defensive behaviors. We will also discuss the regulation of arousal states, which have profound influences on sensory processing and execution of motor actions.

MODULATION OF EXPLORATORY AND FORAGING BEHAVIORS

Animals need to explore their environment to find food, employing foraging strategies aimed at maximizing food procurement and minimizing energy expenditure and risk of encountering predators (Lima and Dill, 1990; Mobbs et al., 2018). Zebrafish larvae start navigating their surroundings immediately after hatching, using a locomotion pattern characterized by alternating rapid bursts of swimming and short intervals of inactivity (Drapeau et al., 2002). Neurons of the reticulospinal network residing in the brainstem, the nucleus of the medial longitudinal fasciculus (nMLF) in the midbrain, and downstream circuits in the spinal cord are responsible for regulating locomotion (Orger et al., 2008; Fetcho and Mclean, 2010; Severi et al., 2014; Berg et al., 2018). Brain and spinal motor circuits are under the influence of neuromodulators. For example, the dopaminergic system is an important player in the motor control of vertebrates (Grillner and Robertson, 2016), including zebrafish larvae (Lambert et al., 2012; McPherson et al., 2016; Barrios et al., 2020). Both in mammals and teleost fish, dopaminergic neurons can be identified by the expression of the gene *tyrosine hydroxylase* (*th*), encoding one of the enzymes necessary for dopamine synthesis. Zebrafish has two paralogous *th* genes (*th1* and *th2*) displaying partially non-overlapping expression patterns (Filippi et al., 2010). The activity of subpopulations of hypothalamic th1$^+$ and th2$^+$ dopaminergic neurons is correlated with swimming (Jay et al., 2015; Reinig et al., 2017; Barrios et al., 2020). Ablation of hypothalamic dopaminergic neurons decreased the frequency of swimming bouts (McPherson et al., 2016; Barrios et al., 2020). Consistently, optogenetic activation of th2$^+$ cells increased locomotor activity (McPherson et al., 2016; Barrios et al., 2020). Together, these data suggest that hypothalamic dopaminergic neurons modulate locomotion, and may be part of a neuronal circuit controlling exploratory behavior. It would be interesting to know if and how motivational systems controlling energy balance communicate with these dopaminergic neurons to regulate foraging-related exploration in response to internal homeostatic needs.

The main function of exploratory behavior in a young zebrafish is to find food. When a zebrafish larva encounters a potentially edible object, it needs to switch its behavior from exploration, when it travels relatively large distances, to prey hunting in its immediate surroundings. Larvae hunt preys (in laboratory settings most often unicellular organisms such as paramecia, or small moving visual stimuli simulating them) with a well-coordinated series of fin, tail, eye, and jaw movements performed in sequential steps of prey detection, approach, and ingestion (Budick and O'Malley, 2000; Bianco et al., 2011; Preuss et al., 2014; Semmelhack et al., 2014; Antinucci et al., 2019; Mearns et al., 2020). By using a microscope capable of performing whole-brain calcium imaging at cellular resolution in freely swimming zebrafish larvae (Kim D. H. et al., 2017), Marques et al. identified neuronal correlates of exploration and hunting behavior (Marques et al., 2020). Notably, serotonergic neurons in the dorsal raphe nucleus were active during hunting, suggesting that they may be involved in triggering the transition from exploration to hunting behavior (**Figure 1**). This hypothesis is in agreement with a reduction of hunting attempts made by larvae lacking a functional serotonergic system (Filosa et al., 2016). In the same study, Marques et al. revealed correlations of activity of other neuromodulatory populations of neurons with specific steps of the hunting sequence. For example, tectal cholinergic neurons were active during prey detection. Other neurons including dopaminergic ones in the hindbrain, noradrenergic cells of the locus coeruleus, and cholinergic neurons in the cerebellum were preferentially activated by hunting success, possibly suggesting their involvement in reward systems. It would be worthwhile to follow up this study with interventional methods (optogenetic manipulation or neuronal ablations) to test a causative link between the activity of different types of neuromodulatory neurons and subcomponents of hunting behavior.

The dorsal raphe nucleus was also found to be involved in the decision process of approaching or avoiding visual stimuli that could possibly represent food (Filosa et al., 2016). Foraging animals search for food, and at the same time

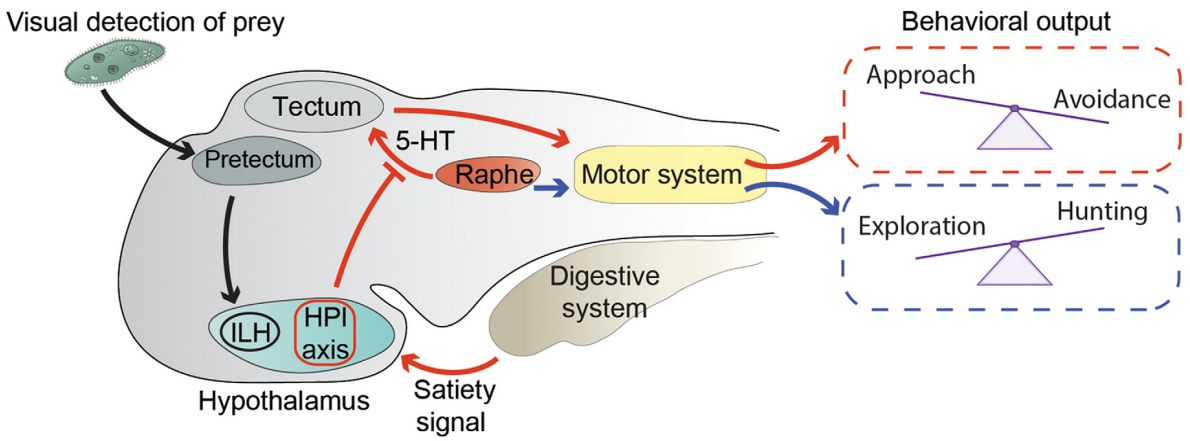

FIGURE 1 | Neuronal circuits modulating exploration and hunting behavior. Black arrows represent the circuit conveying visual information about prey from the pretectum to the inferior lobe of the hypothalamus (ILH; Muto et al., 2017). Red arrows summarize the way information about energy status modulates the hunting/escape decision (Filosa et al., 2016). An unidentified satiety signal activates the hypothalamus-pituitary-interrenal (HPI) axis. In addition, satiety leads to inhibition of serotonergic (5-HT) neurons in the dorsal raphe nucleus, possibly through the action of the HPI axis. Activation of the HPI axis and inhibition of the dorsal raphe lead to altered processing in the tectum of visual stimuli representing preys or potential threats. Changes in visual processing are then likely translated into motor commands controlling the selection of motor actions required to either approach a prey or escape from a threat. Blue arrows represent the correlation between hunting behavior and activity of 5-HT neurons of the dorsal raphe, and their possible involvement in the transition from exploration to hunting behavior (Marques et al., 2020).

must try not to become food for predators by employing effective threat-avoidance strategies (Lima and Dill, 1990). In zebrafish larvae, the choice between prey-approach and threat-avoidance behavior is strongly influenced by their feeding state (**Figure 1**). When confronted with ambiguous visual stimuli that could either indicate the presence of food or a potential threat, satiated larvae tend to avoid them, displaying a loss-aversion strategy, while food-deprived fish are more prone to approach them, suggesting that they adopt a more risk-taking approach (Filosa et al., 2016). At the circuit level, modulation of feeding state of the approach/avoidance decision is mediated by the serotonergic system and the hypothalamus-pituitary-interrenal (HPI) axis (homologous to the mammalian hypothalamus-pituitary-adrenal axis), a neuroendocrine hub regulating responses to stress (Löhr and Hammerschmidt, 2011). Indeed, food intake activated the HPI axis, and boosting activation of the HPI axis by mutating the gene encoding the transcription factor glucocorticoid receptor (Ziv et al., 2012) mimicked the effect of satiation on behavioral choice (Filosa et al., 2016). On the other hand, food deprivation led to increased activity of serotonergic neurons of the dorsal raphe nucleus, and pharmacological enhancement of serotonergic transmission with the selective serotonin reuptake inhibitor fluoxetine in satiated larvae induced them to behave like food-deprived ones. Ablation of the serotonergic system in food-deprived fish had the opposite effect on behavioral selection (Filosa et al., 2016). The serotonergic system and the HPI axis are able to influence the approach/avoidance decision at early stages of sensory-motor transformations (**Figure 1**). Indeed, they both alter the representation of small (prey-like) and large (predator-like) visual stimuli in the optic tectum, the major visual-processing structure in the zebrafish brain, involved in both prey capture and threat avoidance behaviors (Roeser and Baier, 2003; Del Bene et al., 2010; Nevin et al., 2010; Preuss et al., 2014; Barker and Baier, 2015; Temizer et al., 2015; Dunn et al., 2016; Bollmann, 2019). Food intake or activation of the HPI axis decreased, while pharmacological enhancement of serotonergic transmission increased, the number of tectal neurons responding to small visual stimuli (Filosa et al., 2016). In addition to the tectum, feeding-state might also modulate the activity of other visual processing and motor-initiating centers involved in prey capture and avoidance behavior. Further work will be required to test this hypothesis. It is also likely that other modulatory systems, apart from the HPI axis and the dorsal raphe nucleus, regulate sensory-motor transformation according to energy balance. At least some of these circuits probably reside in the hypothalamus, since it is a brain structure important for regulating food intake in zebrafish and other vertebrates (Löhr and Hammerschmidt, 2011; Sternson, 2013). In agreement with this hypothesis, it was shown that neurons in the inferior lobe of the hypothalamus (ILH) are activated once a paramecium appears in the visual field of a zebrafish larva (Muto et al., 2017; **Figure 1**). In the same study, prey-detecting pretectal neurons projecting axons to the ILH were identified, demonstrating the existence in zebrafish of a direct neuronal circuit linking a center processing prey-related visual cues, such as the pretectum (Semmelhack et al., 2014; Antinucci et al., 2019), with the hypothalamus. Neuronal circuits conveying information in the opposite direction, from the hypothalamus to visual-processing areas, also exist. A population of neurons in the rostral hypothalamus was shown to establish connections with the neuropil region of the tectum (Heap et al., 2017). These cells appear to inhibit tectal neurons, although it is not clear if through direct monosynaptic connections or via an indirect

multisynaptic pathway. Taken together, these data suggest that, like in other vertebrates, in zebrafish larvae, hypothalamic circuits integrate sensory inputs with homeostatic information to fine-tune behavioral responses to external stimuli according to internal needs.

The circuits and molecular pathways sensing metabolic status and controlling food intake in zebrafish are likely very similar to the ones present in mammals. Several neuropeptides important for controlling food intake in mammals, such as agouti-related peptide (Agrp), neuropeptide Y (Npy), and hypocretin (Hcrt, also known as orexin) were shown to have conserved roles in zebrafish (Song and Cone, 2007; Yokobori et al., 2011, 2012). However, most of these studies were conducted in adult fish, and the neuronal circuits mediating the actions of the neuropeptides were not studied in detail. Few recent studies investigated how food intake and energy balance are regulated in larval zebrafish (Jordi et al., 2018; Shainer et al., 2019; Wee et al., 2019b). For example, two subpopulations of hypothalamic serotonergic neurons, differentially activated by prey detection and ingestion, were shown to be important to regulate food consumption (Wee et al., 2019b). More research at the circuit and molecular levels is required to have a complete picture of the hypothalamic networks regulating food intake in the larval zebrafish. Moreover, in order to have a better understanding of how hypothalamic circuits modulate behavioral flexibility, it is crucial to know how they interact with brain areas processing sensory information or generating motor commands. The optical accessibility and small size of the larval zebrafish hypothalamus are definitively great advantages for obtaining such information.

Learning and memory systems are crucial regulators of an animal's behavior, enabling the comparison of current situations with stored information acquired in the past to avoid perpetuating erroneous actions and to improve motor outputs and behavioral choices through practice (Milner et al., 1998; McGaugh, 2000). Although some studies reported that zebrafish larvae appear to possess poor associative learning and memory capabilities (Valente et al., 2012; Yashina et al., 2019), several lines of evidence suggest that they are indeed able to learn associative tasks (Aizenberg and Schuman, 2011; Hinz et al., 2013; Lin et al., 2020). In accord with these latter reports, it was shown that learning is involved in prey-capture behavior performed by young fish. Larvae exposed to live prey (paramecia or rotifers) displayed elevated capture success compared to naïve larvae or controls raised with inert food (Lagogiannis et al., 2020; Oldfield et al., 2020). Moreover, compared to controls, prey-experienced fish had higher visually-evoked neuronal activity in the telencephalon and the habenula, suggesting that the two brain structures may contain neurons regulating learning processes required for refining motor sequences involved in hunting behavior (Oldfield et al., 2020). In support of this hypothesis, the ablation of habenular neurons led to a reduction of capture efficiency (Oldfield et al., 2020). More work is needed to identify the precise forebrain circuits responsible for this form of learning. Moreover, it would be interesting to know how neurons in the telencephalon and the habenula interact with sensory, motor, and homeostatic circuits to regulate behavioral performance.

CONTROL OF DEFENSIVE BEHAVIORS

Defensive behaviors are a class of innate responses fundamental for survival that involve detection of threatening stimuli and initiation of specific actions to avoid or eliminate the threat. Defensive strategies are influenced by external and internal factors, such as type and proximity of a threat and current metabolic needs, and elicit different behavioral responses including orienting the body away from the source of the hostile stimulus, freezing, hiding to avoid detection by predators, escaping to prevent capture, and suppressing foraging behavior to reduce risk of predation (Evans et al., 2019; Headley et al., 2019). These behaviors are associated with changes in the autonomic nervous system, which increases heart rate and blood pressure, as well as endocrine pathways mobilizing energy resources, that together allow proper responses to threats (Headley et al., 2019). Threat-avoidance behaviors require activation of sensory mechanisms that identify the type and intensity of the stimulus, hypothalamic circuits for both initiation of motor actions and activation of neuroendocrine responses, habenular circuits that promote aversive learning, and midbrain and hindbrain motor circuits that mediate fast escape responses.

Zebrafish has emerged as an excellent model organism for dissecting the neuronal circuits mediating defensive strategies. Indeed, stimuli that threaten fish homeostasis (e.g., exposure to hyperosmotic medium, temperature, and pH fluctuations), nociceptive stimuli (e.g., mustard oil, electric shock), and stimuli mimicking approaching predators (e.g., visual looming or acoustic/vibrational stimuli) are commonly used and well established (Burgess and Granato, 2007; Temizer et al., 2015; Dunn et al., 2016; Ryu and De Marco, 2017; Wee et al., 2019a; Yashina et al., 2019).

Detection of approaching predators in zebrafish larvae is mediated mainly by visual, somatosensory, and auditory systems (Korn and Faber, 2005; Medan and Preuss, 2014; Temizer et al., 2015; Dunn et al., 2016). Vibrational and acoustic stimuli activate hindbrain sensory circuits, which in turn relay information to a reticulospinal network of neurons, including the Mauthner cells, that trigger escape responses (O'Malley et al., 1996; Liu and Fetcho, 1999; Korn and Faber, 2005; Medan and Preuss, 2014). Looming visual stimuli activate neurons in the tectum and pretectum, and lesioning the tectum impairs efficient escape behavior (Temizer et al., 2015). Visual information about potential threats is also conveyed to reticulospinal escape circuits (Dunn et al., 2016).

While escape responses need to be very fast to be effective, they can also be fine-tuned by neuromodulatory circuits. For example, the threshold for the stimulus intensity capable of eliciting an acoustic startle response (ASR), a fast unilateral C-bend of the tail which turns the animal away from the stimulus (Korn and Faber, 2005), and the speed of escape are not constant and can be regulated by several neuromodulators (**Figures 2A–D**). A forward genetic screen identified zebrafish mutants having increased startle sensitivity (Marsden et al., 2018). The authors mapped one of the mutations to the gene *cytoplasmic Fragile X mental retardation protein (FMRP)-interacting protein 2* (*cyfip2*), coding for a cytoskeleton-

interacting protein which controls activity of excitatory spiral fiber neurons innervating the Mauthner cells (Marsden et al., 2018). The molecular mechanisms linking this protein regulating cytoskeletal functions to neuronal excitability are currently unknown. Another study showed that the serotonergic and dopaminergic systems regulate in opposite ways the speed of escape, with serotonergic agonists promoting slow escapes and dopaminergic receptor activators biasing behavior selection toward fast ones (Jain et al., 2018).

Escape behavior can be altered also by previous sensory experiences, such as in the case of pre-pulse inhibition (PPI) and habituation of the ASR. PPI is a sensorimotor gating phenomenon characterized by an attenuation of the startle response when it is preceded by a weak non-startling stimulus (Burgess and Granato, 2007; **Figure 2B**). The dopamine agonist apomorphine suppressed PPI of startle in larval zebrafish, while the dopamine D2 receptor antagonist haloperidol reduced the apomorphine effect, suggesting that the dopaminergic system inhibits PPI (Burgess and Granato, 2007). The exact populations of dopaminergic neurons responsible for this type of modulation have not been identified yet. A genetic screen identified hindbrain glutamatergic neurons, labeled by expression of the gene encoding the transcription factor Genomic Screen Homeobox 1 (*gsx1*), capable of promoting PPI (Bergeron et al., 2015). However, more work is required to have a complete picture of the neuronal circuits mediating PPI of startle responses in larval zebrafish.

Another way for previous sensory experience to modulate startle responses is through habituation, a form of non-associative learning, which leads to reduced response probability when the startling stimulus is presented repeatedly at short intervals (Wolman et al., 2011; López-Schier, 2019; Randlett et al., 2019; **Figure 2C**). Depression of dendritic excitability of the Mauthner cells is responsible for a short–term form of habituation of the ASR (Marsden and Granato, 2015). A forward genetic screen revealed some of the molecular mechanisms mediating habituation of the ASR by identifying the metalloprotease pregnancy-associated plasma protein-aa (Papp-aa) and the palmitoyltransferase Huntingtin interacting protein 14 (Hip14) as important regulators of this form of learning (Wolman et al., 2015; Nelson et al., 2020). Papp-aa modulates habituation by enhancing insulin-like growth factor (IGF) signaling (Wolman et al., 2015), while Hip14 regulates depression of sensory inputs onto dendrites of the Mauthner cells through palmitoylation of the Shaker-like K^+ voltage-gated channel subunit Kv1.1 (Nelson et al., 2020). An interesting work showed that habituation of the ASR varies between different zebrafish larvae and that these inter-individual differences are stable over days and heritable (Pantoja et al., 2016). Notably, dorsal raphe serotonergic neurons, which project into the vicinity of the Mauthner cells and are also activated by acoustic stimuli, decrease their activity during habituation, and the amount of this decrease cosegregates with behavioral habituation between generations (Pantoja et al., 2016). These results suggest that inter-individual differences in the activity of dorsal raphe neurons might impact ASR habituation through the Mauthner cells network. Likely, other brain regions are involved in modulating inter-individual variability of escape responses. In a follow up study, Pantoja et al. (2020) raised two generations of fish selected for innate differences in the ASR habituation and mapped their whole-brain neuronal activity using immunostaining of phosphorylated extracellular signal-regulated kinase (pERK) as a readout of neuronal activation (Randlett et al., 2015). Larvae habituating faster to acoustic stimuli showed increased baseline activity in several brain regions including the caudal hypothalamus, which was previously reported to be involved in the modulation of ASR (Mu et al., 2012). In addition, fast-habituating individuals displayed a higher frequency of spontaneous activity in dopaminergic neurons of the caudal hypothalamus (Pantoja et al., 2020).

Neurons regulating arousal levels (discussed in the next section) and stress are also involved in modulating escape behavior in zebrafish. Indeed, it was shown that larvae with elevated activation of the HPI axis due to mutation of the glucocorticoid receptor (Ziv et al., 2012) display augmented ASR (Griffiths et al., 2012).

In fish, like in other vertebrates, the perception of threatening stimuli triggers the activation in the hypothalamus of the HPI axis, which leads ultimately to the synthesis and release of cortisol (Wendelaar Bonga, 1997; Alderman and Bernier, 2009). The key coordination center of the HPI axis is the neurosecretory preoptic region of the hypothalamus, analogous to the mammalian paraventricular nucleus (Herget and Ryu, 2015). Perception of stressors leads to activation in this region of corticotropin-releasing-hormone-producing (Crh^+) neurons, which project directly to the pituitary and stimulate the corticotroph cells to release adrenocorticotropic hormone (Acth), which in turn triggers the secretion of cortisol from the interrenal gland (Ulrich-Lai and Herman, 2009; Löhr and Hammerschmidt, 2011). In support of the role of neuroendocrine systems in threat-evoked defensive behaviors, it was shown that enhancing the activity of pituitary corticotroph cells with optogenetic stimulation is sufficient to modulate locomotion and avoidance behavior immediately after the onset of a stressful stimulus (De Marco et al., 2016). Although endocrine responses are indubitably important to modulate behavior, several studies have revealed previously unknown roles for hypothalamic neurons in stress-related behaviors that are independent of hormonal actions (Fox and Lowry, 2013; Füzesi et al., 2016; Daviu et al., 2020). For example, Lovett-Barron et al. recently demonstrated that Crh^+ neurons and oxytocin-producing neurons in the preoptic hypothalamus of zebrafish larvae can modulate fast behavioral responses to different homeostatic threats despite chemogenetic ablation of corticotroph cells in the anterior pituitary (Lovett-Barron et al., 2020). An interesting finding from this study is that different types of homeostatic threats—heat, salinity, acidity—and visual looming stimuli activate in the preoptic hypothalamus multiple populations of peptidergic neurons, rather than individual cell classes, which synergistically modulate rapid avoidance responses. This fast modulation of behavior might occur via glutamatergic synapses between the preoptic peptidergic neurons and brainstem spinal-projecting neurons (Lovett-Barron et al., 2020).

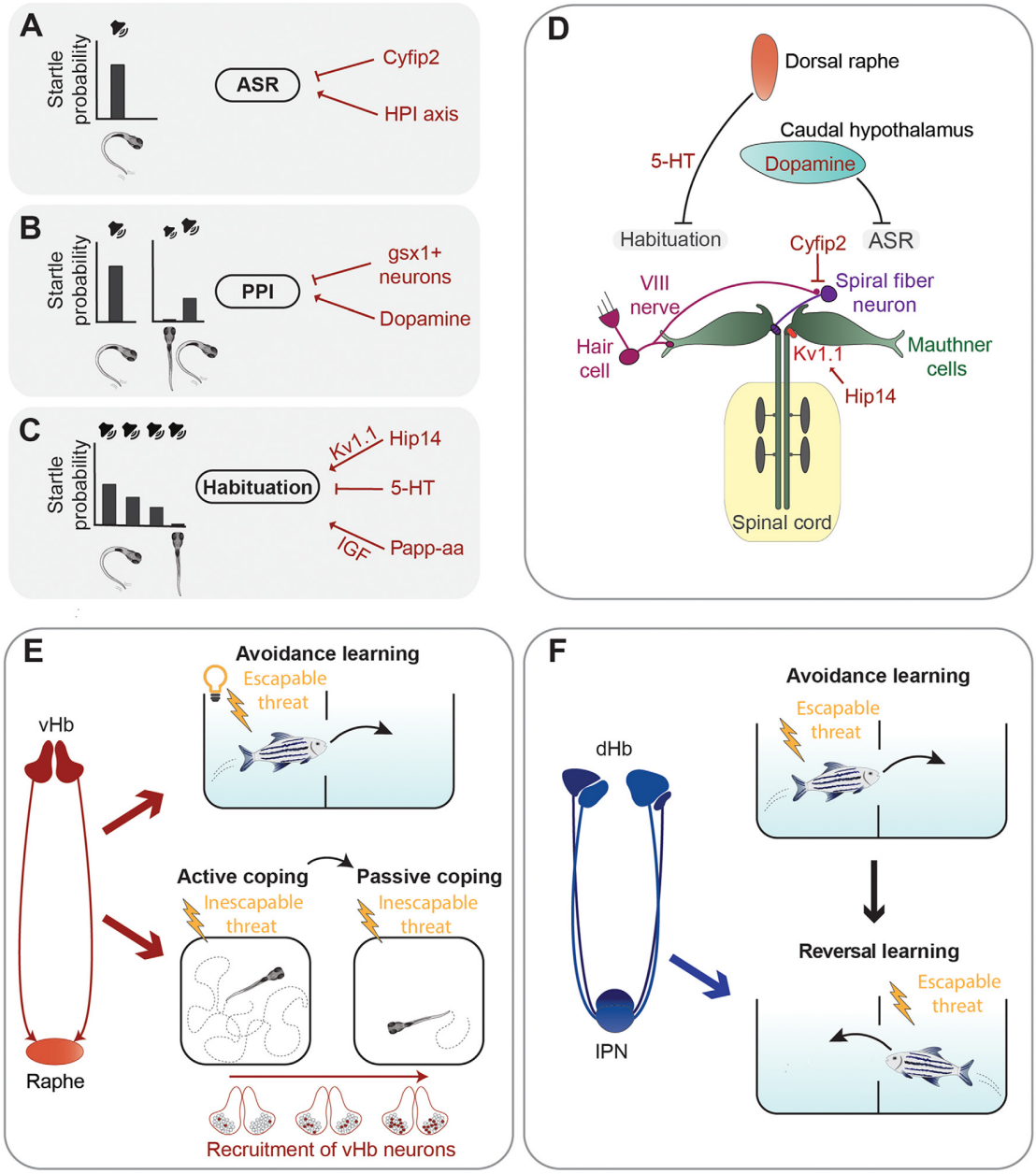

FIGURE 2 | Summary of neuronal circuits and molecules regulating defensive behavior. **(A–C)** Left are representations of the acoustic stimuli and related probabilities to trigger an acoustic startle response (ASR). A loud sound efficiently triggers ASR **(A)**. When the acoustic stimulus is shortly preceded by a sub-threshold sound, the probability of triggering an ASR is reduced due to pre-pulse inhibition (PPI) **(B)**. Repetition of a supra-threshold sound with short intervals also leads to a reduction of the probability of triggering an ASR due to habituation **(C)**. Several neurotransmitters, proteins, and the HPI axis (in red) were found to control the execution of the ASR, PPI, or habituation **(A–C)**. **(D)** Graphical summary of the main circuits mediating the ASR and examples of neuromodulators regulating them. **(E)** The ventral habenula (vHb)–raphe network mediates avoidance learning in the presence of an aversive escapable stimulus (electric shock) and a conditioned stimulus (light; Amo et al., 2014). Sequential recruitment of vHb neurons controls the switch from active coping to passive coping behavior in the presence of an inescapable threat (electric shock; Andalman et al., 2019). **(F)** The dorsal habenula (dHb) is required for reversal learning (Palumbo et al., 2020), which involves updating previously acquired learning rules when new information is available (in this case change of the tank compartment associated with electric shock).

In addition to neuronal circuits promoting a certain motor action, systems must exist to suppress alternative conflicting behaviors happening at the same time (Kennedy et al., 2014). Circuits regulating stress may also work in this way. For example, it was shown that food intake is also affected by activation of the HPI axis (Carr, 2002; De Marco et al., 2014), as exposure to stressors, such as hyperosmotic medium or water motion, led to suppression of food consumption in zebrafish larvae (De Marco et al., 2014), possibly a mechanism to inhibit foraging

behavior and let an animal concentrate on avoidance of potential threats.

Learning is another fundamental mechanism for survival as it confers behavioral flexibility for selecting threat-avoidance strategies. The habenula (Hb) has been implicated in the process of learning how to respond to aversive stimuli (Bianco and Wilson, 2009; Hu et al., 2020). In zebrafish, this structure is divided into dorsal habenula (dHb) and ventral habenula (vHb), which are homologous to the mammalian medial and lateral portions, respectively (Agetsuma et al., 2010; Amo et al., 2010). Zebrafish Hb receives inputs from the entopeduncular nucleus, hypothalamus, and median raphe (Beretta et al., 2012; Turner et al., 2016; Roberson and Halpern, 2018). While the dHb region projects to the interpeduncular nucleus (IPN), the vHb projects to the raphe (Agetsuma et al., 2010; Amo et al., 2010, 2014; Beretta et al., 2012; Roberson and Halpern, 2018). Most of the studies investigating the role of the habenula in zebrafish behavior have been performed with juvenile or adult fish.

Amo et al. (2014) demonstrated involvement of neurons in the vHb in active avoidance learning in adult zebrafish. The learning process investigated in this study was based on a conditioning protocol in which a light cue is presented as a conditioned stimulus to freely swimming fish, followed by an electrical shock. After several trials, fish eventually learned to associate the cue with the shock, the unconditioned stimulus, and to actively swim in another compartment of the tank to avoid the potential danger (**Figure 2E**). As the animal learned to associate the cue with the electric shock the authors observed, by using *in vivo* electrophysiology techniques, an increase of tonic activity of vHb neurons. Interestingly, optogenetic activation of vHb neurons led to increased activity of serotonergic neurons in the median raphe, which receives glutamatergic inputs from the vHb. Specific inactivation of the vHb-median raphe pathway abrogated the increase of tonic activity and impaired avoidance learning. Thus, tonic activity of vHb neurons, together with its projections to the median raphe, seems to be essential in encoding the reward expectation value of an aversive stimulus and thus induce escape from a potentially dangerous environment (Amo et al., 2014).

In the conditioning protocol used by Amo et al. (2014), fish are presented with an escapable harmful threat and learn to actively avoid it, using an active coping strategy. Most animals, when repeatedly exposed to inescapable aversive stimuli, eventually stop trying to avoid them and switch from active coping behavior to a passive one, usually characterized by reduced locomotion and a state that in mammals is often referred to as "helpless" (Maier and Seligman, 2016). A recent study revealed that in zebrafish the vHb is involved not only in the process of active coping in the presence of stressful conditions, as just described, but also in switching from active to passive coping (**Figure 2E**). Andalman et al. (2019) induced this behavioral transition in juvenile zebrafish using continuous inescapable mild electric shocks and analyzed whole-brain neuronal activity during the switch from active to passive coping behavior. Not only the vHb increased its activity after the inescapable aversive stimuli but, intriguingly, this effect was due to the sequential recruitment of habenular neurons during the aversive experience. During the transition from active to passive coping an overall decrease of neuronal activity in the raphe nucleus was observed. To prove a causal relationship between passive coping and the vHb-raphe circuit, the authors showed that optogenetic activation of vHb neurons or inhibition of serotonergic neurons of the dorsal raphe reduced swimming speed, consistent with a passive coping state. Moreover, stimulation of the vHb led to a significant increase of the number of inhibitory responses in the raphe suggesting a model wherein inescapable shock activates vHb neurons, causing inhibition of raphe neurons and passive coping behavior. In a recent study, Mu et al. (2019) discovered interactions between noradrenergic neurons and radial glia in the hindbrain that trigger passivity to prevent futile actions in response to unsuccessful behavior. It would be interesting to know whether habenular circuits and the hindbrain neuronal-glia network trigger passivity independently in response to different types of stimuli, or if they are both parts of a larger system regulating passivity regardless of behavioral context.

While the vHb is symmetric, the dHb shows a pronounced left-right asymmetry with differences in size, gene expression, neuronal populations, and innervation (Beretta et al., 2012; Turner et al., 2016; Roberson and Halpern, 2018). This neuroanatomical asymmetry correlates in young larvae with functional differences, as olfactory stimuli mostly activate the right Hb whereas the left Hb responds to changes in light (Dreosti et al., 2014). However, this asymmetry of sensory inputs disappears at later stages (Fore et al., 2020). Disruption of habenular asymmetry led to the elevation of cortisol levels and anxiety-like behavior in adult zebrafish (Facchin et al., 2015). The dHb has also been linked to defensive behaviors in zebrafish, as disruption of the dHb abrogated the execution of innate and experience-dependent fear responses (Agetsuma et al., 2010; Lee et al., 2010; Duboué et al., 2017).

A recent study in juvenile zebrafish used a conditioned place avoidance learning protocol similar to the one used by Amo et al. (2014) to demonstrate that the dorsolateral habenula (dlHb) is not important for conditioned avoidance learning, but instead mediates reversal learning, which involves the ability to use new information to modify associations learned in the past (Palumbo et al., 2020; **Figure 2F**). These results, together with another study showing that silencing the dlHb-IPN pathway impairs decision-making in a foraging task (Cherng et al., 2020), suggest that the dlHb in zebrafish is not only critically involved in aversive responses but is also an important regulator of behavioral flexibility.

In summary, the studies described in this section have shed light on the molecular and cellular identities of some of the major components of neuronal circuits essential for the flexibility of aversive behavior in zebrafish. The challenge for the near future, in addition to better characterize their molecular and functional properties, is to understand how each of these brain subcomponents communicates with each other in order to coordinate the selection of the most appropriate defensive strategy in response to external and internal conditions.

REGULATION OF AROUSAL STATES

A critical prerequisite for an animal to hunt preys and defend itself from predators is to be alert in order to quickly process information from the environment and react accordingly. An animal's arousal level can be operationally defined by the frequency and/or intensity of spontaneous locomotor activity and responsiveness to sensory stimuli: states of high arousal are associated with elevated locomotion and/or sensory sensitivity (Pfaff et al., 2008).

Several monoaminergic circuits play critical roles in regulating arousal in zebrafish. Among them is the noradrenergic system, as a homozygous mutation in the gene coding for the noradrenaline-synthesizing enzyme dopamine-beta-hydroxylase (*dbh*) leads to higher sensitivity to mechanoacoustic stimuli (Singh et al., 2015). Furthermore, serotonergic neurons of the dorsal raphe nucleus regulate arousal state and sensitivity to whole-field visual motion stimuli, which trigger the optomotor response (Yokogawa et al., 2012), a behavior involved in stabilization of body position in flowing water (Neuhauss et al., 1999). Indeed, it was shown that neuronal activity in the raphe increases when zebrafish larvae were exposed to sudden changes of water flow velocity, and ablation of serotonergic neurons in the raphe abolished the increase of visual sensitivity (Yokogawa et al., 2012; **Figure 3A**). Interestingly, water flow affected only the visual system, without altering other sensory modalities, suggesting the existence of neuronal mechanisms limiting the activation of sensory systems based on the relevant behavioral task. This is not an isolated case, since some neuropeptides were also found to have modality-specific arousal properties. For example, using an inducible overexpression method, Woods et al. showed that the neuropeptides Hcrt and Nociceptin modulate sensitivity to visual stimuli (Hcrt increases, while Nociceptin decreases responses to dark-flashes), but not to acoustic and thermal ones (Woods et al., 2014). This type of modality-selective arousal, a form of which was also observed in the mouse cerebral cortex (Shimaoka et al., 2018), is a very intriguing phenomenon that should be studied in more detail.

The regulation of visual sensitivity by a somatosensory stimulus mediated by the serotonergic system (Yokogawa et al., 2012) is not the only example of a cross-modal modulatory effect in zebrafish, as it was shown that a light flash stimulus is able to enhance sound-evoked escape behavior triggered by a subsequent auditory stimulus (Mu et al., 2012). The increase of escape probability was shown to be caused by light-responsive dopaminergic neurons residing in the caudal hypothalamus, which increased responsiveness of the Mauthner cells to auditory stimuli through activation of dopamine D1 receptors (Mu et al., 2012). The role of this type of cross-sensory modulatory effect is likely to increase the alertness of an animal following alterations of the visual environment, for example a flash of light that could signify the movement of a predator nearby, and react swiftly in response to further signals of potential danger, such as a suddenly appearing sound.

As mentioned earlier, one of the major advantages of using zebrafish larvae for studying neuromodulation is the fact that they have a small brain amenable to large-scale

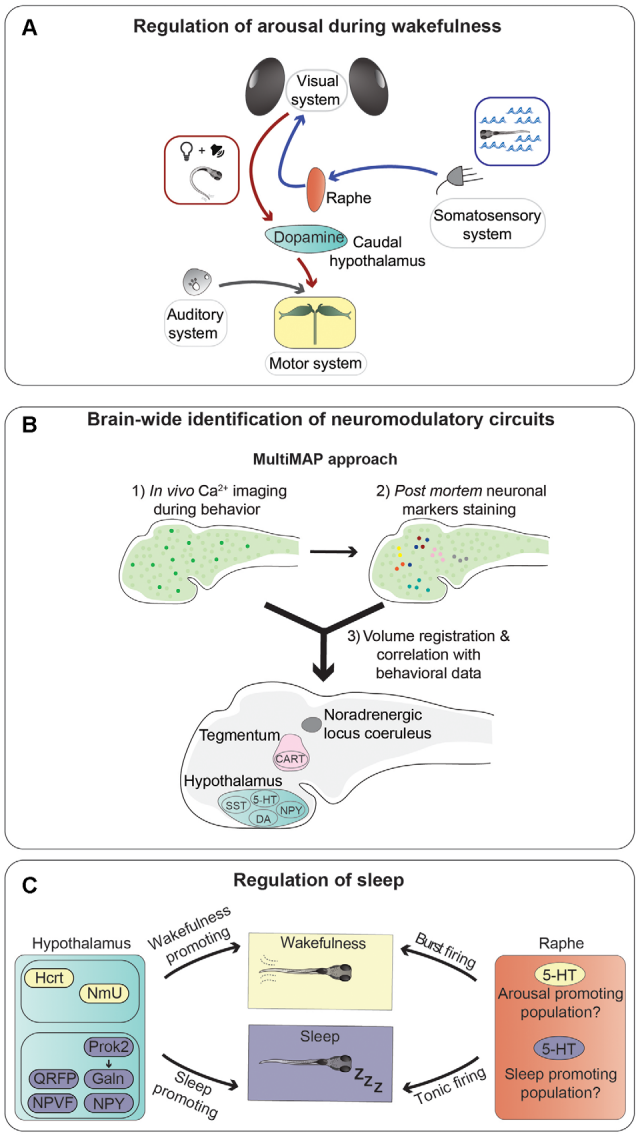

FIGURE 3 | Neurotransmitters and neuronal populations controlling arousal and sleep. **(A)** Summary of the information flow involved in regulating trans-modal arousal. Water flow, through the somatosensory system, activates serotonergic neurons of the dorsal raphe nucleus, which in turn increase the sensitivity of the visual system to whole-field motion stimuli (blue arrows; Yokogawa et al., 2012). A flash of light preceding a sound facilitates the acoustic startle response by increasing responsiveness of the Mauthner cells, via activation of dopaminergic neurons in the hypothalamus (red arrows; Mu et al., 2012). **(B)** Novel whole-brain imaging techniques are facilitating the discovery of neuromodulatory circuits. This scheme summarizes a method (MultiMAP) combining *in vivo* calcium imaging with *post mortem* staining of neuronal markers to identify neurons whose activity correlates with specific brain states and/or behavioral tasks (Lovett-Barron et al., 2017). **(C)** Sleep is controlled by multiple brain regions and neurotransmitters. This graphical summary depicts the influences of several neuropeptides secreted by hypothalamic neurons (sleep-promoting in violet and wakefulness-promoting in yellow), and serotonergic cells of the raphe nucleus on sleep regulation. It was shown that the raphe can induce both arousal and sleep, possibly through different types of firing (tonic or burst), or maybe thanks to the presence of different populations of serotonergic neurons with specific connectivity patterns.

analysis of neuronal activity. Lovett-Barron et al. developed a semi-high-throughput technique, which they termed MultiMAP (Multiplexed alignment of Molecular and Activity Phenotypes), to identify molecularly-labeled populations of neurons whose activity correlates with specific behaviors (Lovett-Barron et al., 2017; **Figure 3B**). Using this method, the authors were able to identify several groups of neuromodulatory neurons regulating arousal in zebrafish larvae. They showed to the fish looming dark circles, simulating approaching predators, and measured reaction times of escape responses as a readout of alertness. Sensorimotor reaction times are inversely proportional to alertness: the higher the state of alertness, the faster the reaction time. First, calcium imaging was used to record the activity of large numbers of neurons right before the visual stimuli were presented, directly linking pre-stimulus neuronal activity to reaction times (arousal state). *Post mortem* immunofluorescence staining was then used to label several populations of neuromodulatory neurons. Volume registration of the calcium imaging and immunofluorescence data allowed to assign specific identities to neurons whose activity correlated with different arousal states. In this way, the authors were able to identify several groups of neurons active during high alertness states: cocaine- and amphetamine-regulated transcript (Cart) and cholinergic neurons in the tegmentum, noradrenergic cells of the locus coeruleus, and serotonergic, dopaminergic, and Npy-positive neurons in the hypothalamus. On the other hand, somatostatin-positive cells in the hypothalamus were correlated with low-alertness states. In the same study, several of the neuromodulatory systems identified in zebrafish were shown to have a conserved function also in mice. This work nicely shows the potential of using zebrafish larvae for the brain-wide discovery of evolutionarily conserved neuromodulatory networks.

The majority of animals cannot be on high alert for very long periods of time, and their arousal level needs to be tuned down in order to rest. Sleep is a resting behavioral state characterized by very low levels of arousal, in which thresholds for detection of sensory stimuli are lower compared to wakefulness. During sleep, behavioral activities including foraging and feeding are suppressed, while others, such as threat avoidance, can still be evoked but not as efficiently as during wakefulness. Sleep, or at least some form of rest, is present in a large variety of animals including mammals, birds, arthropods, worms, and even cnidarians (Campbell and Tobler, 1984; Anafi et al., 2019). Zebrafish larvae also display a clear alternation of high (diurnal) and low (nocturnal) motor activity during the day (Zhdanova et al., 2001; Chiu and Prober, 2013; Barlow and Rihel, 2017; Oikonomou and Prober, 2017). Zebrafish larvae exhibit the three criteria for sleep in non-mammalian animals (Campbell and Tobler, 1984; Anafi et al., 2019): a quiescent state under control of the circadian clock, increased arousal threshold (reduced responsiveness to sensory stimuli), and homeostatic regulation leading to sleep rebound after sleep deprivation. In some animals, such as mammals, birds, and reptiles, in addition to these behavioral manifestations, well-defined signatures of neuronal activity are also associated with sleep (Siegel, 2008; Shein-Idelson et al., 2016). However, until recently no data were reported about brain activity during sleep in zebrafish. By using whole-brain calcium imaging techniques, Leung et al. identified in the dorsal pallium of zebrafish neuronal signatures of sleep similar to those of slow-wave and rapid eye movement phases of mammals (Leung et al., 2019), suggesting that these patterns of neuronal activity might have evolved before the appearance of tetrapods.

Not surprisingly, there seems to be a functional overlap between some of the circuits modulating arousal during wakefulness and the ones regulating sleep. In some cases, they act in the same direction. For example, Hcrt increases arousal and decreases sleep. In other cases, the same brain structures and neurotransmitter systems can be involved in regulating both arousal and sleep in opposite directions. For instance, the serotonergic raphe nucleus was implicated in promoting arousal (Yokogawa et al., 2012), as mentioned earlier, but also in promoting initiation and maintenance of sleep (Oikonomou et al., 2019). Indeed, it was shown that serotonin receptor agonists or optogenetic stimulation of the raphe promote sleep, while pharmacological antagonization of serotonin signaling, inhibition of serotonin synthesis by mutating the gene coding for the serotonin-producing enzyme tryptophan hydroxylase 2 (*tph2*), or ablation of the raphe, reduce sleep. These seemingly contradictory results can be possibly explained by different patterns of neuronal firing required for the two functions. It was suggested that tonic activity of serotonergic neurons could have a sleep-promoting role, while burst firing would instead lead to increased arousal (Oikonomou et al., 2019; **Figure 3C**). In line with this hypothesis, in other species, distinct or even opposite consequences of tonic and burst firing have been reported for monoaminergic systems, including dopaminergic and noradrenergic ones (Aston-Jones and Cohen, 2005; Goto et al., 2007). Alternatively, or concomitantly, subpopulations of serotonergic neurons with different functions may exist within the raphe, as shown in mice (Okaty et al., 2015; Ren et al., 2018). It would be interesting to characterize, possibly in a systematic way, such diversity of subcomponents of neuromodulatory systems in zebrafish.

Another sleep-promoting molecule is melatonin produced by cells of the pineal gland (Kazimi and Cahill, 1999). Application of exogenous melatonin was shown to induce sleep in zebrafish (Zhdanova et al., 2001), while ablation of the pineal gland or mutating the gene coding for the melatonin-synthesizing enzyme (*aanat2*) caused a reduction of sleep (Gandhi et al., 2015). Molecular and behavioral circadian rhythms were not altered in *aanat2* homozygous mutants, suggesting that melatonin signaling is downstream of the circadian clock.

Neuropeptidergic signaling plays a major role in regulating sleep (**Figure 3C**). For example, the neuropeptide Hcrt has evolutionarily conserved functions in sleep regulation in both mammals and zebrafish (Sutcliffe and de Lecea, 2002; Prober et al., 2006). Overexpression of *hcrt* in zebrafish larvae has a wake-promoting effect (Prober et al., 2006), and chemogenetic activation of Hcrt-producing neurons reduces sleep (Chen S. et al., 2016). On the other hand, homozygous mutation of the *hypocretin receptor* (*hcrtr*) gene in adult zebrafish (Yokogawa et al., 2007), and ablation of Hcrt-producing neurons in larvae (Chen A. et al., 2016), caused sleep fragmentation.

One further neuropeptide involved in sleep regulation is Galanin (Galn), which is secreted by neurons located in the preoptic area and posterior region of the hypothalamus (Podlasz et al., 2012). The activity of Galn-positive neurons and levels of *galn* mRNA increase after administration of wake-promoting drugs or forced wakefulness (Reichert et al., 2019). Moreover, mutant fish larvae lacking Galn displayed a stark reduction of rebound sleep after sleep deprivation (Reichert et al., 2019). Together, these data suggest that this peptide may be involved in regulating the homeostatic component of sleep. However, Galn might be involved also in other aspects of sleep, since it was shown that it mediates the action of the neuropeptide Prokineticin 2 (Prok2) in promoting sleep in a light-dependent, but circadian-independent manner (Chen et al., 2017).

Several other neuropeptides were shown to control sleep. Among them, neuropeptide VF (NPVF; Lee et al., 2017), QRFP (Chen A. et al., 2016), and Npy (Singh et al., 2017) promote sleep, while Neuromedin U (NmU) is wake-promoting (Chiu et al., 2016). The presence of such a large variety of sleep-regulating neuropeptides suggests a complex role of neuropeptidergic transmission in inducing or inhibiting sleep. One of the factors contributing to this complexity is the existence of interactions between different populations of peptidergic neurons and signaling pathways and between neuropeptidergic and monoaminergic systems. While some of these interactions have been discovered, for example between Npy and noradrenergic neurons (Singh et al., 2017), NmU and Crh signaling (Chiu et al., 2016), or Hcrt-producing neurons with the melatonin-secreting pineal gland (Appelbaum et al., 2009) and with noradrenergic neurons of the locus coeruleus (Singh et al., 2015), a large amount of them very likely remains to be uncovered.

CONCLUDING REMARKS AND FUTURE DIRECTIONS

Innate behaviors are often thought as consisting of stereotypic and inflexible actions. However, this view has been challenged by studies demonstrating that even the most simple behaviors are flexible and can be altered by neuromodulatory systems in response to changes of external conditions or internal needs (Bargmann, 2012; Lee and Dan, 2012; Marder, 2012; Kennedy et al., 2014; Kim S. M. et al., 2017). A vast amount of this pioneering work was done in invertebrates. A current challenge is to apply the general principles of neuromodulation discovered in invertebrates to the specific functions of modulatory systems in vertebrates since neuronal circuits differ substantially between the two groups of animals. The zebrafish larva is an ideal model organism for bridging this gap, by combining some advantages of invertebrates, e.g., large numbers of progenies useful for screenings, and a small brain ideal for optical probing, with conserved anatomical and physiological properties in common with other vertebrates. In the past few years, important groundwork has been carried out to characterize the neuronal circuits mediating innate behaviors in zebrafish. Now is the time to investigate how neuromodulatory systems interact with these circuits to regulate behavioral flexibility.

The best-characterized circuit performing a sensorimotor transformation in zebrafish is the one responsible for the ASR. Therefore, it is not surprising that the first studies addressing the role of neuromodulation in zebrafish behavior focused on this particular circuit (Burgess and Granato, 2007; Wolman et al., 2011; López-Schier, 2019). This work showed that even a stereotypic and hardwired behavior such as the ASR is amenable to modification by several neuromodulators, and can be altered by non-associative forms of learning, such as habituation. The circuits responsible for more complex behaviors in zebrafish, such as hunting, are still not fully understood. However, brain regions and neuronal populations involved in hunting have been identified (Roeser and Baier, 2003; Semmelhack et al., 2014; Antinucci et al., 2019; Gebhardt et al., 2019; Förster et al., 2020), and recent work showed that at least some of them are influenced by neuromodulators (Filosa et al., 2016). Both hunting and threat avoidance are strongly influenced by arousal states, which regulate alertness levels and sensitivity to sensory stimuli, and can be regulated by learning and memory processes. It is still not clear how neuromodulatory processes, including arousal and learning, affect the full spectrum of behaviors in young zebrafish. Indeed, the behavioral repertoire of larval and juvenile zebrafish is not limited to hunting and threat avoidance. For example, they also display several aspects of social behavior (Dreosti et al., 2015; Hinz and de Polavieja, 2017; Larsch and Baier, 2018; Groneberg et al., 2020; Stednitz and Washbourne, 2020; Tunbak et al., 2020). However, the neuronal circuits mediating social behavior in zebrafish, and the modulatory systems regulating their activity, are still largely unknown. Moreover, we still don't have a full catalog of all the molecules with neuromodulatory action, and complete knowledge of their functions is still lacking.

It is important to understand how neuromodulatory systems regulate the circuits controlling various types of behavior at different scales, from molecular alterations of signaling pathways to the activity of large ensembles of neurons. Strategies combining mutagenesis methods, behavioral screens, and whole-brain activity mapping in zebrafish larvae have the potential to reveal the whole picture of neuromodulation, from the micro to the macro scale, and to speed up the discovery of the mechanisms behind it. However, several challenges must be overcome before reaching a full understanding of the complexity of neuromodulatory systems. The first source of such intricacy is the large diversity of modulatory neurons and neurotransmitters. Often, the same neuronal circuit can influence multiple behaviors. This is the case, for example, of the serotonergic raphe nucleus, which in zebrafish larvae is involved in foraging (Marques et al., 2020), decision making during hunting (Filosa et al., 2016), regulation of visual sensitivity (Yokogawa et al., 2012), and sleep (Oikonomou et al., 2019). In other instances, multiple neuromodulatory systems are simultaneously engaged in regulating a single behavior, such as defensive responses to homeostatic threats (Lovett-Barron et al., 2020). A systems approach will be required to disentangle the intricate relationships between different types of neuromodulatory networks and the consequences of these interactions on

different behaviors. The small and translucent brain of the young zebrafish will certainly have a central stage in this endeavor, also thanks to new techniques for whole-brain imaging of neuronal activity (Keller and Ahrens, 2015; Mu et al., 2020; Bruzzone et al., 2021), possibly in freely moving larvae (Kim D. H. et al., 2017), and novel behavioral tracking and classification methods (Marques et al., 2018). The second layer of complexity is presented by the fact that neuromodulatory neurons often project their axons to large areas of the brain and identifying their many downstream targets is challenging. Recent efforts to obtain information about the connectomes of large numbers of neurons in the central nervous system of zebrafish (Wanner et al., 2016; Hildebrand et al., 2017; Kunst et al., 2019) will certainly help in identifying connectivity patterns of neuromodulatory neurons. However, the application of these approaches to the study of neuromodulation is hindered by the fact that several neuromodulators can act far away from synapses or can be released at extrasynaptic sites (van den Pol, 2012). Novel strategies will likely be required to identify the neuronal targets of modulatory circuits in an efficient manner. Finally, the fact that multiple neuropeptides and non-protein neurotransmitters often coexist in the same neuron further complicates the study of neuromodulatory systems. Indeed, different neurotransmitters can be coreleased at the same synapse, or individually secreted from different axonal or dendritic locations (Ludwig and Leng, 2006; Vaaga et al., 2014; Nusbaum et al., 2017). Precise molecular manipulations for altering a single neurotransmitter signaling at a time in specific subgroups of neurons will be necessary to disentangle the functions of sympatric neuromodulators.

AUTHOR CONTRIBUTIONS

All authors contributed to the article and approved the submitted version.

FUNDING

The work was supported by the Helmholtz Association of German Research Centers and by a grant from the German Research Foundation (Deutsche Forschungsgemeinschaft, project ID: FI 2339/1-1).

ACKNOWLEDGMENTS

We thank Suphansa Sawamiphak for critically reading and commenting on the manuscript.

REFERENCES

Agetsuma, M., Aizawa, H., Aoki, T., Nakayama, R., Takahoko, M., Goto, M., et al. (2010). The habenula is crucial for experience-dependent modification of fear responses in zebrafish. *Nat. Neurosci.* 13, 1354–1356. doi: 10.1038/nn.2654

Ahrens, M. B., Li, J. M., Orger, M. B., Robson, D. N., Schier, A. F., Engert, F., et al. (2012). Brain-wide neuronal dynamics during motor adaptation in zebrafish. *Nature* 485, 471–477. doi: 10.1038/nature11057

Aizenberg, M., and Schuman, E. M. (2011). Cerebellar-dependent learning in larval zebrafish. *J. Neurosci.* 31, 8708–8712. doi: 10.1523/JNEUROSCI.6565-10.2011

Alderman, S. L., and Bernier, N. J. (2009). Ontogeny of the corticotropin-releasing factor system in zebrafish. *Gen. Comp. Endocrinol.* 164, 61–69. doi: 10.1016/j.ygcen.2009.04.007

Amo, R., Aizawa, H., Takahoko, M., Kobayashi, M., Takahashi, R., Aoki, T., et al. (2010). Identification of the zebrafish ventral habenula as a homolog of the mammalian lateral habenula. *J. Neurosci.* 30, 1566–1574. doi: 10.1523/JNEUROSCI.3690-09.2010

Amo, R., Fredes, F., Kinoshita, M., Aoki, R., Aizawa, H., Agetsuma, M., et al. (2014). The habenulo-raphe serotonergic circuit encodes an aversive expectation value essential for adaptive active avoidance of danger. *Neuron* 84, 1034–1048. doi: 10.1016/j.neuron.2014.10.035

Anafi, R. C., Kayser, M. S., and Raizen, D. M. (2019). Exploring phylogeny to find the function of sleep. *Nat. Rev. Neurosci.* 20, 109–116. doi: 10.1038/s41583-018-0098-9

Andalman, A. S., Burns, V. M., Lovett-Barron, M., Broxton, M., Poole, B., Yang, S. J., et al. (2019). Neuronal dynamics regulating brain and behavioral state transitions. *Cell* 177, 970–985. doi: 10.1016/j.cell.2019.02.037

Antinucci, P., Folgueira, M., and Bianco, I. H. (2019). Pretectal neurons control hunting behavior. *eLife* 8:e48114. doi: 10.7554/eLife.48114

Appelbaum, L., Wang, G. X., Maro, G. S., Mori, R., Tovin, A., Marin, W., et al. (2009). Sleep-wake regulation and hypocretin-melatonin interaction in zebrafish. *Proc. Natl. Acad. Sci. U S A* 106, 21942–21947. doi: 10.1073/pnas.906637106

Aston-Jones, G., and Cohen, J. D. (2005). An integrative theory of locus coeruleus-norepinephrine function: adaptive gain and optimal performance. *Annu. Rev. Neurosci.* 28, 403–450. doi: 10.1146/annurev.neuro.28.061604.135709

Baier, H., and Scott, E. K. (2009). Genetic and optical targeting of neural circuits and behavior—zebrafish in the spotlight. *Curr. Opin. Neurobiol.* 19, 553–560. doi: 10.1016/j.conb.2009.08.001

Bargmann, C. I. (2012). Beyond the connectome: how neuromodulators shape neural circuits. *Bioessays* 34, 458–465. doi: 10.1002/bies.201100185

Barker, A. J., and Baier, H. (2015). Sensorimotor decision making in the zebrafish tectum. *Curr. Biol.* 25, 2804–2814. doi: 10.1016/j.cub.2015.09.055

Barlow, I. L., and Rihel, J. (2017). Zebrafish sleep: from geneZZZ to neuronZZZ. *Curr. Opin. Neurobiol.* 44, 65–71. doi: 10.1016/j.conb.2017.02.009

Barrios, J. P., Wang, W.-C., England, R., Reifenberg, E., and Douglass, A. D. (2020). Hypothalamic dopamine neurons control sensorimotor behavior by modulating brainstem premotor nuclei in zebrafish. *Curr. Biol.* 30, 4606.e4–4618.e4. doi: 10.1016/j.cub.2020.09.002

Beretta, C. A., Dross, N., Guiterrez-Triana, J. A., Ryu, S., and Carl, M. (2012). Habenula circuit development: past, present, and future. *Front. Neurosci.* 6:51. doi: 10.3389/fnins.2012.00051

Berg, E. M., Björnfors, E. R., Pallucchi, I., Picton, L. D., and Manira, A. E. (2018). Principles governing locomotion in vertebrates: lessons from zebrafish. *Front. Neural Circuits* 12:73. doi: 10.3389/fncir.2018.00073

Bergeron, S. A., Carrier, N., Li, G. H., Ahn, S., and Burgess, H. A. (2015). Gsx1 expression defines neurons required for prepulse inhibition. *Mol. Psychiatry* 20, 974–985. doi: 10.1038/mp.2014.106

Bianco, I. H., Kampff, A. R., and Engert, F. (2011). Prey capture behavior evoked by simple visual stimuli in larval zebrafish. *Front. Syst. Neurosci.* 5:101. doi: 10.3389/fnsys.2011.00101

Bianco, I. H., and Wilson, S. W. (2009). The habenular nuclei: a conserved asymmetric relay station in the vertebrate brain. *Philos. Trans. R. Soc. Lond. B Biol. Sci.* 364, 1005–1020. doi: 10.1098/rstb.2008.0213

Bollmann, J. H. (2019). The zebrafish visual system: from circuits to behavior. *Annu. Rev. Vis. Sci.* 5, 269–293. doi: 10.1146/annurev-vision-091718-014723

Bruzzone, M., Chiarello, E., Albanesi, M., Miletto Petrazzini, M. E., Megighian, A., Lodovichi, C., et al. (2021). Whole brain functional recordings at cellular

resolution in zebrafish larvae with 3D scanning multiphoton microscopy. *Sci. Rep.* 11:11048. doi: 10.1038/s41598-021-90335-y

Budick, S., and O'Malley, D. M. (2000). Locomotor repertoire of the larval zebrafish: swimming, turning and prey capture. *J. Exp. Biol.* 203, 2565–2579. doi: 10.1242/jeb.203.17.2565

Burgess, H. A., and Granato, M. (2007). Sensorimotor gating in larval zebrafish. *J. Neurosci.* 27, 4984–4994. doi: 10.1523/JNEUROSCI.0615-07.2007

Campbell, S. S., and Tobler, I. (1984). Animal sleep: a review of sleep duration across phylogeny. *Neurosci. Biobehav. Rev.* 8, 269–300. doi: 10.1016/0149-7634(84)90054-x

Carr, J. A. (2002). Stress, neuropeptides, and feeding behavior: a comparative perspective. *Integr. Comp. Biol.* 42, 582–590. doi: 10.1093/icb/42.3.582

Chen, S., Chiu, C. N., McArthur, K. L., Fetcho, J. R., and Prober, D. A. (2016). TRP channel mediated neuronal activation and ablation in freely behaving zebrafish. *Nat. Methods* 13, 147–150. doi: 10.1038/nmeth.3691

Chen, A., Chiu, C. N., Mosser, E. A., Kahn, S., Spence, R., and Prober, D. A. (2016). QRFP and its receptors regulate locomotor activity and sleep in zebrafish. *J. Neurosci.* 36, 1823–1840. doi: 10.1523/JNEUROSCI.2579-15.2016

Chen, S., Reichert, S., Singh, C., Oikonomou, G., Rihel, J., and Prober, D. A. (2017). Light-dependent regulation of sleep and wake states by prokineticin 2 in zebrafish. *Neuron* 95, 153.e6–168.e6. doi: 10.1016/j.neuron.2017.06.001

Cherng, B.-W., Islam, T., Torigoe, M., Tsuboi, T., and Okamoto, H. (2020). The dorsal lateral habenula-interpeduncular nucleus pathway is essential for left-right-dependent decision making in zebrafish. *Cell Rep.* 32:108143. doi: 10.1016/j.celrep.2020.108143

Chiu, C. N., and Prober, D. A. (2013). Regulation of zebrafish sleep and arousal states: current and prospective approaches. *Front. Neural Circuits* 7:58. doi: 10.3389/fncir.2013.00058

Chiu, C. N., Rihel, J., Lee, D. A., Singh, C., Mosser, E. A., Chen, S., et al. (2016). A zebrafish genetic screen identifies neuromedin U as a regulator of sleep/wake states. *Neuron* 89, 842–856. doi: 10.1016/j.neuron.2016.01.007

Curado, S., Stainier, D. Y. R., and Anderson, R. M. (2008). Nitroreductase-mediated cell/tissue ablation in zebrafish: a spatially and temporally controlled ablation method with applications in developmental and regeneration studies. *Nat. Protoc.* 3, 948–954. doi: 10.1038/nprot.2008.58

Dal Maschio, M., Donovan, J. C., Helmbrecht, T. O., and Baier, H. (2017). Linking neurons to network function and behavior by two-photon holographic optogenetics and volumetric imaging. *Neuron* 94, 774–789. doi: 10.1016/j.neuron.2017.04.034

Daviu, N., Füzesi, T., Rosenegger, D. G., Rasiah, N. P., Sterley, T.-L., Peringod, G., et al. (2020). Paraventricular nucleus CRH neurons encode stress controllability and regulate defensive behavior selection. *Nat. Neurosci.* 23, 398–410. doi: 10.1038/s41593-020-0591-0

De Marco, R. J., Groneberg, A. H., Yeh, C. M., Treviño, M., and Ryu, S. (2014). The behavior of larval zebrafish reveals stressor-mediated anorexia during early vertebrate development. *Front. Behav. Neurosci.* 8:367. doi: 10.3389/fnbeh.2014.00367

De Marco, R. J., Thiemann, T., Groneberg, A. H., Herget, U., and Ryu, S. (2016). Optogenetically enhanced pituitary corticotroph cell activity post-stress onset causes rapid organizing effects on behavior. *Nat. Commun.* 7:12620. doi: 10.1038/ncomms12620

Del Bene, F., Wyart, C., Robles, E., Tran, A., Looger, L. L., Scott, E. K., et al. (2010). Filtering of visual information in the tectum by an identified neural circuit. *Science* 330, 669–673. doi: 10.1126/science.1192949

Drapeau, P., Saint-Amant, L., Buss, R. R., Chong, M., McDearmid, J. R., and Brustein, E. (2002). Development of the locomotor network in zebrafish. *Prog. Neurobiol.* 68, 85–111. doi: 10.1016/s0301-0082(02)00075-8

Dreosti, E., Llopis, N. V., Carl, M., Yaksi, E., and Wilson, S. W. (2014). Left-right asymmetry is required for the habenulae to respond to both visual and olfactory stimuli. *Curr. Biol.* 24, 440–445. doi: 10.1016/j.cub.2014.01.016

Dreosti, E., Lopes, G., Kampff, A. R., and Wilson, S. W. (2015). Development of social behavior in young zebrafish. *Front. Neural Circuits* 9:39. doi: 10.3389/fncir.2015.00039

Duboué, E. R., Hong, E., Eldred, K. C., and Halpern, M. E. (2017). Left habenular activity attenuates fear responses in larval zebrafish. *Curr. Biol.* 27, 2154.e3–2162.e3. doi: 10.1016/j.cub.2017.06.017

Dunn, T. W., Gebhardt, C., Naumann, E. A., Riegler, C., Ahrens, M. B., Engert, F., et al. (2016). Neural circuits underlying visually evoked escapes in larval zebrafish. *Neuron* 89, 613–628. doi: 10.1016/j.neuron.2015.12.021

Evans, D. A., Stempel, A. V., Vale, R., and Branco, T. (2019). Cognitive control of escape behavior. *Trends Cogn. Sci.* 23, 334–348. doi: 10.1016/j.tics.2019.01.012

Facchin, L., Duboué, E. R., and Halpern, M. E. (2015). Disruption of epithalamic left-right asymmetry increases anxiety in zebrafish. *J. Neurosci.* 35, 15847–15859. doi: 10.1523/JNEUROSCI.2593-15.2015

Fetcho, J. R., and Mclean, D. L. (2010). Some principles of organization of spinal neurons underlying locomotion in zebrafish and their implications. *Ann. N Y Acad. Sci.* 1198, 94–104. doi: 10.1111/j.1749-6632.2010.05539.x

Filippi, A., Mahler, J., Schweitzer, J., and Driever, W. (2010). Expression of the paralogous tyrosine hydroxylase encoding genes th1 and th2 reveals the full complement of dopaminergic and noradrenergic neurons in zebrafish larval and juvenile brain. *J. Comp. Neurol.* 518, 423–438. doi: 10.1002/cne.22213

Filosa, A., Barker, A. J., Dal Maschio, M., and Baier, H. (2016). Feeding state modulates behavioral choice and processing of prey stimuli in the zebrafish tectum. *Neuron* 90, 596–608. doi: 10.1016/j.neuron.2016.03.014

Fore, S., Acuña-Hinrichsen, F., Mutlu, K. A., Bartoszek, E. M., Serneels, B., Faturos, N. G., et al. (2020). Functional properties of habenular neurons are determined by developmental stage and sequential neurogenesis. *Sci. Adv.* 6:eaaz3173. doi: 10.1126/sciadv.aaz3173

Förster, D., Arnold-Ammer, I., Laurell, E., Barker, A. J., Fernandes, A. M., Finger-Baier, K. C., et al. (2017). Genetic targeting and anatomical registration of neuronal populations in the zebrafish brain with a new set of BAC transgenic tools. *Sci. Rep.* 7:5230. doi: 10.1038/s41598-017-04657-x

Förster, D., Helmbrecht, T. O., Mearns, D. S., Jordan, L., Mokayes, N., and Baier, H. (2020). Retinotectal circuitry of larval zebrafish is adapted to detection and pursuit of prey. *eLife* 9:e58596. doi: 10.7554/eLife.58596

Fox, J. H., and Lowry, C. A. (2013). Corticotropin-releasing factor-related peptides, serotonergic systems, and emotional behavior. *Front. Neurosci.* 7:169. doi: 10.3389/fnins.2013.00169

Freeman, J., Vladimirov, N., Kawashima, T., Mu, Y., Sofroniew, N. J., Bennett, D. V., et al. (2014). Mapping brain activity at scale with cluster computing. *Nat. Methods* 11, 941–950. doi: 10.1038/nmeth.3041

Friedrich, R. W., Jacobson, G. A., and Zhu, P. (2010). Circuit neuroscience in zebrafish. *Curr. Biol.* 20, R371–R381. doi: 10.1016/j.cub.2010.02.039

Füzesi, T., Daviu, N., Wamsteeker Cusulin, J. I., Bonin, R. P., and Bains, J. S. (2016). Hypothalamic CRH neurons orchestrate complex behaviors after stress. *Nat. Commun.* 7:11937. doi: 10.1038/ncomms11937

Gandhi, A. V., Mosser, E. A., Oikonomou, G., and Prober, D. A. (2015). Melatonin is required for the circadian regulation of sleep. *Neuron* 85, 1193–1199. doi: 10.1016/j.neuron.2015.02.016

Gebhardt, C., Auer, T. O., Henriques, P. M., Rajan, G., Duroure, K., Bianco, I. H., et al. (2019). An interhemispheric neural circuit allowing binocular integration in the optic tectum. *Nat. Commun.* 10:5471. doi: 10.1038/s41467-019-13484-9

Goto, Y., Otani, S., and Grace, A. A. (2007). The Yin and Yang of dopamine release: a new perspective. *Neuropharmacology* 53, 583–587. doi: 10.1016/j.neuropharm.2007.07.007

Griffiths, B. B., Schoonheim, P. J., Ziv, L., Voelker, L., Baier, H., and Gahtan, E. (2012). A zebrafish model of glucocorticoid resistance shows serotonergic modulation of the stress response. *Front. Behav. Neurosci.* 6:68. doi: 10.3389/fnbeh.2012.00068

Grillner, S., and Robertson, B. (2016). The basal ganglia over 500 million years. *Curr. Biol.* 26, R1088–R1100. doi: 10.1016/j.cub.2016.06.041

Groneberg, A. H., Marques, J. C., Martins, A. L., Diez Del Corral, R., de Polavieja, G. G., and Orger, M. B. (2020). Early-life social experience shapes social avoidance reactions in larval zebrafish. *Curr. Biol.* 30, 4009–4021. doi: 10.1016/j.cub.2020.07.088

Headley, D. B., Kanta, V., Kyriazi, P., and Paré, D. (2019). Embracing complexity in defensive networks. *Neuron* 103, 189–201. doi: 10.1016/j.neuron.2019.05.024

Heap, L. A., Vanwalleghem, G. C., Thompson, A. W., Favre-Bulle, I., Rubinsztein-Dunlop, H., and Scott, E. K. (2017). Hypothalamic projections to the optic tectum in larval zebrafish. *Front. Neuroanat.* 11:135. doi: 10.3389/fnana.2017.00135

Herget, U., and Ryu, S. (2015). Coexpression analysis of nine neuropeptides in the neurosecretory preoptic area of larval zebrafish. *Front. Neuroanat.* 9:2. doi: 10.3389/fnana.2015.00002

Hildebrand, D. G. C., Cicconet, M., Torres, R. M., Choi, W., Quan, T. M., Moon, J., et al. (2017). Whole-brain serial-section electron microscopy in larval zebrafish. *Nature* 545, 345–349. doi: 10.1038/nature22356

Hinz, F. I., Aizenberg, M., Tushev, G., and Schuman, E. M. (2013). Protein synthesis-dependent associative long-term memory in larval zebrafish. *J. Neurosci.* 33, 15382–15387. doi: 10.1523/JNEUROSCI.0560-13.2013

Hinz, R. C., and de Polavieja, G. G. (2017). Ontogeny of collective behavior reveals a simple attraction rule. *Proc. Natl. Acad. Sci. U S A* 114, 2295–2300. doi: 10.1073/pnas.1616926114

Hu, H., Cui, Y., and Yang, Y. (2020). Circuits and functions of the lateral habenula in health and in disease. *Nat. Rev. Neurosci.* 21, 277–295. doi: 10.1038/s41583-020-0292-4

Jain, R. A., Wolman, M. A., Marsden, K. C., Nelson, J. C., Shoenhard, H., Echeverry, F. A., et al. (2018). A forward genetic screen in zebrafish identifies the G-protein-coupled receptor CaSR as a modulator of sensorimotor decision making. *Curr. Biol.* 28, 1357–1369. doi: 10.1016/j.cub.2018.03.025

Jay, M., De Faveri, F., and McDearmid, J. R. (2015). Firing dynamics and modulatory actions of supraspinal dopaminergic neurons during zebrafish locomotor behavior. *Curr. Biol.* 25, 435–444. doi: 10.1016/j.cub.2014.12.033

Jordi, J., Guggiana-Nilo, D., Bolton, A. D., Prabha, S., Ballotti, K., Herrera, K., et al. (2018). High-throughput screening for selective appetite modulators: a multibehavioral and translational drug discovery strategy. *Sci. Adv.* 4:eaav1966. doi: 10.1126/sciadv.aav1966

Kaslin, J., and Panula, P. (2001). Comparative anatomy of the histaminergic and other aminergic systems in zebrafish (Danio rerio). *J. Comp. Neurol.* 440, 342–377. doi: 10.1002/cne.1390

Kastenhuber, E., Kratochwil, C. F., Ryu, S., Schweitzer, J., and Driever, W. (2010). Genetic dissection of dopaminergic and noradrenergic contributions to catecholaminergic tracts in early larval zebrafish. *J. Comp. Neurol.* 518, 439–458. doi: 10.1002/cne.22214

Kawakami, K., Abe, G., Asada, T., Asakawa, K., Fukuda, R., Ito, A., et al. (2010). zTrap: zebrafish gene trap and enhancer trap database. *BMC Dev. Biol.* 10:105. doi: 10.1186/1471-213X-10-105

Kazimi, N., and Cahill, G. M. (1999). Development of a circadian melatonin rhythm in embryonic zebrafish. *Brain Res. Dev. Brain Res.* 117, 47–52. doi: 10.1016/s0165-3806(99)00096-6

Keller, P. J., and Ahrens, M. B. (2015). Visualizing whole-brain activity and development at the single-cell level using light-sheet microscopy. *Neuron* 85, 462–483. doi: 10.1016/j.neuron.2014.12.039

Kennedy, A., Asahina, K., Hoopfer, E., Inagaki, H., Jung, Y., Lee, H., et al. (2014). Internal states and behavioral decision-making: toward an integration of emotion and cognition. *Cold Spring Harb. Symp. Quant. Biol.* 79, 199–210. doi: 10.1101/sqb.2014.79.024984

Kim, D. H., Kim, J., Marques, J. C., Grama, A., Hildebrand, D. G. C., Gu, W., et al. (2017). Pan-neuronal calcium imaging with cellular resolution in freely swimming zebrafish. *Nat. Methods* 14, 1107–1114. doi: 10.1038/nmeth.4429

Kim, S. M., Su, C.-Y., and Wang, J. W. (2017). Neuromodulation of innate behaviors in *Drosophila*. *Annu. Rev. Neurosci.* 40, 327–348. doi: 10.1146/annurev-neuro-072116-031558

Korn, H., and Faber, D. S. (2005). The Mauthner cell half a century later: a neurobiological model for decision-making? *Neuron* 47, 13–28. doi: 10.1016/j.neuron.2005.05.019

Kunst, M., Laurell, E., Mokayes, N., Kramer, A., Kubo, F., Fernandes, A. M., et al. (2019). A cellular-resolution atlas of the larval zebrafish brain. *Neuron* 103, 21–38. doi: 10.1016/j.neuron.2019.04.034

Lagogiannis, K., Diana, G., and Meyer, M. P. (2020). Learning steers the ontogeny of an efficient hunting sequence in zebrafish larvae. *eLife* 9:e55119. doi: 10.7554/eLife.55119

Lambert, A. M., Bonkowsky, J. L., and Masino, M. A. (2012). The conserved dopaminergic diencephalospinal tract mediates vertebrate locomotor development in zebrafish larvae. *J. Neurosci.* 32, 13488–13500. doi: 10.1523/JNEUROSCI.1638-12.2012

Larsch, J., and Baier, H. (2018). Biological motion as an innate perceptual mechanism driving social affiliation. *Curr. Biol.* 28, 3523–3532. doi: 10.1016/j.cub.2018.09.014

Lee, D. A., Andreev, A., Truong, T. V., Chen, A., Hill, A. J., Oikonomou, G., et al. (2017). Genetic and neuronal regulation of sleep by neuropeptide VF. *eLife* 6:e25727. doi: 10.7554/eLife.25727

Lee, S.-H., and Dan, Y. (2012). Neuromodulation of brain states. *Neuron* 76, 209–222. doi: 10.1016/j.neuron.2012.09.012

Lee, A., Mathuru, A. S., Teh, C., Kibat, C., Korzh, V., Penney, T. B., et al. (2010). The habenula prevents helpless behavior in larval zebrafish. *Curr. Biol.* 20, 2211–2216. doi: 10.1016/j.cub.2010.11.025

Leung, L. C., Wang, G. X., Madelaine, R., Skariah, G., Kawakami, K., Deisseroth, K., et al. (2019). Neural signatures of sleep in zebrafish. *Nature* 571, 198–204. doi: 10.1038/s41586-019-1336-7

Li, M., Zhao, L., Page-McCaw, P. S., and Chen, W. (2016). Zebrafish genome engineering using the CRISPR-Cas9 system. *Trends Genet.* 32, 815–827. doi: 10.1016/j.tig.2016.10.005

Lima, S. L., and Dill, L. M. (1990). Behavioral decisions made under the risk of predation: a review and prospectus. *Canad. J. Zool.* 68, 619–640. doi: 10.1139/z90-092

Lin, Q., Manley, J., Helmreich, M., Schlumm, F., Li, J. M., Robson, D. N., et al. (2020). Cerebellar neurodynamics predict decision timing and outcome on the single-trial level. *Cell* 180, 536–551. doi: 10.1016/j.cell.2019.12.018

Liu, K. S., and Fetcho, J. R. (1999). Laser ablations reveal functional relationships of segmental hindbrain neurons in zebrafish. *Neuron* 23, 325–335. doi: 10.1016/s0896-6273(00)80783-7

Löhr, H., and Hammerschmidt, M. (2011). Zebrafish in endocrine systems: recent advances and implications for human disease. *Annu. Rev. Physiol.* 73, 183–211. doi: 10.1146/annurev-physiol-012110-142320

López-Schier, H. (2019). Neuroplasticity in the acoustic startle reflex in larval zebrafish. *Curr. Opin. Neurobiol.* 54, 134–139. doi: 10.1016/j.conb.2018.10.004

Lovett-Barron, M., Andalman, A. S., Allen, W. E., Vesuna, S., Kauvar, I., Burns, V. M., et al. (2017). Ancestral circuits for the coordinated modulation of brain state. *Cell* 171, 1411–1423. doi: 10.1016/j.cell.2017.10.021

Lovett-Barron, M., Chen, R., Bradbury, S., Andalman, A. S., Wagle, M., Guo, S., et al. (2020). Multiple convergent hypothalamus-brainstem circuits drive defensive behavior. *Nat. Neurosci.* 23, 959–967. doi: 10.1038/s41593-020-0655-1

Ludwig, M., and Leng, G. (2006). Dendritic peptide release and peptide-dependent behaviors. *Nat. Rev. Neurosci.* 7, 126–136. doi: 10.1038/nrn1845

Maier, S. F., and Seligman, M. E. P. (2016). Learned helplessness at fifty: insights from neuroscience. *Psychol. Rev.* 123, 349–367. doi: 10.1037/rev0000033

Marder, E. (2012). Neuromodulation of neuronal circuits: back to the future. *Neuron* 76, 1–11. doi: 10.1016/j.neuron.2012.09.010

Marques, J. C., Lackner, S., Félix, R., and Orger, M. B. (2018). Structure of the zebrafish locomotor repertoire revealed with unsupervised behavioral clustering. *Curr. Biol.* 28, 181–195. doi: 10.1016/j.cub.2017.12.002

Marques, J. C., Li, M., Schaak, D., Robson, D. N., and Li, J. M. (2020). Internal state dynamics shape brainwide activity and foraging behavior. *Nature* 577, 239–243. doi: 10.1038/s41586-019-1858-z

Marsden, K. C., and Granato, M. (2015). *in vivo* Ca^{2+} imaging reveals that decreased dendritic excitability drives startle habituation. *Cell Rep.* 13, 1733–1740. doi: 10.1016/j.celrep.2015.10.060

Marsden, K. C., Jain, R. A., Wolman, M. A., Echeverry, F. A., Nelson, J. C., Hayer, K. E., et al. (2018). A Cyfip2-dependent excitatory interneuron pathway establishes the innate startle threshold. *Cell Rep.* 23, 878–887. doi: 10.1016/j.celrep.2018.03.095

McGaugh, J. L. (2000). Memory—a century of consolidation. *Science* 287, 248–251. doi: 10.1126/science.287.5451.248

McLean, D. L., and Fetcho, J. R. (2004). Ontogeny and innervation patterns of dopaminergic, noradrenergic, and serotonergic neurons in larval zebrafish. *J. Comp. Neurol.* 480, 38–56. doi: 10.1002/cne.20280

McPherson, A. D., Barrios, J. P., Luks-Morgan, S. J., Manfredi, J. P., Bonkowsky, J. L., Douglass, A. D., et al. (2016). Motor behavior mediated by continuously generated dopaminergic neurons in the zebrafish hypothalamus recovers after cell ablation. *Curr. Biol.* 26, 263–269. doi: 10.1016/j.cub.2015.11.064

Mearns, D. S., Donovan, J. C., Fernandes, A. M., Semmelhack, J. L., and Baier, H. (2020). Deconstructing hunting behavior reveals a tightly coupled stimulus-response loop. *Curr. Biol.* 30, 54–69. doi: 10.1016/j.cub.2019.11.022

Medan, V., and Preuss, T. (2014). The Mauthner-cell circuit of fish as a model system for startle plasticity. *J. Physiol. Paris* 108, 129–140. doi: 10.1016/j.jphysparis.2014.07.006

Milner, B., Squire, L. R., and Kandel, E. R. (1998). Cognitive neuroscience and the study of memory. *Neuron* 20, 445–468. doi: 10.1016/s0896-6273(00)80987-3

Mobbs, D., Trimmer, P. C., Blumstein, D. T., and Dayan, P. (2018). Foraging for foundations in decision neuroscience: insights from ethology. *Nat. Rev. Neurosci.* 19, 419–427. doi: 10.1038/s41583-018-0010-7

Mu, Y., Bennett, D. V., Rubinov, M., Narayan, S., Yang, C. T., Tanimoto, M., et al. (2019). Glia accumulate evidence that actions are futile and suppress unsuccessful behavior. *Cell* 178, 27–43. doi: 10.1016/j.cell.2019.05.050

Mu, Y., Li, X.-Q., Zhang, B., and Du, J.-L. (2012). Visual input modulates audiomotor function *via* hypothalamic dopaminergic neurons through a cooperative mechanism. *Neuron* 75, 688–699. doi: 10.1016/j.neuron.2012.05.035

Mu, Y., Narayan, S., Mensh, B. D., and Ahrens, M. B. (2020). Brain-wide, scale-wide physiology underlying behavioral flexibility in zebrafish. *Curr. Opin. Neurobiol.* 64, 151–160. doi: 10.1016/j.conb.2020.08.013

Muto, A., Lal, P., Ailani, D., Abe, G., Itoh, M., and Kawakami, K. (2017). Activation of the hypothalamic feeding center upon visual prey detection. *Nat. Commun.* 8:15029. doi: 10.1038/ncomms15029

Nelson, J. C., Witze, E., Ma, Z., Ciocco, F., Frerotte, A., Randlett, O., et al. (2020). Acute regulation of habituation learning *via* posttranslational palmitoylation. *Curr. Biol.* 30, 2729–2738. doi: 10.1016/j.cub.2020.05.016

Neuhauss, S. C. F., Biehlmaier, O., Seeliger, M. W., Das, T., Kohler, K., Harris, W. A., et al. (1999). Genetic disorders of vision revealed by a behavioral screen of 400 essential loci in zebrafish. *J. Neurosci.* 19, 8603–8615. doi: 10.1523/JNEUROSCI.19-19-08603.1999

Nevin, L. M., Robles, E., Baier, H., and Scott, E. K. (2010). Focusing on optic tectum circuitry through the lens of genetics. *BMC Biol.* 8:126. doi: 10.1186/1741-7007-8-126

Nusbaum, M. P., Blitz, D. M., and Marder, E. (2017). Functional consequences of neuropeptide and small-molecule co-transmission. *Nat. Rev. Neurosci.* 18, 389–403. doi: 10.1038/nrn.2017.56

Oikonomou, G., Altermatt, M., Zhang, R.-W., Coughlin, G. M., Montz, C., Gradinaru, V., et al. (2019). The serotonergic raphe promote sleep in zebrafish and mice. *Neuron* 103, 686.e8–701.e8. doi: 10.1016/j.neuron.2019.05.038

Oikonomou, G., and Prober, D. A. (2017). Attacking sleep from a new angle: contributions from zebrafish. *Curr. Opin. Neurobiol.* 44, 80–88. doi: 10.1016/j.conb.2017.03.009

Okaty, B. W., Freret, M. E., Rood, B. D., Brust, R. D., Hennessy, M. L., deBairos, D., et al. (2015). Multi-scale molecular deconstruction of the serotonin neuron system. *Neuron* 88, 774–791. doi: 10.1016/j.neuron.2015.10.007

Oldfield, C. S., Grossrubatscher, I., Chávez, M., Hoagland, A., Huth, A. R., Carroll, E. C., et al. (2020). Experience, circuit dynamics, and forebrain recruitment in larval zebrafish prey capture. *eLlife* 9:e56619. doi: 10.7554/eLife.56619

O'Malley, D. M., Kao, Y. H., and Fetcho, J. R. (1996). Imaging the functional organization of zebrafish hindbrain segments during escape behaviors. *Neuron* 17, 1145–1155. doi: 10.1016/s0896-6273(00)80246-9

Orger, M. B., and de Polavieja, G. G. (2017). Zebrafish behavior: opportunities and challenges. *Annu. Rev. Neurosci.* 40, 125–147. doi: 10.1146/annurev-neuro-071714-033857

Orger, M. B., Kampff, A. R., Severi, K. E., Bollmann, J. H., and Engert, F. (2008). Control of visually guided behavior by distinct populations of spinal projection neurons. *Nat. Neurosci.* 11, 327–333. doi: 10.1038/nn2048

Palumbo, F., Serneels, B., Pelgrims, R., and Yaksi, E. (2020). The zebrafish dorsolateral habenula is required for updating learned behaviors. *Cell Rep.* 32:108054. doi: 10.1016/j.celrep.2020.108054

Pantoja, C., Hoagland, A., Carroll, E. C., Karalis, V., Conner, A., and Isacoff, E. Y. (2016). Neuromodulatory regulation of behavioral individuality in zebrafish. *Neuron* 91, 587–601. doi: 10.1016/j.neuron.2016.06.016

Pantoja, C., Larsch, J., Laurell, E., Marquart, G., Kunst, M., and Baier, H. (2020). Rapid effects of selection on brain-wide activity and behavior. *Curr. Biol.* 30, 3647–3656. doi: 10.1016/j.cub.2020.06.086

Panula, P., Chen, Y.-C., Priyadarshini, M., Kudo, H., Semenova, S., Sundvik, M., et al. (2010). The comparative neuroanatomy and neurochemistry of zebrafish CNS systems of relevance to human neuropsychiatric diseases. *Neurobiol. Dis.* 40, 46–57. doi: 10.1016/j.nbd.2010.05.010

Pfaff, D., Ribeiro, A., Matthews, J., and Kow, L.-M. (2008). Concepts and mechanisms of generalized central nervous system arousal. *Ann. N Y Acad. Sci.* 1129, 11–25. doi: 10.1196/annals.1417.019

Podlasz, P., Sallinen, V., Chen, Y.-C., Kudo, H., Fedorowska, N., and Panula, P. (2012). Galanin gene expression and effects of its knock-down on the development of the nervous system in larval zebrafish. *J. Comp. Neurol.* 520, 3846–3862. doi: 10.1002/cne.23131

Preuss, S. J., Trivedi, C. A., vom Berg-Maurer, C. M., Ryu, S., and Bollmann, J. H. (2014). Classification of object size in retinotectal microcircuits. *Curr. Biol.* 24, 2376–2385. doi: 10.1016/j.cub.2014.09.012

Prober, D. A., Rihel, J., Onah, A. A., Sung, R.-J., and Schier, A. F. (2006). Hypocretin/orexin overexpression induces an insomnia-like phenotype in zebrafish. *J. Neurosci.* 26, 13400–13410. doi: 10.1523/JNEUROSCI.4332-06.2006

Randlett, O., Haesemeyer, M., Forkin, G., Shoenhard, H., Schier, A. F., Engert, F., et al. (2019). Distributed plasticity drives visual habituation learning in larval zebrafish. *Curr. Biol.* 29, 1337–1345. doi: 10.1016/j.cub.2019.02.039

Randlett, O., Wee, C. L., Naumann, E. A., Nnaemeka, O., Schoppik, D., Fitzgerald, J. E., et al. (2015). Whole-brain activity mapping onto a zebrafish brain atlas. *Nat. Methods* 12, 1039–1046. doi: 10.1038/nmeth.3581

Reichert, S., Pavón Arocas, O., and Rihel, J. (2019). The neuropeptide galanin is required for homeostatic rebound sleep following increased neuronal activity. *Neuron* 104, 370–384. doi: 10.1016/j.neuron.2019.08.010

Reinig, S., Driever, W., and Arrenberg, A. B. (2017). The descending diencephalic dopamine system is tuned to sensory stimuli. *Curr. Biol.* 27, 318–333. doi: 10.1016/j.cub.2016.11.059

Ren, J., Friedmann, D., Xiong, J., Liu, C. D., Ferguson, B. R., Weerakkody, T., et al. (2018). Anatomically defined and functionally distinct dorsal raphe serotonin sub-systems. *Cell* 175, 472–487. doi: 10.1016/j.cell.2018.07.043

Rink, E., and Wullimann, M. F. (2002). Development of the catecholaminergic system in the early zebrafish brain: an immunohistochemical study. *Brain Res. Dev. Brain Res.* 137, 89–100. doi: 10.1016/s0165-3806(02)00354-1

Roberson, S., and Halpern, M. E. (2018). Development and connectivity of the habenular nuclei. *Semin. Cell Dev. Biol.* 78, 107–115. doi: 10.1016/j.semcdb.2017.10.007

Roeser, T., and Baier, H. (2003). Visuomotor behaviors in larval zebrafish after GFP-guided laser ablation of the optic tectum. *J. Neurosci.* 23, 3726–3734. doi: 10.1523/JNEUROSCI.23-09-03726.2003

Ryu, S., and De Marco, R. J. (2017). Performance on innate behavior during early development as a function of stress level. *Sci. Rep.* 7:7840. doi: 10.1038/s41598-017-08400-4

Semenova, S. A., Chen, Y.-C., Zhao, X., Rauvala, H., and Panula, P. (2014). The tyrosine hydroxylase 2 (TH2) system in zebrafish brain and stress activation of hypothalamic cells. *Histochem. Cell Biol.* 142, 619–633. doi: 10.1007/s00418-014-1240-z

Semmelhack, J. L., Donovan, J. C., Thiele, T. R., Kuehn, E., Laurell, E., and Baier, H. (2014). A dedicated visual pathway for prey detection in larval zebrafish. *eLlife* 3:e04878. doi: 10.7554/eLife.04878

Severi, K. E., Portugues, R., Marques, J. C., O'Malley, D. M., Orger, M. B., and Engert, F. (2014). Neural control and modulation of swimming speed in the larval zebrafish. *Neuron* 83, 692–707. doi: 10.1016/j.neuron.2014.06.032

Shainer, I., Michel, M., Marquart, G. D., Bhandiwad, A. A., Zmora, N., Ben-Moshe Livne, Z., et al. (2019). Agouti-related protein 2 is a new player in the teleost stress response system. *Curr. Biol.* 29, 2009–2019. doi: 10.1016/j.cub.2019.05.021

Shein-Idelson, M., Ondracek, J. M., Liaw, H.-P., Reiter, S., and Laurent, G. (2016). Slow waves, sharp waves, ripples, and REM in sleeping dragons. *Science* 352, 590–595. doi: 10.1126/science.aaf3621

Shimaoka, D., Harris, K. D., and Carandini, M. (2018). Effects of arousal on mouse sensory cortex depend on modality. *Cell Rep.* 22, 3160–3167. doi: 10.1016/j.celrep.2018.02.092

Siegel, J. M. (2008). Do all animals sleep? *Trends Neurosci.* 31, 208–213. doi: 10.1016/j.tins.2008.02.001

Singh, C., Oikonomou, G., and Prober, D. A. (2015). Norepinephrine is required to promote wakefulness and for hypocretin-induced arousal in zebrafish. *eLlife* 4:e07000. doi: 10.7554/eLife.07000

Singh, C., Rihel, J., and Prober, D. A. (2017). Neuropeptide Y regulates sleep by modulating noradrenergic signaling. *Curr. Biol.* 27, 3796–3811. doi: 10.1016/j.cub.2017.11.018

Song, Y., and Cone, R. D. (2007). Creation of a genetic model of obesity in a teleost. *FASEB J.* 21, 2042–2049. doi: 10.1096/fj.06-7503com

Stednitz, S. J., and Washbourne, P. (2020). Rapid progressive social development of zebrafish. *Zebrafish* 17, 11–17. doi: 10.1089/zeb.2019.1815

Sternson, S. M. (2013). Hypothalamic survival circuits: blueprints for purposive behaviors. *Neuron* 77, 810–824. doi: 10.1016/j.neuron.2013.02.018

Sutcliffe, J. G., and de Lecea, L. (2002). The hypocretins: setting the arousal threshold. *Nat. Rev. Neurosci.* 3, 339–349. doi: 10.1038/nrn808

Tay, T. L., Ronneberger, O., Ryu, S., Nitschke, R., and Driever, W. (2011). Comprehensive catecholaminergic projectome analysis reveals single-neuron integration of zebrafish ascending and descending dopaminergic systems. *Nat. Commun.* 2:171. doi: 10.1038/ncomms1171

Temizer, I., Donovan, J. C., Baier, H., and Semmelhack, J. L. (2015). A visual pathway for looming-evoked escape in larval zebrafish. *Curr. Biol.* 25, 1823–1834. doi: 10.1016/j.cub.2015.06.002

Tunbak, H., Vazquez-Prada, M., Ryan, T. M., Kampff, A. R., and Dreosti, E. (2020). Whole-brain mapping of socially isolated zebrafish reveals that lonely fish are not loners. *eLlife* 9:e55863. doi: 10.7554/eLife.55863

Turner, K. J., Hawkins, T. A., Yáñez, J., Anadón, R., Wilson, S. W., and Folgueira, M. (2016). Afferent connectivity of the zebrafish habenulae. *Front. Neural Circuits* 10:30. doi: 10.3389/fncir.2016.00030

Ulrich-Lai, Y. M., and Herman, J. P. (2009). Neural regulation of endocrine and autonomic stress responses. *Nat. Rev. Neurosci.* 10, 397–409. doi: 10.1038/nrn2647

Vaaga, C. E., Borisovska, M., and Westbrook, G. L. (2014). Dual-transmitter neurons: functional implications of co-release and co-transmission. *Curr. Opin. Neurobiol.* 29, 25–32. doi: 10.1016/j.conb.2014.04.010

Valente, A., Huang, K.-H., Portugues, R., and Engert, F. (2012). Ontogeny of classical and operant learning behaviors in zebrafish. *Learn. Mem.* 19, 170–177. doi: 10.1101/lm.025668.112

van den Pol, A. N. (2012). Neuropeptide transmission in brain circuits. *Neuron* 76, 98–115. doi: 10.1016/j.neuron.2012.09.014

Vanwalleghem, G. C., Ahrens, M. B., and Scott, E. K. (2018). Integrative whole-brain neuroscience in larval zebrafish. *Curr. Opin. Neurobiol.* 50, 136–145. doi: 10.1016/j.conb.2018.02.004

Wanner, A. A., Genoud, C., Masudi, T., Siksou, L., and Friedrich, R. W. (2016). Dense EM-based reconstruction of the interglomerular projectome in the zebrafish olfactory bulb. *Nat. Neurosci.* 19, 816–825. doi: 10.1038/nn.4290

Wee, C. L., Nikitchenko, M., Wang, W. C., Luks-Morgan, S. J., Song, E., Gagnon, J. A., et al. (2019a). Zebrafish oxytocin neurons drive nocifensive behavior *via* brainstem premotor targets. *Nat. Neurosci.* 22, 1477–1492. doi: 10.1038/s41593-019-0452-x

Wee, C. L., Song, E. Y., Johnson, R. E., Ailani, D., Randlett, O., Kim, J.-Y., et al. (2019b). A bidirectional network for appetite control in larval zebrafish. *eLlife* 8:e43775. doi: 10.7554/eLife.43775

Wendelaar Bonga, S. E. (1997). The stress response in fish. *Physiol. Rev.* 77, 591–625. doi: 10.1152/physrev.1997.77.3.591

Wolman, M. A., Jain, R. A., Liss, L., and Granato, M. (2011). Chemical modulation of memory formation in larval zebrafish. *Proc. Natl. Acad. Sci. U S A* 108, 15468–15473. doi: 10.1073/pnas.1107156108

Wolman, M. A., Jain, R. A., Marsden, K. C., Bell, H., Skinner, J., Hayer, K. E., et al. (2015). A genome-wide screen identifies PAPP-AA-mediated IGFR signaling as a novel regulator of habituation learning. *Neuron* 85, 1200–1211. doi: 10.1016/j.neuron.2015.02.025

Woods, I. G., Schoppik, D., Shi, V. J., Zimmerman, S., Coleman, H. A., Greenwood, J., et al. (2014). Neuropeptidergic signaling partitions arousal behaviors in zebrafish. *J. Neurosci.* 34, 3142–3160. doi: 10.1523/JNEUROSCI.3529-13.2014

Wyart, C., and Del Bene, F. (2011). Let there be light: zebrafish neurobiology and the optogenetic revolution. *Rev. Neurosci.* 22, 121–130. doi: 10.1515/RNS.2011.013

Yashina, K., Tejero-Cantero, Á., Herz, A., and Baier, H. (2019). Zebrafish exploit visual cues and geometric relationships to form a spatial memory. *iScience* 19, 119–134. doi: 10.1016/j.isci.2019.07.013

Yokobori, E., Azuma, M., Nishiguchi, R., Kang, K. S., Kamijo, M., Uchiyama, M., et al. (2012). Neuropeptide Y stimulates food intake in the Zebrafish, Danio rerio. *J. Neuroendocrinol.* 24, 766–773. doi: 10.1111/j.1365-2826.2012.02281.x

Yokobori, E., Kojima, K., Azuma, M., Kang, K. S., Maejima, S., Uchiyama, M., et al. (2011). Stimulatory effect of intracerebroventricular administration of orexin A on food intake in the zebrafish, Danio rerio. *Peptides* 32, 1357–1362. doi: 10.1016/j.peptides.2011.05.010

Yokogawa, T., Hannan, M. C., and Burgess, H. A. (2012). The dorsal raphe modulates sensory responsiveness during arousal in zebrafish. *J. Neurosci.* 32, 15205–15215. doi: 10.1523/JNEUROSCI.1019-12.2012

Yokogawa, T., Marin, W., Faraco, J., Pézeron, G., Appelbaum, L., Zhang, J., et al. (2007). Characterization of sleep in zebrafish and insomnia in hypocretin receptor mutants. *PLoS Biol.* 5:e277. doi: 10.1371/journal.pbio.0050277

Zhdanova, I. V., Wang, S. Y., Leclair, O. U., and Danilova, N. P. (2001). Melatonin promotes sleep-like state in zebrafish. *Brain Res.* 903, 263–268. doi: 10.1016/s0006-8993(01)02444-1

Ziv, L., Muto, A., Schoonheim, P. J., Meijsing, S. H., Strasser, D., Ingraham, H. A., et al. (2012). An affective disorder in zebrafish with mutation of the glucocorticoid receptor. *Mol. Psychiatry* 18, 681–691. doi: 10.1038/mp.2012.64

Conflict of Interest: The authors declare that the research was conducted in the absence of any commercial or financial relationships that could be construed as a potential conflict of interest.

Copyright © 2021 Corradi and Filosa. This is an open-access article distributed under the terms of the Creative Commons Attribution License (CC BY). The use, distribution or reproduction in other forums is permitted, provided the original author(s) and the copyright owner(s) are credited and that the original publication in this journal is cited, in accordance with accepted academic practice. No use, distribution or reproduction is permitted which does not comply with these terms.

frontiers in Molecular Neuroscience

REVIEW
published: 19 July 2021
doi: 10.3389/fnmol.2021.714768

From Junk to Function: LncRNAs in CNS Health and Disease

*Rafaela Policarpo[1,2,3], Annerieke Sierksma[1,2], Bart De Strooper[1,2,4] and Constantin d'Ydewalle[3]**

[1] VIB-KU Leuven Center For Brain & Disease Research, Leuven, Belgium, [2] Laboratory for the Research of Neurodegenerative Diseases, Department of Neurosciences, Leuven Brain Institute (LBI), KU Leuven, Leuven, Belgium, [3] Neuroscience Discovery, Janssen Research & Development, Janssen Pharmaceutica N.V., Beerse, Belgium, [4] UK Dementia Research Institute, University College London, London, United Kingdom

Recent advances in RNA sequencing technologies helped to uncover the existence of tens of thousands of long non-coding RNAs (lncRNAs) that arise from the dark matter of the genome. These lncRNAs were originally thought to be transcriptional noise but an increasing number of studies demonstrate that these transcripts can modulate protein-coding gene expression by a wide variety of transcriptional and post-transcriptional mechanisms. The spatiotemporal regulation of lncRNA expression is particularly evident in the central nervous system, suggesting that they may directly contribute to specific brain processes, including neurogenesis and cellular homeostasis. Not surprisingly, lncRNAs are therefore gaining attention as putative novel therapeutic targets for disorders of the brain. In this review, we summarize the recent insights into the functions of lncRNAs in the brain, their role in neuronal maintenance, and their potential contribution to disease. We conclude this review by postulating how these RNA molecules can be targeted for the treatment of yet incurable neurological disorders.

Keywords: long non-coding RNAs, central nervous system, neuronal development, neurological disorders, gene regulation

OPEN ACCESS

Edited by:
Inmaculada Segura, Ludwig Maximilian University of Munich, Germany

Reviewed by:
Massimiliano Caiazzo, University of Naples Federico II, Italy
Masato Yano, Niigata University, Japan

***Correspondence:**
Constantin d'Ydewalle
cvanoutr@ITS.JNJ.com

***Received:** 25 May 2021*
***Accepted:** 25 June 2021*
***Published:** 19 July 2021*

Citation:
Policarpo R, Sierksma A, De Strooper B and d'Ydewalle C (2021) From Junk to Function: LncRNAs in CNS Health and Disease. Front. Mol. Neurosci. 14:714768. doi: 10.3389/fnmol.2021.714768

INTRODUCTION

The sequencing of the ∼3.1 billion base pairs of the human genome marked the completion of the Human Genome Project in April 2003 after a little over 10 years of research. One of the main findings of this large scale project was that only a fraction of the genome encoded in total ∼22,300 protein-coding genes, whereas the remaining fraction was considered "junk DNA" (Human Genome Project, 2003). Since then, our perception of the complexity of the human genome changed dramatically (Frankish et al., 2021). In the past 20 years, advances in RNA sequencing technology pointed out that approximately 80% of our genome is actually transcribed, whereas only around 2% is subsequently translated into proteins (Carninci et al., 2005; Dunham et al., 2012; Hon et al., 2017; Zhao et al., 2021). Besides protein-coding messenger RNAs (mRNAs), transfer RNA (tRNAs) and ribosomal RNAs (rRNAs), other essential RNA species include long non-coding RNAs (lncRNAs), circular RNAs (circRNAs), and small non-coding RNAs (sncRNA) such as microRNAs (miRNAs) and small-interfering RNAs (siRNAs) (Mattick and Rinn, 2015; Quan et al., 2017; Lorenzi et al., 2021).

Remarkably, the majority of our DNA generates a large number of lncRNAs (Iyer et al., 2015; Bonetti and Carninci, 2017; Yao et al., 2019; Zhao et al., 2021). By definition, lncRNAs contain more

than 200 nucleotides in length and lack protein-coding potential. Based on their genomic location and orientation relative to neighboring protein-coding genes, lncRNAs are broadly categorized into intergenic lncRNAs, intronic lncRNAs, bidirectional lncRNAs, sense lncRNAs, antisense lncRNAs and enhancer RNAs (**Figure 1**) (Ma et al., 2013; Youse et al., 2020).

LncRNA promoters are structurally similar to those from protein-coding genes, exhibiting characteristic profiles of transcriptional activity markers (e.g., histone acetylation, methylation, ubiquitination, etc.) around their transcription start sites (Derrien et al., 2012; Djebali et al., 2012; Roberts et al., 2014). Consistent with their promoter structure, lncRNAs are generally transcribed by RNA polymerase II (Hon et al., 2017). Additionally, many lncRNAs share some features of messenger RNAs (mRNAs) at the transcript level including the presence of a 5′-cap, 3′-polyadenylation, and the occurrence of alternative splicing events that give rise to alternative transcript isoforms (Derrien et al., 2012; Djebali et al., 2012; Roberts et al., 2014). The mechanisms that regulate these post-transcriptional events in lncRNAs are not well documented; the limited amount of evidence available suggests that the same mechanisms are used as for protein-coding genes albeit with different efficiency (Gil and Ulitsky, 2018; Statello et al., 2021). There are also marked differences between lncRNAs and protein-coding genes. LncRNAs are generally expressed at lower levels although there are examples of highly expressed lncRNAs (e.g., *TUG1* and *MALAT1*) (Derrien et al., 2012; Washietl et al., 2014; Jiang et al., 2016). LncRNAs also exhibit a more highly specific spatiotemporal expression pattern, and display poorer sequence conservation across species compared to protein-coding genes (Derrien et al., 2012; Djebali et al., 2012; Jiang et al., 2016). The high level of orchestrated regulation at the transcriptional and post-transcriptional level suggests that lncRNAs are at least as functionally relevant as protein-coding genes despite low conservation and expression levels.

The lncRNA *Xist* (X-inactive-specific transcript) was one of the first lncRNAs identified when it was isolated in the early 1990s from a female placental complementary DNA library screening (Brown et al., 1991). This lncRNA remains the most studied nuclear lncRNA to date. *Xist* is exclusively expressed from one of the two X chromosomes in females during early embryonic development. The transcript "*coats*" the X chromosome in *cis* and triggers a series of events that results in chromosome-wide transcriptional silencing and heterochromatinization acting in concert with many other lncRNAs, RNA binding proteins and DNA (Rocha and Heard, 2017). As such, *Xist* ensures X chromosome inactivation and dosage compensation between females and males in mammals (Brown et al., 1991).

Xist is an archetypical example on the functional relevance of lncRNAs. Evolutionary biologists uncovered that the amount of transcribed DNA (as lncRNAs) correlates with the organisms' complexity and genome size (Rubin et al., 2000; Mattick, 2001; Taft et al., 2007; Liu et al., 2013; Kapusta and Feschotte, 2014). These observations further suggest that despite low sequence conservation across species, lncRNAs may contribute to the development of complex organisms and organs including the central nervous system (CNS) (Aprea and Calegari, 2015). In this review, we will summarize the current knowledge on the role of lncRNAs in brain physiology and disease; and discuss the future perspectives and challenges of using lncRNAs as RNA-based therapeutic targets in neurological disorders.

LncRNAs IN THE CNS

The observation that most of the mammalian genome is actively transcribed, that much of this pervasive transcription is likely functional, and that lncRNA loci are linked to key biological functions has boosted the interest in lncRNAs (Dunham et al., 2012; Kopp and Mendell, 2018; Lorenzi et al., 2021; Statello et al., 2021; Zhao et al., 2021). However, the first challenge in understanding the physiological relevance of lncRNAs is the difficulty to annotate these transcripts (Uszczynska-Ratajczak et al., 2018). The development of recent sequencing technologies has been key for the emergence of different annotation methods and databases that continue to improve our knowledge of these genes. A few examples are the GENCODE geneset, which combines manual with automated annotation from two pipelines (Ensembl-HAVANA and Ensembl-Genebuild) for protein-coding genes annotation, but uses mostly manual annotation for lncRNA genes (Frankish et al., 2021); NONCODE, an integrative database exclusively dedicated to the annotation of non-coding RNAs, in particular lncRNAs in animals (Zhao et al., 2021); or FANTOM CAT, a meta-assembly mostly based on CAGE (Cap Analysis of Gene Expression) data and annotations from diverse sources (**Figure 2**) (Hon et al., 2017). Thus, while the number of functional lncRNAs is still a matter of debate, between 15,000 and 100,000 lncRNAs have recently been reported to exist in the human genome. Similar numbers have been annotated in the mouse genome (Uszczynska-Ratajczak et al., 2018). In comparison, approximately 20,000 protein-coding genes have been mapped (Salzberg, 2018). Thus, given their relative quantities, it is hypothesized that lncRNAs contribute to the organism's complexity.

The development and maintenance of the nervous system in particular is a complex process that must rely on highly coordinated spatiotemporal gene expression programs to finetune the balance between cell proliferation and differentiation and ensure these cell populations give rise to a functional network. A remarkable amount of 40% of all annotated tissue-specific lncRNA genes are specifically enriched in particular brain regions or cell types and participate in many aspects of brain function and development (Derrien et al., 2012; Francescatto et al., 2014; Briggs et al., 2015; Zimmer-Bensch, 2019). In this section, we will discuss some features of lncRNAs that support a widespread functional role for this RNA subclass in mediating CNS development and function.

Brain LncRNAs Are Evolutionary Conserved

Accumulating data suggest that conserved lncRNAs are more likely to be functionally relevant. While lncRNAs exhibit higher sequence conservation in their promoter regions, splice-junction motifs and small functional domains, lncRNA gene bodies exhibit

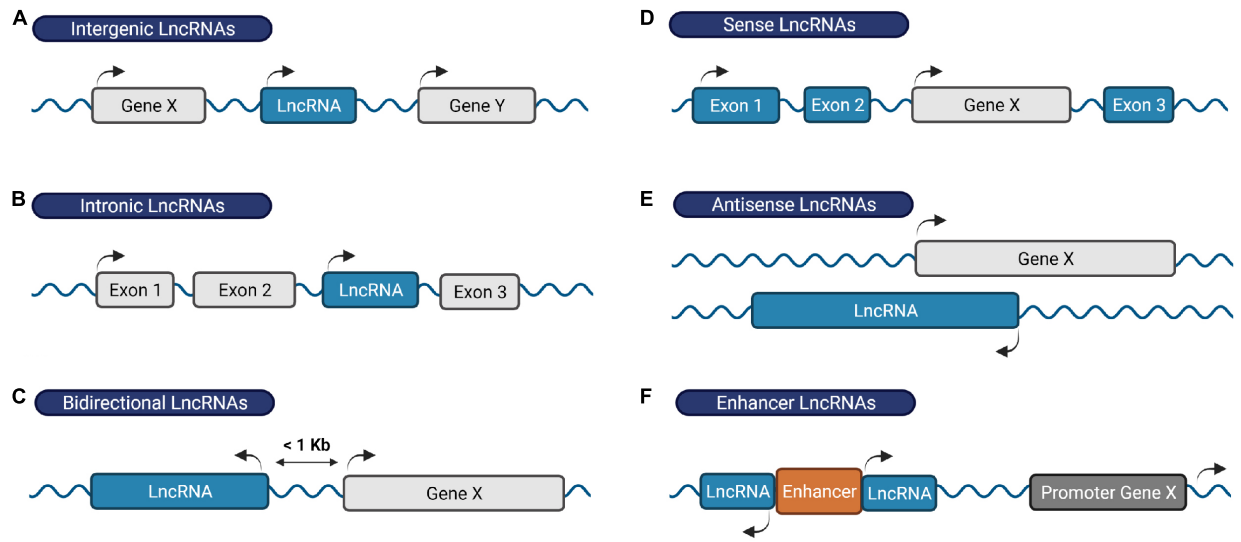

FIGURE 1 | Classification of lncRNAs based on their genomic location. **(A)** Intergenic RNAs are located between two protein-coding genes, **(B)** intronic lncRNAs are transcribed within an intronic region of a protein-coding gene, **(C)** bidirectional lncRNAs are located on the opposite strand of a protein-coding gene whose transcription initiates less than 1,000 base pairs away, **(D)** sense lncRNAs are transcribed from and overlap with the sense strand of a protein-coding gene, **(E)** antisense lncRNAs originate from the antisense strand of a protein coding-gene, and **(F)** enhancer RNAs derive from enhancer regions and play a role in gene transcription activation. Protein-coding genes/exons shown in gray; LncRNA genes/exons shown in blue.

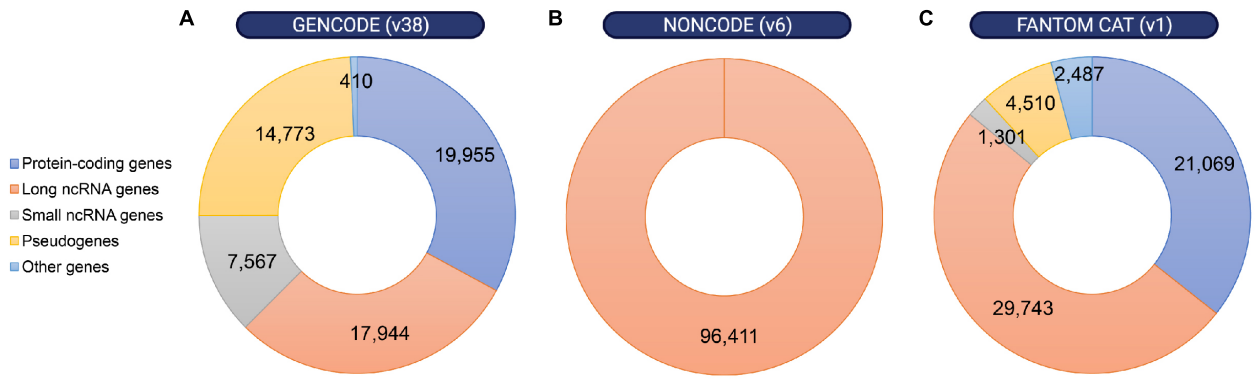

FIGURE 2 | Distribution of annotated loci in the human genome according to different gene map databases. Despite the discrepancies between different annotation methods, non-coding RNA loci are remarkably abundant within the human genome. Number of protein-coding genes, long or small non-coding RNA genes, pseudogenes and other genes were obtained from **(A)** GENCODE release 38 (https://www.gencodegenes.org/human/stats.html), **(B)** NON-CODE v6.0 (http://www.noncode.org/analysis.php), and **(C)** FANTOM CAT v1 (https://fantom.gsc.riken.jp/cat/v1/#/genes).

an overall lower evolutionary conservation relative to protein-coding genes (Chodroff et al., 2010; Ulitsky et al., 2011; Derrien et al., 2012; Necsulea and Kaessmann, 2014; Nitsche et al., 2015). A possible explanation is the fact that many lncRNAs have a recent evolutionary origin, and approximately one third of human lncRNAs has been reported to be restricted to the primate lineage (Derrien et al., 2012; Necsulea and Kaessmann, 2014; Washietl et al., 2014). Accordingly, these lncRNAs seem to have less exonic sequence constraints compared to ancestral and conserved lncRNAs (Necsulea and Kaessmann, 2014; Washietl et al., 2014). Moreover, several lncRNAs have been shown to be under positive evolutionary selection in human compared to other mammalian species (Tay et al., 2009; Lindblad-Toh et al., 2011; Grossman et al., 2013; Francescatto et al., 2014; Washietl et al., 2014; Sarropoulos et al., 2019).

Nonetheless, brain-specific lncRNAs display the strongest evolutionary conservation compared to those expressed in other tissues (Ponjavic et al., 2009; He et al., 2014), and their levels of sequence conservation correlate very well with the levels of brain complexity (Johnson et al., 2015). Intergenic lncRNAs that show strong evolutionary conservation (when evaluating mouse and human genomes) are particularly enriched in the brain (Ponjavic et al., 2009). Moreover, these enriched lncRNAs are located adjacent to protein-coding genes that are co-expressed in the brain and involved in transcriptional regulation or CNS development (Ponjavic et al., 2009).

Other studies indicate that some lncRNAs with relevant functional roles in the brain have been subjected to higher sequence constraints throughout evolution. For instance, the lncRNAs *linc-Brn1b*, *Dali,* and *Pnky* are 3 conserved lncRNAs located in close proximity of and co-expressed with *Brn1* and *Brn2* (Sauvageau et al., 2013; Chalei et al., 2014; Ramos et al., 2015). These two genes encode the POU-homeodomain transcription factors POU3F3 and POU3F2, respectively, that play crucial roles in neocortex development (Sugitani et al., 2002). *Linc-Brn1b* and *Dali* are located downstream of *Brn1* and loss-of-function studies demonstrated that these lncRNAs are required for correct brain development (Sauvageau et al., 2013; Chalei et al., 2014). *Pnky* is a lncRNA transcribed in the opposite strand of *Brn2* with two regions conserved in vertebrates, and its expression is upregulated in neural stem cells in the developing mouse and human cortex. *Pnky* controls neuronal differentiation in dividing neural stem cells by interacting with PTBP1, a splicing factor that represses the inclusion of neural exons in non-neural cells (Ramos et al., 2015). Additional examples of well-conserved lncRNA genes with a role in neurogenesis include the lncRNA *Rmst* and *Tuna*; knockdown of these lncRNAs suppresses neuronal differentiation in mouse embryonic stem cells (Ng et al., 2013; Lin et al., 2014).

Structural features rather than the primary sequence can contribute to functional relevance of lncRNAs (Torarinsson et al., 2006; Seemann et al., 2012; Smith et al., 2013; Diederichs, 2014; Johnsson et al., 2014; Kapusta and Feschotte, 2014). For example, the lncRNA *MALAT1* contains a large number of helices that are highly conserved across vertebrates and even more in mammalian *MALAT1* homologs, indicating the presence of an evolutionary conserved core with predicted functional roles in mammals and vertebrates (McCown et al., 2019).

LncRNA Genes Exhibit Highly Specific Expression Patterns in the CNS

The CNS is one of the most complex organs in mammals, exhibiting a tight spatial and temporal organization and gene expression profile during development and homeostasis. Several studies showed that lncRNA expression is spatially more restricted than mRNAs in multiple brain regions suggesting that lncRNAs may play crucial roles in the coordination of the complex gene expression in distinct CNS regions (Belgard et al., 2011; Luo et al., 2013; Ramos et al., 2013; Kadakkuzha et al., 2015).

A systematic *in situ* hybridization analysis demonstrated that the expression of the majority of lncRNAs in the mouse brain is restricted to distinct neuroanatomical loci (Mercer et al., 2008). The lncRNA *MIAT*/*Gomafu* was identified as a nuclear retained lncRNA that is specifically expressed in a distinct set of postmitotic neurons within the mouse nervous system (Sone et al., 2007). *Gomafu*-deficient mice develop normally but demonstrate mild hyperactivity associated with an increase in dopamine levels specifically in the nucleus accumbens (Ip et al., 2016). Recently, *Abhd11os* (*ABHD11-AS1* in human) has been identified as a striatal-specific lncRNA and proposed to play a neuroprotective role against mutant Huntingtin (HTT), a protein implicated in Huntington's Disease (Francelle et al., 2015). Studies combining bulk tissue RNA sequencing with single-cell RNA sequencing approaches confirmed cell-type and region specificity (Liu et al., 2016; Fan et al., 2020).

Taken together, expression analyses and functional studies have demonstrated that the spatial expression of a large number of lncRNAs is tightly regulated in various brain regions. However, the mechanisms that control this restricted expression pattern are not yet fully understood.

LncRNAs Are Dynamically Regulated in the CNS

The expression of many lncRNAs is temporally regulated during CNS development and several of them are linked to the regulation of protein-coding genes that play crucial roles in neurodevelopment (Briggs et al., 2015). Expression profiling of both protein-coding and non-coding transcripts during differentiation of mouse embryonic forebrain-derived neural stem cells indicated that 5% of approximately 3,600 analyzed lncRNAs are differentially expressed during neuronal-glial fate specification and oligodendrocyte lineage maturation (Mercer et al., 2010). Many of these lncRNAs exhibit coordinated expression with protein-coding genes involved in neuronal and glial lineage differentiation at distinct developmental stages, suggesting that these ncRNAs might regulate the expression of their associated protein-coding genes (Mercer et al., 2010).

Several reports also demonstrated that lncRNA expression is thoroughly regulated in processes such as synaptogenesis and in response to neuronal activity and plasticity (Zalfa et al., 2003; Bernard et al., 2010; Barry et al., 2014). For instance, the lncRNA *ADEPTR* is upregulated in an activity-dependent manner and consequently transported to synapses where it modulates the structural plasticity of dendritic spines in mouse hippocampal neurons (Grinman et al., 2021). Keihani et al. (2019) also identified *NeuroLNC* as a nuclear and neuron-specific lncRNA involved in the regulation of genes with crucial roles in neuronal physiology including neurotransmitter release, synapse organization and neuronal migration in rat models.

Is the expression of lncRNAs also temporally regulated in the human CNS? Lipovich et al. (2014) profiled the expression of thousands of lncRNAs in the human neocortex using microarray technology and identified 8 lncRNA genes with specific developmental expression patterns. The majority of these lncRNAs are located antisense and/or close to known protein-coding genes. Moreover, these loci exhibit primate-specific gene structure features. A transcriptomic analysis of human neurons derived from induced pluripotent stem cells revealed the presence of more than 1,500 lncRNAs whose expression is regulated during their transition to early differentiating neurons (Lin et al., 2011). Many of these lncRNAs are associated with chromatin-remodeling complexes such as RE1-Silencing Transcription factor (REST), REST corepressor 1 (CoREST) and Polycomb Repressive Complex 2 (PRC2) (Lin et al., 2011).

Widespread changes in the transcriptome, including in the expression of lncRNAs, also occur during aging (Wood et al., 2013; Barry et al., 2015; Kour and Rath, 2015; Chen et al.,

2017). Several studies demonstrated that lncRNAs can be either up- or downregulated in senescent cells. These lncRNAs are typically associated to protein-coding genes that play a role in cell cycle arrest, cellular growth/tumor suppression, telomere organization and p53 signaling (Grammatikakis et al., 2014; Quinodoz and Guttman, 2014; Angrand et al., 2015; Xu C. L. et al., 2020). These molecular functions all have a clear link to aging. Finally, genome-wide association studies identified single-nucleotide polymorphisms associated with neurological diseases including Schizophrenia, Bipolar Disorder and Autism Spectrum Disorder, and that map to lncRNA genes that are dynamically expressed in the CNS (Lin et al., 2011). Together, the expression of lncRNAs in the brain are tightly regulated during neuronal development and aging. Changes in their expression levels during aging and in neurodegenerative diseases further imply that lncRNAs can play crucial roles in pathological events in the brain and underscore their functional importance in brain development and homeostasis.

MECHANISMS OF lncRNAs IN NEUROLOGICAL DISORDERS

Perhaps the most intriguing feature of lncRNAs is their association with disease. Emerging evidence emphasizes the importance of lncRNAs in CNS development and (dys)function. Genome-wide association studies and comparative transcriptomic analyses link lncRNA deregulation and dysfunction to multiple human diseases, including a wide range of neurodevelopmental, neuropsychiatric, and neurodegenerative conditions (Salta and De Strooper, 2017; Salvatori et al., 2020). The identification of multiple natural antisense transcripts (NATs), a class of lncRNAs, at distinct human loci associated with hereditary neurodegenerative disorders including Alzheimer's Disease, Frontotemporal Dementia, Parkinson's Disease, Amyotrophic Lateral Sclerosis and Huntington's Disease further illustrates the potential role of lncRNAs in the expression regulation of neurodegeneration-related genes (Zucchelli et al., 2019).

However, the association of altered expression of specific lncRNAs in brain disorders is not hard proof of biological relevance, and functional studies investigating the role of these lncRNAs are still needed. Since lncRNA function is intrinsically influenced by their subcellular localization (Chen, 2016; Bridges et al., 2021), we will separately discuss lncRNAs that exert their function at the epigenetic or transcriptional level in the nucleus, and those responsible for post-transcriptional regulatory mechanisms in the cytoplasm (**Table 1** and **Figure 3**). Nevertheless, some lncRNAs might be present in both compartments and exert different functions depending on their location (Bridges et al., 2021).

Epigenetic Regulation

Numerous nuclear lncRNAs with potential roles in neurological disorders associate with chromatin where they interact with a wide variety of proteins to enhance or repress their binding and activity at specific DNA regions (Guttman et al., 2011; Roberts et al., 2014; Yao et al., 2019). Specifically, lncRNAs can recruit chromatin modifiers to their target-gene promoters and activate or inhibit their transcription in *cis* (close to their transcription sites) or in *trans* (regulation is exerted at distant loci). Alternatively, they can act as molecular decoys, sequestering specific chromatin modulators from the promoters of target genes. Finally, they can directly interact with DNA and generate DNA-RNA hybrid structures, such as R-loops, which ultimately influence chromatin accessibility and remodeling (Yao et al., 2019; Statello et al., 2021).

LncRNAs Interact With the PRC2 Complex

Many lncRNAs interact with the PRC2 complex, constituted by a group of polycomb proteins that mediate epigenetic silencing in diverse biological processes (Davidovich and Cech, 2015; Balas et al., 2021). The NAT *BDNF-AS* is transcribed antisense to the *BDNF* gene, which encodes a neurotrophic factor essential for neuronal development and maintenance (Modarresi et al., 2012; Miranda et al., 2019). Moreover, BDNF protein levels are reduced in various neurodegenerative disorders including Alzheimer's Disease (Laske et al., 2011), Huntington's Disease (Ferrer et al., 2000; Zuccato and Cattaneo, 2007), and Major Depressive Disorder (Molendijk et al., 2011; Emon et al., 2020). *BDNF-AS* knockdown leads to an increase in *BDNF* mRNA and protein levels both *in vitro* and *in vivo* by reducing the recruitment of the histone lysine methyltransferase EZH2, a component of PRC2, and consequently decreasing the levels of the repressive chromatin mark in the *BDNF* promoter region. Even though it remains unclear how *BDNF-AS* recruits the PRC2 components to the *BDNF* locus, this interaction could be of relevance in disorders where an upregulation of BDNF protein levels in the brain is needed (Modarresi et al., 2012).

Two independent studies identified *SMN-AS1* as an antisense lncRNA that arises from the *SMN* locus and recruits the PRC2 complex to transcriptionally repress *SMN* expression and to have relevant implications for Spinal Muscular Atrophy (SMA) (d'Ydewalle et al., 2017; Woo et al., 2017). SMA is a genetic disorder caused by an autosomal recessive mutation of deletion of the *SMN1* gene which results in atrophy of skeletal muscles due to a progressive motor neuron loss. Increasing the expression of the homologous *SMN2* gene has been shown to functionally compensate for the loss of *SMN1* and ameliorate disease severity by upregulating SMN protein levels (d'Ydewalle and Sumner, 2015). Knockdown of *SMN-AS1* with antisense oligonucleotides (ASOs) can dissociate PRC2 from the *SMN* promoter and increase SMN expression in both *in vitro* and *in vivo* SMA models (d'Ydewalle et al., 2017; Woo et al., 2017). Combining *SMN2* splice-switching oligonucleotides and ASOs targeting *SMN-AS1* further boosted the levels of SMN protein and improved survival of SMA mice compared to either therapy by itself. These findings suggest that targeting this lncRNA combined with the FDA approved *SMN2* splice-switching oligonucleotides (*Spinraza*) could represent a valuable therapeutic approach for severe SMA cases characterized by very low SMN levels (U.S. Food & Drug Administration, 2016; d'Ydewalle et al., 2017).

TABLE 1 | LncRNA regulatory mechanisms and their contribution to CNS disorders.

Function	LncRNA	Binding partners	Mode of action	Associated disease	References
Epigenetic regulation	*BDNF-AS*	PRC2	Act as scaffolds to recruit chromatin modifiers to *BDNF or SMN* promoter region, respectively, and transcriptionally repress their targets	AD, HD, MDD	Modarresi et al., 2012
	SMN-AS1	PRC2		SMA	d'Ydewalle et al., 2017; Woo et al., 2017
	HAR1F/HAR1R	REST	Mutant HTT re-locates REST to the nucleus and represses *HAR1* non-coding locus	HD	Johnson et al., 2010
	TUG1, MEG3	REST, PRC2	ND	HD	Johnson, 2012; Khalil et al., 2009; Myers et al., 2011;
	DGCR5	REST	ND	HD, SZ	Myers et al., 2011; Johnson, 2012; Meng et al., 2018
Transcriptional regulation	*UBE3A-ATS*	ND	Represses paternal copy of *UBE3A* (unclear whether due to the presence of the antisense lncRNA or due to locus transcription)	AS	Meng et al., 2012
	LRP1-AS	HMGB2	Acts as molecular decoy by binding to HMGB2 and inhibiting its ability to promote SREBP1a-dependent transcription of *LRP1*	AD	Yamanaka et al., 2015
	FMR4	ND	Proposed to negatively regulate *MBD4* transcription, a transcriptional repressor involved in DNA repair and apoptosis, via a *trans*-acting mechanism	FXS, FXTAS	Khalil et al., 2008; Peschansky et al., 2015
	C9orf72	Multiple RBPs	Sense and antisense transcripts accumulate in RNA foci and might function as molecular decoys for RBPs, including splicing factors, affecting their function	c9FTD/ALS	Lee et al., 2013; Barker et al., 2017
	MIAT/Gomafu	QKI, SRSF1	Acts as a splicing factor scaffold by binding to QK1 and SRSF1 and regulate alternative splicing of *DISC1* and *ERBB4* genes	SZ	Barry et al., 2014
	51A/SORL1-AS	*SORL1*	Downregulates canonical *SORL1* variant A through alternative splicing, increasing Aβ formation	AD	Ciarlo et al., 2013
	17A	*GPR51*	Shifts alternative splicing of *GPR51* toward an isoform that abolishes GABA B2 intracellular signaling	AD	Massone et al., 2011
Post-transcriptional regulation	*BACE1-AS*	*BACE1*	Positively regulates the levels of *BACE1* mRNA by masking binding site for miR-485-5p, promoting Aβ synthesis	AD	Faghihi et al., 2008, 2010;
	SHANK2-AS	*SHANK2*	Directly binds to *SHANK2* mRNA, decreasing its mRNA stability and expression	ASD, SZ	Luo et al., 2018
	PINK1-AS	*PINK1*	Directly binds to the mRNA of the *svPINK1* splice variant, stabilizing its expression by formation of an RNA duplex	PD	Scheele et al., 2007
	HOTAIR	*LRRK2*	Directly binds to *LRKK2* mRNA, stabilizing its expression by formation of an RNA duplex and inducing neuronal apoptosis	PD	Wang S. et al., 2017
	HTT-AS	*HTT*	Represses mutant *HTT* expression via a RISC-dependent mechanism	HD	Chung et al., 2011
	AS UCHL1	*UCHL1*	Makes use of a SINE B2 sequence to upregulate translation of *UCHL1*, therefore belonging to the SINEUP subclass of lncRNAs	AD, PD	Carrieri et al., 2012; Zucchelli et al., 2015
	MAPT-AS1	*MAPT*	Short elements within *MAPT-AS1* MIR sequence interfere with the binding of *MAPT* mRNA to ribosomes, thus blocking translation	AD, PD	Simone et al., 2021
Structural function	MALAT1, NEAT1	Multiple (splicing factors, miRNAs, epigenetic regulators,	Structural components of nuclear speckles (MALAT1)	FTLD-TDP, PD FTLD-TDP, ALS, HD, SZ	Tollervey et al., 2011; Nishimoto et al., 2013; Sunwoo et al., 2017;

(Continued)

TABLE 1 | Continued

Function	LncRNA	Binding partners	Mode of action	Associated disease	References
		transcription factors, chromatin)	and paraspeckles (NEAT1); multiple roles in gene regulation at epigenetic, transcriptional and post-transcriptional levels in a context-dependent manner		Shelkovnikova et al., 2018; Katsel et al., 2019; Xia et al., 2019

BDNF-AS, brain-derived neurotrophic factor-antisense; SMN-AS1, survival motor neuron-antisense 1; HAR1F, human accelerated region 1 forward; HAR1, human accelerated region 1 reverse (F-forward; R-reverse); TUG1, taurine upregulated gene 1; MEG3, maternally expressed 3; DGCR5, DiGeorge syndrome critical region gene 5 UBE3A-ATS, ubiquitin ligase E3A-antisense, LRP1-AS, low-density lipoprotein receptor-related protein 1-antisense; FMR4, fragile X mental retardation 4; c9orf72, chromosome 9 open reading frame 72; MIAT, myocardial infarction associated transcript; SORL1-AS, sortilin related receptor 1-antisense; BACE1-AS, β-site APP cleaving enzyme 1-antisense; SHANK2-AS, SH3 and multiple ankyrin repeat domains 2-antisense; PINK1-AS, PTEN-induced kinase 1-antisense; HOTAIR, HOX transcript antisense intergenic RNA; HTT-AS, huntingtin-antisense; AS UCHL1, antisense to ubiquitin carboxy-terminal hydrolase L1; MAPT-AS1, microtubule associated protein transcript antisense 1; MALAT1, metastasis-associated lung adenocarcinoma transcript 1; NEAT1, nuclear paraspeckle assembly transcript 1; PRC2, polycomb repressive complex 2; REST, RE1-silencing transcription factor; ND, not defined; RBPs, RNA-binding proteins; HMGB2, high mobility group Box 2; QKI, quaking homolog, KH domain RNA binding; SRSF1, serine and arginine rich splicing factor 1; SORL1, sortilin related receptor 1; BACE1-AS, β-site APP cleaving enzyme 1; SHANK2, SH3 and multiple ankyrin repeat domains 2; PINK1, PTEN-induced kinase 1, GPR51, G protein-coupled receptor 51; LRRK2, leucine-rich repeat kinase 2; SREBP1a, sterol regulatory element binding protein 1a; MBD4, methyl-CpG binding domain 4; DISC1, disrupted-in-schizophrenia 1; ERBB4, Erb-B2 receptor tyrosine kinase 4; SINEUP, SINE B2 sequence to UP-regulate translation; MIR, mammalian-wide interspersed repeat; AD, Alzheimer's disease; HD, Huntington's disease; MDD, major depressive disorder; SMA, spinal muscular atropy; SZ, schizophrenia; AS, Angelman Syndrome; FXS, Fragile X Syndrome; FXTAS, Fragile X-associated Tremor/Ataxia Syndrome; c9FTD/ALS, c9orf72-associated Frontotemporal Dementia and Amyotrophic Lateral Sclerosis (ALS); ASD, autism spectrum disorders; PD, Parkinson's disease; FTLD-TDP, frontotemporal lobar degeneration associated with TDP-43.

LncRNAs Interact With Other Chromatin Modifiers

Chromatin-remodeling complexes other than PRC2 might be involved in neurological disorders through their interaction with lncRNAs. Huntington's Disease (HD) is a polyglutamine (PolyQ)-related disorder caused by an expanded CAG repeat (>36) in the first exon of the *HTT* gene. The repeat expansion results in the production of a mutant neurotoxic form of the HTT protein that triggers a progressive degeneration of cortical and striatal neurons. Although the mechanisms behind neuronal loss in HD are not yet completely understood, aberrant chromatin remodeling and transcriptional dysregulation seem to represent key features in the pathogenesis (Benn et al., 2008). For instance, during HD pathology, the transcriptional repressor REST is abnormally relocated to the nucleus by a mutant HTT-dependent mechanism, resulting in the repression of many REST target genes (Zuccato et al., 2007). The *HAR1* non-coding locus is directly targeted by REST, which might explain the reduction in *HAR1F* and *HAR1R* transcript levels observed in the striatum of HD patients (Johnson et al., 2010). The expression of other lncRNAs with potential epigenetic regulatory functions is dysregulated in the brains of HD patients (Johnson, 2012). These include the putative REST targets *DGCR5*, *NEAT1,* and *MEG3* (Myers et al., 2011), and *TUG1* (Johnson, 2012). Interestingly, *TUG1* and *MEG3* can interact with PRC2 (Khalil et al., 2009). Therefore, it is likely that altered levels of some of these lncRNAs might influence gene expression patterns during disease. Similarly, *DGCR5* has recently also been proposed to regulate the expression of genes associated with Schizophrenia (Meng et al., 2018).

Transcriptional Regulation

Multiple lncRNAs regulate their target genes at the transcriptional level. Importantly, two mechanisms may play a role in this regulation: the lncRNA transcript can influence the transcription of neighboring loci, and/or the act of transcription of the lncRNA itself can drive chromatin remodeling and affect the expression of other genes (Statello et al., 2021).

Is It the Transcript or Transcription?

UBE3A-ATS is a nuclear lncRNA that has been implicated in Angelman syndrome (AS), a severe neurodevelopmental disorder caused by a maternal deficiency of the imprinted gene *UBE3A* (Meng et al., 2012). Although patients carry at least one functional copy of the paternal *UBE3A*, in neurons this allele is silenced by the antisense lncRNA. Whether silencing of *UBE3A* by *UBE3A-ATS* occurs due to the presence of the antisense lncRNA or due to transcription of this locus is unclear (Meng et al., 2012). Nonetheless, reducing *UBE3A-ATS* levels to restore UBE3A protein levels has been proposed as a potential therapeutic intervention for AS (Meng et al., 2013, 2015; Wolter et al., 2020).

LncRNAs Act as Molecular Decoys

LncRNAs can also act as molecular decoys for other RNA-binding proteins (RBPs) including transcription and splicing factors. For example, Yamanaka et al. (2015) identified a NAT associated with the *LRP1* gene, designated as *LRP1*-AS (*Lrp1-AS* in mouse), which has been implicated in Alzheimer's Disease (AD) pathology. AD is the main cause of dementia worldwide and two hallmarks of this neurodegenerative disorder are the accumulation of extracellular amyloid-β (Aβ)-containing plaques and intracellular neurofibrillary tangles composed of hyperphosphorylated and aggregated Tau protein within the patients' brains (Scheltens et al., 2021). LRP1 protein plays a major role in different aspects of AD (Tachibana et al., 2019; Rauch et al., 2020). Modulation of *Lrp1-AS* levels in a mouse cell line revealed that this lncRNA negatively regulates *Lrp1* expression both at the mRNA and protein levels. *Lrp1-AS* directly binds to HMGB2, a non-histone chromatin modifier, inhibiting

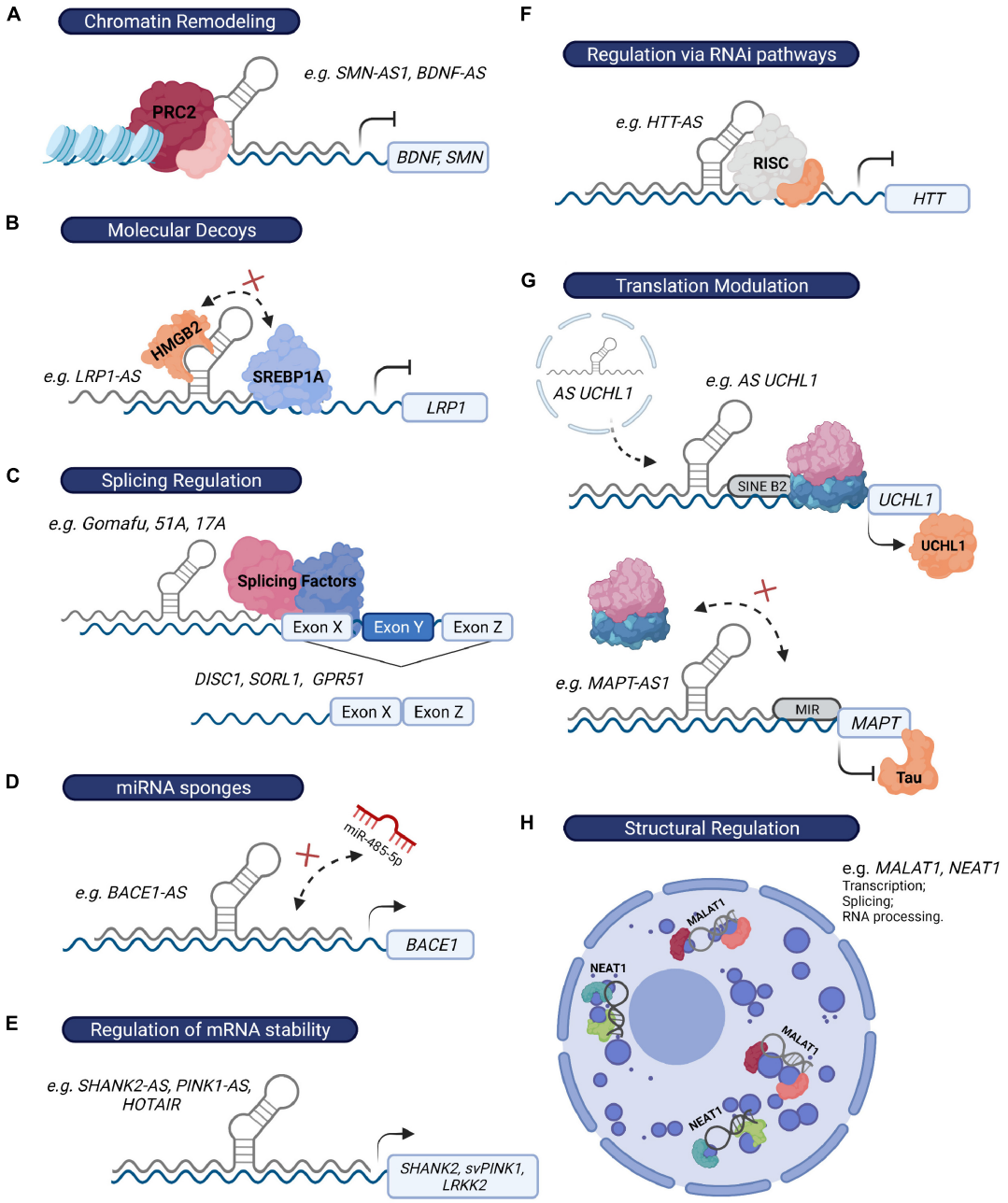

FIGURE 3 | LncRNAs regulate gene expression through multiple mechanisms. **(A)** LncRNAs can recruit chromatin modifiers (e.g., PRC2 complex) to their target-gene promoters and epigenetically influence their expression (e.g., *BDNF-AS* and *SMN-AS1*). **(B)** Alternatively, they can modulate transcription by acting as molecular decoys and sequester specific chromatin and non-chromatin modulators, transcription factors, or other regulatory proteins from the promoters of their target genes (e.g., *LRP1-AS*). **(C)** LncRNAs can also influence transcription by affecting the alternative splicing of their target genes (e.g., *Gomafu, 51A, 17A*). **(D)** Some lncRNAs regulate mRNA turnover by acting as miRNA "sponges" (e.g., *BACE1-AS*), as they prevent miRNAs from binding their target genes. **(E)** Additionally, they can directly bind to their target mRNAs, leading to the formation of an RNA-RNA duplex and therefore influencing mRNA stability (*SHANK2-AS*, *PINK1-AS*, and *HOTAIR*). **(F)** LncRNAs can also exert their function via recruitment of the RISC complex to their target mRNA (e.g., *HTT-AS*). **(G)** Some lncRNAs directly modulate translation efficiency of their target genes through the presence of specific sequences that either promote (e.g., SINE B2 element in *AS UCHL1*) or prevent (e.g., MIR sequence in *MAPT-AS1*) the association of ribosome machinery with their target mRNAs. **(H)** Finally, *NEAT1* and *MALAT1* exert a crucial structural function in the formation of paraspeckles and speckles, respectively, two nuclear structures that regulate multiple mechanisms, including RNA transcription, splicing and processing.

its ability to promote SREBP1A-dependent transcription of *Lrp1*. Accordingly, increased levels of *LRP1*-AS and a reduction in *LRP1* expression in human AD brain samples compared to age-matched controls were observed (Yamanaka et al., 2015). However, further studies are needed to specifically investigate the role of *LRP1-AS* in the transcriptional regulation of *LRP1* in the human brain and its functional effects in AD pathogenesis.

Development of Fragile X Syndrome (FXS) or the related disease Fragile X-associated Tremor/Ataxia Syndrome (FXTAS) is caused by the presence of a triple CGG repeat motif in the 5′ untranslated region (5′-UTR) of the *FMR1* gene (Khalil et al., 2008; Peschansky et al., 2015; Huang et al., 2019). Unaffected individuals typically carry 5–54 repeats while 55–200 repeats are considered a premutation leading to the development of FXTAS. A full mutation occurs when > 200 repeats are present, and this is necessary to develop FXS. In most FXS patients, *FMR1* is hypermethylated and transcriptionally silenced resulting in decreased *FMR1* mRNA and FMRP protein levels, impacting neurogenesis (Sunamura et al., 2018). Intriguingly, the *FMR1* locus is particularly complex and encodes several lncRNAs. The expression of these lncRNAs are differentially affected by the repeat expansion mutations suggesting that they could potentially explain the distinct clinical features of FXS and FXTAS (Ladd et al., 2007; Khalil et al., 2008; Pastori et al., 2014; Vittal et al., 2018; Huang et al., 2019). One of these lncRNAs, *FMR4*, overlaps with the repeat region and is silenced in FXS patients but upregulated in premutation carriers (Khalil et al., 2008; Peschansky et al., 2015). Previously, Khalil et al. (2008) have shown that even though *FMR4* does not regulate *FMR1* expression, it exhibits anti-apoptotic functions in human cell lines. Later on, and consistent with a role at the transcriptional level, *FMR4* was found to be primarily associated with chromatin, and a discordant expression between the lncRNA and *MBD4,* a transcriptional repressor involved in DNA repair mechanisms and regulation of apoptosis (Bellacosa, 2001), was observed during human neuronal precursor cells development. This suggests a *trans*-acting regulatory role for *FMR4* independent of *FMR1* which might be impaired in Fragile X repeat expansion-associated diseases (Peschansky et al., 2015).

The presence of hexanucleotide GGGGCC (G4C2) repeat expansions in the *C9orf72* gene represents the most common genetic cause of Frontotemporal Dementia (FTD) and Amyotrophic Lateral Sclerosis (ALS), two devastating neurodegenerative disorders commonly designated as c9FTD/ALS (Barker et al., 2017). While the mechanisms by which these repeat expansions lead to c9FTD/ALS are not fully understood, both sense and antisense RNA foci comprising *C9orf72* RNA are widely distributed across the CNS of these patients (Gendron et al., 2013; Zu et al., 2013; Cooper-Knock et al., 2015). A potential mechanism by which RNA foci are thought to cause neurotoxicity is by directly sequestering specific RBPs and disrupting their function (Barker et al., 2017). Ultimately, this leads to a wide range of RNA misprocessing events, including aberrant alternative splicing. In support of this, Lee et al. (2013) transfected human neuroblastoma cells with different G4C2 repeat lengths and revealed that longer repeat lengths originate RNA foci that co-localize with a subset of RBPs involved in alternative splicing, which include SF2, SC35 and hnRNP-H. Furthermore, hnRNP-H directly binds to G4C2 repeat sequences and associate with RNA foci in both transfected cells and in the brains of c9FTD/ALS patients (Lee et al., 2013).

LncRNAs Influence Alternative Splicing

Another mechanism by which lncRNAs can influence transcription is by affecting the alternative splicing of their target genes (Yao et al., 2019). Schizophrenia is a complex mental disorder that affects about 1% of the population, and it is likely to result from different genetic, epigenetic and environmental factors that culminate in neurodevelopmental abnormalities and brain dysfunction (Morikawa and Manabe, 2010; Barry et al., 2014). Many genes associated with Schizophrenia are aberrantly spliced, including *DISC1* (Nakata et al., 2009) and *ERBB4* (Law et al., 2007). In line with this, *Gomafu* can act as a splicing factor scaffold, directly binding to the splicing factors QKI and SRSF1 to regulate alternative splicing of *DISC1* and *ERBB4* in human neurons derived from induced pluripotent stem cells (Barry et al., 2014). Notably, abnormal alternative splicing patterns upon ASO-mediated knockdown of *Gomafu in vitro* match those observed for these two genes in post-mortem brains from individuals affected by Schizophrenia. Finally, *Gomafu* levels are reduced in cortical samples from patients compared to controls further suggesting a role for *Gomafu* in Schizophrenia pathology (Barry et al., 2014).

In AD, the lncRNAs *51A*/*SORL1*-AS and *17A* have both been suggested to interfere with the alternative splicing of their neighboring genes - *SORL1* encoding Sortilin-1 and *GPR51* encoding GABA receptor B2, respectively - and their expression is upregulated in the brain tissue from AD patients (Massone et al., 2011; Ciarlo et al., 2013).

Post-transcriptional Regulation

LncRNAs can be exported to the cytoplasm, where they regulate gene expression at the post-transcriptional level by influencing mRNA turnover, modulating translation or by interfering with post-translational modifications (Yao et al., 2019; Salvatori et al., 2020).

LncRNAs "Sponge" miRNAs

Some lncRNAs regulate mRNA turnover of their target genes by competing with *miRNA* binding sites by acting as *miRNA* "sponges" (Su et al., 2018; Yao et al., 2019). For instance, *BACE1-AS* has been identified as an antisense lncRNA associated with the *BACE1* gene (Faghihi et al., 2008). *BACE1-AS* regulates the levels of *BACE1* mRNA by masking *BACE1* mRNA binding site for miR-485-5p (Faghihi et al., 2010). *BACE1* encodes a secretase involved in the biosynthesis of Aβ and plays a central role in the amyloid cascade in AD pathophysiology (Hampel et al., 2020). In the presence of cell stressors including $A\beta_{1-42}$, *BACE1-AS* levels increase thereby raising the levels of both *BACE1* mRNA and protein. This in turn stimulates the production of $A\beta_{1-42}$, at least *in vitro,* which may lead to a detrimental accumulation of toxic Aβ aggregates (Faghihi et al., 2008). Moreover, different brain regions from AD patients exhibit

increased levels of this lncRNA compared to control subjects indicating a direct role for *BACE1-AS* in driving AD pathology (Faghihi et al., 2008).

LncRNAs Regulate mRNA Stability

Another possibility is that lncRNA transcripts directly bind to their target mRNA, originating an RNA duplex and affecting mRNA stability by either recruiting proteins that promote mRNA degradation or, on the contrary, by acting as molecular decoys for RBPs involved in mRNA decay (Yao et al., 2019). Autism Spectrum Disorder (ASD) comprises a range of heterogeneous neurodevelopmental disorders characterized by cognitive, social and sensory impairments (Lord et al., 2020). Many are co-expressed with ASD risk genes in the developing brain (Cogill et al., 2018). For instance, the expression *SHANK2-AS*, a lncRNA transcribed antisense to the *SHANK2* gene, is upregulated and its levels negatively correlate with *SHANK2* mRNA and protein levels in ASD patients compared to control individuals (Wang et al., 2015; Luo et al., 2018). Mutations in the *SHANK2* gene, which encodes a post-synaptic density scaffold protein, have been identified as risk factors for ASD (Sato et al., 2012; Zaslavsky et al., 2019) and Schizophrenia (Peykov et al., 2015). *SHANK2-AS* can directly bind to *SHANK2* mRNA, consequently decreasing its expression *in vitro* (Luo et al., 2018). Furthermore, overexpression of *SHANK2-AS* or downregulation of *SHANK2* reduces neurite length and number in a human neuronal cell line suggesting that abnormal expression of *SHANK2*-AS may affect neuronal structure and growth by downregulating *SHANK2* expression, and thus directly contribute to ASD pathology (Luo et al., 2018).

Parkinson's Disease (PD) is a neurodegenerative disorder generally characterized by the accumulation of α-synuclein (encoded by the *SNCA* gene) aggregates within Lewy bodies or Lewy neurites and degeneration of dopaminergic neurons, particularly in the substantia nigra. While most PD cases are sporadic, familial forms of the disease can occur and result from mutations in a group of genes that include *LRRK2*, *PARK2*, *PARK7*, *PINK1* or the *SNCA* gene itself (Bandres-Ciga et al., 2020). The antisense lncRNA *PINK1-AS* stabilizes the expression of a *PINK1* splice variant (svPINK1) *in vivo* through the formation of an RNA duplex (Scheele et al., 2007). This interaction might have important implications in multiple disorders besides PD (Wilhelmus et al., 2011), as *PINK1* is thought to have a neuroprotective role against stress-induced mitochondrial dysfunction, oxidative stress and apoptosis (Deas et al., 2009). In addition, the lncRNA *HOTAIR* has also been implicated in PD pathology by increasing *LRKK2* mRNA stability and inducing dopaminergic neuronal apoptosis in a human neuroblastoma cell line (Wang S. et al., 2017). There are also several lncRNAs identified that can arise from the antisense strand in the *SNCA* locus either overlapping with the SNCA gene in the 5′ or 3′end (Zucchelli et al., 2019). Although their role in regulating *SNCA* expression is still enigmatic, expression analysis confirmed that some of these lncRNAs are co-expressed with *SNCA,* including in the substantia nigra (Zucchelli et al., 2019).

LncRNAs Act via the RNAi Pathway

The lncRNA *HTT-AS* originates from the HD repeat locus containing the repeat region and represses mutant HTT expression via an RNA-induced silencing complex (RISC)-dependent mechanism (Chung et al., 2011). In human cells, overexpression of the *HTT-AS* transcript reduces *HTT* mRNA levels, while knocking down the lncRNA upregulates *HTT* transcripts. Interestingly, reduced levels of *HTT-AS* were observed in the frontal cortex from HD patients compared to control individuals suggesting a potential protective role in HD in which the presence of expanded repeats reduces *HTT-AS* expression, removing its inhibitory effect on *HTT* expression (Chung et al., 2011).

LncRNAs Modulate Translation

Finally, some lncRNAs directly modulate translation efficiency of genes associated with neurological disorders (Muddashetty et al., 2002; Salta and De Strooper, 2017). Carrieri et al. (2012) have identified *AS Uchl1* as an antisense lncRNA associated with the *Uchl1* gene. UCHL1 is a highly abundant neuronal protein involved in neuronal development (Reinicke et al., 2019), dopaminergic neuron differentiation (Carrieri et al., 2015) and regulation of the ubiquitin-proteasome pathway (Yichin et al., 2002). *UCHL1* gene variants are associated with susceptibility to PD (Ying et al., 2015), and oxidative modifications and downregulation of UCHL1 protein are observed in sporadic cases of both AD and PD patients (Choi et al., 2004). *AS Uchl1* shuttles from the nucleus to the cytoplasm upon rapamycin induced mTOR activity in a dopaminergic cellular model, where it targets *Uchl1* mRNA to active polysomes to facilitate its translation and upregulate Uchl1 protein levels (Carrieri et al., 2012). Owing to the presence of an embedded repetitive sequence SINE B2 in the inverted orientation at the non-overlapping part of the transcript, *AS Uchl1* has been considered the representative member of a recently identified functional NAT class designated as SINEUPs. These molecules require a SINE B2 sequence to UP-regulate translation of their target mRNA. Importantly, due to their ability to increase the translation of virtually any gene of interest, the development of synthetic SINEUPs that target the antisense sequence of the target mRNA might constitute an interesting therapeutic approach to enhance protein synthesis (Zucchelli et al., 2015).

The very recent identification of NATs with embedded mammalian-wide interspersed repeat (MIR) sequences – referred to as MIR-NATs – associated with protein-coding genes tied to neurodegenerative disorders has revealed a new class of lncRNAs that mediate gene regulation at the translational level through a MIR-dependent mechanism (Simone et al., 2021). One of these MIR-NATs, *MAPT-AS1*, is associated with the *MAPT* gene – encoding the Tau protein - and has been suggested to repress Tau translation by competing for ribosomal RNA pairing with the *MAPT* mRNA internal ribosome entry site (Simone et al., 2021).

The Nucleus Takes It All

NEAT1 and *MALAT1* (also known as *NEAT2*) are two human lncRNAs conserved within the mammalian lineage

which regulate key nuclear functions (Hutchinson et al., 2007; Zhang et al., 2017; An et al., 2018). Despite displaying an adjacent genomic location, these two RNAs exert their function in related but distinct nuclear subdomains (West et al., 2014). *MALAT1* is localized in nuclear speckles which are enriched in serine- and arginine-rich (SR) splicing factors, while *NEAT1* is a structural component of nuclear bodies called paraspeckles, also composed by multiple proteins with reported roles in transcription and RNA processing (West et al., 2014). Therefore, both lncRNAs play important regulatory roles in many cellular pathways that are commonly affected in neurological diseases (Zhang et al., 2017; An et al., 2018). The expression of both *MALAT1* and *NEAT1* is markedly upregulated in the brains from Frontotemporal Lobar Degeneration associated with TDP-43 (FTLD-TDP) patients (Tollervey et al., 2011). Moreover, this differential expression can explain an increased binding of TDP-43 protein to these lncRNAs in FTLD-TDP patient samples, supporting a role for lncRNAs and TDP-43 in the regulation of splicing in the brain with direct implications for neurodegenerative diseases (Tollervey et al., 2011).

Although a large proportion of the genetic risk for familial ALS (fALS) is still elusive, mutations in *SOD1*, *TARDBP* (TDP-43), *FUS* and *C9orf72* genes are linked to the onset of fALS (Mejzini et al., 2019). Both TDP-43 and FUS/TLS are enriched in paraspeckles in cultured cells where they directly bind *NEAT1_2* transcript. Analysis of human spinal motor neurons revealed upregulated levels of *NEAT1_2,* and enhanced paraspeckle formation was confirmed in two independent cohorts of ALS cases compared to controls (Nishimoto et al., 2013; Shelkovnikova et al., 2018). The formation of paraspeckles has been linked to the loss of TDP-43 function in cells, suggesting a protective role for these structures (Shelkovnikova et al., 2018).

A microarray analysis demonstrated upregulated levels of *NEAT1* in human HD postmortem brain patients and in a mouse model of HD (Sunwoo et al., 2017). Transfection of *NEAT1* in a mouse cell line increases cell viability under oxidative stress, an observation that aligns with a previous report describing the involvement of *NEAT1* in cell survival pathways under stress conditions (Choudhry et al., 2015). Thus, these studies support the idea of a protective role for this lncRNA in non-physiological settings (Sunwoo et al., 2017). Conversely, expression of *NEAT1* is reduced in cortical brain regions from Schizophrenia patients. Furthermore, RNA-seq analysis performed in the frontal cortex of *NEAT1* deficient mice indicated that pathways related to oligodendrocytes differentiation and RNA post-translational modifications are significantly impacted (Katsel et al., 2019). These results are in line with previously discussed data indicating that *NEAT1* expression is dramatically changed during mouse oligodendrocyte-lineage specification (Mercer et al., 2010). Additionally, *NEAT1*$^{-/-}$ mice displayed a significant reduction in the numbers of oligodendrocyte-lineage cells and impaired expression of genes related to myelination, supporting a role for *NEAT1* in oligodendrocyte function and related abnormalities in Schizophrenia pathology (Haroutunian et al., 2014; Katsel et al., 2019).

Finally, *MALAT1* was found to bind to α-synuclein protein and increase its stability in a human neuroblastoma cell line (Zhang et al., 2016). Accordingly, inhibition of *MALAT1* using resveratrol was found to increase miR-129 levels, consequently downregulating *SNCA* expression and improving disease-related phenotypes in a PD mouse model (Xia et al., 2019).

TARGETING lncRNAs IN NEUROLOGICAL DISORDERS: TRASH OR TREASURE?

Around 30 years ago, gene transcription was perceived as a process mostly regulated by protein transcription factors and RNA was largely seen as an intermediary between DNA and protein; RNA had merely a supportive role in the translation of genetic information into diverse functional programs within the cells. However, the recent identification of multiple endogenous RNA classes with unexpected functions in gene regulation, including lncRNAs, has raised the interest to exploit RNA-based therapies (Wahlestedt, 2013; Roovers et al., 2018). To date, the biological functions of many annotated lncRNAs remain largely unexplored. The high unmet need for efficacious disease-modifying therapies for many of the neurodegenerative diseases mentioned in this review underscores the necessity to take bold steps and invest more in lncRNA research in order to open up innovative therapeutic opportunities for disorders of the brain.

Targeting LncRNAs at the DNA Level

Recent progress in genome-editing techniques, such as CRISPR-based methods including CRISPR-interference (CRISPRi) and CRISPR-activation (CRISPRa), has brought the exciting possibility of transcriptionally silence or activate lncRNA expressing loci, and clearly demonstrate that these tools will be crucial for a better understanding of lncRNA biology (Jinek et al., 2012; Cong et al., 2013; Mali et al., 2013; Qi et al., 2013; Gilbert et al., 2014; Thakore et al., 2015; Zhu et al., 2016; Abudayyeh et al., 2017; Liu S. J. et al., 2017; Chen et al., 2019; Phelan and Staudt, 2020; Wolter et al., 2020; Xu D. et al., 2020; Zhang et al., 2021). One way to achieve such transcriptional modulation is to use a dead-Cas9 approach. In this approach, a mutant form of Cas9 without endonuclease activity is fused to transcriptional repressors or activators to achieve transcriptional silencing or activation, respectively, of a specific gene promoter (Liu S. J. et al., 2017; Arun et al., 2018) (**Figure 4A**). Furthermore, Cas9-based gene therapy was shown to successfully reduce the expression of *UBE3A-ATS* and activate the paternal *UBE3A* in a mouse model of AS. Early treatment with an adeno-associated viral (AAV) delivery system designed to activate the expression of paternal *UBE3A* for at least 17 months ameliorated disease phenotype in AS mice and provided proof of concept that this approach is therapeutically relevant (Wolter et al., 2020). Onasemnogene abeparvovec, an AAV-based therapy carrying a functional copy of the *SMN* gene, was approved in May 2019 as the first gene therapy for SMA in the United States and illustrates that

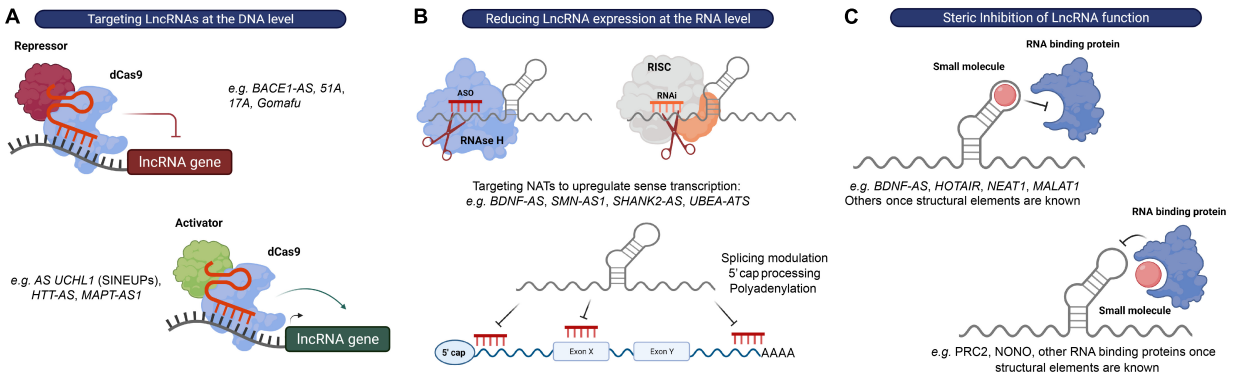

FIGURE 4 | Strategies to target lncRNAs. **(A)** DNA editing: CRISPRi and CRISPRa tools can be used to transcriptionally silence or activate lncRNA expressing loci, respectively. **(B)** Modulation of RNA levels: ASOs and siRNAs can be used to reduce lncRNA levels in order to alter the expression of their associated protein-coding genes. recruits RBPs that mediate RNA processing events, such as 5′ capping, splicing or polyadenylation, to modulate expression or RNAse H to promote degradation of the lncRNA transcript, respectively, while RNAi induces RISC-mediated cleavage of the lncRNA transcript. **(C)** Steric inhibition: small molecules target secondary and tertiary structures of lncRNAs and/or their binding partners to block their interaction.

AAV approaches can lead to clinical successes for devastating neurological diseases (Hoy, 2019). While recent advances in CRISPR-based techniques demonstrate great potential for the discovery of disease mechanisms and identification of new therapeutic targets, there are still some challenges and risks that need to be considered prior to their use as therapy for neurological disorders. These include finding an effective CNS delivery method, the irreversibility of DNA editing, and safety concerns related to undesired on-target and off-target effects (Sun and Roy, 2021). For instance, a genome-wide association analysis found that almost two-thirds of lncRNA loci are at risk of inadvertently influencing the expression of neighboring genes upon CRISPR-mediated targeting (Goyal et al., 2017). Thus, future research will be crucial to explore the full potential of these modalities as therapeutics.

Reducing LncRNA Expression at the RNA Level

The possibility of modulating RNA expression with oligonucleotides provides a relatively straightforward strategy to impact virtually any RNA of interest and to target previously "undruggable" portions of our genome (Arun et al., 2018). At the moment, there are two major strategies employing oligonucleotide-based therapeutics: ASOs and RNA-mediated interference (RNAi), which share the fundamental principle of exerting their catalytic activity by binding their target RNA through Watson-Crick base pairing (Watts and Corey, 2012). ASOs are single stranded nucleotide sequences that bind RNA primary sequences to either affect RNA processing events, such as 5′-cap formation, splicing and polyadenylation, induce RNA degradation via the recruitment of Ribonuclease H (RNase H), or repress translation (in the case of protein-coding genes) (DeVos and Miller, 2013). Alternatively, a complementary hybrid RNA strand will engage with the target RNA in the RISC complex to initiate its degradation in the RNAi mechanism (Hannon and Rossi, 2004) (**Figure 4B**).

Remarkably, both ASO- and siRNA-based strategies have been proven successful in reducing the expression of several lncRNAs with potential roles in neurological disorders (Scheele et al., 2007; Chung et al., 2011; Carrieri et al., 2012; Modarresi et al., 2012; Barry et al., 2014; Meng et al., 2015; Peschansky et al., 2015; Yamanaka et al., 2015; d'Ydewalle et al., 2017; Wang X. et al., 2017; Woo et al., 2017; Luo et al., 2018). However, their efficiency is at least partially dependent on the subcellular compartment in which the target lncRNA localizes (Lennox and Behlke, 2016). Specifically, while lncRNAs primarily located within the nucleus were shown to be easier to target using ASOs, the expression of cytoplasmic lncRNAs was more efficiently reduced using RNAi methods. Additionally, both strategies were able to suppress the levels of lncRNAs residing in both compartments, although ASOs performed overall better in this case (Lennox and Behlke, 2016). In line with these observations, RNAse H1-dependent ASOs robustly exert their function in both the nucleus and the cytoplasm (Liang et al., 2017). These studies highlight the importance of better understanding how and where lncRNAs play their functional roles to select the most appropriate therapeutic approach to target these molecules.

A particular attractive class of candidate targets for these approaches is the previously mentioned NATs. Most of these NATs affect the transcription and/or translation of their neighboring genes. Furthermore, many of these antisense lncRNAs have been shown to act as repressors of sense coding genes in a locus-specific manner (e.g., *SMN-AS1, BDNF-AS, SHANK2-AS*, and *UBE3A-ATS*). Since there is still a considerable lack of therapeutic approaches to upregulate gene expression, inhibition of these transcripts with siRNAs or ASOs (called "antagoNATs") might be of particular interest to increase the expression of genes found downregulated in CNS disorders (Wahlestedt, 2013) (**Figure 4B**).

The recent approval of several ASOs and siRNAs for clinical intervention clearly demonstrates the huge therapeutic potential of RNA-based therapies for a wide range of human diseases, including HD, ALS, AD and

FTD (Roberts et al., 2020). However, two main limitations need to be considered. First, systemic delivery to the CNS remains a limitation since oligonucleotides are unable to cross the blood-brain barrier (Roberts et al., 2020). Additionally, due to the presence of complex secondary and tertiary structures, their incorporation into large protein complexes, or their specific intracellular location, some lncRNAs might be hard to target using these tools (Gutschner et al., 2011; Wilusz et al., 2012; Brown et al., 2014; Pegueroles and Gabaldón, 2016).

Steric Inhibition of LncRNA Function

Interfering with lncRNA function(s) rather than modulating its expression levels may represent an alternative therapeutic approach. An increasing body of evidence suggests that the function of many lncRNAs is largely mediated by their interaction with RBPs or protein complexes. Thus, a promising therapeutic option for targeting lncRNAs is the use of steric hindering antisense oligonucleotides or small molecules that affect these interactions by either (1) blocking the RNA-binding domain of the protein, or (2) directly binding to and disrupting secondary and tertiary structures in the lncRNA molecule (Meyer et al., 2020) (**Figure 4C**).

The variety of lncRNA binding partners and their unique structural features offer exceptional opportunities to target these RNAs using small molecules. Importantly, the development of new RNA sequencing techniques and structure determination assays such as SHAPE (Wilkinson et al., 2006), SHAPE-MaP (Smola et al., 2015), PARIS (Lu et al., 2016), or CROSSalign (Ponti et al., 2018) have made it possible to map the secondary and tertiary structures of lncRNAs. In addition, a database tool called LNCmap has been recently developed to explore correlations among diseases, small molecules and lncRNA signatures (Yang et al., 2017). Indeed, structural domains of several lncRNAs that interact with proteins or protein complexes, continue to be revealed (Smith et al., 2013; Mondal et al., 2015; Somarowthu et al., 2015; Liu F. et al., 2017; McCown et al., 2019; Balas et al., 2021).

MALAT1 has been proposed to contain a bipartite triple helix at the 3′ end and single-point mutations that destabilize this structure have been shown to reduce *MALAT1* levels in cells, implying a crucial role for this structure in enabling *MALAT1* expression (Brown et al., 2014, 2016). The secondary structure of the inverted SINE B2 element embedded in the mouse *AS Uchl1* has also been recently revealed by Podbevšek et al. (2018). The authors found that removal of a structural motif containing a short hairpin abolishes the ability of *AS Uchl1* to upregulate UCHL1 protein levels, highlighting the importance of specific structural determinants of the SINE B2 sequence in the functionality of *AS Uchl1* (Podbevšek et al., 2018). Furthermore, the RBP NONO is an important component of paraspeckles and was shown to be recruited to these structures by specifically binding to highly abundant and conserved G-quadruplex motifs in the lncRNA *NEAT1* (Simko et al., 2020). These motifs represent the main structural element recognized by the catalytic subunit of PRC2 (Wang X. et al., 2017), which we already discussed as an important binding partner for many lncRNAs, including *HOTAIR* (Rinn et al., 2007), *XIST* (Bousard et al., 2019), *SMN-AS1* (d'Ydewalle et al., 2017), *BDNF-AS* (Modarresi et al., 2012), and others. Moreover, the observation that stable G-quadruplexes are present at the G-rich region of *C9orf72* repeat RNA suggests a link between these motifs and neurodegeneration (Cammas and Millevoi, 2017). Several groups are currently exploring the potential of small molecules to modulate the function of lncRNAs, including some lncRNAs previously implicated in neurological disorders such as *BDNF-AS*, *HOTAIR*, *NEAT1* or *MALAT1* (Pedram Fatemi et al., 2015; Donlic et al., 2018; Abulwerdi et al., 2019; Ren et al., 2019; Simko et al., 2020; Khaled et al., 2021). While the field of RNA-targeting small molecules is still in its infancy, efforts toward understanding the fundamental dynamics between small molecule and lncRNAs recognition together with methodology development will likely contribute to unlock the full potential of using these compounds to treat complex brain disorders by targeting lncRNAs.

Although still early, it has been shown that small molecules can target several classes of RNA besides lncRNAs, including *miRNAs*, repeat expansion regions, mRNAs encoding for intrinsically disordered proteins, splicing modifiers and motifs located at the 5′- and 3′- untranslated regions (5′- and 3′- UTRs, respectively) (Meyer et al., 2020; Yu et al., 2020). Recently, *Risdiplam* received FDA approval for the treatment of SMA (U.S. Food & Drug Administration, 2020), and *Branaplam* is undergoing clinical trials as a therapy for the same disease as well as a for HD (ClinicalTrials. gov, 2021). Both *Risdiplam* and *Branaplam* increase SMN protein levels by acting as *SMN2* splicing modulators (Meyer et al., 2020). Other small molecules have been identified as potential therapeutic agents for neurological disorders but are still in early discovery stages. These include *Synucleozid* for PD (Zhang et al., 2020), *Mitoxantrone* for primary tauopathies (Zheng et al., 2009), and at least one compound with the ability to target expanded repeat regions of *FMR1* mRNA and *C9orf72* mRNA, involved in FXTAS and c9FTD/ALS, respectively (Colak et al., 2014; Su et al., 2014; Wang et al., 2019).

CONCLUSION AND FUTURE PERSPECTIVES

Supported by their characteristics including high cell- and specificity and dynamic regulation of specific cellular pathways at the transcriptional and post-transcriptional level, lncRNA-based therapies could bring important clinical advantages. These include their superior potential as new targets, reduced toxic effects derived from off-target mechanisms, and the possibility to have a biologically meaningful effect with lower compound doses due to their lack of translation, fast turnover, and general low expression levels (Barry, 2014; Bonetti and Carninci, 2017). The fact that most disease-linked single-nucleotide polymorphisms have been shown to map to the non-coding genome further emphasizes the point that exploring non-coding loci can be relevant to identify new potential therapeutic targets (Tak and Farnham, 2015).

However, there are still some challenges to overcome in the field of lncRNAs research. First and foremost, more basic research is needed to address the exact roles of lncRNAs in the brain and identify their related disease-relevant signaling pathways. Second, and related to the first point, further investigation is needed to develop therapeutic strategies that efficiently alter lncRNA transcript levels or repress their function(s) using ASOs and siRNAs provided that the delivery of these molecules to the CNS is tackled. Though impressive progress occurred in the past years regarding the use of oligonucleotide-based therapies, a deeper appreciation of lncRNA structural features and their interactions with DNA, RNA and proteins will open the exciting possibility of targeting these RNAs using small molecules with unprecedented specificity as agonists or antagonists. On the long term, development of orally available, brain-penetrant lncRNA-targeting small molecules could represent a new therapeutic modality for genomic imprinting diseases, neurodevelopmental and neurodegenerative diseases. As new RNA-targeted therapeutic strategies continue to emerge, we believe that unraveling the functional roles of lncRNAs will pave the way to transform lncRNAs originally perceived as "junk" DNA to a therapeutic treasure for patients affected by CNS diseases.

AUTHOR CONTRIBUTIONS

RP, AS, and Cd'Y were responsible for the conception of the article. RP did the scientific literature review, created the figures, and wrote the first draft of the review. Cd'Y contributed to the scientific literature review. AS and Cd'Y critically revised the entire review. All authors approved the final version.

FUNDING

RP holds a doctoral student fellowship from VLAIO, the Flemish Agency for Innovation and Entrepeneurship (Vlaams Agentschap Innoveren en Ondernemen). This work was supported by VLAIO (R&D grants HBC.2018.2290 and HBC.2020.3236) and VIB-KU Leuven.

ACKNOWLEDGMENTS

Illustrations were created with BioRender.com.

REFERENCES

Abudayyeh, O. O., Gootenberg, J. S., Essletzbichler, P., Han, S., Joung, J., Belanto, J. J., et al. (2017). RNA targeting with CRISPR-Cas13. *Nature* 550, 280–284. doi: 10.1038/nature24049

Abulwerdi, F. A., Xu, W., Ageeli, A. A., Yonkunas, M. J., Arun, G., Nam, H., et al. (2019). Selective small-molecule targeting of a triple helix encoded by the long noncoding RNA, MALAT1. *ACS Chem. Biol.* 14, 223–235. doi: 10.1021/acschembio.8b00807

An, H., Williams, N. G., and Shelkovnikova, T. A. (2018). NEAT1 and paraspeckles in neurodegenerative diseases: a missing lnc found? Non-coding. *RNA Res.* 3, 243–252. doi: 10.1016/j.ncrna.2018.11.003

Angrand, P.-O., Vennin, C., Le Bourhis, X., and Adriaenssens, E. (2015). The role of long non-coding RNAs in genome formatting and expression. *Front. Genet.* 6:165. doi: 10.3389/fgene.2015.00165

Aprea, J., and Calegari, F. (2015). Long non-coding RNAs in corticogenesis: deciphering the non-coding code of the brain. *EMBO J.* 34, 2865–2884. doi: 10.15252/embj.201592655

Arun, G., Diermeier, S. D., and Spector, D. L. (2018). Therapeutic targeting of long non-coding RNAs in cancer. *Trends Mol. Med.* 24, 257–277. doi: 10.1016/j.molmed.2018.01.001

Balas, M. M., Hartwick, E. W., Barrington, C., Roberts, J. T., Wu, S. K., Bettcher, R., et al. (2021). Establishing RNA-RNA interactions remodels lncRNA structure and promotes PRC2 activity. *Sci. Adv.* 7:eabc9191. doi: 10.1126/sciadv.abc9191

Bandres-Ciga, S., Diez-Fairen, M., Kim, J. J., and Singleton, A. B. (2020). Genetics of Parkinson's disease: an introspection of its journey towards precision medicine. *Neurobiol. Dis.* 137:104782. doi: 10.1016/j.nbd.2020.104782

Barker, H. V., Niblock, M., Lee, Y., and Shaw, C. E. (2017). RNA misprocessing in C9orf72 - linked neurodegeneration. *Front. Cell. Neurosci.* 11:195. doi: 10.3389/fncel.2017.00195

Barry, G. (2014). Integrating the roles of long and small non-coding RNA in brain function and disease. *Mol. Psychiatry* 19, 410–416. doi: 10.1038/mp.2013.196

Barry, G., Briggs, J. A., Vanichkina, D. P., Poth, E. M., Beveridge, N. J., Ratnu, V. S., et al. (2014). The long non-coding RNA Gomafu is acutely regulated in response to neuronal activation and involved in schizophrenia-associated alternative splicing. *Mol. Psychiatry* 19, 486–494. doi: 10.1038/mp.2013.45

Barry, G., Guennewig, B., Fung, S., Kaczorowski, D., and Weickert, C. S. (2015). Long non-coding RNA expression during aging in the human subependymal zone. *Front. Neurol.* 6:45. doi: 10.3389/fneur.2015.00045

Belgard, T. G., Marques, A. C., Oliver, P. L., Abaan, H. O., Sirey, T. M., Hoerder-Suabedissen, A., et al. (2011). A transcriptomic atlas of mouse neocortical layers. *Neuron* 71, 605–616. doi: 10.1016/j.neuron.2011.06.039

Bellacosa, A. (2001). Role of MED1 (MBD4) Gene in DNA repair and human cancer. *J. Cell. Physiol.* 187, 137–144. doi: 10.1002/jcp.1064

Benn, C. L., Sun, T., Sadri-Vakili, G., McFarland, K. N., DiRocco, D. P., Yohrling, G. J., et al. (2008). Huntingtin modulates transcription, occupies gene promoters in vivo, and binds directly to DNA in a polyglutamine-dependent manner. *J. Neurosci.* 28, 10720–10733. doi: 10.1523/JNEUROSCI.2126-08.2008

Bernard, D., Prasanth, K. V., Tripathi, V., Colasse, S., Nakamura, T., Xuan, Z., et al. (2010). A long nuclear-retained non-coding RNA regulates synaptogenesis by modulating gene expression. *EMBO J.* 29, 3082–3093. doi: 10.1038/emboj.2010.199

Bonetti, A., and Carninci, P. (2017). From bench to bedside: the long journey of long. *Curr. Opin. Syst. Biol.* 3, 119–124. doi: 10.1016/j.coisb.2017.04.016

Bousard, A., Raposo, A. C., Zylicz, J. J., Picard, C., Pires, V. B., Qi, Y., et al. (2019). The role of Xist-mediated Polycomb recruitment in the initiation of X-chromosome inactivation. *EMBO Rep.* 20, 1–18. doi: 10.15252/embr.201948019

Bridges, M. C., Daulagala, A. C., and Kourtidis, A. (2021). LNCcation: lncRNA localization and function. *J. Cell Biol.* 220, 1–17. doi: 10.1083/JCB.202009045

Briggs, J. A., Wolvetang, E. J., Mattick, J. S., Rinn, J. L., and Barry, G. (2015). Mechanisms of Long Non-coding RNAs in mammalian nervous system development, plasticity, disease, and evolution. *Neuron* 88, 861–877. doi: 10.1016/j.neuron.2015.09.045

Brown, C. J., Ballabio, A., Rupert, J. L., Lafreniere, R. G., Grompe, M., Tonlorenzi, R., et al. (1991). A gene from the region of the human X inactivation centre is expressed exclusively from the inactive X chromosome. *Nature* 349, 38–44. doi: 10.1038/349038a0

Brown, J. A., Bulkley, D., Wang, J., Valenstein, M. L., Yario, T. A., Steitz, T. A., et al. (2014). Structural insights into the stabilization of MALAT1 noncoding RNA by a bipartite triple helix. *Nat. Struct. Mol. Biol.* 21, 633–640. doi: 10.1038/nsmb.2844

Brown, J. A., Kinzig, C. G., Degregorio, S. J., and Steitz, J. A. (2016). Hoogsteen-position pyrimidines promote the stability and function of the MALAT1 RNA triple helix. *RNA* 22, 743–749. doi: 10.1261/rna.055707.115.1

Cammas, A., and Millevoi, S. (2017). RNA G-quadruplexes: emerging mechanisms in disease. *Nucleic Acid Ther.* 45, 1584–1595. doi: 10.1093/nar/gkw1280

Carninci, P., Kasukawa, T., Katayama, S., Gough, J., Frith, M. C., Maeda, N., et al. (2005). The transcriptional landscape of the mammalian genome. *Science* 309, 1559–1563. doi: 10.1126/science.1112014

Carrieri, C., Cimatti, L., Biagioli, M., Beugnet, A., Zucchelli, S., Fedele, S., et al. (2012). Long non-coding antisense RNA controls Uchl1 translation through an embedded SINEB2 repeat. *Nature* 491, 454–457. doi: 10.1038/nature11508

Carrieri, C., Forrest, A. R. R., Santoro, C., Persichetti, F., Carninci, P., Zucchelli, S., et al. (2015). Expression analysis of the long non-coding RNA antisense to Uchl1 (AS Uchl1) during dopaminergic cells' differentiation in vitro and in neurochemical models of Parkinson's disease. *Front. Cell. Neurosci.* 9:114. doi: 10.3389/fncel.2015.00114

Chalei, V., Sansom, S. N., Kong, L., Lee, S., Montiel, J. F., Vance, K. W., et al. (2014). The long non-coding RNA Dali is an epigenetic regulator of neural differentiation. *eLife* 3, 1–24. doi: 10.7554/eLife.04530

Chen, B. J., Ueberham, U., Mills, J. D., Kirazov, L., Kirazov, E., Knobloch, M., et al. (2017). RNA sequencing reveals pronounced changes in the noncoding transcriptome of aging synaptosomes. *Neurobiol. Aging* 56, 67–77. doi: 10.1016/j.neurobiolaging.2017.04.005

Chen, L.-L. (2016). Linking long noncoding RNA localization and function. *Trends Biochem. Sci.* 41, 761–772. doi: 10.1016/j.tibs.2016.07.003

Chen, W., Zhang, G., Li, J., Zhang, X., Huang, S., Xiang, S., et al. (2019). CRISPRlnc: a manually curated database of validated sgRNAs for lncRNAs. *Nucleic Acids Res.* 47, D63–D68. doi: 10.1093/nar/gky904

Chodroff, R. A., Goodstadt, L., Sirey, T. M., Oliver, P. L., Davies, K. E., Green, E. D., et al. (2010). Long noncoding RNA genes: conservation of sequence and brain expression among diverse amniotes. *Genome Biol.* 11:R72. doi: 10.1186/gb-2010-11-7-r72

Choi, J., Levey, A. I., Weintraub, S. T., Rees, H. D., Gearing, M., Chin, L.-S., et al. (2004). Oxidative modifications and down-regulation of ubiquitin carboxyl-terminal hydrolase L1 associated with idiopathic Parkinson's and Alzheimer's diseases. *J. Biol. Chem.* 279, 13256–13264. doi: 10.1074/jbc.M314124200

Choudhry, H., Albukhari, A., Morotti, M., Haider, S., Moralli, D., Smythies, J., et al. (2015). Tumor hypoxia induces nuclear paraspeckle formation through HIF-2α dependent transcriptional activation of NEAT1 leading to cancer cell survival. *Oncogene* 34, 4482–4490. doi: 10.1038/onc.2014.378

Chung, D. W., Rudnicki, D. D., Yu, L., and Margolis, R. L. (2011). A natural antisense transcript at the Huntington's disease repeat locus regulates HTT expression. *Hum. Mol. Genet.* 20, 3467–3477. doi: 10.1093/hmg/ddr263

Ciarlo, E., Massone, S., Penna, I., Nizzari, M., Gigoni, A., Dieci, G., et al. (2013). An intronic ncRNA-dependent regulation of SORL1 expression affecting Aβ formation is upregulated in post-mortem Alzheimer's disease brain samples. *DMM Dis. Model. Mech.* 6, 424–433. doi: 10.1242/dmm.009761

ClinicalTrials. gov (2021). Available online at: https://clinicaltrials.gov/ct2/show/results/NCT02268552 (accessed May 20, 2021).

Cogill, S. B., Srivastava, A. K., Yang, M. Q., and Wang, L. (2018). Co-expression of long non-coding RNAs and autism risk genes in the developing human brain. *BMC Syst. Biol.* 12:91. doi: 10.1186/s12918-018-0639-x

Colak, D., Zaninovic, N., Cohen, M. S., Rosenwaks, Z., Yang, W.-Y., Gerhardt, J., et al. (2014). Promoter-bound trinucleotide repeat mRNA drives epigenetic silencing in fragile X syndrome. *Science* 343, 1002–1005. doi: 10.1126/science.1245831

Cong, L., Ran, F. A., Cox, D., Lin, S., Barretto, R., Habib, N., et al. (2013). Multiplex genome engineering using CRISPR/Cas systems. *Science* 339, 819–823. doi: 10.1126/science.1231143

Cooper-Knock, J., Higginbottom, A., Stopford, M. J., Highley, J. R., Ince, P. G., Wharton, S. B., et al. (2015). Antisense RNA foci in the motor neurons of C9ORF72-ALS patients are associated with TDP-43 proteinopathy. *Acta Neuropathol.* 130, 63–75. doi: 10.1007/s00401-015-1429-9

Davidovich, C., and Cech, T. R. (2015). The recruitment of chromatin modifiers by long noncoding RNAs: lessons from PRC2. *RNA* 21, 2007–2022. doi: 10.1261/rna.053918.115.Kuzmichev

Deas, E., Plun-Favreau, H., and Wood, N. W. (2009). PINK1 function in health and disease. *EMBO Mol. Med.* 1, 152–165. doi: 10.1002/emmm.200900024

Derrien, T., Johnson, R., Bussotti, G., Tanzer, A., Djebali, S., Tilgner, H., et al. (2012). The GENCODE v7 catalog of human long noncoding RNAs: analysis of their gene structure, evolution, and expression. *Genome Res.* 22, 1775–1789. doi: 10.1101/gr.132159.111

DeVos, S. L., and Miller, T. M. (2013). Antisense oligonucleotides: treating neurodegeneration at the level of RNA. *Neurotherapeutics* 10, 486–497. doi: 10.1007/s13311-013-0194-5

Diederichs, S. (2014). The four dimensions of noncoding RNA conservation. *Trends Genet.* 30, 121–123. doi: 10.1016/j.tig.2014.01.004

Djebali, S., Davis, C. A., Merkel, A., Dobin, A., Lassmann, T., Mortazavi, A., et al. (2012). Landscape of transcription in human cells. *Nature* 489, 101–108. doi: 10.1038/nature11233

Donlic, A., Morgan, B. S., Xu, J. L., Liu, A., Roble, C., and Hargrove, A. E. (2018). Discovery of small molecule ligands for MALAT1 by tuning an RNA-binding scaffold. *Angew. Chemie Int. Ed.* 57, 13242–13247. doi: 10.1002/anie.201808823

Dunham, I., Kundaje, A., Aldred, S. F., Collins, P. J., Davis, C. A., Doyle, F., et al. (2012). An integrated encyclopedia of DNA elements in the human genome. *Nature* 489, 57–74. doi: 10.1038/nature11247

d'Ydewalle, C., Ramos, D. M., Pyles, N. J., Ng, S. Y., Gorz, M., Pilato, C. M., et al. (2017). The antisense transcript SMN-AS1 regulates SMN expression and is a novel therapeutic target for spinal muscular atrophy. *Neuron* 93, 66–79. doi: 10.1016/j.neuron.2016.11.033

d'Ydewalle, C., and Sumner, C. J. (2015). Spinal muscular atrophy therapeutics: where do we stand? *Neurotherapeutics* 12, 303–316. doi: 10.1007/s13311-015-0337-y

Emon, P. Z., Das, R., Nishuty, N. L., Qusar, M. M. A. S., Bhuiyan, M. A., and Islam, R. (2020). Reduced serum BDNF levels are associated with the increased risk for developing MDD: a case-control study with or without antidepressant therapy. *BMC Res. Notes* 13:9. doi: 10.1186/s13104-020-04952-3

Faghihi, M. A., Modarresi, F., Khalil, A. M., Wood, D. E., Sahagan, B. G., Morgan, T. E., et al. (2008). Expression of a noncoding RNA is elevated in Alzheimer's disease and drives rapid feed-forward regulation of beta-secretase. *Nat. Med.* 14, 723–730. doi: 10.038/nm1784

Faghihi, M. A., Zhang, M., Huang, J., Modarresi, F., Van der Brug, M. P., Nalls, M. A., et al. (2010). Evidence for natural antisense transcript-mediated inhibition of microRNA function. *Genome Biol.* 11, 1–13. doi: 10.1186/gb-2010-11-5-r56

Fan, X., Fu, Y., Zhou, X., Sun, L., Yang, M., Wang, M., et al. (2020). Single-cell transcriptome analysis reveals cell lineage specification in temporal-spatial patterns in human cortical development. *Sci. Adv.* 6, 1–16. doi: 10.1126/sciadv.aaz2978

Ferrer, I., Goutan, E., Marín, C., Rey, M. J., and Ribalta, T. (2000). Brain-derived neurotrophic factor in Huntington disease. *Brain Res.* 866, 257–261. doi: 10.1016/s0006-8993(00)02237-x

Francelle, L., Galvan, L., Gaillard, M., Petit, F., Bernay, B., Guillermier, M., et al. (2015). Neurobiology of Aging The striatal long noncoding RNA Abhd11os is neuroprotective against an N-terminal fragment of mutant huntingtin in vivo. *Neurobiol. Aging* 36, e7–e16. doi: 10.1016/j.neurobiolaging.2014.11.014

Francescatto, M., Vitezic, M., Heutink, P., and Saxena, A. (2014). Brain-specific noncoding RNAs are likely to originate in repeats and may play a role in up-regulating genes in cis. *Int. J. Biochem. Cell Biol.* 54, 331–337. doi: 10.1016/j.biocel.2014.06.014

Frankish, A., Diekhans, M., Jungreis, I., Lagarde, J., Loveland, J. E., Mudge, J. M., et al. (2021). Gencode 2021. *Nucleic Acids Res.* 49, D916–D923. doi: 10.1093/nar/gkaa1087

Gendron, T. F., Bieniek, K. F., Zhang, Y.-J., Jansen-West, K., Ash, P. E. A., Caulfield, T., et al. (2013). Antisense transcripts of the expanded C9ORF72 hexanucleotide repeat form nuclear RNA foci and undergo repeat-associated non-ATG translation in c9FTD/ALS. *Acta Neuropathol.* 126, 829–844. doi: 10.1007/s00401-013-1192-8

Gil, N., and Ulitsky, I. (2018). Production of Spliced Long Noncoding RNAs specifies regions with increased enhancer activity. *Cell Syst.* 7, 537.e3–547.e3. doi: 10.1016/j.cels.2018.10.009

Gilbert, L. A., Horlbeck, M. A., Adamson, B., Villalta, J. E., Chen, Y., Whitehead, E. H., et al. (2014). Genome-scale CRISPR-mediated control of gene repression and activation. *Cell* 159, 647–661. doi: 10.1016/j.cell.2014.09.029

Goyal, A., Myacheva, K., Groß, M., Klingenberg, M., Duran Arqué, B., and Diederichs, S. (2017). Challenges of CRISPR/Cas9 applications for long non-coding RNA genes. *Nucleic Acids Res.* 45:e12. doi: 10.1093/nar/gkw883

Grammatikakis, I., Panda, A. C., Abdelmohsen, K., and Gorospe, M. (2014). Long noncoding RNAs(lncRNAs) and the molecular hallmarks of aging. *Aging* 6, 992–1009. doi: 10.18632/aging.100710

Grinman, E., Nakahata, Y., Avchalumov, Y., Espadas, I., Swarnkar, S., Yasuda, R., et al. (2021). Activity-regulated synaptic targeting of lncRNA ADEPTR mediates structural plasticity by localizing Sptn1 and AnkB in dendrites. *Sci. Adv.* 7:eabf0605. doi: 10.1126/sciadv.abf0605

Grossman, S. R., Andersen, K. G., Shlyakhter, I., Tabrizi, S., Winnicki, S., Yen, A., et al. (2013). Identifying recent adaptations in large-scale genomic data. *Cell* 152, 703–713. doi: 10.1016/j.cell.2013.01.035

Gutschner, T., Baas, M., and Diederichs, S. (2011). Noncoding RNA gene silencing through genomic integration of RNA destabilizing elements using zinc finger nucleases. *Genome Res.* 21, 1944–1954. doi: 10.1101/gr.122358.111

Guttman, M., Donaghey, J., Carey, B. W., Garber, M., Grenier, J. K., Munson, G., et al. (2011). LincRNAs act in the circuitry controlling pluripotency and differentiation. *Nature* 477, 295–300. doi: 10.1038/nature10398

Hampel, H., Vassar, R., De Strooper, B., Hardy, J., Willem, M., Singh, N., et al. (2020). The β-Secretase BACE1 in Alzheimer's disease. *Biol. Psychiatry* 89, 745–756. doi: 10.1016/j.biopsych.2020.02.001

Hannon, G. J., and Rossi, J. J. (2004). Unlocking the potential of the human genome with RNA interference. *Nature* 431, 371–378. doi: 10.1038/nature02870

Haroutunian, V., Katsel, P., Roussos, P., Davis, K. L., Altshuler, L. L., and Bartzokis, G. (2014). Myelination, oligodendrocytes, and serious mental illness. *Glia* 62, 1856–1877. doi: 10.1002/glia.22716

He, Z., Bammann, H., Han, D., and Xie, G. (2014). Conserved expression of lincRNA during human and macaque prefrontal cortex development and maturation. *RNA* 20, 1103–1111. doi: 10.1261/rna.043075.113

Hon, C., Ramilowski, J. A., Harshbarger, J., Bertin, N., Rackham, O. J. L., Gough, J., et al. (2017). An atlas of human long non-coding RNAs with accurate 5' ends. *Nat. Publ. Gr.* 543, 199–204. doi: 10.1038/nature21374

Hoy, S. M. (2019). Onasemnogene abeparvovec: first global approval. *Drugs* 79, 1255–1262. doi: 10.1007/s40265-019-01162-5

Huang, G., Zhu, H., Wu, S., Cui, M., and Xu, T. (2019). Long noncoding RNA can be a probable mechanism and a novel target for diagnosis and therapy in fragile X syndrome. *Front. Genet.* 10:446. doi: 10.3389/fgene.2019.00446

Human Genome Project (2003). Available online at: https://www.genome.gov/human-genome-project (accessed April 26, 2021).

Hutchinson, J. N., Ensminger, A. W., Clemson, C. M., Lynch, C. R., Lawrence, J. B., and Chess, A. (2007). A screen for nuclear transcripts identifies two linked noncoding RNAs associated with SC35 splicing domains. *BMC Genomics* 8:39. doi: 10.1186/1471-2164-8-39

Ip, J. Y., Sone, M., Nashiki, C., Pan, Q., Kitaichi, K., Yanaka, K., et al. (2016). Gomafu lncRNA knockout mice exhibit mild hyperactivity with enhanced responsiveness to the psychostimulant methamphetamine. *Sci. Rep.* 6:27204. doi: 10.1038/srep27204

Iyer, M. K., Niknafs, Y. S., Malik, R., Singhal, U., Sahu, A., Hosono, Y., et al. (2015). The landscape of long noncoding RNAs in the human transcriptome. *Nat. Genet.* 47, 199–208. doi: 10.1038/ng.3192

Jiang, C., Li, Y., Zhao, Z., Lu, J., Chen, H., Ding, N., et al. (2016). Identifying and functionally characterizing tissue-specific and ubiquitously expressed human lncRNAs. *Oncotarget* 7, 7120–7133. doi: 10.18632/oncotarget.6859

Jinek, M., Chylinski, K., Fonfara, I., Hauer, M., Doudna, J. A., and Charpentier, E. (2012). A programmable dual-RNA-guided DNA endonuclease in adaptive bacterial immunity. *Science* 337, 816–821. doi: 10.1126/science.1225829

Johnson, M. B., Wang, P. P., Atabay, K. D., Murphy, E. A., Doan, R. N., Hecht, J. L., et al. (2015). Single-cell analysis reveals transcriptional heterogeneity of neural progenitors in human cortex. *Nat. Neurosci.* 18, 637–646. doi: 10.1038/nn.3980

Johnson, R. (2012). Long non-coding RNAs in Huntington's disease neurodegeneration. *Neurobiol. Dis.* 46, 245–254. doi: 10.1016/j.nbd.2011.12.006

Johnson, R., Richter, N., Jauch, R., Gaughwin, P. M., Zuccato, C., Cattaneo, E., et al. (2010). Human accelerated region 1 noncoding RNA is repressed by REST in Huntington's disease. *Physiol. Genomics* 41, 269–274. doi: 10.1152/physiolgenomics.00019.2010

Johnsson, P., Lipovich, L., Grandér, D., and Morris, K. V. (2014). Evolutionary conservation of long non-coding RNAs; sequence, structure, function. *Biochim. Biophys. Acta* 1840, 1063–1071. doi: 10.1016/j.bbagen.2013.10.035

Kadakkuzha, B. M., Liu, X. A., McCrate, J., Shankar, G., Rizzo, V., Afinogenova, A., et al. (2015). Transcriptome analyses of adult mouse brain reveal enrichment of lncRNAs in specific brain regions and neuronal populations. *Front. Cell. Neurosci.* 9:63. doi: 10.3389/fncel.2015.00063

Kapusta, A., and Feschotte, C. (2014). Volatile evolution of long noncoding RNA repertoires: mechanisms and biological implications. *Trends Genet.* 30, 439–452. doi: 10.1016/j.tig.2014.08.004

Katsel, P., Roussos, P., Fam, P., Khan, S., Tan, W., Hirose, T., et al. (2019). The expression of long noncoding RNA NEAT1 is reduced in schizophrenia and modulates oligodendrocytes transcription. *NPJ Schizophr.* 5:3. doi: 10.1038/s41537-019-0071-2

Keihani, S., Kluever, V., Mandad, S., Bansal, V., Rahman, R., Fritsch, E., et al. (2019). The long noncoding RNA neuroLNC regulates presynaptic activity by interacting with the neurodegeneration-associated protein TDP-43. *Sci. Adv.* 5:eaay2670. doi: 10.1126/sciadv.aay2670

Khaled, H. G., Feng, H., Hu, X., Sun, X., Zheng, W., Li, P. P., et al. (2021). A high-throughput screening to identify small molecules that suppress huntingtin promoter activity or activate huntingtin-antisense promoter activity. *Sci. Rep.* 11, 1–13. doi: 10.1038/s41598-021-85279-2

Khalil, A. M., Faghihi, M. A., Modarresi, F., Brothers, S. P., and Wahlestedt, C. (2008). A novel RNA transcript with antiapoptotic function is silenced in fragile X syndrome. *PLoS One* 3:e0001486. doi: 10.1371/journal.pone.0001486

Khalil, A. M., Guttman, M., Huarte, M., Garber, M., Raj, A., Rivea Morales, D., et al. (2009). Many human large intergenic noncoding RNAs associate with chromatin-modifying complexes and affect gene expression. *PNAS* 106, 11667–11672. doi: 10.1073/pnas.0904715106

Kopp, F., and Mendell, J. T. (2018). Functional classification and experimental dissection of long noncoding RNAs. *Cell* 172, 393–407. doi: 10.1016/j.cell.2018.01.011

Kour, S., and Rath, P. C. (2015). Age-dependent differential expression profile of a novel intergenic long noncoding RNA in rat brain. *Int. J. Dev. Neurosci. Off. J. Int. Soc. Dev. Neurosci.* 46, 55–66. doi: 10.1016/j.ijdevneu.2015.07.011

Ladd, P. D., Smith, L. E., Rabaia, N. A., Moore, J. M., Georges, S. A., Hansen, R. S., et al. (2007). An antisense transcript spanning the CGG repeat region of FMR1 is upregulated in premutation carriers but silenced in full mutation individuals. *Hum. Mol. Genet.* 16, 3174–3187. doi: 10.1093/hmg/ddm293

Laske, C., Stellos, K., Hoffmann, N., Stransky, E., Straten, G., Eschweiler, G. W., et al. (2011). Higher BDNF serum levels predict slower cognitive decline in Alzheimer's disease patients. *Int. J. Neuropsychopharmacol.* 14, 399–404. doi: 10.1017/S1461145710001008

Law, A. J., Kleinman, J. E., Weinberger, D. R., and Weickert, C. S. (2007). Disease-associated intronic variants in the ErbB4 gene are related to altered ErbB4 splice-variant expression in the brain in schizophrenia. *Hum. Mol. Genet.* 16, 129–141. doi: 10.1093/hmg/ddl449

Lee, Y.-B., Chen, H.-J., Joao, N., Peres, Gomez-Deza, J., Attig, J., et al. (2013). Hexanucleotide repeats in ALS/FTD form length-dependent RNA foci, sequester RNA binding proteins, and are neurotoxic. *Cell Rep.* 5, 1178–1186. doi: 10.1016/j.celrep.2013.10.049

Lennox, K. A., and Behlke, M. A. (2016). Cellular localization of long non-coding RNAs affects silencing by RNAi more than by antisense oligonucleotides. *Nucleic Acids Res.* 44, 863–877. doi: 10.1093/nar/gkv1206

Liang, X. H., Sun, H., Nichols, J. G., and Crooke, S. T. (2017). RNase H1-dependent antisense oligonucleotides are robustly active in directing RNA cleavage in both the cytoplasm and the nucleus. *Mol. Ther.* 25, 2075–2092. doi: 10.1016/j.ymthe.2017.06.002

Lin, M., Pedrosa, E., Shah, A., Hrabovsky, A., Maqbool, S., Zheng, D., et al. (2011). RNA-Seq of human neurons derived from iPS cells reveals candidate long non-coding RNAs involved in neurogenesis and neuropsychiatric disorders. *PLoS One* 6:e0023356. doi: 10.1371/journal.pone.0023356

Lin, N., Chang, K., Li, Z., Gates, K., Rana, Z. A., Dang, J., et al. (2014). An evolutionarily conserved long noncoding RNA TUNA controls pluripotency and neural lineage commitment. *Mol. Cell* 53, 1005–1019. doi: 10.1016/j.molcel.2014.01.021

Lindblad-Toh, K., Garber, M., Zuk, O., Lin, M. F., Parker, B. J., Washietl, S., et al. (2011). A high-resolution map of human evolutionary constraint using 29 mammals. *Nature* 478, 476–482. doi: 10.1038/nature10530

Lipovich, L., Tarca, A. L., Cai, J., Jia, H., Chugani, H. T., Sterner, K. N., et al. (2014). Developmental changes in the transcriptome of human cerebral cortex tissue: long noncoding RNA transcripts. *Cereb. Cortex* 24, 1451–1459. doi: 10.1093/cercor/bhs414

Liu, F., Somarowthu, S., and Pyle, A. M. (2017). Visualizing the secondary and tertiary architectural domains of lncRNA RepA. *Nat. Chem. Biol.* 13, 282–289. doi: 10.1038/nchembio.2272

Liu, G., Mattick, J. S., and Taft, R. J. (2013). A meta-analysis of the genomic and transcriptomic composition of complex life. *Cell Cycle* 12, 2061–2072. doi: 10.4161/cc.25134

Liu, S. J., Horlbeck, M. A., Cho, S. W., Birk, H. S., Malatesta, M., He, D., et al. (2017). CRISPRi-based genome-scale identification of functional long noncoding RNA loci in human cells. *Science* 355:aah7111. doi: 10.1126/science.aah7111

Liu, S. J., Nowakowski, T. J., Pollen, A. A., Lui, J. H., Horlbeck, M. A., Attenello, F. J., et al. (2016). Single-cell analysis of long non-coding RNAs in the developing human neocortex. *Genome Biol.* 17:67. doi: 10.1186/s13059-016-0932-1

Lord, C., Brugha, T. S., Charman, T., Cusack, J., Dumas, G., Frazier, T., et al. (2020). Autism spectrum disorder. *Nat. Rev. Dis. Prim.* 6:5. doi: 10.1038/s41572-019-0138-4

Lorenzi, L., Chiu, H., Cobos, F. A., Gross, S., Volders, P., Cannoodt, R., et al. (2021). The RNA Atlas expands the catalog of human non-coding RNAs. *Nat. Biotechnol.* [Epub ahead of print]. doi: 10.1038/s41587-021-00936-1

Lu, Z., Zhang, Q. C., Lee, B., Flynn, R. A., Smith, M. A., Robinson, J. T., et al. (2016). RNA duplex map in living cells reveals higher-order transcriptome structure. *Cell* 165, 1267–1279. doi: 10.1016/j.cell.2016.04.028

Luo, H., Sun, S., Li, P., Bu, D., Cao, H., and Zhao, Y. (2013). Comprehensive characterization of 10,571 mouse large intergenic noncoding RNAs from whole transcriptome sequencing. *PLoS One* 8:e0070835. doi: 10.1371/journal.pone.0070835

Luo, T., Liu, P., Wang, X.-Y., Li, L., Li-Ping, Zao, Huang, J., et al. (2018). Effect of the autism-associated lncRNA Shank2-AS on architecture and growth of neurons. *J. Cell. Biochem.* [Epub ahead of print]. doi: 10.1002/jcb.27471

Ma, L., Bajic, V. B., Zhang, Z., Ma, L., Bajic, V. B., and Zhang, Z. (2013). On the classification of long non-coding RNAs. *RNA Biol.* 10, 925–933. doi: 10.4161/rna.24604

Mali, P., Yang, L., Esvelt, K. M., Aach, J., Guell, M., DiCarlo, J. E., et al. (2013). RNA-guided human genome engineering via Cas9. *Science* 339, 823–826. doi: 10.1126/science.1232033

Massone, S., Vassallo, I., Fiorino, G., Castelnuovo, M., Barbieri, F., Borghi, R., et al. (2011). 17A, a novel non-coding RNA, regulates GABA B alternative splicing and signaling in response to inflammatory stimuli and in Alzheimer disease. *Neurobiol. Dis.* 41, 308–317. doi: 10.1016/j.nbd.2010.09.019

Mattick, J. S. (2001). Non-coding RNAs: the architects of eukaryotic complexity. *EMBO Rep.* 2, 986–991. doi: 10.1093/embo-reports/kve230

Mattick, J. S., and Rinn, J. L. (2015). Discovery and annotation of long noncoding RNAs. *Nat. Struct. Mol. Biol.* 22, 5–7. doi: 10.1038/nsmb.2942

McCown, P. J., Wang, M. C., and Jaeger, L. (2019). Secondary structural model of human MALAT1 reveals multiple structure - function relationships. *Int. J. Mol. Sci.* 20, 1–19.

Mejzini, R., Flynn, L. L., Pitout, I. L., Fletcher, S., Wilton, S. D., and Akkari, P. A. (2019). ALS genetics, mechanisms, and therapeutics: where are we now? *Front. Neurosci.* 13:1310. doi: 10.3389/fnins.2019.01310

Meng, L., Person, R. E., and Beaudet, A. L. (2012). Ube3a-ATS is an atypical RNA polymerase II transcript that represses the paternal expression of Ube3a. *Hum. Mol. Genet.* 21, 3001–3012. doi: 10.1093/hmg/dds130

Meng, L., Person, R. E., Huang, W., Zhu, P. J., Costa-Mattioli, M., and Beaudet, A. L. (2013). Truncation of Ube3a-ATS unsilences paternal Ube3a and ameliorates behavioral defects in the angelman syndrome mouse model. *PLoS Genet.* 9:e1004039. doi: 10.1371/journal.pgen.1004039

Meng, L., Ward, A. J., Chun, S., Bennett, C. F., Beaudet, A. L., and Rigo, F. (2015). Towards a therapy for Angelman syndrome by targeting a long non-coding RNA. *Nature* 518, 409–412. doi: 10.1038/nature13975

Meng, Q., Wang, K., Brunetti, T., Xia, Y., Jiao, C., Dai, R., et al. (2018). The DGCR5 long noncoding RNA may regulate expression of several schizophrenia-related genes. *Sci. Transl. Med.* 10, 1–11. doi: 10.1126/scitranslmed.aat6912

Mercer, T. R., Dinger, M. E., Sunkin, S. M., Mehler, M. F., and Mattick, J. S. (2008). Specific expression of long noncoding RNAs in the mouse brain. *PNAS* 105, 716–721. doi: 10.1073/pnas.0706729105

Mercer, T. R., Qureshi, I. A., Gokhan, S., Dinger, M. E., Li, G., Mattick, J. S., et al. (2010). Long noncoding RNAs in neuronal-glial fate specification and oligodendrocyte lineage maturation. *BMC Neurosci.* 11:14. doi: 10.1186/1471-2202-11-14

Meyer, S. M., Williams, C. C., Akahori, Y., Tanaka, T., Aikawa, H., Tong, Y., et al. (2020). Small molecule recognition of disease-relevant RNA structures. *Chem. Soc. Rev.* 49, 7167–7199. doi: 10.1039/d0cs00560f

Miranda, M., Morici, J. F., Zanoni, M. B., and Bekinschtein, P. (2019). Brain-derived neurotrophic factor: a key molecule for memory in the healthy and the pathological brain. *Front. Cell. Neurosci.* 13:363. doi: 10.3389/fncel.2019.00363

Modarresi, F., Faghihi, M. A., Lopez-Toledano, M. A., Fatemi, R. P., Magistri, M., Brothers, S. P., et al. (2012). Inhibition of natural antisense transcripts in vivo results in gene-specific transcriptional upregulation. *Nat. Biotechnol.* 30, 453–459. doi: 10.1038/nbt.2158

Molendijk, M. L., Bus, B. A. A., Spinhoven, P., Penninx, B., Kenis, G., and Prickaerts, J. (2011). Serum levels of brain-derived neurotrophic factor in major depressive disorder: state-trait issues, clinical features and pharmacological treatment. *Mol. Psychiatry* 16, 1088–1095. doi: 10.1038/mp.2010.98

Mondal, T., Subhash, S., Vaid, R., Enroth, S., Uday, S., Mitra, S., et al. (2015). MEG3 long noncoding RNA regulates the TGF-beta pathway genes through formation of RNA-DNA triplex structures. *Nat. Commun.* 6:7743. doi: 10.1038/ncomms8743

Morikawa, T., and Manabe, T. (2010). Aberrant regulation of alternative pre-mRNA splicing in schizophrenia. *Neurochem. Int.* 57, 691–704. doi: 10.1016/j.neuint.2010.08.012

Muddashetty, R., Khanam, T., Kondrashov, A., Bundman, M., Iacoangeli, A., Kremerskothen, J., et al. (2002). Poly(A)-binding protein is associated with neuronal BC1 and BC200 ribonucleoprotein particles. *J. Mol. Biol.* 321, 433–445. doi: 10.1016/s0022-2836(02)00655-1

Myers, R. M., Stamatoyannopoulos, J., Snyder, M., Dunham, I., Hardison, R. C., Bernstein, B. E., et al. (2011). A user's guide to the Encyclopedia of DNA elements (ENCODE). *PLoS Biol.* 9:e1001046. doi: 10.1371/journal.pbio.1001046

Nakata, K., Lipska, B. K., Hyde, T. M., Ye, T., Newburn, E. N., Morita, Y., et al. (2009). DISC1 splice variants are upregulated in schizophrenia and associated with risk polymorphisms. *PNAS* 106, 15873–15878. doi: 10.1073/pnas.0903413106

Necsulea, A., and Kaessmann, H. (2014). Evolutionary dynamics of coding and non-coding transcriptomes. *Nat. Rev. Genet.* 15, 734–748. doi: 10.1038/nrg3802

Ng, S., Bogu, G. K., Soh, B. S., and Stanton, L. W. (2013). The long noncoding RNA RMST interacts with SOX2 to regulate neurogenesis. *Mol. Cell* 51, 349–359. doi: 10.1016/j.molcel.2013.07.017

Nishimoto, Y., Nakagawa, S., Hirose, T., Okano, H. J., Takao, M., Shibata, S., et al. (2013). The long non-coding RNA nuclear-enriched abundant transcript 1_2 induces paraspeckle formation in the motor neuron during the early phase of amyotrophic lateral sclerosis. *Mol. Brain* 6:31. doi: 10.1186/1756-6606-6-31

Nitsche, A., Rose, D., Fasold, M., Reiche, K., and Stadler, P. F. (2015). Comparison of splice sites reveals that long noncoding RNAs are evolutionarily well conserved. *RNA* 21, 801–812. doi: 10.1261/rna.046342.114

Pastori, C., Peschansky, V. J., Barbouth, D., Mehta, A., Silva, J. P., and Wahlestedt, C. (2014). Comprehensive analysis of the transcriptional landscape of the human FMR1 gene reveals two new long noncoding RNAs differentially expressed in Fragile X syndrome and Fragile X-associated tremor/ataxia syndrome. *Hum. Genet.* 133, 59–67. doi: 10.1007/s00439-013-1356-6

Pedram Fatemi, R., Salah-Uddin, S., Modarresi, F., Khoury, N., Wahlestedt, C., and Faghihi, M. A. (2015). Screening for small-molecule modulators of long noncoding RNA-protein interactions using alphascreen. *J. Biomol. Screen.* 20, 1132–1141. doi: 10.1177/1087057115594187

Pegueroles, C., and Gabaldón, T. (2016). Secondary structure impacts patterns of selection in human lncRNAs. *BMC Biol.* 14:13. doi: 10.1186/s12915-016-0283-0

Peschansky, V. J., Pastori, C., Zeier, Z., Motti, D., Katya, W., Velmeshev, D., et al. (2015). Changes in expression of the long non-coding RNA FMR4 associate with altered gene expression during differentiation of human neural precursor cells. *Front. Genet.* 6:263. doi: 10.3389/fgene.2015.00263

Peykov, S., Berkel, S., Schoen, M., Weiss, K., Degenhardt, F., Strohmaier, J., et al. (2015). Identification and functional characterization of rare SHANK2 variants in schizophrenia. *Mol. Psychiatry* 20, 1489–1498. doi: 10.1038/mp.2014.172

Phelan, J. D., and Staudt, L. M. (2020). CRISPR-based technology to silence the expression of lncRNAs. *PNAS* 117, 8225–8227. doi: 10.1073/pnas.2003702117

Podbevšek, P., Fasolo, F., Bon, C., Cimatti, L., Reißer, S., Carninci, P., et al. (2018). Structural determinants of the SINE B2 element embedded in the long non-coding RNA activator of translation AS Uchl1. *Sci. Rep.* 8:3189. doi: 10.1038/s41598-017-14908-6

Ponjavic, J., Oliver, P. L., Lunter, G., and Ponting, C. P. (2009). Genomic and transcriptional co-localization of protein-coding and long non-coding RNA pairs in the developing brain. *PLoS Genet.* 5:e1000617. doi: 10.1371/journal.pgen.1000617

Ponti, R. D., Armaos, A., Marti, S., and Tartaglia, G. G. (2018). A method for RNA structure prediction shows evidence for structure in lncRNAs. *Front. Mol. Biosci.* 5:111. doi: 10.3389/fmolb.2018.00111

Qi, L. S., Larson, M. H., Gilbert, L. A., Doudna, J. A., Weissman, J. S., Arkin, A. P., et al. (2013). Repurposing CRISPR as an RNA-γuided platform for sequence-specific control of gene expression. *Cell* 152, 1173–1183. doi: 10.1016/j.cell.2013.02.022

Quan, Z., Zheng, D., and Qing, H. (2017). Regulatory roles of long non-coding rnas in the central nervous system and associated neurodegenerative diseases. *Front. Cell. Neurosci.* 11:175. doi: 10.3389/fncel.2017.00175

Quinodoz, S., and Guttman, M. (2014). Long noncoding RNAs: an emerging link between gene regulation and nuclear organization. *Trends Cell Biol.* 24, 651–663. doi: 10.1016/j.tcb.2014.08.009

Ramos, A. D., Andersen, R. E., Kriegstein, A. R., Lim, D. A., Ramos, A. D., Andersen, R. E., et al. (2015). The long noncoding RNA Pnky regulates neuronal differentiation of embryonic and postnatal neural stem cells. *Stem Cell* 16, 439–447. doi: 10.1016/j.stem.2015.02.007

Ramos, A. D., Diaz, A., Nellore, A., Delgado, R. N., Park, K. Y., Gonzales-Roybal, G., et al. (2013). Integration of genome-wide approaches identifies lncRNAs of adult neural stem cells and their progeny in vivo. *Cell Stem Cell* 12, 616–628. doi: 10.1016/j.stem.2013.03.003

Rauch, J. N., Luna, G., Guzman, E., Audouard, M., Challis, C., Sibih, Y. E., et al. (2020). LRP1 is a master regulator of tau uptake and spread. *Nature* 580, 381–385. doi: 10.1038/s41586-020-2156-5

Reinicke, A. T., Laban, K., Sachs, M., Kraus, V., Walden, M., Damme, M., et al. (2019). Ubiquitin C-terminal hydrolase L1 (UCH-L1) loss causes neurodegeneration by altering protein turnover in the first postnatal weeks. *PNAS* 116, 7963–7972. doi: 10.1073/pnas.1812413116

Ren, Y., Wang, Y. F., Zhang, J., Wang, Q. X., Han, L., Mei, M., et al. (2019). Targeted design and identification of AC1NOD4Q to block activity of HOTAIR by abrogating the scaffold interaction with EZH2. *Clin. Epigenetics* 11, 1–16. doi: 10.1186/s13148-019-0624-2

Rinn, J. L., Kertesz, M., Wang, J. K., Squazzo, S. L., Xu, X., Brugmann, S. A., et al. (2007). Functional demarcation of active and silent chromatin domains in human HOX loci by noncoding RNAs. *Cell* 129, 1311–1323. doi: 10.1016/j.cell.2007.05.022

Roberts, T. C., Langer, R., and Wood, M. J. A. (2020). Advances in oligonucleotide drug delivery. *Nat. Rev. Drug Discov.* 19, 673–694. doi: 10.1038/s41573-020-0075-7

Roberts, T. C., Morris, K. V., and Wood, M. J. A. (2014). The role of long non-coding RNAs in neurodevelopment, brain function and neurological disease. *Philos. Trans. R. Soc. B Biol. Sci.* 369:20130507. doi: 10.1098/rstb.2013.0507

Rocha, S. T., and Heard, E. (2017). Novel players in X inactivation: insights into Xist -mediated gene silencing and chromosome conformation. *Nat. Struct. Mol. Biol.* 24, 197–204. doi: 10.1038/nsmb.3370

Roovers, J., De Jonghe, P., and Weckhuysen, S. (2018). Expert opinion on therapeutic targets the therapeutic potential of RNA regulation in neurological disorders. *Expert Opin. Ther. Targets* 22, 1017–1028. doi: 10.1080/14728222.2018.1542429

Rubin, G. M., Yandell, M. D., Wortman, J. R., Gabor, G. L., Miklos, Nelson, C. R., et al. (2000). Comparative genomics of the eukaryotes. *Science* 287, 2204–2215. doi: 10.1126/science.287.5461.2204

Salta, E., and De Strooper, B. (2017). Noncoding RNAs in neurodegeneration. *Nat. Rev. Neurosci.* 18, 627–640. doi: 10.1038/nrn.2017.90

Salvatori, B., Biscarini, S., and Morlando, M. (2020). Non-coding RNAs in nervous system development and disease. *Front. Cell Dev. Biol.* 8:273. doi: 10.3389/fcell.2020.00273

Salzberg, S. L. (2018). Open questions: how many genes do we have? *BMC Biol.* 16:12. doi: 10.1186/s12915-018-0564-x

Sarropoulos, I., Marin, R., Cardoso-Moreira, M., and Kaessmann, H. (2019). Developmental dynamics of lncRNAs across mammalian organs and species. *Nature* 571, 510–514. doi: 10.1038/s41586-019-1341-x

Sato, D., Lionel, A. C., Leblond, C. S., Prasad, A., Pinto, D., Walker, S., et al. (2012). SHANK1 deletions in males with autism spectrum disorder. *Am. J. Hum. Genet.* 90, 879–887. doi: 10.1016/j.ajhg.2012.03.017

Sauvageau, M., Goff, L. A., Lodato, S., Bonev, B., Groff, A. F., Gerhardinger, C., et al. (2013). Multiple knockout mouse models reveal lincRNAs are required for life and brain development. *eLife* 2:e01749. doi: 10.7554/eLife.01749

Scheele, C., Petrovic, N., Faghihi, M. A., Lassmann, T., Fredriksson, K., Rooyackers, O., et al. (2007). The human PINK1 locus is regulated in vivo by a non-coding natural antisense RNA during modulation of mitochondrial function. *BMC Genomics* 8:74. doi: 10.1186/1471-2164-8-74

Scheltens, P., De Strooper, B., Kivipelto, M., Holstege, H., Chételat, G., Teunissen, C. E., et al. (2021). Alzheimer's disease. *Lancet* 397, 1577–1590. doi: 10.1016/S0140-6736(20)32205-4

Seemann, S. E., Sunkin, S. M., Hawrylycz, M. J., Ruzzo, W. L., and Gorodkin, J. (2012). Transcripts with in silico predicted RNA structure are enriched everywhere in the mouse brain. *BMC Genomics* 13:214. doi: 10.1186/1471-2164-13-214

Shelkovnikova, T. A., Kukharsky, M. S., An, H., Dimasi, P., Alexeeva, S., Shabir, O., et al. (2018). Protective paraspeckle hyper-assembly downstream of TDP-43 loss of function in amyotrophic lateral sclerosis. *Mol. Neurodegener.* 13:30. doi: 10.1186/s13024-018-0263-7

Simko, E. A. J., Liu, H., Zhang, T., Velasquez, A., Teli, S., Haeusler, A. R., et al. (2020). G-quadruplexes offer a conserved structural motif for NONO recruitment to NEAT1 architectural lncRNA. *Nucleic Acids Res.* 48, 7421–7438. doi: 10.1093/nar/gkaa475

Simone, R., Javad, F., Emmett, W., Wilkins, O. G., Almeida, F. L., Barahona-Torres, N., et al. (2021). MIR-NATs repress MAPT translation and aid proteostasis in neurodegeneration. *Nature* 594, 117–123. doi: 10.1038/s41586-021-03556-6

Smith, M. A., Gesell, T., Stadler, P. F., and Mattick, J. S. (2013). Widespread purifying selection on RNA structure in mammals. *Nucleic Acids Res.* 41, 8220–8236. doi: 10.1093/nar/gkt596

Smola, M. J., Rice, G. M., Busan, S., Siegfried, N. A., and Weeks, K. M. (2015). Selective 2'-hydroxyl acylation analyzed by primer extension and mutational profiling (SHAPE-MaP) for direct, versatile and accurate RNA structure analysis. *Nat. Protoc.* 10, 1643–1669. doi: 10.1038/nprot.2015.103

Somarowthu, S., Legiewicz, M., Chillón, I., Marcia, M., Liu, F., and Pyle, A. M. (2015). HOTAIR forms an intricate and modular secondary structure. *Mol. Cell* 58, 353–361. doi: 10.1016/j.molcel.2015.03.006

Sone, M., Hayashi, T., Tarui, H., Agata, K., Takeichi, M., and Nakagawa, S. (2007). The mRNA-like noncoding RNA Gomafu constitutes a novel nuclear domain in a subset of neurons. *J. Cell Sci.* 120, 2498–2506. doi: 10.1242/jcs.009357

Statello, L., Guo, C. J., Chen, L. L., and Huarte, M. (2021). Gene regulation by long non-coding RNAs and its biological functions. *Nat. Rev. Mol. Cell Biol.* 22, 96–118. doi: 10.1038/s41580-020-00315-9

Su, L., Wang, C., Zheng, C., Wei, H., and Song, X. (2018). A meta-analysis of public microarray data identifies biological regulatory networks in Parkinson's disease. *BMC Med. Genomics* 11:40. doi: 10.1186/s12920-018-0357-7

Su, Z., Zhang, Y., Gendron, T. F., Bauer, P. O., Chew, J., Yang, W.-Y., et al. (2014). Discovery of a biomarker and lead small molecules to target r(GGGGCC)-associated defects in c9FTD/ALS. *Neuron* 84:239. doi: 10.1016/j.neuron.2014.09.019

Sugitani, Y., Nakai, S., Minowa, O., Nishi, M., Jishage, K.-I., Kawano, H., et al. (2002). Brn-1 and Brn-2 share crucial roles in the production and positioning of mouse neocortical neurons. *Genes Dev.* 16, 1760–1765. doi: 10.1101/gad.978002

Sun, J., and Roy, S. (2021). Gene-based therapies for neurodegenerative diseases. *Nat. Neurosci.* 24, 297–311. doi: 10.1038/s41593-020-00778-1

Sunamura, N., Iwashita, S., Enomoto, K., Kadoshima, T., and Isono, F. (2018). Loss of the fragile X mental retardation protein causes aberrant differentiation in human neural progenitor cells. *Sci. Rep.* 8:11585. doi: 10.1038/s41598-018-30025-4

Sunwoo, J.-S., Lee, S.-T., Im, W., Lee, M., Byun, J.-I., Jung, K.-H., et al. (2017). Altered expression of the long noncoding RNA NEAT1 in Huntington's disease. *Mol. Neurobiol.* 54, 1577–1586. doi: 10.1007/s12035-016-9928-9

Tachibana, M., Holm, M., Liu, C., Shinohara, M., Aikawa, T., Oue, H., et al. (2019). APOE4-mediated amyloid-β pathology depends on its neuronal receptor LRP1. *J. Clin. Invest.* 129, 1272–1277. doi: 10.1172/jci124853

Taft, R. J., Pheasant, M., and Mattick, J. S. (2007). The relationship between non-protein-coding DNA and eukaryotic complexity. *Bioessays* 29, 288–299. doi: 10.1002/bies.20544

Tak, Y. G., and Farnham, P. J. (2015). Making sense of GWAS: using epigenomics and genome engineering to understand the functional relevance of SNPs in non-coding regions of the human genome. *Epigenetics Chromatin* 8, 1–18. doi: 10.1186/s13072-015-0050-4

Tay, S.-K., Blytheb, J., and Lipovicha, L. (2009). Global discovery of primate-specific genes in the human genome. *PNAS* 106:14180. doi: 10.1073/pnas.0908685106

Thakore, P. I., D'Ippolito, A. M., Song, L., Safi, A., Shivakumar, N. K., Kabadi, A. M., et al. (2015). Highly specific epigenome editing by CRISPR-Cas9 repressors for silencing of distal regulatory elements. *Nat. Methods* 12, 1143–1149. doi: 10.1038/nmeth.3630

Tollervey, J. R., Curk, T., Rogelj, B., Briese, M., Cereda, M., Kayikci, M., et al. (2011). Characterizing the RNA targets and position-dependent splicing regulation by TDP-43. *Nat. Neurosci.* 14, 452–458. doi: 10.1038/nn.2778

Torarinsson, E., Sawera, M., Havgaard, J. H., Fredholm, M., and Gorodkin, J. (2006). Thousands of corresponding human and mouse genomic regions unalignable in primary sequence contain common RNA structure. *Genome Res.* 16, 885–889. doi: 10.1101/gr.5226606

U.S. Food & Drug Administration (2016). Available online at: https://www.fda.gov/news-events/press-announcements/fda-approves-first-drug-spinal-muscular-atrophy (accessed May 11, 2021).

U.S. Food & Drug Administration (2020). Available online at: https://www.fda.gov/news-events/press-announcements/fda-approves-oral-treatment-spinal-muscular-atrophy (accessed May 11, 2021).

Ulitsky, I., Shkumatava, A., Jan, C. H., Sive, H., and Bartel, D. P. (2011). Conserved function of lincRNAs in vertebrate embryonic development despite rapid sequence evolution. *Cell* 147, 1537–1550. doi: 10.1016/j.cell.2011.11.055

Uszczynska-Ratajczak, B., Lagarde, J., Frankish, A., Guigó, R., and Johnson, R. (2018). Towards a complete map of the human long non-coding RNA transcriptome. *Nat. Rev. Genet.* 19, 535–548. doi: 10.1038/s41576-018-0017-y

Vittal, P., Pandya, S., Sharp, K., Berry-kravis, E., Zhou, L., Ouyang, B., et al. (2018). ASFMR1 splice variant. A predictor of fragile X-associated tremor/ataxia syndrome. *Neurol. Genet.* 4:e246. doi: 10.1212/NXG.0000000000000246

Wahlestedt, C. (2013). Targeting long non-coding RNA to therapeutically upregulate gene expression. *Nat. Rev. Drug Discov.* 12, 433–446. doi: 10.1038/nrd4018

Wang, S., Zhang, X., Guo, Y., Rong, H., and Liu, T. (2017). The long noncoding RNA HOTAIR promotes Parkinson's disease by upregulating LRRK2 expression. *Oncotarget* 8, 24449–24456. doi: 10.18632/oncotarget.15511

Wang, X., Goodrich, K. J., Gooding, A. R., Youmans, D. T., Cech, T. R., Wang, X., et al. (2017). Targeting of polycomb repressive complex 2 to RNA by short repeats of consecutive guanines article targeting of polycomb repressive complex 2 to RNA by short repeats of consecutive guanines. *Mol. Cell* 65, 1056.e5–1067.e5. doi: 10.1016/j.molcel.2017.02.003

Wang, Y., Zhao, X., Ju, W., Flory, M., Zhong, J., Jiang, S., et al. (2015). Genome-wide differential expression of synaptic long noncoding RNAs in autism spectrum disorder. *Transl. Psychiatry* 5:e660. doi: 10.1038/tp.2015.144

Wang, Z.-F., Ursu, A., Childs-Disney, J. L., Guertler, R., Yang, W.-Y., Bernat, V., et al. (2019). The Hairpin Form of r(G(4)C(2))(exp) in c9ALS/FTD Is Repeat-Associated Non-ATG translated and a target for bioactive small molecules. *Cell Chem. Biol.* 26, 179.e12–190.e12. doi: 10.1016/j.chembiol.2018.10.018

Washietl, S., Kellis, M., and Garber, M. (2014). Evolutionary dynamics and tissue specificity of human long noncoding RNAs in six mammals. *Genome Res.* 24, 616–628. doi: 10.1101/gr.165035.113

Watts, J. K., and Corey, D. R. (2012). Silencing disease genes in the laboratory and the clinic. *J. Pathol.* 226, 365–379. doi: 10.1002/path.2993

West, J. A., Davis, C. P., Sunwoo, H., Simon, M. D., Sadreyev, R. I., Wang, P. I., et al. (2014). The long noncoding RNAs NEAT1 and MALAT1 bind active chromatin sites. *Mol. Cell* 55, 791–802. doi: 10.1016/j.molcel.2014.07.012

Wilhelmus, M. M. M., Van Der Pol, S. M. A., Jansen, Q., Witte, M. E., Van Der Valk, P., Rozemuller, A. J. M., et al. (2011). Association of Parkinson disease-related protein PINK1 with Alzheimer disease and multiple sclerosis brain lesions. *Free Radic. Biol. Med.* 50, 469–476. doi: 10.1016/j.freeradbiomed.2010.11.033

Wilkinson, K. A., Merino, E. J., and Weeks, K. M. (2006). Selective 2'-hydroxyl acylation analyzed by primer extension (SHAPE): quantitative RNA structure analysis at single nucleotide resolution. *Nat. Protoc.* 1, 1610–1616. doi: 10.1038/nprot.2006.249

Wilusz, J. E., JnBaptiste, C. K., Lu, L. Y., Kuhn, C. D., Joshua-Tor, L., and Sharp, P. A. (2012). A triple helix stabilizes the 3' ends of long noncoding RNAs that lack poly(A) tails. *Genes Dev.* 26, 2392–2407. doi: 10.1101/gad.204438.112

Wolter, J. M., Mao, H., Fragola, G., Simon, J. M., Krantz, J. L., Bazick, H. O., et al. (2020). Cas9 gene therapy for Angelman syndrome traps Ube3a-ATS long non-coding RNA. *Nature* 587, 281–284. doi: 10.1038/s41586-020-2835-2

Woo, C. J., Maier, V. K., Davey, R., Brennan, J., Li, G., Brothers, J., et al. (2017). Gene activation of SMN by selective disruption of lncRNA-mediated recruitment of PRC2 for the treatment of spinal muscular atrophy. *PNAS* 114, E1509–E1518. doi: 10.1073/pnas.1616521114

Wood, S. H., Craig, T., Li, Y., Merry, B., and de Magalhães, J. P. (2013). Whole transcriptome sequencing of the aging rat brain reveals dynamic RNA changes in the dark matter of the genome. *Age* 35, 763–776. doi: 10.1007/s11357-012-9410-1

Xia, D., Sui, R., and Zhang, Z. (2019). Administration of resveratrol improved Parkinson's disease-like phenotype by suppressing apoptosis of neurons via modulating the MALAT1/miR-129/SNCA signaling pathway. *J. Cell. Biochem.* 120, 4942–4951. doi: 10.1002/jcb.27769

Xu, C. L., Sang, B., Liu, G. Z., Li, J. M., Zhang, X. D., Liu, L. X., et al. (2020). SENEBLOC, a long non-coding RNA suppresses senescence via p53-dependent and independent mechanisms. *Nucleic Acids Res.* 48, 3089–3102. doi: 10.1093/nar/gkaa063

Xu, D., Cai, Y., Tang, L., Han, X., Gao, F., Cao, H., et al. (2020). A CRISPR/Cas13-based approach demonstrates biological relevance of vlinc class of long non-coding RNAs in anticancer drug response. *Sci. Rep.* 10:1794. doi: 10.1038/s41598-020-58104-5

Yamanaka, Y., Faghihi, M. A., Magistri, M., Alvarez-Garcia, O., Lotz, M., and Wahlestedt, C. (2015). Antisense RNA Controls LRP1 sense transcript expression through interaction with a chromatin-associated protein, HMGB2. *Cell Rep.* 344, 1173–1178. doi: 10.1126/science.1249098

Yang, H., Shang, D., Xu, Y., Zhang, C., Feng, L., Sun, Z., et al. (2017). The LncRNA connectivity map: using LncRNA signatures to connect small molecules, LncRNAs, and diseases. *Sci. Rep.* 7, 1–6. doi: 10.1038/s41598-017-06897-3

Yao, R., Wang, Y., and Chen, L. (2019). Cellular functions of long noncoding RNAs. *Nat. Cell Biol.* 21, 542–551.

Yichin, L., Fallon, L., Lashuel, H. A., Liu, Z., and Lansbury, P. T. J. (2002). The UCH-L1 gene encodes two opposing enzymatic activities that affect alpha-synuclein degradation and Parkinson's disease susceptibility. *Cell* 111, 209–218. doi: 10.1016/s0092-8674(02)01012-7

Ying, L., Chen, Y.-Y., Liu, H., Yao, C.-J., Zhu, X.-X., Chen, D.-J., et al. (2015). Association between ubiquitin carboxy-terminal hydrolase-L1 S18Y variant and risk of Parkinson's disease: the impact of ethnicity and onset age. *Neurol. Sci.* 36, 179–188. doi: 10.1007/s10072-014-1987-y

Youse, H., Fatemeh, M., Ladan, M., Amir, M., and Aref, R. (2020). Long noncoding RNAs and exosomal lncRNAs: classi fi cation, and mechanisms in breast cancer metastasis and drug resistance. *Oncogene* 39, 953–974. doi: 10.1038/s41388-019-1040-y

Yu, A. M., Choi, Y. H., and Tu, M. J. (2020). RNA drugs and RNA targets for small molecules: principles, progress, and challenges. *Pharmacol. Rev.* 72, 862–898. doi: 10.1124/pr.120.019554

Zalfa, F., Giorgi, M., Primerano, B., Moro, A., Di Penta, A., Reis, S., et al. (2003). The fragile X syndrome protein FMRP associates with BC1 RNA and regulates the translation of specific mRNAs at synapses. *Cell* 112, 317–327. doi: 10.1016/s0092-8674(03)00079-5

Zaslavsky, K., Zhang, W.-B., McCready, F. P., Rodrigues, D. C., Deneault, E., Loo, C., et al. (2019). SHANK2 mutations associated with autism spectrum disorder cause hyperconnectivity of human neurons. *Nat. Neurosci.* 22, 556–564. doi: 10.1038/s41593-019-0365-8

Zhang, P., Park, H.-J., Zhang, J., Junn, E., Andrews, R. J., Velagapudi, S. P., et al. (2020). Translation of the intrinsically disordered protein α-synuclein is inhibited by a small molecule targeting its structured mRNA. *PNAS* 117, 1457–1467. doi: 10.1073/pnas.1905057117

Zhang, Q.-S., Wang, Z.-H., Zhang, J.-L., Duan, Y.-L., Li, G.-F., and Zheng, D.-L. (2016). Beta-asarone protects against MPTP-induced Parkinson's disease via regulating long non-coding RNA MALAT1 and inhibiting α-synuclein protein expression. *Biomed. Pharmacother.* 83, 153–159. doi: 10.1016/j.biopha.2016.06.017

Zhang, X., Hamblin, M. H., and Yin, K. J. (2017). The long noncoding RNA Malat1: its physiological and pathophysiological functions. *RNA Biol.* 14, 1705–1714. doi: 10.1080/15476286.2017.1358347

Zhang, Z., Chen, J., Zhu, Z., Zhu, Z., Liao, X., Wu, J., et al. (2021). CRISPR-Cas13-Mediated Knockdown of lncRNA-GACAT3 Inhibited Cell Proliferation and Motility, and Induced Apoptosis by Increasing p21, Bax, and E-cadherin expression in bladder cancer. *Front. Mol. Biosci.* 7:433. doi: 10.3389/fmolb.2020.627774

Zhao, L., Wang, J., Li, Y., Song, T., Wu, Y., Fang, S., et al. (2021). NONCODEV6: an updated database dedicated to long non-coding RNA annotation in both animals and plants. *Nucleic Acids Res.* 49, D165–D171. doi: 10.1093/nar/gkaa1046

Zheng, S., Chen, Y., Donahue, C. P., Wolfe, M. S., and Varani, G. (2009). Structural basis for stabilization of the tau pre-mRNA splicing regulatory element by novantrone (mitoxantrone). *Chem. Biol.* 16, 557–566. doi: 10.1016/j.chembiol.2009.03.009

Zhu, S., Li, W., Liu, J., Chen, C. H., Liao, Q., Xu, P., et al. (2016). Genome-scale deletion screening of human long non-coding RNAs using a paired-guide RNA CRISPR-Cas9 library. *Nat. Biotechnol.* 34, 1279–1286. doi: 10.1038/nbt.3715

Zimmer-Bensch, G. (2019). Emerging roles of long non-coding RNAs as drivers of brain evolution. *Cells* 8:1399. doi: 10.3390/cells8111399

Zu, T., Liu, Y., Bañez-Coronel, M., Reid, T., Pletnikova, O., Lewis, J., et al. (2013). RAN proteins and RNA foci from antisense transcripts in C9ORF72 ALS and frontotemporal dementia. *PNAS* 110, E4968–E4977. doi: 10.1073/pnas.1315438110

Zuccato, C., Belyaev, N., Conforti, P., Ooi, L., Tartari, M., Papadimou, E., et al. (2007). Widespread disruption of repressor element-1 silencing transcription factor/neuron-restrictive silencer factor occupancy at its target genes in Huntington's disease. *J. Neurosci.* 27, 6972–6983. doi: 10.1523/JNEUROSCI.4278-06.2007

Zuccato, C., and Cattaneo, E. (2007). Role of brain-derived neurotrophic factor in Huntington's disease. *Prog. Neurobiol.* 81, 294–330. doi: 10.1016/j.pneurobio.2007.01.003

Zucchelli, S., Cotella, D., Takahashi, H., Carrieri, C., Cimatti, L., Fasolo, F., et al. (2015). SINEUPs: a new class of natural and synthetic antisense long non-coding RNAs that activate translation. *RNA Biol.* 12, 771–779. doi: 10.1080/15476286.2015.1060395

Zucchelli, S., Fedele, S., Vatta, P., Calligaris, R., Heutink, P., Rizzu, P., et al. (2019). Antisense transcription in loci associated to hereditary neurodegenerative diseases. *Mol. Neurobiol.* 56, 5392–5415.

Conflict of Interest: Cd'Y was employed by company Janssen Pharmaceutica N.V.

The remaining authors declare that the research was conducted in the absence of any commercial or financial relationships that could be construed as a potential conflict of interest.

Copyright © 2021 Policarpo, Sierksma, De Strooper and d'Ydewalle. This is an open-access article distributed under the terms of the Creative Commons Attribution License (CC BY). The use, distribution or reproduction in other forums is permitted, provided the original author(s) and the copyright owner(s) are credited and that the original publication in this journal is cited, in accordance with accepted academic practice. No use, distribution or reproduction is permitted which does not comply with these terms.

frontiers in Molecular Neuroscience

REVIEW
published: 16 August 2021
doi: 10.3389/fnmol.2021.695294

Held Up in Traffic—Defects in the Trafficking Machinery in Charcot-Marie-Tooth Disease

*Ronja Markworth[1,2], Mathias Bähr[1] and Katja Burk[1,2]**

[1] Department of Neurology, University Medical Center Göttingen, Göttingen, Germany, [2] Center for Biostructural Imaging of Neurodegeneration, Göttingen, Germany

Charcot-Marie-Tooth disease (CMT), also known as motor and sensory neuropathy, describes a clinically and genetically heterogenous group of disorders affecting the peripheral nervous system. CMT typically arises in early adulthood and is manifested by progressive loss of motor and sensory functions; however, the mechanisms leading to the pathogenesis are not fully understood. In this review, we discuss disrupted intracellular transport as a common denominator in the pathogenesis of different CMT subtypes. Intracellular transport via the endosomal system is essential for the delivery of lipids, proteins, and organelles bidirectionally to synapses and the soma. As neurons of the peripheral nervous system are amongst the longest neurons in the human body, they are particularly susceptible to damage of the intracellular transport system, leading to a loss in axonal integrity and neuronal death. Interestingly, defects in intracellular transport, both in neurons and Schwann cells, have been found to provoke disease. This review explains the mechanisms of trafficking and subsequently summarizes and discusses the latest findings on how defects in trafficking lead to CMT. A deeper understanding of intracellular trafficking defects in CMT will expand our understanding of CMT pathogenesis and will provide novel approaches for therapeutic treatments.

Keywords: Charcot-Marie-Tooth, trafficking, signaling, transport, endosomal system

OPEN ACCESS

Edited by:
Inmaculada Segura, Ludwig Maximilian University of Munich, Germany

Reviewed by:
Albena Jordanova, University of Antwerp, Belgium
Henna Tyynismaa, University of Helsinki, Finland

***Correspondence:**
Katja Burk
kburk@gwdg.de

Specialty section:
This article was submitted to Molecular Signalling and Pathways, a section of the journal Frontiers in Molecular Neuroscience

Received: *14 April 2021*
Accepted: *23 July 2021*
Published: *16 August 2021*

Citation:
Markworth R, Bähr M and Burk K (2021) Held Up in Traffic—Defects in the Trafficking Machinery in Charcot-Marie-Tooth Disease. Front. Mol. Neurosci. 14:695294. doi: 10.3389/fnmol.2021.695294

INTRODUCTION

Charcot-Marie-Tooth disorder (CMT) is a group of hereditary peripheral neuropathies leading to loss of sensation and fine motor control in the extremities with a prevalence of over 1:2,500. Over 100 genes are identified to cause CMT (Timmerman et al., 2014; Rudnik-Schöneborn et al., 2020). CMT is diagnosed and categorized into several subtypes based on clinical presentation including a loss of sensation and fine motor control in the extremities, nerve conduction velocity, neuropathological findings, as well as mode of inheritance and genes involved (Bird, 2020). Classically, CMT1 is a demyelinating neuropathy, CMT2 is an axonal neuropathy, and dominant-intermediate CMT (DI-CMT) is an intermediate type showing both demyelinating and axonal pathologies. Since many more genes causing CMT were discovered showing overlaps of the phenotypes, a gene-based classification of inherited neuropathies has been proposed. Since so far this classification is not established, we stick to the classification by genes with the corresponding alphanumeric classification according to OMIM (Magy et al., 2018).

The observation that so many different mutations lead to a very similar phenotype has stirred the idea for a common pathomechanism and led to a search of a molecular pathway that covers many of the proteins recorded in CMT. Another interesting aspect of CMT is the peripheral nerve specificity, regardless of the ubiquitous expression of many of the proteins associated with CMT. Peripheral neurons stand out due to their length and polarity. Both sensory and motor neurons of the peripheral nervous system (PNS) can be up to over a meter in length and symptoms often arise earliest in the extremities. This, in combination with the post mitotic state of the neurons, makes these cells particularly susceptible to changes in the intracellular transport machinery.

The intracellular transport machinery ranging from endocytosis to protein degradation is a tightly regulated, yet extremely dynamic system that is crucial for energy metabolism, signaling and protein homeostasis. Even though many studies look at trafficking aspects in the different types of CMT, we are lacking studies that look at multiple CMT types at once to benefit from directly comparable results. Here we will give an overview of the different aspects involved in intracellular trafficking (the irony of trying to divide such a dynamic system into clearly defined sections is not lost on us). We briefly mention which CMT-mutations show defects in the respective sections but discuss several CMT disorders, their trafficking defects and similarities between them after presenting the cell biological mechanisms. Our main approach is to link the different pathological mechanisms seen in CMT to find common denominators. An overall summary of how genes causing CMT affect trafficking can be found in **Figure 1** (axonal) and **Figure 2** (Schwann cell).

ENDOCYTOSIS

Arguably, the first step for intracellular transport is endocytosis. The most common and well-studied pathway for the uptake of nutrients, signaling receptors but also ion channels, transporters or pathogens, as well as vesicles is clathrin mediated endocytosis. Upon initiation signal [for many signaling receptors this involves kinase activity and mono-ubiquitination of the intracellular domain (Haglund et al., 2003)] Phosphatidylinositol (PI) 4,5-biphosphate ($PI_{4,5}P_2$) is generated at the plasma membrane, which recruits AP2, an adaptor protein complex. AP2 then recruits clathrin triskella that—with the involvement of several other proteins such as F-BAR domain-containing Fer/Cip4 homology domain-only proteins and Epsins-induce and stabilize membrane curvature and form a clathrin-coated pit, in which cargo gathers. Subsequently, Dynamin is recruited to the neck of the pit and self-polymerizes to induce membrane scission by GTP hydrolysis. The clathrin-coated vesicle pinches off subsequently (reviewed in McMahon and Boucrot, 2011). Upon removal of the clathrin coat, the vesicle is ready to fuse with early endosomes and begins its journey along the intracellular trafficking pathways.

Several genes known to cause CMT have been associated with dysfunctional endocytic processes, namely *MTMR2,13,5, SH3TC2, FGD4, DNM2* (relating to the subtypes CMT4B, CMT4C,CMT4H, and DI-CMTB, respectively), which will be discussed below. Defects in endocytosis have brought consequences on neuronal health for example lack of endocytosis of neurotrophic receptors would eventually affect gene expression of pro survival genes (Scott-Solomon and Kuruvilla, 2018).

From the early endosome, cargo continues its intracellular journey. The early endosome is characterized by the binding of the Rab5 GTPase, a small Rab GTPase that is cytosolic in its inactive GDP bound state. Upon activation by a Guanine nucleotide exchange factor (GEF) Rab5 is membrane tethered and activates several effector proteins, such as early endosome antigen 1 (EEA1; Gorvel et al., 1991; Bucci et al., 1992; Simonsen et al., 1998). The early endosome has a slightly acidic milieu with a pH of 6, which is generated by the vacuolar H-ATPase (Johnson et al., 1993). The membrane contains a high content of PI_3P and its shape is characterized by tubular extensions from its sorting activity (Jovic et al., 2010). The early endosome is also often referred to as the sorting platform. From there, cargo is sorted into one of three possible pathways. The recycling pathway, which is considered the default pathway, the retrograde pathway back to the trans golgi network (TGN) or to the soma, and lastly the degradative pathway (Schreij et al., 2016).

RECYCLING

After the clathrin coat is shed, the early endosome acts as a sorting station where bulk recycling is the default pathway due to probability: The endosome extends tubular domains increasing the amount of membrane in this section. Therefore, more receptors per volume will end up on that tubular domain, which is pinched off and recycled back to the plasma membrane (Maxfield and McGraw, 2004). Due to the acidic lumen of the endosome, many ligands dissociate from their receptors. Consequently, only the receptor is shuttled back to the plasma membrane for another round of signaling. Ligands, however, remain in the endosome for maturation and subsequent degradation. A prime example for this pathway is Transferrin and its receptor (Hopkins and Trowbridge, 1983). Receptors can also be recycled specifically via the so-called retromer complex together with the WASH complex and dynamin 2 (Derivery et al., 2009; Seaman et al., 2013). For example, the β-adrenergic receptor is recycled via a guided retromer sorting nexin (SNx) 27 complex. Where SNx27 recognizes a recycling sequence at the C-terminal of β-adrenergic receptor (Lauffer et al., 2010; Temkin et al., 2011; Seaman, 2012). This recycling mechanism has also been reported for other receptors, using different retromer/SNx combinations (Weeratunga et al., 2020). It is to be expected that many more receptors have specific sorting sequences interacting with different adaptors leading to a highly selective sorting mechanism. Rab4 and Rab11 decorate recycling endosomes undergoing fast and slow recycling, respectively (Jovic et al., 2010). Defects in recycling can either affect re-activation due to decreased surface levels of the receptor or affect downstream signaling from endosomes causing for example growth defects (Pasterkamp and Burk, 2020).

Defects in recycling have been reported for mutations in *DNM2, MTMR2,13,5 SH3TC2*, and *NDRG1*, causing DI-CMT, CMT4B, C and 4D, respectively.

ENDOSOMAL MATURATION

As mentioned above, the early endosome undergoes a maturation process, from so-called early endosomes to late endosomes. This maturation is manifested in a Rab switch, where Rab5 activates effectors that are Rab7 GEFs, which, in turn, activate Rab7 (Rink et al., 2005). The luminal content of the endosome further acidifies (pH between 4.5 and 6) and a shift in PI composition (PI_3P to $PI_{3,5}P_2$) by 1-phosphatidylinositol 3-phosphate 5-kinase (PIKFYVE) is reported (Maxfield and Yamashiro, 1987; Wallroth and Haucke, 2018). Maturation is further manifested by the formation of intra-luminal vesicles (ILVs) by inward budding of the maturing endosomal membrane. These ILVs contain cargos marked for degradation by ubiquitination. At this point, late endosomes are often referred to as multi vesicular bodies (MVBs). Late endosomes/MVBs have also been reported to be involved in retrograde trafficking. The following sections describe the three different pathways that all fall under the category of retrograde transport, namely, retrograde transport for signaling, retrograde transport to the TGN, and retrograde transport for degradation.

RETROGRADE TRANSPORT FOR SIGNALING

While many receptors signal from the plasma membrane, others rely on internalization in signaling endosomes to propagate their signaling cascade. Neurotrophins as well as neurocytokines are retrogradely trafficked, mostly during development. Even though tropomyosin-related kinase A (TrkA) and B (TrkB), the receptors for neurotrophins nerve growth factor (NGF) and brain-derived neurotrophic factor (BDNF), respectively, are mostly studied for their role in neurodevelopment, TrkB has been shown to be import for the maintenance of neurons in the adult neocortex (Xu et al., 2000). In addition, peripheral sympathetic neurons that were treated with an anti-NGF antibody slowly degenerated, indicating that not only TrkB but also TrkA has a role in maintenance of the nervous system (Ruit et al., 1990).

Neurotrophic receptors that were endocytosed after monoubiquitination, have been shown to be transported in early or late endosomes in different model systems (Delcroix et al., 2003; Deinhardt et al., 2006). Recently a study showed that TrkA is transported along the axon of sympathetic neurons in MVBs but signals from small vesicles at the soma (Ye et al., 2018). However, endosomal maturation is a fluent process (e.g., as described during the Rab-switch), making it hard to pinpoint the exact maturation state of endosomes. In addition, static studies without any live-cell imaging, only give very limited insight.

Disruption in retrograde traffic for signaling have been observed in mutations in *RAB7* (CMT2B), *GARS1* (CMT2D), *HSPB1* (CMT2F). Neurotrophic signaling regulating neuronal survival depends on retrograde trafficking (Scott-Solomon and Kuruvilla, 2018).

RETROGRADE TRANSPORT TO THE TGN

When retrograde transport is mentioned in non-neuronal cells, it is referring to the transport of cargo from endosomes to the TGN. In this context, the most studied cargo being the cation-independent mannose 6 phosphate receptor (CIMPR) that delivers hydrolases to late endosomes/lysosomes. The retromer complex, a key player in the endosomal sorting machinery, regulates this process. Composed of a vacuolar protein sorting-associated protein (VPS) trimer (VPS26,29,35), termed cargo recognition complex, and a SNx dimer (SNx1, 2 with SNx5 or 6), this protein complex returns the receptor back to the TGN, where it can pick up a fresh round of hydrolases (Seaman, 2004, 2012). SNxs are BAR-domain containing proteins, which drive membrane binding and curvature via their PI_3P membrane binding domain. The VPS trimer recruits CIMPR into a tubulus, which is stabilized by another protein complex termed WASH complex (Wiskott–Aldrich syndrome protein and SCAR homolog complex). Thoroughly studied in yeast, the exact roles of the VPS trimer and SNxs are still being debated in human cells (Kvainickas et al., 2017; Simonetti et al., 2017). When retrograde vesicles containing CIMPR reach the TGN, they need to dock and fuse for further hydrolase uptake by the receptor. This docking and fusion is orchestrated by Golgi-associated retrograde protein complex (GARP) and Rab29 (Bonifacino and Hierro, 2011; Wang et al., 2014). If this pathway is disrupted no more hydrolases are delivered to lysosomes, leading to a lack in degradation, therefore to an accumulation of neurotoxic waste, a lack of nutrients and triggered apoptosis.

Disruptions of retrograde traffic and accumulations in the TGN were observed for mutations in *GJB1* causing, CMT1X.

RETROGRADE TRANSPORT FOR DEGRADATION

As just discussed, retrograde transport of CIMPR is very important for proper lysosomal function, a process essential for protein degradation. Internalization and subsequent degradation of signaling receptors is an important step in signal termination. Polyubiquitinated proteins at the cell surface that are marked for degradation remain in the early endosome (aka no recycling) while this endosome matures into a late endosome. The ubiquitinated cargo is recognized by Hrs of the endosomal sorting complexes required for transport (ESCRT)-0 complex (Raiborg et al., 2002). Interacting with PI_3P ESCRT-0 recruits ESCRT-I and II, ubiquitinated cargo is concentrated in clathrin coated microdomains (Katzmann et al., 2001; Bache et al., 2003). ESCRT-III recruits membrane curving proteins to generate ILVs

(Adell et al., 2014). Once a late endosome contains such ILVs, it is classified as a MVB. The definition of a MVB throughout the literature is quite vague when it comes to marker proteins—MVBs are only definitely characterized structurally in electron microscopy images. Upon ILV generation, the MVB fuses with lysosomes, degrading its content (Futter et al., 1996). The degradative pathway is not only used by signaling receptors to terminate signaling but also for the degradation of lipids. For example, Rab8 is involved in the regulation of cholesterol efflux via this pathway, an important step for myelination (Linder et al., 2009; Zhou et al., 2019).

Interestingly, the ErbB pathway, a crucial pathway for Schwann cell myelination, relies heavily on proper degradation and recycling. Neuregulin1 signaling through ErbB leads to Schwann cell myelination, both ErbB2 and ErbB3 are expressed in Schwann cells (Michailov et al., 2004; Taveggia et al., 2005). However, both receptors follow different pathways in this process- ErbB2 is recycled, whereas ErbB3 is degraded via the ESCRT pathway. Ubiquitinated ErbB recognizes ESCRT-0, recruits ESCRTI-III and is subsequently incorporated into the invaginations—which bud off ILVs within MVBs (for a good review please see Lee et al., 2017). This process attenuates signal transduction and ends in receptor degradation. Abnormalities in this pathway again lead to increased neurotoxic waste and apoptosis.

Abnormalities in lysosomal degradation have been reported for mutations in *PMP22, LITAF, RAB7, DYNC1H1, LRSAM1, MTMR2,13,5, NDRG1*, and *FIG4* causing CMT1A, 1C, 2B, 2O, 2P, 4B, 4D, and 4J, respectively.

AUTOPHAGY

Another degradative pathway is the one of autophagy. A pathway mostly used for the degradation of aggregated and misfolded proteins but also whole organelles (like mitochondria, termed mitophagy), induced by cellular stress. For this, a double membrane structure called phagophore forms, expands and closes upon itself to generate an autophagosome engulfing protein aggregate. The autophagosome then fuses with a lysosome leading to the degradation of its content and a subsequent nutrient release into the cytosol (also referred to as macroautophagy). Rab1, 4, and 11 are involved in the membrane delivery for the formation of the phagophore, whereas autophagy receptor p62 binds ubiquitinated cargo and Microtubule-associated protein 1A/1B-light chain 3 (LC3) on autophagosomes (Komatsu et al., 2007; Kiral et al., 2018). The class 3 phosphoinositide 3-kinase (PI3K) complex, recruited by Rab5, produces PI_3P for the nucleation of the phagophore, whereas Rab33 is involved in the elongation. Autophagosomes fuse with late endosomes to so called amphisomes that traffic retrogradely- possibly by the same Rab7/Rab-interacting lysosomal protein (RILP)/dynactin complex that regulates the transport of late endosomes (Jordens et al., 2001; Cheng et al., 2015). Rab7 and Rab24 then mediate the fusion with lysosomes (Kiral et al., 2018). The autophagic flux depends on the autophagosomal transport, and fusion with lysosomes. In healthy neurons, few autophagosomes are observed indicating a low level of autophagy or a very quick turnover (Mizushima et al., 2004; Boland et al., 2008).

Autophagy related proteins have also been shown in Schwann cells, where autophagy plays an important role for cell plasticity, myelin maturation, and compaction. Excess cytoplasm is removed by autophagy leading to more compact myelin. Furthermore, Schwann cells rely on autophagy after nerve injury for the phagocytosis of myelin debris (Belgrad et al., 2020).

Alterations in autophagy were seen with mutations in *PMP22, RAB7, HSPB*1, and *FIG4* causing CMT1A, 2B, 2F, and 4J, respectively.

MITOCHONDRIA TRANSPORT

Neuronal cells have a relatively large energy consumption, which is why they rely heavily on a functioning mitochondria system. Trafficking is an important process for mitochondrial maintenance. Mitochondria need to be transported to regions of high energy demand. If mitochondria transport is disturbed this would lead to a local energy crisis and to degradation of the long neurons of the PNS. Transport is regulated by a Miro/Milton complex (Stowers et al., 2002; Fransson et al., 2006; Glater et al., 2006). Miro binds the outer mitochondrial membrane via its carboxyterminal, whereas Milton is the adaptor protein of Miro and the motor proteins. Accumulated damaged mitochondria are degraded by mitophagy as described above. Disruptions in mitochondria transport and location have been described in many sub-types of CMT including mutations in *MFN2* (CMT2A2), *RAB7* (CMT2B), *GARS1* (CMT2D), *NEFL* (CMT2E), *HSPB1* (CMT2F), and *DYNC1H1* (CMT2O). For a recent review on mitochondria transport in a disease context refer to (Schiavon et al., 2021).

CYTOSKELETAL BASIS FOR TRANSPORT

The basic structure or architecture of neurons is provided by its cytoskeleton, which also serves as the tracks for intracellular trafficking. The cytoskeleton is comprised of three building blocks, microfilaments, intermediate filaments, and microtubules. Microfilaments are made by actin and are mostly found in mobile/changing structures like the growth cone or newly formed synapses. Intermediate filaments are made from three different neurofilaments (light, medium, and heavy polypeptide) and peripherin in the PNS. The filaments share a structural organization of a central α-helical rod that drives assembly of dimers, protofilaments, and filaments of 10 nm diameter (Laser-Azogui et al., 2015). Neurofilaments are the most abundant cytoskeletal component in myelinated axons. They have the intrinsic role to form and maintain the axonal architecture, its diameter and the intracellular transport of cargo in dendrites. Posttranslational modifications influence neurofilament assembly, hence the axonal size of large myelinated axons.

Lastly, microtubules are composed of α and β tubulin forming profilaments, where 13 profilaments make 1 microtubule with a diameter of about 25 nm (Prior et al., 2017). Microtubules, also referred to as molecular tracks, are modified by acetylation and detyrosination, which influences trafficking. Acetylation increases the binding of motor proteins thus enhancing transport and is highest in stable and long-lived microtubules, like axons (Reed et al., 2006). Acetylation of α-tubulin improves the binding capacities of kinesins to the microtubules thus enhancing transport (Reed et al., 2006) but has also shown to increase dynein recruitment to microtubules (Dompierre et al., 2007). Whereas, detyrosination guides kinesin-1 to the axon (Konishi and Setou, 2009) and regulates dynein based transport (Nirschl et al., 2016).

Kinesins are the motor proteins involved in the plus-end directed (anterograde) transport. Dyneins are involved in minus-end directed or retrograde transport. Dynein interacts with cargo via a dynein/dynactin complex involving p150glued. Deregulation in microtubule assembly and disassembly has been shown to affect axonal growth (Markworth et al., 2019). Importantly, neurotrophic signaling can affect microtubule stability (Goold and Gordon-Weeks, 2003).

Many types of CMT have shown to have cytoskeletal abnormalities (Brownlees et al., 2002), including mutations in *PMP22* (CMT1A), *MFN2* (CMT2A2), *RAB7* (CMT2B), *GARS1* (CMT2D), *NEFL* (CMT2E), *HSPB1* (CMT2F), *FIG4* (CMT4J), *FGD4* (CMT4H), *DNM2* (DI-CMT), and *GJB1* (CMT1X). Whether these are causative or secondary remains to be shown in many cases.

PHOSPHOLIPIDS

Finally yet importantly, while the phospholipid system is involved in every step of intracellular trafficking, it is worthy of its own section. As already mentioned, the endosomal trafficking journey begins with the synthesis of $PI_{4,5}P_2$ at the site of endocytosis and changes over the course of endosomal maturation, making phospholipids not only a marker for endosomal maturation but an important regulator of the endosomal system (Wallroth and Haucke, 2018). Early endosomes are mostly comprised of PI_3P, generated by class III phosphoinositide VPS34, which, in turn, is recruited by Rab5. PI_3P is then recognized by the FYVE domain of ESCRT-0 subunit Hrs, which is recruited to the endosomes to promote ESCRT sorting and MVB formation. During endosomal maturation PI_3P is phosphorylated by PIKFYVE complex/PI5K to $PI_{3,5}P_2$. PI regulating enzymes can affect endosome to lysosome trafficking and therefore inhibit the degradation of cell surface proteins (Berger et al., 2011).

Interestingly, as a component of the plasma membrane, phospholipids have been shown to play an important role in Schwann cells too. More precisely, phospholipids on Schwann cells have shown to be regulators of compact myelination. As PI3K generates $PI_{3,4,5}P_3$ at the plasma membrane, which then activates the Akt pathway, a promyelinating signaling cascade in the PNS, that is tightly regulated by phosphatase and tensin homolog (PTEN), downregulating $PI_{3,4,5}P_3$ (Lee et al., 2017). This again shows that phosphoinositides do not only function as membrane markers for different organelles, but also hold a signaling and regulating function in the PNS. This makes them interesting candidates to investigate in axonal and demyelinating CMT as a deregulation would affect the whole intracellular trafficking pathway spanning from endocytosis to degradation.

Specifically mutations in *MTMR2,13,5* and *FIG4* causing CMT4B and CMT4J, respectively, have shown to disrupt the phospholipid system.

CMT SUBTYPES SHOWING IMPAIRED INTRACELLULAR TRAFFICKING

While genetic mutations leading to CMT also affect other cellular processes (e.g., genes coding for human aminoacyl tRNA synthetases such as *GARS1* [glycyl-tRNA synthetase (GlyRS)], which catalyzes the first step of protein synthesis), eventually many processes meet at the platform of intracellular trafficking. For example, CMT2D-associated mutants of GlyRS stimulate deacetylase activity on α-tubulin (Mo et al., 2018). Further, even protein synthesis is linked to intracellular trafficking: mRNAs made in the nucleus associate with so-called RNA-binding proteins (RBPs). These RBPs are transported as ribonucleoprotein particles (RNPs) to distal subcellular locations for local translation. To perform local translation, RNPs associate with late endosomes/lysosomes, which are transported along the axons. Finally, These RNP-associated late endosomes have been found to dock at mitochondria sustaining mitochondrial health (Cioni et al., 2019). Intriguingly, this process is disrupted in CMT2B, caused by mutations in the late-endosomal Rab7-GTPase (Cioni et al., 2019). Therefore, rather than listing CMT-causing mutations based on their functions, we deciphered where and how, to today's knowledge, CMT mutations affect intracellular trafficking and how this then could explain the observed phenotypes.

The length, polarity and post-mitotic state make peripheral sensory and motor neurons extremely dependent on intracellular axonal transport for proper function and maintenance. It is therefore understandable that even mutations in ubiquitously expressed proteins cause a cell type specific phenotype in these neurons. Importantly, also subtypes that show both, axonal and demyelinating phenotypes show many mutations involved in intracellular transport in neurons but also in Schwann cells, hindering proper myelination.

Schwann cells have a highly polar structure and rely heavily on membrane transport for myelination. This can be seen in the involvement of the intracellular transport machinery in the pathology of demyelinating CMT1 as described below. Although many other factors are involved in the pathology, the involvement of intracellular traffic in CMT is intriguing as it highlights the importance of the intracellular transport machinery for many aspects of proper cellular function. Further, it sheds light on the importance of considering intracellular dynamics when looking for potential disease mechanisms. The fluidity yet tight regulation of this system is its toughest aspect to study. However, the following examples highlight the importance of considering this system as highly dynamic when interpreting

static results. The CMT subtypes discussed in this review and their corresponding trafficking phenotypes are summarized in **Table 1**.

AXONAL CMT2

CMT2A1-KIF1Bβ

In CMT2, several defects in intracellular trafficking have been reported (**Figure 1**).

CMT2A1 is caused by mutant KIF1Bβ, a kinesin family member that plays a role in neuronal survival and function due to its role in anterograde transport (Zhao et al., 2001). KIF1Bβ directly binds to insulin like growth factor (IGF) receptor (IGFR) 1β, a receptor tyrosine kinase that signals for axonal outgrowth via IGF-I signaling and activation of the PI3K-Akt pathway (Laurino et al., 2005; Scolnick et al., 2008). In one of the studied CMT2A1 mutations (Y1087C) binding of KIF1Bβ to IGFR is significantly reduced, leading to less IGF1R transport, reduced surface expression and reduced axonal outgrowth in mouse hippocampal neurons (Xu et al., 2018). Further, KIF1Bβ is involved in the development of myelinated axons, both in the CNS and PNS (Lyons et al., 2009 in Xu). Other mutations have been reported in the conserved ATP binding site of the kinesin motor (Q98L), leading to a perinuclear accumulation of the protein and defects in cargo transport. This defect in transport was visible by decreased levels of synaptic vesicle proteins including synaptotagmin and synaptic vesicle protein 2 (SV2) in western blots of proximal and distal nerve sections after sciatic nerve ligation of heterozygous *kif1B*± mice in comparison to *kif1B*+/+ mice (Zhao et al., 2001). This study concluded a trafficking defect due to decreased protein levels on western blots of lysed nerve sections comparing distal and proximal parts. Levels of synaptotagmin and SV2 were reduced in both, distal and proximal section of the heterozygous mice compared to control. While the authors concluded a Kif1B-dependent trafficking defect, decreased levels could also occur from downregulation of these proteins or altered degradation instead of altered trafficking. Therefore, to specifically pinpoint trafficking defects, live-imaging using trafficking markers would help to decipher this question. In addition, KIF1Bβ is able to bind to other cargo. Therefore, it would be interesting to see if other intracellular transport systems are also affected, including the transport and signaling of epidermal growth factor receptor (EGFR), mitochondrial transport and autophagic turnover as presented for other CMT types (see below). Lastly, the effect on IGF1R trafficking and signaling in other CMT types would be intriguing to unwrap, to see if it is a common denominator or if commonalities can be found in the effect on the downstream signaling cascade.

CMT2A2

The most common type of CMT2 is CMT2A2, caused by dominantly inherited point mutations in *Mitofusin 2* (*MFN2*; Züchner et al., 2004). MFN2 is a dynamin family GTPase located on the outer mitochondrial membrane protein and part of the Miro/Milton tethering complex, tethering mitochondria to kinesin. MFN2 is further involved in mitochondria morphology, fusion and motility, endoplasmic reticulum tethering and synapse formation (Chen et al., 2003; De Brito and Scorrano, 2008; Misko et al., 2010). CMT2A2 mutations cause a decrease between mitochondria and endoplasmic reticulum tethering and a reduction in neurite length of primary motor neurons. Live cell imaging also revealed fewer mitochondria in the sciatic nerve axons with a higher proportion of very slow-moving mitochondria compared to control (Bernard-Marissal et al., 2019). This is in line with data from primary sensory neurons, where overexpressed mutant MFN2 led to a loss of mitochondria in distal and an aggregation in the proximal axonal segments with fewer mobile mitochondria (Baloh et al., 2007). The phenotype of slower mitochondrial movement was also observed in spinal motor neurons derived from patient induced pluripotent stem cells, but to lesser extent (Saporta et al., 2015). In a CMT2A2 mouse model, loss of mitochondria was observed in the distal part of sciatic nerve axons as well as a loss of tubulin acetylation that worsened with age (Picci et al., 2020). However, since these mice display a neuropathic phenotype before the decrease of acetylation is detected, another pathomechanism has to be in play. Yet treatment with an histone deacetylase 6 (HDAC6) inhibitor ameliorated some of the motor and sensory phenotypes in these mouse models (Picci et al., 2020). It would be very interesting to see if and how the treatment affected mitochondrial transport and how it acted on a molecular level by applying it *in vitro*. This, in turn, would help to put this finding in context with previous studies focusing on the molecular pathomechanisms [like they did for CMT2D causing GlyRS (Benoy et al., 2018)]. Still, the questions that remain are: is the deacetylation of tubulin is a cause of the decreased mitochondrial transport? Would the deacetylation then, in turn, amplify the trafficking defect by decreased motor protein association, or do the pathomechanisms work in parallel? If mitochondria can no longer be transported to sites of high energy demand, like synapses or nodes of Ranvier, this would lead to a local energy crisis and explain neuronal malfunction in the longest and most distal parts as seen in CMT2A. Therefore, future studies on mitochondrial transport, or how to overcome disruptions in kinesin tethering would be an interesting point of investigation.

CMT2B

Autosomal dominant CMT2B, marked by primarily axonal degeneration, is caused by mutations in the late Rab7 GTPase. As of today 6 mutations are known to cause CMT2B, with all mutations being located close to the GTP binding pocket altering the binding kinetics (Spinosa et al., 2008; McCray et al., 2010; Saveri et al., 2020). Rab7 has been shown to transport ligand bound neurotrophic receptors TrkA and TrkB retrogradely to the soma (Deinhardt et al., 2006). Even though the CMT2B-causing Rab7 mutations are no loss of function mutations, alterations in retrograde traffic were observed in a drosophila model and in cultured mouse dorsal root ganglia overexpressing the mutant Rab7 proteins (Zhang et al., 2013; Janssens et al., 2014). The binding of Rab7 and TrkA was not changed by the mutations. However, signaling of TrkA and EGFR was altered in cells expressing CMT2B mutant Rab7, possibly as a result of

TABLE 1 | An overview of the CMT mutations involved in intracellular trafficking discussed in this review, including their relevant phenotypes.

Type	*Gene symbol*	Gene name	Trafficking phenotype	References
CMT1A	*PMP22*	Peripheral myelin protein 22	Autophagy/saturation of proteasome, disrupted PMP22 transport, elevated ErbB levels, reduction in slow axonal transport, altered cytoskeletal organization and NF phosphorylation	De Waegh and Brady, 1990; de Waegh et al., 1992; Massa et al., 2006; Fortun et al., 2007; Rangaraju et al., 2010; Marinko et al., 2020
CMT1C	*LITAF*	Lipopolysaccharide induced TNF factor	Mislocalization from early endosomes to cytosol, reduced ESCRT recruitment, decreased EGFR degradation, enlarged endosomes/lysosomes	Lee et al., 2011, 2012; Edgar et al., 2020
CMTX	*GJB1*	Gap junction protein beta 1	Dysfunctional anterograde trafficking of GJB1, defects in retrograde axonal transport and neurofilament phosphorylation	Deschênes et al., 1997; Yum et al., 2002; Abrams et al., 2003; Kleopa et al., 2006; Vavlitou et al., 2010
CMT2A1	*KIF1B*	Kinesin family member 1B	Defects in IGFR1 transport, perinuclear accumulation and defects in anterograde cargo transport	Zhao et al., 2001; Xu et al., 2018
CMT2A2	*MFN2*	Mitofusin 2	Disturbed mitochondrial transport, mitochondria aggregation in proximal segment, loss of tubulin acetylation	Baloh et al., 2007; Saporta et al., 2015; Bernard-Marissal et al., 2019; Picci et al., 2020
CMT2B	*RAB7A*	Rab7A, Member RAS oncogene family	Altered retrograde traffic, altered TrkA/EGFR signaling, decreased RILP levels, increased peripherin interaction, disturbed retromer binding, reduced autophagic flux	Spinosa et al., 2008; Seaman et al., 2009; Basuray et al., 2010; BasuRay et al., 2013; Cogli et al., 2013; Zhang et al., 2013; Janssens et al., 2014; Colecchia et al., 2018
CMT2D	*GARS1*	Glycyl-tRNA synthetase 1	Reduced acetylated tubulin levels, disrupted mitochondria transport, novel binding to HDAC6 and TrkA, disrupted NGF transport, increased interaction with neuropilin-1→ disrupted interaction with VEGFR	He et al., 2015; Kim et al., 2016; Sleigh et al., 2017; Benoy et al., 2018; Mo et al., 2018
CMT2E/CMT1F	*NEFL*	Neurofilament light	Disrupted anterograde traffic of NF-L (aggregation/accumulation) and mitochondria	Brownlees et al., 2002; Pérez-Ollé et al., 2005; Saporta et al., 2015
CMT2F	*HSPB1*	Heat shock protein family B (small) member 1	Intracellular aggregates NF-M, disturbed retrograde mitochondrial transport, increased binding to α-tubulin, reduced autophagic flux	Ackerley et al., 2006; Almeida-Souza et al., 2011; D'Ydewalle et al., 2011; Kim et al., 2016; Kalmar et al., 2017; Haidar et al., 2019
CMT2O	*DYNC1H1*	Dynein cytoplasmic 1, heavy chain 1	Decreased retrograde transport of lysosomes and trophic factors, reduced mitochondrial transport	Hafezparast et al., 2003; Perlson et al., 2009; Ori-McKenney et al., 2010; Zhao et al., 2016
CMT2P/CMT2G	*LRSAM1*	Leucine-rich repeat- and sterile alpha motif-containing 1	Altered interaction with ESCRT protein TSG101 and altered EGFR degradation	Guernsey et al., 2010; Palaima et al., 2021
DI-CMTB	*DNM2*	Dynamin 2	Blocks dynamin-dependent endocytosis, defects in microtubule stability	Tanabe and Takei, 2009; Sidiropoulos et al., 2012
CMT4B1	*MTMR2*	Myotubularin related protein 2	GluR2 uptake increases upon loss of functional protein, also lack of recycling initiation/missorting into lysosomes, altered EGFR degradation	Bolino et al., 2004; Cao et al., 2008; Lee et al., 2010; Berger et al., 2011
CMT4B2	*MTMR13*	Myotubularin related protein 13		
CMT4B3	*MTMR5*	Myotubularin related protein 5		
CMT4C	*SH3TC2*	SH3 domain and teratricopeptide repeats 2	Decreased ErbB2 internalization, decreased interaction with Rab11, increased recycling of TF	Arnaud et al., 2009; Roberts et al., 2010; Gouttenoire et al., 2013
CMT4D	*NDRG1*	N-myc downstream regulated 1	Disturbed Rab4 endosomes, disturbed TFR, e-cadherin, ErbB and LDL recycling, abnormal endosomal maturation, delayed fusion of MVBs with lysosomes	Kachhap et al., 2007; Pietiäinen et al., 2013; Li et al., 2017
CMT4H	*FGD4*	FYVE, RhoGEF and PH domain containing 4	Defective TF internalization, alterations in microfilament structure	Delague et al., 2007; Horn et al., 2012
CMT4J	*FIG4*	Fig4 phosphoinositide 5-phosphatase	Decreased levels of PI3,5P2 on endosomes, enlarged endosomes and lysosomes, decreased autophagic flux, defective cholesterol transport	Ferguson et al., 2009; Vaccari et al., 2015; Bharadwaj et al., 2016

defective signaling from endosomes (Maxfield and Yamashiro, 1987; Rink et al., 2005; Marat and Haucke, 2016; Bakker et al., 2017)—since signaling from the plasma membrane was still intact (Basuray et al., 2010; BasuRay et al., 2013). In addition, the different mutants showed decreased expression of RILP, a Rab7 effector important for lysosomal transport by recruiting dynein-dynactin motors, as well as an increased interaction with peripherin, an intermediate filament of the PNS (Spinosa et al., 2008; Cogli et al., 2013). Further, one of the mutants showed disturbed binding to the protein sorting complex retromer by co-immunoprecipitation, suggesting a pathomechanism that involves mis-sorting of receptors on their trafficking route (Seaman et al., 2009). A study from 2018 also reported alterations in autophagy in CMT2B. All tested mutants displayed reduced localization on autophagic compartments and reduced autophagic flux in HeLa cells, similarly to a dominant negative mutant of Rab7. Further, basal and induced autophagy were decreased in skin fibroblasts from a CMT2B patient (Colecchia et al., 2018; Romano et al., 2020). As mentioned, local translation by RNPs localizing to late-Rab7 endosomes and mitochondria is disrupted in CMT2B (Cioni et al., 2019). The diverse phenotypes of CMT2B- causing mutations in Rab7 is explainable by the involvement of Rab7 in many aspects of this highly dynamic system (e.g., transport, signaling of receptors, degradation, local translation), which makes pinpointing the causal effect of mutant Rab7 extremely difficult. It would therefore be very interesting to study if within these mechanisms some common modalities are present—e.g., do CMT2B-causing mutations have difficulties binding to dynein which would disrupt trafficking, signaling, maturation and degradation.

CMT2D

Mutant GlyRS encoded by *GARS1* causes autosomal dominant CMT2D and distal hereditary motor neuronopathy (Antonellis et al., 2003). A mutant mouse model shows reduced acetylated α-tubulin levels and disrupted mitochondrial transport (Benoy et al., 2018; Mo et al., 2018). How the molecular mechanism of tRNA generation influences intracellular trafficking is not yet understood. To date, GlyRS mutants have been found to show novel and increased binding properties to cytoskeletal proteins and receptors (He et al., 2015). Mutant but not wild type GlyRS co-immunoprecipitates with HDAC6. HDAC6 deacetylases tubulin leading to unstable tubulin. Therefore, binding of mutant GlyRS to HDAC6 is believed to increase the deacetylase activity. A HDAC6 specific inhibitor has been found to improve mitochondrial axonal transport and relieve both, motor and sensory systems in mice (Benoy et al., 2018; Mo et al., 2018). The similarity to MFN2 causing CMT2A2 is striking, yet needs to be confirmed by producing more comparable studies and results. Both mutant MFN2 and GlyRS show reduced acetylated tubulin levels and decreased mitochondrial transport (Baloh et al., 2007; Benoy et al., 2018; Mo et al., 2018; Picci et al., 2020). Further, mouse models of each show an improvement of motor and sensory phenotypes upon treatment with HDAC6 inhibitors. How mutations in MFN2 lead to decreased acetylated tubulin, which in turn could lead to decreased binding of motor proteins to it and therefore to decreased transport of cargo/mitochondria, is still open. It is possible that MFN2 has a direct impact on the acetylation levels or that it is a secondary effect to the disrupted mitochondrial transport. It would therefore, be of interest if mitochondrial transport was improved upon HDAC6 inhibitor treatment in models of CMT2A2 (MFN2) or if deliberately disrupting mitochondrial transport leads to a decrease in tubulin acetylation.

GlyRS also shows increased interactions with receptors. GlyRS binds neuropilin-1, a co-receptor of the vascular endothelial growth factor receptor (VEGFR). This interaction is enhanced by the GlyRS-CMT2D causing mutations. The increased binding of mutant GlyRS to neuropilin-1 disrupts its interaction with VEGFR. While genetic depletion of neuropilin-1 worsens the CMT phenotype, overexpression of VEGF improves motor problems (He et al., 2015), indicating that this pathway is also involved in the pathogenesis. Interestingly, VEGF signaling has been shown to be regulated by intracellular trafficking (Horowitz and Seerapu, 2012). Whether the altered VEGF pathway contributes to the pathology in parallel or in stream with the altered tubulin acetylation remains unknown. To pinpoint the effects of VEGFR signaling in CMT2D, trafficking and downstream signaling could be followed. For example, does VEGFR change its downstream targets since neuropilin-1 has been found to act as a "gating" protein switching downstream signaling of PlexinD1 to VEGFR2 (Chauvet et al., 2007)?

Lastly, mutant GlyRS but not wild type GlyRS binds to TrkA. There is a correlation between binding intensity and disease severity. Even though the molecular effect on Trk binding is not clear, an increased Trk activation by increased Erk1/2 phosphorylation is indicated (Sleigh et al., 2017). Whether the disrupted transport of NGF (Mo et al., 2018) is a consequence of altered tubulin acetylation and transport defects in general or due to GlyRS' increased binding to NGF-receptor TrkA remains to be answered. The causal relationship of growth factor trafficking and tubulin acetylation needs to be determined. It is known that neurotrophic factor signaling affect microtubule dynamics (Goold and Gordon-Weeks, 2003). Other options are changes in downstream signaling due to increased TrkA/GlyRS binding.

CMT2E

Mutations in *NEFL* are quite intriguing as they cause mostly axonal CMT2E but can also be classified as CMT1F because severely reduced nerve conduction velocity is a reported phenotype. However, the decreased conduction velocity that usually stems from demyelination is proposed to be caused by a decrease in axonal diameters in CMT2E, making it ultimately axonal (Lancaster et al., 2018). The mutations associated with CMT2E/1F are most commonly missense mutations in the head domain or in the central rod domain of neurofilament light polypeptide (NEFL; Mersiyanova et al., 2000; De Jonghe et al., 2001; Lerat et al., 2019). Mutations disturb axonal transport of NEFL that is generated in the soma and transported along the axon, shown by lack of NEFL in the distal part of axons and accumulation in the proximal part and soma (Brownlees et al., 2002). However, live cell imaging of fluorescently tagged mutant NEFL in primary rat neurons did not show any alteration of NEFL movement compared to WT indicating that NEFL

traffic greatly depends on the model being used (Stone et al., 2019). In contrast, transport of mitochondria is disrupted—seen in an accumulation of mitochondria in the cell body region and loss in the distal axon of sympathetic neurons (Brownlees et al., 2002; Pérez-Ollé et al., 2005). In patient derived iPSCs differentiated into spinal motor neurons, mitochondria movement was reported to be slower and shorter distanced (Saporta et al., 2015). Aggregates of mutated NEFL were observed in transfected rat cortical neurons and mouse models, as seen for other neuropathies. However, patient nerve biopsies and patient derived motor neurons only showed disorganized NEFL polymer accumulation not aggregation (Brownlees et al., 2002; Fabrizi et al., 2007; Adebola et al., 2015; Saporta et al., 2015; Zhao et al., 2017). Overall, above studies should be carefully interpreted since data arose from different model systems—as phenotype depends greatly on the accompanying neurofilament proteins available for co-assembly (Stone et al., 2019).

CMT2F

Similar effects as described for CMT2D (mutant GlyRS) on α-tubulin acetylation and axonal transport have also been reported for CMT2F, which is caused by a mutation in heat shock protein family B (small) member 1 (*HSPB1)*. CMT2, causing HSPB1 has been found to cause intracellular aggregates of components including neurofilament medium polypeptide (NEFM) and p150 dynactin (Ackerley et al., 2006). In sensory and motor neurons, expression of mutant HSPB1 lead to disturbed retrograde mitochondrial transport, whereas axonal transport of neurotrophic factor p75 was only minimally affected, indicating a cargo specific defect (D'Ydewalle et al., 2011; Kim et al., 2016; Kalmar et al., 2017). This mitochondrial transport defect was partially rescued by an HDAC6 inhibitor. Almeida-Souza et al. (2011) have shown that mutant HSPB1 reveals an enhanced binding efficiency to α-tubulin leading to stabilization of microtubules without changing the acetylation pattern of tubulin. This seems counterintuitive to the beneficial effect of HDAC6 inhibitors and shows that more studies are needed to figure out the molecular pathway of HSPB1 and HDAC6 inhibitors in the cytoskeleton. Interestingly, the commonalities of phenotypes between CMT2D (*GARS1*), CMT2E (*NEFL*), and CMT2F (*HSPB1*) all share a common defect: disruption in α-tubulin acetylation. A comparison on tubulin dynamics and structure could reveal additional shared phenotypes and increase the understanding of how these common phenotypes occur despite different genes affected. Furthermore, starvation induced autophagic flux was reduced in patient derived motor neurons. The exact molecular pathway of how HSPB1 is involved in autophagy remains to be answered but it has been shown that HSPB1 binds to the autophagy inducing receptor SQSTM1 and that this binding is increased by some mutants of HSPB1. Those mutants failed to induce autophagic pores upon starvation (Haidar et al., 2019).

CMT2O

CMT2O is an autosomal dominant type of CMT, caused by a His306Arg mutation of dynein cytoplasmic 1 heavy chain 1 (*DYNC1H1*). The His306Arg mutation resides in the highly conserved residue of the homodimerization domain of DYNC1H1 (Weedon et al., 2011). As dynein is the main motor protein responsible for minus-end/retrograde transport, a pathomechanism involving defective axonal transport is expected. Indeed, tagged dynein from the Loa mice line, which carries a mutation in the binding domain of DYNC1H1, show decreased run length of retrograde transport of lysosomes (Hafezparast et al., 2003; Ori-McKenney et al., 2010) as well as decreased transport of trophic factors in a sciatic nerve ligation assay (Perlson et al., 2009). In mouse models with a 9bp deletion mutation in the stem domain of DYNC1H1 (responsible for cargo binding and homodimerization), retrograde axonal transport of NGF was reduced, which caused increased apoptosis upon NGF stimulation at the peripheral axon (Zhao et al., 2016). Whether the downstream signaling cascade of TrkA, the receptor for NGF, was altered as reported for mutated Rab7 and GlyRS has not been investigated yet. Further, mitochondrial transport is reduced in these mice as also reported for mutated MFN2, GlyRS and NEFL. The model shows that DYNC1H1 has a crucial role in the transport of both neurotrophic factors and mitochondria a defect shared among several CMT subtypes.

CMT2P

Recessive and dominant axonal CMT2P are caused by mutations in *LRSAM1* (leucine rich and sterile alpha motif containing) encoding a universally expressed RING-type E3 ubiquitin ligase (Guernsey et al., 2010). Thus far, its only known target is TSG101, a member of ESCRT I, involved in the degradation pathway of EGFR (Palaima et al., 2021). Though only known since the last decade, first results already show the involvement of LRSAM1 in the intracellular trafficking pathway and more results regarding its exact involvement in the molecular processes of EGFR degradation and possible other trafficking phenotypes are to be expected in the future.

In summary, the most prominent shared defects in axonal CMT include abnormalities in mitochondrial transport, transport of neurotrophic factors, tubulin acetylation and altered autophagy. These mechanisms, in turn, could affect downstream signaling from endosomes as well as microtubule dynamics via trophic signaling (Goold and Gordon-Weeks, 2003), One downside of interpretation is that experiments conducted vary between model systems used. Further, the level of detail in how the transport mechanisms are studied also shows variability. Therefore, comparative studies focusing on the effect of the different CMT mutated proteins would be ideal to identify common pathologies. Further, checking for phenotypes reported in one subtype (like altered IGFR transported as reported for CMT2A1) in other subtypes will complete the picture of possible shared mechanisms. The same holds true for CMT subtypes not mentioned in this review because not enough data to altered trafficking mechanism were reported as of yet.

CMT SUBTYPES WITH DEMYELINATING AND AXONAL PHENOTYPES

Importantly, not only predominantly axonal types of CMT show intracellular transport defects. In fact, several of the demyelinating subtypes have shown abnormal trafficking

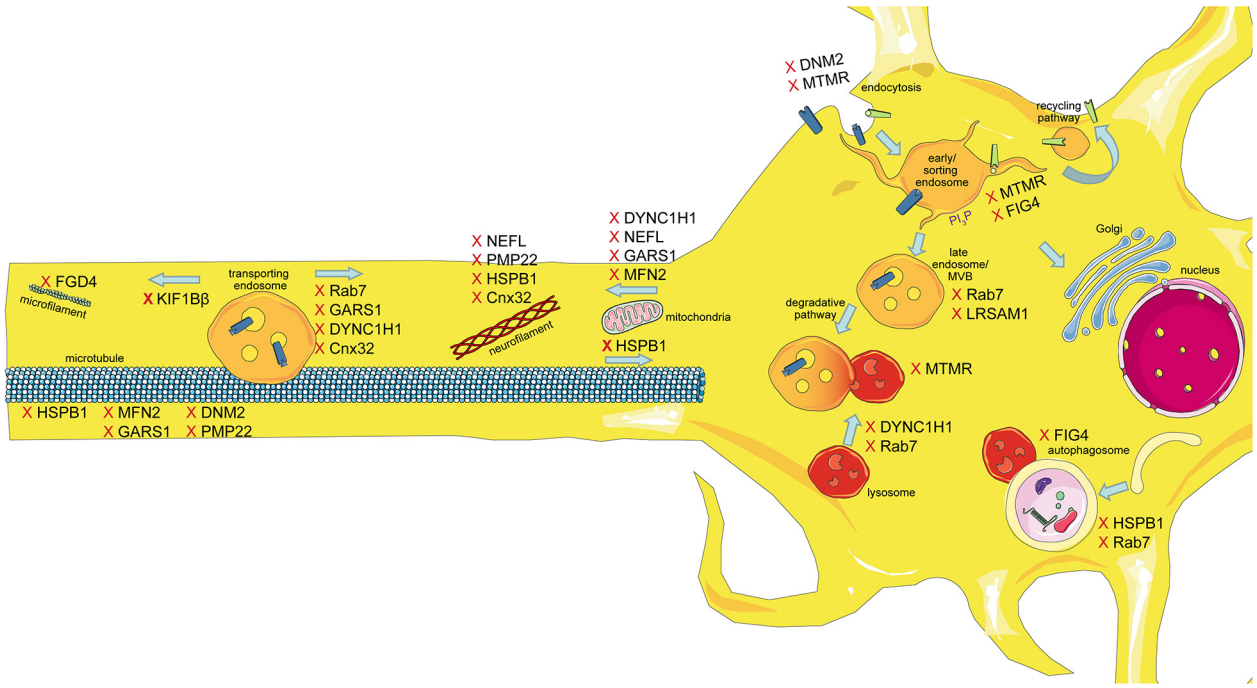

FIGURE 1 | Schematic overview of the intracellular trafficking processes in a neuron of the PNS. Highlighting all the steps where proteins involved in CMT can cause dysregulation. This figure was created using Servier Medical Art templates, which are licensed under a Creative Commons Attribution 3.0 Unported License; https://smart.servier.com.

including CMT1, the most common type of CMT, as well as CMT1X, CMT4, and DI-CMT (**Figures 1**, **2**). This indicates that trafficking is also a crucial step in Schwann cells. Of note is that the majority of trafficking defects in CMT subtypes with more demyelinating phenotypes is seen in the endocytic and recycling pathway indicating these two steps critical in Schwann cell myelination. DI-CMT, CMT4B, 4C, 4D, and 4H all show endocytic alterations, recycling defects or both. On the other hand, CMT4B and CMT4J affect phosphoinositide compositions altering endocytic processes, recycling, maturation, and degradation pathways. This shows that the PI regulation is essential for the complete dynamic process of intracellular trafficking and cannot be pinpointed to a single subsection.

DI-CMTB

Mutations in dynamin 2 cause dominant-intermediate CMT (DI-CMTB) displaying both axonal and demyelinating phenotypes, sometimes also classified as axonal CMT2M (Züchner et al., 2005). Dynamin 2 is a ubiquitously expressed fission protein, responsible for the fission of intracellular vesicles after endocytosis and for the fission from endosomes. The mutations causing Di-CMTB are located in the Pleckstrin homology domain of dynamin 2, which binds to $PI_4{,}_5P_2$ required for membrane localization. One of the DI-CMTB causing mutants (K558E) blocks dynamin-dependent endocytosis in a dominant negative fashion, whereas another (551Δ3) showed defects in microtubule stability, indicating two different pathogenic mechanisms (Tanabe and Takei, 2009). Of note, dynamin 2 also plays a role in receptor trafficking as it is involved in targeting receptors into the recycling pathway from early endosomes (Jovic et al., 2010). Therefore, defects in dynamin 2 could affect receptor signaling by blocking receptor endocytosis as well as re-activation if receptor re-insertion to the plasma membrane is disrupted. Although live cell imaging experiments are sparse for DI-CMTB, the disturbances in three of the main fundaments for intracellular transport—endocytosis, recycling, and microtubules, could lead to trafficking defects and would be ideal candidates to receive further investigation. Interestingly, dynamin 2 is essential for Schwann cell myelination of the peripheral nerves. An induced dynamin 2 deletion in adult Schwann cells leads to a demyelinating neuropathy (Gerber et al., 2019). However, it is unclear if this defect is caused by disrupted endocytosis as seen by a Transferrin uptake assay, or caused by altered levels of ErbB2 receptors on the plasma membrane (Sidiropoulos et al., 2012). The involvement of dynamin 2 in Schwann cell myelin maintenance provides a basis for the intermediate pathogenesis seen in DI-CMTB.

CMT4B

CMT4 is a rather rare subtype of the disease mostly inherited in an autosomal recessive pattern characterized by myelin deformities and a relatively early onset.

CMT4B is caused by autosomal recessive mutations in three of the myotubularin-related protein (MTMR) family of phosphoinositide 3-phosphatases with a mostly demyelinating phenotype with focal hypermyelination. CMT4B1 is caused by

loss-of-function mutations in the catalytically active MTMR2, whereas CMT4B2 and CMT4B3 are caused by mutations in catalytically inactive MTMR13 and MTMR5, respectively (Bolino et al., 2000; Berger et al., 2002; Robinson and Dixon, 2005). MTMR2 dephosphorylates PI_3P (mainly present on early endosomes) to PI, and $PI_{3,5}P_2$ (mainly present on late endosomes) to PI_5P. MTMR5 and MTMR13 directly interact with active MTMR2 and increase its catalytic activity as well as recruit MTMR2 to membrane compartments (Kim et al., 2003; Robinson and Dixon, 2005). Due to faulty phosphatase activity, PI_3P and $PI_{3,5}P_2$ are predicted to accumulate on endosomes in CMT4B.

As discussed above, phosphoinositides are an important regulator of many steps along the intracellular trafficking pathway, as well as of myelination. Therefore, it is of no surprise that several studies have found effects of CMT4B mutations in many different aspects of the intracellular pathways. Even though expression of MTMR in Schwann cells is very low (Berger et al., 2002), mutations in Schwann cells is sufficient to induce CMT4B-like pathology (Bolis et al., 2005).

A study in cortical neurons has located MTMR2 to synapses by interaction with PSD95. Here, MTMR2 seems to function as a negative regulator of endocytosis, as the uptake of AMPAR subunit GluR2 increases upon loss of functional protein (Lee et al., 2010). As MTMR2 has been shown to interact with SAP97/Dlg1 a part of the PSD family in Schwann cells, it is plausible for MTMR to play a regulatory role of endocytosis in Schwann cells (Bolino et al., 2004). Whether this process contributes to the pathology remains to be answered.

Further, loss of MTMR2 promotes the sorting of internalized AMPA receptors to lysosomes, indicating that active MTMR2 plays a role in preventing AMPA degradation, possibly by initiating a recycling pathway (Lee et al., 2010). However, in epithelial cells, knockdown or overexpression of MTMR2 leads to a blockage of EGFR degradation *in vitro* in two different studies, implicating MTMR directly in the degradative pathway (Cao et al., 2008; Berger et al., 2011). Further, MTMR2 shows binding to PI3K adaptor hVPS34/hVPS15 complex that also interacts with Rab7, indicating a possible link in pathology of CMT4B and CMT2B. Although the direct effect of CMT4B mutations on the degradative pathway are not shown, the general involvement of MTMR in the degradative pathway offers many possible pathomechanisms. Normally, MTMR2 recruits RME8 via PI_3P, which, in turn, regulates EGFR traffic from endosomes to lysosomes—a pathway that could be disrupted in CMT4B (Xhabija et al., 2011). Overall, CMT4B shows that misregulation of phospholipid composition can lead to disruptions in endocytosis, recycling and degradation. Since CMT4B shows predominantly demyelinating phenotypes, it will now be interesting to see how CMT4B mutations affect ErbB endocytosis, recycling and degradation in Schwann cells, considering that this is a major signaling pathway for myelination, as well as its downstream promyelinating PI3K/Akt signaling cascade. Interestingly, Akt levels were altered in sciatic nerve sections from MTMR2,13 knockout mice (Berger et al., 2011). The direct effect on phosphoinositide composition could alter the promyelinating signaling cascade and link the mutation to the demyelinating phenotype. [For a good review on ErB signaling and trafficking in CMT we refer the reader to Lee et al. (2017)].

Lastly, MTMR2 has been shown to interact with NEFL, indicating a common pathway could underlie the pathology causing CMT4B and CMT2E explaining the similar phenotypes observed (Previtali et al., 2003).

CMT4C

CMT4C, also an autosomal recessive disorder with an early onset, is characterized by hypomyelination. This hypomyelination is caused by both, nonsense and missense mutations in the *SH3TC2* gene leading to a loss of function (Senderek et al., 2003). Over 20 different mutations have been reported to date. SH3TC2 is expressed in Schwann cells but not neurons of the PNS (Vijay et al., 2016). Although its exact molecular mechanism has not been identified, SH3TC2 has been implicated in the ErbB-neuregulin1 signaling axis, a crucial pathway for PNS myelination. Neuregulin1 binds ErB3, which activates ErbB2. This receptor complex is internalized for downstream promyelin-signaling (Di Guglielmo et al., 1994; Zastrow and Sorkin, 2007; Birchmeier and Bennett, 2016). It has been proposed that SH3TC2 plays a role in endocytosis, as ErbB2 internalization is reduced in SH3TC2 knockout Schwann cells. Moreover, overexpression of SH3TC2 increased internalization of ErbB2, co-immunoprecipitated with ErbB2 and is co-internalized with it upon stimulation (Gouttenoire et al., 2013). To date, the molecular role of SH3TC2 in endocytosis remains undetermined. CMT4C mutations of SH3TC2 impair the localization of SH3TC2 to the plasma membrane (Lupo et al., 2009) and impair ErbB2 uptake in Schwann cells (Gouttenoire et al., 2013). These findings indicate a role for SH3TC2 in receptor uptake and that endocytic dysfunctions in CMT mutants contribute to the pathology. However, many more roles of SH3TC2 at different stages of the endolysosomal pathway have arisen that may contribute to the pathology seen in CMT4C.

Besides localizing to the plasma membrane, SH3TC2 is found on recycling endosomes (the perinuclear recycling compartment in Schwann cells) that bind to active Rab11 (Arnaud et al., 2009; Roberts et al., 2010; Stendel et al., 2010). Interestingly, CMT4C mutants of SH3TC2 showed no interaction with Rab11 and no localization to recycling endosomes. In HeLa cells, mutant SH3TC2 has been shown to promote the recycling of the transferrin receptor (TfR) back to the plasma membrane, whereas transient expression of WT SH3TC2 decreased TfR recycling (Roberts et al., 2010). This suggests that SH3TC2 either acts as a competitor to TfR recycling or negatively regulates the recycling of TfR directly and that this is disrupted by the CMT4C mutations. Lastly, the SH3TC2 mutants show decreased myelin protein synthesis in Schwann cells and dominant negative Rab11 has been shown to lead to myelin defects *in vitro*, whereas constitutively active Rab11 increased myelination (Stendel et al., 2010). This indicates a direct role of Rab11 in the myelination process and therefore a likely role for its effector SH3TC2. Vijay et al. have identified Integrinα6 as a SH3TC2 associated protein in retinal pigment epithelial cells. Integrinα6 is a laminin receptor known to

recycle via Rab11 endosomes involved in maintaining structural integrity of the myelin sheath (Vijay et al., 2016). It would be interesting to see if the recycling of ErB and Integrinα6 is also disrupted by the CMT4C mutations, as ErB2 depends on rapid recycling for proper signaling. Further, it remains to be dissected, whether the effects described for SH3TC2 affecting endocytosis and recycling are shared effects of the same pathway or separate pathways.

CMT4D

CMT4D is a demyelinating, autosomal recessive type of the disorder caused by a mutation in N-myc downstream regulated 1 (NDRG1; Kalaydjieva et al., 2000).The most common truncation mutation (R148X) leads to a loss of function showing similar phenotypes as complete deletion of the protein (King et al., 2011). Its high and exclusive expression in Schwann cells in the PNS suggest a Schwann cell specific role, although the precise role remains to be determined (Okuda et al., 2004). In prostate cancer cell lines, NDRG1 was identified as a Rab4 effector protein. NDRG1 was shown to be involved in the fast recycling of TfR, as recycling was slowed down when NDRG1 was knocked down. Further, NDRG1 binds PI_4P but is recruited to endosomes independently of its effector Rab4 (Kachhap et al., 2007). Yet overexpression of mutant NDRG1 with Rab4 in HeLa cells resulted in enlarged Rab4 endosomes compared to WT NDRG1 (Li et al., 2017). In cancer cell lines, NDRG1 is involved in recycling of e-cadherin (Kachhap et al., 2007). This leads to speculate that other recycling pathways specific to Schwann cell myelination and Schwann cell/axonal communication might be disrupted by loss of NDRG1 function. Recycling of both, ErbB and the low density lipoprotein (LDL) receptor are significantly reduced in CMT4D (Pietiäinen et al., 2013). Investigating this abnormality in LDL receptor recycling showed that NDRG1 has a role as a negative regulator of receptor degradation. The observation of decreased LDL receptor recycling led to the hypothesis that NDRG1 normally prevents ubiquitination of LDL receptor, leading to its recycling back to the plasma membrane. When NDRG1 is dysfunctional, LDL receptor is marked for degradation, therefore the receptor is not recycled back to the plasma membrane. This leads to a shortage of receptors available for endocytosis and thus a shortage of LDL (Pietiäinen et al., 2013). In addition, this experimental set up also showed a second effect of NDRG1 depletion: abnormal endosomal maturation. LDL receptors were found to be trapped in MVBs. These MVBs showed an increased number of ILVs (despite a downregulation of ESCRT proteins), yet were still positive for early endosomal marker EEA1, indicating disturbed endosomal maturation. This phenotype in combination with the observed slowed degradation of LDL receptor indicates a delayed fusion of MVBs with lysosomes. Prenylated Rab Acceptor 1 protein (PRA1) was identified as a NDRG1 interactor (King et al., 2011) and overexpression of PRA1 was able to partially rescue LDL receptor phenotype of NDRG1 depletion (Pietiäinen et al., 2013). PRA1 regulates several Rab GTPases including Rab4, Rab5, Rab7, and Rab9 (Bucci et al., 1999). Since Rabs are key players in intracellular trafficking, it is likely that dysregulation of PRA1 contributes to the pathomechanism of delayed lysosomal fusion. However, how PRA1 function is altered by the loss of function in *NDRG1* remains to be investigated.

Interestingly, NDRG1 showed interaction with ApoA1 and A2, both are proposed to be involved in Schwann cell lipid trafficking (Hunter et al., 2005). Whether a parallel recycling effect based on NDRG1s interaction with Rab4 is involved, how NDRG1 functions as a ubiquitin inhibitor and what mechanisms are altered by PRA1 activity in CMT4D are all questions that remain to be answered.

CMT4H

Another autosomal recessive, early onset disorder is CMT4H caused by mutations in the *FGD4* gene encoding FYVE, RhoGEF and PH domain containing protein 4 (FGD4) (Delague et al., 2007). Over 20 mutations have been reported so far, many of which result in a truncated and loss of function mutation or missense mutations in the PI-recognition domains (two PH domains recognize $PI_{3,4,5}P_3$, $PI_{4,5}P_2$, and $PI_{3,4}P_2$, FYVE domain binds PI_3P) (Argente-Escrig et al., 2019). FGD4 is a GEF for the Rho GTPase Cdc42 and Rac1 (Obaishi et al., 1998; Umikawa et al., 1999). As deletion of Cdc42 in adult Schwann cells of mice shows a similar phenotype to adult deletion of FGD4 and levels of active Cdc42 are reduced in sciatic nerves of adult FGD4 knockouts as well as in cultured Schwann cells (Horn et al., 2012), the Cdc42 pathway is probably disrupted in CMT4H. Even though CMT4H is an early onset disorder and FGD4 expression in Schwann cells is required for proper myelin development it is also important for myelin maintenance as an induced knockout in adult Schwann cells leads to myelin defects. Interestingly and tying FGD4 to the endocytic section of this review: depletion of endogenous FGD4 inhibits the internalization of TfR in rat Schwann cells (Horn et al., 2012). Unfortunately, the molecular mechanism of FGD4's involvement in endocytosis is still unknown. However, Cdc42 has a proposed role in endocytosis, by enabling clathrin mediated endocytosis via actin polymerization (Yang et al., 2001; Bu et al., 2010). This observation opens up the possibility that other internalization processes i.e., ErbB are disrupted leading to the pathology.

When overexpressed in rat motoneurons or rat RT4 schwannoma cells, wild type FGD4 co-localized with f-actin in the growth cone and tips of neurites and increased the number of filopodia-like microspikes. Overexpression of truncated FGD4, still revealed colocalization with f-actin, but showed a reduced number of microspikes with altered curly morphology (Delague et al., 2007). This observation indicates that FGD4 plays a role in the structural organization of microfilaments during cellular growth, which is possibly disrupted by the loss of function mutations in CMT4H. Further, Cdc42 has been implicated in the reorganization of the cytoskeleton (Daub et al., 2001; Nakanishi and Takai, 2008; Li et al., 2021). However, no abnormalities in the organization of microfilaments or microtubules were observed in patient fibroblasts (Delague et al., 2007). It is possible that changes unnoticed in fibroblasts are detrimental for neurons or Schwann cells, considering their long and polarized structure.

CMT4J

CMT4J is caused by a partial loss-of-function mutation on FIG4 phosphoinositide 5-phosphatase (FIG4), a ubiquitously expressed phosphoinositide 5 phosphatase, dephosphorylating $PI_{3,5}P_2$ to PI_3P. CMT4J is a neuropathy with myelin defects and axonal loss in the periphery caused by a compound heterozygotic combination of a missense allele with a null allele. A loss of FIG4 function, counterintuitively, decreases the levels of $PI_{3,5}P_2$ (Chow et al., 2007), as FIG4 also activates PIKFYVE, a PI5K on endosomes (Rudge et al., 2004). The CMT mutant of FIG4 is not stabilized, leading to protein instability and reduced levels of FIG4 (Lenk et al., 2011). In FIG4 deficient cells, lysosomes and endosomes are enlarged, showing that a tight PI regulation is important for proper endosome maturation and following fusion with lysosomes. Interestingly, this phenotype can be rescued in drosophila by overexpression of an enzymatically inactive FIG4, indicating that its loss of function goes beyond its phosphatase activity (Bharadwaj et al., 2016). FIG4 also interacts with MTMR2 in neurons and Schwann cells, indicating a shared pathomechanism in CMT4B and CMT4J. As they both have an effect on $PI_{3,5}P_2$, in Schwann cells the loss of FIG4 function in MTMR2 null mice rescues the myelin outfolding phenotype. As the loss of MTMR2 leads to more $PI_{3,5}P_2$, the reduction of FIG4 and therefore the decrease in PIKFYVE reduces levels of $PI_{3,5}P_2$ (Vaccari et al., 2011). The overlap of these two CMT subtypes working on a shared pathway are a great opportunity to figure out the downstream changes of altered $PI_{3,5}P_2$ levels leading to the pathology and should be investigated in more detail. *In vivo,* conditional inactivation of FIG4 lead to axonal degeneration and Schwann cell demyelination, possibly by a defective transport of cholesterol (Vaccari et al., 2015). Further, altered levels of autophagic markers were observed in neurons and astrocytes of mice models of CMT4J. These altered levels indicate a decrease in autophagic flux, proposed to be due to defective fusion with lysosomes (Ferguson et al., 2009; Vaccari et al., 2015).

CMT1X

CMT1X is caused by mutations in the *GJB1* gene located on the X chromosome encoding Gap junction protein beta 1 (GJB1) also known as Connexin32 (Cnx32) (Bergoffen et al., 1993). Over 400 mutations have been reported to cause CMT1X, with many of them being loss of function mutations, where WT GJB1 normally forms gap junctions in the peripheral nerve ensuring intercellular communication (Kleopa et al., 2012). Abnormal trafficking has been reported for CMT1X in two ways. First, mutant GJB1 is not properly trafficked anterogradely to the plasma membrane. Instead, mutant GJB1accumulates in the endoplasmic reticulum or Golgi leading to a lack of intercellular gap junctions (Deschênes et al., 1997; Yum et al., 2002; Abrams et al., 2003; Kleopa et al., 2006). However, some mutant forms of GJB1 form functional gap junctions indicating a second, parallel pathogenic mechanisms (Castro et al., 1999). Vavlitou et al. (2010) have shown that lack of GJB1 can cause defects in axonal retrograde transport and neurofilament abnormalities before onset of demyelination in mice. Neurofilaments were more densely packed and dephosphorylated in the absence of GJB1, probably leading to deficient axonal transport as indicated by the accumulation of dynein and other markers usually transported along the axon (Vavlitou et al., 2010). Although direct evidence for trafficking defects is missing this indicates a pathomechanism beyond the lack of gap junctions that requires further investigation as to how GJB1 affects neurofilaments and thus trafficking, especially if the trafficking of receptor tyrosine kinases is altered by the neurofilament abnormalities observed. A potentially common pathway could be the altered MEK-ERK signaling observed in GJB1 deficient Schwann cells leading to altered expression profiles of MEK-ERK regulated proteins (Groh et al., 2010).

With all studies targeting the experimental questions using specific approaches (e.g., looking at one receptor or one specific downstream protein related to the affected GEFs), it would be interesting to set up comparative studies between the CMT subtypes targeting potential shared proteins. This would help to reveal if there are common denominators affected.

DEMYELINATING CMT

CMT1A

Also prominently demyelinating subtypes of CMT have shown several transport deficits (**Figure 2**). CMT1A is the most common cause of CMT, an autosomal dominant type caused by a duplication of the gene encoding peripheral myelin protein 22 (PMP22), leading to overexpression and aggregation. Even though not the focus of many studies, intracellular transport is heavily involved in the processing of PMP22 in several aspects. For example, a prominent pathway in the degradation of misfolded proteins and aggregates is autophagy. With the observation of an increase in misfolded PMP22 and its aggregates, it is reasonable to speculate that autophagy plays an important role in protein clearance of CMT1A. Patient derived fibroblasts show increased levels of autophagic markers (Lee et al., 2018). Indeed, autophagy activation by rapamycin was shown to improve myelination in demyelinating CMT mouse DRG cultures (Rangaraju et al., 2010) and in mice (Nicks et al., 2014). Further, a recent study by Marinko et al. shows that the expression of PMP22 is negatively correlated to the trafficking of newly synthetized PMP22 to the plasma membrane. When too much PMP22 is expressed, the proteasomes of the ER's membrane protein quality control become saturated as most of PMP22 is very unstable and needs to be degraded. Upon saturation of the proteasomes, misfolded PMP22 is accumulating and aggregating, leading to a decrease of functional PMP22 being trafficked to the plasma membrane, ultimately leading to demyelination (D'Urso et al., 1998; Marinko et al., 2020). Increasing autophagy can lessen the burden of proteasomes and thus increase PMP22 transport to the plasma membrane, showing how trafficking defects in Schwann cells as secondary mechanisms can lead to demyelination (Fortun et al., 2007; Rangaraju et al., 2010). Further, in patient nerves increased levels of ErbB2/3 were found in Schwann cells, this could potentially mean a defective

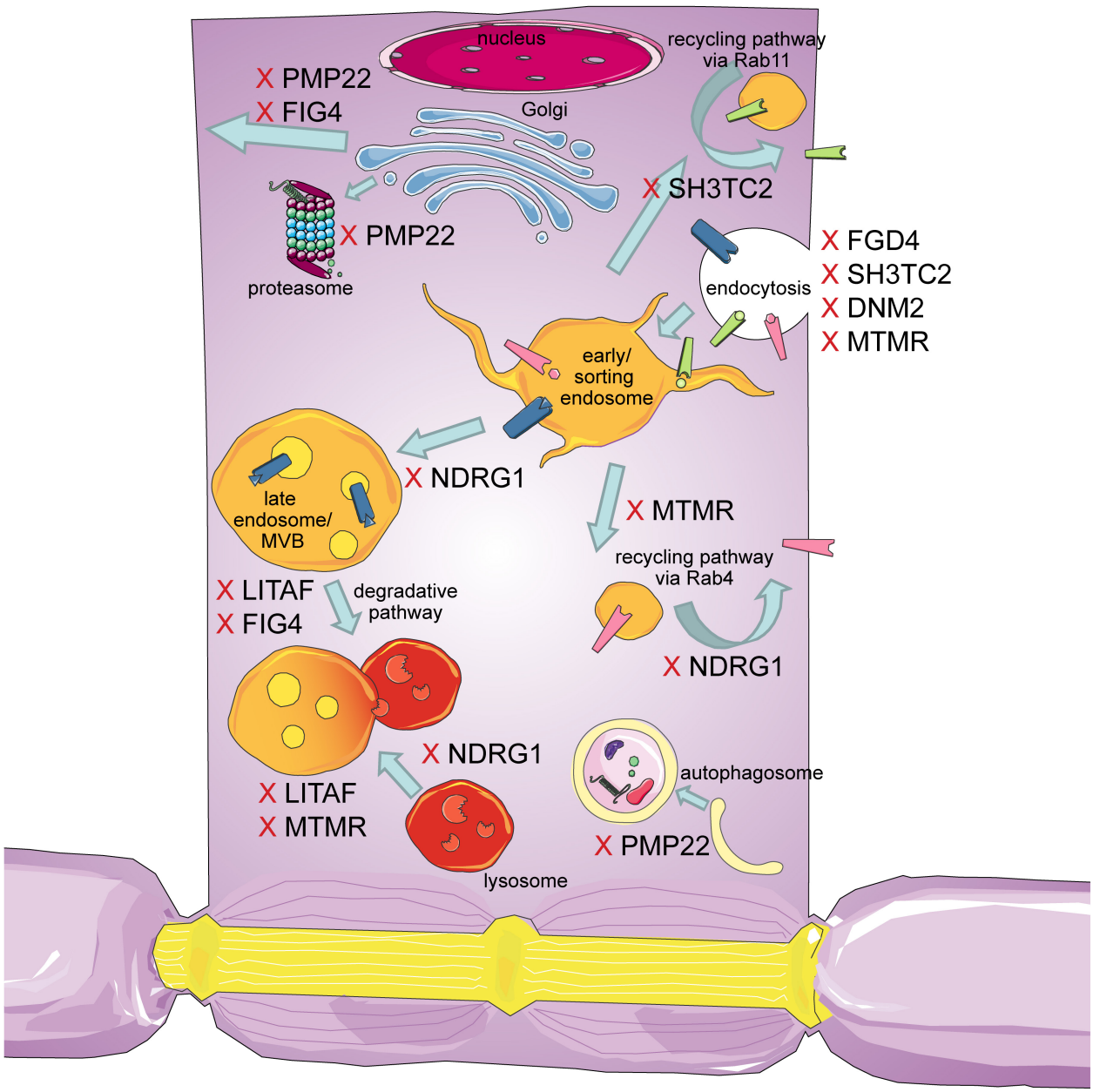

FIGURE 2 | Schematic overview of the intracellular trafficking processes in a myelinating Schwann cell. Highlighting all the steps where proteins involved in CMT can cause dysregulation. This figure was created using Servier Medical Art templates, which are licensed under a Creative Commons Attribution 3.0 Unported License; https://smart.servier.com.

degradation pathway (Massa et al., 2006). Whether the possible defect in degradation is a secondary effect due to a saturated autophagic system or a parallel defect remains to be investigated. Interestingly, early studies report axonal transport defects in mice with mutated PMP22 showing slowed axonal transport of neurofilaments, decreased microtubule stability and abnormal neurofilament phosphorylation opening up the possibility of secondary trafficking defects in demyelinated neurons (De Waegh and Brady, 1990; de Waegh et al., 1992).

CMT1C

In autosomal dominant CMT1C point mutations in *LITAF*, also known as *SIMPLE*, are identified to cause the disease (Street et al., 2003). *LITAF* encodes a 161 amino acid protein (Lipopolysaccharide-induced tumor necrosis factor-alpha factor) with one transmembrane domain that is inserted to the membrane post-translationally, all mutations occur in this domain. Therefore, mutated LITAF no longer localizes to endosomes but is cytosolic (Lee et al., 2011). LITAF interacts with

STAM1, Hrs and TSG101, ESCRT proteins of the degradative pathway (Lee et al., 2012). The cytosolic mutant competes with endosomally located LITAF for Hrs, leading to deficient Hrs recruitment to endosomes and a lack of ESCRT recruitment. This lack of recruitment has been shown to decrease EGFR degradation leading to prolonged ERK1/2 signaling. Late endosomes/lysosomes are enlarged in patients' fibroblasts, similarly to the phenotype reported for mutant FIG4 in CMT4J showing a defect in the degradative pathway (Edgar et al., 2020). By activating cation channel TRPML1, a homeostasis regulator of lysosomes in mammalian cells, the authors were able to rescue the vacuolar phenotype of both LITAF or FIG4 knockout cells demonstrating a common pathway. It will be essential to unravel how the enlarged endolysosomes in both CMT types lead to the pathology. A possibility offers deficient ErbB3 degradation that has been shown in CMT mutants also leading to prolonged ERK1/2 signaling and demyelination (Lee et al., 2012).

An overall summary of how genes causing CMT affect trafficking in Schwann cells is shown in **Figure 2**.

TREATMENTS

Currently there is no cure for CMT, nor is there a treatment that addresses the specific phenotypes of CMT. Patients can only battle the disorder with physical and occupational therapies, as well as with pain-relief medication or surgeries to cope with the symptoms. Pinpointing the specific disruption in intracellular transport can help to identify new therapeutic targets, for current therapeutic prospects in CMT, we refer to two excellent recent reviews (Beijer et al., 2019; Morena et al., 2019). However, since axonal transport is disrupted in many subtypes of CMT, we briefly want to discuss the potential of HDAC6 inhibitors as a treatment for CMT.

HDAC6 inhibitor treatment alleviates many of the trafficking phenotypes in several models of different CMT types. HDAC6 deacetylates tubulin, making it unstable. By inhibiting HDAC6, tubulin remains more stable, which improves the basis for intracellular transport. Other targets of HDAC6's deacteylation function include heat shock protein 90, cortactin and Miro1, linking it to the elimination process of misfolded proteins and mitochondrial transport. HDAC6 is also proposed to play a role in response to eliminate misfolded proteins independent of its deacetylation function. It shows a high binding affinity for ubiquitinated proteins and can interact with dynein motor proteins directly. Especially in different CMT2 types HDAC6 inhibitors have been shown to be beneficial (for a review please see Rossaert and Van Den Bosch, 2020). For example, treatment with HDAC6 inhibitor partially rescued phenotypes displayed by mice with mutant HSPB1, models for CMT2F (D'Ydewalle et al., 2011). But also in mice modeling CMT2D (caused by mutated GlyRS) the treatment with HDAC6 inhibitor has been shown to restore function (Benoy et al., 2018; Mo et al., 2018). Due to its direct interaction with Miro1 HDAC6 inhibitor was also tested as a treatment for CMT2A in a mouse model, where it even rescued motor dysfunction when given after symptom onset, giving it great therapeutic potential (Picci et al., 2020). Its role in misfolded protein clearance has shown a promising treatment strategy for CMT1A, where an HDAC6 inhibitor leads to improved nerve integrity as well as improved motor behavior in C22 mice (Ha et al., 2020). Overall, HDAC6's inhibitors are shown to be promising therapeutic targets for several CMT subtypes that are currently being developed (Shen and Kozikowski, 2020). The beneficial effect of HDAC6 inhibitors on different CMT subtypes also shifts HDAC6's involvement in the pathogenesis into focus of future research, also in the subtypes not yet explored. To develop new therapeutic strategies and model systems we refer to an excellent review by the Timmerman lab, highlighting recent advances in modeling CMT (Juneja et al., 2019).

CONCLUDING REMARKS

Overall, it is fascinating to see that mutations in very diverse proteins can all lead to similar defects in intracellular transport. Whether the mutations cause a direct defect in traffic by affecting the stability of the cytoskeleton, or whether the trafficking defects are secondary due to disrupted signaling (which ultimately also affects the stability of the cytoskeleton) remains to be elucidated for many CMT subtypes. Here we tried to give enough detailed insights into the different trafficking defects observed to encourage more studies that investigate similar defects in multiple CMT disorders for better comparability in the search for a common denominator and to look at the system of intracellular transport as a highly fluid and dynamic system. The sheer number of results indicating trafficking defects in all the different CMT subtypes is a solid basis to suspect abnormal trafficking as the underlying pathomechanism. However, many studies that claim trafficking defects only look at static data and lack comparability with each other. More experiments generally looking at cytoskeletal integrity, mitochondrial transport, retrograde transport of receptors, recycling and degradation for each subtype are needed for a holistic approach to CMT pathology as well as, checking phenotypes reported for one subtype in the others. This also applies for CMT subtypes not mentioned in this review that have, as of yet, no or less reported trafficking phenotypes.

AUTHOR CONTRIBUTIONS

RM wrote the first draft of the manuscript and prepared the figures. KB and MB reviewed and edited the manuscript. All authors contributed to the article and approved the submitted version.

FUNDING

This work was funded by the Deutsche Forschungsgemeinschaft (DFG) (Grant No. 427899738) and the Forschungsförderung of the University Medical Center Göttingen to KB.

REFERENCES

Abrams, C. K., Freidin, M., Bukauskas, F., Dobrenis, K., Bargiello, T. A., Verselis, V. K., et al. (2003). Pathogenesis of X-linked Charcot-Marie-tooth disease: differential effects of two mutations in Connexin 32. *J. Neurosci.* 23, 10548–10558. doi: 10.1523/jneurosci.23-33-10548.2003

Ackerley, S., James, P. A., Kalli, A., French, S., Davies, K. E., and Talbot, K. (2006). A mutation in the small heat-shock protein HSPB1 leading to distal hereditary motor neuronopathy disrupts neurofilament assembly and the axonal transport of specific cellular cargoes. *Hum. Mol. Genet.* 15, 347–354. doi: 10.1093/hmg/ddi452

Adebola, A. A., Di Castri, T., He, C. Z., Salvatierra, L. A., Zhao, J., Brown, K., et al. (2015). Neurofilament light polypeptide gene N98S mutation in mice leads to neurofilament network abnormalities and a Charcot-Marie-Tooth Type 2E phenotype. *Hum. Mol. Genet.* 24, 2163–2174. doi: 10.1093/hmg/ddu736

Adell, M. A. Y., Vogel, G. F., Pakdel, M., Müller, M., Lindner, H., Hess, M. W., et al. (2014). Coordinated binding of Vps4 to ESCRT-III drives membrane neck constriction during MVB vesicle formation. *J. Cell Biol.* 205, 33–49. doi: 10.1083/jcb.201310114

Almeida-Souza, L., Asselbergh, B., d'Ydewalle, C., Moonens, K., Goethals, S., de Winter, V., et al. (2011). Small heat-shock protein HSPB1 mutants stabilize microtubules in Charcot-Marie-Tooth neuropathy. *J. Neurosci.* 31, 15320–15328. doi: 10.1523/JNEUROSCI.3266-11.2011

Antonellis, A., Ellsworth, R. E., Sambuughin, N., Puls, I., Abel, A., Lee-Lin, S. Q., et al. (2003). Glycyl tRNA synthetase mutations in Charcot-Marie-Tooth disease type 2D and distal spinal muscular atrophy type V. *Am. J. Hum. Genet.* 72, 1293–1299. doi: 10.1086/375039

Argente-Escrig, H., Sánchez-Monteagudo, A., Frasquet, M., Millet-Sancho, E., Martínez-Rubio, M. D., Pitarch, I., et al. (2019). A very mild phenotype of Charcot-Marie-Tooth disease type 4H caused by two novel mutations in FGD4. *J. Neurol. Sci.* 402, 156–161. doi: 10.1016/j.jns.2019.05.015

Arnaud, E., Zenker, J., de Preux Charles, A.-S., Stendel, C., Roos, A., Médard, J. J., et al. (2009). SH3TC2/KIAA1985 protein is required for proper myelination and the integrity of the node of Ranvier in the peripheral nervous system. *Proc. Natl. Acad. Sci. U.S.A.* 106, 17528–17533. doi: 10.1073/pnas.1011320107

Bache, K. G., Brech, A., Mehlum, A., and Stenmark, H. (2003). Hrs regulates multivesicular body formation via ESCRT recruitment to endosomes. *J. Cell Biol.* 162, 435–442. doi: 10.1083/jcb.200302131

Bakker, J., Spits, M., Neefjes, J., and Berlin, I. (2017). The EGFR odyssey – from activation to destruction in space and time. *J. Cell Sci.* 130, 4087–4096. doi: 10.1242/jcs.209197

Baloh, R. H., Schmidt, R. E., Pestronk, A., and Milbrandt, J. (2007). Altered axonal mitochondrial transport in the pathogenesis of Charcot-Marie-Tooth disease from mitofusin 2 mutations. *J. Neurosci.* 27, 422–430. doi: 10.1523/JNEUROSCI.4798-06.2007

BasuRay, S., Mukherjee, S., Romero, E. G., Seaman, M. N. J., and Wandinger-Ness, A. (2013). Rab7 mutants associated with Charcot-Marie-Tooth disease cause delayed growth factor receptor transport and altered endosomal and nuclear signaling. *J. Biol. Chem.* 288, 1135–1149. doi: 10.1074/jbc.M112.417766

Basuray, S., Mukherjee, S., Romero, E., Wilson, M. C., and Wandinger-Ness, A. (2010). Rab7 mutants associated with charcot-Marie-tooth disease exhibit enhanced NGF-stimulated signaling. *PLoS One* 5:e15351. doi: 10.1371/journal.pone.0015351

Beijer, D., Sisto, A., Van Lent, J., Baets, J., and Timmerman, V. (2019). Defects in axonal transport in inherited neuropathies. *J. Neuromuscul. Dis.* 6, 401–419. doi: 10.3233/JND-190427

Belgrad, J., de Pace, R., and Douglas Fields, R. (2020). Autophagy in myelinating glia. *J. Neurosci.* 40, 256–266. doi: 10.1523/JNEUROSCI.1066-19.2019

Benoy, V., Van Helleputte, L., Prior, R., D'Ydewalle, C., Haeck, W., Geens, N., et al. (2018). HDAC6 is a therapeutic target in mutant GARS-induced Charcot-Marie-Tooth disease. *Brain* 141, 673–687. doi: 10.1093/brain/awx375

Berger, P., Bonneick, S., Willi, S., Wymann, M., and Suter, U. (2002). Loss of phosphatase activity in myotubularin-related protein 2 is associated with Charcot-Marie-Tooth disease type 4B1. *Hum. Mol. Genet.* 11, 1569–1579. doi: 10.1093/hmg/11.13.1569

Berger, P., Tersar, K., Ballmer-Hofer, K., and Suter, U. (2011). The CMT4B disease-causing proteins MTMR2 and MTMR13/SBF2 regulate AKT signalling. *J. Cell. Mol. Med.* 15, 307–315. doi: 10.1111/j.1582-4934.2009.00967.x

Bergoffen, J., Scherer, S. S., Wang, S., Oronzi Scott, M., Bone, L. J., Paul, D. L., et al. (1993). Connexin mutations in X-linked Charcot-Marie-Tooth disease. *Science* 262, 2039–2042. doi: 10.1126/science.8266101

Bernard-Marissal, N., Van Hameren, G., Juneja, M., Pellegrino, C., Louhivuori, L., Bartesaghi, L., et al. (2019). Altered interplay between endoplasmic reticulum and mitochondria in Charcot-Marie-Tooth type 2A neuropathy. *Proc. Natl. Acad. Sci. U.S.A.* 116, 2328–2337. doi: 10.1073/pnas.1810932116

Bharadwaj, R., Cunningham, K. M., Zhang, K., and Lloyd, T. E. (2016). FIG4 regulates lysosome membrane homeostasis independent of phosphatase function. *Hum. Mol. Genet.* 25, 681–692. doi: 10.1093/HMG/DDV505

Birchmeier, C., and Bennett, D. L. H. (2016). *Neuregulin/ErbB Signaling in Developmental Myelin Formation and Nerve Repair*, 1st Edn. Amsterdam: Elsevier Inc. doi: 10.1016/bs.ctdb.2015.11.009

Bird, T. D. (2020). "Charcot-Marie-Tooth (CMT) hereditary neuropathy overview 1. Clinical characteristics of Charcot-Marie-Tooth (CMT) hereditary neuropathy," in *GeneReviews*, eds M. P. Adam, H. H. Ardinger, R. A. Pagon, S. E. Wallace, L. J. H. Bean, G. Mirzaa, et al. (Seattle, WA: University of Washington), 1–22.

Boland, B., Kumar, A., Lee, S., Platt, F. M., Wegiel, J., Yu, W. H., et al. (2008). Autophagy induction and autophagosome clearance in neurons: relationship to autophagic pathology in Alzheimer's disease. *J. Neurosci.* 28, 6926–6937. doi: 10.1523/JNEUROSCI.0800-08.2008

Bolino, A., Bolis, A., Previtali, S. C., Dina, G., Bussini, S., Dati, G., et al. (2004). Disruption of Mtmr2 CMT4B1-like neuropathy with myelin outfolding and impaired spermatogenesis. *J. Cell Biol.* 167, 711–721. doi: 10.1083/jcb.200407010

Bolino, A., Muglia, M., Conforti, F. L., LeGuern, E., Salih, M. A. M., Georgiou, D. M., et al. (2000). Charcot-Marie-Tooth type 4B is caused by mutations in the gene encoding myotubularin-related protein-2. *Nat. Genet.* 25, 17–19. doi: 10.1038/75542

Bolis, A., Coviello, S., Bussini, S., Dina, G., Pardini, C., Previtali, S. C., et al. (2005). Loss of Mtmr2 phosphatase in Schwann cells but not in motor neurons causes Charcot-Marie-Tooth type 4B1 neuropathy with myelin outfoldings. *J. Neurosci.* 25, 8567–8577. doi: 10.1523/JNEUROSCI.2493-05.2005

Bonifacino, J. S., and Hierro, A. (2011). Transport according to GARP: receiving retrograde cargo at the trans-Golgi network. *Trends Cell Biol.* 21, 159–167. doi: 10.1016/j.tcb.2010.11.003

Brownlees, J., Ackerley, S., Grierson, A. J., Jacobsen, N. J. O., Shea, K., Anderton, B. H., et al. (2002). Charcot-Marie-Tooth disease neurofilament mutations disrupt neurofilament assembly and axonal transport. *Hum. Mol. Genet.* 11, 2837–2844. doi: 10.1093/hmg/11.23.2837

Bu, W., Lim, K. B., Yu, Y. H., Chou, A. M., Sudhaharan, T., and Ahmed, S. (2010). Cdc42 interaction with N-WASP and Toca-1 regulates membrane tubulation, vesicle formation and vesicle motility: implications for endocytosis. *PLoS One* 5:e12153. doi: 10.1371/journal.pone.0012153

Bucci, C., Chiariello, M., Lattero, D., Maiorano, M., and Bruni, C. B. (1999). Interaction cloning and characterization of the cDNA encoding the human prenylated Rab acceptor (PRA1). *Biochem. Biophys. Res. Commun.* 258, 657–662. doi: 10.1006/bbrc.1999.0651

Bucci, C., Parton, R. G., Mather, I. H., Stunnenberg, H., Simons, K., Hoflack, B., et al. (1992). The small GTPase rab5 functions as a regulatory factor in the early endocytic pathway. *Cell* 70, 715–728. doi: 10.1016/0092-8674(92)90306-W

Cao, C., Backer, J. M., Laporte, J., Bedrick, E. J., and Wandinger-Ness, A. (2008). Sequential actions of myotubularin lipid phosphatases regulate endosomal PI(3)P and growth factor receptor trafficking. *Mol. Biol. Cell* 19, 3334–3346. doi: 10.1091/mbc.E08

Castro, C., Gómez-Hernandez, J. M., Silander, K., and Barrio, L. C. (1999). Altered formation of hemichannels and gap junction channels caused by C- terminal connexin-32 mutations. *J. Neurosci.* 19, 3752–3760. doi: 10.1523/jneurosci.19-10-03752.1999

Chauvet, S., Cohen, S., Yoshida, Y., Fekrane, L., Livet, J., Gayet, O., et al. (2007). Gating of Sema3e/PlexinD1 signaling by neuropilin-1 switches axonal repulsion to attraction during brain development. *Neuron* 56, 807–822. doi: 10.1016/j.neuron.2007.10.019

Chen, H., Detmer, S. A., Ewald, A. J., Griffin, E. E., Fraser, S. E., and Chan, D. C. (2003). Mitofusins Mfn1 and Mfn2 coordinately regulate mitochondrial fusion and are essential for embryonic development. *J. Cell Biol.* 160, 189–200. doi: 10.1083/jcb.200211046

Cheng, X. T., Zhou, B., Lin, M. Y., Cai, Q., and Sheng, Z. H. (2015). Axonal autophagosomes recruit dynein for retrograde transport through fusion with late endosomes. *J. Cell Biol.* 209, 377–386. doi: 10.1083/jcb.201412046

Chow, C. Y., Zhang, Y., Dowling, J. J., Jin, N., Adamska, M., Shiga, K., et al. (2007). Mutation of FIG4 causes neurodegeneration in the pale tremor mouse and patients with CMT4J. *Nature* 448, 68–72.

Cioni, J. M., Lin, J. Q., Holtermann, A. V., Koppers, M., Jakobs, M. A. H., Azizi, A., et al. (2019). Late endosomes act as mRNA translation platforms and sustain mitochondria in axons. *Cell* 176, 56–72.e15. doi: 10.1016/j.cell.2018.11.030

Cogli, L., Progida, C., Thomas, C. L., Spencer-Dene, B., Donno, C., Schiavo, G., et al. (2013). Charcot-Marie-Tooth type 2B disease-causing RAB7A mutant proteins show altered interaction with the neuronal intermediate filament peripherin. *Acta Neuropathol.* 125, 257–272. doi: 10.1007/s00401-012-1063-8

Colecchia, D., Stasi, M., Leonardi, M., Manganelli, F., Nolano, M., Veneziani, B. M., et al. (2018). Alterations of autophagy in the peripheral neuropathy Charcot-Marie-Tooth type 2B. *Autophagy* 14, 930–941. doi: 10.1080/15548627.2017.1388475

D'Urso, D., Prior, R., Greiner-Petter, R., Gabreëls-Festen, A. A. W. M., and Müller, H. W. (1998). Overloaded endoplasmic reticulum-golgi compartments, a possible pathomechanism of peripheral neuropathies caused by mutations of the peripheral myelin protein PMP22. *J. Neurosci.* 18, 731–740. doi: 10.1523/jneurosci.18-02-00731.1998

D'Ydewalle, C., Krishnan, J., Chiheb, D. M., Van Damme, P., Irobi, J., Kozikowski, A. P., et al. (2011). HDAC6 inhibitors reverse axonal loss in a mouse model of mutant HSPB1-induced Charcot-Marie-Tooth disease. *Nat. Med.* 17, 968–974. doi: 10.1038/nm.2396

Daub, H., Gevaert, K., Vandekerckhove, J., Sobel, A., and Hall, A. (2001). Rac/Cdc42 and p65PAK regulate the microtubule-destabilizing protein stathmin through phosphorylation at serine 16. *J. Biol. Chem.* 276, 1677–1680. doi: 10.1074/jbc.C000635200

De Brito, O. M., and Scorrano, L. (2008). Mitofusin 2 tethers endoplasmic reticulum to mitochondria. *Nature* 456, 605–610. doi: 10.1038/nature07534

De Jonghe, P., Mersivanova, I., Nelis, E., Favero, J. D., Martin, J. J., Van Broeckhoven, C., et al. (2001). Further evidence that neurofilament light chain gene mutations can cause Charcot-Marie-Tooth disease type 2E. *Ann. Neurol.* 49, 245–249. doi: 10.1002/1531-8249(20010201)49:2<245::AID-ANA45<3.0.CO;2-A

de Waegh, S. M., Lee, V. M. Y., and Brady, S. T. (1992). Local modulation of neurofilament phosphorylation, axonal caliber, and slow axonal transport by myelinating Schwann cells. *Cell* 68, 451–463. doi: 10.1016/0092-8674(92)90183-D

De Waegh, S., and Brady, S. T. (1990). Altered slow axonal transport and regeneration in a myelin-deficient mutant mouse: The trembler as an in vivo model for schwann cell-axon interactions. *J. Neurosci.* 10, 1855–1865. doi: 10.1523/jneurosci.10-06-01855.1990

Deinhardt, K., Salinas, S., Verastegui, C., Watson, R., Worth, D., Hanrahan, S., et al. (2006). Rab5 and Rab7 control endocytic sorting along the axonal retrograde transport pathway. *Neuron* 52, 293–305. doi: 10.1016/j.neuron.2006.08.018

Delague, V., Jacquier, A., Hamadouche, T., Poitelon, Y., Baudot, C., Boccaccio, I., et al. (2007). Mutations in FGD4 encoding the Rho GDP/GTP exchange factor FRABIN cause autosomal recessive Charcot-Marie-Tooth type 4H. *Am. J. Hum. Genet.* 81, 1–16. doi: 10.1086/518428

Delcroix, J. D., Valletta, J. S., Wu, C., Hunt, S. J., Kowal, A. S., and Mobley, W. C. (2003). NGF signaling in sensory neurons: evidence that early endosomes carry NGF retrograde signals. *Neuron* 39, 69–84. doi: 10.1016/S0896-6273(03)00397-0

Derivery, E., Sousa, C., Gautier, J. J., Lombard, B., Loew, D., and Gautreau, A. (2009). The Arp2/3 activator WASH controls the fission of endosomes through a large multiprotein complex. *Dev. Cell* 17, 712–723. doi: 10.1016/j.devcel.2009.09.010

Deschênes, S. M., Walcott, J. L., Wexler, T. L., Scherer, S. S., and Fischbeck, K. H. (1997). Altered trafficking of mutant connexin32. *J. Neurosci.* 17, 9077–9084. doi: 10.1523/jneurosci.17-23-09077.1997

Di Guglielmo, G. M., Baass, P. C., Ou, W. J., Posner, B. I., and Bergeron, J. J. M. (1994). Compartmentalization of SHC, GRB2 and mSOS, and hyperphosphorylation of Raf-1 by EGF but not insulin in liver parenchyma. *EMBO J.* 13, 4269–4277. doi: 10.1002/j.1460-2075.1994.tb06747.x

Dompierre, J. P., Godin, J. D., Charrin, B. C., Cordelières, F. P., King, S. J., Humbert, S., et al. (2007). Histone deacetylase 6 inhibition compensates for the transport deficit in Huntington's disease by increasing tubulin acetylation. *J. Neurosci.* 27, 3571–3583. doi: 10.1523/JNEUROSCI.0037-07.2007

Edgar, J. R., Ho, A. K., Laurá, M., Horvath, R., Reilly, M. M., Luzio, J. P., et al. (2020). A dysfunctional endolysosomal pathway common to two sub-types of demyelinating Charcot–Marie–Tooth disease. *Acta Neuropathol. Commun.* 8:165. doi: 10.1186/s40478-020-01043-z

Fabrizi, G. M., Cavallaro, T., Angiari, C., Cabrini, I., Taioli, F., Malerba, G., et al. (2007). Charcot-Marie-Tooth disease type 2E, a disorder of the cytoskeleton. *Brain* 130, 394–403. doi: 10.1093/brain/awl284

Ferguson, C. J., Lenk, G. M., and Meisler, M. H. (2009). Defective autophagy in neurons and astrocytes from mice deficient in PI(3,5)P2. *Hum. Mol. Genet.* 18, 4868–4878. doi: 10.1093/hmg/ddp460

Fortun, J., Verrier, J. D., Go, J. C., Madorsky, I., Dunn, W. A. J., and Notterpek, L. (2007). The formation of peripheral myelin protein 22 aggregates is hindered by the enhancement of autophagy and expression of cytoplasmic chaperones. *Neurobiol. Dis.* 25, 252–265.

Fransson, Å, Ruusala, A., and Aspenström, P. (2006). The atypical Rho GTPases Miro-1 and Miro-2 have essential roles in mitochondrial trafficking. *Biochem. Biophys. Res. Commun.* 344, 500–510. doi: 10.1016/j.bbrc.2006.03.163

Futter, C. E., Pearse, A., Hewlett, L. J., and Hopkins, C. R. (1996). Multivesicular endosomes containing internalized EGF-EGF receptor complexes mature and then fuse directly with lysosomes. *J. Cell Biol.* 132, 1011–1023. doi: 10.1083/jcb.132.6.1011

Gerber, D., Ghidinelli, M., Tinelli, E., Somandin, C., Gerber, J., Pereira, J. A., et al. (2019). Schwann cells, but not oligodendrocytes, depend strictly on dynamin 2 function. *Elife* 8:e42404. doi: 10.7554/eLife.42404

Glater, E. E., Megeath, L. J., Stowers, R. S., and Schwarz, T. L. (2006). Axonal transport of mitochondria requires milton to recruit kinesin heavy chain and is light chain independent. *J. Cell Biol.* 173, 545–557. doi: 10.1083/jcb.200601067

Goold, R. G., and Gordon-Weeks, P. R. (2003). NGF activates the phosphorylation of MAP1B by GSK3β through the TrkA receptor and not the p75NTR receptor. *J. Neurochem.* 87, 935–946. doi: 10.1046/j.1471-4159.2003.02062.x

Gorvel, J.-P., Chavrier, P., Zerial, M., and Gruenberg, J. (1991). rab5 controls early endosome. *Cell* 64, 915–925.

Gouttenoire, E. A., Lupo, V., Calpena, E., Bartesaghi, L., Schüpfer, F., Médard, J. J., et al. (2013). Sh3tc2 deficiency affects neuregulin-1/ErbB signaling. *Glia* 61, 1041–1051. doi: 10.1002/glia.22493

Groh, J., Heinl, K., Kohl, B., Wessig, C., Greeske, J., Fischer, S., et al. (2010). Attenuation of MCP-1/CCL2 expression ameliorates neuropathy in a mouse model for Charcot-Marie-Tooth 1X. *Hum. Mol. Genet.* 19, 3530–3543. doi: 10.1093/hmg/ddq269

Guernsey, D. L., Jiang, H., Bedard, K., Evans, S. C., Ferguson, M., Matsuoka, M., et al. (2010). Mutation in the gene encoding ubiquitin ligase LRSAM1 in patients with charcot-marie-tooth disease. *PLoS Genet.* 6:e1001081. doi: 10.1371/journal.pgen.1001081

Ha, N., Choi, Y. I, Jung, N., Song, J. Y., Bae, D. K., Kim, M. C., et al. (2020). A novel histone deacetylase 6 inhibitor improves myelination of Schwann cells in a model of Charcot–Marie–Tooth disease type 1A. *Br. J. Pharmacol.* 177, 5096–5113. doi: 10.1111/bph.15231

Hafezparast, M., Klocke, R., Ruhrberg, C., Marquardt, A., Ahmad-Annuar, A., Bowen, S., et al. (2003). Mutations in dynein link motor neuron degeneration to defects in retrograde transport. *Science* 300, 808–812. doi: 10.1126/science.1083129

Haglund, K., Sigismund, S., Polo, S., Szymkiewicz, I., Di Fiore, P. P., and Dikic, I. (2003). Multiple monoubiquitination of RTKs is sufficient for their endocytosis and degradation. *Nat. Cell Biol.* 5, 461–466. doi: 10.1038/ncb983

Haidar, M., Asselbergh, B., Adriaenssens, E., De Winter, V., Timmermans, J. P., Auer-Grumbach, M., et al. (2019). Neuropathy-causing mutations in

HSPB1 impair autophagy by disturbing the formation of SQSTM1/p62 bodies. *Autophagy* 15, 1051–1068. doi: 10.1080/15548627.2019.1569930

He, W., Bai, G., Zhou, H., Wei, N., White, N. M., Lauer, J., et al. (2015). CMT2D neuropathy is linked to the neomorphic binding activity of glycyl-tRNA synthetase. *Nature* 526, 710–714. doi: 10.1038/nature15510.CMT2D

Hopkins, C. R., and Trowbridge, I. S. (1983). Internalization and processing of transferrin and the transferrin receptor in human carcinoma A431 cells. *J. Cell Biol.* 97, 508–521. doi: 10.1083/jcb.97.2.508

Horn, M., Baumann, R., Pereira, J. A., Sidiropoulos, P. N. M., Somandin, C., Welzl, H., et al. (2012). Myelin is dependent on the Charcot-Marie-Tooth Type 4H disease culprit protein FRABIN/FGD4 in Schwann cells. *Brain* 135, 3567–3583. doi: 10.1093/brain/aws275

Horowitz, A., and Seerapu, H. R. (2012). Regulation of VEGF signaling by membrane traffic. *Cell Signal.* 24, 1810–1820. doi: 10.1016/j.cellsig.2012.05.007

Hunter, M., Angelicheva, D., Tournev, I., Ingley, E., Chan, D. C., Watts, G. F., et al. (2005). NDRG1 interacts with APO A-I and A-II and is a functional candidate for the HDL-C QTL on 8q24. *Biochem. Biophys. Res. Commun.* 332, 982–992. doi: 10.1016/j.bbrc.2005.05.050

Janssens, K., Goethals, S., Atkinson, D., Ermanoska, B., Fransen, E., Jordanova, A., et al. (2014). Human Rab7 mutation mimics features of Charcot-Marie-Tooth neuropathy type 2B in drosophila. *Neurobiol. Dis.* 65, 211–219. doi: 10.1016/j.nbd.2014.01.021

Johnson, L. S., Dunn, K. W., Pytowski, B., and McGraw, T. E. (1993). Endosome acidification and receptor trafficking: bafilomycin A1 slows receptor externalization by a mechanism involving the receptor's internalization motif. *Mol. Biol. Cell* 4, 1251–1266. doi: 10.1091/mbc.4.12.1251

Jordens, I., Fernandez-Borja, M., Marsman, M., Dusseljee, S., Janssen, L., Calafat, J., et al. (2001). The Rab7 effector protein RILP controls lysosomal transport by inducing the recruitment of dynein-dynactin motors. *Curr. Biol.* 11, 1680–1685. doi: 10.1016/S0960-9822(01)00531-0

Jovic, M., Sharma, M., Rahajeng, J., and Caplan, S. (2010). The early endosome: a busy sorting station for proteins at the crossroads. *Histol. Histopathol.* 25, 99–112. doi: 10.1007/s12020-009-9266-z.A

Juneja, M., Burns, J., Saporta, M. A., and Timmerman, V. (2019). Challenges in modelling the Charcot-Marie-Tooth neuropathies for therapy development. *J. Neurol. Neurosurg. Psychiatry* 90, 58–67. doi: 10.1136/jnnp-2018-318834

Kachhap, S. K., Faith, D., Qian, D. Z., Shabbeer, S., Galloway, N. L., Pili, R., et al. (2007). The N-Myc down regulated gene1 (NDRG1) is a Rab4a effector involved in vesicular recycling of E-cadherin. *PLoS One* 2:844. doi: 10.1371/journal.pone.0000844

Kalaydjieva, L., Gresham, D., Gooding, R., Heather, L., Baas, F., De Jonge, R., et al. (2000). N-myc downstream-regulated gene 1 is mutated in hereditary motor and sensory neuropathy-Lom. *Am. J. Hum. Genet.* 67, 47–58. doi: 10.1086/302978

Kalmar, B., Innes, A., Wanisch, K., Kolaszynska, A. K., Pandraud, A., Kelly, G., et al. (2017). Mitochondrial deficits and abnormal mitochondrial retrograde axonal transport play a role in the pathogenesis of mutant Hsp27-induced charcot marie tooth disease. *Hum. Mol. Genet.* 26, 3313–3326. doi: 10.1093/hmg/ddx216

Katzmann, D. J., Babst, M., and Emr, S. D. (2001). Ubiquitin-dependent sorting into the multivesicular body pathway requires the function of a conserved endosomal protein sorting complex, ESCRT-I. *Cell* 106, 145–155. doi: 10.1016/S0092-8674(01)00434-2

Kim, J. Y., Woo, S. Y., Hong, Y. B., Choi, H., Kim, J., Choi, H., et al. (2016). HDAC6 inhibitors rescued the defective axonal mitochondrial movement in motor neurons derived from the induced pluripotent stem cells of peripheral neuropathy patients with HSPB1 mutation. *Stem Cells Int.* 2016:9475981. doi: 10.1155/2016/9475981

Kim, S. A., Vacratsis, P. O., Firesteint, R., Clearyt, M. L., and Dixon, J. E. (2003). Regulation of myotubularin-related (MTMR)2 phosphatidylinositol phosphatase by MTMR5, a catalytically inactive phosphatase. *Proc. Natl. Acad. Sci. U.S.A.* 100, 4492–4497. doi: 10.1073/pnas.0431052100

King, R. H. M., Chandler, D., Lopaticki, S., Huang, D., Blake, J., Muddle, J. R., et al. (2011). Ndrg1 in development and maintenance of the myelin sheath. *Neurobiol. Dis.* 42, 368–380. doi: 10.1016/j.nbd.2011.01.030

Kiral, F. R., Kohrs, F. E., Jin, E. J., and Hiesinger, P. R. (2018). Rab GTPases and membrane trafficking in neurodegeneration. *Curr. Biol.* 28, R471–R486. doi: 10.1016/j.cub.2018.02.010

Kleopa, K. A., Abrams, C. K., and Scherer, S. S. (2012). How do mutations in GJB1 cause X-linked Charcot-Marie-Tooth disease? *Brain Res.* 1487, 198–205. doi: 10.1016/j.brainres.2012.03.068

Kleopa, K. A., Zamba-Papanicolaou, E., Alevra, X., Nicolaou, P., Georgiou, D. M., Hadjisavvas, A., et al. (2006). Phenotypic and cellular expression of two novel connexin32 mutations causing CMT1X. *Neurology* 66, 396–402. doi: 10.1212/01.wnl.0000196479.93722.59

Komatsu, M., Waguri, S., Koike, M., Sou, Y. S., Ueno, T., Hara, T., et al. (2007). Homeostatic levels of p62 control cytoplasmic inclusion body formation in autophagy-deficient mice. *Cell* 131, 1149–1163. doi: 10.1016/j.cell.2007.10.035

Konishi, Y., and Setou, M. (2009). Tubulin tyrosination navigates the kinesin-1 motor domain to axons. *Nat. Neurosci.* 12, 559–567. doi: 10.1038/nn.2314

Kvainickas, A., Jimenez-Orgaz, A., Nägele, H., Hu, Z., Dengjel, J., and Steinberg, F. (2017). Cargo-selective SNX-BAR proteins mediate retromer trimer independent retrograde transport. *J. Cell Biol.* 216, 3677–3693. doi: 10.1083/jcb.201702137

Lancaster, E., Li, J., Hanania, T., Liem, R., Scheideler, M. A., and Scherer, S. S. (2018). Myelinated axons fail to develop properly in a genetically authentic mouse model of Charcot-Marie-Tooth disease type 2E. *Exp. Neurol.* 308, 13–25. doi: 10.1016/j.expneurol.2018.06.010

Laser-Azogui, A., Kornreich, M., Malka-Gibor, E., and Beck, R. (2015). Neurofilament assembly and function during neuronal development. *Curr. Opin. Cell Biol.* 32, 92–101. doi: 10.1016/j.ceb.2015.01.003

Lauffer, B. E. L., Melero, C., Temkin, P., Lei, C., Hong, W., Kortemme, T., et al. (2010). SNX27 mediates PDZ-directed sorting from endosomes to the plasma membrane. *J. Cell Biol.* 190, 565–574. doi: 10.1083/jcb.201004060

Laurino, L., Wang, X. X., de la Houssaye, B. A., Sosa, L., Dupraz, S., Cáceres, A., et al. (2005). PI3K activation by IGF-1 is essential for the regulation of membrane expansion at the nerve growth cone. *J. Cell Sci.* 118, 3653–3663. doi: 10.1242/jcs.02490

Lee, H. W., Kim, Y., Han, K., Kim, H., and Kim, E. (2010). The phosphoinositide 3-phosphatase MTMR2 interacts with PSD-95 and maintains excitatory synapses by modulating endosomal traffic. *J. Neurosci.* 30, 5508–5518. doi: 10.1523/JNEUROSCI.4283-09.2010

Lee, S. M., Chin, L.-S., and Li, L. (2012). Charcot-Marie-Tooth disease-linked protein SIMPLE functions with the ESCRT machinery in endosomal trafficking. *J. Cell Biol.* 199, 799–816. doi: 10.1083/jcb.201204137

Lee, S. M., Chin, L.-S., and Li, L. (2017). Dysregulation of ErbB receptor trafficking and signaling in demyelinating Charcot-Marie-Tooth Disease. *Mol. Neurobiol.* 54, 87–100. doi: 10.1007/s12035-015-9668-2.Dysregulation

Lee, S. M., Olzmann, J. A., Chin, L. S., and Li, L. (2011). Mutations associated with Charcot-Marie-Tooth disease cause SIMPLE protein mislocalization and degradation by the proteasome and aggresome-autophagy pathways. *J. Cell Sci.* 124, 3319–3331. doi: 10.1242/jcs.087114

Lee, S., Bazick, H., Chittoor-Vinod, V., Al Salihi, M. O., Xia, G., and Notterpek, L. (2018). Elevated peripheral myelin protein 22, reduced mitotic potential, and proteasome impairment in dermal fibroblasts from Charcot-Marie-Tooth disease type 1A patients. *Am. J. Pathol.* 188, 728–738. doi: 10.1016/j.ajpath.2017.10.021

Lenk, G. M., Ferguson, C. J., Chow, C. Y., Jin, N., Jones, J. M., Grant, A. E., et al. (2011). Pathogenic mechanism of the FIG4 mutation responsible for charcot-marie-tooth disease CMT4J. *PLoS Genet.* 7:e1002104. doi: 10.1371/journal.pgen.1002104

Lerat, J., Magdelaine, C., Beauvais-Dzugan, H., Espil, C., Ghorab, K., Latour, P., et al. (2019). A novel pathogenic variant of NEFL responsible for deafness associated with peripheral neuropathy discovered through next-generation sequencing and review of the literature. *J. Peripher. Nerv. Syst.* 24, 139–144. doi: 10.1111/jns.12310

Li, A., Zhu, H.-M., Chen, Y., Yan, F., Liu, Z.-Y., Li, Z.-L., et al. (2021). Cdc42 facilitates axonogenesis by enhancing microtubule stabilization in primary hippocampal neurons. *Cell. Mol. Neurobiol.* doi: 10.1007/s10571-021-01051-0 [Epub ahead of print].

Li, L. X., Liu, G. L., Liu, Z. J., Lu, C., and Wu, Z. Y. (2017). Identification and functional characterization of two missense mutations in NDRG1 associated with Charcot-Marie-Tooth disease type 4D. *Hum. Mutat.* 38, 1569–1578. doi: 10.1002/humu.23309

Linder, M. D., Mäyränpää, M. I., Peränen, J., Pietilä, T. E., Pietiäinen, V. M., Uronen, R. L., et al. (2009). Rab8 regulates ABCA1 cell surface expression

and facilitates cholesterol efflux in primary human macrophages. *Arterioscler. Thromb. Vasc. Biol.* 29, 883–888. doi: 10.1161/ATVBAHA.108.179481

Lupo, V., Galindo, M. I., Martínez-Rubio, D., Sevilla, T., Vílchez, J. J., Palau, F., et al. (2009). Missense mutations in the SH3TC2 protein causing Charcot-Marie-Tooth disease type 4C affect its localization in the plasma membrane and endocytic pathway. *Hum. Mol. Genet.* 18, 4603–4614. doi: 10.1093/hmg/ddp427

Lyons, D., Naylor, S., Scholze, A., and Talbot, W. S. (2009). Kif1b is essential for mRNA localization in oligodendrocytes and development of myelinated axons. *Nat. Genet.* 41, 854–858. doi: 10.1038/ng.376

Magy, L., Mathis, S., Le Masson, G., Goizet, C., Tazir, M., and Vallat, J.-M. (2018). Updating the classification of inherited neuropathies. *Neurology* 90, e870–e876. doi: 10.1212/wnl.0000000000005074

Marat, A. L., and Haucke, V. (2016). Phosphatidylinositol 3-phosphates—at the interface between cell signalling and membrane traffic. *EMBO J.* 35, 561–579. doi: 10.15252/embj.201593564

Marinko, J. T., Carter, B. D., and Sanders, C. R. (2020). Direct relationship between increased expression and mistrafficking of the Charcot-Marie-Tooth-associated protein PMP22. *J. Biol. Chem.* 295, 11963–11970. doi: 10.1074/jbc.AC120.014940

Markworth, R., Adolfs, Y., Dambeck, V., Steinbeck, L. M., Lizé, M., Pasterkamp, R. J., et al. (2019). Sensory axon growth requires spatiotemporal integration of CaSR and TrkB signaling. *J. Neurosci.* 39, 5842–5860. doi: 10.1523/JNEUROSCI.0027-19.2019

Massa, R., Palumbo, C., Cavallaro, T., Panico, M. B., Bei, R., Terracciano, C., et al. (2006). Overexpression of ErbB2 and ErbB3 receptors in Schwann cells of patients with Charcot-Marie-Tooth disease type 1A. *Muscle Nerve* 33, 342–349. doi: 10.1002/mus.20460

Maxfield, F. R., and McGraw, T. E. (2004). Endocytic recycling. *Nat. Rev. Mol. Cell Biol.* 5, 121–132. doi: 10.1038/nrm1315

Maxfield, F. R., and Yamashiro, D. J. (1987). Endosome acidification and the pathways of receptor-mediated endocytosis. *Adv. Exp. Med. Biol.* 225, 189–198. doi: 10.1007/978-1-4684-5442-0_16

McCray, B. A., Skordalakes, E., and Taylor, J. P. (2010). Disease mutations in Rab7 result in unregulated nucleotide exchange and inappropriate activation. *Hum. Mol. Genet.* 19, 1033–1047. doi: 10.1093/hmg/ddp567

McMahon, H. T., and Boucrot, E. (2011). Molecular mechanism and physiological functions of clathrin-mediated endocytosis. *Nat. Rev. Mol. Cell Biol.* 12, 517–533. doi: 10.1038/nrm3151

Mersiyanova, I. V., Perepelov, A. V., Polyakov, A. V., Sitnikov, V. F., Dadali, E. L., Oparin, R. B., et al. (2000). A new variant of Charcot-Marie-Tooth disease type 2 is probably the result of a mutation in the neurofilament-light gene. *Am. J. Hum. Genet.* 67, 37–46. doi: 10.1086/302962

Michailov, G. V., Sereda, M. W., Brinkmann, B. G., Fischer, T. H., Haug, B., Birchmeier, C., et al. (2004). Axonal neuregulin-1 regulates myelin sheath thickness. *Science* 304, 700–703. doi: 10.1126/science.1095862

Misko, A., Jiang, S., Wegorzewska, I., Milbrandt, J., and Baloh, R. H. (2010). Mitofusin 2 is necessary for transport of axonal mitochondria and interacts with the Miro/Milton complex. *J. Neurosci.* 30, 4232–4240. doi: 10.1523/JNEUROSCI.6248-09.2010

Mizushima, N., Yamamoto, A., Matsui, M., Yoshimori, T., and Ohsumi, Y. (2004). In vivo analysis of autophagy in response to nutrient starvation using transgenic mice expressing a fluorescent autophagosome marker. *Mol. Biol. Cell* 15, 1101–1111.

Mo, Z., Zhao, X., Liu, H., Hu, Q., Chen, X. Q., Pham, J., et al. (2018). Aberrant GlyRS-HDAC6 interaction linked to axonal transport deficits in Charcot-Marie-Tooth neuropathy. *Nat. Commun.* 9:1007. doi: 10.1038/s41467-018-03461-z

Morena, J., Gupta, A., and Hoyle, J. C. (2019). Charcot-marie-tooth: from molecules to therapy. *Int. J. Mol. Sci.* 20, 1–15. doi: 10.3390/ijms20143419

Nakanishi, H., and Takai, Y. (2008). Frabin and other related Cdc42-specific guanine nucleotide exchange factors couple the actin cytoskeleton with the plasma membrane. *J. Cell. Mol. Med.* 12, 1169–1176. doi: 10.1111/j.1582-4934.2008.00345.x

Nicks, J., Lee, S., Harris, A., Falk, D. J., Todd, A. G., Arredondo, K., et al. (2014). Rapamycin improves peripheral nerve myelination while it fails to benefit neuromuscular performance in neuropathic mice. *Neurobiol. Dis.* 70, 224–236. doi: 10.1016/j.nbd.2014.06.023

Nirschl, J. J., Magiera, M. M., Lazarus, J. E., Janke, C., and Holzbaur, E. L. F. (2016). α-tubulin tyrosination and CLIP-170 phosphorylation regulate the initiation of dynein-driven transport in neurons. *Cell Rep.* 14, 2637–2652. doi: 10.1016/j.celrep.2016.02.046

Obaishi, H., Nakanishi, H., Mandai, K., Satoh, K., Satoh, A., Takahashi, K., et al. (1998). Frabin, a novel FGD1-related actin filament-binding protein capable of changing cell shape and activating c-Jun N-terminal kinase. *J. Biol. Chem.* 273, 18697–18700. doi: 10.1074/jbc.273.30.18697

Okuda, T., Higashi, Y., Kokame, K., Tanaka, C., Kondoh, H., and Miyata, T. (2004). Ndrg1-deficient mice exhibit a progressive demyelinating disorder of peripheral nerves. *Mol. Cell. Biol.* 24, 3949–3956. doi: 10.1128/mcb.24.9.3949-3956.2004

Ori-McKenney, K. M., Xu, J., Gross, S. P., and Vallee, R. B. (2010). A cytoplasmic dynein tail mutation impairs motor processivity. *Nat. Cell Biol.* 12, 1228–1234. doi: 10.1038/ncb2127

Palaima, P., Berciano, J., Peeters, K., and Jordanova, A. (2021). LRSAM1 and the RING domain: Charcot–Marie–Tooth disease and beyond. *Orphanet J. Rare Dis.* 16, 1–12. doi: 10.1186/s13023-020-01654-8

Pasterkamp, R. J., and Burk, K. (2020). Axon guidance receptors: endocytosis, trafficking and downstream signaling from endosomes. *Prog. Neurobiol.* 198:101916. doi: 10.1016/j.pneurobio.2020.101916

Pérez-Ollé, R., López-Toledano, M. A., Goryunov, D., Cabrera-Poch, N., Stefanis, L., Brown, K., et al. (2005). Mutations in the neurofilament light gene linked to Charcot-Marie-Tooth disease cause defects in transport. *J. Neurochem.* 93, 861–874. doi: 10.1111/j.1471-4159.2005.03095.x

Perlson, E., Jeong, G. B., Ross, J. L., Dixit, R., Wallace, K. E., Kalb, R. G., et al. (2009). A switch in retrograde signaling from survival to stress in rapid-onset neurodegeneration. *J. Neurosci.* 29, 9903–9917. doi: 10.1523/JNEUROSCI.0813-09.2009

Picci, C., Wong, V. S. C., Costa, C. J., McKinnon, M. C., Goldberg, D. C., Swift, M., et al. (2020). HDAC6 inhibition promotes α-tubulin acetylation and ameliorates CMT2A peripheral neuropathy in mice. *Exp. Neurol.* 328:113281. doi: 10.1016/j.expneurol.2020.113281

Pietiäinen, V., Vassilev, B., Blom, T., Wang, W., Nelson, J., Bittman, R., et al. (2013). NDRG1 functions in LDL receptor trafficking by regulating endosomal recycling and degradation. *J. Cell Sci.* 126, 3961–3971. doi: 10.1242/jcs.128132

Previtali, S. C., Zerega, B., Sherman, D. L., Brophy, P. J., Dina, G., King, R. H. M., et al. (2003). Myotubularin-related 2 protein phosphatase and neurofilament light chain protein, both mutated in CMT neuropathies, interact in peripheral nerve. *Hum. Mol. Genet.* 12, 1713–1723. doi: 10.1093/hmg/ddg179

Prior, R., Van Helleputte, L., Benoy, V., and Van Den Bosch, L. (2017). Defective axonal transport: a common pathological mechanism in inherited and acquired peripheral neuropathies. *Neurobiol. Dis.* 105, 300–320. doi: 10.1016/j.nbd.2017.02.009

Raiborg, C., Bache, K. G., Gillooly, D. J., Madshus, I. H., Stang, E., and Stenmark, H. (2002). Hrs sorts ubiquitinated proteins into clathrin-coated microdomains of early endosomes. *Nat. Cell Biol.* 4, 394–398. doi: 10.1038/ncb791

Rangaraju, S., Verrier, J. D., Madorsky, I., Nicks, J., Dunn, W. A., and Notterpek, L. (2010). Rapamycin activates autophagy and improves myelination in explant cultures from neuropathic mice. *J. Neurosci.* 30, 11388–11397. doi: 10.1523/JNEUROSCI.1356-10.2010

Reed, N. A., Cai, D., Blasius, T. L., Jih, G. T., Meyhofer, E., Gaertig, J., et al. (2006). Microtubule acetylation promotes kinesin-1 binding and transport. *Curr. Biol.* 16, 2166–2172. doi: 10.1016/j.cub.2006.09.014

Rink, J., Ghigo, E., Kalaidzidis, Y., and Zerial, M. (2005). Rab conversion as a mechanism of progression from early to late endosomes. *Cell* 122, 735–749. doi: 10.1016/j.cell.2005.06.043

Roberts, R. C., Peden, A. A., Buss, F., Bright, N. A., Latouche, M., Reilly, M. M., et al. (2010). Mistargeting of SH3TC2 away from the recycling endosome causes Charcot-Marie-Tooth disease type 4C. *Hum. Mol. Genet.* 19, 1009–1018. doi: 10.1093/hmg/ddp565

Robinson, F. L., and Dixon, J. E. (2005). The phosphoinositide-3-phosphatase MTMR2 associates with MTMR13, a membrane-associated pseudophosphatase also mutated in type 4B Charcot-Marie-Tooth disease. *J. Biol. Chem.* 280, 31699–31707. doi: 10.1074/jbc.M505159200

Romano, R., Rivellini, C., De Luca, M., Tonlorenzi, R., Beli, R., Manganelli, F., et al. (2020). Alteration of the late endocytic pathway in Charcot–Marie–Tooth

type 2B disease. *Cell. Mol. Life Sci.* 78, 351–372. doi: 10.1007/s00018-020-03510-1

Rossaert, E., and Van Den Bosch, L. (2020). HDAC6 inhibitors: translating genetic and molecular insights into a therapy for axonal CMT. *Brain Res.* 1733:146692. doi: 10.1016/j.brainres.2020.146692

Rudge, S. A., Anderson, D. M., and Emr, S. D. (2004). Vacuole size control: regulation of PtdIns(3,5)P2 levels by the vacuole-associated Vac14-Fig4 complex, a PtdIns(3,5)P2-specific phosphatase. *Mol. Biol. Cell* 15, 24–36.

Rudnik-Schöneborn, S., Auer-Grumbach, M., and Senderek, J. (2020). Charcot-Marie-Tooth disease and hereditary motor neuropathies – update 2020. *Medizinische Genet.* 32, 207–219. doi: 10.1515/medgen-2020-2038

Ruit, K. G., Osborne, P. A., Schmidt, R. E., Johnson, E. M., and Snider, W. D. (1990). Nerve growth factor regulates sympathetic ganglion cell morphology and survival in the adult mouse. *J. Neurosci.* 10, 2412–2419. doi: 10.1523/jneurosci.10-07-02412.1990

Saporta, M. A., Dang, V., Volfson, D., Zou, B., Xie, X. S., Adebola, A., et al. (2015). Axonal Charcot-Marie-Tooth disease patient-derived motor neurons demonstrate disease-specific phenotypes including abnormal electrophysiological properties. *Exp. Neurol.* 263, 190–199. doi: 10.1016/j.expneurol.2014.10.005

Saveri, P., De Luca, M., Nisi, V., Pisciotta, C., Romano, R., Piscosquito, G., et al. (2020). Charcot-Marie-Tooth Type 2B: a new phenotype associated with a novel RAB7A mutation and inhibited EGFR degradation. *Cells* 9:1028. doi: 10.3390/cells9041028

Schiavon, C. R., Shadel, G. S., and Manor, U. (2021). Impaired mitochondrial mobility in Charcot-Marie-Tooth disease. *Front. Cell Dev. Biol.* 9:624823. doi: 10.3389/fcell.2021.624823

Schreij, A. M. A., Fon, E. A., and McPherson, P. S. (2016). Endocytic membrane trafficking and neurodegenerative disease. *Cell. Mol. Life Sci.* 73, 1529–1545. doi: 10.1007/s00018-015-2105-x

Scolnick, J. A., Cui, K., Duggan, C. D., Xuan, S., Yuan, X. B., Efstratiadis, A., et al. (2008). Role of IGF signaling in olfactory sensory map formation and axon guidance. *Neuron* 57, 847–857. doi: 10.1016/j.neuron.2008.01.027

Scott-Solomon, E., and Kuruvilla, R. (2018). Mechanisms of neurotrophin trafficking via Trk receptors. *Mol. Cell. Neurosci.* 91, 25–33. doi: 10.1016/j.mcn.2018.03.013

Seaman, M. N. J. (2004). Cargo-selective endosomal sorting for retrieval to the Golgi requires retromer. *J. Cell Biol.* 165, 111–122. doi: 10.1083/jcb.200312034

Seaman, M. N. J. (2012). The retromer complex-endosomal protein recycling and beyond. *J. Cell Sci.* 125(Pt 20), 4693–4702. doi: 10.1242/jcs.103440

Seaman, M. N. J. J., Gautreau, A., and Billadeau, D. D. (2013). Retromer-mediated endosomal protein sorting: all WASHed up! *Trends Cell Biol.* 23, 522–528. doi: 10.1016/j.tcb.2013.04.010

Seaman, M. N. J., Harbour, M. E., Tattersall, D., Read, E., and Bright, N. (2009). Membrane recruitment of the cargo-selective retromer subcomplex is catalysed by the small GTPase Rab7 and inhibited by the Rab-GAP TBC1D5. *J. Cell Sci.* 122, 2371–2382.

Senderek, J., Bergmann, C., Stendel, C., Kirfel, J., Verpoorten, N., De Jonghe, P., et al. (2003). Mutations in a gene encoding a novel SH3/TPR domain protein cause autosomal recessive Charcot-Marie-Tooth type 4C neuropathy. *Am. J. Hum. Genet.* 73, 1106–1119. doi: 10.1086/379525

Shen, S., and Kozikowski, A. P. (2020). A patent review of histone deacetylase 6 inhibitors in neurodegenerative diseases (2014-2019). *Expert Opin. Ther. Pat.* 30, 121–136. doi: 10.1080/13543776.2019.1708901

Sidiropoulos, P. N. M., Miehe, M., Bock, T., Tinelli, E., Oertli, C. I., Kuner, R., et al. (2012). Dynamin 2 mutations in Charcot-Marie-Tooth neuropathy highlight the importance of clathrin-mediated endocytosis in myelination. *Brain* 135, 1395–1411. doi: 10.1093/brain/aws061

Simonetti, B., Danson, C. M., Heesom, K. J., and Cullen, P. J. (2017). Sequence-dependent cargo recognition by SNX-BARs mediates retromer-independent transport of CI-MPR. *J. Cell Biol.* 216, 3695–3712. doi: 10.1083/jcb.201703015

Simonsen, A., Lippé, R., Christoforidis, S., Gaullier, J. M., Brech, A., Callaghan, J., et al. (1998). EEA1 links PI(3)K function to Rab5 regulation of endosome fusion. *Nature* 394, 494–498. doi: 10.1038/28879

Sleigh, J. N., Dawes, J. M., West, S. J., Wei, N., Spaulding, E. L., Gómez-Martín, A., et al. (2017). Trk receptor signaling and sensory neuron fate are perturbed in human neuropathy caused by Gars mutations. *Proc. Natl. Acad. Sci. U.S.A.* 114, E3324–E3333. doi: 10.1073/pnas.1614557114

Spinosa, M. R., Progida, C., De Luca, A., Colucci, A. M. R., Alifano, P., and Bucci, C. (2008). Functional characterization of Rab7 mutant proteins associated with Charcot-Marie-Tooth type 2B disease. *J. Neurosci.* 28, 1640–1648. doi: 10.1523/JNEUROSCI.3677-07.2008

Stendel, C., Roos, A., Kleine, H., Arnaud, E., Özçelik, M., Sidiropoulos, P. N. M., et al. (2010). SH3TC2, a protein mutant in Charcot-Marie-Tooth neuropathy, links peripheral nerve myelination to endosomal recycling. *Brain* 133, 2462–2474. doi: 10.1093/brain/awq168

Stone, E. J., Uchida, A., and Brown, A. (2019). Charcot-Marie-Tooth disease type 2E/1F mutant neurofilament proteins assemble into neurofilaments. *Cytoskeleton* 76, 423–439. doi: 10.1002/cm.21566

Stowers, R. S., Megeath, L. J., Górska-Andrzejak, J., Meinertzhagen, I. A., and Schwarz, T. L. (2002). Axonal transport of mitochondria to synapses depends on Milton, a novel *Drosophila* protein. *Neuron* 36, 1063–1077. doi: 10.1016/S0896-6273(02)01094-2

Street, V. A., Bennett, C. L., Goldy, J. D., Shirk, A. J., Kleopa, K. A., Tempel, B. L., et al. (2003). Mutation of a putative protein degradation gene LITAF/SIMPLE in Charcot-Marie-Tooth disease 1C. *Neurology* 60, 22–26. doi: 10.1212/WNL.60.1.22

Tanabe, K., and Takei, K. (2009). Dynamic instability of microtubules requires dynamin 2 and is impaired in a Charcot-Marie-Tooth mutant. *J. Cell Biol.* 185, 939–948. doi: 10.1083/jcb.200803153

Taveggia, C., Zanazzi, G., Petrylak, A., Yano, H., Rosenbluth, J., Einheber, S., et al. (2005). Neuregulin-1 type III determines the ensheathment fate of axons. *Neuron* 47, 681–694. doi: 10.1016/j.neuron.2005.08.017

Temkin, P., Lauffer, B., Jager, S., Cimermacic, P., Krogan, N. J., and Zastrow, M. V. (2011). SNX27 mediates retromer tubule entry and endosome-to-plasma membrane trafficking of signaling receptors. *Nat. Cell Biol.* 13, 715–721. doi: 10.1038/ncb2252.SNX27

Timmerman, V., Strickland, A. V., and Züchner, S. (2014). Genetics of Charcot-Marie-Tooth (CMT) disease within the frame of the human genome project success. *Genes* 5, 13–32. doi: 10.3390/genes5010013

Umikawa, M., Obaishi, H., Nakanishi, H., Satoh-Horikawa, K., Takahashi, K., Hotta, I., et al. (1999). Association of frabin with the actin cytoskeleton is essential for microspike formation through activation of Cdc42 small G protein. *J. Biol. Chem.* 274, 25197–25200. doi: 10.1074/jbc.274.36.25197

Vaccari, I., Carbone, A., Previtali, S. C., Mironova, Y. A., Alberizzi, V., Noseda, R., et al. (2015). Loss of Fig4 in both Schwann cells and motor neurons contributes to CMT4J neuropathy. *Hum. Mol. Genet.* 24, 383–396. doi: 10.1093/hmg/ddu451

Vaccari, I., Dina, G., Tronchère, H., Kaufman, E., Chicanne, G., Cerri, F., et al. (2011). Genetic interaction between MTMR2 and FIG4 phospholipid phosphatases involved in Charcot-Marie-Tooth neuropathies. *PLoS Genet.* 7:e1002319. doi: 10.1371/journal.pgen.1002319

Vavlitou, N., Sargiannidou, I., Markoullis, K., Kyriacou, K., Scherer, S. S., and Kleopa, K. A. (2010). Axonal pathology precedes demyelination in a mouse model of X-linked demyelinating/type i Charcot-Marie Tooth neuropathy. *J. Neuropathol. Exp. Neurol.* 69, 945–958. doi: 10.1097/NEN.0b013e3181efa658

Vijay, S., Chiu, M., Dacks, J. B., and Roberts, R. C. (2016). Exclusive expression of the Rab11 effector SH3TC2 in Schwann cells links integrin-α6 and myelin maintenance to Charcot-Marie-Tooth disease type 4C. *Biochim. Biophys. Acta Mol. Basis Dis.* 1862, 1279–1290. doi: 10.1016/j.bbadis.2016.04.003

Wallroth, A., and Haucke, V. (2018). Phosphoinositide conversion in endocytosis and the endolysosomal system. *J. Biol. Chem.* 293, 1526–1535. doi: 10.1074/jbc.R117.000629

Wang, S., Ma, Z., Xu, X., Wang, Z., Sun, L., Zhou, Y., et al. (2014). A role of Rab29 in the integrity of the trans-golgi network and retrograde trafficking of mannose-6-phosphate receptor. *PLoS One* 9:e96242. doi: 10.1371/journal.pone.0096242

Weedon, M. N., Hastings, R., Caswell, R., Xie, W., Paszkiewicz, K., Antoniadi, T., et al. (2011). Exome sequencing identifies a DYNC1H1 mutation in a large pedigree with dominant axonal Charcot-Marie-Tooth disease. *Am. J. Hum. Genet.* 89, 308–312. doi: 10.1016/j.ajhg.2011.07.002

Weeratunga, S., Paul, B., and Collins, B. M. (2020). Recognising the signals for endosomal trafficking. *Curr. Opin. Cell Biol.* 65, 17–27. doi: 10.1016/j.ceb.2020.02.005

Xhabija, B., Taylor, G. S., Fujibayashi, A., Sekiguchi, K., and Vacratsis, P. O. (2011). Receptor mediated endocytosis 8 is a novel PI (3) P binding protein regulated by myotubularin-related 2. *FEBS Lett.* 585, 1722–1728. doi: 10.1016/j.febslet.2011.04.016

Xu, B., Zang, K., Ruff, N. L., Zhang, Y. A., McConnell, S. K., Stryker, M. P., et al. (2000). Cortical degeneration in the absence of neurotrophin signaling. *Neuron* 26, 233–245. doi: 10.1016/s0896-6273(00)81153-8

Xu, F., Takahashi, H., Tanaka, Y., Ichinose, S., Niwa, S., Wicklund, M. P., et al. (2018). KIF1Bβ mutations detected in hereditary neuropathy impair IGF1R transport and axon growth. *J. Cell Biol.* 217, 3480–3496. doi: 10.1083/JCB.201801085

Yang, W., Lo, C. G., Dispenza, T., and Cerione, R. A. (2001). The Cdc42 target ACK2 directly interacts with clathrin and influences clathrin assembly. *J. Biol. Chem.* 276, 17468–17473. doi: 10.1074/jbc.M010893200

Ye, M., Lehigh, K. M., and Ginty, D. D. (2018). Multivesicular bodies mediate long-range retrograde NGF-TrkA signaling. *Elife* 7:e33012. doi: 10.7554/eLife.33012

Yum, S. W., Kleopa, K. A., Shumas, S., and Scherer, S. S. (2002). Diverse trafficking abnormalities of connexin32 mutants causing CMTX. *Neurobiol. Dis.* 11, 43–52. doi: 10.1006/nbdi.2002.0545

Zastrow, M. V., and Sorkin, A. (2007). Signaling on the endocytic pathway. *Curr. Opin. Cell Biol.* 19, 436–445. doi: 10.1016/j.ceb.2007.04.021

Zhang, K., Kenan, R. F. B., Osakada, Y., Xu, W., Sinit, R. S., Chen, L., et al. (2013). Defective axonal transport of Rab7 GTPase results in dysregulated trophic signaling. *J. Neurosci.* 33, 7451–7462. doi: 10.1523/JNEUROSCI.4322-12.2013

Zhao, C., Takita, J., Tanaka, Y., Setou, M., Nakagawa, T., Takeda, S., et al. (2001). Charcot-Marie-Tooth disease type 2A caused by mutation in a microtubule motor KIF1Bbeta. *Cell* 105, 587–597.

Zhao, J., Brown, K., and Liem, R. K. H. (2017). Abnormal neurofilament inclusions and segregations in dorsal root ganglia of a Charcot-Marie-Tooth type 2E mouse model. *PLoS One* 12:e0180038. doi: 10.1371/journal.pone.0180038

Zhao, J., Wang, Y., Xu, H., Fu, Y., Qian, T., Bo, D., et al. (2016). Dync1h1 mutation causes proprioceptive sensory neuron loss and impaired retrograde axonal transport of dorsal root ganglion neurons. *CNS Neurosci. Ther.* 22, 593–601. doi: 10.1111/cns.12552

Zhou, Y., Miles, J. R., Tavori, H., Lin, M., Khoshbouei, H., Borchelt, D. R., et al. (2019). PMP22 regulates cholesterol trafficking and ABCA1-mediated cholesterol efflux. *J. Neurosci.* 39, 5404–5418. doi: 10.1523/JNEUROSCI.2942-18.2019

Züchner, S., Mersiyanova, I. V., Muglia, M., Bissar-Tadmouri, N., Rochelle, J., Dadali, E. L., et al. (2004). Mutations in the mitochondrial GTPase mitofusin 2 cause Charcot-Marie-Tooth neuropathy type 2A. *Nat. Genet.* 36, 449–451. doi: 10.1038/ng1341

Züchner, S., Noureddine, M., Kennerson, M., Verhoeven, K., Claeys, K., De Jonghe, P., et al. (2005). Mutations in the pleckstrin homology domain of dynamin 2 cause dominant intermediate Charcot-Marie-Tooth disease. *Nat. Genet.* 37, 289–294. doi: 10.1038/ng1514

Conflict of Interest: The authors declare that the research was conducted in the absence of any commercial or financial relationships that could be construed as a potential conflict of interest.

Publisher's Note: All claims expressed in this article are solely those of the authors and do not necessarily represent those of their affiliated organizations, or those of the publisher, the editors and the reviewers. Any product that may be evaluated in this article, or claim that may be made by its manufacturer, is not guaranteed or endorsed by the publisher.

Copyright © 2021 Markworth, Bähr and Burk. This is an open-access article distributed under the terms of the Creative Commons Attribution License (CC BY). The use, distribution or reproduction in other forums is permitted, provided the original author(s) and the copyright owner(s) are credited and that the original publication in this journal is cited, in accordance with accepted academic practice. No use, distribution or reproduction is permitted which does not comply with these terms.

frontiers in Molecular Neuroscience

ORIGINAL RESEARCH
published: 22 October 2021
doi: 10.3389/fnmol.2021.756264

Expression of FLRT2 in Postnatal Central Nervous System Development and After Spinal Cord Injury

*Juntan Li[1], Yo Shinoda[2], Shuhei Ogawa[3], Shunsuke Ikegaya[1], Shuo Li[1,4], Yukihiro Matsuyama[4], Kohji Sato[1] and Satoru Yamagishi[1]**

[1] Department of Organ and Tissue Anatomy, Hamamatsu University School of Medicine, Hamamatsu, Japan, [2] Department of Environmental Health, School of Pharmacy, Tokyo University of Pharmacy and Life Sciences, Tokyo, Japan, [3] Division of Integrated Research, Research Institute for Biomedical Sciences, Tokyo University of Science, Chiba, Japan, [4] Department of Orthopedic Surgery, Hamamatsu University School of Medicine, Hamamatsu, Japan

Fibronectin and leucine-rich transmembrane (FLRT) proteins are necessary for various developmental processes and in pathological conditions. FLRT2 acts as a homophilic cell adhesion molecule, a heterophilic repulsive ligand of Unc5/Netrin receptors, and a synaptogenic molecule; the last feature is mediated by binding to latrophilins. Although the function of FLRT2 in regulating cortical migration at the late gestation stage has been analyzed, little is known about the expression pattern of FLRT2 during postnatal central nervous system (CNS) development. In this study, we used *Flrt2-LacZ* knock-in (KI) mice to analyze FLRT2 expression during CNS development. At the early postnatal stage, FLRT2 expression was largely restricted to several regions of the striatum and deep layers of the cerebral cortex. In adulthood, FLRT2 expression was more prominent in the cerebral cortex, hippocampus, piriform cortex (PIR), nucleus of the lateral olfactory tract (NLOT), and ventral medial nucleus (VM) of the thalamus, but lower in the striatum. Notably, in the hippocampus, FLRT2 expression was confined to the CA1 region and partly localized on pre- and postsynapses whereas only few expression was observed in CA3 and dentate gyrus (DG). Finally, we observed temporally limited FLRT2 upregulation in reactive astrocytes around lesion sites 7 days after thoracic spinal cord injury. These dynamic changes in FLRT2 expression may enable multiple FLRT2 functions, including cell adhesion, repulsion, and synapse formation in different regions during CNS development and after spinal cord injury.

Keywords: FLRT2, axon guidance, synaptic plasticity, development, spinal cord injury

OPEN ACCESS

Edited by:
Joaquim Egea, Biomedical Research Institute of Lleida, Spain

Reviewed by:
Richard Sando, Vanderbilt University, United States
Hailong Hou, Renascent Biosciences, United States

***Correspondence:**
Satoru Yamagishi
yamagish@hama-med.ac.jp

Specialty section:
This article was submitted to Neuroplasticity and Development, a section of the journal Frontiers in Molecular Neuroscience

Received: *10 August 2021*
Accepted: *28 September 2021*
Published: *22 October 2021*

Citation:
Li J, Shinoda Y, Ogawa S, Ikegaya S, Li S, Matsuyama Y, Sato K and Yamagishi S (2021) Expression of FLRT2 in Postnatal Central Nervous System Development and After Spinal Cord Injury. Front. Mol. Neurosci. 14:756264. doi: 10.3389/fnmol.2021.756264

INTRODUCTION

The mammalian cerebral cortex is a highly organized laminar structure with six layers. During development, the cortical plate develops in an inside-out pattern, i.e., later-born neurons migrate outward through neurons born earlier. After arriving at their final destinations, neurons extend their axons and establish synaptic connections with neurons in other layers and regions, allowing

each layer and region to exhibit characteristic features. Axon guidance molecules such as Netrin, Ephrins, Semaphorins, and Slits are involved in organizing the precise positioning and connection of neurons (Chen et al., 2008; Torii et al., 2009; Gonda et al., 2020; Yamagishi et al., 2021). However, the molecular mechanisms involved in axonal guidance and synaptogenesis during development and in response to nerve injury have not yet been fully elucidated.

Fibronectin and leucine-rich transmembrane (FLRT) protein family members are type I transmembrane proteins consisting of extracellular leucine-rich repeat sequences (LRRs), type III fibronectin (FNIII) domains, and cytoplasmic tails with Rnd1 binding motifs (Lacy et al., 1999; Ogata et al., 2007). FLRTs play important roles in cell–cell adhesion, cell migration, axon guidance, and vasculogenesis during development (Akita et al., 2016; Peregrina and Del Toro, 2020; Yamagishi et al., 2021), and they also play pivotal roles in interneuron development and final cortical allocation *in vivo* (Fleitas et al., 2021). Fibronectin and leucine-rich transmembranes can be induced by FGF-mediated signaling cascade in many tissues during mouse embryogenesis, such as in the midbrain/hindbrain boundary, the apical ectodermal ridge, and the developing sclerotome (Haines et al., 2006). Fibronectin and leucine-rich transmembranes also mediate intercellular adhesion through heterophilic interaction with latrophilins expressed on the surface of adjacent cells, as well as homophilic interactions (Muller et al., 2011; O'Sullivan et al., 2012; Seiradake et al., 2014; Jackson et al., 2015; Lu et al., 2015; Del Toro et al., 2020). In the process of cell migration and axon guidance, FLRTs interact with UNC5s to contribute to repulsion in neuron guidance (Yamagishi et al., 2011; Seiradake et al., 2014; Jackson et al., 2015). Moreover, FLRT2 and FLRT3 also play important roles in embryonic development. In mouse, *Flrt3* mutants are lethal due to dysfunction in several aspects of embryonic development: highly disorganized basement membrane in the anterior visceral endoderm region; defects in headfold fusion; and failure of the lateral edges of the ventral body wall to fuse, leading to cardia bifida (Egea et al., 2008; Maretto et al., 2008). Mouse embryos lacking *FLRT2* expression arrest at mid-gestation due to cardiac insufficiency (Muller et al., 2011). Conditional knockout mice lacking FLRT2 in vascular endothelial cells exhibit embryonic lethality at the mid-gestation stage with systemic congestion and hypoxia (Tai-Nagara et al., 2017). FLRT1 and FLRT3 promote increases in neurite number and length (Wheldon et al., 2010). FLRT2 regulates dendritic spine density in CA1 neurons (Schroeder et al., 2018). Crystal structures of FLRT proteins imply that distinct binding sites can trigger adhesive and/or repulsive signals in the same receiving cell, leading to an integrative response (Seiradake et al., 2014). Recent work showed that the TEN2–LPHN3–FLRT3 ternary complex is important for the formation of synaptic properties (Sando et al., 2019; Li et al., 2020).

In humans, FLRT2 is expressed in pancreas, skeletal muscle, brain, and heart (Lacy et al., 1999). During embryogenesis, FLRT2 is expressed in endothelial cells in the placental labyrinth (Tai-Nagara et al., 2017). During cortical development, FLRT2 expression is confined to the cortical plate, especially in deep layers, starting from E15.5 (Yamagishi et al., 2011). However, the expression pattern of FLRT2 in the brain in later postnatal stages remains largely unknown. In this study, using *Flrt2-LacZ* knock-in (KI) and Nestin-Cre;FLRT2$^{lx/lx}$ cKO mice, we investigated the detailed expression pattern of FLRT2 in the brain of neonatal and adult mice. In addition, we also performed electrophysiological analyses of synaptic function by deleting FLRT2 in excitatory neurons in the hippocampus using Emx1-Cre mice. Finally, we analyzed FLRT2 expression in response to spinal cord injury.

MATERIALS AND METHODS

Animals

Flrt2-LacZ KI mice were obtained and maintained on a CD1 background (Tai-Nagara et al., 2017). P0, P7, and adulthood (>6 weeks old) *Flrt2-LacZ* KI mice were used for LacZ staining. For electrophysiological and immunohistochemistry experiments, *Flrt2*$^{lox/lox}$ mice (Tai-Nagara et al., 2017) were crossed with Emx1-Cre (Iwasato et al., 2000) and Nestin-Cre (Isaka et al., 1999), respectively. For validating the conditional allele, FLRT2$^{+/-}$ (Yamagishi et al., 2011), FLRT2$^{lox/+}$ and Nestin-Cre mice were crossed. Male mice aged 2–4 months were used for electrophysiological experiments. Primers pairs for genotyping were as follows: *Flrt2-LacZ* KI mice, 5′-TTACACAG ACTGCCACATCC, 5′-CCTGCAGCCCAAGCTGATCC and 5′-GAGCCCACCTGACATTATCC; (2) *Flrt2*$^{lox/lox}$ mice, 5′-GT GGAAGGAAGGAATTGTCTCAGG and 5′-GGAGCCAGGTT GGCAGGAGTTGGC; and (3) Cre mice, 5′-GCCTGCAT TACCGGTCGATGCAACGA and 5′-GTGGCAGATGGCG CGGCAACACCATT-3′. All animal experiments were approved by the Animal Research Committee of Hamamatsu University School of Medicine and were carried out in accordance with the in-house guidelines for the care and use of laboratory animals of the university.

LacZ Staining

LacZ staining was performed as previously reported (Tai-Nagara et al., 2017). Briefly, mice were anesthetized with a mixture containing medetomidine hydrochloride, midazolam, and butorphanol tartrate (0.1 ml/10 g delivered by intraperitoneal injection), and then fixed via cardiac perfusion with 0.01 M sodium phosphate-buffered saline (pH 7.4) for 1 min followed by 4% paraformaldehyde in 0.01 M PBS (pH 7.4) for 5 min. The brains were dissected and placed in cold PBS. Then, the brains were embedded in BSA (Sigma-Aldrich, MO, United States) solution cross-linked with glutaraldehyde (Nacalai Tesque Inc, Kyoto, Japan). After solidification, sagittal and coronal sections were cut at a thickness of 100 μm on a Vibratome (Dosaka EM Co Ltd, Kyoto, Japan), and then stained at 37°C overnight for X-gal (5-bromo-4-chloro-3-indolyl-β-galactoside) (Fuji-Wako, Osaka, Japan). Images of sections were acquired using a transmission light microscope (Eclipse E600; Nikon, Tokyo, Japan).

Immunostaining

Immunostaining of tissue sections was performed as described previously (Ikegaya et al., 2020) with some modifications.

Briefly, the mice were deeply anesthetized and intracardially perfused with phosphate-buffered saline (PBS), and then the brain and spinal cord were dissected. Dissected tissues were immediately frozen with dry ice. Sagittal and coronal sections (20 μm thickness) were prepared using a cryostat and stored at −80°C until use. Before staining, the sections were fixed in 2% PFA/PBS for 5 min, washed with PBS, and permeabilized in 0.3% Triton X-100/PBS for 5 min. The permeabilized sections were incubated for 1 h at room temperature with blocking solution containing either 3%BSA or 10% donkey serum in 0.1% Triton X-100/PBS, followed by incubation with primary antibodies in either 3% BSA or 10% donkey serum/0.1% Triton X-100/PBS overnight at 4°C. The sections were then incubated with Alexa Fluor-conjugated secondary antibodies for 30 min at room temperature, followed by nuclear staining with DAPI. Images of the sections were acquired with a confocal microscope (TCS SP8; Leica, Wetzlar, Germany). The primary antibodies used were goat anti-FLRT2 (1:350; R&D Systems, Minneapolis, MN, United States), rabbit anti-PSD95 (1:200; Cell Signaling Technology, Danvers, MA, United States), guinea pig anti-VGLUT1 (1:1000; Millipore; Darmstadt, Germany) and mouse anti-GFAP-Cy3 conjugated (1:500; Sigma-Aldrich, Burlington, MA, United States) antibodies. Secondary antibodies were donkey anti-rabbit, donkey anti-goat and goat anti-guinea pig (conjugated to Alexa Fluor 488 and 568, respectively; Thermo Fisher Scientific, Waltham, MA, United States), used at a dilution of 1:500.

Electrophysiology

Electrophysiology was performed as reported previously with minor modifications (Ishii et al., 2021). Briefly, deeply anesthetized mice were decapitated and their brains were rapidly removed into ice-cold high-sucrose Ringer's solution (234 mM sucrose, 2.5 mM KCl, 1.25 mM NaH_2PO_4, 10 mM $MgSO_4$, 0.5 mM $CaCl_2$, 26 mM $NaHCO_3$, and 11 mM glucose; pH 7.5). Hippocampi were transversely sliced (thickness, 400 μm) on a vibratome Pro-7 (Dosaka, Kyoto, Japan), and slices were recovered in ACSF (125 mM NaCl, 2.5 mM KCl, 1.25 mM NaH_2PO_4, 1 mM $MgCl_2$, 2 mM $CaCl_2$, 26 mM $NaHCO_3$, and 11 mM D-glucose; pH 7.5) at room temperature for at least 2 h. All solutions were constantly bubbled with 95% O_2/5% CO_2. Recovered slices were placed in a recording chamber and immersed in ACSF at 26°C. A bipolar platinum–iridium stimulation electrode (WPI, Sarasota, FL, United States) was placed in the CA1 stratum radiatum region. Field excitatory postsynaptic potentials (fEPSPs) were recorded from the CA1 stratum radiatum using an Ag/AgCl recording electrode placed in a glass pipette (Harvard Apparatus, Holliston, MA, United States) filled with ACSF following a 0.05 Hz test pulse generated by pulse generator Master-8 (AMPI, Jerusalem, Israel). Long-term potentiation (LTP) was induced by using theta-burst stimulation (TBS) consisting of four trains with 10 s intervals between trains; each train had five bursts separated by 200 ms, and each burst included four pulses delivered at 100 Hz at 20% of maximal stimulus intensity. Data were amplified using a MultiClamp 700A (Molecular Devices, San Jose, CA, United States), and digitized at 10 kHz and filtered at 2 kHz using a Digidata 1440 system with the pCLAMP10 software (Molecular Devices).

Spinal Cord Injury

Eight- to nine-week-old *Flrt2-LacZ* KI and Nestin-Cre;FLRT2$^{lx/lx}$ cKO mice were anesthetized with medetomidine hydrochloride, midazolam, and butorphanol tartrate (0.1 ml/10 g). Spinal cord injury at the tenth thoracic vertebra (T10) was induced using an Infinite Horizons impactor (IH impactor; Muromachi, Tokyo, Japan) with an impact force of 60 kdyn, as described previously (Arima et al., 2014). Animals in the sham group were conducted to laminectomy alone. These animals were sacrificed at 3, 7, 14, and 28 days post-injury.

Western Blot Analysis

Brain lysates were obtained as previously described (Yamagishi et al., 2011). Glycoproteins were pulled down from 1000 μg of protein lysate using wheat germ agglutinin (lectin) agarose beads (Sigma). Western blots in lectin pull downs or total cell lysates were performed as indicated: goat anti-FLRT2 antibody (1:1000; R&D Systems, Minneapolis, MN, United States) and rabbit anti-tubulin antibody (1:1000; Thermo Fisher Scientific, Waltham, MA, United States).

RESULTS

General Expression Patterns of FLRT2 in the Brain at P0, P7, and Adulthood

Expression patterns of FLRT2 in the developing brain were examined using *Flrt2-LacZ* KI heterozygote mice at P0, P7, and adulthood (>6 weeks old). Although LacZ staining was very intense in homozygotes, we used heterozygotes for the analysis because the homozygotes were embryonic lethal (Muller et al., 2011; Tai-Nagara et al., 2017). We observed intense FLRT2 expression in the anterior part of the cortex at P0 and P7 (**Figures 1A,B**). The expression decreased in adult mice (**Figure 1C** and **Supplementary Figure 1**). FLRT2 was expressed in the neural epithelium at P0, but not at P7 or adulthood (**Figures 1D–F**). By contrast, LacZ staining was observed in the piriform area (PIR), mainly in the pyramidal layer (PIR2) at P7 and adulthood, but not at P0. In the cortex, the deep layer neurons expressed FLRT2 at the early stages, but FLRT2 expression was expanded in the adult mice (**Figures 1G–I** and **Supplementary Figure 2**). In CA1 of the hippocampus, FLRT2 expression was prominent after P7. In the brain stem and cerebellum, except for several nuclei, the intensity of LacZ staining was much weaker than in the cortex (**Figures 1J–O**). We could observe weak staining in the Purkinje layer of the posterior cerebellum in the adult mice (**Supplementary Figures 3A–C**). In the amygdala, weak and moderate FLRT2 expression was observed in the lateral amygdala nucleus (LA) at P7 and adulthood, respectively. In addition, a shift from moderate to weak FLRT2 expression was observed

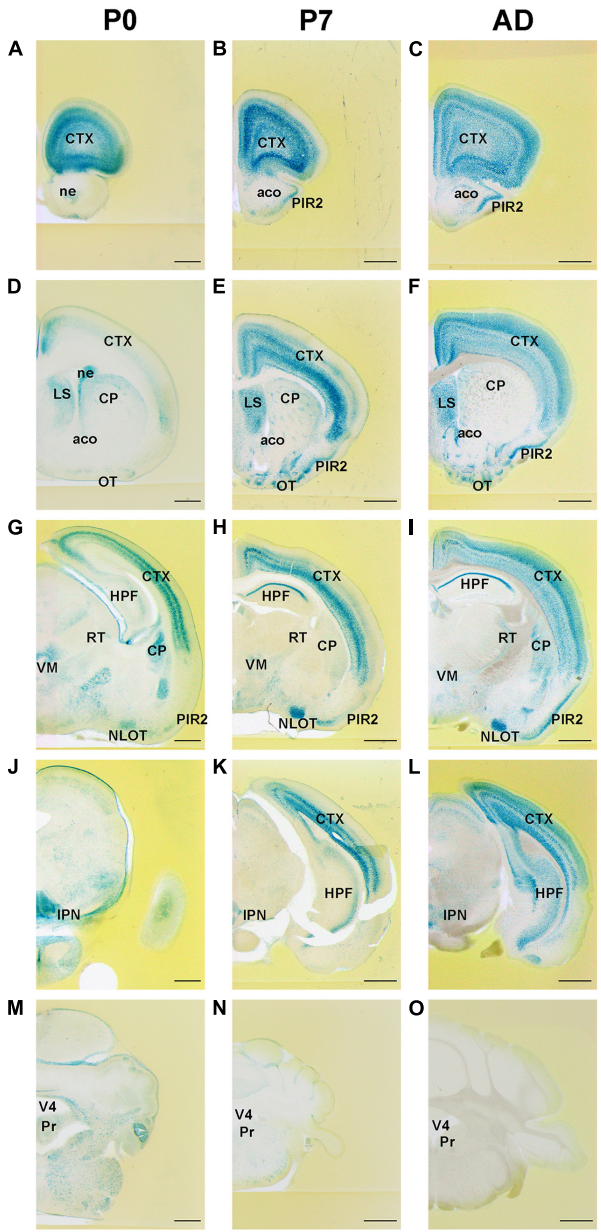

FIGURE 1 | Expression pattern of *Flrt2-lacZ* in the postnatal stages of brain development. *Flrt2-lacZ* expression was observed on the planes of the prefrontal cortex **(A–C)**, LS **(D–F)**, HPF **(G–I)**, midbrain **(J–L)**, and cerebellum **(M–O)** at P0 **(A,D,G,J,M)**, P7 **(B,E,H,K,N)**, and adulthood **(C,F,I,L,O)**. aco, anterior commissure, olfactory limb; ACB, nucleus accumbens; CP, caudate putamen; CTX, cerebral cortex; HPF, hippocampal formation; IPN, interpeduncular nucleus; LS, lateral septal nucleus; ne, neuroepithelium; NLOT, nucleus of the lateral olfactory tract; OT, olfactory tubercle; PIR2, piriform area, pyramidal layer; Pr, prepositus nucleus; RT, reticular nucleus of the thalamus; VM, ventral medial nucleus of thalamus; V4, fourth ventricle. Scale bars, 500 μm **(A,D,G,J,M)**; 1 mm **(B,C,E,F,H,I,K,L,N,O)**. *n* = 3, 3, and 4 for P0, P7 and adulthood, respectively.

in the basolateral amygdala nucleus, anterior part (BLAa) at P0, P7, and adulthood (**Supplementary Figures 3D–F**). During development, intermediate staining was consistently observed in some areas of the pons, such as the parabrachial nucleus ventral lateral part (PBlv), parabrachial nucleus external lateral part (PBle), and locus ceruleus (LC) (**Table 1**).

Within the basal forebrain, no LacZ staining was observed at P0 and a weak expression was observed at both P7 and adulthood (**Table 1**). In the diencephalon, LacZ staining was observed in the medial habenula (MH), the lateral habenula (LH) (**Supplementary Figures 4A–C**), and the ventromedial hypothalamic nucleus (VMH) (**Table 1**). In addition, LacZ staining was observed in the interpeduncular nucleus (IPN) at P0, P7, and adulthood (**Supplementary Figures 4D–F**) and the midbrain reticular nucleus (MRN) (**Table 1**).

Postnatal FLRT2 Expression in the Primary Somatosensory Area of Cortex and During Hippocampal Formation

As age increased, FLRT2 expression in the primary somatosensory area of cerebral cortex gradually spread from the deep layer to the superficial layers, except for layer I (**Figures 2A–C**). In layer II/III, moderate FLRT2 expression was observed at adulthood but not at P0 or P7, consistent with our previous report (Yamagishi et al., 2011). In adulthood, the strongest expression was observed in layer IV, where thalamocortical axons project. In layer V, moderate expression was observed at adulthood, whereas expression in this region was stronger at P0 and P7. In layer VI, as age increased, expression decreased from strong to moderate, as in layer V (**Figures 2A–C**). In addition, we also observed intense FLRT2 expression in the rostral part of the cerebral cortex at P0, but not at P7 or adulthood (**Supplementary Figure 1**). FLRT2 was expressed in Ctip2 + layer V at P0 (**Supplementary Figure 2**). In addition, we observed strong expression of FLRT2 on the pia surface at P0 that decreased at P7 and adulthood (**Figures 2A–C**).

During formation of CA1 of the hippocampus, although weak expression of FLRT2 was observed at P0, strong and specific expression was observed in pyramidal cell layers at P7 and adulthood (**Figures 2D–F**). In CA2, weak expression was observed at P0, and moderate expression was observed in the pyramidal cell layer at P7 and adulthood. In CA3 and DG, very faint expression was observed at all three stages.

Postnatal FLRT2 Expression in the Caudate Putamen, Lateral Septal Nucleus, and Nucleus of the Lateral Olfactory Tract

At P0, FLRT2 was widely expressed in the caudate putamen (CP) and in sparse clusters of the CP (**Figure 3A**). At P7, the clusters of medium LacZ staining were more prominent (**Figure 3B**). However, expression was dramatically reduced at adulthood (**Figure 3C**). On the other hand, in the lateral septal nucleus (LS), moderate expression was also observed at P0, P7, and adulthood (**Figures 3A–C**). Strong expression was observed in the neuroepithelium (ne) on the lateral side of the lateral ventricle at P0, but not at P7 or adulthood (**Figures 3A–C**). In addition, intense LacZ expression was observed in nucleus of the lateral olfactory tract (NLOT) at P7 and adulthood (**Figures 3D–F**).

TABLE 1 | Distribution and intensity of FLRT2-LacZ expression in the mouse CNS.

	***Flrt2-LacZ* expression**		
	P0	**P7**	**adulthood**
Telencephalon			
Olfactory system			
Olfactory bulb (OB)	−	−	−
Piriform area (PIR) layer 2	−	+ +	+ + +
Anterior olfactory nucleus (AON)	−	−	+
Olfactory tubercle (OT)	+	+ +	+ +
Nucleus of the lateral olfactory tract (NLOT)	+ +	+ + +	+ + +
Taenia tecta (TT) layer 2	+ +	+	+
Cerebral cortex			
Primary somatosensory area			
Layer I	−	−	−
Layer II/III	−	−	+
Layer IV	+ +	+	+ + +
Layer V	+ +	+ +	+ +
Layer VI	+	+ + +	+ +
Agranular insular area	+ +	+ +	+
Basal forebrain			
Bed nucleus of stria terminalis (BST)	−	+	+
Endopiriform nucleus (EP)	−	+	+
Claustrum (CLA)	−	+	+
Substantia innominata (SI)	−	+	+
Septum			
Lateral septal nucleus (LS)	+ +	+ +	+ +
Medial septal nucleus (MS)	−	−	−
Basal ganglia			
Caudate putamen (CP)	+ + +	+ +	+
Nucleus accumbens (ACB)	+ + +	+	+
Globus pallidus external segment (GPe)	+	−	−
Globus pallidus internal segment (GPi)	+	−	−
Subthalamic nucleus (STN)	+	+	+
Substantia nigra reticular part (SNr)	−	+	−
Substantia nigra compact part (SNc)	−	+	+
Hippocampal formation (HPF)			
CA1			
oriens	−	+	+
pyramidal layer	+	+ + +	+ + +
radiatum	−	−	−
lacunosum-moleculare	−	−	−
CA2			
oriens	−	−	+
pyramidal layer	−	+ + +	+ + +
radiatum	−	+	+
lacunosum-moleculare	−	−	+
CA3			
oriens	−	−	+
pyramidal layer	−	+	+
radiatum	−	−	+
lacunosum-moleculare	−	−	+
Dentate gyrus (DG)			
polymorph layer	+	+	+
granule cell layer	−	−	+
molecular layer	−	−	+

(Continued)

TABLE 1 | (Continued)

	***Flrt2-LacZ* expression**		
	P0	**P7**	**adulthood**
Amygdala			
Lateral amygdala nucleus (LA)	−	+	+ +
Basolateral amygdala nucleus, anterior part (BLAa)	+ +	+ +	+
Basolateral amygdala nucleus, posterior part (BLAp)	−	+ +	+
Basolateral amygdala nucleus, ventral part (BLAv)	−	+ +	+
Cortical amygdala area (COA)	+ +	+ +	+ +
Piriform-amygdala area (PAA)	−	+	+
Diencephalon			
Medial habenula (MH)	+ +	+	+
Lateral habenula (LH)	+ +	+	+
Reticular nucleus of the thalamus (RT)	−	−	+
Ventral medial nucleus of the thalamus (VM)	+ + +	+	+
Hypothalamus			
Paraventricular hypothalamic nucleus (PVH)	−	−	+
Ventromedial hypothalamic nucleus (VMH)	+ +	+ +	+
Arcuate hypothalamic nucleus (ARH)	−	−	+
Lateral hypothalamic area (LHA)	+	+	+
Suprachiasmatic nucleus (SCH)	−	−	+
Midbrain			
Superior colliculus superficial gray layer (SCsg)	−	+	+ +
Superior colliculus intermediate gray layer (SCig)	−	+	+
Superior colliculus deep gray layers (SCdg)	−	−	+
Interpeduncular nucleus (IPN)	+ + +	+ +	+
Periaqueductal gray (PAG)	+	+	+
Midbrain reticular nucleus (MRN)	+ +	+	+
Hindbrain			
Cerebellum granular layer	−	−	−
Cerebellum Purkinje layer	−	−	+
Cerebellum molecular layer	−	−	−
Pontine reticular nucleus (PRNr)	+	+	−
Parabrachial nucleus ventral lateral part (PBlv)	+ +	+ +	+ +
Parabrachial nucleus external lateral part (PBle)	+ +	+ +	+ +
Locus ceruleus (LC)	+ +	+	+
Laterodorsal tegmental nucleus (LDT)	+	+	+
Dorsal tegmental nucleus (DTN)	+ + +	+ + +	+ +

FLRT2 Expression in the Ventral Medial Nucleus, the Reticular Nucleus of the Thalamus, and the Dorsal Tegmental Nucleus

Although strong expression was observed at the ventral medial nucleus of the thalamus (VM) at P0, expression decreased at P7 and adulthood (**Figures 4A–C**). Additionally, in the reticular nucleus of the thalamus (RT), no expression was observed at P0 or P7, but weak expression was observed at adulthood. In the dorsal tegmental nucleus (DTN) in the midbrain, strong expression was observed at P0 and P7, but at adulthood,

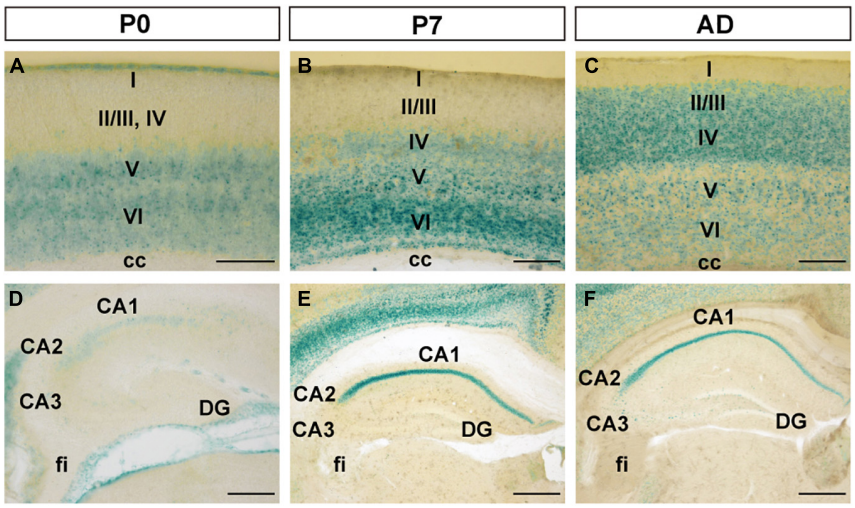

FIGURE 2 | FLRT2 expression in the cortical region (CTX) and during hippocampal formation (HPF) at P0, P7, and adulthood. **(A–C)** In the cerebral cortex, FLRT2 was expressed at deep layers at P0 **(A)**, followed by layer IV at P7 **(B)** and superficial layers II/III at adulthood **(C)**. **(D–F)** In the hippocampus, FLRT2 was expressed at a lower level in the CA1 at P0 **(D)**, becoming more intense at P7 **(E)** and adulthood **(F)**, concentrated in the pyramidal layer of CA1 but not CA2, CA3, or DG. cc, corpus callosum; CA1, Ammon's horn field 1; CA2, Ammon's horn field 2; CA3, Ammon's horn field 3; DG, dentate gyrus; I–VI, layers of cortical region. Scale bars, 100 μm **(A)**; 200 μm **(B,C,D)**; 500 μm **(E,F)**. *n* = 3, 3, and 4 for P0, P7 and adulthood, respectively.

expression was weakened (**Figures 4D–F**). Expression in the laterodorsal tegmental nucleus (LDT) was constantly weaker than in DTN. In other areas of the thalamus and midbrain, FLRT2 expression level was very low (**Figures 1G–L** and **Table 1**).

FLRT2 Is Expressed in Pre- and Postsynapses in the CA1, but Is Dispensable for CA3-CA1 Schaffer Collateral Synaptic Transmission

Because LacZ staining was confined to the CA1 region in the adult hippocampus (**Figures 2F**, **5A**), we next sought to visualize FLRT2 protein expression by immunostaining. FLRT2 immunoreactivity was high in the layers of the stratum oriens (SO), stratum radiatum (SR), and stratum lacunosum-moleculare (SLM), but not in the stratum pyramidale (SP) (**Figure 5B**). Reactivity was dramatically diminished in the Nestin-Cre;FLRT2$^{lx/lx}$ cKO as expected, indicating the specificity of the antibody (**Figure 5C**). Higher magnification revealed that in the SR, FLRT2 localized in globular dot patterns and was partially colocalized with the presynapses (vGLUT1; 30.6%) and postsynapses (PSD95; 15.7%), respectively (**Figures 5E–I**). The postsynaptic localization was consistent with previous findings (Schroeder et al., 2018). In addition, FLRT2 was expressed in the vascular endothelial cells on the border between the SLM and DG, and this expression could not be abolished by crossing with Nestin-Cre mice. We could not detect any signal in the SR or SO of the cKO mice, indicating that the endothelial cells of capillary vessels do not express FLRT2. Recombination of FLRT2 allele by Nestin-Cre was also confirmed by western blotting (**Supplementary Figure 5**).

Next, we investigated electrophysiological properties to determine whether FLRT2 expression on postsynapses is involved in synaptic transmission in the CA3–CA1 Schaffer collateral pathway (**Supplementary Figures 6A–D**). However, relative to the control group, we could not detect any alteration in either the amplitude or slope of fEPSP in the Emx1-Cre; FLRT2$^{lx/lx}$ cKO mice (**Supplementary Figures 6A,B**). Furthermore, we observed no significant differences in paired-pulse facilitation before or after LTP induction or in TBS-induced LTP (**Supplementary Figures 6C,D**). These results indicate that FLRT2 is dispensable for CA3-CA1 Schaffer collateral synaptic transmission.

FLRT2 Expression Is Elevated in Response to Spinal Cord Injury

In the spinal cord, we observed down-regulation of FLRT2 during development (**Supplementary Figures 3G–I**). Next, because many axon guidance molecules, including FLRT3 and RGMa, are upregulated upon central and peripheral nervous system injury (Robinson et al., 2004; Tsuji et al., 2004; Hata et al., 2006; Yamada et al., 2019), we investigated whether FLRT2 is upregulated after spinal cord injury. FLRT2 was highly upregulated around lesion sites 7 days after thoracic spinal cord injury (**Figures 6A–D**); weak expression was maintained until day 14, but was no longer visible by day 28 (**Figures 6C,D**). In the uninjured spinal cord gray matter, FLRT2 expression was weak in wild type mice (**Figures 6F,I**), which is consistent with the result of LacZ staining (**Supplementary Figure 3I**), and a relatively small number of GFAP + cells was observed (**Figures 6G,J**). Expression of FLRT2, induced at the subacute phase, was localized on GFAP + reactive astrocytes (**Figures 6K–M**). Interestingly, the provocation of GFAP at 7 days after the injury was decreased in Nestin-Cre; FLRT2$^{lx/lx}$ cKO mice (**Figures 6N–P**). These results suggest that FLRT2

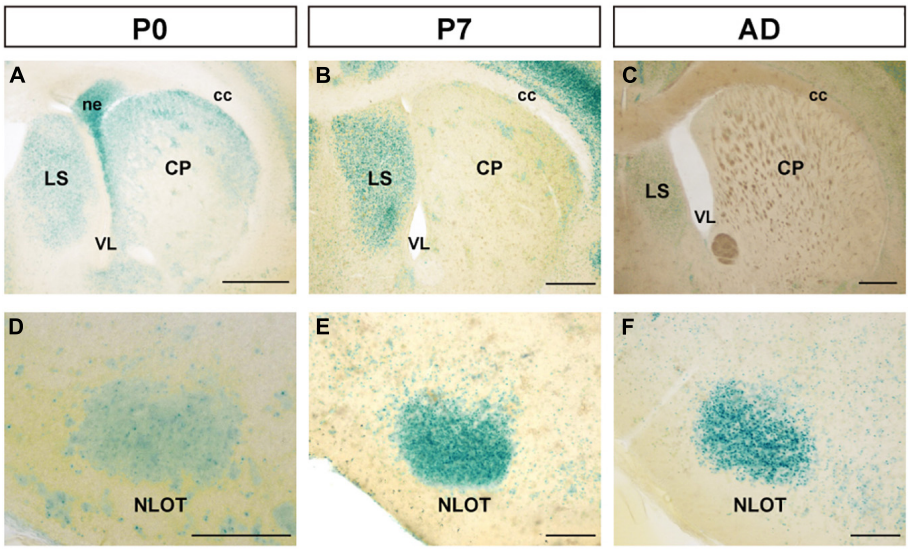

FIGURE 3 | Expression pattern in the caudate putamen (CP), lateral septal nucleus (LS), and nucleus of the lateral olfactory tract (NLOT) at P0, P7, and adult mouse. **(A–C)** In the caudate putamen (CP), FLRT2 signals decreased during development. Note that strong expression was observed in the neuroepithelium at P0 **(A)** and the lateral septum at P7 **(B)**. **(D–F)** In the nucleus of the lateral olfactory tract (NLOT), intermediate expression of FLRT2 was observed at P0 **(D)**, and high expression was observed at P7 **(E)** and adulthood **(F)**. cc, corpus callosum; CP, caudate putamen; LS, lateral septal nucleus; ne, neuroepithelium; NLOT, nucleus of the lateral olfactory tract; VL, lateral ventricle. Scale bars, 500 μm **(A–C)**; 200 μm **(D–F)**. *n* = 3, 3, and 4 for P0, P7 and adulthood, respectively.

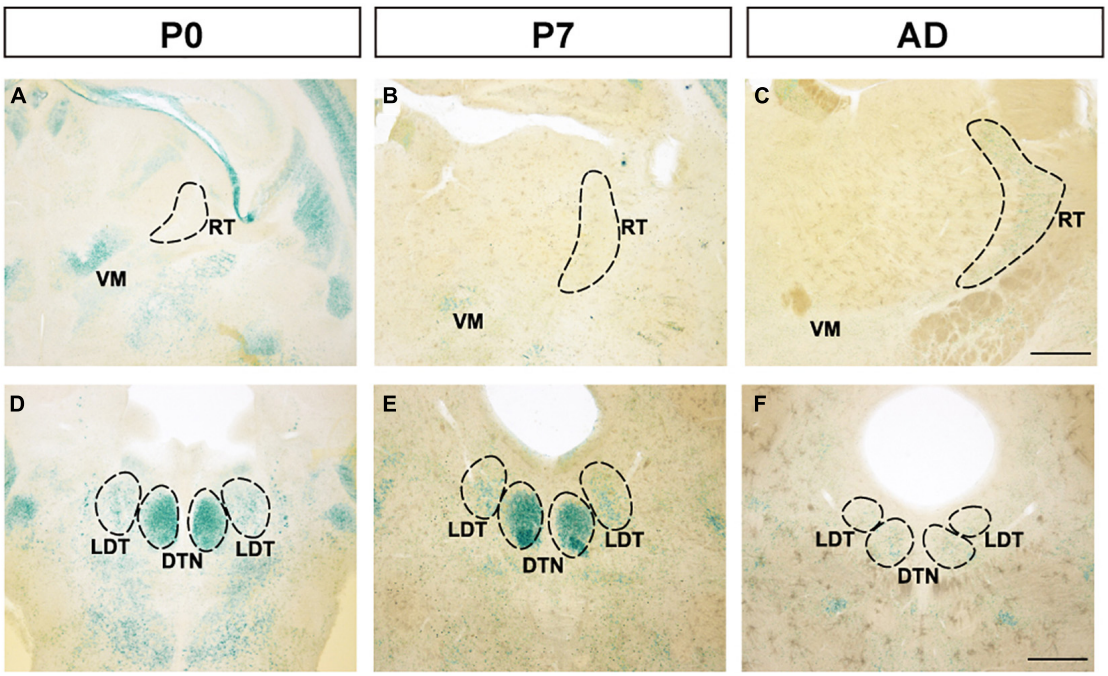

FIGURE 4 | Expression patterns in the thalamus and midbrain at P0, P7, and adulthood, revealed by X-gal staining. **(A–C)** FLRT2 expression levels changed from absent to weak in the ventral medial nucleus of the thalamus (VM) and from strong to weak in the reticular nucleus of the thalamus (RT) during development. **(D–F)** In the dorsal tegmental nucleus (DTN), expression of FLRT2 was high at P0 and P7, but decreased by adulthood. DTN, dorsal tegmental nucleus; LDT, laterodorsal tegmental nucleus; RT, reticular nucleus of the thalamus; VM, ventral medial nucleus of the thalamus. Scale bars, 500 μm **(A–F)**. *n* = 3, 3, and 4 for P0, P7 and adulthood, respectively.

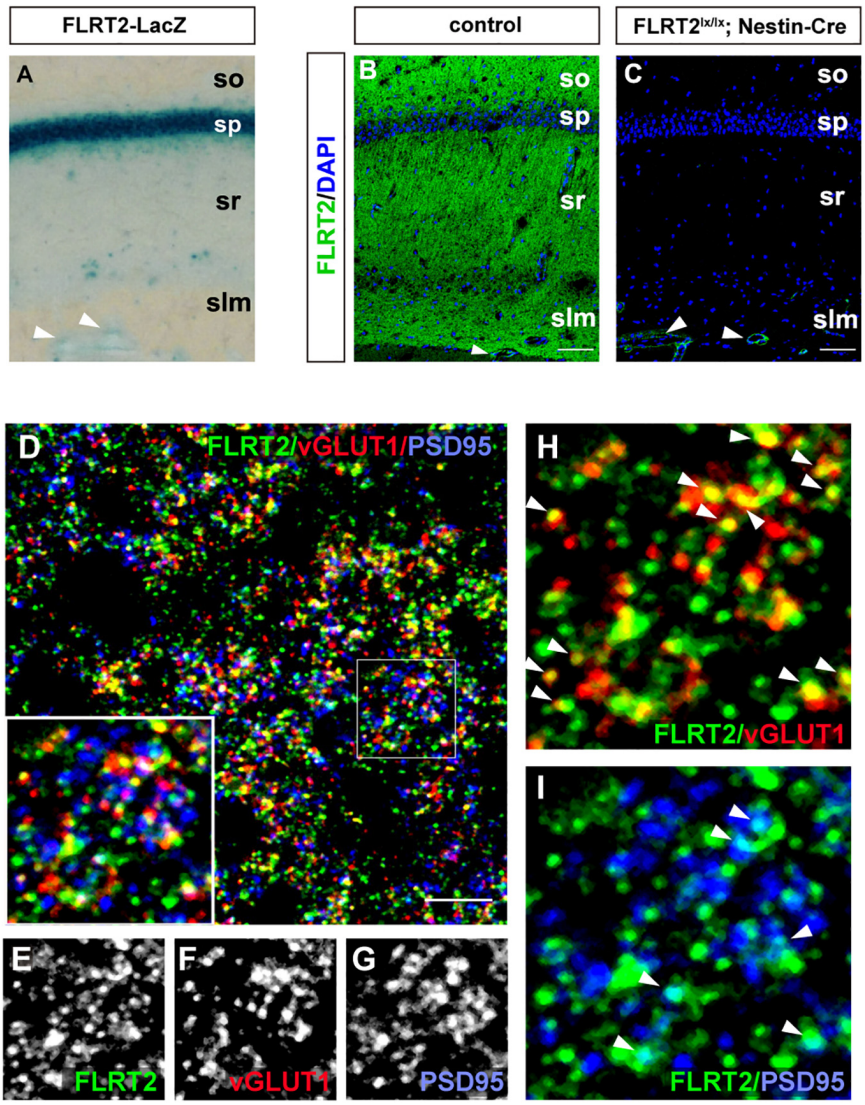

FIGURE 5 | Synaptic localization of FLRT2 in the CA1 of adult mice. **(A)** FLRT2-*LacZ* expression was strong in the pyramidal layer. **(B)** FLRT2 protein expression was distributed in the layers of so, sr, and slm but not in sp. **(C)** FLRT2 was specifically knocked out in CA1 neurons in conditional knockout mice, but not in blood vessels (arrowheads). **(D–I)** FLRT2 partly colocalized with vGLUT1 and PSD95 (arrowheads in **H** and **I**). Inset: higher magnification. so, stratum oriens; sp, stratum pyramidale; sr, stratum radiatum; slm, stratum lacunosum-moleculare. Scale bars, 100 μm **(B,C)**, 5 μm **(D)**. *n* = 4 for *Flrt2-LacZ* KI adulthood mice.

serves as a repulsive guidance molecule like RGMa, inhibits CNS regeneration, acts as an adhesive molecule, and contributes to form glial scar.

DISCUSSION

In this study, we observed FLRT2 expression in multiple regions of the CNS at these three time points (**Figure 1**). Confined FLRT2 expression in CA1 at the postnatal stage suggested a pivotal role for FLRT2 in synaptic function (**Figure 2**). In addition, FLRT2 expression was confined to the CA1 region and partly localized on pre- and postsynapses whereas only few expression was observed in CA3 and dentate gyrus (DG) (**Figure 5**). Furthermore, astrocytes transiently expressed FLRT2 in the penumbra region after spinal cord injury (**Figure 6**).

In the early postpartum period, the cortex is still rapidly developing. We observed that FLRT2 expression was confined to deep layers of the cortex at P0, consistent with our previous report (Yamagishi et al., 2011). Because FLRT2 acts as both a repulsive guidance cue and an adhesive molecule (Yamagishi et al., 2011), it may play a role in fine tuning of cortical circuits. Eventually, in adult mouse brain, cells expressing FLRT2 appeared mainly in layer IV, which is occupied by spiny stellate cells (Lefort et al., 2009). This region is where thalamocortical axons predominantly terminate (White and Keller, 1989), suggesting that FLRT2 may play an important role in the formation of neural networks. Interestingly, we observed expression of FLRT2 in the RT only

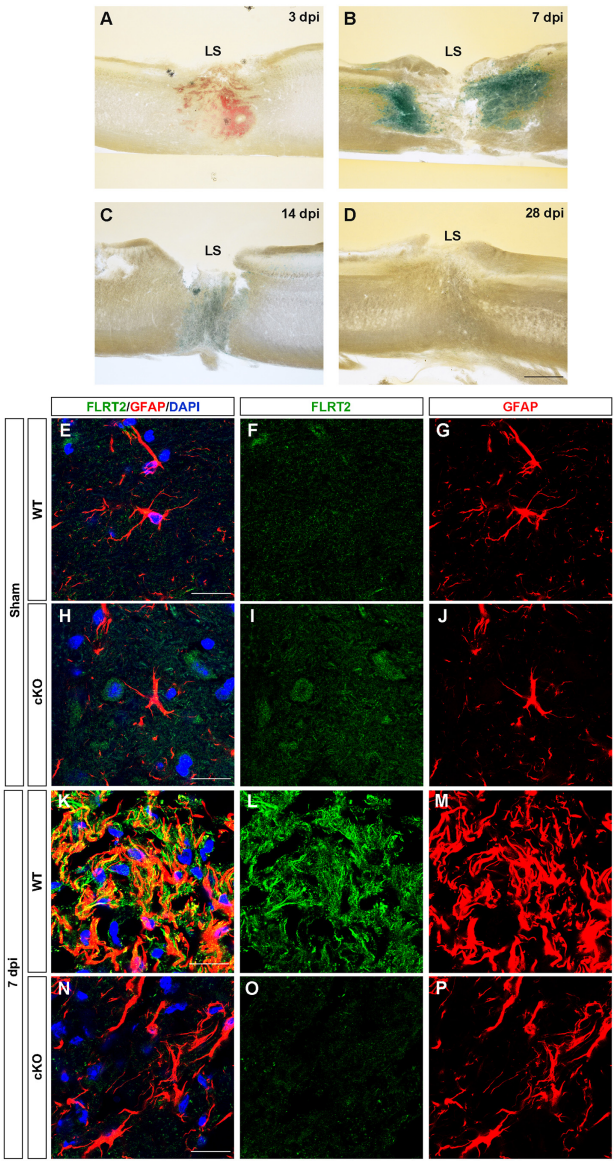

FIGURE 6 | FLRT2 is strongly expressed in astrocytes 7 days after spinal cord injury. **(A–D)** Sagittal slices 3, 7, 14, and 28 days after spinal cord injury, subjected to X-gal staining. Strong FLRT2 expression was observed at 7 dpi and decreased rapidly. **(E–P)** FLRT2 was expressed in GFAP + astrocytes at 7 dpi in wild type mice. GFAP induction after spinal cord injury was decreased in FLRT2 cKO. $n = 3$ for each group. dpi, days post-injury; LS, lesion site. Scale bars, 500 μm **(A–D)**; 20 μm **(E–M)**.

in the brains of adult mice. Because it mainly receives projections from the cortex, this may be intrinsically related to expression of FLRT2 in the cortex. On the other hand, in the VM, which receives afferent input from the basal ganglia and relays to the cerebral motor cortex (Kuramoto et al., 2015), the expression of FLRT2 at P7 and adulthood was much lower than at P0. In addition, we also observed reduced FLRT2 expression during development in the CP, a part of the basal ganglia. Based on these observations, FLRT2 may play a key role not only in the development of specific brain regions but also in intricate inter-regional connections such as the cortico-basal ganglia-thalamo-cortical loop.

Notably, we observed FLRT2 expression in vessels in the hippocampus that could not be abolished by Nestin-Cre (**Figure 5C**). Our previous studies showed that mice lacking FLRT2 in vascular endothelial cells exhibit embryonic lethality at mid-gestation with systemic congestion and hypoxia (Tai-Nagara et al., 2017). Notably, FLRT3 is a newly identified member of a family of axon guidance-related factors that participate in VEGF-signaling and regulation of endothelial cell functions (Jauhiainen et al., 2019). We observed that FLRT2 is expressed in the vascular endothelial cells of the hippocampus in adult mice, indicating that FLRT2 may play a key role in maintenance of vascular morphology and function at various stages of development. However, the function of FLRT2 in vascular endothelium in the CNS remains unclear and requires further study.

In contrast to weak expression in the hippocampal CA1 at P0, high expression in the pyramidal layer limited to CA1 began to be observed at P7 and was maintained till adulthood. Our results showed that FLRT2 is expressed by CA1 pyramidal neurons, consistent with the Allen Brain Atlas. Electrophysiology revealed that the CA1 postsynaptic localization of FLRT2 is dispensable in the Schaffer collateral synaptic connection (**Supplementary Figure 6**). Electrophysiological studies revealed that basal synaptic transmission of CA3-CA1 Schaffer collateral synapses in hippocampus did not altered in Emx1-Cre; FLRT2$^{lox/lox}$ cKO, indicating dispensability of FLRT2. Consistent to our result, Cicvaric et al. reported that in haplodeficient *FLRT2*$^{+/-}$ male mice don't show any defect in synaptic transmission and plasticity in the hippocampal CA1, although *FLRT2*$^{+/-}$ female mice showed reduced synaptic transmission and enhanced LTP because of decreased expression levels of EAAT2 and estrogen receptor β (Cicvaric et al., 2018). In the present study, we did not analyze female mice so that synaptic properties in the gender difference in the mutant mice are still unclear. On the other hand, knocking down postsynaptic FLRT2 in the CA1 caused decreased synaptic density at SC inputs, decreasing the frequency of EPSPs and the amplitude of AMPA and NMDA EPSCs (Schroeder et al., 2018). Because we used FLRT2 conditional knockout mice, there may have been developmental compensation by another molecule, e.g., FLRT1. Recent studies revealed that the TEN2–LPHN3–FLRT3 ternary complex plays a key role in the formation of synaptic properties (Sando et al., 2019; Li et al., 2020), but it remains unclear how FLRT2 plays a role in the complex. Further studies are required for clarify detailed function of FLRT2 in the synaptic transmission.

In terms of the olfactory system, FLRT2 expression changed from postpartum to adulthood in layer 2 of the PIR and NLOT. Layer 2 of the PIR is mainly composed of semilunar cells and superficial pyramidal cells. These two main types of primary neurons in the densely populated input layer (layer II) of the PIR have markedly different synaptic and firing characteristics, and they may provide the basis of coding strategies used to represent odors (Suzuki and Bekkers, 2006). This finding indicates that FLRT2 may participate in the coding strategy of PIR during the development of the nervous system. Rat studies have

demonstrated that normal functioning of the olfactory system requires NLOT integrity (Vaz et al., 2017). Therefore, FLRT2 may be involved in the development of the olfactory system.

Expression of FLRT2 in the DTN in the early postpartum period was strong, but the expression dropped to a lower level in adulthood. The only known function of the DTN is to generate head-direction cell signals (Sharp et al., 2001; Bassett et al., 2007). In addition, a recent study showed that bilateral lesions of the DTN promote awakening at the expense of sleep (Chazalon et al., 2018). These findings indicate that FLRT2 contributes to establishment of the DTN neural network, and is involved in the sleep and awakening mechanism. Recent studies in rats indicate that the habenula is linked with LDT, either via direct reciprocal projections from/to the medial division of the lateral habenula (LHbM) or indirectly via the medial habenula (MHb)–interpeduncular nucleus (IPN) axis, supporting a functional role for LDT in the regulation of aversive behaviors, and for LHb as a master controller of ascending brainstem state-setting modulatory projection systems (Bueno et al., 2019). We also observed changes in FLRT2 expression in habenula and IPN, as observed in the LDT. Therefore, FLRT2 may play a role in formation of the neural network among the LDT, habenula, and IPN.

Here, we observed that FLRT2 is strongly expressed on GFAP + astrocytes, and the induction of GFAP was decreased in FLRT2 cKO mice at 7 days after spinal cord injury. The glial component of the scar after spinal cord injury consists of reactive astrocytes, NG2 + oligodendrocyte precursors, and microglia in the penumbra (Tran et al., 2018). Reactive astrocytes rapidly proliferate and densely populate the area around the lesion core within 7–10 days after glial scar formation (Wanner et al., 2013). In addition, a neutralizing antibody against repulsive guidance molecule a (RGMa) can dramatically facilitate locomotor improvement and axon regeneration after spinal cord injury in rats (Hata et al., 2006). Our results suggested that FLRT2 expressed on reactive astrocytes contributes to formation of glial scars as an adhesive molecule and induction of GFAP and inhibits axonal regeneration as a repulsive molecule. Thus, inhibiting FLRT2 function by applying neutralization antibodies may ameliorate scar formation after spinal cord injury and promotes CNS regeneration.

CONCLUSION

FLRT2 exhibits different expression patterns at various stages from the early postnatal stage to maturity, indicating that it plays important roles in mouse development. In addition, FLRT2 expression is confined to the CA1 region and partly localized on pre- and postsynapses. We also observed FLRT2 signal at the boundary of lesion sites 7 and 14 days after spinal cord injury. These results provide some useful information about the role of FLRT2 in the developmental mechanisms of the CNS, the mechanism of regulation of synaptic plasticity, and other central neuropathy processes.

DATA AVAILABILITY STATEMENT

The original contributions presented in the study are included in the article/**Supplementary Material**, further inquiries can be directed to the corresponding author.

ETHICS STATEMENT

The animal study was reviewed and approved by The Animal Research Committee of Hamamatsu University School of Medicine.

AUTHOR CONTRIBUTIONS

JL and SY designed, analyzed, and wrote the manuscript. YS, SO, SI, and SL performed the research. YM and KS analyzed the data. All authors have seen and agreed with the content of the manuscript.

FUNDING

This work was supported by grants from JSPS KAKENHI (Grant Number 17K08512, 20K21499, and 21H02655), the Takeda Science Foundation, the Hamamatsu Foundation for Science and Technology Promotion, and an HUSM Grant-in-Aid.

ACKNOWLEDGMENTS

We would like to thank Rüdiger Klein (Max-Planck Institute), Takuji Iwasato (National Institute of Genetics), Ryuichi Kageyama (Kyoto University) for providing mice, and Makiko Kato (Hamamatsu University School of Medicine) for providing excellent technical support. Confocal imaging was obtained with the kind support of the Advanced Research Facilities and Services, Preeminent Medical Photonics Education and Research Center, Hamamatsu University School of Medicine.

SUPPLEMENTARY MATERIAL

The Supplementary Material for this article can be found online at: https://www.frontiersin.org/articles/10.3389/fnmol.2021.756264/full#supplementary-material

REFERENCES

Akita, T., Kumada, T., Yoshihara, S., Egea, J., and Yamagishi, S. (2016). Ion channels, guidance molecules, intracellular signaling and transcription factors regulating nervous and vascular system development. *J. Physiol. Sci.* 66, 175–188. doi: 10.1007/s12576-015-0416-1

Arima, H., Hanada, M., Hayasaka, T., Masaki, N., Omura, T., Xu, D., et al. (2014). Blockade of IL-6 signaling by MR16-1 inhibits reduction of docosahexaenoic

acid-containing phosphatidylcholine levels in a mouse model of spinal cord injury. *Neuroscience* 269, 1–10. doi: 10.1016/j.neuroscience.2014.03.012

Bassett, J. P., Tullman, M. L., and Taube, J. S. (2007). Lesions of the tegmentomammillary circuit in the head direction system disrupt the head direction signal in the anterior thalamus. *J. Neurosci.* 27, 7564–7577. doi: 10.1523/jneurosci.0268-07.2007

Bueno, D., Lima, L. B., Souza, R., Goncalves, L., Leite, F., Souza, S., et al. (2019). Connections of the laterodorsal tegmental nucleus with the habenular-interpeduncular-raphe system. *J. Comp. Neurol.* 527, 3046–3072. doi: 10.1002/cne.24729

Chazalon, M., Dumas, S., Bernard, J. F., Sahly, I., Tronche, F., De Kerchove D'exaerde, A., et al. (2018). The GABAergic Gudden's dorsal tegmental nucleus: a new relay for serotonergic regulation of sleep-wake behavior in the mouse. *Neuropharmacology* 138, 315–330. doi: 10.1016/j.neuropharm.2018.06.014

Chen, G., Sima, J., Jin, M., Wang, K. Y., Xue, X. J., Zheng, W., et al. (2008). Semaphorin-3A guides radial migration of cortical neurons during development. *Nat. Neurosci.* 11, 36–44. doi: 10.1038/nn2018

Cicvaric, A., Yang, J., Bulat, T., Zambon, A., Dominguez-Rodriguez, M., Kühn, R., et al. (2018). Enhanced synaptic plasticity and spatial memory in female but not male FLRT2-haplodeficient mice. *Sci. Rep.* 8:3703.

Del Toro, D., Carrasquero-Ordaz, M. A., Chu, A., Ruff, T., Shahin, M., Jackson, V. A., et al. (2020). Structural basis of teneurin-latrophilin interaction in repulsive guidance of migrating neurons. *Cell* 180, 323.e19–339.e19.

Egea, J., Erlacher, C., Montanez, E., Burtscher, I., Yamagishi, S., Hess, M., et al. (2008). Genetic ablation of FLRT3 reveals a novel morphogenetic function for the anterior visceral endoderm in suppressing mesoderm differentiation. *Genes Dev.* 22, 3349–3362. doi: 10.1101/gad.486708

Fleitas, C., Marfull-Oromi, P., Chauhan, D., Del Toro, D., Peguera, B., Zammou, B., et al. (2021). FLRT2 and FLRT3 cooperate in maintaining the tangential migratory streams of cortical interneurons during development. *J. Neurosci.* 41, 7350–7362.

Gonda, Y., Namba, T., and Hanashima, C. (2020). Beyond axon guidance: roles of slit-robo signaling in neocortical formation. *Front. Cell Dev. Biol.* 8:607415. doi: 10.3389/fcell.2020.607415

Haines, B. P., Wheldon, L. M., Summerbell, D., Heath, J. K., and Rigby, P. W. (2006). Regulated expression of FLRT genes implies a functional role in the regulation of FGF signalling during mouse development. *Dev. Biol.* 297, 14–25. doi: 10.1016/j.ydbio.2006.04.004

Hata, K., Fujitani, M., Yasuda, Y., Doya, H., Saito, T., Yamagishi, S., et al. (2006). RGMa inhibition promotes axonal growth and recovery after spinal cord injury. *J. Cell Biol.* 173, 47–58. doi: 10.1083/jcb.200508143

Ikegaya, S., Iga, Y., Mikawa, S., Zhou, L., Abe, M., Sakimura, K., et al. (2020). Decreased proliferation in the neurogenic niche, disorganized neuroblast migration, and increased oligodendrogenesis in adult netrin-5-deficient mice. *Front. Neurosci.* 14:570974. doi: 10.3389/fnins.2020.570974

Isaka, F., Ishibashi, M., Taki, W., Hashimoto, N., Nakanishi, S., and Kageyama, R. (1999). Ectopic expression of the bHLH gene Math1 disturbs neural development. *Eur. J. Neurosci.* 11, 2582–2588. doi: 10.1046/j.1460-9568.1999.00699.x

Ishii, C., Shibano, N., Yamazaki, M., Arima, T., Kato, Y., Ishii, Y., et al. (2021). CAPS1 is involved in hippocampal synaptic plasticity and hippocampus-associated learning. *Sci. Rep.* 11:8656.

Iwasato, T., Datwani, A., Wolf, A. M., Nishiyama, H., Taguchi, Y., Tonegawa, S., et al. (2000). Cortex-restricted disruption of NMDAR1 impairs neuronal patterns in the barrel cortex. *Nature* 406, 726–731. doi: 10.1038/35021059

Jackson, V. A., Del Toro, D., Carrasquero, M., Roversi, P., Harlos, K., Klein, R., et al. (2015). Structural basis of latrophilin-FLRT interaction. *Structure* 23, 774–781. doi: 10.1016/j.str.2015.01.013

Jauhiainen, S., Laakkonen, J. P., Ketola, K., Toivanen, P. I., Nieminen, T., Ninchoji, T., et al. (2019). Axon guidance-related factor FLRT3 regulates VEGF-signaling and endothelial cell function. *Front. Physiol.* 10:224. doi: 10.3389/fphys.2019.00224

Kuramoto, E., Ohno, S., Furuta, T., Unzai, T., Tanaka, Y. R., Hioki, H., et al. (2015). Ventral medial nucleus neurons send thalamocortical afferents more widely and more preferentially to layer 1 than neurons of the ventral anterior-ventral lateral nuclear complex in the rat. *Cereb. Cortex* 25, 221–235. doi: 10.1093/cercor/bht216

Lacy, S. E., Bönnemann, C. G., Buzney, E. A., and Kunkel, L. M. (1999). Identification of FLRT1, FLRT2, and FLRT3: a novel family of transmembrane leucine-rich repeat proteins. *Genomics* 62, 417–426. doi: 10.1006/geno.1999.6033

Lefort, S., Tomm, C., Floyd Sarria, J. C., and Petersen, C. C. (2009). The excitatory neuronal network of the C2 barrel column in mouse primary somatosensory cortex. *Neuron* 61, 301–316. doi: 10.1016/j.neuron.2008.12.020

Li, J., Xie, Y., Cornelius, S., Jiang, X., Sando, R., Kordon, S. P., et al. (2020). Alternative splicing controls teneurin-latrophilin interaction and synapse specificity by a shape-shifting mechanism. *Nat. Commun.* 11:2140.

Lu, Y. C., Nazarko, O. V., Sando, R., Salzman, G. S., Li, N.-S., Südhof, T. C., et al. (2015). Structural basis of latrophilin-FLRT-UNC5 interaction in cell adhesion. *Structure* 23, 1678–1691. doi: 10.1016/j.str.2015.06.024

Maretto, S., Muller, P. S., Aricescu, A. R., Cho, K. W., Bikoff, E. K., and Robertson, E. J. (2008). Ventral closure, headfold fusion and definitive endoderm migration defects in mouse embryos lacking the fibronectin leucine-rich transmembrane protein FLRT3. *Dev. Biol.* 318, 184–193. doi: 10.1016/j.ydbio.2008.03.021

Muller, P. S., Schulz, R., Maretto, S., Costello, I., Srinivas, S., Bikoff, E., et al. (2011). The fibronectin leucine-rich repeat transmembrane protein Flrt2 is required in the epicardium to promote heart morphogenesis. *Development* 138, 1297–1308. doi: 10.1242/dev.059386

Ogata, S., Morokuma, J., Hayata, T., Kolle, G., Niehrs, C., Ueno, N., et al. (2007). TGF-beta signaling-mediated morphogenesis: modulation of cell adhesion via cadherin endocytosis. *Genes Dev.* 21, 1817–1831. doi: 10.1101/gad.1541807

O'Sullivan, M. L., De Wit, J., Savas, J. N., Comoletti, D., Otto-Hitt, S., Yates, J. R. III, et al. (2012). FLRT proteins are endogenous latrophilin ligands and regulate excitatory synapse development. *Neuron* 73, 903–910. doi: 10.1016/j.neuron.2012.01.018

Peregrina, C., and Del Toro, D. (2020). FLRTing neurons in cortical migration during cerebral cortex development. *Front. Cell Dev. Biol.* 8:578506. doi: 10.3389/fcell.2020.578506

Robinson, M., Parsons Perez, M. C., Tebar, L., Palmer, J., Patel, A., Marks, D., et al. (2004). FLRT3 is expressed in sensory neurons after peripheral nerve injury and regulates neurite outgrowth. *Mol. Cell. Neurosci.* 27, 202–214. doi: 10.1016/j.mcn.2004.06.008

Sando, R., Jiang, X., and Sudhof, T. C. (2019). Latrophilin GPCRs direct synapse specificity by coincident binding of FLRTs and teneurins. *Science* 363:eaav7969. doi: 10.1126/science.aav7969

Schroeder, A., Vanderlinden, J., Vints, K., Ribeiro, L. F., Vennekens, K. M., Gounko, N. V., et al. (2018). A modular organization of LRR protein-mediated synaptic adhesion defines synapse identity. *Neuron* 99, 329.e7–344.e7.

Seiradake, E., Del Toro, D., Nagel, D., Cop, F., Hartl, R., Ruff, T., et al. (2014). FLRT structure: balancing repulsion and cell adhesion in cortical and vascular development. *Neuron* 84, 370–385. doi: 10.1016/j.neuron.2014.10.008

Sharp, P. E., Tinkelman, A., and Cho, J. (2001). Angular velocity and head direction signals recorded from the dorsal tegmental nucleus of gudden in the rat: implications for path integration in the head direction cell circuit. *Behav. Neurosci.* 115, 571–588. doi: 10.1037/0735-7044.115.3.571

Suzuki, N., and Bekkers, J. M. (2006). Neural coding by two classes of principal cells in the mouse piriform cortex. *J. Neurosci.* 26, 11938–11947. doi: 10.1523/jneurosci.3473-06.2006

Tai-Nagara, I., Yoshikawa, Y., Numata, N., Ando, T., Okabe, K., Sugiura, Y., et al. (2017). Placental labyrinth formation in mice requires endothelial FLRT2/UNC5B signaling. *Development* 144, 2392–2401.

Torii, M., Hashimoto-Torii, K., Levitt, P., and Rakic, P. (2009). Integration of neuronal clones in the radial cortical columns by EphA and ephrin-A signalling. *Nature* 461, 524–528. doi: 10.1038/nature08362

Tran, A. P., Warren, P. M., and Silver, J. (2018). The biology of regeneration failure and success after spinal cord injury. *Physiol. Rev.* 98, 881–917. doi: 10.1152/physrev.00017.2017

Tsuji, L., Yamashita, T., Kubo, T., Madura, T., Tanaka, H., Hosokawa, K., et al. (2004). FLRT3, a cell surface molecule containing LRR repeats and a FNIII domain, promotes neurite outgrowth. *Biochem. Biophys. Res. Commun.* 313, 1086–1091. doi: 10.1016/j.bbrc.2003.12.047

Vaz, R. P., Cardoso, A., Sa, S. I., Pereira, P. A., and Madeira, M. D. (2017). The integrity of the nucleus of the lateral olfactory tract is essential for the normal functioning of the olfactory system. *Brain Struct. Funct.* 222, 3615–3637.

Wanner, I. B., Anderson, M. A., Song, B., Levine, J., Fernandez, A., Gray-Thompson, Z., et al. (2013). Glial scar borders are formed by newly proliferated, elongated astrocytes that interact to corral inflammatory and fibrotic cells via STAT3-dependent mechanisms after spinal cord injury. *J. Neurosci.* 33, 12870–12886. doi: 10.1523/jneurosci.2121-13.2013

Wheldon, L. M., Haines, B. P., Rajappa, R., Mason, I., Rigby, P. W., and Heath, J. K. (2010). Critical role of FLRT1 phosphorylation in the interdependent regulation of FLRT1 function and FGF receptor signalling. *PLoS One* 5:e10264. doi: 10.1371/journal.pone.0010264

White, E. L., and Keller, A. (1989). *Cortical Circuits: Synaptic Organization of the Cerebral Cortex: Structure, Function, and Theory*. Berlin: Springer.

Yamada, M., Fujita, Y., Hayano, Y., Hayakawa, H., Baba, K., Mochizuki, H., et al. (2019). Increased expression of fibronectin leucine-rich transmembrane protein 3 in the dorsal root ganglion induces neuropathic pain in rats. *J. Neurosci.* 39, 7615–7627.

Yamagishi, S., Bando, Y., and Sato, K. (2021). Involvement of netrins and their receptors in neuronal migration in the cerebral cortex. *Front. Cell Dev. Biol.* 8:590009. doi: 10.3389/fcell.2020.590009

Yamagishi, S., Hampel, F., Hata, K., Del Toro, D., Schwark, M., Kvachnina, E., et al. (2011). FLRT2 and FLRT3 act as repulsive guidance cues for Unc5-positive neurons. *EMBO J.* 30, 2920–2933.

Conflict of Interest: The authors declare that the research was conducted in the absence of any commercial or financial relationships that could be construed as a potential conflict of interest.

Publisher's Note: All claims expressed in this article are solely those of the authors and do not necessarily represent those of their affiliated organizations, or those of the publisher, the editors and the reviewers. Any product that may be evaluated in this article, or claim that may be made by its manufacturer, is not guaranteed or endorsed by the publisher.

Copyright © 2021 Li, Shinoda, Ogawa, Ikegaya, Li, Matsuyama, Sato and Yamagishi. This is an open-access article distributed under the terms of the Creative Commons Attribution License (CC BY). The use, distribution or reproduction in other forums is permitted, provided the original author(s) and the copyright owner(s) are credited and that the original publication in this journal is cited, in accordance with accepted academic practice. No use, distribution or reproduction is permitted which does not comply with these terms.

frontiers in Molecular Neuroscience

REVIEW
published: 30 November 2021
doi: 10.3389/fnmol.2021.755686

The Fine Art of Writing a Message: RNA Metabolism in the Shaping and Remodeling of the Nervous System

María Landínez-Macías[1,2]* *and Olivier Urwyler*[1,2,3]*

[1] Department of Molecular Life Sciences, University of Zurich, Zurich, Switzerland, [2] Molecular Life Sciences Program, Life Science Zurich Graduate School, University of Zurich and Eidgenössische Technische Hochschule (ETH) Zurich, Zurich, Switzerland, [3] Neuroscience Center Zurich (ZNZ), University of Zurich, Zurich, Switzerland

Neuronal morphogenesis, integration into circuits, and remodeling of synaptic connections occur in temporally and spatially defined steps. Accordingly, the expression of proteins and specific protein isoforms that contribute to these processes must be controlled quantitatively in time and space. A wide variety of post-transcriptional regulatory mechanisms, which act on pre-mRNA and mRNA molecules contribute to this control. They are thereby critically involved in physiological and pathophysiological nervous system development, function, and maintenance. Here, we review recent findings on how mRNA metabolism contributes to neuronal development, from neural stem cell maintenance to synapse specification, with a particular focus on axon growth, guidance, branching, and synapse formation. We emphasize the role of RNA-binding proteins, and highlight their emerging roles in the poorly understood molecular processes of RNA editing, alternative polyadenylation, and temporal control of splicing, while also discussing alternative splicing, RNA localization, and local translation. We illustrate with the example of the evolutionary conserved Musashi protein family how individual RNA-binding proteins are, on the one hand, acting in different processes of RNA metabolism, and, on the other hand, impacting multiple steps in neuronal development and circuit formation. Finally, we provide links to diseases that have been associated with the malfunction of RNA-binding proteins and disrupted post-transcriptional regulation.

Keywords: RNA-binding proteins, neuronal wiring, RNA metabolism, Musashi, neuronal development, neurological diseases, post-transcriptional control of gene expression

OPEN ACCESS

Edited by:
Inmaculada Segura, Ludwig Maximilian University of Munich, Germany

Reviewed by:
Sandra Maria Fernández Moya, Institut d'Investigacio Biomedica de Bellvitge (IDIBELL), Spain
Takatoshi Iijima, Tokai University, Japan

***Correspondence:**
María Landínez-Macías
maria.landinezmacias@uzh.ch
orcid.org/0000-0003-0304-5629
Olivier Urwyler
olivier.urwyler@uzh.ch
orcid.org/0000-0001-8334-8667

Specialty section:
This article was submitted to Neuroplasticity and Development, a section of the journal Frontiers in Molecular Neuroscience

Received: *09 August 2021*
Accepted: *18 October 2021*
Published: *30 November 2021*

Citation:
Landínez-Macías M and Urwyler O (2021) The Fine Art of Writing a Message: RNA Metabolism in the Shaping and Remodeling of the Nervous System. Front. Mol. Neurosci. 14:755686. doi: 10.3389/fnmol.2021.755686

1. INTRODUCTION

Developmental assembly of neural circuits occurs through precisely orchestrated cellular events for the specification, differentiation, and morphogenesis of neurons. Neurons typically develop an elaborate dendritic tree and an elongated axon to reach their target area(s) and their specific synaptic partners. Through axon branch formation, neurons can, on the one hand, project to distinct target areas, and, on the other hand, increase the number of presynapses that they can form at a particular location (i.e., the local synaptogenic potential). Dendritic, axonal, and synaptic morphogenesis depend on the ability of the neuron to integrate and to appropriately respond to intrinsic and extrinsic cues. Different neuronal types can use the same set of proteins to respond to these cues. Moreover, these proteins can be reused by a given neuron at different developmental

stages and throughout distinct steps in circuit assembly, sometimes with different or even opposing outcomes on neuronal morphogenesis. The response of a neuron thereby depends on the combination of proteins that it expresses at a given time and place. For example, depending on the specific co-receptor that it binds to, a cell-surface receptor can elicit either an attractive or a repulsive cellular response (Dalpé et al., 2004; Chauvet et al., 2007). Proper circuit assembly therefore highly depends on precisely regulated temporal changes of the global cellular proteome, but also on the spatially and temporally controlled composition of local proteomes in dendrites, axons and at synapses. Beyond transcriptional control of gene expression, post-transcriptional mechanisms confer multiple additional layers and means of regulation for achieving protein synthesis at the right time and place in developing neurons. We refer to these mechanisms, which are introduced below, as "RNA metabolism." RNA-binding proteins (RBPs) are key regulators of RNA metabolism. RBPs are, therefore, critically involved in the expansion of proteome diversity and of proteome function in neurons, and in the rapid and localized control of neuronal gene expression. In turn, these processes are essential for coordinating axon and dendrite growth, guidance, targeting, and synapse formation. In this review, we will discuss how RNA metabolism and its control by RBPs guide key steps of neuronal wiring, with a special focus on axon and synapse development. Given their essential functions in neural circuit assembly, it is not surprising that mutations in RBPs have been associated with neurodevelopmental disorders in humans. We will exemplify this for several RBPs in the last section of this article.

RNA metabolism encompasses all the controllable molecular processes that determine the properties of an RNA during its life cycle, from synthesis to degradation (**Figure 1**). As we are focusing on post-transcriptional regulation of RNAs, we will not discuss RNA biogenesis (i.e., transcription) here. Moreover, we will limit our review to the metabolism of protein-coding RNAs, i.e., messenger RNAs (mRNAs). After transcription, maturation of a pre-mRNA to an mRNA occurs through splicing, 5′ end capping, and 3′ end polyadenylation. The process of splicing allows for a multitude of ways to control the function of an mRNA. First, alternative splicing (AS) of coding exons generates different protein isoforms from a single gene. Such expansion of proteome diversity through AS is prominent for example for neuronal cell-surface adhesion and signaling receptors such as the vertebrate Neurexins and the invertebrate Dscam1 protein (Ushkaryov et al., 1992; Ushkaryov and Südhof, 1993; Schmucker et al., 2000). Second, AS of untranslated regions (UTRs) can modify, which cis-regulatory elements are included in an mRNA molecule. Third, regulated splicing can contribute to the temporal control of gene expression (Mauger et al., 2016). Polyadenylation, i.e., the addition of a poly(A) tail at the 3′ end of the mRNA, also impacts mRNA function in different ways. On the one hand, the choice of the position of poly(A) tail addition determines the length of the 3′-UTR, and thus the inclusion of specific cis-regulatory elements. On the other hand, the length of the poly(A) tail itself contributes to the control of mRNA stability and to its translation rate. After nuclear export, cytoplasmic polyadenylation can lead to further elongation of the poly(A) tail, while cytoplasmic deadenylases are catalyzing poly(A) tail shortening (Wiederhold and Passmore, 2010). Both the 5′ end cap structure and the 3′ end poly(A) tail are important for the stability of the mRNA, and their removal leads to rapid mRNA degradation in most cell types. At the pre-mRNA stage, or after mRNA maturation, coding and regulatory sequences of the mRNA can be altered by post-transcriptional editing through RNA editing enzymes (Savva et al., 2012; Lerner et al., 2018), and such editing can also affect mRNA structure. RNA editing enzymes belong either to the "adenosine deaminases that act on RNA" (ADAR) family or to the "Apolipoprotein B mRNA editing enzyme, catalytic polypeptide-like" (APOBEC) family, and they catalyze the deamination of adenosine to inosine (decoded as guanosine) and cytosine to uracil, respectively. Moreover, RNA modification, of which the most prominent example is adenosine methylation at position N^6 (m^6A) (Dominissini et al., 2012; Meyer et al., 2012), impinges on mRNA metabolism, including splicing, translation, and stability (Frye et al., 2018). A further aspect that we include here as part of RNA metabolism is the localization of mRNA molecules to specific subcellular compartments, either through passive diffusion and trapping at a particular location, or through active transport by motor proteins along microtubules or the actin cytoskeleton. Such RNA localization can target the synthesis of specific proteins to defined subcellular locations through local translation. Finally, the output of a given mRNA molecule is determined by its translational rate, which is highly regulated by different means and through different molecular players. We will present in the following sections different examples for these various facets of mRNA metabolism, and how they individually, or in combination, impact neuronal development. Given the breadth of identified mechanisms and molecules, we are thereby focusing on chosen examples rather than aiming at providing a comprehensive review of the field.

2. ROLES OF RNA METABOLISM IN NEURONAL WIRING AND REMODELING

2.1. Alternative Cleavage and Polyadenylation

During transcription, the recognition of a polyadenylation signal (PAS) triggers the downstream cleavage of the nascent transcript, and thus the release of a pre-mRNA molecule. Concomitantly, the PAS induces nuclear polyadenylation of the pre-mRNA. The recognition and usage of alternative transcript termination sites/PASs, known as alternative cleavage and polyadenylation (APA), diversifies the 3′UTRs of mRNA isoforms and their regulatory potential. Indeed, changing the 3′UTR length directs the exclusion or inclusion of more downstream structural and cis-regulatory elements. APA patterns are tissue-specific, and even mRNAs that are ubiquitously expressed in many tissues have alternative 3′UTRs that are used at different ratios in each tissue (Lianoglou et al., 2013). Overall, neuronal tissues are biased toward expressing isoforms with longer 3′UTRs (Miura et al., 2013; Guvenek and Tian, 2018). For instance, during embryogenesis in *Drosophila*, some mRNAs in neuronal tissues

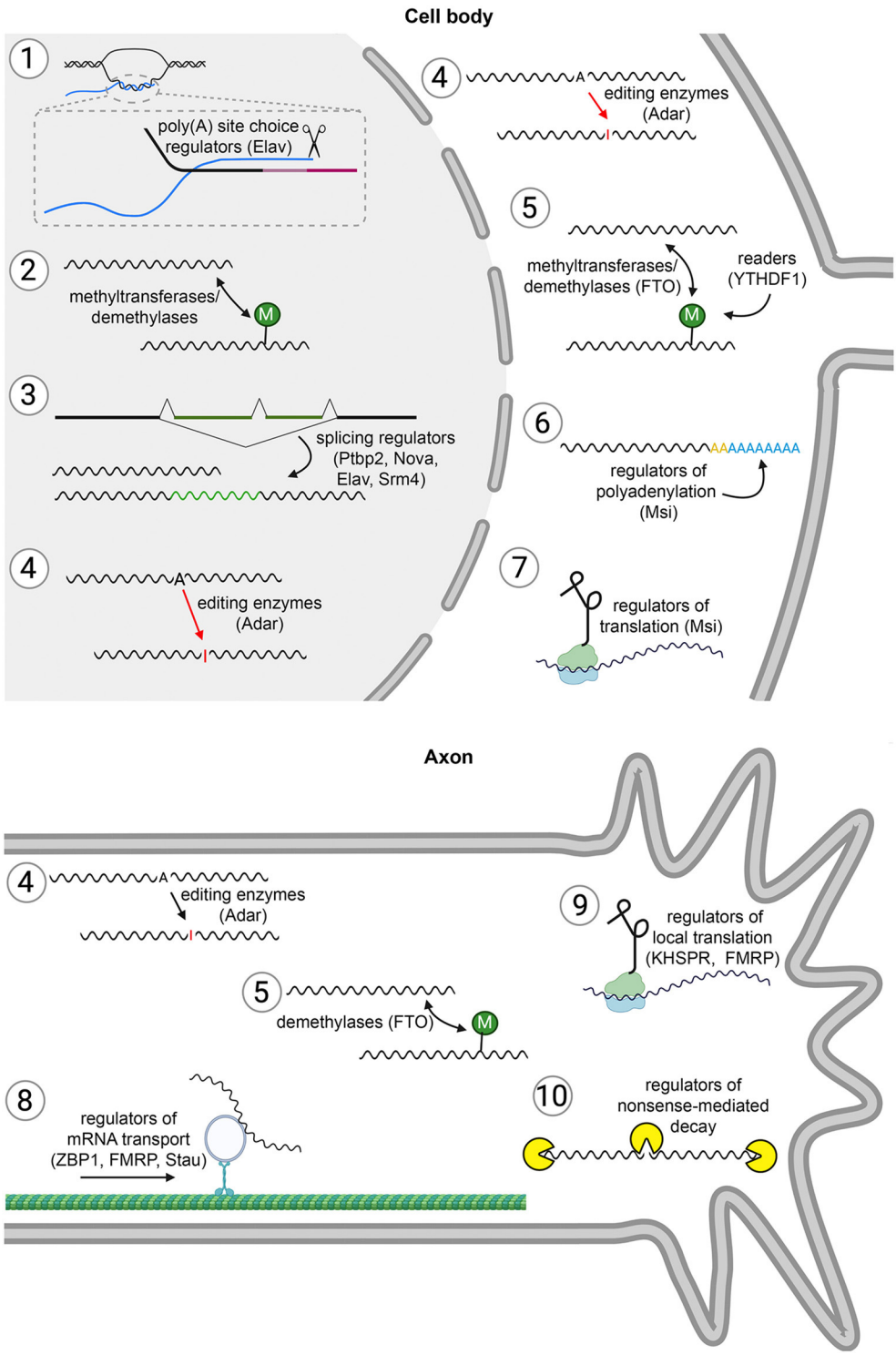

FIGURE 1 | Different steps of mRNA metabolism. (1) Alternative cleavage and polyadenylation. The choice between alternative polyadenylation signals diversifies 3′UTRs and thereby determines, which regulatory motifs are included in an mRNA molecule. Thus, this process expands the potential for post-transcriptional regulation of gene expression. As in the rest of the figure, an example of an RNA-binding protein that controls the process, and which we discuss in this article, is indicated in brackets. Blue: mRNA. Shades of pink: alternative 3′UTRs encoded in the DNA. (2) RNA modification. Nucleotides are modified for example by methyltransferases and demethylases. RNA modification can occur both in the nucleus and in the cytoplasm. This impacts on splicing, translation, and stability of an mRNA. (3) Alternative splicing (AS). Regulation of gene expression by AS is a means to increase proteome diversity, and also to include or exclude

(Continued)

FIGURE 1 | regulatory elements that for example can provide temporal or spatial control of expression. (4) RNA editing. The coding and regulatory regions in an mRNA molecule can be edited in the nucleus or in the cytoplasm, for example by conversion of adenosines (A) into inosines (I). (5) Dynamic RNA modifications. In the cell body and axonal cytoplasm, modifications can be added or removed from mRNA molecules. RBPs that recognize the modifications ("readers") can then for example modulate translation. (6) Polyadenylation. This dynamic process can occur in the nucleus [yellow poly(A) tails] and in the cytoplasm [blue poly(A) tails]. Polyadenylation is a means to regulate translation and mRNA stability. (7) Translation. In neurons, protein synthesis is heavily regulated to provide temporal and spatial control of proteome composition during development. (8) Localization. mRNA molecules can be transported to axon terminals, and (9) locally translated. (10) Degradation. Different pathways, such as nonsense-mediated decay, degrade mRNAs after translation.

can have 3′UTRs up to 20-fold longer than the 3′UTRs of the same mRNAs in other tissues (Hilgers et al., 2011). Elongation of the 3′UTR starts early in the development of the nervous system, with neuronal stem cells already having longer 3′UTRs, which is required for correct neuronal differentiation (Grassi et al., 2018). During the development of specific neuronal tissues, such as the mouse retina, long 3′UTRs are also enriched (Hu et al., 2016). The lengthening of the 3′UTRs in neurons is coordinated by the Elav/Hu family of RBPs (Soller and White, 2004). *Drosophila* Elav binds to proximal alternative PASs and thereby promotes the selection of more distal PASs (Hilgers et al., 2012; Carrasco et al., 2020). Interestingly, this process is linked to transcription initiation (Oktaba et al., 2015): Elav binds both to the promoter region, where the RNA polymerase II pauses during transcription initiation, and to the nascent 3'UTR. Both the promoter regions and the RNA polymerase II pausing are necessary for Elav- mediated 3′UTR elongation (Oktaba et al., 2015). Remarkably, in *Drosophila*, upon loss of Elav, a specific splice variant, which is normally repressed by Elav, of the mRNA encoding the RBP "Found in Neurons" (FNE) is produced. The FNE protein encoded by this splice variant can translocate to the nucleus and take over Elav's role in promoting neuronal 3′UTR lengthening (Carrasco et al., 2020).

Why do neurons favor longer 3′UTRs? Since 3′UTRs contain sequences and structural elements that can determine mRNA stability, localization, and translation efficiency, the extension of 3′UTRs increases the number of cis-elements for post-transcriptional regulation of gene expression. Due to the elaborate and complex morphology of neuronal cells and their dendritic and axonal processes, one post-transcriptional mechanism that has prominent functions in neurons is the differential localization and local translation of transcripts, often at very long distances from the cell body. Different 3′UTR isoforms of the same mRNA can thereby localize differentially. In mouse embryonic stem cells and in rat brains, some 3′UTR isoforms are specifically enriched in neuropil regions, i.e., in dendrites and axons, while other isoforms are enriched in the soma or are distributed uniformly (Ciolli et al., 2018; Tushev et al., 2018). Interestingly, the mRNA isoforms with a specific localization usually have a longer 3′UTR, indicating that 3′UTR lengthening confers an enhanced potential for spatial regulation (Tushev et al., 2018). mRNA stabilization and localization are controlled by different RBPs that bind to the 3′UTR, together forming macromolecular complexes called RNA granules. mRNA granules contain several RBPs, such as ZBP1, FMRP, or Staufen2, which are responsible for localization, stabilization, and regulation of translation (Kiebler and Bassell, 2006). mRNA localization and local translation are essential for neuronal development and plasticity (Lin and Holt, 2008; Holt and Schuman, 2013; Shigeoka et al., 2013; Jung et al., 2014; Glock et al., 2017; Cioni et al., 2018a; Biever et al., 2019; Holt et al., 2019), and will be discussed in more detail below.

Alternative cleavage and polyadenylation of specific transcripts controls correct neuronal wiring. Transcripts coding for the murine brain-derived neurotrophic factor (BDNF), which has well-studied roles in axon and dendrite growth and dendrite branching, has either a short or a long 3′UTR (Segal et al., 1995; Cheung et al., 2007; An et al., 2008; Lazo et al., 2013). The neuronal RBP HuD binds specifically to *BDNF* transcripts with the long 3′UTR, and this interaction is necessary and sufficient for selective stabilization of these mRNA molecules, and for elevated expression of BDNF protein (Allen et al., 2013). Moreover, *BDNF* transcripts with short 3′UTRs are restricted to the soma, while the transcripts with long 3′UTR are localized to dendrites. In a mouse mutant with a truncated long 3′UTR, dendritic targeting of *BDNF* mRNAs is impaired (An et al., 2008). This impairment of the long *BDNF* 3′UTR leads to deficits in the pruning of dendritic spines in young mice, suggesting that dendritic targeting of the long *BDNF* isoform controls synaptic connectivity (An et al., 2008).

Interestingly, APA is involved in controlling distinct stages and even opposing processes during axon morphogenesis. Selection of the most distal PAS of the *Drosophila* cell surface receptor Dscam1 is required for axon growth and terminal branching (see below). Conversely, toward the end of axon morphogenesis, selection of the most distal PAS in a component of the cytoskeleton, Ankyrin, mediates stabilization of mature axons and synapses, and growth arrest (Knobel et al., 2001; Pielage et al., 2008). In *Caenorhabditis elegans*, at the end of axon morphogenesis, the casein kinase 1δ (CK1δ) localizes to the nucleus and inhibits transcription termination of *ankyrin*, leading to the production of the longer isoform (LaBella et al., 2020). CK1δ regulates APA by phosphorylating several components of the RNA polymerase-II termination complex (LaBella et al., 2020). Gamma-aminobutyric acid (GABA) motor neurons extend axons from the ventral nerve cord to the dorsal nerve cord during a specific developmental window, after which axon outgrowth stops. Mutations in CK1δ do not affect axon growth, branching, or synaptogenesis during development of GABA motor neurons (LaBella et al., 2020). However, CK1δ mutations lead to continuous elongation of their growth cones after the late larval L1 stage, which leads to a highly branched nervous system (LaBella et al., 2020). The overgrowth phenotype can be suppressed by expression of the giant isoform of Ankyrin, or mutations in the RNA polymerase-II termination complex (LaBella et al., 2020).

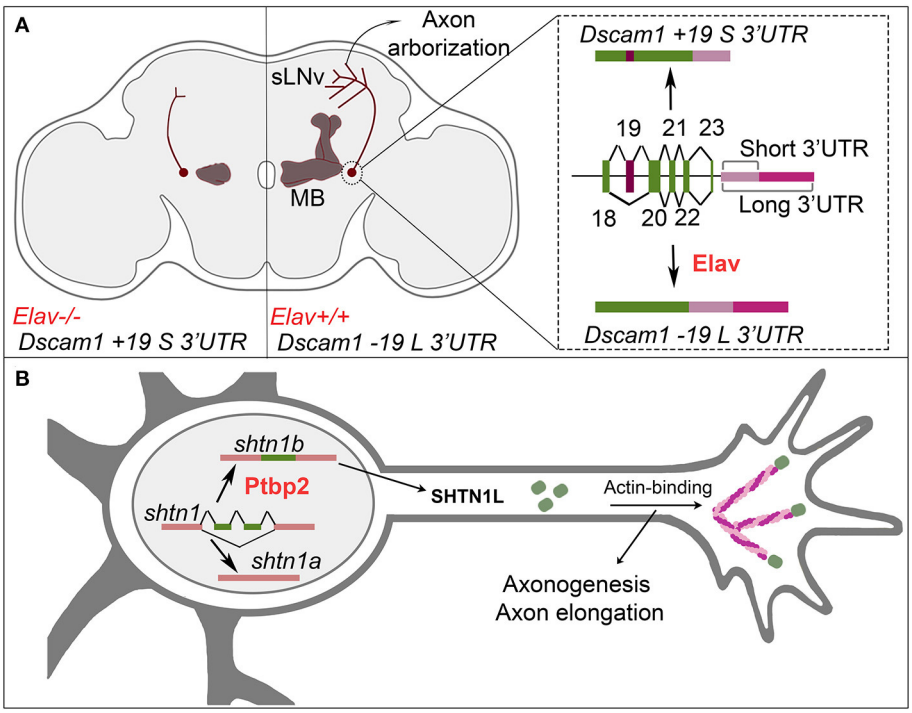

FIGURE 2 | Alternative cleavage/polyadenylation and AS control neuronal wiring. **(A)** Regulation of alternative cleavage/polyadenylation and exon skipping control axon branching and axon arborization. (Right) The RBP Elav mediates the skiping of exon 19 and the selection of the long 3′UTR isoform for *Dscam1*. (Center) The *Dscam1 -19 L 3′UTR* is required for bifurcation of *Drosophila* mushroom body (MB) axons, and correct formation of axon arborizations in sLNv neurons. (Left) Loss of Elav or loss of the long 3′UTR of *Dscam1* leads to bifurcation and growth defects in mushroom body axons, and loss of axonal arborizations in sLNv neurons. **(B)** Regulation of AS of *shtn1* coordinates axonogenesis and axon elongation. AS of *shtn1* leads to two different isoforms via the inclusion/exclusion of two exons. The RBP Ptbp2 mediates the inclusion of two exons to produce the *shtn1b/shtn1L* isoform. The SHTN1L isoform binds actin to allow the formation of actin filaments, which leads to axonogenesis and axon elongation. In absence of Ptbp2 or *shtn1L*, axonogenesis is impaired.

3′UTR choice in the mRNA coding for the *Drosophila* Dscam1 cell-surface receptor provides another compelling example of the role of APA in axon morphogenesis. The Dscam1 long 3′UTR is required at a late stage of axon development in the ventral lateral neurons in the fly brain (Zhang et al., 2019b; **Figure 2A**). Upon specific deletion of the long 3′UTR, the axons of these neurons properly reach their target area, however, they fail to elaborate the typical extensive terminal arborizations in that target area (Zhang et al., 2019b). The RBP Elav binds to the proximal PAS and inhibits its use, thereby promoting the inclusion of the long 3′UTR in the Dscam1 mRNA (Zhang et al., 2019b). Remarkably, the inclusion of the long UTR is coupled by Elav to the exclusion of an alternatively spliced upstream coding exon (Zhang et al., 2019b). It will be exciting to determine in the future whether coupling of APA and AS is a widespread feature during mRNA biogenesis in the developing nervous system.

2.2. Alternative Splicing

Alternative splicing is a means to drastically increase the coding potential of genomes. Indeed, many transcripts undergo AS for diversification of the encoded gene products, with the controlled inclusion or exclusion of specific coding exons, or the use of alternative homologous coding exons, ultimately determining the properties of the produced protein isoforms. One of the most remarkable cases of AS in the regulation of neuronal wiring is found for the mRNA encoding the *Drosophila* cell surface receptor Dscam1. Through AS of three alternative exon clusters, more than 18,000 protein isoforms differing in their extracellular domains can be generated from one single gene (12 × 48 × 33 alternative exons for each respective cluster; Schmucker et al., 2000). Dscam1 proteins interact homophilically in a highly isoform-specific manner, with each isoform binding only to itself but not (or very poorly) to other isoforms (Wojtowicz et al., 2004). These interactions mediate neurite self-repulsion, which is required for the assembly of many neuronal circuits. The knowledge on the Dscam1 function has been extensively discussed in several excellent reviews (e.g., Schmucker, 2007; Hattori et al., 2008), and will therefore not be further discussed here. Similarly, in mammals, the Neurexin gene family also encodes a high number of protein isoforms through the use of AS. These presynaptic adhesion molecules instruct synapse formation and the acquisition of cell type-specific and synapse-specific functional properties. A detailed description of Neurexin functions and regulation can be found for example in a recent review (Gomez et al., 2021).

Beyond expanding the coding potential of genes, the AS of both coding exons and of 3′UTRs exons can alter the regulatory elements included in an mRNA, and thus its stability,

localization, and translational dynamics. AS events are controlled by RBPs and are often cell-type specific: individual neuron types have highly selective AS programs. These programs were found to control the expression of specific isoforms of proteins that determine intrinsic neuronal excitability, synapse formation and differentiation, pre-synaptic neurotransmitter release, and postsynaptic neurotransmitter sensing (Traunmüller et al., 2016; Furlanis et al., 2019). Through the mRNAs encoding these proteins, AS therefore directly impacts the functional properties of neurons. Remarkably, even closely related neuronal cell types can be reliably distinguished based on their transcript isoform profiles (Furlanis et al., 2019). Importantly, as we will exemplify below, the temporal regulation of AS is an important means to time the expression of specific protein isoforms that will have different effects on neuronal development. The AS programs in most neuronal types are controlled by RBPs from the Nova, Rbfox, Ptbp, Hu/Elav, nSR100, and MbnL families (Raj and Blencowe, 2015; Vuong et al., 2016).

Some RBPs can regulate the splicing of corresponding/paralogous exons in distinct, functionally related genes (Ule et al., 2005; Jacko et al., 2018). Moreover, RBPs direct switch-like changes of the AS program during neuronal development, and the use of specific splicing patterns that are associated either with different stages of neuronal development or of neuronal maturation. For example, in mice, the RBP Ptbp antagonizes more mature splicing programs. This means that for most developmentally regulated exons, it promotes the generation of splicing patterns that are required earlier during development (around 80% of Ptbp-dependent exons). By contrast, Nova, Rbfox, and Mbnl families are generally associated with facilitating splicing programs that are found in more mature neurons (80–96% of target exons of these RBPs; Weyn-Vanhentenryck et al., 2018). The maturation of the AS program is functionally relevant for fundamental aspects of neuronal development. For instance, murine Ptbp2 controls the complex process of axon formation by regulating the AS of axonogenesis-associated genes. In particular, Ptbp2 inhibits the AS switches that stop axon growth, such as for the *shootin1* gene product (**Figure 2B**). Two isoforms of SHTN1 can be produced by AS. SHTN1L (encoded by the *shootin1b* mRNA isoform) is a protein that binds to both the cell-surface receptor L1-CAM and to actin. By contrast, the isoform SHTN1S (encoded by the *shootin1a* mRNA isoform) does not bind actin (Ergin and Zheng, 2020). SHTN1L promotes actin polymerization in the axonal growth cone and thereby provides a driving force for growth (Toriyama et al., 2006; Zhang et al., 2019a). In early axonogenesis, Ptbp2 inhibits the switch from *shootin1b* to *shootin1a* mRNA isoform usage (Zhang et al., 2019a). The inhibition of this switch maintains axonal growth, and, accordingly, Ptbp2 mutant neurons grow short axons (Zhang et al., 2019a). According to the model, the switch from *shootin1b* to *shootin1a* expression at a later developmental time point (i.e., after axon growth) induces axon specification/maturation mediated by SHTN1S. It is important to note here that the sequence and interdependence of neuritogenesis, axon growth, specification, and maturation remains poorly understood particularly *in vivo*, and that Ptbp2 controls the splicing of other mRNAs coding for proteins involved in these processes. Getting a more complete picture of how switches in alternative splicing programs contribute to axonogenesis represents an exciting challenge for future studies.

Later steps of neuronal development are also controlled by changes in the AS programs. For example, during murine cortical development, Nova2 switches the splicing patterns of mRNAs coding for axon guidance cues and receptors, such as *Dcc, Robo1, Robo2, Slit2*, and *Epha5* (Leggere et al., 2016; Saito et al., 2016; Johnson et al., 2019). Given the essential functions of these cues and receptors, it is not surprising that the loss of *Nova2* leads to severe defects in different parts of the nervous system, such as agenesis of the corpus callosum and impairment of axonal pathfinding of motoneurons and of auditory efferents (Saito et al., 2016). In the murine spinal cord, the two family members Nova 1 and 2 have common RNA targets and function redundantly in regulating the migration of dorsal commissural interneurons, and outgrowth and guidance of their axons toward the ventral midline (Leggere et al., 2016). In this context, Nova1/2 function through *Dcc* splicing (Leggere et al., 2016). Nova1/2 catalyzes the production of a *Dcc-long* isoform through the choice of an alternative splice acceptor at the 3′ end of a specific intron. Thereby, compared to *Dcc-short*, *Dcc-long* encodes an additional 20 amino acids in a linker region between two extracellular fibronectin repeats (Leggere et al., 2016). It is not yet fully clear what functional consequences this insertion has. The two murine Dcc isoforms have similar affinities for the Netrin ligand, yet they seem to adopt different conformations upon binding to Netrin (Xu et al., 2014). The Dcc-long isoform is clearly implicated downstream of Nova1/2 in spinal cord interneuron axon guidance, as supplying Dcc-long suppresses the guidance defects in Nova1/2 double knockout mice (Leggere et al., 2016). Moreover, Nova1/2 provides a typical example of how RNA-binding proteins can be involved in subsequent steps of neuronal development (more precisely, in this case even subsequent steps of axon guidance). After guidance of commissural axons to the ventral part of the spinal cord, they cross the midline to project to the contralateral side of the CNS. The midline represents a typical intermediate target in axon guidance. Intermediate targets need to first attract the axons, before a switch to repulsion happens so that the axons can leave the target and continue their journey. After their function in promoting axon outgrowth and ventral guidance, Nova1/2 promotes midline crossing of spinal cord commissural axons (and thus, axons do not cross the midline in Nova1/2 knockout mice). This is achieved through splicing regulation of a conserved microexon in the transcripts coding for Robo1/2 proteins (Johnson et al., 2019), which are receptors for the classical repulsive cue Slit (Brose et al., 1999; Kidd et al., 1999). Exons that are 3-27 nt long are considered as microexons; in this case, they code for 3 and 4 amino acids in the extracellular domain of Robo1 and Robo2, respectively. Nova1/2 binds to intronic sequences flanking the microexon, and inhibits its inclusion in the *Robo* transcripts. Therefore, in Nova1/2 double knockout animals, only *Robo* transcripts that contain the microexon are expressed. In an elegant genetic experiment, Johnson et al. (2019) deleted the microexon from one allele of each of the *Robo1* and the *Robo2* gene, and thereby restored the expression of both transcript isoforms for

each gene in Nova1/2 double knockout mice. Remarkably, this deletion of the microexon in one allele of each *Robo1/2* gene efficiently rescued normal midline crossing, establishing a causal link between Nova1/2-mediated *Robo1/2* splicing and midline crossing. The authors of the study report that the presence or absence of the amino acids encoded by the microexon alter the molecular signaling properties of the Robo receptors. *In vivo*, the Robo1 receptor containing the amino acids encoded by the microexon leads to more axon repulsion than the Robo1 receptor without these amino acids. Consistent with this finding, the microexon splicing is remarkably dynamic in commissural axons, demonstrating the potential of temporal control of AS during neuronal wiring: first, the microexon is included when the axons are guided ventrally, to prevent a premature crossing of the midline. It subsequently gets excluded to allow midline crossing, before it gets included again when the axons have reached the contralateral side, to prevent re-crossing (Johnson et al., 2019).

The third Robo family member, the Robo3 receptor, is also involved in controlling axon midline crossing, and it is also critically regulated by AS (Friocourt and Chédotal, 2017). Robo3 was first identified as generally promoting midline crossing, in contrast to its Robo1/2 paralogs (Sabatier et al., 2004). Later studies however identified a more intricate mechanism. Namely, murine *Robo3* produces 2 isoforms by a rather unusual form of AS: alternative retention of an intron results in different intracellular C-terminal regions between the two encoded receptor isoforms. One of them, Robo 3.1, is expressed in pre-crossing axons of commissural neurons, while the Robo 3.2 isoform is expressed in post-crossing axons (Chen et al., 2008 and see also below). Robo 3.1 is required for midline crossing, while Robo 3.2 contributes to expelling axons from the midline and preventing their recrossing. These data together led to the model that the Robo 3.1 isoform inhibits Robo1/2-mediated repulsion from the midline in pre-crossing axons, while the Robo 3.2 isoform acts in concert with Robo1/2 to mediate repulsion from the midline in post-crossing axons (Chen et al., 2008). Intriguingly, an additional level of complexity is added through a switch that occurred during mammalian evolution, and which eliminated Slit binding to mammalian Robo3 receptors (while Slits bind to Robo3 in non-mammalian vertebrates; Zelina et al., 2014). Instead, mammalian Robo3 interacts with the Netrin-1 receptor DCC and promotes the attraction of commissural neurons to the midline in response to Netrin-1 (Zelina et al., 2014). Therefore, Robo 3.1 could function in pre-crossing axons both by attenuating repulsion and, in mammals, by boosting attraction to midline cues (Blockus and Chédotal, 2016). The precise mechanism of Robo3.2-mediated repulsion in post-crossing mammalian axons and differences in Robo3 functions in distinct types of commissural neurons, remain to be fully addressed.

Alternative splicing also crucially regulates proteins that control synapse formation, specification, and maturation. For example, the "signal transduction and activation of RNA" (STAR) family RBP Sam68 participates in transforming the splicing program of genes involved in synapse development and synaptic transmission in the developing mammalian CNS, including the presynaptic Neurexin cell-surface receptors and several postsynaptic scaffolding proteins (Iijima et al., 2011; Witte et al., 2019; Farini et al., 2020). Sam68 mainly functions by preventing exon inclusion. In the cerebellum of mice lacking Sam68, there is increased inclusion of exons, and this impairs the maturation of cerebellar Purkinje cells and leads to a reduction of synaptic contacts between Purkinje cells and granule cells (Farini et al., 2020). The mammalian cerebellum critically contributes to motor and social behaviors. Therefore, it is not surprising that the connectivity defects in cerebellar circuits lead to dysfunction in these behaviors (Farini et al., 2020), and that they could contribute to the association between alternatively spliced Sam68 targets and autism-spectrum disorders.

Liquid-liquid phase separation has recently emerged as a cellular mechanism implicated in synapse formation, function, and plasticity (Milovanovic et al., 2018; McDonald et al., 2020; Hosokawa et al., 2021). AS can contribute to the regulation of liquid-liquid phase separation, as exemplified by the SynGAP protein, an abundant component of the postsynaptic density (Zeng et al., 2016). SynGAP negatively regulates synaptic strength, and downregulation of SynGAP leads to premature formation of enlarged spines in the hippocampus of young mice (Vazquez et al., 2004; Clement et al., 2012). Moreover, some forms of long-term synaptic potentiation lead to SynGAP dispersion from the postsynaptic density. Rat SynGAP binds to another postsynaptic density protein, PSD95. This interaction induces phase separation of the SynGAP/PSD95 complex, and it is required for maintaining SynGAP localization in the postsynaptic density (Zeng et al., 2016). Complex AS of murine *SynGAP* pre-mRNA generates protein isoforms with differences in their C-terminal domain (McMahon et al., 2012). Of these, only the isoform $\alpha 1$ was able to induce liquid-liquid phase separation in a heterologous cellular assay, while the $\alpha 2$, β, and γ isoforms were not (Araki et al., 2020). Consistent with these biochemical properties, synaptically localized murine SynGAP $\alpha 1$ was rapidly dispersed upon LTP induction, while SynGAP β was less enriched at synapses and did not disperse during LTP. SynGAP $\alpha 1$ dispersion from the synapse is required to allow dendritic spine enlargement and insertion of AMPA-type glutamate receptors during LTP, suggesting that SynGAP $\alpha 1$ is the main isoform involved in this type of synaptic plasticity, while the other isoforms play at best modest roles in this process. By contrast, the "division of labor" between isoforms is different in another major neuronal SynGAP function, namely the control of developmental dendrite morphogenesis and maturation (Aceti et al., 2015; Araki et al., 2020). Indeed, only the SynGAP β isoform supports the normal branching of distal dendrites (Araki et al., 2020). Remarkably, disrupting the propensity of SynGAP $\alpha 1$ to undergo liquid-liquid phase separation rendered this isoform capable of taking over the function of SynGAP β in controlling distal dendrite morphogenesis. These results directly link the different phase separation characteristics to separable neuronal functions of SynGAP isoforms, and exemplify how AS can generate protein isoforms with distinct biochemical properties that underlie different cellular functions.

Moreover, the case of the SynGAPs provides an additional example of how AS can contribute to the regulation of protein biogenesis beyond generating mRNAs with different

coding sequences and thus proteins with different properties: *syngap* mRNA isoforms are differentially stabilized post-transcriptionally, which contributes to regulating relative expression levels of the different isoforms, potentially underlying differences in expression of the SynGAP isoforms at distinct developmental stages. More specifically, the 3′UTR of the murine *syngap α2* mRNA includes binding elements for the RBP FUS, which are not present in the *syngap α1* mRNA (Yokoi et al., 2017). The binding of FUS and also ELAV4 to the *syngap α2* 3′UTR leads to stabilization of *syngap α2* mRNA and higher SynGAP α2 protein levels (Yokoi et al., 2017). In the absence of ELAV4 binding, FUS dissociates from *syngap α2* mRNA (Yokoi et al., 2017). In this situation, the ELAV1 family member binds to the *syngap α2* mRNA, which correlates with a decrease in SynGAP α2 protein levels (Yokoi et al., 2017). Interestingly, murine FUS also regulates the stability of the *GluA1* mRNA. FUS binds to the 3′UTR of *GluA1* and enhances polyadenylation of the mRNA, which correlates with higher GluA1 protein levels (Udagawa et al., 2015). Functionally, the absence of FUS leads to impaired maturation of dendritic spines, and this phenotype can be rescued by the expression of SynGAP α2 or GluA1 (Udagawa et al., 2015; Yokoi et al., 2017). Thus, a common RBP regulates the metabolism of different mRNA targets whose products are involved in a common neurodevelopmental process.

2.3. RNA Localization and Local Translation

Local translation has long been recognized to account for site-specific protein production in dendrites and at post-synapses. *In vivo* evidence for local translation in (developing) axons has however emerged more recently, but has been the subject of several excellent reviews. We will thus not discuss it extensively here. In axonal compartments, local translation allows for a localized and fast remodeling of the axonal proteome (Lin and Holt, 2008; Holt and Schuman, 2013; Shigeoka et al., 2013; Jung et al., 2014; Glock et al., 2017; Cioni et al., 2018a; Biever et al., 2019; Holt et al., 2019). Local translation occurs at many steps of axonal wiring. In the early steps, during axon growth and targeting, specific guidance cues rapidly up- or down-regulate a large number of locally translated proteins. Repulsive and attractive cues can thereby generate opposite remodeling of axonal proteins (Cagnetta et al., 2018).

A prerequisite for local translation is, obviously, the localization of mRNAs to specific subcellular compartments. mRNA localization and local translation have a large impact on the proteome in neuronal processes. Indeed, nearly half of the proteins in the neurite-enriched proteome are locally translated (Zappulo et al., 2017). Thereby, axonal mRNAs that encode key regulators of axonal outgrowth, branching and synaptogenesis are dynamically localized and translated during CNS development (Shigeoka et al., 2016). This mRNA localization is developmentally regulated: growing axons contain a different set of mRNAs than mature axons (Gumy et al., 2011). In neurons, the distribution of mRNA is differentially regulated not only between dendrites, cell body, and axons, but also to a finer spatial level within axons: sub-axonal compartments, such as the axon shaft, the central domain of the growth cone, and the peripheral domain of the growth cone, respectively, contain different subsets of localized mRNAs (Zivraj et al., 2010; Wang et al., 2014). Active transport contributes to the differential localization of mRNAs in sub-axonal compartments (Turner-Bridger et al., 2018). In this section, we will first introduce general mechanisms for mRNA localization, highlighting some examples that have emerged recently. We will then discuss instances of mRNA localization and local translation in developing neurons.

mRNAs are transported in ribonucleoprotein (RNP) complexes that typically contain a couple dozen RBPs, such as helicases and regulators of translation, and also non-coding RNAs with regulatory functions (Fritzsche et al., 2013; Mitchell and Parker, 2014). RNP complexes can be further assembled into bigger structures for transport, known as RNP granules (Mitchell and Parker, 2014). The formation of RNP complexes is mediated by protein-protein interactions leading to oligomerization, or liquid-liquid phase separation driven by intrinsically disordered protein domains (IDDs; also known as low complexity regions). RBPs typically contain IDDs (Weber and Brangwynne, 2012). In the context of RNPs, IDDs have functions beyond assembly: for example, the IDD of *Drosophila* IMP (a homolog of the vertebrate ZBP1) is not required for RNP assembly, but rather for the regulation of the dynamics and other properties of RNPs (Vijayakumar et al., 2019). The Imp IDD modulates the size, the number and the motility of RNP granules, and in the *Drosophila* CNS, it regulates the transport of RNP granules to axons during development. This is a key mechanism for the proper remodeling of the axons of mushroom body γ neurons (Vijayakumar et al., 2019).

The localization of mRNAs to neurites can be achieved through different mechanisms of transport. One of them is the directional transport to axons and dendrites *via* RNP anchoring to motor proteins (Abouward and Schiavo, 2021). Motor proteins, such as the Dynein and Kinesin families, move along the microtubule cytoskeleton, and can deliver RNA cargo to distal neuronal processes (Kanai et al., 2004). The minimal array of elements described to be sufficient for proper mRNA localization to axons consists of a kinesin motor protein (Kinesin-2), an adaptor protein (KAP3), and an RBP (adenomatous polyposis coli, APC; Baumann et al., 2020). *In vitro*, these components are sufficient for delivering β-actin and β2B-tubulin mRNAs to the axonal terminal. Baumann et al. (2020) further identified that one to three mRNA molecules are found in a single RNP transport complex. Moreover, it suggests that other proteins, which are present in a single RNP, may have functions that are not directly related to transport.

Recently, two more mechanisms of transport were described in neurons. First, in mammalian cells, RNAs can be transported by hitchhiking onto motile late endosomal/lysosomal organelles (Liao et al., 2019). Using a proximity ligation assay, Liao et al. (2019) identified that one of the proteins mediating the anchoring of RNP complexes to late endosomes is annexin A11 (ANXA11). ANXA11 contains an IDD in its N-terminal domain that mediates liquid-liquid phase separation and formation of the RNP complexes. In the C-terminal part of ANXA11, a membrane binding domain tethers the protein to the membrane of endosomes (Liao et al., 2019). Tethering of RNPs to endosomes for transport and local translation in *X. laevis* retinal ganglion cell

axons suggest that this mechanism is shared among vertebrates (Cioni et al., 2019). The second unconventional mechanism of transport is mediated by extracellular vesicles. Here, proteins, RNA, and other molecules are encapsulated in secreted vesicles and transported between different cells and cell types in the nervous system (Morel et al., 2013; Xu et al., 2017; Ashley et al., 2018; Pastuzyn et al., 2018). For instance, mammalian and *Drosophila* Arc have properties resembling retroviral Gag proteins: Arc proteins form structures similar to virus capsids, which are used to encapsulate mRNA. The *Arc* mRNA is deposited inside an Arc capsid, and the capsid is transported in extracellular vesicles across synaptic partners (Ashley et al., 2018; Pastuzyn et al., 2018). This transport mechanism is required for developmental and activity-dependent synapse morphogenesis at the *Drosophila* NMJ (Ashley et al., 2018). However, how intercellular RNA transfer contributes to the axonal and dendritic proteome, as well as its impact on neuronal wiring and synaptogenesis, remains to be fully addressed.

All three above-mentioned mechanisms of transport involve at least one RBP that selects mRNA targets based on specific binding elements in the RNA sequence. The incorporation of these elements is developmentally and spatially regulated by different mechanisms, such as AS. For example, this is the case of the Staufen (Stau)-mediated transport of *calmodulin3* (*calm3*) and *CaMKII* α mRNAs in the mammalian brain (Ortiz et al., 2017, Sharangdhar et al., 2017). The mRNA of *calm3* localizes to dendrites upon binding of Stau2 to an intron retained in the *calm3* isoform with the longest 3′UTR (Sharangdhar et al., 2017). Similarly, the mRNA of the *CaMKII* α isoform that retains intron 16 is bound by Stau2 and subsequently localized to dendrites (Ortiz et al., 2017). Importantly, active mechanisms are also used to avoid erroneous transport to neuronal processes. For instance, in the mammalian brain, mRNAs containing Pumilio2 (Pum2) binding elements are retained in the cell body, and ectopic translation of these mRNAs is avoided during the early stages of development. Later, at the adult stage, when the expression of Pum2 decreases, these mRNAs become enriched in the axonal compartment and locally translated (Martinez et al., 2019). Thus, the regulation of RNA localization is a key feature of CNS development. In the next section, we will illustrate how several steps of neuronal wiring, namely axon growth, axon branching, and synaptogenesis, are controlled by differential localization and translation of mRNAs.

Directional switches during axon guidance are based on axonal growth cone turning toward attractive cues and away from repulsive cues. These responses are mediated by the stabilization of cytoskeletal elements in the growth cone compartment that is exposed to attractive cues, and, conversely, to the destabilization of the cytoskeleton in the compartment that is exposed to repulsive cues (Terenzio et al., 2017). During axon guidance, *β-actin* mRNA undergoes local translation *in vivo* in axons of *X. laevis* (Wong et al., 2017). The zip-code binding protein 1 (ZBP1) homolog Vg1RBP binds to the 3′UTR of *β-actin*, and transports the *β-actin* mRNA to growth cones and within growth cones (Leung et al., 2006). Vg1RBP and *β-actin* transcripts move into filopodial protrusions of growth cones upon Netrin-1 induced attraction. Moreover, Netrin-1 or BDNF can induce asymmetrical β-actin translation in the growth cone, which leads to directional turning of growth cones during axon guidance (Leung et al., 2006; Yao et al., 2006; Welshhans and Bassell, 2011). Mediators of actin disassembly are also regulated by cue-induced local translation. For instance, in *X. laevis*, transcripts encoding the actin filament-severing protein Cofilin are locally translated upon exposure to the repulsive cue Slit-2, inducing growth cone collapse (Piper et al., 2006). Moreover, in chicken, upon semaphorin-3A (Sema3A) exposure, the GTPase RhoA and the RhoA-kinase on the one hand inhibit actin polymerization-dependent formation of protrusions, thereby enhancing growth cone collapse. On the other hand, chicken RhoA-kinase promotes the formation of intra-axonal F-actin bundles that mediate myosin II-dependent retraction (Dontchev and Letourneau, 2002; Wu et al., 2005; Gallo, 2006). In the rat, the activation of this pathway occurs through local axonal translation: transcripts of *RhoA* localize to developing growth cones, and Sema3A induces its local translation, and thus growth cone collapse (Wu et al., 2005).

Local translation is also key for axon branching. In *X. laevis* retinal ganglion cells, Vg1RBP/ZBP1 localizes to regions of filopodia sprouting and it is required for the formation of terminal arborizations (while it is not required for long–range axon navigation; Kalous et al., 2014). Likewise, *β-actin* mRNA is transported in RNA granules that dock at sites of new branch emergence, and its local translation is required for terminal axon branching (Wong et al., 2017). Moreover, in chicken embryonic sensory axons, the formation of new branches is supported by the local translation of the actin-nucleation complexes Arp2, WAVE1, and cortactin, which are essential for both the formation of actin patches and for filopodia emergence from them (Spillane et al., 2012). Interestingly, another regulator of actin assembly, Mena (also called ENAH; Krause et al., 2003), interacts with several RBPs and mRNAs in murine axonal growth cones, forming ribonucleoprotein complexes that also include *Mena* mRNA itself (Vidaki et al., 2017). Mena is required for local translation of the mRNAs present in those complexes (Vidaki et al., 2017). Therefore, Mena regulates both, actin dynamics and local translation, linking the two processes. Besides mRNAs coding for regulators of actin remodeling, other mRNAs, mitochondria, and ribosomes are located to axon branch points. The local translation of mitochondrial and ribosomal proteins, as well as ribosome assembly and mitochondria function in axons, support branch formation (Courchet et al., 2013; Spillane et al., 2013; Wong et al., 2017; Cioni et al., 2019; Shigeoka et al., 2019).

Recent studies showed how key components of the synapse are locally translated during synapse assembly. For example, rat *SNAP25* (encoding a component of the SNARE complex that is involved in the release of synatic vesicles) and *β-catenin* (encoding a subunit of the Cadherin/β-Catenin complex that is involved in cell adhesion) are locally translated during the formation of presynapses, and their protein products cluster with presynaptic proteins (Taylor et al., 2013; Batista et al., 2017). However, relatively little is known about the functions of local translation in other aspects of synapse formation, such as the subcellular control of synaptogenesis, synapse specification, and synaptic partner choice. Intriguingly, a recent study on the

Drosophila membrane-associated dual-specificity "phosphatase of regenerating liver-1" (Prl-1) suggests that local translation may be involved in controlling axon compartment-specific synaptic connectivity (Urwyler et al., 2019). Prl-1 promotes high local synapse number in one specific collateral branch of a *Drosophila* CNS axon. Both, this function and Prl-1 protein enrichment in this axon collateral branch, depend on the UTRs of the *prl-1* mRNA. UTR-dependent localization of the Prl-1 protein to a specific axon compartment thus suggests that local translation may be a key mechanism to confer spatial specificity of Prl-1 function to this compartment. Remarkably, for promoting high local synapse number, *prl-1* genetically interacts with components of the InR/Akt signaling pathway and its downstream effector, the mTOR complex (Urwyler et al., 2019). One major output of the InR/Akt/mTOR axis is the control of translation (Roux and Topisirovic, 2018), suggesting that Prl-1 may contribute to the regulation of local translation of both its own mRNA (in a positive feedback loop) and of other mRNAs localized to that axon compartment. This is reminiscent of mTOR-dependent local translation of *mTOR* mRNA, and other mRNAs, in injured axons (Terenzio et al., 2018). Further studies are required to test this model of compartmentalization of Prl-1 localization and function through local translation. Moreover, it will be exciting in the future to decipher additional mechanisms that depend on local translation for controlling axon compartment-specific synaptogenesis, synapse specification, and synaptic partner matching in the CNS.

2.4. RNA Modification, Non-Coding RNAs, and Decay Mechanisms in the Control of Local Axonal Translation

Internal chemical modification of mRNAs, often referred to as "epitranscriptomics," is a major way to control gene expression (Frye et al., 2018). Of the more than 170 different known RNA modifications, N^6-methyladenosine (m^6A) has attracted particular attention as a major regulator of translation. m^6A is a reversible and dynamic modification that is controlled by methyltransferases ("writers," which add the modification) and demethylases ("erasers," which remove the modification; Roundtree et al., 2017). Within specific sequence contexts, the modification is recognized by RBPs called "readers" (Roundtree et al., 2017). "Writing and erasing" of m^6A in mRNA is involved in controlling local translation in axons (Yu et al., 2017). For example, in rat dorsal root ganglion (DRG) neurons, the local translation of *Gap-43* mRNA, which is required for axon elongation, is regulated by N^6A methylation (Donnelly et al., 2013). Intracellular, cell membrane-associated GAP-43 protein induces growth *via* regulation of actin dynamics (Laux et al., 2000; Denny, 2006). The murine *Gap-43* mRNA is N^6A-methylated in the cell body and then transported to the axon in a translationally repressed state (**Figure 3A**; Yu et al., 2017). An m^6A eraser, FTO, is locally translated in axons, and locally removes the N^6A methylation from *Gap-43* mRNA, which derepresses its translation (**Figure 3A**; Yu et al., 2017). Upon loss of FTO, m^6A modifications in *Gap-43* mRNA remains present, and *Gap-43*$^{m^6A}$ mRNA accumulates (Yu et al., 2017). This modified mRNA is not translated locally, which results in reduced GAP-43 protein levels in the axon and failure of axon elongation (Yu et al., 2017). Interestingly, there is a second, independent mechanism regulating the local translation of *Gap-43* mRNA. ALAE, an axon-enriched long intergenic non-coding RNA, also controls *Gap-43* local translation, as observed in rat DRG axons (**Figure 3A**; Wei et al., 2021). More specifically, under normal conditions, ALAE binds to an RBP called KHSRP in the axonal compartment. KHSRP that is not bound to ALAE can bind to the 3′UTR of *Gap-43* mRNA and inhibit *Gap-43* translation without affecting its mRNA levels (Wei et al., 2021). ALAE functions as an "RNA-decoy" for KHSRP because ALAE-bound KHSRP cannot bind to the 3′UTR of *Gap-43* mRNA. Consistent with this model, in the absence of ALAE, protein levels of rat GAP-43 are reduced and axon elongation is impaired. These phenotypes are recapitulated by a disruption of the ALAE-KHSRP interaction, which does not affect RNA levels of either ALAE or *Gap-43* (Wei et al., 2021). Therefore, ALAE promotes axon elongation by preventing KHSRP-mediated inhibition of *Gap-43* mRNA translation (Wei et al., 2021). Together, these mechanisms exemplify the dynamic control of local translation in the axon, which in turn is crucial for local regulation of the axon cytoskeleton during neuronal wiring. In the cell body and possibly during the transport of *Gap-43* mRNA, translation is inhibited both by N^6A methylation and by KHSRP binding. Once the *Gap-43* mRNA has reached the axon, m^6A- and KHSRP-mediated inhibition of translation are both removed by FTO and ALAE action, respectively. More studies are required to investigate whether these two mechanisms interact, and how ALAE is localized to the axon. Both m^6A modification and KHSRP binding occur in the 3′UTR of *Gap-43* mRNA (Yu et al., 2017; Wei et al., 2021), highlighting again the pivotal role of 3′UTRs as regulatory hubs in neuronal wiring.

Methylation of *Robo3* mRNA further exemplifies the role of RNA modification in neuronal wiring. In mice, the guidance of commissural neuron axons across the midline is regulated by the Robo 3 receptor, for which two isoforms are produced by AS (Chen et al., 2008). As described above, Robo 3.1 localizes to the pre-crossing axonal segment of commissural neurons, while the Robo 3.2 isoform localizes to the post-crossing axonal segment (Chen et al., 2008). The spatial regulation of Robo 3.1 and 3.2 is achieved by local translation (**Figure 3B**; Colak et al., 2013). Both mRNA isoforms are present in the growth cone. Before midline crossing, Robo 3.2 translation is repressed, and only Robo 3.1 is expressed (Colak et al., 2013). Expression of the Robo 3.1 protein needs continuous local translation, because of the short half-life of the protein (Zhuang et al., 2019). To increase Robo 3.1 protein levels in pre-crossing axons, *Robo 3.1* mRNA is N^6A-methylated and bound by the m^6A reader YTH domain-containing family 1 (YTHDF1), which positively regulates *Robo 3.1* mRNA translation (Zhuang et al., 2019; note that in this case, m^6A is stimulating translation, while in the case of GAP-43 described above, m^6A is inhibitory). When axons reach and cross the midline, floor plate signaling down-regulates YTHDF1 and thereby reduces *Robo 3.1* expression (Zhuang et al., 2019). As a result, Robo 3.1 levels are higher in the pre-crossing axon segment than in the post-crossing segment. At

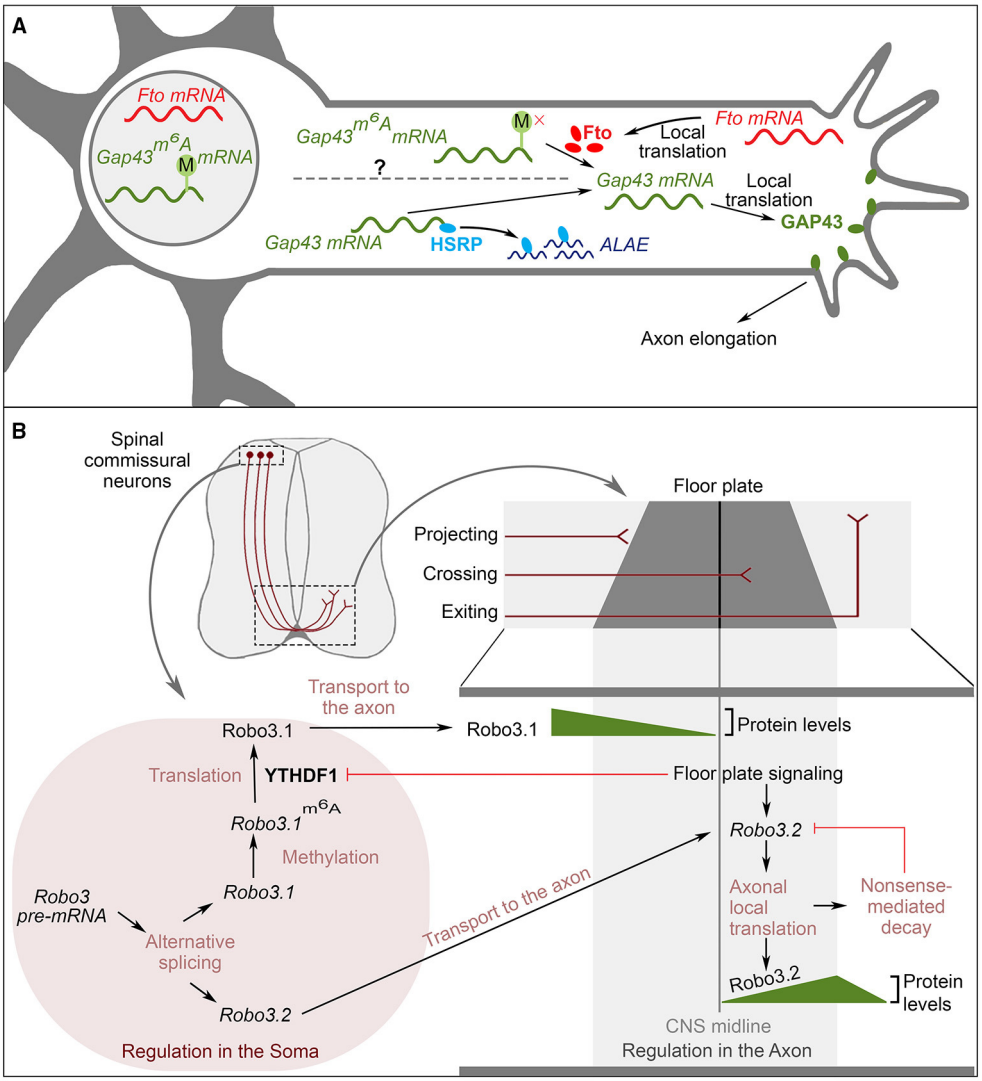

FIGURE 3 | The interplay of RNA modification and local translation for neuronal wiring **(A)** Regulation of local translation of *Gap43* mRNA for axon elongation. *FTO* mRNA is locally translated in axons. The eraser FTO mediates the de-methylation of *Gap43*$^{m^6A}$ *mRNA* in axons. This leads to local translation of *Gap43* mRNA. *Via* an alternative pathway, HSRP binds to the 3′UTR of *Gap43* mRNA to repress its translation. The non-coding RNA ALAE is enriched in the axon and sequesters HSRP. Released *Gap43* mRNA can then be translated locally. *Gap43* associates with the plasma membrane and regulates actin dynamics to promote axon elongation. The question mark on the dotted line highlights that it is unknown whether these two pathways interact. **(B)** RNA metabolism of Robo3 involved in midline crossing of commissural neurons. (Top) Cross-section of spinal cord showing the trajectory of commissural neurons. During development, these neurons project their axons ventrally, where they cross the midline to target the contralateral side. (Bottom) *Robo3* RNA metabolism leads to spatially and temporally controlled expression of Robo3 during navigation of commissural axons. (Left) Events occurring in the soma. (Right) events occurring in the axons. *Robo3* can produce 2 isoforms *via* AS, *Robo3.1* and *Robo3.2*. From these isoforms, *Robo3.1* is methylated, and the m^{6}A modification is read by YTHDF1, which stimulates translation of *Robo3.1*$^{m^6A}$ in the soma. When commissural axons reach the floor plate, signaling from the floor plate downregulates YTHDF1 expression, thus inhibiting *Robo3.1* expression in post-crossing axons. At this point, floor plate signaling induces the local translation of the *Robo3.2* isoform. After translation, *Robo3.2* is degraded by nonsense-mediated decay. Growth cones projecting to the floor plate express Robo3.1 only. After reaching the floor plate, the protein levels of Robo3.1 decrease and Robo3.2 protein levels increase. Shortly after crossing the midline, Robo3.2 protein levels are downregulated.

the same time, floor plate signaling induces local translation of Robo 3.2 transcripts (Colak et al., 2013). After the first round of translation, however, mRNAs are targeted for nonsense-mediated decay (NMD), which gradually reduces Robo 3.2 protein levels in post-crossing axons (Colak et al., 2013). These sophisticated regulatory mechanisms ensure that *Robo 3.1/3.2* expression is spatially tightly restricted: only *Robo 3.1* is expressed before crossing the midline, and *Robo 3.2* is expressed only in a short post-crossing axonal segment. Robo 3.1 attracts the axons to the midline, and allows midline crossing (Zelina et al., 2014). Robo 3.2 was suggested to mediate repulsion from the midline (Colak et al., 2013). Its localization only in the post-crossing segment avoids early repulsion (Colak et al., 2013). The expression of Robo 3.2 induced by the floor plate allows axons to exit the midline

(Colak et al., 2013). In turn, the continuous decay of Robo 3.2 in the post-crossing axonal segment prevents over-repulsion from the midline, and sets the distance from the midline, at which the axons will turn rostrally and continue their journey in the contralateral side of the CNS (Chen et al., 2008; Colak et al., 2013; Zhuang et al., 2019).

Another molecular mechanism involving m^6A reading was identified in *Drosophila*, where the YTHDF1 homolog (YTHDF) interacts with the RBP FMRP. Murine FMRP binds polyribosome-associated mRNAs and can inhibit translation by promoting ribosome stalling (Darnell et al., 2011). *Via* this, and other mechanisms, FMRP is a negative regulator of local translation with large impacts on neuronal wiring (Davis and Broadie, 2017). FMRP is expressed in almost all neuronal cell types and localizes to axons and to pre-synapses during synaptogenesis (Christie et al., 2009). At the *Drosophila* neuromuscular junction (NMJ), loss of FMRP leads to increased axonal growth due to increased translation of the *chic* mRNA (Zhang et al., 2001; Reeve et al., 2005). *chic* encodes Profilin, an actin-binding protein that promotes axonal outgrowth (Wills et al., 1999). A recent study identified several shared mRNA targets of YTHDF and FMRP, including *chic* and *futsch* (the latter encoding a microtubule-associated protein that regulates axon growth at the NMJ; Worpenberg et al., 2021). YTHDF stabilizes FMRP binding to these mRNAs, which represses their translation. This interaction thereby limits axon growth both at the NMJ and in the CNS (Worpenberg et al., 2021). A major open question to tackle in the future is whether YTHDF homologs in mammals can also repress translation depending on the involved target and interaction partners, and, conversely, whether *Drosophila* YTHDF can also stimulate translation (Worpenberg et al., 2021).

2.5. RNA Editing

The most frequent form of RNA editing is adenosine deamination (Adenosine-to-Inosine, A-to-I editing), catalyzed by the ADAR family of RBPs. The produced inosines are read as guanosines by cellular proteins, and this can alter codons and splicing events, thus leading to changes in protein function (Tariq and Jantsch, 2012; Nishikura, 2016; Walkley and Li, 2017). A to I editing is most abundant in the CNS (Ramaswami et al., 2013) and increases progressively during development (Hwang et al., 2016). Like other regulatory mechanisms of RNA metabolism, RNA editing is cell type-specific (Lundin et al., 2020). ADARs are enriched in the nucleus at different stages of brain development (Desterro et al., 2003; Behm et al., 2017). This led to the hypothesis that mRNA editing is restricted to the nucleus. However, RNA editing can also occur in the cytoplasm, such as in adult axons of the squid (Vallecillo-Viejo et al., 2020). Surprisingly, in these neurons, the rate of editing is higher in axons than in cell bodies (Vallecillo-Viejo et al., 2020). The presence and function of RNA editing in developing axons, such as at the stage of axon outgrowth and targeting, are still to be discovered.

Among the neuronal proteins recoded by editing, neurotransmitter receptors, ion channels and other genes involved in rapid electrical and chemical transmission are the principal identified targets of ADARs (Hoopengardner et al., 2003). The rat 2C subtype of serotonin receptors (5-HT2CR) is edited in the intracellular domain, which leads to a dramatic decrease in signaling downstream of the receptor (Burns et al., 1997). In mice, the α3 subunit (*Gabra-3*) of the $GABA_A$ receptor is edited by ADARs, replacing isoleucine with methionine in the transmembrane region of the protein (Ohlson et al., 2007). This editing event depends on an intronic stem loop 150 nt downstream of the edited site (Daniel et al., 2012). The amino acid change decreases α3 protein levels and trafficking to the cell membrane (Daniel et al., 2011). The reduction of cell surface presentation of the edited α3 subunit is mediated by both, higher receptor internalization from the membrane and degradation by the lysosomal pathway (Daniel et al., 2011). The recoding also affects the biophysical properties of the channel: editing leads to higher sensitivity to GABA and faster deactivation (Nimmich et al., 2009). The *Drosophila* homolog of the GABA receptor is formed by homomers of RDL (resistance to dieldrin), whose encoding transcript is diversified into 4 alternative variants due to AS (Ffrench-Constant and Rocheleau, 1993). Additional isoform diversity is given by RNA editing that changes four amino acid residues (Hoopengardner et al., 2003; Jones et al., 2009). The recoding and the choice of alternative exons are linked, and depend on the developmental stage, although the underlying molecular mechanisms are unknown (Jones et al., 2009). As in the mammalian receptor, the combination of AS and amino acid recoding determine the functional properties of the receptor in *Drosophila* (Jones et al., 2009). In mammals, the glutamate receptors GluA1, GluA2, GluA3, GluA4, GluA5, and GluA6 (encoded by *Gria1, Gria2, Gria3, Gria4, Gria5, and Gria6*, respectively) are also edited by ADARs (Bernard and Khrestchatisky, 1994; Bass, 2003). The RNA editing rates of the transcripts of these receptors change from early development until adulthood, leading to the expression of distinct receptors that differ in single amino acids across development (Wahlstedt et al., 2009). Similarly to GABA receptors, recoding of glutamate receptors also leads to changes in functional properties, namely lower permeability (Egebjerg and Heinemann, 1993), faster recovery after desensitization (Lomeli et al., 1994), and also a decrease in the insertion rate into the plasma membrane (Araki et al., 2010).

Besides their function in synaptic transmission, neurotransmitter receptors also have functions in synaptogenesis and neuronal wiring. In chicken, the GluA2 subunit of AMPA receptors is required for the formation of dendritic arborizations (Yoon et al., 2012), and in mammalian brains, it can modulate spine formation (Saglietti et al., 2007; Lee et al., 2016). The murine $GABA_A$ receptor can induce synaptogenesis (Oh et al., 2016), and it is also required for spine formation (Heinen et al., 2003). Since RNA editing modifies the properties and membrane insertion of GluA2 and $GABA_A$, RNA editing could potentially affect neuronal wiring *via* these neurotransmitter receptors. Whether and how this is the case remains a major unsolved question that should be addressed in future studies.

Adenosine deaminases that act on RNA also have other targets with more evident functions in neuronal wiring. Among them are *Filamin-α* (FLNa), *Filamin-β* (FLNb), and *Nova1*

(Tariq and Jantsch, 2012; Nishikura, 2016). FLNa and FLNb are actin binding proteins that control actin reorganization and are required for neurogenesis, neuronal migration, and axon guidance (Fox et al., 1998; Zheng et al., 2011; Zhang et al., 2013; Oliva et al., 2015). *Drosophila* FLNa and FLNb interact with the cell surface receptors Teneurin-2 (Ten-m) and Semaphorin-1a (Sema-1a) and mediate responses downstream of receptor activity (Zheng et al., 2011; Jeong et al., 2017; DePew et al., 2019). *Via* interactions with FLN, Ten-m controls growth cone guidance (Zheng et al., 2011; DePew et al., 2019). Moreover, a bioactive peptide corresponding to the C-terminal region of the protein is produced from the Ten-m locus, and it strongly induces filopodia formation and growth cone enlargement through interaction with FLN (Rubin et al., 1999). Sema-1a promotes axon outgrowth and, depending on the context, is an attractive axon guidance cue (such as in grasshoppers; Wong et al., 1997, 1999), or a repulsive axon guidance cue through interaction with FLN (such as in *Drosophila*; Jeong et al., 2017). However, it is still unknown if editing of *FLN* mRNA affects its response to receptor activity. Nova1 regulates AS of several receptors required for correct neuronal wiring (see section above), and although the editing of murine *Nova1* had no direct impact on the splicing activity in a heterologous system, it leads to reduced proteasome targeting and extended half-life of Nova1 (Irimia et al., 2012). How Nova1 editing is regulated to control neuronal wiring remains elusive.

Although it is not yet known if its editing affects its function in neuronal wiring, the mRNA encoding the cytoplasmic FMRP-interacting protein 2 (CYFIP2) constitutes an intriguing target of ADARs in the contexts of circuit development (Tariq and Jantsch, 2012; Nishikura, 2016). CYFIP2 is a member of the WAVE complex that can trigger actin nucleation, and it is required for axon guidance and synaptogenesis (Schenck et al., 2003; Zhao et al., 2013). Interestingly, CYFIP2 interacts with the RBP FMRP (see above) in the growth cone and mediates actin remodeling, for example in the context of optic tract axon sorting (Schenck et al., 2001, 2003, 2004; Cioni et al., 2018b). Remarkably, in both vertebrates and invertebrates, FMRP interacts directly with ADAR and regulates ADAR RNA editing activity, particularly of synaptic proteins (Shamay-Ramot et al., 2015; Filippini et al., 2017). In zebrafish, ADAR and FMRP interact biochemically, and FMRP limits axon branching and synapse density in different projection, sensory and motor neurons (Shamay-Ramot et al., 2015). At the *Drosophila* NMJ, the knockout of either *Fmr1* or *Adar* leads to an increase both in axon branching and in synaptic boutons, and a reduction of postsynaptic GluRIIA receptor levels (Bhogal et al., 2011; Maldonado et al., 2013). Yet, FMRP is not the only RBP that modulates ADAR activity: a recent *in vivo* genetic screen in *Drosophila* identified several such RBPs, including Rbp6, a Musashi family protein (see below), and Pasilla, a Nova1/2-homolog best described as a splicing regulator (Sapiro et al., 2020). The evolutionarily conserved zinc finger protein Zn72D, however, turned out as the major regulator of ADAR-mediated RNA editing, affecting almost 60% of the investigated editing sites, mostly stimulating their editing. Consistently, knockout of Zn72D leads to a similar reduction of GluRIIA receptor levels at the *Drosophila* NMJ as ADAR knockout (Sapiro et al., 2020). In total, this study identified more than 1,200 editing sites in introns, untranslated regions, and coding sequences, with editing efficiencies (i.e., the fraction of mRNA molecules with an edited nucleotide) ranging from a few percent to a hundred percent. A major challenge for the field of RNA editing is the investigation of the effects on protein expression and function, and neuronal wiring, of each of these editing sites.

3. THE MUSASHI RNA BINDING PROTEIN FAMILY AS MASTER REGULATORS OF NEURONAL DEVELOPMENT

A intriguing and debated question in the field of neuronal wiring is how the differential regulation of gene expression can generate the highly specialized protein repertoires, which are needed for correct circuit formation, in a cell type-specific and temporally controlled manner. Individual RBPs typically act on hundreds of RNA targets to post-transcriptionally regulate different aspects of mRNA metabolism, and, concomitantly, different stages of neuronal wiring. The evolutionary conserved Musashi (Msi) protein family constitutes a prime example of this diversity in RBP molecular function and repeated involvement in neuronal development. Msi proteins control neural stem cell maintenance, neuronal proliferation and differentiation, neuronal morphology, axon guidance, sub-cellular synaptic connectivity, and synapse maintenance. To control these diverse cellular processes, the Musashi proteins can fully rely on their versatility in terms of molecular function. Namely, Msi proteins can inhibit or stimulate mRNA translation, enhance polyadenylation, and regulate splicing (Sutherland et al., 2013; Fox et al., 2015; Murphy et al., 2016). In this section, we discuss how the versatility of Msi is exploited for neuronal wiring in different systems. First, we will introduce the well-described essential Msi functions in neuronal stem cell maintenance, cell proliferation, and cell fate determination. Subsequently, we will discuss Msi functions in neuronal morphology, axon guidance, synaptic connectivity and synapse maintenance.

Two homologues form the Msi protein family, which is conserved from invertebrates to vertebrates (Nakamura et al., 1994; Sakakibara et al., 1996, 2001; Nagata et al., 1999; Shibata et al., 2012). Msi proteins are highly enriched in the developing CNS, with prominent expression in embryonic, fetal, and adult neural stem cells (Nakamura et al., 1994; Sakakibara et al., 1996, 2001; Kaneko et al., 2000; Shibata et al., 2012). The name of the Msi protein was inspired by the samurai Miyamoto Musashi, who used to fight with two swords simultaneously: in *Drosophila*, where Msi was originally identified (Nakamura et al., 1994), disrupted asymmetric division of sensory organ precursors in *msi* null mutants leads to the duplication of large thoracic sensory bristles, and these duplicated bristles resemble the two swords that Musashi used (Nakamura et al., 1994).

Msi proteins contain two RNA binding domains (Sakakibara et al., 1996, 2001; Nagata et al., 1999; Ohyama et al., 2008; Iwaoka et al., 2017). Close to their C-terminus, an intrinsically disordered region can promote RNA binding (Iwaoka et al., 2017). Msi can bind to the pentamers-heptamers

(G/A)$U_{1\text{-}3}$AGU in RNA (Ohyama et al., 2012; Zearfoss et al., 2014; Schneider and Wolfinger, 2019). RNA-protein immunoprecipitation assays have uncovered more than 1,000 potential RNA targets of Msi (Vo et al., 2012; Uren et al., 2015; Bennett et al., 2016). This high number of targets explains the versatility of Msi function in different cellular processes.

3.1. Function of Msi Proteins in Neural Stem Cell Maintenance and Neuronal Proliferation

In the context of neural stem cell maintenance, cell proliferation, and cell fate determination, Msi functions by inhibiting translation of target mRNAs (Sutherland et al., 2013; Fox et al., 2015). Murine Musashi 1 (Msi1) is key to maintaining multipotent neuronal progenitors in the proliferative state, and it also influences cell differentiation (Sakakibara and Okano, 1997). Neuronal progenitors have high levels of Msi1, while differentiated neurons have lower Msi1 levels (Sakakibara and Okano, 1997). *In vitro* studies showed that Msi1 controls the proliferative state of neuronal stem cells *via* the cyclin-dependent kinase inhibitor $p21^{WAF\text{-}1}$. In HEK293 cells, Msi1 binds to the 3′UTR of $p21^{WAF\text{-}1}$ mRNA and represses its translation (Battelli et al., 2006). p21 is important to maintain cellular quiescence. Its regulation by murine Msi1 is a means to control quiescence vs. proliferation of (neural) stem cells (Qiu et al., 2004; Battelli et al., 2006). In the absence of murine *msi1*, the differentiation potential of neuronal precursors is lost (Sakakibara et al., 2002). *In vitro* studies showed that during cell differentiation, Msi1 modulates the Notch pathway by binding to the 3′UTR of *numb* mRNA, which results in inhibition of *numb* mRNA translation and thereby an increase in Notch signaling (Imai et al., 2001; Berdnik et al., 2002; das Chagas et al., 2020). Based on information collected from mammalian model systems, the mechanism proposed for this type of inhibition is mediated by Msi1 physically interacting with the Poly(A) binding protein (PABP), both bound to *numb* mRNA (Kawahara et al., 2008). Thus, Msi sequesters PABP and prevents its interaction with the eukaryotic translation initiation factor eIF4G. Reduced binding of eIF4G to PABP impedes the formation of the 80S ribosome and inhibits the initiation of translation (Kawahara et al., 2008).

As revealed by the study of Zika virus-induced microcephaly, the roles of Msi in stem cell maintenance, cell proliferation, and cell fate determination appear relevant to understanding the pathophysiology of this developmental disorder of the brain. The emergence of a Zika virus (ZIKV) epidemic in Brazil in 2016 showed that children that were exposed to the virus infection in the uterus developed defects ranging from mild developmental delay to severe microcephaly and other severe brain abnormalities (Kindhauser et al., 2016; Caldas-Garcia et al., 2020). Resulting from multiple efforts to understand the mechanisms of action of the virus, mammalian Msi1 was eventually shown to interact with the Zika genome (Chavali et al., 2017). The genomic RNA of the Brazilian ZIKV strain, PE243, has 3 Musashi binding elements (MBEs; Chavali et al., 2017). Msi1, but not Msi2, binds to the 3′UTR of the ZIKV and enhances ZIKV protein expression, which enables viral replication, at least in cultured neuronal cell lines (Chavali et al., 2017). The concomitant finding that Msi1 is mutated in individuals with autosomal recessive primary microcephaly suggested the following working model: because of binding of Msi1 to ZIKV RNA, ZIKV infection could induce microcephaly by titrating Msi1 protein. Thus, less Msi1 protein is available for binding to endogenous targets, leading to de-regulation of these endogenous targets during brain development (Chavali et al., 2017). This could lead to aberrant stem cell maintenance, cell proliferation, and cell fate determination in the CNS (Chavali et al., 2017). *In silico* studies showed that Msi1 can also bind to the 3′UTR of other, related flavoviruses (Schneider and Wolfinger, 2019). Therefore, several emerging viruses could cause the same developmental defects in children as the ZIKV (Schneider and Wolfinger, 2019).

Of note, Msi proteins have also been associated with neurodegenerative diseases. Msi proteins have intrinsically disordered regions that could lead to their aggregation and interaction with Tau (Chen and Huang, 2020; Montalbano et al., 2020), and Msi1/2 were found to form oligomers in brains of patients with Alzheimer's disease, amyotrophic lateral sclerosis, and frontotemporal dementia (Sengupta et al., 2018; Montalbano et al., 2020).

3.2. Functions of Msi Proteins in Neural Circuit Formation

Surprisingly little is known about the roles of Msi in neural circuit formation beyond stem cell maintenance, cell cycle progression, and cell fate specification. Only few studies have investigated the functions of Msi in later steps of neuronal development that could contribute to the patterning of neuronal connectivity. Yet, it appears that Msi can regulate various aspects of postmitotic neuronal morphogenesis, axon guidance, the establishment of synaptic connectivity, and synapse maintenance (**Figure 4**), with dramatic impacts on neuronal wiring. Examples thereof are discussed below.

3.2.1. Functions of Msi Proteins in Neuronal Morphogenesis

Murine Msi1/2 are involved in shaping the morphology of photoreceptors (**Figure 4A**): upon loss of Msi1/2, the outer segment of the photoreceptors is not formed (Sundar et al., 2020; **Figure 4A**). This phenotype seems to be due to the dysregulation of a specialized splicing program: Msi1/2 promote the inclusion of photoreceptor-specific exons in at least half a dozen transcripts that are critical for morphogenesis of the outer segment, and for synaptic transmission in mice and *X. laevis* (Murphy et al., 2016; Sundar et al., 2020). Remarkably, overexpression of Msi1 in liver cancer cells can induce the inclusion of photoreceptor-specific exons (Ling et al., 2020). However, the effect of Msi1/2 on AS in photoreceptors may be indirect: Msi1/2 could potentially have a broad impact on AS by regulating translation of RBPs that in turn regulate splicing. Finally, Msi1 is not a general regulator of splicing, but rather its function in splicing is restricted to specific cell types and/or specific genes. For example, in cellular models

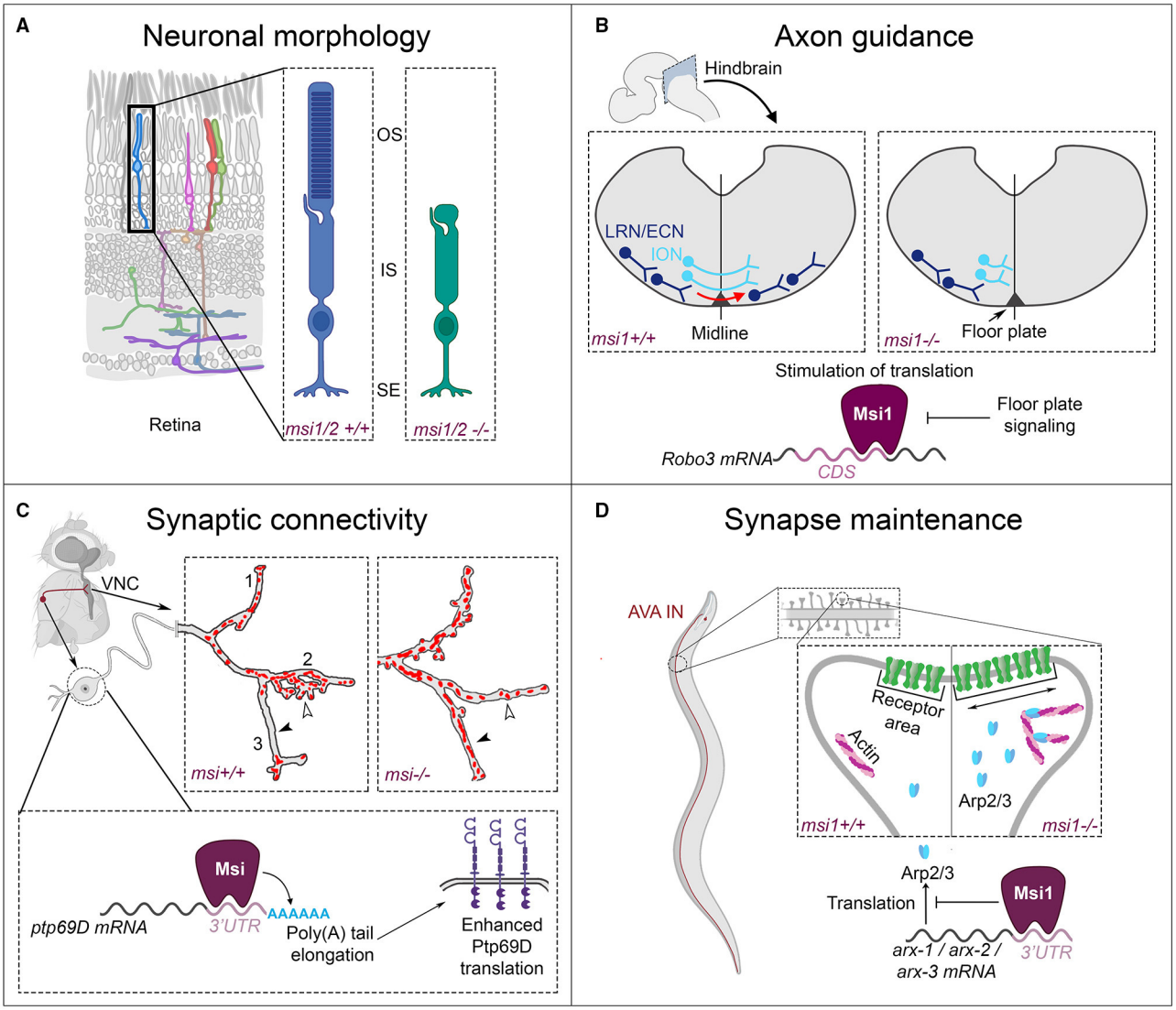

FIGURE 4 | The RBP Musashi as a master regulator of neuronal wiring. **(A)** Msi proteins control the morphology of photoreceptors. In the mouse retina, Msi1 and Msi2 are required for the correct formation of the outer segment (OS) in photoreceptors. Moreover, in animals lacking Msi1/2, photoreceptors have impaired light response and increased degeneration. These phenotypes are attributed to dysregulation of a Msi1/2-dependent splicing program. IS, inner segment; SE, synaptic ending. Cartoon of retina reproduced from Baden, Tom (2020); Zebrafish retina (adult); Zenodo; https://doi.org/10.5281/zenodo.3926525. **(B)** Msi1 controls midline crossing of precerebellar neurons in mice. The precerebellar lateral reticular neurons (LRN) and external cuneate nucleous neurons (ECN) migrate toward the ventral midline and both the processes and the cell bodies cross the ventral midline. The inferior olivary neurons (ION) also migrate toward the ventral midline, but only their processes cross the midline. In animals lacking Msi1, midline crossing and neuronal migration of IO and LR/EC neurons are impaired. Msi1 binds to the coding sequence (CDS) of the *Robo3* mRNA to enhance protein levels of the Robo3 receptor. When the neurons are approaching the ventral midline, signaling from the floor plate inhibits Msi1 expression, which reduces *Robo3* translation. The temporal and spatial regulation of *Robo3* translation is required for the midline crossing of precerebellar neurons. **(C)** Msi controls axon collateral branch-specific synaptic connectivity of mechanosensory neurons in *Drosophila*. The mechanosensory neurons innervate bristles on the dorsal thorax of the fly and extend their axon to the ventral nerve cord (VNC). The axon forms three collateral branches that innervate the anterior (1), contralateral (2), and posterior (3) regions of the VNC, respectively. Msi specifically promotes the formation of terminal arborizations and a high number of synapses in branch 2 (open arrowhead). By contrast, in branch 3, Msi prevents ectopic synaptogenesis (filled arrowhead). These antagonistic, compartment-specific functions of Msi may depend on the regulation of different mRNA targets. For the function observed in branch 2, Msi binds to the 3′UTR of the mRNA encoding the receptor protein tyrosine phosphatase Ptp69D (bottom). Msi enhances poly(A) tailing and stability/translation of the *ptp69D mRNA*. For the function observed in branch 3, the relevant target(s) have not yet been identified. **(D)** Msi1 controls synapse size after associative learning in the *Caenorhabditis elegans* AVA interneuron. In wild-type animals, synapse/dendritic spine size increases during learning, and it is decreased *via* a Msi1-dependent mechanism during forgetting. Msi1 binds to the 3′UTR of transcripts coding for components of the actin branching regulator Arp2/3 to down-regulate its translation. The decrease in levels of the ARP2/3 complex leads to a reduced ramification of actin filaments, which correlates with the decrease in synapse size. In animals lacking Msi1, the translation of Arp2/3 complex components is not inhibited and synapse size remains high, leading to a failure to forget.

of glioblastoma, only the splicing of very few genes is controlled by Msi1 (Uren et al., 2015).

3.2.2. Functions of Msi Proteins in Neuronal Migration and Axon Guidance

The evolutionary conserved Msi1 is also involved in regulating cell migration and axon guidance in mice. In pre-cerebellar neurons, this occurs *via* post-transcriptional regulation of the Robo3 cell-surface receptor (Kuwako et al., 2010; **Figure 4B**). Msi1 binds to the mRNA of *Robo3* at binding elements in the coding sequence, in contrast to the vast majority of confirmed Msi1 targets, for which binding occurs in the 3′UTR. Interestingly, *Robo3* binding is not mediated by consensus MBEs, but by alternative elements that are unknown (Kuwako et al., 2010). Loss of *msi1* leads to a decrease in Robo3 protein levels, without affecting the *Robo3* mRNA levels (Kuwako et al., 2010), suggesting that Msi1 directly stimulates *Robo3* translation. Very similar neuronal migration and axon guidance phenotypes are observed in precerebellar neurons of animals either lacking *Robo3* or *msi1* (Kuwako et al., 2010). Moreover, it is worth noting that Msi1 was found to positively regulate YTHDF1 expression in glioblastoma (Yarmishyn et al., 2020). Since YTHDF1 positively regulates Robo3 expressions in spinal commissural neurons (see above), it will be an interesting avenue for future studies to determine if YTHDF1 regulation is a second, parallel Msi1-dependent or -independent pathway to control Robo3 expression in developing neurons.

3.2.3. Functions of Msi Proteins in Establishing Synaptic Connectivity

In the *Drosophila* CNS, we recently identified a role for Msi in the sub-cellular control of synaptic connectivity. Msi specifically promotes a high number of synapses in one axon collateral of mechanosensory neurons, while in a different compartment of the same axon, Msi limits synapse number and prevents ectopic synaptogenesis. Thus, Msi has opposing, compartment-specific functions (Landínez-Macías et al., 2021; **Figure 4C**). Moreover, Msi has an additional function in promoting the formation/growth of a specific axon collateral branch. Msi binds to the 3′UTR of the mRNA encoding the type IIA receptor protein tyrosine phosphatase Ptp69D and enhances its poly(A) tailing (Landínez-Macías et al., 2021). Our study proposes that the regulation of polyadenylation is a means to control translation of the *ptp69D* mRNA. In turn, precisely set levels of Ptp69D protein determine synaptic connectivity in one specific axon compartment (Landínez-Macías et al., 2021). The different compartment-specific functions downstream of an RBP present a concept of how a single "master" regulator can confer subcellular specificity of morphogenesis (in this case, synaptogenesis), thereby reducing the complexity required for the regulation of gene expression. Molecularly, we propose that Msi regulates different mRNA targets in mechanosensory neurons, which, in turn, have opposing functions in the control of synapse numbers in different subcellular compartments. As previously described for non-neuronal cells (Arumugam et al., 2012; Cragle and MacNicol, 2014; Weill et al., 2017), our findings further support that Msi proteins can not only function in the inhibition of translation but can also be translational activators for specific target mRNAs. How is this activation achieved on the molecular level? Different mechanisms were identified by studies in *X. laevis* oocytes. Msi1 induces oocyte maturation by activating translation of target mRNAs at specific time points during meiotic progressions (Arumugam et al., 2012). This translational activation can be achieved by stimulation of polyadenylation. In one scenario, the binding of Msi1 to the 3′UTR of target mRNAs can elicit structural changes that lead to preferential exposure of adjacent cytoplasmic polyadenylation elements (CPEs), and induction of polyadenylation (Cragle and MacNicol, 2014; Weill et al., 2017). CPEs are recognized by the cytoplasmic polyadenylation element binding protein (CPEB), which on the one hand dictates, which mRNAs undergo cytoplasmic polyadenylation, and on the other hand impacts on the strength of polyadenylation. In another scenario, *via* a mechanism independent of CPEB, Msi1 can associate with Gld2 (germline development 2), a protein that catalyzes poly(A) addition (Cragle and MacNicol, 2014). Msi1 bound to Gld2 directs cytoplasmic polyadenylation and activation of translation of Msi targets (Cragle and MacNicol, 2014). These mechanisms could be conserved in the mammalian brain: CPEB and Gld2 were shown to elicit polyadenylation of neuronal mRNAs in mouse hippocampal neurons (Zearfoss et al., 2008; Udagawa et al., 2012). However, it remains to be tested if in neuronal tissues Msi1 also interacts with Gld2 or CPEB to enhance polyadenylation of specific targets. Surprisingly, while Msi1 can *inhibit* translation by binding to PABP and thus decrease PABP interactions with the translation initiation complex (see above), Msi1-mediated translational *activation* in *X. laevis* oocytes can also be achieved *via* an interaction with an embryonic PABP, or the canonical somatic cell PABPC1 (Cragle and MacNicol, 2014).

In general, it remains largely unknown how RBPs shape neuronal circuits through the specific control of poly(A) tailing. Besides the cytoplasmic polyadenylation element binding protein and other general regulators of polyadenylation, only a few RBPs with functions linked to the poly(A) tail have been involved in neuronal wiring. One of them is the Nab2 poly(A) binding protein, which controls the guidance of *Drosophila* mushroom body (MB) axons (Bienkowski et al., 2017). Thus, the control of mRNA polyadenylation is an underappreciated mechanism for the translational regulation of specific mRNAs in developing neurons, and an interesting avenue for future studies.

3.2.4. Function of Msi Proteins in Synapse Maintenance

In *C. elegans*, Msi has been linked to the control of synapse size and of time-dependent memory loss (**Figure 4D**). Msi1 (the only Msi paralog in *C. elegans*) binds to the 3′UTR of the mRNAs encoding three different subunits of the Arp2/3 complex (Hadziselimovic et al., 2014). Thereby, Msi1 elicits downregulation of Arp2/3 expression. This mechanism causes the reversal of learning-induced increases in synapse size. Hence, synapse size cannot be reduced in animals lacking *msi1*, which leads to deficits in forgetting. These findings thus

link the translational control of cytoskeletal components to forgetting (Hadziselimovic et al., 2014). Forgetting is an essential physiological process whose regulation/dysregulation is at the core of neurological syndromes such as post-traumatic stress disorder or the extremely rare Hyperthymestic Syndrome/Highly Superior Autobiographical Memory (Parker et al., 2006; LePort et al., 2012). Interestingly, the most prominent targets of the Msi family of proteins, identified by transcriptome-wide mapping of RNA targets, are key regulators of the actin cytoskeleton and of focal adhesions (Vo et al., 2012; Uren et al., 2015; Bennett et al., 2016; Lin et al., 2019). In particular, Filamin, Rac, WAVE1, α-catenin, and actin can be bound by Msi (Uren et al., 2015). These proteins have key roles in axon outgrowth, branching and targeting, and synapse formation and maintenance, and are interesting putative targets to further study Msi-mediated mechanisms that control neuronal wiring.

4. MALFUNCTION OF RNA BINDING PROTEINS AND ASSOCIATED DISEASES

Neurodevelopmental and psychiatric disorders affect a considerable proportion of the population worldwide, with prevalences of several percent for certain syndromes, and they are highly driven by genetic determinants (Parenti et al., 2020). Yet, our understanding of the molecular etiology of these disorders is still very limited. Risk loci identified in genome wide association studies have paved the way for investigating these underlying molecular mechanisms. As illustrated so far in this article, gene expression in the central nervous system is highly regulated during development and in a tissue and cell type-specific manner and this control is essential for the formation of complex neural circuits. Thus, not surprisingly, an important number of risk loci for neurodevelopmental and psychiatric disorders are present in non-coding and regulatory regions of the genome (Schizophrenia Working Group of the Psychiatric Genomics Consortium, 2014; Parikshak et al., 2016). In particular, genetic variants in RBP binding sites (required for RBP-mediated post-transcriptional regulation of gene expression) are drivers of psychiatric disorder risk, with, remarkably, an even stronger impact than genetic variants in coding regions (Park et al., 2021). In this section, we exemplify how dysregulation of RBP-RNA interactions, at several steps of RNA metabolism, can lead to disease. We will highlight the molecular and cellular functions of some RBPs and how their loss/reduction of function can lead to disease. Given that RBPs can have thousands of targets, we will specially emphasize non-monogenic disorders. Several "infamous" RBPs, such as TDP-43, FUS, FMR1/FMRP, and SMN, are causally linked to different neurological disorders. The function of these proteins has been extensively reviewed elsewhere (Hagerman et al., 2018; Bagni and Zukin, 2019; Gao et al., 2019; Prasad et al., 2019; Wirth et al., 2020; Zbinden et al., 2020; Portz et al., 2021) and although many questions regarding the cellular and molecular consequences of their dysregulation remain open, we will not discuss them here.

4.1. Alternative Splicing

Genetic variants in loci linked to splicing have a big impact on the risk for disorders of brain development (Parikshak et al., 2016; Walker et al., 2019), and altered function of splicing factors can lead to neurodevelopmental disorders, such as intellectual disability (ID; Mattioli et al., 2020). For example, a point mutation in *Nova2* that is found in patients with ID leads to a reading frame shift that changes the C-terminal part of the protein (Mattioli et al., 2020). This mutation impairs Nova2 RNA binding activity and causes dysregulation of AS events, with, among the affected targets, an enrichment of mRNAs coding for regulators of the cytoskeleton. The C-terminal frame shift also elicits aberrant axon tract formation *in vivo* in the zebrafish visual system, suggesting that axonal wiring defects may underlie the human neurodevelopmental disorders caused by mutations in *Nova2* (Mattioli et al., 2020).

An intriguing feature of gene expression in the nervous system is the alternative use of microexons (3-27 nt long). These microexons are frequently neuron-specific, and generate in-frame changes in the coding sequence, which lead to variant protein surfaces and modulation of protein-protein interactions (Irimia et al., 2014). Dysregulation of microexon splicing is present in many disease-associated proteins, including proteins linked to autism spectrum disorders (ASD; Irimia et al., 2014). One of the key regulators of inclusion of microexons in neuronal cells that has been linked to ASD is Srrm4 (also known as nSR100; Irimia et al., 2014; Quesnel-Vallières et al., 2015; Gonatopoulos-Pournatzis et al., 2018). Quesnel-Vallières et al. developed a mouse model of ASD with a reduction of Srrm4 expression to 50% of wild-type levels, in order to study the molecular functions of this splicing regulator. They found that reduction of Srrm4 protein levels leads to deficits in social behavior as observed in ASD (Quesnel-Vallières et al., 2016). Also, the 50% reduction of Srrm4 is sufficient to alter the splicing of microexons in targets of Srrm4 that are associated with ASD, including cues and receptors involved in axon guidance and synaptic maturation/transmission, such as Slit2, Dnm2, and Nrxn2 (Quesnel-Vallières et al., 2016). The impact of these changes on the neural circuitry was demonstrated in pyramidal neurons of the somatosensory cortex: upon reduction of Srrm4 levels, these neurons had a strong reduction in synaptic transmission and neuronal excitability. At the morphological level, only minor changes were observed upon 50% reduction of Srrm4 levels, namely in the morphology of dendritic spines (Quesnel-Vallières et al., 2016). By contrast, full knockout of Srrm4 leads to severe wiring defects, such as impairment of neurite outgrowth in motor neurons, disruption of cortical layering, premature neurogenesis, and midline crossing defects (Quesnel-Vallières et al., 2015).

Mechanistically, Srrm4 regulates splicing of microexons in association with the SR-related proteins Srsf11 and Rnps1 (Gonatopoulos-Pournatzis et al., 2018). *In vitro* studies showed that Srrm4, Rnps1, and Srsf11 form a specialized splicing enhancer complex that binds to intronic sequences upstream of neuronal microexons and promote early steps in spliceosome assembly (Gonatopoulos-Pournatzis et al., 2018). This complex

regulates several microexons that are affected in patients with ASD (Gonatopoulos-Pournatzis et al., 2018), including a specific microexon in the mRNA encoding the translation initiation factor eIF4G1 (Gonatopoulos-Pournatzis et al., 2020). Recapitulating defects observed in ASD, lack of inclusion of this microexon in a mouse model leads to impaired social behavior and abnormal protein synthesis-dependent synaptic plasticity (Gonatopoulos-Pournatzis et al., 2020). Molecularly, in the same mouse model, the steady-state levels of several proteins with key synaptic functions are increased upon exclusion of the microexon in eIF4G1, such as a subunit of NMDA-type ionotropic glutamate receptors, and the postsynaptic components of inhibitory synapses Gephyrin and Neuroligin-2 (Gonatopoulos-Pournatzis et al., 2020). Inclusion of the microexon in *eIF4G1* increases the propensity of eIF4G to undergo phase separation, which allows the formation of neuronal RNP granules with Fxr1, Ataxin-2, Larp1, and Stau2, and causes ribosome stalling (Gonatopoulos-Pournatzis et al., 2020). Hence, the absence of the microexon in *Eif4g1* mRNA leads to enhanced translation of synaptic proteins and alterations in synaptic transmission (Gonatopoulos-Pournatzis et al., 2020). Remarkably, another general regulator of translation that is associated with ASD risk and regulated by Srrm4/Srrm3/Srsf11-dependent microexon splicing is the cytoplasmic polyadenylation element binding protein 4 (CPEB4; Quesnel-Vallières et al., 2015; Parras et al., 2018). CPEB4 AS is altered in patients with ASD, with a decrease of microexon 4 inclusion and a reduction of protein levels (Parras et al., 2018). In a mouse model recapitulating *CPEB4* microexon 4 skipping, deadenylation is enhanced and translation is reduced for mRNAs of ASD risk genes (Parras et al., 2018). These mice also show a decreased spine density in dendrites of pyramidal neurons in the somatosensory cortex, and behavioral changes recapitulating the hallmarks of ASD (Parras et al., 2018). It is not clear if the eIF4G and CPEB4 proteins converge to control the translation of the same mRNA targets, and the formation of neuronal granules in the same cell types/developmental stages. However, insights into the (dys)regulation of eIF4G, CPEB4, and the Srrm4/Srrm3/Srsf11 complex together could strengthen our understanding of the root causes of ASD, and provide an entry point for tackling the disorder.

4.2. Regulation of Translation

RNA-binding proteins control the translation of a plethora of targets at different stages in the process, namely the initiation, elongation, or termination of translation, or ribosome recycling (Sonenberg and Hinnebusch, 2009). Not surprisingly, mutations altering the function and/or expression levels of RBPs with functions in translational regulation can be at the core of different neurodevelopmental disorders and also elicit accompanying syndromes. For example, a mutation that affects the C-terminal domain of the eukaryotic translation initiation factor eIF2γ was identified as a possible cause of MEHMO syndrome (Young-Baird et al., 2020). This syndrome is characterized by intellectual disability (ID), epilepsy, hypogenitalism, microcephaly, and obesity. In patient-derived induced pluripotent stem cells, the eIF2γ mutation decreases global translation levels due to defective assembly of eIF2 complexes (Young-Baird et al., 2020), which under normal circumstances assist in the selection of the translation initiation site and the delivery of the initiation methionyl-tRNA (Hinnebusch, 2014).

As another example, DDX3X is an RNA helicase of the DEAD-box family that is associated with ASD, amyotrophic lateral sclerosis, frontotemporal dementia (Cheng et al., 2019), and Toriello Carey (Lennox et al., 2020). Toriello Carey is a disease characterized by ID, corpus callosum agenesis, facial malformations, abnormal postnatal brain development leading to microcephaly, respiratory distress, and cardiovascular anomalies (Toriello et al., 2016). DDX3X is involved in the regulation of canonical translation, repeat-associated non-AUG translation, and formation of RNP granules (Cheng et al., 2019; Hondele et al., 2019; Lennox et al., 2020). Lennox et al. (2020) generated a mouse model with the DDX3X mutations found in patients with ID, which reduce DDX3X helicase activity. In this model, the degree of impairment in the helicase activity correlates with the severity of the symptoms found in patients. Cellularly, reduced DDX3X helicase activity leads to a decrease in cortical neuron generation and in neuronal differentiation during mouse prenatal development. Molecularly, the disruption of DDX3X helicase activity alters the translation of some mRNA targets and elicits ectopic RNP granules in neuronal progenitors (Lennox et al., 2020). In addition, in these mutants, the translation of proteins with repeat-associated non-AUG translation fails to be repressed, which leads to the accumulation of cytotoxic dipeptide repeat proteins (Cheng et al., 2019).

Other RBPs associated with complex neurological disease phenotypes have more specific effects in regulating a smaller group of genes. For example, mutations in Cold Shock Domain-containing E1 (CSDE1) are associated with ASD and ID (Xia et al., 2014; Guo et al., 2019). This RBP was initially studied in the context of stem cell maintenance and the inhibition of neuronal differentiation (Ju Lee et al., 2017). Similarly as our previous example Msi, roles for CSDE1 in later steps of neuronal development have emerged more recently. Downregulation of *CSDE1* in mouse cortical pyramidal neurons leads to neurite overgrowth and reduced branching, decreased spine density, immature spine morphology, reduced number of synapses, and defects in synaptic transmission (Guo et al., 2019). The molecular mechanism mediating these defects is proposed to be the dysregulation of components of the Wnt/β-catenin cell adhesion pathway, including β-catenin, APCDD1, and CDH2 (Guo et al., 2019; El Khouri et al., 2021). Remarkably, expression of β-catenin is sufficient to rescue the developmental defects observed upon downregulation of *CSDE1* (Guo et al., 2019). The function of CSD1 in synapse development is conserved for Unr (the *Drosophila* homolog of mammalian CSD1; Guo et al., 2019).

The transcription factor Ataxin-1 is a good example underscoring the importance of precise regulation of protein levels. Changes in Ataxin1 levels cause spinocerebellar ataxia type 1 (SCA1), which is characterized by cerebellar degeneration due to the accumulation of the protein Ataxin1. Mutated Ataxin1 can contain expanded polyglutamine repeats, which protect the protein from degradation by the proteasome and thus lead to higher protein levels in mice models of SCA1 (Cummings et al., 1999). Increased Ataxin1 levels can also arise from insufficient

translational repression. The Pumilio1 RBP binds to the 3′UTR of *Ataxin1* mRNA, and, under normal conditions, decreases the stability of the mRNA, which reduces both mRNA and protein levels of Ataxin1 (Gennarino et al., 2015). In mice models of SCA1, reduction of Pumilio1 protein levels can lead to SCA1 due to overexpression of wild-type Ataxin1, a phenotype that can be rescued by decreasing Ataxin1 levels. However, additional neurological features in Pumilio1 mutants cannot be rescued by this manipulation, suggesting additional pathways (Gennarino et al., 2015). Interestingly, human *Pumilio1* mutations that differentially reduce its protein levels lead to a different time of disease onset, with lower Pumilio1 levels correlating with earlier onset time and stronger symptoms in patients. A 50% reduction in Pumilio1 causes developmental delay and ID in addition to ataxia (Gennarino et al., 2018), highlighting the developmental roles of Pumilio1 in addition to its roles in the maintenance of neuronal circuits.

RBPs, such as FMRP, Ataxin-2, and SMN (linked to the neurological diseases fragile X mental retardation, spinocerebellar ataxia type 2, and spinal muscular atrophy, respectively) are implicated in the control of mRNA localization and local translation in neurons (Dictenberg et al., 2008; Akten et al., 2011; Fallini et al., 2011; Sudhakaran et al., 2014). The precise causal relationships between defects in mRNA localization/local translation and neurological diseases are however only beginning to be unraveled. As these advances have been discussed in two recent reviews (Wang et al., 2016; Thelen and Kye, 2019), we will not further elaborate on them here.

4.3. RNA Editing

Impairment of ADAR-mediated RNA editing activity has been associated with different neurological disorders, including ALS (Aizawa et al., 2010; Hideyama et al., 2012), epilepsy (Srivastava et al., 2017), Alzheimer's disease (Khermesh et al., 2016), autoimmune disorders (Rice et al., 2012), and ASD (Eran et al., 2013; Tran et al., 2019). Interestingly, in mammals, ADAR expression can be stimulated by interferon (IFN) activity (Patterson and Samuel, 1995), and at the same time, ADAR can suppress IFN signaling (Hartner et al., 2009), suggesting a negative feedback loop. In a mouse model of viral infection that recapitulates ASD-associated behavioral changes, ADAR activity is increased, possibly due to IFN-induced ADAR expression (Tsivion-Visbord et al., 2020). As a consequence, the levels of RNA editing are increased in transcripts coding for proteins involved in neuronal development, metabolism, and the immune response. *FLN-α* and *FLN-β* were among the identified ADAR targets with altered levels of editing (Tsivion-Visbord et al., 2020). As discussed before, an interesting model is that dysregulation of editing in *FLN-α* and *FLN-β* could lead to changes in neuronal wiring, which in turn could be the cause of the observed behavioral changes.

Mutations in ADAR have been found in patients with Aicardi-Goutéres syndrome (Rice et al., 2012), an autoimmune disease characterized by brain inflammation due to increased IFN signaling (Crow and Livingston, 2008). In these patients, the mutations found in ADAR can lead to a decrease of its catalytic activity (Rice et al., 2012). Aicardi-Goutéres syndrome patients have an increase in expression of IFN stimulated genes. However, the authors discuss that it is not clear whether loss of ADAR catalytic activity is the cause of increased IFN signaling (Rice et al., 2012). Can the inflammation elicited by increased IFN signaling induce neuronal wiring defects? This is just one of the many open questions regarding the role of RNA editing, and the underlying cellular and molecular principles, in patients with neurodevelopmental and psychiatric disorders.

Changes in ADAR activity are found in individuals with ASD, also independently of IFN signaling. A postmortem study comparing the editing activity in cerebellar tissue of individuals diagnosed with ASD to the editing activity in individuals without diagnosis showed differences in editing of proteins involved in synaptic transmission (Eran et al., 2013). Interestingly, alterations could go into either direction: for the same editing site, a percentage of editing higher or lower than the average values found in undiagnosed individuals were found in samples from individuals with ASD (Eran et al., 2013). The observed changes might be due in part to the altered expression of ADAR (Eran et al., 2013). In ASD samples, an ADAR isoform with defective binding to dsRNA is expressed at higher levels, and simultaneously, there is downregulation of the ADAR isoform that can actually bind dsRNA (Eran et al., 2013). The study also found that altered RNA editing is correlated with alternative exon retention, affecting *FLN-α*, among others. More specifically, editing at the 3′ end of exon 43 in *FLN-α* mRNA leads to higher exon retention (Eran et al., 2013). It remains to be elucidated if and how increased variability in the editing of *FLN-α*, and therefore increased variability in exon 43 retention, altogether affect neuronal wiring. A second study, with a larger cohort of patients, studied the editing patterns in the frontal cortex, temporal cortex, and cerebellum (Tran et al., 2019). This study also found that ASD samples had higher variability of editing, although there was a higher proportion of sites with lower editing rates (Tran et al., 2019). The genes with larger changes in editings have functions in synaptic transmission, corroborating previous studies describing ADAR function. Several of these editing sites belong to genes that are regulated by FMRP and FXR1P (Tran et al., 2019). The ADAR-edited sites are found in close proximity to the binding sites of these RBPs, and both, FMR1 and FXR1P function regulate the editing of these sites. Remarkably, samples from Fragile X patients, an ID with phenotypes overlapping ASD, showed similar changes in RNA editing as ASD sample (Tran et al., 2019).

These studies provide an entry point to understand the role of ADAR in neurodevelopmental diseases. However, more efforts are needed to further characterize other proteins that interact with ADAR and that modulate its activity. Also, it is required to dissect how changes in RNA editing of ADAR targets affect their cellular and molecular functions, and if and how this could modify neuronal wiring.

5. CONCLUSIONS AND FUTURE PERSPECTIVES

Wiring of the nervous system, with several 100,000 neurons (*Drosophila*) to billions of neurons (86 billions for humans, 200

billions for elephants) is a daunting task. Division of the process into temporally and spatially separated, successive steps, and the application of "simple" pattern formation rules, reduces the complexity that needs to be encoded in the genome (Hassan and Hiesinger, 2015). This breaking down of neural circuit formation into several steps requires precise, localized control of gene expression, often on a timescale of minutes. As we have discussed, local translation in neuronal processes has emerged as a crucial component of this regulation. Thereby, neurons need to rapidly integrate extrinsic and intrinsic cues. While clear *in vivo* evidence for local translation has now been provided for dendrites, (developing) axons and both, pre- and postsynapses, much about its extent and functions in developmental processes, such as axon branching and targeting, remains elusive. A large body of knowledge on local translation in the axon is derived from studies of cultured cells, or of bulk isolates of axons from brain tissue. Studies of single, defined cells (/cell types) and even subcellular compartments *in vivo* will be required to tackle questions such as: how do neurons integrate many extrinsic and intrinsic cues in a rapid way? How are the global and the subcellular proteome changing in response to the specific set of cues that an axon/growth cone is exposed to? Why do different axons respond differently? What are the molecular transduction mechanisms, i.e., how does the (in)activation of a particular cell-surface receptor lead to increases or decreases in global translation, or of only a specific set of RNAs? What is the role of RBPs in this context, do they act as all-or-nothing "molecular switches," or rather in dose-dependent gradual changes in the response? The latter is a major question not only in the context of local translation, but generally in the post-transcriptional control of gene expression.

Despite the mechanisms for reducing the complexity of nervous system wiring and thus of the genomic coding potential required for it, proteome expansion at the post-transcriptional level is essential for correct nervous system development. Except for select genes, some of which we have discussed here, the molecular underpinnings and roles of AS and APA, and their potential coupling (i.e., specific exons being linked to specific 3′UTR isoforms), remain unexplored for many genes and many neurodevelopmental processes. The same applies to other post-transcriptional events. For example, how much RNA editing is present in axons? Can RNA editing even be specific for subcellular compartments? Does this depend on levels of the Adar enzyme, or the localization of specific modulators of its activity? Or could edited RNAs be recognized and transported selectively to specific places in the cell? Likewise, the coupling between mRNA poly(A) tail length and protein production, which was found to differ between different developmental stages/cell types (Xiang and Bartel, 2021), remains unexplored for different neuronal subcellular compartments and wiring stages. Finally, a major question in our opinion is which RNA degradation pathways, besides the NMD pathway described above for control of Robo3.2 expression, are present in axons and dendrites and how they contribute to neuronal morphogenesis and connectivity. The tackling of these and other questions will be greatly facilitated by recent technological advances for the study of RNA metabolism, such as tools to visualize local translation *in situ*, and improved high-throughput sequencing approaches that can also be applied for epitranscriptomics, i.e., the study of RNA modifications. We will need to apply these techniques to study post-transcriptional events not only individually, but also how they are coupled and to what extent there is crosstalk between them. Such studies will provide major insights into how RNA metabolism shapes the nervous system under both, physiological and pathophysiological conditions.

AUTHOR CONTRIBUTIONS

ML-M and OU wrote, discussed, and edited the manuscript. All authors contributed to the article and approved the submitted version.

FUNDING

This work was supported by grants from the Swiss National Science Foundation (SNSF; Ambizione PZ00P3_161448), from the Promotor Stiftung and from the Julius Klaus Stiftung to OU, and by funding from the University of Zurich.

ACKNOWLEDGMENTS

We thank Carlos Oliva (Pontificia Universidad Católica de Chile, Santiago, Chile) for critical reading and feedback on the manuscript.

REFERENCES

Abouward, R., and Schiavo, G. (2021). Walking the line: mechanisms underlying directional mRNA transport and localisation in neurons and beyond. *Cell. Mol. Life Sci*. 78, 2665–2681. doi: 10.1007/s00018-020-03724-3

Aceti, M., Creson, T. K., Vaissiere, T., Rojas, C., Huang, W.-C., Wang, Y.-X., et al. (2015). Syngap1 haploinsufficiency damages a postnatal critical period of pyramidal cell structural maturation linked to cortical circuit assembly. *Biol. Psychiatry* 77, 805–815. doi: 10.1016/j.biopsych.2014.08.001

Aizawa, H., Sawada, J., Hideyama, T., Yamashita, T., Katayama, T., Hasebe, N., et al. (2010). TDP-43 pathology in sporadic ALS occurs in motor neurons lacking the RNA editing enzyme ADAR2. *Acta Neuropathol*. 120, 75–84. doi: 10.1007/s00401-010-0678-x

Akten, B., Kye, M. J., Hao, L. T., Wertz, M. H., Singh, S., Nie, D., et al. (2011). Interaction of survival of motor neuron (SMN) and HuD proteins with mRNA CPG15 rescues motor neuron axonal deficits. *Proc. Natl. Acad. Sci. U.S.A*. 108, 10337–10342. doi: 10.1073/pnas.1104928108

Allen, M., Bird, C., Feng, W., Liu, G., Li, W., Perrone-Bizzozero, N. I., et al. (2013). HuD promotes BDNF expression in brain neurons *via* selective stabilization of the BDNF long 3′UTR mRNA. *PLoS ONE* 8:e55718. doi: 10.1371/journal.pone.0055718

An, J. J., Gharami, K., Liao, G.-Y., Woo, N. H., Lau, A. G., Vanevski, F., et al. (2008). Distinct role of long 3′UTR BDNF mRNA in spine morphology and synaptic plasticity in hippocampal neurons. *Cell* 134, 175–187. doi: 10.1016/j.cell.2008.05.045

Araki, Y., Hong, I., Gamache, T. R., Ju, S., Collado-Torres, L., Shin, J. H., et al. (2020). SynGAP isoforms differentially regulate synaptic plasticity and dendritic development. *eLife* 9:56273. doi: 10.7554/eLife.56273.sa2

Araki, Y., Lin, D.-T., and Huganir, R. L. (2010). Plasma membrane insertion of the AMPA receptor GluA2 subunit is regulated by NSF binding and Q/R editing of the ion pore. *Proc. Natl. Acad. Sci. U.S.A.* 107, 11080–11085. doi: 10.1073/pnas.1006584107

Arumugam, K., MacNicol, M. C., Wang, Y., Cragle, C. E., Tackett, A. J., Hardy, L. L., et al. (2012). Ringo/cyclin-dependent kinase and mitogen-activated protein kinase signaling pathways regulate the activity of the cell fate determinant Musashi to promote cell cycle re-entry in Xenopus oocytes. *J. Biol. Chem.* 287, 10639–10649. doi: 10.1074/jbc.M111.300681

Ashley, J., Cordy, B., Lucia, D., Fradkin, L. G., Budnik, V., and Thomson, T. (2018). Retrovirus-like gag protein Arc1 binds RNA and traffics across synaptic boutons. *Cell* 172, 262.e11–270.e11. doi: 10.1016/j.cell.2017.12.022

Bagni, C., and Zukin, R. S. (2019). A synaptic perspective of fragile X syndrome and autism spectrum disorders. *Neuron* 101, 1070–1088. doi: 10.1016/j.neuron.2019.02.041

Bass, B. L. (2003). RNA editing by adenosine deaminases that act on RNA. *Annu. Rev.* 71, 817–846. doi: 10.1146/annurev.biochem.71.110601.135501

Batista, A. F. R., Martinez, J. C., and Hengst, U. (2017). Intra-axonal synthesis of SNAP25 is required for the formation of presynaptic terminals. *Cell Rep.* 20, 3085–3098. doi: 10.1016/j.celrep.2017.08.097

Battelli, C., Nikopoulos, G. N., Mitchell, J. G., and Verdi, J. M. (2006). The RNA-binding protein Musashi-1 regulates neural development through the translational repression of p21WAF-1. *Mol. Cell. Neurosci.* 31, 85–96. doi: 10.1016/j.mcn.2005.09.003

Baumann, S., Komissarov, A., Gili, M., Ruprecht, V., Wieser, S., and Maurer, S. P. (2020). A reconstituted mammalian APC-kinesin complex selectively transports defined packages of axonal mRNAs. *Sci. Adv.* 6:eaaz1588. doi: 10.1126/sciadv.aaz1588

Behm, M., Wahlstedt, H., Widmark, A., Eriksson, M., and Öhman, M. (2017). Accumulation of nuclear ADAR2 regulates adenosine-to-inosine RNA editing during neuronal development. *J. Cell Sci.* 130, 745–753. doi: 10.1242/jcs.200055

Bennett, C. G., Riemondy, K., Chapnick, D. A., Bunker, E., Liu, X., Kuersten, S., et al. (2016). Genome-wide analysis of Musashi-2 targets reveals novel functions in governing epithelial cell migration. *Nucleic Acids Res.* 44, 3788–3800. doi: 10.1093/nar/gkw207

Berdnik, D., Török, T., González-Gaitán, M., and Knoblich, J. A. (2002). The endocytic protein alpha-Adaptin is required for numb-mediated asymmetric cell division in Drosophila. *Dev. Cell* 3, 221–231. doi: 10.1016/S1534-5807(02)00215-0

Bernard, A., and Khrestchatisky, M. (1994). Assessing the extent of RNA editing in the TMII regions of GluR5 and GluR6 kainate receptors during rat brain development. *J. Neurochem.* 62, 2057–2060. doi: 10.1046/j.1471-4159.1994.62052057.x

Bhogal, B., Jepson, J. E., Savva, Y. A., Pepper, A. S.-R., Reenan, R. A., and Jongens, T. A. (2011). Modulation of dADAR-dependent RNA editing by the Drosophila fragile X mental retardation protein. *Nat. Neurosci.* 14, 1517–1526. doi: 10.1038/nn.2950

Bienkowski, R. S., Banerjee, A., Rounds, J. C., Rha, J., Omotade, O. F., Gross, C., et al. (2017). The conserved, disease-associated RNA binding protein dNab2 interacts with the fragile X protein ortholog in Drosophila neurons. *Cell Rep.* 20, 1372–1384. doi: 10.1016/j.celrep.2017.07.038

Biever, A., Donlin-Asp, P. G., and Schuman, E. M. (2019). Local translation in neuronal processes. *Curr. Opin. Neurobiol.* 57, 141–148. doi: 10.1016/j.conb.2019.02.008

Blockus, H., and Chédotal, A. (2016). Slit-Robo signaling. *Development* 143, 3037–3044. doi: 10.1242/dev.132829

Brose, K., Bland, K. S., Wang, K. H., Arnott, D., Henzel, W., Goodman, C. S., et al. (1999). Slit proteins bind Robo receptors and have an evolutionarily conserved role in repulsive axon guidance. *Cell* 96, 795–806. doi: 10.1016/S0092-8674(00)80590-5

Burns, C. M., Chu, H., Rueter, S. M., Hutchinson, L. K., Canton, H., Sanders-Bush, E., et al. (1997). Regulation of serotonin-2C receptor G-protein coupling by RNA editing. *Nature* 387, 303–308. doi: 10.1038/387303a0

Cagnetta, R., Frese, C. K., Shigeoka, T., Krijgsveld, J., and Holt, C. E. (2018). Rapid cue-specific remodeling of the nascent axonal proteome. *Neuron* 99, 29.e4–46.e4. doi: 10.1016/j.neuron.2018.06.004

Caldas-Garcia, G. B., Schüler-Faccini, L., Pissinatti, A., Paix ao-Côrtes, V. R., and Bortolini, M. C. (2020). Evolutionary analysis of the Musashi family: What can it tell us about Zika? *Infect. Genet. Evol.* 84:104364. doi: 10.1016/j.meegid.2020.104364

Carrasco, J., Rauer, M., Hummel, B., Grzejda, D., Alfonso-Gonzalez, C., Lee, Y., et al. (2020). ELAV and FNE determine neuronal transcript signatures through EXon-activated rescue. *Mol. Cell* 80, 156.e6–163.e6. doi: 10.1016/j.molcel.2020.09.011

Chauvet, S., Cohen, S., Yoshida, Y., Fekrane, L., Livet, J., Gayet, O., et al. (2007). Gating of Sema3E/PlexinD1 signaling by neuropilin-1 switches axonal repulsion to attraction during brain development. *Neuron* 56, 807–822. doi: 10.1016/j.neuron.2007.10.019

Chavali, P. L., Stojic, L., Meredith, L. W., Joseph, N., Nahorski, M. S., Sanford, T. J., et al. (2017). Neurodevelopmental protein Musashi-1 interacts with the Zika genome and promotes viral replication. *Science* 357, 83–88. doi: 10.1126/science.aam9243

Chen, T.-C., and Huang, J.-R. (2020). Musashi-1: an example of how polyalanine tracts contribute to self-association in the intrinsically disordered regions of RNA-binding proteins. *Int. J. Mol. Sci.* 21:2289. doi: 10.3390/ijms21072289

Chen, Z., Gore, B. B., Long, H., Ma, L., and Tessier-Lavigne, M. (2008). Alternative splicing of the Robo3 axon guidance receptor governs the midline switch from attraction to repulsion. *Neuron* 58, 325–332. doi: 10.1016/j.neuron.2008.02.016

Cheng, W., Wang, S., Zhang, Z., Morgens, D. W., Hayes, L. R., Lee, S., et al. (2019). CRISPR-Cas9 screens identify the RNA helicase DDX3X as a repressor of C9ORF72 (GGGGCC)n repeat-associated non-AUG translation. *Neuron* 104, 885.e8–898.e8. doi: 10.1016/j.neuron.2019.09.003

Cheung, Z. H., Chin, W. H., Chen, Y., Ng, Y. P., and Ip, N. Y. (2007). Cdk5 is involved in BDNF-stimulated dendritic growth in hippocampal neurons. *PLoS Biol.* 5:e63. doi: 10.1371/journal.pbio.0050063

Christie, S. B., Akins, M. R., Schwob, J. E., and Fallon, J. R. (2009). The FXG: a presynaptic fragile X granule expressed in a subset of developing brain circuits. *J. Neurosci.* 29, 1514–1524. doi: 10.1523/JNEUROSCI.3937-08.2009

Ciolli, C., Rom, A., Franke, V., Imami, K., Arrey, G., Terne, M., et al. (2018). Alternative 3′ UTRs direct localization of functionally diverse protein isoforms in neuronal compartments. *Nucleic Acids Res.* 47, 2560–2573. doi: 10.1093/nar/gky1270

Cioni, J.-M., Koppers, M., and Holt, C. E. (2018a). Molecular control of local translation in axon development and maintenance. *Curr. Opin. Neurobiol.* 51, 86–94. doi: 10.1016/j.conb.2018.02.025

Cioni, J.-M., Lin, J. Q., Holtermann, A. V., Koppers, M., Jakobs, M. A. H., Azizi, A., et al. (2019). Late endosomes act as mRNA translation platforms and sustain mitochondria in axons. *Cell* 176, 56.e15–72.e15. doi: 10.1016/j.cell.2018.11.030

Cioni, J.-M., Wong, H. H.-W., Bressan, D., Kodama, L., Harris, W. A., and Holt, C. E. (2018b). Axon-axon interactions regulate topographic optic tract sorting *via* CYFIP2-dependent WAVE complex function. *Neuron* 97:1078.e6–1093.e6. doi: 10.1016/j.neuron.2018.01.027

Clement, J. P., Aceti, M., Creson, T. K., Ozkan, E. D., Shi, Y., Reish, N. J., et al. (2012). Pathogenic SYNGAP1 mutations impair cognitive development by disrupting maturation of dendritic spine synapses. *Cell* 151, 709–723. doi: 10.1016/j.cell.2012.08.045

Colak, D., Ji, S.-J., Porse, B. T., and Jaffrey, S. R. (2013). Regulation of axon guidance by compartmentalized nonsense-mediated mRNA decay. *Cell* 153, 1252–1265. doi: 10.1016/j.cell.2013.04.056

Courchet, J., Lewis, T. L. Jr., Lee, S., Courchet, V., Liou, D.-Y., et al. (2013). Terminal axon branching is regulated by the LKB1-NUAK1 kinase pathway *via* presynaptic mitochondrial capture. *Cell* 153, 1510–1525. doi: 10.1016/j.cell.2013.05.021

Cragle, C. E., and MacNicol, A. M. (2014). Musashi protein-directed translational activation of target mRNAs is mediated by the poly(A) polymerase, germ line development defective-2. *J. Biol. Chem.* 289, 14239–14251. doi: 10.1074/jbc.M114.548271

Crow, Y. J., and Livingston, J. H. (2008). Aicardi-Goutiéres syndrome: an important Mendelian mimic of congenital infection. *Dev. Med. Child Neurol.* 50, 410–416. doi: 10.1111/j.1469-8749.2008.02062.x

Cummings, C. J., Reinstein, E., Sun, Y., Antalffy, B., Jiang, Y., Ciechanover, A., et al. (1999). Mutation of the E6-AP ubiquitin ligase reduces nuclear inclusion frequency while accelerating polyglutamine-induced pathology in SCA1 mice. *Neuron* 24, 879–892. doi: 10.1016/S0896-6273(00)81035-1

Dalpé, G., Zhang, L. W., Zheng, H., and Culotti, J. G. (2004). Conversion of cell movement responses to Semaphorin-1 and Plexin-1 from attraction to repulsion by lowered levels of specific RAC GTPases in *C. elegans*. *Development* 131, 2073–2088. doi: 10.1242/dev.01063

Daniel, C., Venø, M. T., Ekdahl, Y., Kjems, J., and Öhman, M. (2012). A distant cis acting intronic element induces site-selective RNA editing. *Nucleic Acids Res*. 40, 9876–9886. doi: 10.1093/nar/gks691

Daniel, C., Wahlstedt, H., Ohlson, J., Björk, P., and Öhman, M. (2011). Adenosine-to-inosine RNA editing affects trafficking of the gamma-aminobutyric acid type A (GABA(A)) receptor. *J. Biol. Chem*. 286, 2031–2040. doi: 10.1074/jbc.M110.130096

Darnell, J. C., Van Driesche, S. J., Zhang, C., Hung, K. Y. S., Mele, A., Fraser, C. E., et al. (2011). FMRP stalls ribosomal translocation on mRNAs linked to synaptic function and autism. *Cell* 146, 247–261. doi: 10.1016/j.cell.2011.06.013

das Chagas, P. F., Baroni, M., Brassesco, M. S., and Tone, L. G. (2020). Interplay between the RNA binding-protein Musashi and developmental signaling pathways. *J. Gene Med*. 22:e3136. doi: 10.1002/jgm.3136

Davis, J. K., and Broadie, K. (2017). Multifarious functions of the fragile X mental retardation protein. *Trends Genet*. 33, 703–714. doi: 10.1016/j.tig.2017.07.008

Denny, J. B. (2006). Molecular mechanisms, biological actions, and neuropharmacology of the growth-associated protein GAP-43. *Curr. Neuropharmacol*. 4, 293–304. doi: 10.2174/157015906778520782

DePew, A. T., Aimino, M. A., and Mosca, T. J. (2019). The tenets of teneurin: conserved mechanisms regulate diverse developmental processes in the Drosophila nervous system. *Front. Neurosci*. 13:2185. doi: 10.3389/fnins.2019.00027

Desterro, J. M. P., Keegan, L. P., Lafarga, M., Berciano, M. T., O'Connell, M., and Carmo-Fonseca, M. (2003). Dynamic association of RNA-editing enzymes with the nucleolus. *J. Cell Sci*. 116, 1805–1818. doi: 10.1242/jcs.00371

Dictenberg, J. B., Swanger, S. A., Antar, L. N., Singer, R. H., and Bassell, G. J. (2008). A direct role for FMRP in activity-dependent dendritic mRNA transport links filopodial-spine morphogenesis to fragile X syndrome. *Dev. Cell* 14, 926–939. doi: 10.1016/j.devcel.2008.04.003

Dominissini, D., Moshitch-Moshkovitz, S., Schwartz, S., Salmon-Divon, M., Ungar, L., Osenberg, S., et al. (2012). Topology of the human and mouse m6A RNA methylomes revealed by m6A-seq. *Nature* 485, 201–206. doi: 10.1038/nature11112

Donnelly, C. J., Park, M., Spillane, M., Yoo, S., Pacheco, A., Gomes, C., et al. (2013). Axonally synthesized β-actin and GAP-43 proteins support distinct modes of axonal growth. *J. Neurosci*. 33, 3311–3322. doi: 10.1523/JNEUROSCI.1722-12.2013

Dontchev, V. D., and Letourneau, P. C. (2002). Nerve growth factor and semaphorin 3A signaling pathways interact in regulating sensory neuronal growth cone motility. *J. Neurosci*. 22, 6659–6669. doi: 10.1523/JNEUROSCI.22-15-06659.2002

Egebjerg, J., and Heinemann, S. F. (1993). Ca2+ permeability of unedited and edited versions of the kainate selective glutamate receptor GluR6. *Proc. Natl. Acad. Sci. U.S.A*. 90, 755–759. doi: 10.1073/pnas.90.2.755

El Khouri, E., Ghoumid, J., Haye, D., Giuliano, F., Drevillon, L., Briand-Suleau, A., et al. (2021). Wnt/β-catenin pathway and cell adhesion deregulation in CSDE1-related intellectual disability and autism spectrum disorders. *Mol. Psychiatry* 26, 3572–3585. doi: 10.1038/s41380-021-01072-7

Eran, A., Li, J. B., Vatalaro, K., McCarthy, J., Rahimov, F., Collins, C., et al. (2013). Comparative RNA editing in autistic and neurotypical cerebella. *Mol. Psychiatry* 18, 1041–1048. doi: 10.1038/mp.2012.118

Ergin, V., and Zheng, S. (2020). Putative coiled-coil domain-dependent autoinhibition and alternative splicing determine SHTN1's actin-binding activity. *J. Mol. Biol*. 432, 4154–4166. doi: 10.1016/j.jmb.2020.04.025

Fallini, C., Zhang, H., Su, Y., Silani, V., Singer, R. H., Rossoll, W., et al. (2011). The survival of motor neuron (SMN) protein interacts with the mRNA-binding protein HuD and regulates localization of poly(A) mRNA in primary motor neuron axons. *J. Neurosci*. 31, 3914–3925. doi: 10.1523/JNEUROSCI.3631-10.2011

Farini, D., Cesari, E., Weatheritt, R. J., La Sala, G., Naro, C., Pagliarini, V., et al. (2020). A dynamic splicing program ensures proper synaptic connections in the developing cerebellum. *Cell Rep*. 31:107703. doi: 10.1016/j.celrep.2020.107703

Ffrench-Constant, R. H., and Rocheleau, T. A. (1993). Drosophila gamma-aminobutyric acid receptor gene Rdl shows extensive alternative splicing. *J. Neurochem*. 60, 2323–2326. doi: 10.1111/j.1471-4159.1993.tb03523.x

Filippini, A., Bonini, D., Lacoux, C., Pacini, L., Zingariello, M., Sancillo, L., et al. (2017). Absence of the fragile X mental retardation protein results in defects of RNA editing of neuronal mRNAs in mouse. *RNA Biol*. 14, 1580–1591. doi: 10.1080/15476286.2017.1338232

Fox, J. W., Lamperti, E. D., Ekşioğlu, Y. Z., Hong, S. E., Feng, Y., Graham, D. A., et al. (1998). Mutations in filamin 1 prevent migration of cerebral cortical neurons in human periventricular heterotopia. *Neuron* 21, 1315–1325. doi: 10.1016/S0896-6273(00)80651-0

Fox, R. G., Park, F. D., Koechlein, C. S., Kritzik, M., and Reya, T. (2015). Musashi signaling in stem cells and cancer. *Annu. Rev. Cell Dev. Biol*. 31, 249–267. doi: 10.1146/annurev-cellbio-100814-125446

Friocourt, F., and Chédotal, A. (2017). The Robo3 receptor, a key player in the development, evolution, and function of commissural systems. *Dev. Neurobiol*. 77, 876–890. doi: 10.1002/dneu.22478

Fritzsche, R., Karra, D., Bennett, K. L., Ang, F. Y., Heraud-Farlow, J. E., Tolino, M., et al. (2013). Interactome of two diverse RNA granules links mRNA localization to translational repression in neurons. *Cell Rep*. 5, 1749–1762. doi: 10.1016/j.celrep.2013.11.023

Frye, M., Harada, B. T., Behm, M., and He, C. (2018). RNA modifications modulate gene expression during development. *Science* 361, 1346–1349. doi: 10.1126/science.aau1646

Furlanis, E., Traunmüller, L., Fucile, G., and Scheiffele, P. (2019). Landscape of ribosome-engaged transcript isoforms reveals extensive neuronal-cell-class-specific alternative splicing programs. *Nat. Neurosci*. 22, 1709–1717. doi: 10.1038/s41593-019-0465-5

Gallo, G. (2006). RhoA-kinase coordinates F-actin organization and myosin II activity during semaphorin-3A-induced axon retraction. *J. Cell Sci*. 119, 3413–3423. doi: 10.1242/jcs.03084

Gao, J., Wang, L., Yan, T., Perry, G., and Wang, X. (2019). TDP-43 proteinopathy and mitochondrial abnormalities in neurodegeneration. *Mol. Cell. Neurosci*. 100:103396. doi: 10.1016/j.mcn.2019.103396

Gennarino, V. A., Palmer, E. E., McDonell, L. M., Wang, L., Adamski, C. J., Koire, A., et al. (2018). A mild PUM1 mutation is associated with adult-onset ataxia, whereas haploinsufficiency causes developmental delay and seizures. *Cell* 172, 924.e11–936.e11. doi: 10.1016/j.cell.2018.02.006

Gennarino, V. A., Singh, R. K., White, J. J., De Maio, A., Han, K., Kim, J.-Y., et al. (2015). Pumilio1 haploinsufficiency leads to SCA1-like neurodegeneration by increasing wild-type Ataxin1 levels. *Cell* 160, 1087–1098. doi: 10.1016/j.cell.2015.02.012

Glock, C., Heumüller, M., and Schuman, E. M. (2017). mRNA transport & local translation in neurons. *Curr. Opin. Neurobiol*. 45, 169–177. doi: 10.1016/j.conb.2017.05.005

Gomez, A. M., Traunmüller, L., and Scheiffele, P. (2021). Neurexins: molecular codes for shaping neuronal synapses. *Nat. Rev. Neurosci*. 22, 137–151. doi: 10.1038/s41583-020-00415-7

Gonatopoulos-Pournatzis, T., Niibori, R., Salter, E. W., Weatheritt, R. J., Tsang, B., Farhangmehr, S., et al. (2020). Autism-misregulated eIF4G microexons control synaptic translation and higher order cognitive functions. *Mol. Cell* 77:1176.e16–1192.e16. doi: 10.1016/j.molcel.2020.01.006

Gonatopoulos-Pournatzis, T., Wu, M., Braunschweig, U., Roth, J., Han, H., Best, A. J., et al. (2018). Genome-wide CRISPR-Cas9 interrogation of splicing networks reveals a mechanism for recognition of autism-misregulated neuronal microexons. *Mol. Cell* 72, 510.e12–524.e12. doi: 10.1016/j.molcel.2018.10.008

Grassi, E., Santoro, R., Umbach, A., Grosso, A., Oliviero, S., Neri, F., et al. (2018). Choice of alternative polyadenylation sites, mediated by the RNA-binding protein Elavl3, plays a role in differentiation of inhibitory neuronal progenitors. *Front. Cell. Neurosci*. 12:518. doi: 10.3389/fncel.2018.00518

Gumy, L. F., Yeo, G. S. H., Tung, Y. C. L., Zivraj, K. H., Willis, D., Coppola, G., et al. (2011). Transcriptome analysis of embryonic and adult sensory axons reveals changes in mRNA repertoire localization. *RNA* 17, 85–98. doi: 10.1261/rna.2386111

Guo, H., Li, Y., Shen, L., Wang, T., Jia, X., Liu, L., et al. (2019). Disruptive variants of CSDE1 associate with autism and interfere with neuronal development and synaptic transmission. *Sci. Adv*. 5:eaax2166. doi: 10.1126/sciadv.aax2166

Guvenek, A., and Tian, B. (2018). Analysis of alternative cleavage and polyadenylation in mature and differentiating neurons using RNA-seq data. *Quant. Biol*. 6, 253–266. doi: 10.1007/s40484-018-0148-3

Hadziselimovic, N., Vukojevic, V., Peter, F., Milnik, A., Fastenrath, M., Fenyves, B. G., et al. (2014). Forgetting is regulated *via* musashi-mediated translational control of the Arp2/3 complex. *Cell* 156, 1153–1166. doi: 10.1016/j.cell.2014.01.054

Hagerman, R. J., Protic, D., Rajaratnam, A., Salcedo-Arellano, M. J., Aydin, E. Y., and Schneider, A. (2018). Fragile X-associated neuropsychiatric disorders (FXAND). *Front. Psychiatry* 9:564. doi: 10.3389/fpsyt.2018.00564

Hartner, J. C., Walkley, C. R., Lu, J., and Orkin, S. H. (2009). ADAR1 is essential for the maintenance of hematopoiesis and suppression of interferon signaling. *Nat. Immunol*. 10, 109–115. doi: 10.1038/ni.1680

Hassan, B. A., and Hiesinger, P. R. (2015). Beyond molecular codes: simple rules to wire complex brains. *Cell* 163, 285–291. doi: 10.1016/j.cell.2015.09.031

Hattori, D., Millard, S. S., Wojtowicz, W. M., and Zipursky, S. L. (2008). Dscam-mediated cell recognition regulates neural circuit formation. *Annu. Rev. Cell Dev. Biol*. 24, 597–620. doi: 10.1146/annurev.cellbio.24.110707.175250

Heinen, K., Baker, R. E., Spijker, S., Rosahl, T., van Pelt, J., and Brussaard, A. B. (2003). Impaired dendritic spine maturation in GABAA receptor $\alpha 1$ subunit knock out mice. *Neuroscience* 122, 699–705. doi: 10.1016/S0306-4522(03)00477-9

Hideyama, T., Yamashita, T., Aizawa, H., Tsuji, S., Kakita, A., Takahashi, H., et al. (2012). Profound downregulation of the RNA editing enzyme ADAR2 in ALS spinal motor neurons. *Neurobiol. Dis*. 45, 1121–1128. doi: 10.1016/j.nbd.2011.12.033

Hilgers, V., Lemke, S. B., and Levine, M. (2012). ELAV mediates 3′ UTR extension in the Drosophila nervous system. *Genes Dev*. 26, 2259–2264. doi: 10.1101/gad.199653.112

Hilgers, V., Perry, M. W., Hendrix, D., Stark, A., Levine, M., and Haley, B. (2011). Neural-specific elongation of 3′ UTRs during Drosophila development. *Proc. Natl. Acad. Sci. U.S.A*. 108, 15864–15869. doi: 10.1073/pnas.1112672108

Hinnebusch, A. G. (2014). The scanning mechanism of eukaryotic translation initiation. *Annu. Rev. Biochem*. 83, 779–812. doi: 10.1146/annurev-biochem-060713-035802

Holt, C. E., Martin, K. C., and Schuman, E. M. (2019). Local translation in neurons: visualization and function. *Nat. Struct. Mol. Biol*. 26, 557–566. doi: 10.1038/s41594-019-0263-5

Holt, C. E., and Schuman, E. M. (2013). The central dogma decentralized: new perspectives on RNA function and local translation in neurons. *Neuron* 80, 648–657. doi: 10.1016/j.neuron.2013.10.036

Hondele, M., Sachdev, R., Heinrich, S., Wang, J., Vallotton, P., Fontoura, B. M. A., et al. (2019). DEAD-box ATPases are global regulators of phase-separated organelles. *Nature* 573, 144–148. doi: 10.1038/s41586-019-1502-y

Hoopengardner, B., Bhalla, T., Staber, C., and Reenan, R. (2003). Nervous system targets of RNA editing identified by comparative genomics. *Science* 301, 832–836. doi: 10.1126/science.1086763

Hosokawa, T., Liu, P.-W., Cai, Q., Ferreira, J. S., Levet, F., Butler, C., et al. (2021). CaMKII activation persistently segregates postsynaptic proteins *via* liquid phase separation. *Nat. Neurosci*. 24, 777–785. doi: 10.1038/s41593-021-00843-3

Hu, W., Li, S., Park, J. Y., Boppana, S., and Ni, T. (2016). Dynamic landscape of alternative polyadenylation during retinal development. *Cell. Mol. Life Sci*. 74, 1721–1739. doi: 10.1007/s00018-016-2429-1

Hwang, T., Park, C.-K., Leung, A. K. L., Gao, Y., Hyde, T. M., Kleinman, J. E., et al. (2016). Dynamic regulation of RNA editing in human brain development and disease. *Nat. Neurosci*. 19, 1093–1099. doi: 10.1038/nn.4337

Iijima, T., Wu, K., Witte, H., Hanno-Iijima, Y., Glatter, T., Richard, S., et al. (2011). SAM68 regulates neuronal activity-dependent alternative splicing of neurexin-1. *Cell* 147, 1601–1614. doi: 10.1016/j.cell.2011.11.028

Imai, T., Tokunaga, A., Yoshida, T., Hashimoto, M., Mikoshiba, K., Weinmaster, G., et al. (2001). The neural RNA-binding protein Musashi1 translationally regulates mammalian numb gene expression by interacting with its mRNA. *Mol. Cell. Biol*. 21, 3888–3900. doi: 10.1128/MCB.21.12.3888-3900.2001

Irimia, M., Denuc, A., Ferran, J. L., Pernaute, B., Puelles, L., Roy, S. W., et al. (2012). Evolutionarily conserved A-to-I editing increases protein stability of the alternative splicing factor Nova1. *RNA Biol*. 9, 12–21. doi: 10.4161/rna.9.1.18387

Irimia, M., Weatheritt, R. J., Ellis, J. D., Parikshak, N. N., Gonatopoulos-Pournatzis, T., Babor, M., et al. (2014). A highly conserved program of neuronal microexons is misregulated in autistic brains. *Cell* 159, 1511–1523. doi: 10.1016/j.cell.2014.11.035

Iwaoka, R., Nagata, T., Tsuda, K., Imai, T., Okano, H., Kobayashi, N., et al. (2017). Structural insight into the recognition of r(UAG) by Musashi-1 RBD2, and construction of a model of Musashi-1 RBD1-2 bound to the minimum target RNA. *Molecules* 22, 1207–1216. doi: 10.3390/molecules22071207

Jacko, M., Weyn-Vanhentenryck, S. M., Smerdon, J. W., Yan, R., Feng, H., Williams, D. J., et al. (2018). Rbfox splicing factors promote neuronal maturation and axon initial segment assembly. *Neuron* 97, 853.e6–868.e6. doi: 10.1016/j.neuron.2018.01.020

Jeong, S., Yang, D.-,s., Hong, Y. G., Mitchell, S. P., Brown, M. P., and Kolodkin, A. L. (2017). Varicose and cheerio collaborate with pebble to mediate semaphorin-1a reverse signaling in Drosophila. *Proc. Natl. Acad. Sci. U.S.A*. 114, E8254–E8263. doi: 10.1073/pnas.1713010114

Johnson, V., Junge, H. J., and Chen, Z. (2019). Temporal regulation of axonal repulsion by alternative splicing of a conserved microexon in mammalian Robo1 and Robo2. *eLife* 8:994. doi: 10.7554/eLife.46042

Jones, A. K., Buckingham, S. D., Papadaki, M., Yokota, M., Sattelle, B. M., Matsuda, K., et al. (2009). Splice-variant- and stage-specific RNA editing of the Drosophila GABA receptor modulates agonist potency. *J. Neurosci*. 29, 4287–4292. doi: 10.1523/JNEUROSCI.5251-08.2009

Ju Lee, H., Bartsch, D., Xiao, C., Guerrero, S., Ahuja, G., Schindler, C., et al. (2017). A post-transcriptional program coordinated by CSDE1 prevents intrinsic neural differentiation of human embryonic stem cells. *Nat. Commun*. 8, 1456–1419. doi: 10.1038/s41467-017-01744-5

Jung, H., Gkogkas, C. G., Sonenberg, N., and Holt, C. E. (2014). Remote control of gene function by local translation. *Cell* 157, 26–40. doi: 10.1016/j.cell.2014.03.005

Kalous, A., Stake, J. I., Yisraeli, J. K., and Holt, C. E. (2014). RNA-binding protein Vg1RBP regulates terminal arbor formation but not long-range axon navigation in the developing visual system. *Dev. Neurobiol*. 74, 303–318. doi: 10.1002/dneu.22110

Kanai, Y., Dohmae, N., and Hirokawa, N. (2004). Kinesin transports RNA: isolation and characterization of an RNA-transporting granule. *Neuron* 43, 513–525. doi: 10.1016/j.neuron.2004.07.022

Kaneko, Y., Sakakibara, S., Imai, T., Suzuki, A., Nakamura, Y., Sawamoto, K., et al. (2000). Musashi1: an evolutionally conserved marker for CNS progenitor cells including neural stem cells. *Dev. Neurosci*. 22, 139–153. doi: 10.1159/000017435

Kawahara, H., Imai, T., Imataka, H., Tsujimoto, M., Matsumoto, K., and Okano, H. (2008). Neural RNA-binding protein Musashi1 inhibits translation initiation by competing with eIF4G for PABP. *J. Cell Biol*. 181, 639–653. doi: 10.1083/jcb.200708004

Khermesh, K., D'Erchia, A. M., Barak, M., Annese, A., Wachtel, C., Levanon, E. Y., et al. (2016). Reduced levels of protein recoding by A-to-I RNA editing in Alzheimer's disease. *RNA* 22, 290–302. doi: 10.1261/rna.054627.115

Kidd, T., Bland, K. S., and Goodman, C. S. (1999). Slit is the midline repellent for the robo receptor in Drosophila. *Cell* 96, 785–794. doi: 10.1016/S0092-8674(00)80589-9

Kiebler, M. A., and Bassell, G. J. (2006). Neuronal RNA granules: movers and makers. *Neuron* 51, 685–690. doi: 10.1016/j.neuron.2006.08.021

Kindhauser, M. K., Allen, T., Frank, V., Santhana, R. S., and Dye, C. (2016). Zika: the origin and spread of a mosquito-borne virus. *Bull. World Health Organ*. 94, 675–686C. doi: 10.2471/BLT.16.171082

Knobel, K. M., Davis, W. S., Jorgensen, E. M., and Bastiani, M. J. (2001). UNC-119 suppresses axon branching in *C. elegans*. *Development* 128, 4079–4092. doi: 10.1242/dev.128.20.4079

Krause, M., Erik, W., Dent, James, E., Bear, L., J., and Gertler, F. (2003). Ena/VASP proteins: regulators of the actin cytoskeleton and cell migration. *Annu. Rev*. 19, 541–564. doi: 10.1146/annurev.cellbio.19.050103.103356

Kuwako, K.-,i., Kakumoto, K., Imai, T., Igarashi, M., Hamakubo, T., Sakakibara, S.-I., et al. (2010). Neural RNA-binding protein musashi1 controls midline crossing of precerebellar neurons through posttranscriptional regulation of Robo3/Rig-1 expression. *Neuron* 67, 407–421. doi: 10.1016/j.neuron.2010.07.005

LaBella, M. L., Hujber, E. J., Moore, K. A., Rawson, R. L., Merrill, S. A., Allaire, P. D., et al. (2020). Casein kinase 1δ stabilizes mature axons by inhibiting transcription termination of ankyrin. *Dev Cell* 52, 88.e18–103.e18. doi: 10.1016/j.devcel.2019.12.005

Landínez-Macías, M., Qi, W., Bratus-Neuenschwander, A., Müller, M., and Urwyler, O. (2021). The RNA-binding protein Musashi controls axon compartment-specific synaptic connectivity through ptp69D mRNA poly(A)-tailing. *Cell Rep*. 36:109713. doi: 10.1016/j.celrep.2021.109713

Laux, T., Fukami, K., Thelen, M., Golub, T., Frey, D., and Caroni, P. (2000). Gap43, Marcks, and Cap23 Modulate Pi(4,5)p2 at plasmalemmal rafts, and regulate cell cortex actin dynamics through a common mechanism. *J. Cell Biol*. 149, 1455–1472. doi: 10.1083/jcb.149.7.1455

Lazo, O. M., Gonzalez, A., Ascano, M., Kuruvilla, R., Couve, A., and Bronfman, F. C. (2013). BDNF regulates Rab11-mediated recycling endosome dynamics to induce dendritic branching. *J. Neurosci*. 33, 6112–6122. doi: 10.1523/JNEUROSCI.4630-12.2013

Lee, F. H. F., Su, P., Xie, Y.-F., Wang, K. E., Wan, Q., and Liu, F. (2016). Disrupting GluA2-GAPDH interaction affects axon and dendrite development. *Sci. Rep*. 6, 1–15. doi: 10.1038/srep30458

Leggere, J. C., Saito, Y., Darnell, R. B., Tessier-Lavigne, M., Junge, H. J., and Chen, Z. (2016). NOVA regulates Dcc alternative splicing during neuronal migration and axon guidance in the spinal cord. *eLife* 5:2567. doi: 10.7554/eLife.14264

Lennox, A. L., Hoye, M. L., Jiang, R., Johnson-Kerner, B. L., Suit, L. A., Venkataramanan, S., et al. (2020). Pathogenic DDX3X mutations impair RNA metabolism and neurogenesis during fetal cortical development. *Neuron* 106, 404.e8–420.e8. doi: 10.1016/j.neuron.2020.01.042

LePort, A. K. R., Mattfeld, A. T., Dickinson-Anson, H., Fallon, J. H., Stark, C. E. L., Kruggel, F., et al. (2012). Behavioral and neuroanatomical investigation of Highly Superior Autobiographical Memory (HSAM). *Neurobiol. Learn. Memory* 98, 78–92. doi: 10.1016/j.nlm.2012.05.002

Lerner, T., Papavasiliou, F. N., and Pecori, R. (2018). RNA editors, cofactors, and mRNA targets: an overview of the C-to-U RNA editing machinery and its implication in human disease. *Genes* 10:13. doi: 10.3390/genes10010013

Leung, K. M., van Horck, F. P., Lin, A. C., Allison, R., Standart, N., and Holt, C. E. (2006). Asymmetrical β-actin mRNA translation in growth cones mediates attractive turning to netrin-1. *Nat. Neurosci*. 9, 1247–1256. doi: 10.1038/nn1775

Lianoglou, S., Garg, V., Yang, J. L., Leslie, C. S., and Mayr, C. (2013). Ubiquitously transcribed genes use alternative polyadenylation to achieve tissue-specific expression. *Genes Dev*. 27, 2380–2396. doi: 10.1101/gad.229328.113

Liao, Y.-C., Fernandopulle, M. S., Wang, G., Choi, H., Hao, L., Drerup, C. M., et al. (2019). RNA granules hitchhike on lysosomes for long-distance transport, using annexin A11 as a molecular tether. *Cell* 179, 147.e20–164.e20. doi: 10.1016/j.cell.2019.08.050

Lin, A. C., and Holt, C. E. (2008). Function and regulation of local axonal translation. *Curr. Opin. Neurobiol*. 18, 60–68. doi: 10.1016/j.conb.2008.05.004

Lin, J.-C., Tsai, J.-T., Chao, T.-Y., Ma, H.-I., and Liu, W.-H. (2019). Musashi-1 enhances glioblastoma migration by promoting ICAM1 translation. *Neoplasia* 21, 459–468. doi: 10.1016/j.neo.2019.02.006

Ling, J. P., Wilks, C., Charles, R., Leavey, P. J., Ghosh, D., Jiang, L., et al. (2020). ASCOT identifies key regulators of neuronal subtype-specific splicing. *Nat. Commun*. 11, 1–12. doi: 10.1038/s41467-019-14020-5

Lomeli, H., Mosbacher, J., Melcher, T., Höger, T., Geiger, J. R., Kuner, T., et al. (1994). Control of kinetic properties of AMPA receptor channels by nuclear RNA editing. *Science* 266, 1709–1713. doi: 10.1126/science.7992055

Lundin, E., Wu, C., Widmark, A., Behm, M., Hjerling-Leffler, J., Daniel, C., et al. (2020). Spatiotemporal mapping of RNA editing in the developing mouse brain using *in situ* sequencing reveals regional and cell-type-specific regulation. *BMC Biol*.18:6. doi: 10.1186/s12915-019-0736-3

Maldonado, C., Alicea, D., Gonzalez, M., Bykhovskaia, M., and Marie, B. (2013). Adar is essential for optimal presynaptic function. *Mol. Cell. Neurosci*. 52, 173–180. doi: 10.1016/j.mcn.2012.10.009

Martinez, J. C., Randolph, L. K., Iascone, D. M., Pernice, H. F., Polleux, F., and Hengst, U. (2019). Pum2 shapes the transcriptome in developing axons through retention of target mRNAs in the cell body. *Neuron* 104, 931.e5–946.e5. doi: 10.1016/j.neuron.2019.08.035

Mattioli, F., Hayot, G., Drouot, N., Isidor, B., Courraud, J., Hinckelmann, M.-V., et al. (2020). *De novo* frameshift variants in the neuronal splicing factor NOVA2 result in a common c-terminal extension and cause a severe form of neurodevelopmental disorder. *Am. J. Hum. Genet*. 106, 438–452. doi: 10.1016/j.ajhg.2020.02.013

Mauger, O., Lemoine, F., and Scheiffele, P. (2016). Targeted intron retention and excision for rapid gene regulation in response to neuronal activity. *Neuron* 92, 1266–1278. doi: 10.1016/j.neuron.2016.11.032

McDonald, N. A., Fetter, R. D., and Shen, K. (2020). Assembly of synaptic active zones requires phase separation of scaffold molecules. *Nature* 588, 454–458. doi: 10.1038/s41586-020-2942-0

McMahon, A. C., Barnett, M. W., O'Leary, T. S., Stoney, P. N., Collins, M. O., Papadia, S., et al. (2012). SynGAP isoforms exert opposing effects on synaptic strength. *Nat. Commun*. 3, 900–909. doi: 10.1038/ncomms1900

Meyer, K. D., Saletore, Y., Zumbo, P., Elemento, O., Mason, C. E., and Jaffrey, S. R. (2012). Comprehensive analysis of mRNA methylation reveals enrichment in 3′ UTRs and near stop codons. *Cell* 149, 1635–1646. doi: 10.1016/j.cell.2012.05.003

Milovanovic, D., Wu, Y., Bian, X., and De Camilli, P. (2018). A liquid phase of synapsin and lipid vesicles. *Science* 361, 604–607. doi: 10.1126/science.aat5671

Mitchell, S. F., and Parker, R. (2014). Principles and properties of eukaryotic mRNPs. *Mol. Cell* 54, 547–558. doi: 10.1016/j.molcel.2014.04.033

Miura, P., Shenker, S., Andreu-Agullo, C., Westholm, J. O., and Lai, E. C. (2013). Widespread and extensive lengthening of 3′ UTRs in the mammalian brain. *Genome Res*. 23, 812–825. doi: 10.1101/gr.146886.112

Montalbano, M., McAllen, S., Puangmalai, N., Sengupta, U., Bhatt, N., Johnson, O. D., et al. (2020). RNA-binding proteins Musashi and tau soluble aggregates initiate nuclear dysfunction. *Nat. Commun*. 11, 4305–4316. doi: 10.1038/s41467-020-18022-6

Morel, L., Regan, M., Higashimori, H., Ng, S. K., Esau, C., Vidensky, S., et al. (2013). Neuronal exosomal miRNA-dependent translational regulation of astroglial glutamate transporter GLT1. *J. Biol. Chem*. 288, 7105–7116. doi: 10.1074/jbc.M112.410944

Murphy, D., Cieply, B., Carstens, R., Ramamurthy, V., and Stoilov, P. (2016). The Musashi 1 controls the splicing of photoreceptor-specific exons in the vertebrate retina. *PLoS Genet*. 12:e1006256. doi: 10.1371/journal.pgen.1006256

Nagata, T., Kanno, R., Kurihara, Y., Uesugi, S., Imai, T., Sakakibara, S., et al. (1999). Structure, backbone dynamics and interactions with RNA of the C-terminal RNA-binding domain of a mouse neural RNA-binding protein, Musashi1. *J. Mol. Biol*. 287, 315–330. doi: 10.1006/jmbi.1999.2596

Nakamura, M., Okano, H., Blendy, J. A., and Montell, C. (1994). Musashi, a neural RNA-binding protein required for drosophila adult external sensory organ development. *Neuron* 13, 67–81. doi: 10.1016/0896-6273(94)90460-X

Nimmich, M. L., Heidelberg, L. S., and Fisher, J. L. (2009). RNA editing of the GABA(A) receptor alpha3 subunit alters the functional properties of recombinant receptors. *Neurosci. Res*. 63, 288–293. doi: 10.1016/j.neures.2009.01.003

Nishikura, K. (2016). A-to-I editing of coding and non-coding RNAs by ADARs. *Nat. Struct. Mol. Biol*. 17, 83–96. doi: 10.1038/nrm.2015.4

Oh, W. C., Lutzu, S., Castillo, P. E., and Kwon, H.-B. (2016). De novo synaptogenesis induced by GABA in the developing mouse cortex. *Science* 353, 1037–1040. doi: 10.1126/science.aaf5206

Ohlson, J., Pedersen, J. S., Haussler, D., and Öhman, M. (2007). Editing modifies the GABA(A) receptor subunit alpha3. *RNA* 13, 698–703. doi: 10.1261/rna.349107

Ohyama, T., Furukawa, A., Mashima, T., Sugiyama, T., Ohgara, S., Yamazaki, T., et al. (2008). Structural analysis of Musashi-RNA complex on the basis of long-range structural information. *Nucleic Acids Symp. Ser*. 52, 193–194. doi: 10.1093/nass/nrn098

Ohyama, T., Nagata, T., Tsuda, K., Kobayashi, N., Imai, T., Okano, H., et al. (2012). Structure of Musashi1 in a complex with target RNA: the role of aromatic stacking interactions. *Nucleic Acids Res*. 40, 3218–3231. doi: 10.1093/nar/gkr1139

Oktaba, K., Zhang, W., Lotz, T. S., Jun, D. J., Lemke, S. B., Ng, S. P., et al. (2015). ELAV links paused Pol II to alternative polyadenylation in the drosophila nervous system. *Mol. Cell* 57, 341–348. doi: 10.1016/j.molcel.2014.11.024

Oliva, C., Molina-Fernandez, C., Maureira, M., Candia, N., López, E., Hassan, B., et al. (2015). Hindsight regulates photoreceptor axon targeting through transcriptional control of jitterbug/Filamin and multiple genes involved in axon guidance in Drosophila. *Dev. Neurobiol*. 75, 1018–1032. doi: 10.1002/dneu.22271

Ortiz, R., Georgieva, M. V., Gutiérrez, S., Pedraza, N., Fernández-Moya, S. M., and Gallego, C. (2017). Recruitment of Staufen2 enhances dendritic localization of an intron-containing CaMKIIα mRNA. *Cell Rep*. 20, 13–20. doi: 10.1016/j.celrep.2017.06.026

Parenti, I., Rabaneda, L. G., Schoen, H., and Novarino, G. (2020). Neurodevelopmental disorders: from genetics to functional pathways. *Trends Neurosci*. 43, 608–621. doi: 10.1016/j.tins.2020.05.004

Parikshak, N. N., Swarup, V., Belgard, T. G., Irimia, M., Ramaswami, G., Gandal, M. J., et al. (2016). Genome-wide changes in lncRNA, splicing, and regional gene expression patterns in autism. *Nature* 540, 423–427. doi: 10.1038/nature20612

Park, C. Y., Zhou, J., Wong, A. K., Chen, K. M., Theesfeld, C. L., Darnell, R. B., et al. (2021). Genome-wide landscape of RNA-binding protein target site dysregulation reveals a major impact on psychiatric disorder risk. *Nat. Genet*. 53, 166–173. doi: 10.1038/s41588-020-00761-3

Parker, E. S., Cahill, L., and McGaugh, J. L. (2006). A case of unusual autobiographical remembering. *Neurocase* 12, 35–49. doi: 10.1080/13554790500473680

Parras, A., Anta, H., Santos-Galindo, M., Swarup, V., Elorza, A., Nieto-González, J. L., et al. (2018). Autism-like phenotype and risk gene mRNA deadenylation by CPEB4 mis-splicing. *Nature* 560, 441–446. doi: 10.1038/s41586-018-0423-5

Pastuzyn, E. D., Day, C. E., Kearns, R. B., Kyrke-Smith, M., Taibi, A. V., McCormick, J., et al. (2018). The neuronal gene arc encodes a repurposed retrotransposon gag protein that mediates intercellular RNA transfer. *Cell* 172, 275.e19–278.e19. doi: 10.1016/j.cell.2017.12.024

Patterson, J. B., and Samuel, C. E. (1995). Expression and regulation by interferon of a double-stranded-RNA-specific adenosine deaminase from human cells: evidence for two forms of the deaminase. *Mol. Cell. Biol*. 15, 5376–5388. doi: 10.1128/MCB.15.10.5376

Pielage, J., Cheng, L., Fetter, R. D., Carlton, P. M., Sedat, J. W., and Davis, G. W. (2008). A presynaptic giant ankyrin stabilizes the NMJ through regulation of presynaptic microtubules and transsynaptic cell adhesion. *Neuron* 58, 195–209. doi: 10.1016/j.neuron.2008.02.017

Piper, M., Anderson, R., Dwivedy, A., Weinl, C., van Horck, F., Leung, K. M., et al. (2006). Signaling mechanisms underlying Slit2-induced collapse of xenopus retinal growth cones. *Neuron* 49, 215–228. doi: 10.1016/j.neuron.2005.12.008

Portz, B., Lee, B. L., and Shorter, J. (2021). FUS and TDP-43 phases in health and disease. *Trends Biochem. Sci*. 46, 550–563. doi: 10.1016/j.tibs.2020.12.005

Prasad, A., Bharathi, V., Sivalingam, V., Girdhar, A., and Patel, B. K. (2019). Molecular mechanisms of TDP-43 misfolding and pathology in amyotrophic lateral sclerosis. *Front. Mol. Neurosci*. 12:25. doi: 10.3389/fnmol.2019.00025

Qiu, J., Takagi, Y., Harada, J., Rodrigues, N., Moskowitz, M. A., Scadden, D. T., et al. (2004). Regenerative response in ischemic brain restricted by p21cip1/waf1. *J. Exp. Med*. 199, 937–945. doi: 10.1084/jem.20031385

Quesnel-Valliéres, M., Dargaei, Z., Irimia, M., Gonatopoulos-Pournatzis, T., Ip, J. Y., Wu, M., et al. (2016). Misregulation of an activity-dependent splicing network as a common mechanism underlying autism spectrum disorders. *Mol. Cell* 64, 1023–1034. doi: 10.1016/j.molcel.2016.11.033

Quesnel-Valliéres, M., Irimia, M., Cordes, S. P., and Blencowe, B. J. (2015). Essential roles for the splicing regulator nSR100/SRRM4 during nervous system development. *Genes Dev*. 29, 746–759. doi: 10.1101/gad.256115.114

Raj, B., and Blencowe, B. J. (2015). Alternative splicing in the mammalian nervous system: recent insights into mechanisms and functional roles. *Neuron* 87, 14–27. doi: 10.1016/j.neuron.2015.05.004

Ramaswami, G., Zhang, R., Piskol, R., Keegan, L. P., Deng, P., O'Connell, M. A., et al. (2013). Identifying RNA editing sites using RNA sequencing data alone. *Nat. Methods* 10, 128–132. doi: 10.1038/nmeth.2330

Reeve, S. P., Bassetto, L., Genova, G. K., Kleyner, Y., Leyssen, M., Jackson, F. R., et al. (2005). The Drosophila fragile X mental retardation protein controls actin dynamics by directly regulating profilin in the brain. *CURBIO* 15, 1156–1163. doi: 10.1016/j.cub.2005.05.050

Rice, G. I., Kasher, P. R., Forte, G. M. A., Mannion, N. M., Greenwood, S. M., Szynkiewicz, M., et al. (2012). Mutations in ADAR1 cause Aicardi-Goutiéres syndrome associated with a type I interferon signature. *Nat. Genet*. 44, 1243–1248. doi: 10.1038/ng.2414

Roundtree, I. A., Evans, M. E., Pan, T., and He, C. (2017). Dynamic RNA modifications in gene expression regulation. *Cell* 169, 1187–1200. doi: 10.1016/j.cell.2017.05.045

Roux, P. P., and Topisirovic, I. (2018). Signaling pathways involved in the regulation of mRNA translation. *Mol. Cell. Biol*. 38:e00070-18. doi: 10.1128/MCB.00070-18

Rubin, B. P., Tucker, R. P., Martin, D., and Chiquet-Ehrismann, R. (1999). Teneurins: a novel family of neuronal cell surface proteins in vertebrates, homologous to the drosophila pair-rule gene product ten-m. *Dev. Biol*. 216, 195–209. doi: 10.1006/dbio.1999.9503

Sabatier, C., Plump, A. S., Ma, L., Brose, K., Tamada, A., Murakami, F., et al. (2004). The divergent Robo family protein rig-1/Robo3 is a negative regulator of slit responsiveness required for midline crossing by commissural axons. *Cell* 117, 157–169. doi: 10.1016/S0092-8674(04)00303-4

Saglietti, L., Dequidt, C., Kamieniarz, K., Rousset, M.-C., Valnegri, P., Thoumine, O., et al. (2007). Extracellular Interactions between GluR2 and N-Cadherin in spine regulation. *Neuron* 54, 461–477. doi: 10.1016/j.neuron.2007.04.012

Saito, Y., Miranda-Rottmann, S., Ruggiu, M., Park, C. Y., Fak, J. J., Zhong, R., et al. (2016). NOVA2-mediated RNA regulation is required for axonal pathfinding during development. *eLife* 5:487. doi: 10.7554/eLife.14371

Sakakibara, S., and Okano, H. (1997). Expression of neural RNA-binding proteins in the postnatal CNS: implications of their roles in neuronal and glial cell development. *J. Neurosci*. 17, 8300–8312. doi: 10.1523/JNEUROSCI.17-21-08300.1997

Sakakibara, S.-I., Imai, T., Hamaguchi, K., Okabe, M., Aruga, J., Nakajima, K., et al. (1996). Mouse-Musashi-1, a neural RNA-binding protein highly enriched in the mammalian CNS stem cell. *Dev. Biol*. 176, 230–242. doi: 10.1006/dbio.1996.0130

Sakakibara, S.-I., Nakamura, M., Satoh, H., and Okano, H. (2001). RNA-binding protein Musashi2: developmentally regulated expression in neural precursor cells and subpopulations of neurons in mammalian CNS. *J. Neurosci*. 21, 8091–8107. doi: 10.1523/JNEUROSCI.21-20-08091.2001

Sakakibara, S.-I., Nakamura, Y., Yoshida, T., Shibata, S., Koike, M., Takano, H., et al. (2002). RNA-binding protein Musashi family: roles for CNS stem cells and a subpopulation of ependymal cells revealed by targeted disruption and antisense ablation. *Proc. Natl. Acad. Sci. U.S.A*. 99, 15194–15199. doi: 10.1073/pnas.232087499

Sapiro, A. L., Freund, E. C., Restrepo, L., Qiao, H.-H., Bhate, A., Li, Q., et al. (2020). Zinc finger RNA-binding protein Zn72D regulates ADAR-mediated RNA editing in neurons. *Cell Rep*. 31:107654. doi: 10.1016/j.celrep.2020.107654

Savva, Y. A., Rieder, L. E., and Reenan, R. A. (2012). The ADAR protein family. *Genome Biol*. 13, 252–210. doi: 10.1186/gb-2012-13-12-252

Schenck, A., Bardoni, B., Langmann, C., Harden, N., Mandel, J.-L., and Giangrande, A. (2003). CYFIP/Sra-1 controls neuronal connectivity in drosophila and links the Rac1 GTPase pathway to the fragile X protein. *Neuron* 38, 887–898. doi: 10.1016/S0896-6273(03)00354-4

Schenck, A., Bardoni, B., Moro, A., Bagni, C., and Mandel, J.-L. (2001). A highly conserved protein family interacting with the fragile X mental retardation protein (FMRP) and displaying selective interactions with FMRP-related proteins FXR1P and FXR2P. *Proc. Natl. Acad. Sci. U.S.A*. 98, 8844–8849. doi: 10.1073/pnas.151231598

Schenck, A., Qurashi, A., Carrera, P., Bardoni, B., Diebold, C., Schejter, E., et al. (2004). WAVE/SCAR, a multifunctional complex coordinating different aspects of neuronal connectivity. *Dev. Biol*. 274, 260–270. doi: 10.1016/j.ydbio.2004.07.009

Schizophrenia Working Group of the Psychiatric Genomics Consortium (2014). Biological insights from 108 schizophrenia-associated genetic loci. *Nature* 511, 421–427. doi: 10.1038/nature13595

Schmucker, D. (2007). Molecular diversity of Dscam: recognition of molecular identity in neuronal wiring. *Nat. Rev. Neurosci*. 8, 915–920. doi: 10.1038/nrn2256

Schmucker, D., Clemens, J. C., Shu, H., Worby, C. A., Xiao, J., Muda, M., et al. (2000). Drosophila Dscam is an axon guidance receptor exhibiting extraordinary molecular diversity. *Cell* 101, 671–684. doi: 10.1016/S0092-8674(00)80878-8

Schneider, A. D. B., and Wolfinger, M. T. (2019). Musashi binding elements in Zika and related Flavivirus 3′UTRs: a comparative study *in silico*. *Sci. Rep*. 9, 6911–6912. doi: 10.1038/s41598-019-43390-5

Segal, R. A., Pomeroy, S. L., and Stiles, C. D. (1995). Axonal growth and fasciculation linked to differential expression of BDNF and NT3 receptors

in developing cerebellar granule cells. *J. Neurosci*. 15(7 Pt 1), 4970–4981. doi: 10.1523/JNEUROSCI.15-07-04970.1995

Sengupta, U., Montalbano, M., McAllen, S., Minuesa, G., Kharas, M., and Kayed, R. (2018). Formation of toxic oligomeric assemblies of RNA-BINDING PROTEIN: Musashi in Alzheimer's disease. *Acta Neuropathol. Commun*. 6:113. doi: 10.1186/s40478-018-0615-0

Shamay-Ramot, A., Khermesh, K., Porath, H. T., Barak, M., Pinto, Y., Wachtel, C., et al. (2015). Fmrp Interacts with Adar and regulates RNA editing, synaptic density and locomotor activity in zebrafish. *PLoS Genet*. 11:e1005702. doi: 10.1371/journal.pgen.1005702

Sharangdhar, T., Sugimoto, Y., Heraud-Farlow, J., Fernández-Moya, S. M., Ehses, J., Ruiz de Los Mozos, I., et al. (2017). A retained intron in the 3′-UTR of Calm3 mRNA mediates its Staufen2- and activity-dependent localization to neuronal dendrites. *EMBO Rep*. 18, 1762–1774. doi: 10.15252/embr.201744334

Shibata, S., Umei, M., Kawahara, H., Yano, M., Makino, S., and Okano, H. (2012). Characterization of the RNA-binding protein Musashi1 in zebrafish. *Brain Res*. 1462, 162–173. doi: 10.1016/j.brainres.2012.01.068

Shigeoka, T., Jung, H., Jung, J., Turner-Bridger, B., Ohk, J., Lin, J. Q., et al. (2016). Dynamic axonal translation in developing and mature visual circuits. *Cell* 166, 181–192. doi: 10.1016/j.cell.2016.05.029

Shigeoka, T., Koppers, M., Wong, H. H.-W., Lin, J. Q., Cagnetta, R., Dwivedy, A., et al. (2019). On-site ribosome remodeling by locally synthesized ribosomal proteins in axons. *Cell Rep*. 29:3605.e10–3619.e10. doi: 10.1016/j.celrep.2019.11.025

Shigeoka, T., Lu, B., and Holt, C. E. (2013). RNA-based mechanisms underlying axon guidance. *J. Cell Biol*. 202, 991–999. doi: 10.1083/jcb.201305139

Soller, M., and White, K. (2004). ELAV. *CURBIO* 14:R53. doi: 10.1016/j.cub.2003.12.041

Sonenberg, N., and Hinnebusch, A. G. (2009). Regulation of translation initiation in eukaryotes: mechanisms and biological targets. *Cell* 136, 731–745. doi: 10.1016/j.cell.2009.01.042

Spillane, M., Ketschek, A., Donnelly, C. J., Pacheco, A., Twiss, J. L., and Gallo, G. (2012). Nerve growth factor-induced formation of axonal filopodia and collateral branches involves the intra-axonal synthesis of regulators of the actin-nucleating Arp2/3 complex. *J. Neurosci*. 32, 17671–17689. doi: 10.1523/JNEUROSCI.1079-12.2012

Spillane, M., Ketschek, A., Merianda, T. T., Twiss, J. L., and Gallo, G. (2013). Mitochondria coordinate sites of axon branching through localized intra-axonal protein synthesis. *Cell Rep*. 5, 1564–1575. doi: 10.1016/j.celrep.2013.11.022

Srivastava, P. K., Bagnati, M., Delahaye-Duriez, A., Ko, J.-H., Rotival, M., Langley, S. R., et al. (2017). Genome-wide analysis of differential RNA editing in epilepsy. *Genome Res*. 27, 440–450. doi: 10.1101/gr.210740.116

Sudhakaran, I. P., Hillebrand, J., Dervan, A., Das, S., Holohan, E. E., Hülsmeier, J., et al. (2014). FMRP and Ataxin-2 function together in long-term olfactory habituation and neuronal translational control. *Proc. Natl. Acad. Sci. U.S.A*. 111, E99–E108. doi: 10.1073/pnas.1309543111

Sundar, J., Matalkah, F., Jeong, B., Stoilov, P., and Ramamurthy, V. (2020). A critical role for MSI1 and MSI2 in photoreceptor morphogenesis. *bioRxiv* 296:100048. doi: 10.1074/jbc.RA120.015714

Sutherland, J. M., McLaughlin, E. A., Hime, G. R., and Siddall, N. A. (2013). "The Musashi family of RNA binding proteins: master regulators of multiple stem cell populations," in *Transcriptional and Translational Regulation of Stem Cells*, eds G. Hime and H. Abud (Dordrecht: Springer), 233–245. doi: 10.1007/978-94-007-6621-1_13

Tariq, A., and Jantsch, M. F. (2012). Transcript diversification in the nervous system: a to I RNA-editing in CNS function and disease development. *Front. Neurosci*. 6:99. doi: 10.3389/fnins.2012.00099

Taylor, A. M., Wu, J., Tai, H.-C., and Schuman, E. M. (2013). Axonal translation of β-catenin regulates synaptic vesicle dynamics. *J. Neurosci*. 33, 5584–5589. doi: 10.1523/JNEUROSCI.2944-12.2013

Terenzio, M., Koley, S., Samra, N., Rishal, I., Zhao, Q., Sahoo, P. K., et al. (2018). Locally translated mTOR controls axonal local translation in nerve injury. *Science* 359, 1416–1421. doi: 10.1126/science.aan1053

Terenzio, M., Schiavo, G., and Fainzilber, M. (2017). Compartmentalized signaling in neurons: from cell biology to neuroscience. *Neuron* 96, 667–679. doi: 10.1016/j.neuron.2017.10.015

Thelen, M. P., and Kye, M. J. (2019). The role of RNA binding proteins for local mRNA translation: implications in neurological disorders. *Front. Mol. Biosci*. 6:161. doi: 10.3389/fmolb.2019.00161

Toriello, H. V., Colley, C., and Bamshad, M. (2016). Update on the Toriello-Carey syndrome. *Am. J. Med. Genet. A* 170, 2551–2558. doi: 10.1002/ajmg.a.37735

Toriyama, M., Shimada, T., Kim, K. B., Mitsuba, M., Nomura, E., Katsuta, K., et al. (2006). Shootin1: a protein involved in the organization of an asymmetric signal for neuronal polarization. *J. Cell Biol*. 175, 147–157. doi: 10.1083/jcb.200604160

Tran, S. S., Jun, H.-I., Bahn, J. H., Azghadi, A., Ramaswami, G., Van Nostrand, E. L., et al. (2019). Widespread RNA editing dysregulation in brains from autistic individuals. *Nat. Neurosci*. 22, 25–36. doi: 10.1038/s41593-018-0287-x

Traunmüller, L., Gomez, A. M., Nguyen, T.-M., and Scheiffele, P. (2016). Control of neuronal synapse specification by a highly dedicated alternative splicing program. *Science* 352, 982–986. doi: 10.1126/science.aaf2397

Tsivion-Visbord, H., Kopel, E., Feiglin, A., Sofer, T., Barzilay, R., Ben-Zur, T., et al. (2020). Increased RNA editing in maternal immune activation model of neurodevelopmental disease. *Nat. Commun*. 11, 5236–5213. doi: 10.1038/s41467-020-19048-6

Turner-Bridger, B., Jakobs, M., Muresan, L., Wong, H. H.-W., Franze, K., Harris, W. A., et al. (2018). Single-molecule analysis of endogenous β-actin mRNA trafficking reveals a mechanism for compartmentalized mRNA localization in axons. *Proc. Natl. Acad. Sci. U.S.A*. 115, E9697–E9706. doi: 10.1073/pnas.1806189115

Tushev, G., Glock, C., Heumüller, M., Biever, A., Jovanovic, M., and Schuman, E. M. (2018). Alternative 3′ UTRs modify the localization, regulatory potential, stability, and plasticity of mRNAs in neuronal compartments. *Neuron* 98, 495.e6–511.e6. doi: 10.1016/j.neuron.2018.03.030

Udagawa, T., Fujioka, Y., Tanaka, M., Honda, D., Yokoi, S., Riku, Y., et al. (2015). FUS regulates AMPA receptor function and FTLD/ALS-associated behaviour *via* GluA1 mRNA stabilization. *Nat. Commun*. 6, 7098–7013. doi: 10.1038/ncomms8098

Udagawa, T., Swanger, S. A., Takeuchi, K., Kim, J. H., Nalavadi, V., Shin, J., et al. (2012). Bidirectional control of mRNA translation and synaptic plasticity by the cytoplasmic polyadenylation complex. *Mol. Cell* 47, 253–266. doi: 10.1016/j.molcel.2012.05.016

Ule, J., Ule, A., Spencer, J., Williams, A., Hu, J.-S., Cline, M., et al. (2005). Nova regulates brain-specific splicing to shape the synapse. *Nat. Genet*. 37, 844–852. doi: 10.1038/ng1610

Uren, P. J., Vo, D. T., de Araujo, P. R., Pötschke, R., Burns, S. C., Bahrami-Samani, E., et al. (2015). RNA-binding protein Musashi1 is a central regulator of adhesion pathways in glioblastoma. *Mol. Cell. Biol*. 35, 2965–2978. doi: 10.1128/MCB.00410-15

Urwyler, O., Izadifar, A., Vandenbogaerde, S., Sachse, S., Misbaer, A., and Schmucker, D. (2019). Branch-restricted localization of phosphatase Prl-1 specifies axonal synaptogenesis domains. *Science* 364:eaau9952. doi: 10.1126/science.aau9952

Ushkaryov, Y. A., Petrenko, A. G., Geppert, M., and Südhof, T. C. (1992). Neurexins: synaptic cell surface proteins related to the alpha-latrotoxin receptor and laminin. *Science* 257, 50–56. doi: 10.1126/science.1621094

Ushkaryov, Y. A., and Südhof, T. C. (1993). Neurexin III alpha: extensive alternative splicing generates membrane-bound and soluble forms. *Proc. Natl. Acad. Sci. U.S.A*. 90, 6410–6414. doi: 10.1073/pnas.90.14.6410

Vallecillo-Viejo, I. C., Liscovitch-Brauer, N., Quiroz, J. F. D., Montiel-Gonzalez, M. F., Nemes, S. E., Rangan, K. J., et al. (2020). Spatially regulated editing of genetic information within a neuron. *Nucleic Acids Res*. 48, 3999–4012. doi: 10.1093/nar/gkaa172

Vazquez, L. E., Chen, H.-J., Sokolova, I., Knuesel, I., and Kennedy, M. B. (2004). SynGAP regulates spine formation. *J. Neurosci*. 24, 8862–8872. doi: 10.1523/JNEUROSCI.3213-04.2004

Vidaki, M., Drees, F., Saxena, T., Lanslots, E., Taliaferro, M. J., Tatarakis, A., et al. (2017). A requirement for mena, an actin regulator, in local mRNA translation in developing neurons. *Neuron* 95, 608.e5–622.e5. doi: 10.1016/j.neuron.2017.06.048

Vijayakumar, J., Perrois, C., Heim, M., Bousset, L., Alberti, S., and Besse, F. (2019). The prion-like domain of Drosophila Imp promotes axonal transport of RNP granules *in vivo*. *Nat. Commun*. 10, 275–214. doi: 10.1038/s41467-019-10554-w

Vo, D. T., Subramaniam, D., Remke, M., Burton, T. L., Uren, P. J., Gelfond, J. A., et al. (2012). The RNA-binding protein Musashi1 affects medulloblastoma growth

via a network of cancer- related genes and is an indicator of poor prognosis. *AJPA* 181, 1762–1772. doi: 10.1016/j.ajpath.2012.07.031

Vuong, C. K., Black, D. L., and Zheng, S. (2016). The neurogenetics of alternative splicing. *Nat. Rev. Neurosci*. 17, 265–281. doi: 10.1038/nrn.2016.27

Wahlstedt, H., Daniel, C., Ensterö, M., and Öhman, M. (2009). Large-scale mRNA sequencing determines global regulation of RNA editing during brain development. *Genome Res*. 19, 978–986. doi: 10.1101/gr.089409.108

Walker, R. L., Ramaswami, G., Hartl, C., Mancuso, N., Gandal, M. J., de la Torre-Ubieta, L., et al. (2019). Genetic control of expression and splicing in developing human brain informs disease mechanisms. *Cell* 179, 750.e22–771.e22. doi: 10.1016/j.cell.2019.09.021

Walkley, C. R., and Li, J. B. (2017). Rewriting the transcriptome: adenosine-to-inosine RNA editing by ADARs. *Genome Biol*. 18, 1–13. doi: 10.1186/s13059-017-1347-3

Wang, E. T., Taliaferro, J. M., Lee, J.-A., Sudhakaran, I. P., Rossoll, W., Gross, C., et al. (2016). Dysregulation of mRNA localization and translation in genetic disease. *J. Neurosci*. 36, 11418–11426. doi: 10.1523/JNEUROSCI.2352-16.2016

Wang, Y.-Y., Wu, H.-I., Hsu, W.-L., Chung, H.-W., Yang, P.-H., Chang, Y.-C., et al. (2014). In vitro growth conditions and development affect differential distributions of RNA in axonal growth cones and shafts of cultured rat hippocampal neurons. *Mol. Cell. Neurosci*. 61, 141–151. doi: 10.1016/j.mcn.2014.06.011

Weber, S. C., and Brangwynne, C. P. (2012). Getting RNA and protein in phase. *Cell* 149, 1188–1191. doi: 10.1016/j.cell.2012.05.022

Wei, M., Huang, J., Li, G.-W., Jiang, B., Cheng, H., Liu, X., et al. (2021). Axon-enriched lincRNA ALAE is required for axon elongation *via* regulation of local mRNA translation. *Cell Rep*. 35:109053. doi: 10.1016/j.celrep.2021.109053

Weill, L., Belloc, E., Castellazzi, C. L., and Méndez, R. (2017). Musashi 1 regulates the timing and extent of meiotic mRNA translational activation by promoting the use of specific CPEs. *Nat. Struct. Mol. Biol*. 24, 672–681. doi: 10.1038/nsmb.3434

Welshhans, K., and Bassell, G. J. (2011). Netrin-1-induced local β-actin synthesis and growth cone guidance requires zipcode binding protein 1. *J. Neurosci*. 31, 9800–9813. doi: 10.1523/JNEUROSCI.0166-11.2011

Weyn-Vanhentenryck, S. M., Feng, H., Ustianenko, D., Duffié, R., Yan, Q., Jacko, M., et al. (2018). Precise temporal regulation of alternative splicing during neural development. *Nat. Commun*. 9, 1–17. doi: 10.1038/s41467-018-04559-0

Wiederhold, K., and Passmore, L. A. (2010). Cytoplasmic deadenylation: regulation of mRNA fate. *Biochem. Soc. Trans*. 38, 1531–1536. doi: 10.1042/BST0381531

Wills, Z., Marr, L., Zinn, K., Goodman, C. S., and Van Vactor, D. (1999). Profilin and the Abl tyrosine kinase are required for motor axon outgrowth in the Drosophila embryo. *Neuron* 22, 291–299. doi: 10.1016/S0896-6273(00)81090-9

Wirth, B., Karakaya, M., Kye, M. J., and Mendoza-Ferreira, N. (2020). Twenty-five years of spinal muscular atrophy research: from phenotype to genotype to therapy, and what comes next. *Annu. Rev. Genomics Hum. Genet*. 21, 231–261. doi: 10.1146/annurev-genom-102319-103602

Witte, H., Schreiner, D., and Scheiffele, P. (2019). A Sam68-dependent alternative splicing program shapes postsynaptic protein complexes. *Eur. J. Neurosci*. 49, 1436–1453. doi: 10.1111/ejn.14332

Wojtowicz, W. M., Flanagan, J. J., Millard, S. S., Zipursky, S. L., and Clemens, J. C. (2004). Alternative splicing of Drosophila Dscam generates axon guidance receptors that exhibit isoform-specific homophilic binding. *Cell* 118, 619–633. doi: 10.1016/j.cell.2004.08.021

Wong, H. H.-W., Lin, J. Q., Ströhl, F., Roque, C. G., Cioni, J.-M., Cagnetta, R., et al. (2017). RNA docking and local translation regulate site-specific axon remodeling *in vivo*. *Neuron* 95, 852.e8–868.e8. doi: 10.1016/j.neuron.2017.07.016

Wong, J. T., Yu, W. T., and O'Connor, T. P. (1997). Transmembrane grasshopper Semaphorin I promotes axon outgrowth *in vivo*. *Development* 124, 3597–3607. doi: 10.1242/dev.124.18.3597

Wong, J. T. W., Wong, S. T. M., and O'Connor, T. P. (1999). Ectopic semaphorin-1a functions as an attractive guidance cue for developing peripheral neurons. *Nat. Neurosci*. 2, 798–803. doi: 10.1038/12168

Worpenberg, L., Paolantoni, C., Longhi, S., Mulorz, M. M., Lence, T., Wessels, H.-H., et al. (2021). Ythdf is a N6-methyladenosine reader that modulates Fmr1 target mRNA selection and restricts axonal growth in Drosophila. *EMBO J*. 40:e104975. doi: 10.15252/embj.2020104975

Wu, K. Y., Hengst, U., Cox, L. J., Macosko, E. Z., Jeromin, A., Urquhart, E. R., et al. (2005). Local translation of RhoA regulates growth cone collapse. *Nature* 436, 1020–1024. doi: 10.1038/nature03885

Xia, K., Guo, H., Hu, Z., Xun, G., Zuo, L., Peng, Y., et al. (2014). Common genetic variants on 1p13.2 associate with risk of autism. *Mol. Psychiatry* 19, 1212–1219. doi: 10.1038/mp.2013.146

Xiang, K., and Bartel, D. P. (2021). The molecular basis of coupling between poly(A)-tail length and translational efficiency. *eLife* 10:66493. doi: 10.7554/eLife.66493.sa2

Xu, B., Zhang, Y., Du, X.-F., Li, J., Zi, H.-X., Bu, J.-W., et al. (2017). Neurons secrete miR-132-containing exosomes to regulate brain vascular integrity. *Cell Res*. 27, 882–897. doi: 10.1038/cr.2017.62

Xu, K., Wu, Z., Renier, N., Antipenko, A., Tzvetkova-Robev, D., Xu, Y., et al. (2014). Neural migration. structures of netrin-1 bound to two receptors provide insight into its axon guidance mechanism. *Science* 344, 1275–1279. doi: 10.1126/science.1255149

Yao, J., Sasaki, Y., Wen, Z., Bassell, G. J., and Zheng, J. Q. (2006). An essential role for β-actin mRNA localization and translation in Ca 2+ -dependent growth cone guidance. *Nat. Neurosci*. 9, 1265–1273. doi: 10.1038/nn1773

Yarmishyn, A. A., Yang, Y.-P., Lu, K.-H., Chen, Y.-C., Chien, Y., Chou, S.-J., et al. (2020). Musashi-1 promotes cancer stem cell properties of glioblastoma cells *via* upregulation of YTHDF1. *Cancer Cell Int*. 20, 597–515. doi: 10.1186/s12935-020-01696-9

Yokoi, S., Udagawa, T., Fujioka, Y., Honda, D., Okado, H., Watanabe, H., et al. (2017). 3′UTR length-dependent control of SynGAP isoform α2 mRNA by FUS and ELAV-like proteins promotes dendritic spine maturation and cognitive function. *Cell Rep*. 20, 3071–3084. doi: 10.1016/j.celrep.2017.08.100

Yoon, Y. J., White, S. L., Ni, X., Gokin, A. P., and Martin-Caraballo, M. (2012). Downregulation of GluA2 AMPA receptor subunits reduces the dendritic arborization of developing spinal motoneurons. *PLoS ONE* 7:e49879. doi: 10.1371/journal.pone.0049879

Young-Baird, S. K., Lourenço, M. B., Elder, M. K., Klann, E., Liebau, S., and Dever, T. E. (2020). Suppression of MEHMO syndrome mutation in eIF2 by small molecule ISRIB. *Mol. Cell* 77, 875.e7–886.e7. doi: 10.1016/j.molcel.2019.11.008

Yu, J., Chen, M., Huang, H., Zhu, J., Song, H., Zhu, J., et al. (2017). Dynamic m6A modification regulates local translation of mRNA in axons. *Nucleic Acids Res*. 46, 1412–1423. doi: 10.1093/nar/gkx1182

Zappulo, A., van den Bruck, D., Ciolli, C., Franke, V., Imami, K., McShane, E., et al. (2017). RNA localization is a key determinant of neurite-enriched proteome. *Nat. Commun*. 8, 583–513. doi: 10.1038/s41467-017-00690-6

Zbinden, A., Pérez-Berlanga, M., De Rossi, P., and Polymenidou, M. (2020). Phase separation and neurodegenerative diseases: a disturbance in the force. *Dev. Cell* 55, 45–68. doi: 10.1016/j.devcel.2020.09.014

Zearfoss, N. R., Alarcon, J. M., Trifilieff, P., Kandel, E., and Richter, J. D. (2008). A molecular circuit composed of CPEB-1 and c-Jun controls growth hormone-mediated synaptic plasticity in the mouse hippocampus. *The J. Neurosci*. 28, 8502–8509. doi: 10.1523/JNEUROSCI.1756-08.2008

Zearfoss, N. R., Deveau, L. M., Clingman, C. C., Schmidt, E., Johnson, E. S., Massi, F., et al. (2014). A conserved three-nucleotide core motif defines Musashi RNA binding specificity. *J. Biol. Chem*. 289, 35530–35541. doi: 10.1074/jbc.M114.597112

Zelina, P., Blockus, H., Zagar, Y., Péres, A., Friocourt, F., Wu, Z., et al. (2014). Signaling switch of the axon guidance receptor Robo3 during vertebrate evolution. *Neuron* 84, 1258–1272. doi: 10.1016/j.neuron.2014.11.004

Zeng, M., Shang, Y., Araki, Y., Guo, T., Huganir, R. L., and Zhang, M. (2016). Phase transition in postsynaptic densities underlies formation of synaptic complexes and synaptic plasticity. *Cell* 166:1163.e12–1175.e12. doi: 10.1016/j.cell.2016.07.008

Zhang, J., Neal, J., Lian, G., Hu, J., Lu, J., and Sheen, V. (2013). Filamin A regulates neuronal migration through brefeldin A-inhibited guanine exchange factor 2-dependent Arf1 activation. *J. Neurosci*. 33, 15735–15746. doi: 10.1523/JNEUROSCI.1939-13.2013

Zhang, M., Ergin, V., Lin, L., Stork, C., Chen, L., and Zheng, S. (2019a). Axonogenesis is coordinated by neuron-specific alternative splicing programming and splicing regulator PTBP2. *Neuron* 101, 690.e10–706.e10. doi: 10.1016/j.neuron.2019.01.022

Zhang, Y. Q., Bailey, A. M., Matthies, H. J. G., Renden, R. B., Smith, M. A., Speese, S. D., et al. (2001). Drosophila fragile X-related gene regulates the MAP1B

homolog futsch to control synaptic structure and function. *Cell* 107, 591–603. doi: 10.1016/S0092-8674(01)00589-X

Zhang, Z., So, K., Peterson, R., Bauer, M., Ng, H., Zhang, Y., et al. (2019b). Elav-mediated exon skipping and alternative polyadenylation of the Dscam1 gene are required for axon outgrowth. *Cell Rep*. 27:3808.e7–3817.e7. doi: 10.1016/j.celrep.2019.05.083

Zhao, L., Wang, D., Wang, Q., Rodal, A. A., and Zhang, Y. Q. (2013). Drosophila cyfip regulates synaptic development and endocytosis by suppressing filamentous actin assembly. *PLoS Genet*. 9:e1003450. doi: 10.1371/journal.pgen.1003450

Zheng, L., Michelson, Y., Freger, V., Avraham, Z., Venken, K. J. T., Bellen, H. J., et al. (2011). Drosophila Ten-m and filamin affect motor neuron growth cone guidance. *PLoS ONE* 6:e22956. doi: 10.1371/journal.pone.0022956

Zhuang, M., Li, X., Zhu, J., Zhang, J., Niu, F., Liang, F., et al. (2019). The m6A reader YTHDF1 regulates axon guidance through translational control of Robo3.1 expression. *Nucleic Acids Res*. 47, 4765–4777. doi: 10.1093/nar/gkz157

Zivraj, K. H., Tung, Y. C. L., Piper, M., Gumy, L., Fawcett, J. W., Yeo, G. S. H., et al. (2010). Subcellular profiling reveals distinct and developmentally regulated repertoire of growth cone mRNAs. *J. Neurosci* 30, 15464–15478. doi: 10.1523/JNEUROSCI.1800-10.2010

Conflict of Interest: The authors declare that the research was conducted in the absence of any commercial or financial relationships that could be construed as a potential conflict of interest.

Publisher's Note: All claims expressed in this article are solely those of the authors and do not necessarily represent those of their affiliated organizations, or those of the publisher, the editors and the reviewers. Any product that may be evaluated in this article, or claim that may be made by its manufacturer, is not guaranteed or endorsed by the publisher.

Copyright © 2021 Landínez-Macías and Urwyler. This is an open-access article distributed under the terms of the Creative Commons Attribution License (CC BY). The use, distribution or reproduction in other forums is permitted, provided the original author(s) and the copyright owner(s) are credited and that the original publication in this journal is cited, in accordance with accepted academic practice. No use, distribution or reproduction is permitted which does not comply with these terms.

frontiers in Molecular Neuroscience

ORIGINAL RESEARCH
published: 01 December 2021
doi: 10.3389/fnmol.2021.754393

Refinement of Active and Passive Membrane Properties of Layer V Pyramidal Neurons in Rat Primary Motor Cortex During Postnatal Development

*Patricia Perez-García[1,2†], Ricardo Pardillo-Díaz[2,3†], Noelia Geribaldi-Doldán[3,4], Ricardo Gómez-Oliva[2,3], Samuel Domínguez-García[2,3], Carmen Castro[2,3], Pedro Nunez-Abades[1,3] and Livia Carrascal[1,3]**

[1] Department of Physiology, School of Pharmacy, University of Seville, Seville, Spain, [2] Division of Physiology, School of Medicine, University of Cádiz, Cádiz, Spain, [3] Biomedical Research and Innovation Institute of Cádiz (INiBICA), Cádiz, Spain, [4] Department of Human Anatomy and Embriology, University of Cádiz, Cádiz, Spain

OPEN ACCESS

Edited by:
Inmaculada Segura,
Ludwig Maximilian University of Munich, Germany

Reviewed by:
Yann Zerlaut,
Institut du Cerveau (ICM), France
Scott D. Moore,
Duke University, United States

***Correspondence:**
Livia Carrascal
livia@us.es

† These authors have contributed equally to this work and share first authorship

Specialty section:
This article was submitted to Neuroplasticity and Development, a section of the journal Frontiers in Molecular Neuroscience

Received: 06 August 2021
Accepted: 19 October 2021
Published: 01 December 2021

Citation:
Perez-García P, Pardillo-Díaz R, Geribaldi-Doldán N, Gómez-Oliva R, Domínguez-García S, Castro C, Nunez-Abades P and Carrascal L (2021) Refinement of Active and Passive Membrane Properties of Layer V Pyramidal Neurons in Rat Primary Motor Cortex During Postnatal Development. Front. Mol. Neurosci. 14:754393. doi: 10.3389/fnmol.2021.754393

Achieving the distinctive complex behaviors of adult mammals requires the development of a great variety of specialized neural circuits. Although the development of these circuits begins during the embryonic stage, they remain immature at birth, requiring a postnatal maturation process to achieve these complex tasks. Understanding how the neuronal membrane properties and circuits change during development is the first step to understand their transition into efficient ones. Thus, using whole cell patch clamp recordings, we have studied the changes in the electrophysiological properties of layer V pyramidal neurons of the rat primary motor cortex during postnatal development. Among all the parameters studied, only the voltage threshold was established at birth and, although some of the changes occurred mainly during the second postnatal week, other properties such as membrane potential, capacitance, duration of the post-hyperpolarization phase or the maximum firing rate were not defined until the beginning of adulthood. Those modifications lead to a decrease in neuronal excitability and to an increase in the working range in young adult neurons, allowing more sensitive and accurate responses. This maturation process, that involves an increase in neuronal size and changes in ionic conductances, seems to be influenced by the neuronal type and by the task that neurons perform as inferred from the comparison with other pyramidal and motor neuron populations.

Keywords: development, motor cortex, motor neurons, pyramidal neurons, membrane properties, patch clamp

INTRODUCTION

The development of a large variety of specialized neuronal circuits is needed to achieve all the complex behaviors found in adult mammals. These neuronal circuits are mostly immature at birth and postnatal refinement is required in both neuronal properties and connectivity to effectively manage such a complicated task (Kriegstein et al., 1987; McCormick and Prince, 1987; Burgard and Hablitz, 1993; Ramoa and McCormick, 1994; Picken Bahrey and Moody, 2003;

Carrascal et al., 2006, 2009; Smith and Brownstone, 2020). The degree to which these mature electrophysiological properties are determined by cell-intrinsic *vs*. extrinsic factors is not clear. Thus, in order to understand how neural circuits are ultimately tuned, it is necessary to investigate how the properties of their neurons develop.

The neocortex is the largest part of the mammalian brain, and it is the seat of higher cognitive functions, including fine motor tasks. Accordingly, defects in neocortical development commonly result in severe intellectual, motor and social deficits. Therefore, understanding the mechanisms that underlie the development of the neocortex facilitates the comprehension of its evolution and disease and the disclosure of their triggering mechanisms [reviewed in Borrell (2019)]. In the mammalian neocortex different cell types have been described, based on dendritic and axonal arborization patterns (Amaral and Strick, 2013). The two general cell types, pyramidal and non-pyramidal, represent projection neurons and interneurons, respectively, (Molnár and Cheung, 2006; Molyneaux et al., 2007; Amaral and Strick, 2013). Pyramidal neurons generally have long axonal projections to distant cortical and subcortical targets and are therefore thought to be important in communication between neural networks (Yuste, 2005; Chomiak et al., 2008; Chomiak and Hu, 2013), capable of supplying information that can be rapidly and synchronously reconstituted across remote sensorimotor networks (Chomiak and Hu, 2013). Neocortical neurons undergo an extensive change in their dendritic morphology during postnatal development (Petit et al., 1988; Kasper et al., 1994) and few studies in layer V pyramidal neurons from neocortex demonstrate postnatal changes in its electrophysiological properties during the first 4 postnatal weeks (Zhu, 2000; Zhang, 2004; Christophe et al., 2005; Etherington and Williams, 2011; Elston and Fujita, 2014). However, these studies are mainly focused in prefrontal and visual cortex or somatosensorial cortex. In this work we hypothesize that layer V pyramidal neurons from the primary motor cortex are tuned during postnatal development, and we wonder whether the temporal course of such changes is similar to that of other pyramidal neurons or on the contrary each population of pyramidal neurons evolves with a different temporal course dependent on their final tasks and inputs. Furthermore, previous works from our laboratory have demonstrated considerable postnatal changes in electrophysiological and morphological properties of oculomotor and genioglossal motor neurons during the first month following birth (Nunez-Abades et al., 1993; Nunez-Abades et al., 1994; Nunez-Abades and Cameron, 1995; Carrascal et al., 2006; Carrascal et al., 2009; Carrascal et al., 2010). Additionally, it has also been reported in detail the electrophysiological postnatal maturation of cervical and lumbar motor neurons showing great changes (Smith and Brownstone, 2020).

The aim of this work was to study, through whole cell patch clamp techniques in brain slices, if electrophysiological properties of layer V pyramidal neurons from the primary motor cortex are established at birth or they are refined during the first month of age, with special attention to the temporal course of maturation.

MATERIALS AND METHODS

Animals and Brain Slices Preparation

Wistar rats of both sexes and aged between days 2 and 44 postnatal were used in the study. Rats were classified into four groups for the purpose of including data in a table: newborn (P2–P7); infantile (P11–P17); young adult (P22–P30), and adult (P31–44). A total of 23 animals were used in this study (P1–10, $N = 5$; P11–20, $N = 5$; P21–30; $N = 7$; P21–44, $N = 6$). Only one cell was recorded per slice, using 2–4 slices per animal. Experiments were performed strictly following the recommendations given by the Guide for the Care and Use of Laboratory Animals of the European Community Directive 2010/63/UE and the Spanish Royal Decree 53/2013. In addition, all the procedures were approved by the Animal Ethics Committee of the University of Seville. Overall, newborn rats were sacrificed directly by decapitation, while infantile, young adult, and adult rats were previously sure with sodium pentobarbital (50 mg/kg), ensuring that both the retraction reflex of the limb and the blinking reflex disappeared, and perfused with ice-cold low-calcium artificial cerebral spinal fluid (ACSF), to obtain the best possible preservation of the brain tissue. To guarantee that the results are not influenced by the anesthesia, two infantile animals were directly decapitated using slices obtained from these rats, 5 cells were recorded, and no significant differences were found with respect to the cells recorded from anesthetized rats of the infantile group. In all cases, the brain was rapidly extracted and placed in a dish with the same cutting solution, where the cerebellum and the most rostral part of the telencephalon was removed. The part of the brain that contained the area of interest -i.e., the motor cortex- was cut transversely into 300 μm slices using a vibratome (Leica VT1000 S, Leica Biosystems, United Kingdom). The slices were incubated in a chamber containing ACSF at 33°C for 30 min and then maintained in the same chamber at room temperature until use. The composition of the ACSF was as follows (data in mM): 126 NaCl, 2 KCl, 1.25 Na_2HPO_4, 26 $NaHCO_3$, 10 glucose, 2 $MgCl_2$, and 2 $CaCl_2$; ACSF used for brain perfusion, extraction and slicing contained a lower concentration of calcium and a higher concentration of magnesium (data in mM): 4 $MgCl_2$, 0.1 $CaCl_2$. Both ACSF and low-calcium-ACSF solutions were bubbled with 95% O_2 – 5% CO_2 (pH 7.4, adjusted with HCl).

Whole-Cell Patch Clamp Recordings and Analysis

Single slices were transferred to the recording chamber, where they were continuously superfused with aerated ACSF (∼33°C) at 1 ml/min using a peristaltic pump (Harvard Apparatus MPII, Holliston, MA, United States). As visual guidance, a Nikon Eclipse FN1 microscope equipped with infrared-differential interference contrast (IR-DIC) optics, a 40 × water immersion objective and a WAT-902H2 Ultimate Camera was used. Patch clamp micropipettes were obtained from borosilicate glass capillaries (inner diameter 0.6 mm, outer diameter 1 mm, Narishige) and a vertical puller (PC-10, Narishige, Tokyo, Japan), adjusting its resistance to 3–6 MΩ.

Micropipettes were filled with a K^+-gluconate solution (in mM): 120 K-gluconate, 10 KCl, 10 phosphocreatine disodium salt, 2 MgATP, 0.3 NaGTP, 0.1 EGTA, 10 HEPES. pH was adjusted to 7.3 using KOH and an osmolarity of 285 mosmol/kg was adjusted with sucrose. Using a micromanipulator (MP-225, Sutter Instrument, CA, United States), micropipettes were visually placed in the motor cortex area. Within this region the pyramidal neurons were identified based on their characteristic morphology (Pardillo-Díaz et al., 2016; Carrascal et al., 2020). An amplified (MultiClamp 700B, Axon Instruments, Molecular Devices, Sunnyvale, CA, United States) was also used to achieve the whole-cell patch clamp configuration. Recordings were low-pass Bessel-filtered at 10 kHz; data were digitized at 2–20 kHz using a Digidata 1550 analog-to-digital converter and acquired with the pCLAMP 10 software (Molecular Devices). For the data analysis, Clampfit 10.4 software (Molecular Devices) was used.

As performed in previous studies from our laboratory (Torres-Torrelo et al., 2012; Pardillo-Díaz et al., 2015), both passive and active properties of the cells were studied: resting membrane potential, input resistance, membrane time constant, rheobase, voltage threshold, depolarization voltage, action potential amplitude and duration, AHP duration, maximum frequency of discharge, frequency gain, and cancelation current. All cells selected for analysis had a stable resting membrane potential and did not show spontaneous action potentials.

The resting membrane potential was calculated as the difference between the intracellular and extracellular potential after the removal of the recording electrode from the cell. The input resistance was measured by injecting positive and negative square current pulses (500 ms, 1 Hz, with 10 pA increments) and calculated offline as the slope of the current-voltage relationship, following Ohm's law. Membrane time constant was defined as the time needed for the membrane voltage to reach 2/3 of its final value. When there was evidence of inward rectification (*sag*) the voltage value achieved at the peak was used for the calculation of input resistance. For the measurement of the membrane time constant, single pulses of −30 pA were used, a current intensity that did not elicit inward rectification. Rheobase was defined as the minimum intensity of current necessary to provoke an action potential in 50% of the cases; it was calculated by applying square pulses of 100 ms, 1 Hz, with 5–20 pA increments.

The voltage threshold was the minimum voltage required by the cell to trigger an action potential (spike threshold), while the voltage depolarization was the increase in membrane potential needed to reach the voltage threshold. Thus, the depolarization voltage could be calculated as the difference between the voltage threshold and the resting membrane potential. To determine the spike threshold, the action potential recording was differentiated, with the spike onset taken as the value of the membrane potential at which the first derivative exceeded 10 V/s (Carrascal et al., 2006). Action potential amplitude was calculated as the difference between the spike voltage peak and the threshold voltage, while its duration was calculated as the width of the action potential at half its amplitude. Duration of afterhyperpolarization phase (AHP) was measured as the time elapsed between the repolarizing phase at the resting potential level and the point in which this potential is totally recovered.

Repetitive firing properties were evoked by the application of depolarizing current steps (1 s, 0.5 Hz, with 10–50 pA increments). The maximum firing frequency was taken as the highest number of spikes that cells could achieve during the repetitive discharge, independently of the current intensity. Frequency gain was defined as the slope of the relationship between firing frequency and applied current. All the neurons from this study achieved a plateau after the reaching of the maximum frequency that was not consider for the calculation of this parameter. Cancelation current was the intensity of the 1s depolarizing pulse at which the neuron began to fail in the discharge, after reaching its maximum frequency.

To confirm that soma morphology in IR-DIC was an appropriate neuronal selection method for our study, we chose a random sample of neurons within the studied population to verify their morphology through a dye-filling technique. In total, 6 neurons were intracellularly labeled with neurobiotin after performing electrophysiological recordings. For this purpose, iontophoretic injection of 1% neurobiotin (Neurobiotin tracer; Vector Laboratories, Burlingame, CA, United States) contained in the internal pipette solution was carried out by applying current steps of 400 pA of 500 ms at 0.5 Hz for 20 min. Slices containing labeled cells were deposited in a 4% paraformaldehyde solution at 4°C and left overnight, then transferred to 30% sucrose in phosphate buffer at 4°C overnight. Thereafter, dye-filled neurons were revealed with monoclonal antibiotin FITC conjugated antibody (1:120) from Sigma (Darmstadt, Germany). A Zeiss LSM 900 Airyscan 2 confocal microscope was used for the visualization and reconstruction of the labeled pyramidal cells. Stacks of 30–70 photographs were performed, using a 1 μm interval. Images were processed with ZEN 3.2 Blue Edition software. Neurons were reconstructed using the Neurolucida 360 version 2020 3.1 system (MicroBrightField, Williston, VT, United States).

Statistical Analysis

All statistical analyses were carried out on the raw data. Results were expressed as the mean ± standard error of the mean; n indicates the number of cells included; N indicates the number of animals. GraphPad Prism software was used for the statistical calculations. A normality test (Shapiro-Wilk Test) was applied in order to check the data distribution. A variance analysis (ANOVA) with repeated measures was used to compare the means between groups. If significant differences were shown, Bonferroni test was carried out to make paired comparisons between groups. In all cases, a 95% confidence interval was considered, therefore two groups were statistically different if $p \leq 0.05$. Correlation among two variables was measured using Pearson's correlation coefficient (r). Fisher's exact test was used to determine if there were non-random associations between two categorical variables (presence of sag and age groups). In figures and tables, asterisks (*) indicate statistical dissimilarities between consecutive age groups, while crosses (+) indicate statistical differences when comparing first and last age groups. Finally, black lines in figures represent the best fit to the raw data.

RESULTS

All neurons included were identified as layer V pyramidal neurons based on their morphological characteristics (**Figure 1**), a large triangular-shaped cell body with a prominent apical dendrite projecting vertically to the pial surface and smaller basal dendrites. Cells were discarded if they did not present a stable resting membrane potential or if they were not silent at rest.

Passive Membrane Properties of Layer V Pyramidal Neurons From the Motor Cortex During Postnatal Development

Pyramidal neurons from the motor cortex exhibited a stable membrane potential that progressively hyperpolarized during postnatal development. The best fit to the raw data was a linear regression (slope = −0.30 mV/day; r = 0,51; $p < 0.0001$; **Figure 2C**). This difference was statistically significant when the mean of newborn (−64.10 ± 1.75 mV) and adult (−73.90 ± 1.49 mV) age groups were compared (**Figures 2A,C** and **Table 1**). Input resistance also changed with postnatal maturation. The input resistance of neurons from the newborn group were the highest, being 2.6-fold greater than those of the infantile group and 5–6-fold greater than those of the young adult and adult groups (**Figure 2A**). All the statistical comparisons among group means showed significant differences except the two older ones, meaning that input resistance was established at the third week (**Figure 2D** and **Table 1**). Those changes are also observable in **Figure 2D**, which depicts the raw data (open symbols) fitting a single exponential decay (r = 0.90; τ = 8.572 days). The time constant of this fit demonstrates that the major changes of this parameter occur between the first and the beginning of the second week after birth. This fact is also supported by the comparison between the means of the newborn and the infantile groups: 744.59 ± 46.10 MΩ and 285.40 ± 12.67 MΩ, respectively (**Table 1**). As shown in **Figure 2A**, the voltage response to hyperpolarizing current pulses was nearly linear and exponentially approached a steady-state level. However, although this linearity was observable in all groups, the neurons from adult, young adult and infantile groups exhibited a membrane potential rectification at the more hyperpolarizing current pulse. This depolarizing shift in membrane potential or sag was voltage dependent and more evident at more hyperpolarizing currents (see in **Figure 2A**). When we examined the presence or absence of sag in the four groups, we found that only the 6,67% of neurons from the newborn group showed sag, while the 66,67% of neurons from the infantile, the 80% of neurons from the young adult, and the 85,71% neurons from the adult group exhibited sag. These differences were significant when the three older groups were compared with the newborn group without differences neither between infantile and young adult groups nor between young adult and adult groups (**Table 1**).

Membrane capacitance increased almost 2-fold during maturation. This increase was progressive and only significant differences were found when the adult group was compared with the newborn one, which is consistent with a linear regression as the best fit for the raw data (slope = 0.97 pF/day; r = 0.43; $p = 0.001$; **Figure 2E** and **Table 1**). When we analyzed if membrane capacitance co-varied with input resistance, as expected by the neuronal cable theory, a weak but significant linear relationship was found (r = 0.43; $p = 0.0009$; **Figure 2F**). Hence, membrane capacitance increase is not the sole cause of the input resistance reduction. As membrane capacitance

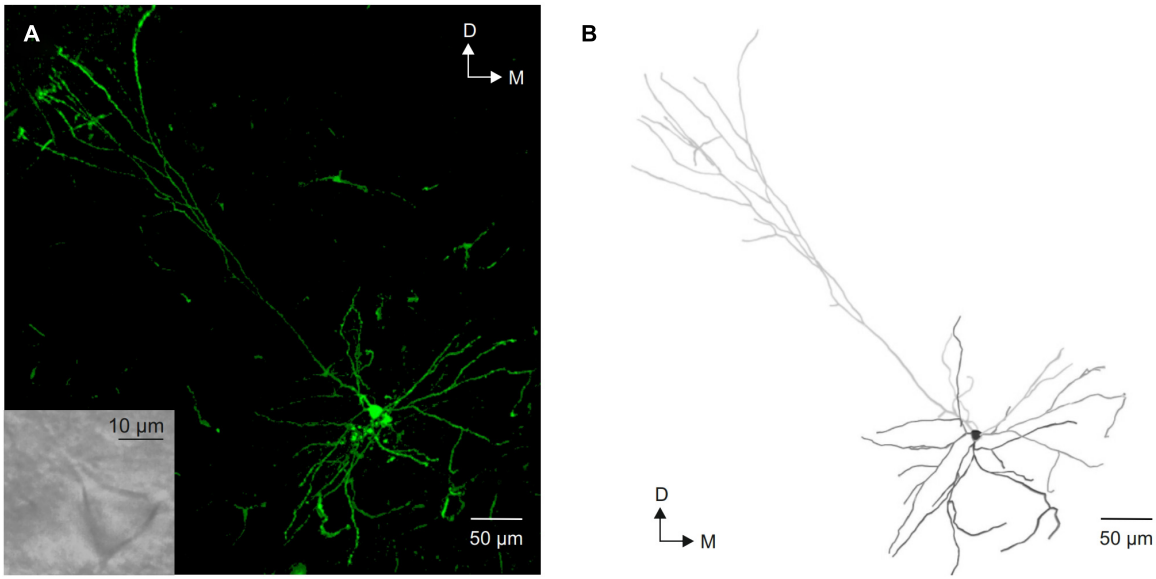

FIGURE 1 | Morphological identification of layer V pyramidal neurons from the motor cortex. **(A)** Photomicrograph of a intracellular labeled layer V pyramidal neuron showing its typical morphology. The inset shows an image of this neuron under infrared microscope visualization. **(B)** Neurolucida reconstruction of the neuron shown in **(A)**. D, dorsal; M, medial.

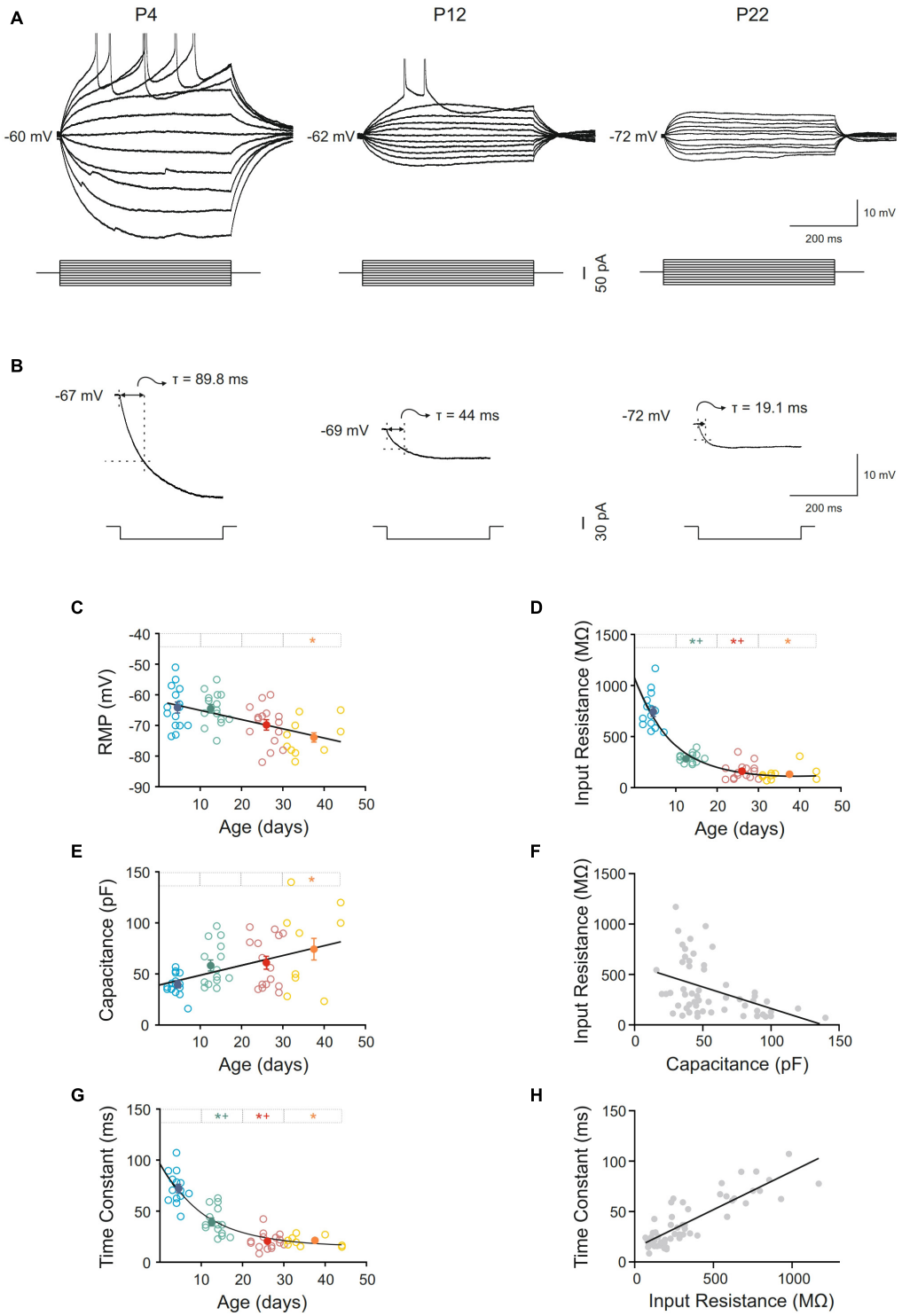

FIGURE 2 | Postnatal development of passive membrane properties of motor cortex pyramidal neurons. **(A)** Membrane voltage responses to depolarizing and hyperpolarizing current pulses in representative neurons of different ages. **(B)** Average ($n = 10$) of the membrane voltage response to a hyperpolarizing current pulse (300 ms, –20 pA) in the representative neurons show in **(A)**. **(C–E,G)** Scatter plots showing the changes in resting membrane potential (RMP) **(C)**, input resistance **(D)**, capacitance **(E),** and time constant **(G)** as a function of postnatal age. Open symbols represent the raw data, while filled symbols are the means of the four different age groups and their standard errors. Each age group is represented by a color (blue = newborn, $n = 15$; green = infantile, $n = 15$; red = young adult, $n = 15$; yellow = adult, $n = 10$). An asterisk indicates a significant difference from the newborn group; a cross indicates a difference between adjacent groups. The significance level was established as $p \leq 0.05$ **(F,H)**. Correlation between input resistance and capacitance, r = –0.43; $p < 0.0009$ **(F)** and time constant and input resistance, r = 0.86; $p < 0.0001$ **(H)**.

TABLE 1 | Electrophysiological properties of pyramidal neurons from the motor cortex during postnatal development.

Membrane properties	Newborn $n = 15$	Infantile $n = 15$	Young adult $n = 15$	Adult $n = 10$
Capacitance (pF)	39.80 ± 2.67	58.40 ± 5.29	61.13 ± 6.36	74.30 ± 10.51*
Membrane Resting Potential (mV)	−64.10 ± 1.75	−64.50 ± 1.37	−69.80 ± 1.67	−73.90 ± 1.49*
Input Resistance (MΩ)	744.59 ± 46.10	285.40 ± 12.67*+	161.80 ± 20.09*+	133.40 ± 17.37*
Time Constant (ms)	72.40 ± 3.98	39.50 ± 3.40*+	20.80 ± 2.10*+	21.50 ± 1.38*
Rheobase (pA)	34.67 ± 4.94	110.00 ± 14.65*+	197.30 ± 26.32*+	209.00 ± 13.26*
Voltage Depolarization (mV)	21.67 ± 2.05	23.90 ± 1.46	33.20 ± 1.78*+	31.20 ± 1.33*
Voltage Threshold (mV)	−43.50 ± 2.83	−42.00 ± 1.12	−36.70 ± 2.31	−42.80 ± 1.63
Action Potential Amplitude (mV)	92.40 ± 0.96	104.10 ± 2.92*+	121.10 ± 2.69*+	118.80 ± 1.31*
Action Potential Duration (ms)	2.98 ± 0.16	1.96 ± 0.11*+	1.47 ± 0.11*+	1.48 ± 0.06*
Ahp Duration (ms)	264.68 ± 16.60	270.44 ± 23.49	159.39 ± 13.85*+	144.23 ± 11.61*
Frequency Gain ($AP \cdot s^{-1} \cdot nA^{-1}$)	91.11 ± 6.47	53.81 ± 6.98*+	48.30 ± 4.50*	33.64 ± 3.04*
Maximum Frequency ($AP \cdot s^{-1}$)	18.07 ± 1.35	20.60 ± 2.25	33.93 ± 3.66*+	32.30 ± 2.95*
Cancelation Current (pA)	174.33 ± 17.24	437.00 ± 64.57	987.00 ± 105.50*+	1060.00 ± 101.62*
Cells with Sag (%)	6.67	66.67*	80.00*	85.71*

An asterisk indicates a significant difference from the newborn group; a cross indicates a difference between adjacent groups. The significance level was established as $p \leq 0.05$. All data are presented as mean ± standard error of the mean.
AP, action potential.

is a measure of neuron size, this indicates that motor cortex pyramidal neurons increase their size beyond the first month.

Membrane time constant also decreased with postnatal age and showed a temporal course similar to that of input resistance (**Figures 2B,G**). As for the input resistance, the raw data of the time constant fitted a single exponential decay ($r = 0.88$; $\tau = 10.92$ days), occurring the 63% of the total decrease in the first two postnatal weeks, as it is shown by the time constant of the fit. Thus, we demonstrated a significant drop in this parameter between newborn and infantile group. Plus, comparisons between the means of age groups demonstrate differences between infantile and young adult group and newborn and young adult group too, without any differences between the two last groups (**Figure 2G** and **Table 1**). To know whether time constant decreased as a function of input resistance, we studied the co-variation between both parameters for the whole population. A significant well-fitted linear relationship was found between the two parameters ($r = 0.86$; $p < 0.0001$: **Figure 2H**).

Characteristics of the Action Potentials of Layer V Pyramidal Neurons From the Motor Cortex During Postnatal Development

The rheobase or minimum current able to elicit an action potential increased during postnatal development, the best fit adjusting a single exponential decay ($r = 0.74$; $\tau = 17.33$). Indeed, neurons from infantile group displayed a rheobase more than 3-fold higher than the newborn ones. In young adult and adult groups, the rheobase was almost 6-fold higher than in this youngest group. Statistical differences were found in the comparisons between the first three age groups being the last one only statistically different with respect to the control group (**Figures 3A,B** and **Table 1**). The increase in rheobase presented a quite similar temporal course, although delayed, respect to the decrease in input resistance, accordingly, we analyzed if these two parameters co-varied during postnatal development. A significant linear relationship was found between these two parameters ($r = -0{,}71$; $p < 0.0001$; **Figure 3C**).

As well as input resistance, other parameters such as membrane potential, depolarization voltage or voltage threshold could be influencing the rheobase. As mentioned above, resting membrane potential was hyperpolarized during development and furthermore, it could be contributing to the rheobase increase. When we analyzed the relationship between these parameters a weak but significant correlation was found ($r = -0.44$; $p = 0.0008$; **Figure 3D**), suggesting an influence of the membrane potential to the rheobase decrease during development.

Regarding voltage threshold and depolarization voltage, the first cannot be influencing the change in rheobase since we have described that it is established at birth (**Figures 3A,E** and **Table 1**). About the latter, we found that there was an increase in this parameter during development, this increase being statistically significant when newborn (21.67 ± 2.05 mV) or infantile (23.90 ± 1.46 mV) groups were compared with the oldest one (33.2 ± 1.78 mV). No differences were found between the two older groups (**Figures 3A,F** and **Table 1**), meaning that depolarization voltage was established at the end of the first month. **Figure 3F** shows the depolarization voltage values for each neuron along the postnatal days (open symbols) and those raw data fit a linear regression with a slope of 0.37 mV/day ($r = 0.54$; $p < 0.0001$). According to this, the increase in depolarization voltage could be underlying the increase in rheobase and a good relationship was found when we analyzed the correlation between both parameters during development ($r = 0.56$; $p < 0.0001$: **Figure 3G**).

Furthermore, action potential duration and amplitude and AHP duration were measured, and intense changes were found (**Figure 4** and **Table 1**). Action potential amplitude increased during postnatal maturation, fitting a single exponential decay ($r = 0.78$; $\tau = 17.44$) and being statistically significant between

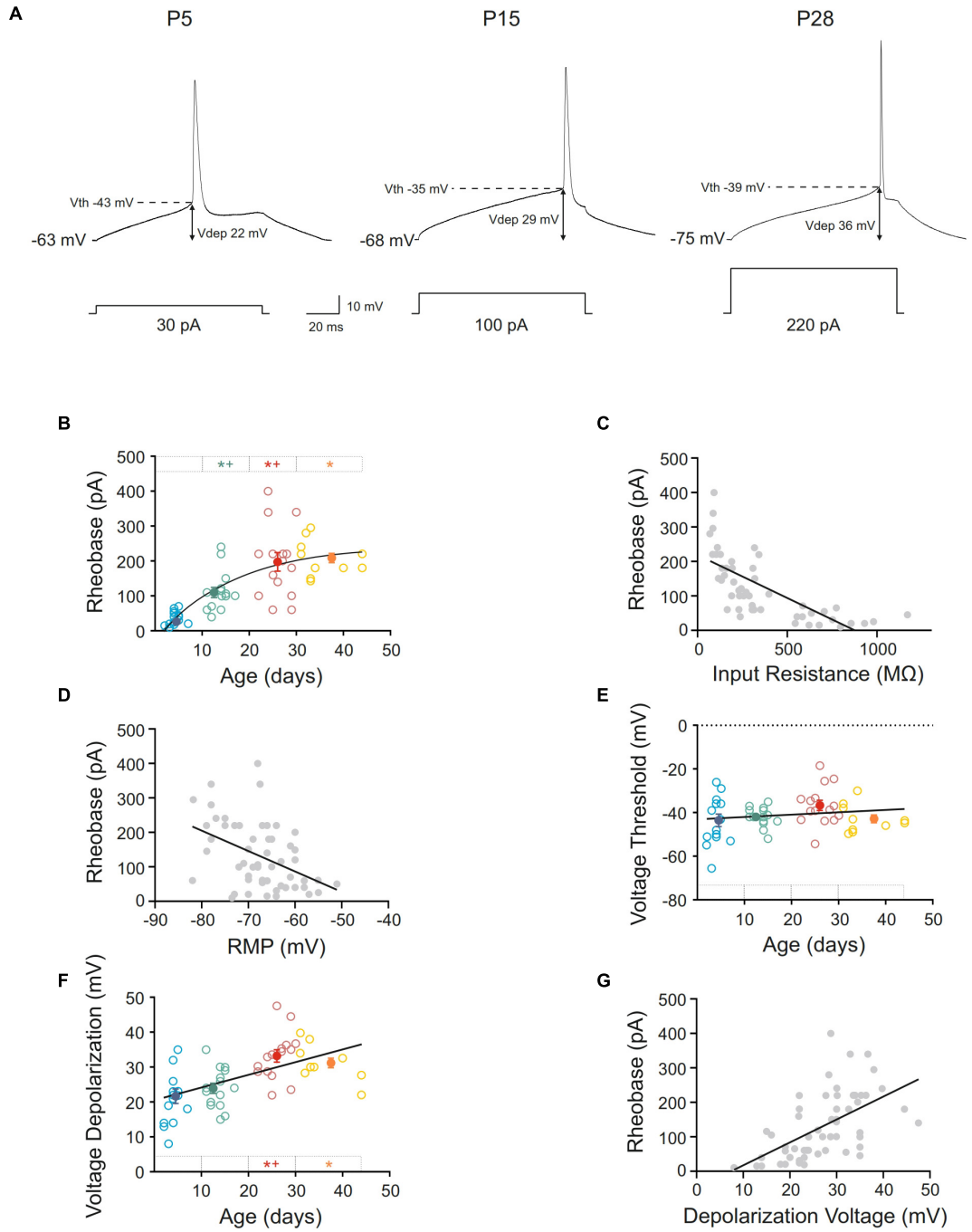

FIGURE 3 | Postnatal development of rheobase and threshold and depolarization voltages of motor cortex pyramidal neurons. **(A)** Membrane voltage responses to the minimum current (rheobase) required to evoke an action potential in representative neurons of different postnatal ages. **(B,E,F)** Scatter plots showing the changes in rheobase **(B)**, voltage threshold **(E),** and voltage depolarization **(F)** as a function of postnatal age. Open symbols represent the raw data, while filled symbols are the means of the four different age groups and their standard errors. Each group is represented by a color (blue = newborn, $n = 15$; green = infantile, $n = 15$; red = young adult, $n = 15$; yellow = adult, $n = 10$). An asterisk indicates a significant difference from the newborn group; a cross indicates a difference between adjacent groups. The significance level was established as $p \leq 0.05$. **(C,D,G)** Correlation between rheobase and input resistance, $r = -0.71$; $p < 0.0001$ **(C)**, rheobase and RMP, $r = -0.44$; $p < 0.0008$ **(D)** and rheobase, and depolarization voltage, $r = 0.56$; $p < 0.0001$ **(G)**.

newborn (92.40 ± 0.96 pA), infantile (104.10 ± 2.92 pA) and young adult (121.10 ± 2.69 pA) groups when compared to each other (**Figures 4A,B**). As illustrated in **Figure 4B** and showed by the fitting time constant ($\tau = 17.44$ days), major changes take place during the first three weeks and no changes were observed between the two older groups. Action

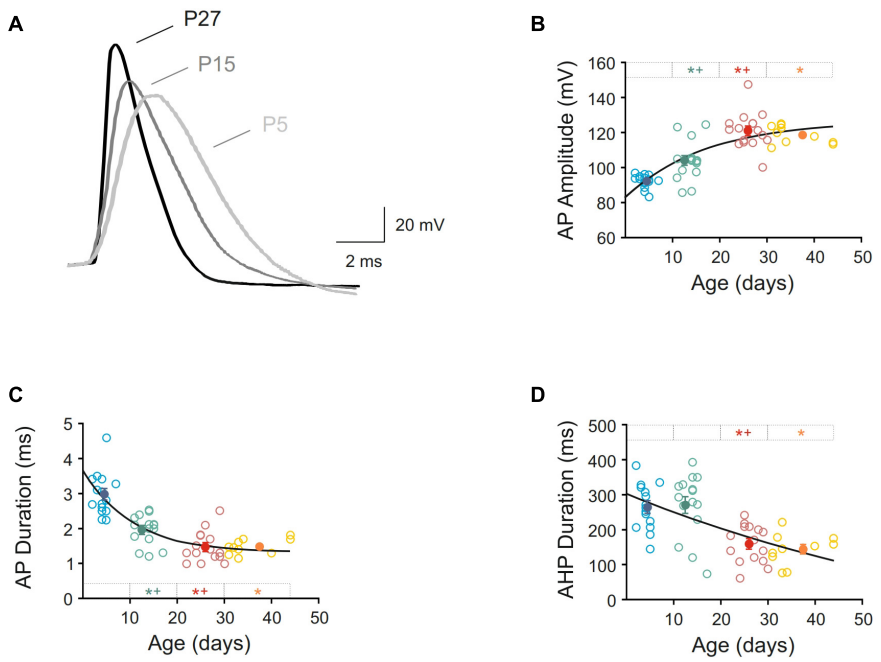

FIGURE 4 | Postnatal development of action potential characteristics of motor cortex pyramidal neurons. **(A)** Membrane voltage responses to suprathreshold stimuli in three representative neurons from newborn, infantile and young adult age groups. Action potentials were synchronized at the beginning of the rising phase to show the differences in amplitude and duration. **(B–D)** Scatter plots showing the amplitude of action potential **(B)**, duration of action potential **(C),** and duration of afterhyperpolarization phase or AHP **(D)** as a function of postnatal age. Open symbols represent the raw data, while filled symbols are the means of the four different age groups and their standard errors. Each group is represented by a color (blue = newborn, $n = 15$; green = infantile, $n = 15$; red = young adult, $n = 15$; yellow = adult, $n = 10$). An asterisk indicates a significant difference from the newborn group; a cross indicates a difference between adjacent groups. The significance level was established as $p \leq 0.05$.

potential duration decreased during development and significant differences were found between newborn, infantile and young adult groups. Nevertheless, the oldest group did not differ from the young adult one, also maturing this parameter in the first month after birth (**Figures 4A,C** and **Table 1**). Finally, the AHP duration also decreased with age being this reduction statistically significant when newborn (264.68 ± 16.60 ms) or infantile (270.44 ± 23.49 ms) groups were compared with the adult one (159.39 ± 13.85 ms). No differences were found neither between newborn and infantile groups nor between young adult and adult groups for this parameter (**Figure 4D** and **Table 1**). The raw data along age fit a linear regression with an adjustment of r = 0.60 (slope = −4.42 ms/day; $p < 0.0001$).

Repetitive Firing Properties of Pyramidal Neurons From the Motor Cortex During Postnatal Development

All recorded pyramidal neurons were silent at resting membrane potential and repetitively discharged when long lasting current pulses were applied. Neurons from this study showed a regular spiking discharge with some grade of adaptation and reached a firing frequency plateau at high intensity currents (**Figure 5A**). To know if repetitive firing properties were established or not at birth several parameters were studied. Thus, frequency gain was measured and a decline in this parameter was found with age. The raw data for this parameter fitted a single exponential decay (r = 0.71). The fitting time constant shows that major changes occur before the beginning of the second week ($\tau = 8.81$ days; **Figure 5B**). Statistical analyses were consistent with these findings, demonstrating that the diminution was significant in the second group of age, with any posterior changes (**Figures 5A,B** and **Table 1**). Subsequently, the frequency gain matured in the first two postnatal weeks. Frequency gain could be influenced by several parameters, being the AHP duration one of the most important; however, no correlation was found between these membrane properties during development (r = 0.20 and $p = 0.14$; **Figure 5C**). Otherwise, one possible explanation of the decrease in frequency gain is the demonstrated fall in input resistance, subsequently, we wondered whether their co-varied. A significant well-fitted linear relationship was found between these two parameters (r = 0.67; $p < 0.0001$; **Figure 5D**).

Additionally, the maximum frequency of the discharge of motor cortex neurons incremented with age. Neurons from adult and young adult groups reached a maximum frequency almost 2-fold higher than neurons from the newborn and infantile groups (**Figure 5A**). Raw data for this parameter is represented by open symbols in **Figure 5E**, showing that this parameter increased linearly with age, with a slope of 0.52 AP · s^{-1}/day (r = 0.51; $p < 0.0001$). However, even this linearity, statistical analysis of the age group means (filled symbols in **Figure 5E** and **Table 1**) showed differences between infantile and young adult groups,

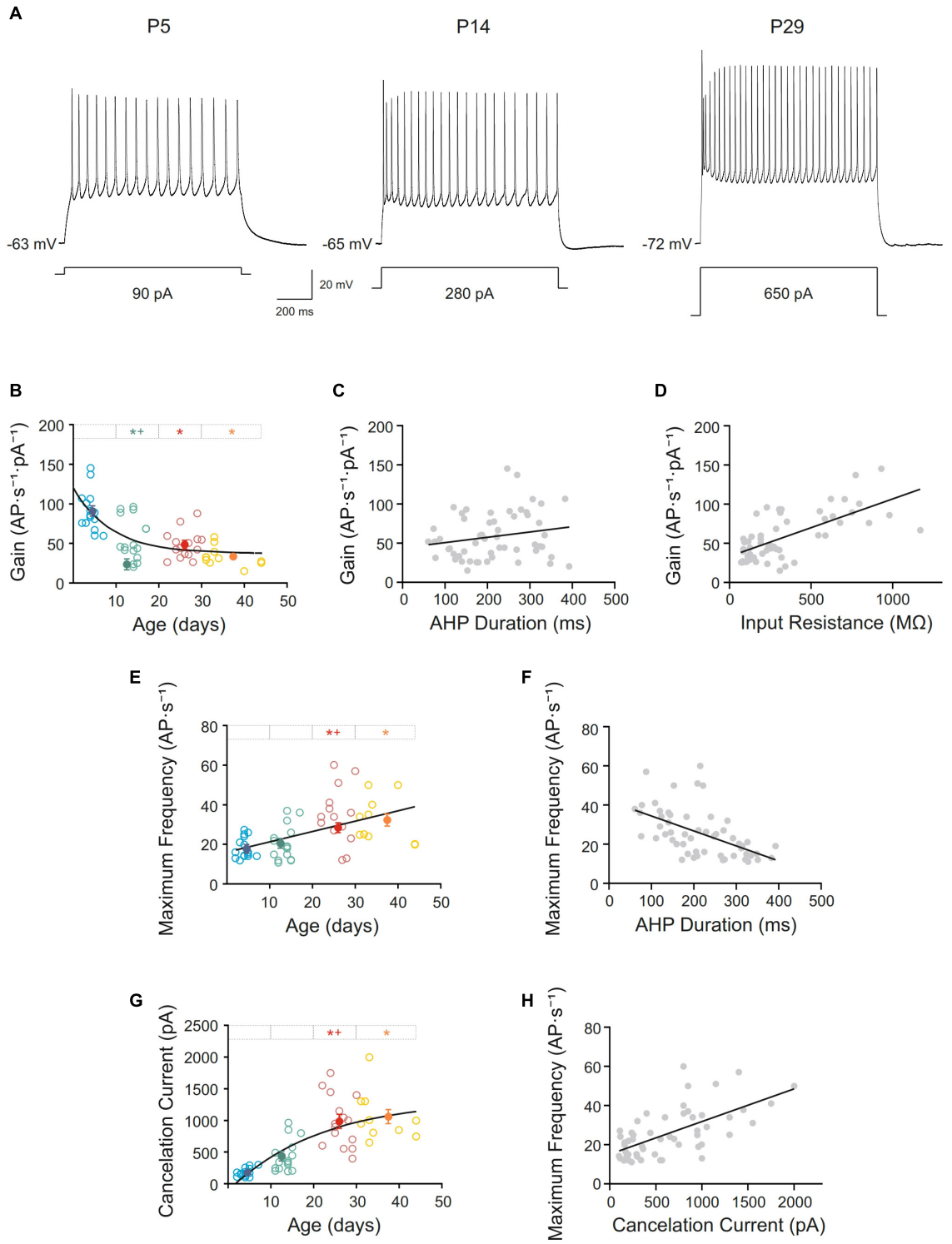

FIGURE 5 | Postnatal development of repetitive firing properties of motor cortex pyramidal neurons. **(A)** Membrane voltage responses to long-lasting current pulse (1s) in representative neurons of different ages. **(B,E,G)** Scatter plots showing the firing frequency gain **(B)**, maximum frequency **(E),** and cancelation current **(G)** as a function of postnatal age. Open symbols represent the raw data, while filled symbols are the means of the four different age groups and their standard errors. Each group is represented by a color (blue = newborn, $n = 15$; green = infantile, $n = 15$; red = young adult, $n = 15$; yellow = adult, $n = 10$). An asterisk indicates a significant difference from the newborn group; a cross indicates a difference between adjacent groups. The significance level was established as $p \leq 0.05$. **(C,D,F,H)** Correlation between gain and the afterhyperpolarization phase (AHP) duration, $r = 0.20$, $p = 0.14$ **(C)**, gain and input resistance, $r = 0.67$, $p < 0.0001$ **(D)** and maximum frequency and AHP duration, $r = -0.54$, $p < 0.0001$, **(F)** and maximum frequency and cancelation current, $r = 0.64$, $p < 0.001$ **(H)**.

implying that this parameter matured within the second and the third weeks of development. No significant differences were found between newborn and infantile groups or between the last two groups. This increase in maximum frequency presented a temporal course close to the decrease on AHP and a good correlation was found between them ($r = -0.54$; $p < 0.0001$; **Figure 5F**).

Finally, cancelation current was also analyzed, showing an increase during postnatal development from 174.33 ± 17.24 pA in newborn group to 1060.00 ± 101.62 pA in adult group (Filled symbols in **Figure 5G** and **Table 1**). The best fit for the raw data was a single exponential decay ($r = 0.75$; $\tau = 21.58$ days). Regarding group means, this increase was significant between the second and third groups, which is consistent with a fitting time constant of 21.58 days (see **Figure 5G**), reaching the parameter a stable level from that moment on, without statistical differences between the third and the fourth groups (**Figures 5A,G** and **Table 1**). This rise in cancelation current could also be underlying the increase in maximum frequency and, in fact, both parameters showed a good correlation during development ($r = 0.64$; $p < 0.001$; **Figure 5H**).

DISCUSSION

This work shows that the passive membrane properties of layer V pyramidal neurons of the motor cortex are not established at birth. On the contrary, they evolve along the first month after birth. We also show that the characteristics of the action potentials as well as the repetitive firing properties in these neurons are refined during postnatal development leading to a reduction in neuronal excitability and to an increase in the working range in adult neurons, allowing more sensitive and accurate responses.

Methodological Considerations

Pyramidal neurons of layer V were identified and differentiated from non-pyramidal cells using soma morphology in IR-DIC before the patch recording. In addition, some of the neurons were intracellularly injected and post-patch identified, being all of them pyramidal neurons. Besides, pyramidal neurons were also identified by their firing behavior characterized by an accommodating regular spiking discharge. Non-pyramidal cells were classically described as fast spiking cells that display tonic discharges of fast action potentials with no accommodation. However, other two populations of non-pyramidal cells have been described. One of them is characterized by an irregular spiking with bursts of action potentials at an irregular frequency and the other population displayed a firing behavior characterized by a marked accommodation. This latter population of non-pyramidal cells could be confused with pyramidal neurons. However, they can be differentiated by other electrophysiological parameters as the presence of a rebound of action potentials after a hyperpolarizing current pulse or larger amplitude of AHP (Cauli et al., 1997). Nevertheless, we cannot discard the possibility that a few of these cells could be included as pyramidal neurons in our work.

Furthermore, no bursting discharge was observed in our work for pyramidal neurons so we cannot differentiate by their firing behavior, as in other studies, between cortico-cortical projecting pyramidal neurons (regular spiking neurons) and pyramidal neurons projecting to subcortical regions (burst neurons) (Molnár and Cheung, 2006). This could be due to the fact that in our study the period between the induction of the anesthesia and the decapitation usually did not exceed 2–4 min and, as has been shown, under this condition cells did not display differences in their action potential behavior (Christophe et al., 2005). This short period of anesthesia did not affect the electrophysiological properties of the cells either, since recordings with and without anesthesia were performed in the infantile group with similar results.

Passive Membrane Properties of Layer V Pyramidal Neurons From the Motor Cortex Are Not Established at Birth

The present results show a hyperpolarization of the resting membrane potential during postnatal development. This fact seems to be a general trend among neocortical pyramidal neurons (Zhu, 2000; Zhang, 2004; Christophe et al., 2005; Etherington and Williams, 2011; Kroon et al., 2019) since in other motor neurons such as genioglossal, oculomotor and spinal it remains constant (Nunez-Abades et al., 1993; Carrascal et al., 2006; Smith and Brownstone, 2020). This drift could be explained by, at least, three different mechanisms. First, a developmental increase of K^+ leak conductances. Second, a postnatal GABA shift from depolarizing to hyperpolarizing, given by a greater activity of the $Na^+/K^+/2Cl^-$ cotransporter (NKCC1) in younger neurons and a higher expression of the K^+/Cl^- cotransporter (KCC2) in mature ones (Yamada et al., 2004; Kilb et al., 2013; Luhmann et al., 2014; Peerboom and Wierenga, 2021). Third, it has been proven that tonic GABAergic currents produce membrane hyperpolarization (Torres-Torrelo et al., 2014). Therefore, an increase in GABAergic synaptic input, efficiency and/or in the number of extrasynaptic $GABA_A$ receptors during development could explain, at least in part, the membrane potential hyperpolarization observed in the neurons of this study.

Furthermore, input resistance decreased during the first postnatal month, especially during the first two weeks, in pyramidal motor neurons. This decline is a characteristic common to most neuronal populations, including not only pyramidal and motor neurons, but also other populations. However, in genioglossal and oculomotor nucleus this parameter is already established at the second postnatal week, while in spinal and neocortical neurons continue to decrease during the whole month (Nunez-Abades et al., 1993; Perez Velazquez and Carlen, 1996; Vincent and Tell, 1997; Ahuja and Wu, 2000; Belleau and Warren, 2000; Zhu, 2000; Murphy and du Lac, 2001; Zhang, 2004; Christophe et al., 2005; Carrascal et al., 2006; Etherington and Williams, 2011; Smith and Brownstone, 2020). The decrease in input resistance could be due to an increase or redistribution of the K^+ leak channels as well as GABAergic synaptic inputs (Cameron and Nunez-Abades, 2000; Torres-Torrelo et al., 2014).

Neuronal size increased during postnatal development as in other studies (Nunez-Abades and Cameron, 1995; Zhu, 2000; Zhang, 2004; Carrascal et al., 2009; Kroon et al., 2019; Smith and Brownstone, 2020) and it could also be the underlying cause of the decrease in input resistance found in our study. In fact, a relationship between input resistance decay and neuronal size increment was found except for genioglossal motoneurons where neurons grow during the 3rd week (Nunez-Abades et al., 1994). In our populations the relationship between input resistance and capacitance, an indirect measure of neuronal size, was weak meaning that the increase in size is not the sole cause of input resistance decrease. The time constant, that reflects integrative properties of the cells, also decreased in pyramidal motor neurons during postnatal maturation, showing a strong correlation with the input resistance decay. This finding is also consistent with those reported for the aforementioned neuronal populations, occurring mainly during the first two postnatal weeks (Nunez-Abades et al., 1993; Perez Velazquez and Carlen, 1996; Vincent and Tell, 1997; Ahuja and Wu, 2000; Belleau and Warren, 2000; Murphy and du Lac, 2001; Zhang, 2004; Carrascal et al., 2006; Etherington and Williams, 2011; Smith and Brownstone, 2020) although in our population the time constant continues to decrease during the whole month, being the parameter stable from this date on. Finally, it has been found that the number of neurons showing voltage rectification is more than 10 fold higher in adults than in neonates, this tendency being common to most studied neurons. The increasing frequency of sag with age found in here could be parallel to a larger density of channels carrying inward rectification currents (Ih). This current is largely carried by sodium ions, and it is activated by a hyperpolarizing input, allowing the repolarization of the cell membrane (Berger et al., 1996; Carrascal et al., 2015).

The Action Potential Characteristics Are Refined During Postnatal Development

Rheobase increased in motor cortex pyramidal neurons during postnatal development as much as in other neocortical areas (Zhu, 2000; Etherington and Williams, 2011; Kroon et al., 2019). These changes in rheobase implies a decrease in developmental neuronal excitability (Nunez-Abades et al., 1993; Etherington and Williams, 2011). However, different trends in rheobase modifications with postnatal maturation have also been reported in other motor and non-motor neuronal pools. Thus, the rheobase increases in accumbens (Belleau and Warren, 2000), decreases in oculomotor (Carrascal et al., 2006), and is already established at birth in dorsal horn neurons (Baccei and Fitzgerald, 2005). These results lead to the suggestion that the postnatal development of this parameter depends on each neuronal pool. Regarding voltage threshold and voltage depolarization, the present study has shown that, while the former was established at birth, the latter increased with the developmental process. Voltage threshold also remains constant in genioglossal and spinal neurons (Nunez-Abades et al., 1993; Smith and Brownstone, 2020) while it decreases in oculomotor, prefrontal, and visual neurons (Zhang, 2004; Christophe et al., 2005; Carrascal et al., 2006; Etherington and Williams, 2011; Kroon et al., 2019). Voltage depolarization remains constant in some populations such as prefrontal pyramidal neurons and genioglossal motoneurons (Nunez-Abades et al., 1993; Zhang, 2004) and decreases in others such as vestibular neurons (Straka et al., 2005; Carrascal et al., 2006).

The present results show, as in all studied pyramidal neurons from layer V, an increase in the action potential amplitude and a decay in the action potential duration and AHP (Zhu, 2000; Zhang, 2004; Christophe et al., 2005; Etherington and Williams, 2011). The decrease in action potential duration and AHP is also demonstrated in non-pyramidal cells, being firstly established in genioglossal motoneurons (Nunez-Abades et al., 1993; Vincent and Tell, 1997; Murphy and du Lac, 2001; Carrascal et al., 2006; Smith and Brownstone, 2020). Nevertheless, the increase in the amplitude of action potential during development found in here and other studies (Etherington and Williams, 2011; Kroon et al., 2019) is not universal among neuronal pools because in other populations this parameter is already established at birth such is genioglossal and oculomotor motoneurons (Nunez-Abades et al., 1993; Carrascal et al., 2006). The refinement in action potential shape is mainly given by an increase in density and/or a faster activation of the voltage-gated Na^+ and K^+ channels (Nunez-Abades et al., 1993; Carrascal et al., 2006, 2015; Smith and Brownstone, 2020). A decrement in voltage-activated Ca^{2+} channels could also contribute to the decrease in spike duration, and these conductances could also be responsible of the decay in AHP duration, since this phase is dependent on Ca^{2+}-dependent K^+ currents (Nunez-Abades et al., 1993; Carrascal et al., 2006).

Repetitive Firing Properties of Pyramidal Neurons From the Motor Cortex Are Adjusted During Postnatal Development

Pyramidal neurons from the primary motor cortex underwent wide modifications in their repetitive firing properties, a measurement of neuronal responsiveness. It can be stated that all the neuronal populations studied to date modified their firing properties, although with different patterns of change. Frequency gain decreases in neocortical pyramidal neurons (Zhang, 2004), including those from the present work, as well as in lumbar and cervical motoneurons (Smith and Brownstone, 2020) while increases in other motor (Nunez-Abades et al., 1993; Carrascal et al., 2006) and non-motor pools (Tennigkeit et al., 1998). However, in all studied neurons the maximum frequency of discharge increased with postnatal development (Nunez-Abades et al., 1993; Zhang, 2004; Carrascal et al., 2006; Smith and Brownstone, 2020), although it does not mature at the same time. Thus, while in pyramidal neurons of the motor cortex the maximum firing frequency increases from the third week, in prefrontal pyramidal neurons and genioglossal motoneurons it occurs earlier (Zhang, 2004). This higher firing frequency in adult neurons could be due to the decrease in the duration of action potential and AHP (Smith and Brownstone, 2020). In fact, the good correlation between AHP duration and the maximum firing frequency seen in here indicates that both parameters mature in parallel. Other studies (Nunez-Abades et al., 1993;

Carrascal et al., 2006) propose that this increase in maximum firing frequency would be more linked to a faster activation of the delay rectifier or to a shorter inactivation stage of the voltage-gated Na^+ channels. Regardless of the ionic nature that underlies these changes, this increase in the maximum firing frequency would be influenced by a greater cancelation current in the adult population, which increases the working range of these motor cortex neurons. The combination of increased working range and decreased frequency gain allow neurons to respond with greater precision to a greater range of current intensities (Smith and Brownstone, 2020).

Comparing our study with those reported for other pyramidal neurons, and mentioned above, it seems that the electrophysiological parameters for these neurons maturated during postnatal development in the same way independently of the cortex region and reaching similar final values. Overall, all these changes led to a decrease in excitability in most of the pyramidal and motor neuron populations except in oculomotor nucleus, this increase being consistent with the task of this motoneurons that must reach higher discharge to control eye movement (Carrascal et al., 2010). On the other hand, in genioglossal motoneurons the postanal refinement of electrophysiological properties is established earlier than in the other populations being the spinal and above all the motor cortex populations the last ones. The fact that electrophysiological properties of genioglossal motoneurons were established earlier than those of other populations is also consistent with the task that they develop. This pool of neurons innervates the tongue, a muscle that is implicate in several motor tasks, such as suckling, swallowing, and breathing, tasks that must be operative soon after birth (Nunez-Abades et al., 1993). In contrast, the locomotor function develops later in time, since neither the musculoskeletal system nor the nervous system that innervates it is sufficiently developed in rodents until at least the second-third postnatal weeks, when quadruped ambulation begins (Smith and Brownstone, 2020). Therefore, the maturation of the electrophysiological properties of motor neurons is more related to the specific motor task that they perform than to their location along the rostro-caudal axis.

CONCLUSION

The electrophysiological properties of layer V pyramidal neurons from the primary motor cortex are tuned during the first postnatal month, although the time course of these changes depends on each specific electrophysiological parameter. These electrophysiological modifications lead to a decrease in excitability and an increase in the working range. This allows mature neurons to generate more precise and graded responses and contributes to the development of the great variety of specialized neuronal circuits founding the complex behaviors of adult mammals. By comparing the evolution of the different neuronal properties in different motor neuron populations during postnatal development, we hypothesize that the temporal course of the acquisition of motor neuron functional properties does not depend on the anteroposterior localization of the nuclei but on the specific motor task that they perform.

DATA AVAILABILITY STATEMENT

The raw data supporting the conclusions of this article will be made available by the authors, without undue reservation.

ETHICS STATEMENT

The animal study was reviewed and approved by the Animal Ethics Committee of the University of Seville.

AUTHOR CONTRIBUTIONS

PP-G and RP-D: data acquisition and analysis of electrophysiological experiments, discussion of results, and manuscript preparation and figure design. NG-D, RG-O, and SD-G: data analysis, discussion of results, and figure design. CC and PN-A: experimental design, data analysis, discussion of results, and manuscript preparation and writing. LC: conception of the work, experimental design, data acquisition and analysis, discussion of results, manuscript preparation, and writing. All authors contributed to the article and approved the submitted version.

FUNDING

This work was partially supported by Spanish Ministerio de Ciencia, Innovación y Universidades (RTI2018-099908-B-C21) and co-financed by the 2014–2020 ERDF Operational Programme and by the Department of Economy, Knowledge, Business and University of the Regional Government of Andalusia (FEDER-UCA18-106647).

ACKNOWLEDGMENTS

We sincerely thank Ella Gorton, a visiting fellow of the University of Manchester, United Kingdom, supported by an Erasmus Practices grant, for her initial contribution to this work.

REFERENCES

Ahuja, T. K., and Wu, S. H. (2000). Developmental changes in physiological properties in the rat's dorsal nucleus of the lateral lemniscus. *Hear. Res.* 149, 33–45. doi: 10.1016/S0378-5955(00)00159-3

Amaral, D. G., and Strick, P. L. (2013). "The Organization of the Central Nervous System" in *Principles of Neural Sciences*. eds E. R. Kandel, J. H. Schawrtz, T. M.

Jessel, S. A. Siegelbaum, and A. J. Hudspethc (United States: McGraw-Hill). 337–355.

Baccei, M. L., and Fitzgerald, M. (2005). Intrinsic firing properties of developing rat superficial dorsal horn neurons. *Neuroreport* 16, 1325–8.

Belleau, M. L., and Warren, R. A. (2000). Postnatal development of electrophysiological properties of nucleus accumbens neurons. *J. Neurophysiol.* 84, 2204–2216. doi: 10.1152/jn.2000.84.5.2204

Berger, A. J., Bayliss, D. A., and Viana, F. (1996). Development of hypoglossal motoneurons. *J. Appl. Physiol.* 81, 1039–1048. doi: 10.1152/jappl.1996.81.3.1039

Borrell, V. (2019). Recent advances in understanding neocortical development. *F1000Res*. 8:1791. doi: 10.12688/f1000research.20332.1

Burgard, E. C., and Hablitz, J. J. (1993). Developmental changes in NMDA and non-NMDA receptor-mediated synaptic potentials in rat neocortex. *J. Neurophysiol.* 69, 230–240. doi: 10.1152/jn.1993.69.1.230

Cameron, W. E., and Nunez-Abades, P. A. (2000). Physiological changes accompanying anatomical remodeling of mammalian motoneurons during postnatal development. *Brain Res. Bull.* 53, 523–527. doi: 10.1016/S0361-9230(00)00385-3

Carrascal, L., Gorton, E., Pardillo-Díaz, R., Perez-García, P., Gómez-Oliva, R., Castro, C., et al. (2020). Age-Dependent Vulnerability to Oxidative Stress of Postnatal Rat Pyramidal Motor Cortex Neurons. *Antioxidants* 9:1307. doi: 10.3390/antiox9121307

Carrascal, L., Luque, M. A., Sobrino, V., Torres, B., and Nunez-Abades, P. (2010). Postnatal development enhances the effects of cholinergic inputs on recruitment threshold and firing rate of rat oculomotor nucleus motoneurons. *Neuroscience* 171, 613–621. doi: 10.1016/j.neuroscience.2010.09.001

Carrascal, L., Nieto-Gonzalez, J. L., Núñez-Abades, P., and Torres, B. (2006). Temporal sequence of changes in electrophysiological properties of oculomotor motoneurons during postnatal development. *Neuroscience* 140, 1223–1237. doi: 10.1016/j.neuroscience.2006.03.006

Carrascal, L., Nieto-González, J. L., Pardillo-Díaz, R., Pásaro, R., Barrionuevo, G., Torres, B., et al. (2015). Time windows for postnatal changes in morphology and membrane excitability of genioglossal and oculomotor motoneurons. *World J. Neurol.* 5, 113–131. doi: 10.5316/wjn.v5.i4.113

Carrascal, L., Nieto-Gonzalez, J. L., Torres, B., and Nunez-Abades, P. (2009). Changes in somatodendritic morphometry of rat oculomotor nucleus motoneurons during postnatal development. *J. Compar. Neurol.* 514, 189–202. doi: 10.1002/cne.21996

Cauli, B., Audinat, E., Lambolez, B., Angulo, M. C., Ropert, N., Tsuzuki, K., et al. (1997). Molecular and Physiological Diversity of Cortical Nonpyramidal Cells. *J. Neurosci.* 17, 3894L–906. doi: 10.1523/JNEUROSCI.17-10-03894.1997

Chomiak, T., and Hu, B. (2013). Alterations of neocortical development and maturation in autism: insight from valproic acid exposure and animal models of autism. *Neurotoxicol. Teratol.* 36, 57–66. doi: 10.1016/j.ntt.2012.08.005

Chomiak, T., Peters, S., and Hu, B. (2008). Functional architecture and spike timing properties of corticofugal projections from rat ventral temporal cortex. *J. Neurophysiol.* 100, 327–335. doi: 10.1152/jn.90392.2008

Christophe, E., Doerflinger, N., Lavery, D. J., Molnár, Z., Charpak, S., and Audinat, E. (2005). Two populations of layer V pyramidal cells of the mouse neocortex: development and sensitivity to anesthetics. *J. Neurophysiol.* 94, 3357–3367. doi: 10.1152/jn.00076.2005

Elston, G. N., and Fujita, I. (2014). Pyramidal cell development: postnatal spinogenesis, dendritic growth, axon growth, and electrophysiology. *Front. Neuroanat.* 8, 1–20. doi: 10.3389/fnana.2014.00078

Etherington, S. J., and Williams, S. R. (2011). Postnatal development of intrinsic and synaptic properties transforms signaling in the layer 5 excitatory neural network of the visual cortex. *J. Neurosci.* 31, 9526–9537. doi: 10.1523/JNEUROSCI.0458-11.2011

Kasper, E. M., Larkman, A., and Lubke, J. (1994). Pyramidal Neurons in Layer 5 of the Rat Visual Cortex . I . Correlation Among Cell Morphology, Intrinsic Electrophysiological Properties, and Axon Targets. *J. Compar. Neurol.* 339, 459–474. doi: 10.1002/cne.903390402

Kilb, W., Kirischuk, S., and Luhmann, H. J. (2013). Role of tonic GABAergic currents during pre- and early postnatal rodent development. *Front. Neural Circuits* 7:139. doi: 10.3389/fncir.2013.00139

Kriegstein, A. R., Suppes, T., and Prince, D. A. (1987). Cellular and synaptic physiology and epileptogenesis of developing rat neocortical neurons in vitro. *Dev. Brain Res.* 34, 161–171. doi: 10.1016/0165-3806(87)90206-9

Kroon, T., van Hugte, E., van Linge, L., Mansvelder, H. D., and Meredith, R. M. (2019). Early postnatal development of pyramidal neurons across layers of the mouse medial prefrontal cortex. *Sci. Rep.* 9, 1–16. doi: 10.1038/s41598-019-41661-9

Luhmann, H. J., Kirischuk, S., Sinning, A., and Kilb, W. (2014). Early GABAergic circuitry in the cerebral cortex. *Curr. Opin. Neurobiol.* 26, 72–78. doi: 10.1016/j.conb.2013.12.014

McCormick, D. A., and Prince, D. A. (1987). Post-natal development of electrophysiological properties of rat cerebral cortical pyramidal neurones. *J. Physiol.* 393, 743–762. doi: 10.1113/jphysiol.1987.sp016851

Molnár, Z., and Cheung, A. F. P. (2006). Towards the classification of subpopulations of layer V pyramidal projection neurons. *Neurosci. Res.* 55, 105–115. doi: 10.1016/j.neures.2006.02.008

Molyneaux, B. J., Arlotta, P., Menezes, J. R. L., and Macklis, J. D. (2007). Neuronal subtype specification in the cerebral cortex. *Nat. Rev. Neurosci.* 8, 427–437. doi: 10.1038/nrn2151

Murphy, G. J., and du Lac, S. (2001). Postnatal development of spike generation in rat medial vestibular nucleus neurons. *J. Neurophysiol.* 85, 1899–1906. doi: 10.1152/jn.2001.85.5.1899

Nunez-Abades, P. A., Spielmann, J. M., Barrionuevo, G., and Cameron, W. E. (1993). In vitro electrophysiology of developing genioglossal motoneurons in the rat. *J. Neurophysiol.* 70, 1401–1411. doi: 10.1152/jn.1993.70.4.1401

Nunez-Abades, P. A., Barrionuevo, G., and Cameron, W. E. (1994). Morphology of developing rat genioglossal motoneurons studied in vitro: changes in Length, Branching Pattern, and Spatial Distribution of Dendrites. *J. Compar. Neurol.* 339, 401–420. doi: 10.1002/cne.903390308

Nunez-Abades, P. A., and Cameron, W. E. (1995). Morphology of developing rat genioglossal motoneurons studied in vitro: relative changes in diameter and surface area of somata and dendrites. *J. Compar. Neurol.* 353, 129–142. doi: 10.1002/cne.903530112

Pardillo-Díaz, R., Carrascal, L., Ayala, A., and Nunez-Abades, P. (2015). Oxidative stress induced by cumene hydroperoxide evokes changes in neuronal excitability of rat motor cortex neurons. *Neuroscience* 289, 85–98. doi: 10.1016/j.neuroscience.2014.12.055

Pardillo-Díaz, R., Carrascal, L., Muñoz, M. F., Ayala, A., and Nunez-Abades, P. (2016). Time and dose dependent effects of oxidative stress induced by cumene hydroperoxide in neuronal excitability of rat motor cortex neurons. *Neurotoxicology* 53, 201–214. doi: 10.1016/j.neuro.2016.02.005

Peerboom, C., and Wierenga, C. J. (2021). The postnatal GABA shift: a developmental perspective. *Neurosci. Biobehav. Rev.* 124, 179–192. doi: 10.1016/j.neubiorev.2021.01.024

Perez Velazquez, J. L., and Carlen, P. L. (1996). Development of firing patterns and electrical properties in neurons of the rat ventrobasal thalamus. *Dev. Brain Res.* 91, 164–170. doi: 10.1016/0165-3806(95)00171-9

Petit, T. L., Leboutillier, J. C., Gregorio, A., and Libstug, H. (1988). The pattern of dendritic development in the cerebral cortex of the rat. *Dev. Brain Res.* 41, 209–219. doi: 10.1016/0165-3806(88)90183-6

Picken Bahrey, H. L., and Moody, W. J. (2003). Early development of voltage-gated ion currents and firing properties in neurons of the mouse cerebral cortex. *J. Neurophysiol.* 89, 1761–1773. doi: 10.1152/jn.00972.2002

Ramoa, A. S., and McCormick, D. A. (1994). Developmental changes in electrophysiological properties of LGNd neurons during reorganization of retinogeniculate connections. *J. Neurosci.* 14, 2089–2097. doi: 10.1523/jneurosci.14-04-02089.1994

Smith, C. C., and Brownstone, R. M. (2020). Spinal motoneuron firing properties mature from rostral to caudal during postnatal development of the mouse. *J. Physiol.* 598, 5467–5485. doi: 10.1113/JP280274

Straka, H., Vibert, N., Vidal, P. P., Moore, L. E., and Dutia, M. B. (2005). Intrinsic membrane properties of vertebrate vestibular neurons: function, development and plasticity. *Progr. Neurobiol.* 76, 349–392. doi: 10.1016/j.pneurobio.2005.10.002

Tennigkeit, F., Schwarz, D. W. F., and Puil, E. (1998). Postnatal development of signal generation in auditory thalamic neurons. *Dev. Brain Res.* 109, 255–263. doi: 10.1016/S0165-3806(98)00056-X

Torres-Torrelo, J., Rodriguez-Rosell, D., Nunez-Abades, P., Carrascal, L., and Torres, B. (2012). Glutamate modulates the firing rate in oculomotor nucleus motoneurons as a function of the recruitment threshold current. *J. Physiol.* 13, 3113–3127. doi: 10.1113/jphysiol.2011.226985

Torres-Torrelo, J., Torres, B., and Carrascal, L. (2014). Modulation of the input-output function by GABAA receptor-mediated currents in rat oculomotor nucleus motoneurons. *J. Physiol.* 592, 5047–5064. doi: 10.1113/jphysiol.2014.276576

Vincent, A., and Tell, F. (1997). Postnatal changes in electrophysiological properties of rat nucleus tractus solitarii neurons. *Eur. J. Neurosci.* 9, 1612–1624. doi: 10.1111/j.1460-9568.1997.tb01519.x

Yamada, J., Okabe, A., Toyoda, H., Kilb, W., Luhmann, H. J., and Fukuda, A. (2004). Cl- uptake promoting depolarizing GABA actions in immature rat neocortical neurones is mediated by NKCC1. *J. Physiol.* 557, 829–841. doi: 10.1113/jphysiol.2004.062471

Yuste, R. (2005). Origin and classification of neocortical interneurons. *Neuron* 48, 524–527. doi: 10.1016/j.neuron.2005.11.012

Zhang, Z. W. (2004). Maturation of Layer V Pyramidal Neurons in the Rat Prefrontal Cortex: intrinsic Properties and Synaptic Function. *J. Neurophysiol.* 91, 1171–1182. doi: 10.1152/jn.00855.2003

Zhu, J. J. (2000). Maturation of layer 5 neocortical pyramidal neurons: amplifying salient layer 1 and layer 4 inputs by Ca2+ action potentials in adult rat tuft dendrites. *J. Physiol.* 526, 571–587. doi: 10.1111/j.1469-7793.2000.00571.x

Conflict of Interest: The authors declare that the research was conducted in the absence of any commercial or financial relationships that could be construed as a potential conflict of interest.

Publisher's Note: All claims expressed in this article are solely those of the authors and do not necessarily represent those of their affiliated organizations, or those of the publisher, the editors and the reviewers. Any product that may be evaluated in this article, or claim that may be made by its manufacturer, is not guaranteed or endorsed by the publisher.

Copyright © 2021 Perez-García, Pardillo-Díaz, Geribaldi-Doldán, Gómez-Oliva, Domínguez-García, Castro, Nunez-Abades and Carrascal. This is an open-access article distributed under the terms of the Creative Commons Attribution License (CC BY). The use, distribution or reproduction in other forums is permitted, provided the original author(s) and the copyright owner(s) are credited and that the original publication in this journal is cited, in accordance with accepted academic practice. No use, distribution or reproduction is permitted which does not comply with these terms.

frontiers in Molecular Neuroscience

REVIEW
published: 02 December 2021
doi: 10.3389/fnmol.2021.759404

With the Permission of Microtubules: An Updated Overview on Microtubule Function During Axon Pathfinding

Carlos Sánchez-Huertas and Eloísa Herrera*

Instituto de Neurociencias, Consejo Superior de Investigaciones Científicas-Universidad Miguel Hernández (CSIC-UMH), Alicante, Spain

During the establishment of neural circuitry axons often need to cover long distances to reach remote targets. The stereotyped navigation of these axons defines the connectivity between brain regions and cellular subtypes. This chemotrophic guidance process mostly relies on the spatio-temporal expression patterns of extracellular proteins and the selective expression of their receptors in projection neurons. Axon guidance is stimulated by guidance proteins and implemented by neuronal traction forces at the growth cones, which engage local cytoskeleton regulators and cell adhesion proteins. Different layers of guidance signaling regulation, such as the cleavage and processing of receptors, the expression of co-receptors and a wide variety of intracellular cascades downstream of receptors activation, have been progressively unveiled. Also, in the last decades, the regulation of microtubule (MT) assembly, stability and interactions with the submembranous actin network in the growth cone have emerged as crucial effector mechanisms in axon pathfinding. In this review, we will delve into the intracellular signaling cascades downstream of guidance receptors that converge on the MT cytoskeleton of the growing axon. In particular, we will focus on the microtubule-associated proteins (MAPs) network responsible of MT dynamics in the axon and growth cone. Complementarily, we will discuss new evidences that connect defects in MT scaffold proteins, MAPs or MT-based motors and axon misrouting during brain development.

Keywords: microtubules, microtubule-associate proteins, growth cone, neuronal cytoskeleton, axon guidance and pathfinding, +TIP

OPEN ACCESS

Edited by:
Joaquim Egea,
Biomedical Research Institute of Lleida, Spain

Reviewed by:
Aurnab Ghose,
Indian Institute of Science Education and Research, Pune, India
Carsten Theiss,
Ruhr University Bochum, Germany

****Correspondence:***
Carlos Sánchez-Huertas
chuertas@umh.es

Specialty section:
This article was submitted to Molecular Signalling and Pathways, a section of the journal Frontiers in Molecular Neuroscience

Received: *16 August 2021*
Accepted: *01 November 2021*
Published: *02 December 2021*

Citation:
Sánchez-Huertas C and Herrera E (2021) With the Permission of Microtubules: An Updated Overview on Microtubule Function During Axon Pathfinding. Front. Mol. Neurosci. 14:759404. doi: 10.3389/fnmol.2021.759404

INTRODUCTION

The navigation of neural axons to find appropriate synaptic partners is one of the most extraordinary events that take place during the development of the nervous system. Axon extension is led by an amoeboid-like cytoplasmic enlargement at the tip, denominated the growth cone (GC). This is a small but extremely dynamic and sensitive cellular structure that integrates extracellular guidance information and transduces the mechanical forces necessary for the steering and propulsion movements during axonal navigation. At the leading edge, the growth cone is composed

of motile sheet-like lamellipodia and narrow filopodia that are sensitive to external guidance cues or ligands because they express specific receptors at the surface. Ligand-receptor signaling activates intracellular transduction pathways that primarily converge over growth cone cytoskeleton remodeling, which in coordination with substrate adhesions turnover and membrane trafficking, orchestrates the steering movements of the axon (Geraldo and Gordon-Weeks, 2009; Lowery and Vactor, 2009; Vitriol and Zheng, 2012; Kerstein et al., 2015).

The highly conserved collection of axon guidance proteins consists of attractive/repulsive membrane-anchored and secreted molecules. Five large families of canonical guidance proteins have been identified: netrins that signal through the deleted in colorectal cancer (DCC), Neogenin and UNC-5 receptors; Slits, that bind to their roundabout (Robo) receptors; Semaphorins, that activate both Neuropilin and Plexin receptors; Ephrins and Ephs; and Repulsive Guidance Molecule family (RGMs) that bind to Neogenin. Besides these initially identified families of guidance proteins, cell-adhesion molecules, growth factors and morphogens, such as the Wnts, Sonic hedgehog (Shh), TGF-β/BMP, neurotrophins or endocannabinoids have been implicated in axonal navigation (Kolodkin and Tessier-Lavigne, 2011; Yam and Charron, 2013; Zhou et al., 2014; Short et al., 2021). These guidance ligand-receptor modules have been identified and reported as essential for the formation of the commissural tracts in the spinal cord and forebrain, the retinotopic maps, the thalamocortical connections or the sensory motor innervation of the limbs, among other systems (Chedotal and Richards, 2010; Leyva-Díaz and López-Bendito, 2013; Chédotal, 2019; Herrera et al., 2019a).

During pathfinding GCs are simultaneously exposed to various signaling proteins and the final guidance decision relies on the spatial-temporal repertoire of guidance receptors expressed at the surface and the computation of their downstream signaling pathways. In addition, neuron-intrinsic molecular mechanisms including response-modulating co-receptors, receptor-receptor interactions, receptor clustering and oligomerization, proteolytic processing of receptors, or the trafficking of signaling receptors-carrying endosomes, contribute to the diversification of axonal responses to a same guidance cue (Dudanova and Klein, 2013; Pasterkamp and Burk, 2021; Zang et al., 2021). These intracellular pathways ultimately converge on proteins managing the cytoskeleton remodeling in the axon and GC.

The major networks constituting the mature neuronal cytoskeleton are formed by microtubules (MTs), actin fibers (F-actin) and neurofilaments, but axon pathfinding is mainly governed by F-actin and MTs acting coordinately in response to extracellular guidance signaling (Geraldo and Gordon-Weeks, 2009; Lowery and Vactor, 2009; Dent et al., 2011; Coles and Bradke, 2015). Seminal studies on the effects of F-actin disrupting drugs over invertebrate neurons in culture, revealed the critical role of the actin cytoskeleton in filopodia maintenance, GC turning and axonal pathfinding (Bentley and Toroian-Raymond, 1986; Zheng et al., 1996). Thereafter, an intricate network of actin-binding and regulatory proteins mediating the axonal response to guidance molecules has been progressively disclosed [see Table 1 in Dent et al. (2011) and Kolodkin and Pasterkamp (2013) for detailed information on actin-binding proteins steering the GC]. Most axon guidance pathways engage the Rho family of small GTPases, mainly represented by RhoA, Rac1 and Cdc42, via their activating guanine nucleotide exchange factors (RhoGEFs) and deactivating GTPase activating proteins (RhoGAPs) (Hall and Lalli, 2010). RhoGTPases, in turn, drive the activity of F-actin regulators, such as the nucleating Arp2/3 complex (Strasser et al., 2004; Shakir et al., 2008), the WASP nucleation factors (Shekarabi et al., 2005; Shakir et al., 2008), the polymerization regulators formins or the Ena/VASP family (Goode and Eck, 2007), the molecular motor Myosin II (Amano et al., 1998; Medeiros et al., 2006) or the severing protein ADF/cofilin (Kuhn et al., 2000), to modulate the actin-based filopodia and lamellipodia dynamics. The essential contribution of actin dynamics to axon guidance signal transduction in the GC has been reviewed recently by other authors (Omotade et al., 2017; Niftullayev and Lamarche-Vane, 2019) and, therefore, will not be the main focus of this review. For years, the long-standing view in the field was that the GC turns as a result of the stabilization/destabilization balance of the actin-rich filopodia and lamellipodia in the presence of a guidance cue and the MT cytoskeleton just provided structural support via MT-dependent transport to consolidate the actin-dependent turning events. However, the role of MTs in cellular functioning is continuously expanding and accumulating evidence indicate that MTs are not just passive regulators of GC dynamics. Instead, MTs can actively control GC protrusion and steering and, along with MT-associated proteins (MAPs), are direct targets of axon guidance signaling pathways (Gordon-Weeks, 2004; Dent et al., 2011; Kalil et al., 2011; Liu and Dwyer, 2014; Bearce et al., 2015; Cammarata et al., 2016; Kahn and Baas, 2016).

In the first part of this review we provide an overview on the configurations of the MT cytoskeleton in the axon and growth cone and describe the cytoskeletal mechanisms that drive GC directional responses, focusing on the contribution of MTs. In the second half of this article, we highlight recent evidences suggesting that guidance cues directly control the activity and localization of MT-associated proteins (MAPs) and discuss how alterations in genes encoding MT network regulators may cause an abnormal development of neural networks *in vivo*.

THE NEURONAL MICROTUBULE CYTOSKELETON

Microtubules are hollow cylindrical structures composed of 13 laterally-associated protofilaments of α-tubulin and β-tubulin heterodimers assembled in a head-to-tail manner, conferring an intrinsic polarity characterized by a stable/slow-growing "minus-end" and a dynamic/fast-growing "plus-end" (Desai and Mitchison, 1997). In eukaryotic cells, the MT nucleation – the *de novo* MT formation from its minus end – is initiated by the γ-tubulin ring complex (γTuRC) in cooperation with additional proteins that regulate MT-nucleation kinetics. MT nucleation events are spatially restricted to MT-organizing centers (MTOC), which concentrate the γ-TuRCs, and the centrosome is a major

MTOC in animal cells (Paz and Lüders, 2018). MT minus-ends are stabilized by a γTuRC cap (Wiese and Zheng, 2000) or by calmodulin-regulated spectrin-associated proteins (CAMSAPs) (Jiang et al., 2014). Instead, the MT plus-ends are more dynamic, alternating polymerization and shrinkage phases (catastrophes), a property commonly referred to as "dynamic instability" (Walker et al., 1989; Tran et al., 1997; Zhang et al., 2015). These MT-intrinsic dynamic plus-end transitions between growth and shrinkage can be externally regulated by the activity of other MAPs, that control the supply of soluble tubulin-heterodimers, the speed and duration of the polymerization/depolymerization events and the plus-ends resilience to collapse (reviewed in Akhmanova and Steinmetz, 2015).

At the onset of neuron differentiation, MTs nucleation takes place mainly at the centrosome. To meet axon growth needs, MTs are subsequently released from the centrosome, sorted into the axon and anterogradely transported by means of molecular motor forces (Kapitein and Hoogenraad, 2015). During maturation the neuron centrosome progressively loses its MT-nucleating and MT-organizing skills to such an extent that axonal MT growth, axonal extension or overall neural development do not require a centrosome (Basto et al., 2006; Stiess et al., 2010; Nguyen et al., 2011). Indeed, during the last years centrosome-independent MT nucleation activities has been identified within the axon and dendrites of mammalian and invertebrate neurons (Stiess et al., 2010; Ori-McKenney et al., 2012; Nguyen et al., 2014; Sánchez-Huertas et al., 2016; Cunha-Ferreira et al., 2018; Qu et al., 2019; Liang et al., 2020). MT configurations display differently in axons and dendrites. In mammalian neurons, MTs are uniformly oriented in the axons, with their plus-ends toward the tip, while in dendrites MTs are arranged with mixed polarity. The uniform MT plus-end-out polarity of axons is mainly established and maintained by motor-dependent MT sliding mechanisms (Miller and Suter, 2018) and the spatial-temporal control of non-centrosomal MT nucleation (Wilkes and Moore, 2020). For example, the cytoplasmic dynein motor promotes bulk forward translocation of MTs into the axon and clears the minus-end-out MTs from axons by soma-directed sliding (Roossien et al., 2014; Rao et al., 2017). In addition, new plus-end-out MTs are locally generated from the lateral surface of pre-existing axonal MTs by the Augmin-γTuRC module (Sánchez-Huertas et al., 2016; Cunha-Ferreira et al., 2018) and TRIM46 bundles these plus-end-out MTs (van Beuningen et al., 2015), to strengthen the axonal identity.

Neuronal MTs show specific physical and dynamic features enabled by their differential tubulin isotype composition, assorted post-translational tubulin modifications – including tyrosination, acetylation or polyglutamylation – and a neuron-specific MAP network unevenly distributed over the axonal and somatodendritic compartments (Moutin et al., 2021). Within the axon shaft, MTs are heavily stabilized and organized in dense, parallel and overlapping bundles. This longitudinally aligned MT network enable the directional transport of organelles, vesicles, other MTs and cargoes along the axon, mediated by MT-based motor proteins of the kinesin superfamily and cytoplasmic dynein (Hirokawa et al., 2010; Leterrier et al., 2017). By virtue of the differential MT layouts in neuron compartments, uniform in axons and mixed in dendrites, specific motor-driven cargos are selectively sorted, determining axonal specification, maturation and navigation (Guillaud et al., 2020).

MICROTUBULE CYTOSKELETON IN THE GROWTH CONE

At the axon tip, the growth cone (GC) can be subdivided in several areas: a mobile peripheral (P) domain, containing filopodia and lamellipodia, a central (C) domain and a transition zone (TZ) in between. The cytoskeletal networks are organized in a highly segregated fashion among these GC subdomains (**Figure 1A**). The P-domain is mainly made of actin fibers organized in dense bundles or loose F-actin meshworks, originating the filopodia and lamellipodia, respectively. The C-domain is populated by thickly bundled MTs, which are continuously pushed by actin-based Myosin II-dependent rearwards forces working at the TZ. Only isolated MTs can pass this actomyosin-mediated barrier to MT assembly and invade the actin-rich P-domain, where MTs display "dynamic instability" (**Figures 1A,B**) (Letourneau, 1983; Forscher and Smith, 1988; Dent and Kalil, 2001; Schaefer et al., 2002; Zhou et al., 2002). F-actin bundles at the GC P-domain experience a sustained retrograde flow (RF) product of: (i) the continuous F-actin polymerization at the submembranous cortex, (ii) the retrograde Myosin-dependent pulling forces and (iii) the F-actin depolymerizing activity of ADF/Cofilin at the transition zone. Actomyosin arcs contribute to MT bundling and advance into the C-domain by exerting forces along the side of the neck of the GC (**Figure 1B**) (Medeiros et al., 2006; Burnette et al., 2008). In addition, once entering the P-domain, MTs tend to unfasciculate, bend and loop due to a dynamic MT-F-actin interplay enabled by MT-F-actin coupling proteins, including MAPs or MT plus-tip interacting proteins (+TIPs) (Coles and Bradke, 2015; Cammarata et al., 2016). This transient MT-F-actin coupling mechanism mediated by MAPs enables MT capture and guidance by F-actin bundles at the P-domain, but also exposes MTs to the continuous F-actin retrograde flow, influencing the orientation and speed of MT growth. This F-actin retrograde flow drags MTs backward and clears the GC periphery of MTs, by attenuating and buckling the MT trajectories. Opposing to these retrograde forces over MT dynamics, the cytoplasmic dynein motor exerts anterograde MT-sliding movements to introduce MTs in the P-domain (**Figure 1B**) (Forscher and Smith, 1988; Zhou et al., 2002; Suter et al., 2004; Myers et al., 2006; Grabham et al., 2007; Schaefer et al., 2008; Marx et al., 2013). Therefore, MT distribution in the GC is partially determined by F-actin network at the same time that the F-actin-based filopodia and lamellipodia dynamics is also known to be strongly influenced by MT capture and stabilization at the GC periphery (Sabry et al., 1991; Tanaka et al., 1995; Gallo, 1998). Such intense reciprocal regulation between MT and F-actin networks in the GC highlights the importance of an expanding family of MT-actin crosslinking proteins in axon guidance decisions, but the precise nature of MT-actin interlinking mechanisms remain to be elucidated.

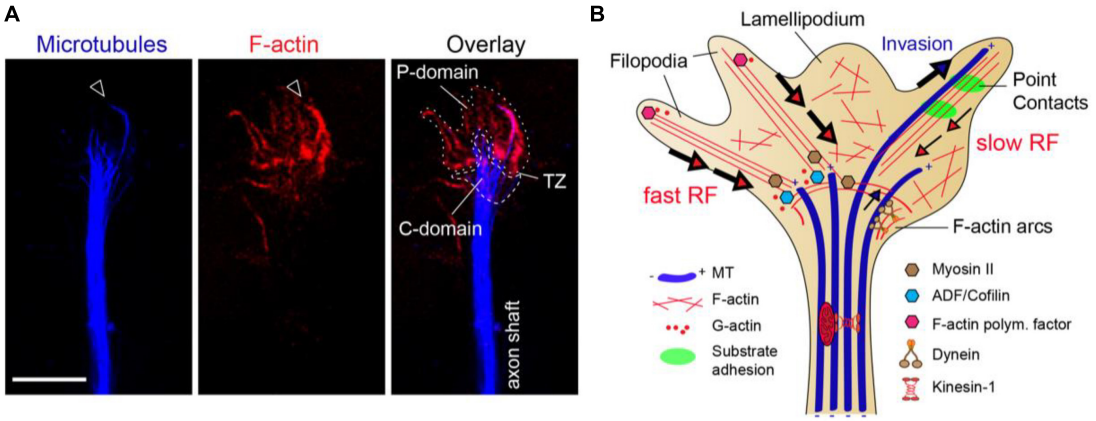

FIGURE 1 | The growth cone cytoskeleton. **(A)** High-resolution image of an axonal growth cone labeled with phalloidin (red) and α-tubulin (blue) from a hippocampal neuron culture. Actin filaments (F-actin) and microtubules (MTs) are segregated amid the peripheral (P-domain) and central regions (C-domain), respectively. Arrowhead marks isolated MTs invading the P-domain aligned with F-actin bundles. P-domain and C-domain are outlined using a dotted or dashed lines, respectively. TZ, transition zone. Scale bar, 5 μm. **(B)** The clutch model for growth cone protrusion and steering. F-actin (red lines), microtubules (blue thick tubes), MT plus-ends (+), point contacts of adhesion (green). Filopodia is formed by F-actin bundles and lamellipodia by F-actin meshworks. The F-actin retrograde flow at the P-domain is balanced between F-actin polymerization and depolymerization rates, and myosin-based pulling forces at the TZ. Actomyosin forces at the TZ restrain MT entry into the P-domain. The engagement of F-actin to adhesion point contacts slows the F-actin retrograde flow rate and facilitates MT invasion to the growth cone periphery, determining outgrowth and steering.

Traction forces that propel axon outgrowth rely on clutching forces exerted at substrate adhesion points, which generally assemble within growth cone filopodia. At these point contact adhesions, extracellular matrix (ECM) proteins activate integrin receptors that recruit scaffolding and signaling proteins, which physically link to the F-actin cytoskeleton (Suter et al., 1998; Woo and Gomez, 2006; Bard et al., 2008; Shimada et al., 2008; Myers and Gomez, 2011; Toriyama et al., 2013). This molecular "clutch" restrains myosin-II mediated F-actin contractile forces and increases the pushing forces of actin polymerization toward the leading edge membrane, producing GC protrusion. Then, taking advantage of the attenuated F-actin retrograde flow, pioneer MTs invade the filopodia and eventually get captured and stabilized. The stabilized MTs enable the entry of organelles and vesicles to the GC periphery, powered by MT-based motor forces, and the GC stepwise progresses toward the engorgement and consolidation stages (**Figure 1B**) (Suter et al., 1998; Zhou et al., 2002; Gomez and Letourneau, 2014; Kerstein et al., 2015). This is the currently accepted mechanistic model for axon outgrowth, although recent data has revealed some inconsistencies (Santos et al., 2020; Turney et al., 2020). By analyzing GC protrusion and axon growth over three-dimensional (3D) matrices, Santos et al. (2020) showed that actomyosin forces do not restrain MTs at the C-domain of GCs in this environment. Instead, MTs widely populate the P-domain of the GCs, enabling a rapid axon elongation. In addition, the authors showed that axons can polarize and extend in adhesion-inert 3D matrices, suggesting that cell adhesions may be dispensable for axon growth in a 3D environment (Santos et al., 2020). GC motility and axon advance has also been analyzed over non-adhesive substrate gaps in a 2D environment. This study revealed that axons transiently stop at gaps, but GC protrusive activity continued, with MTs entering the filopodium extending across the gap. These MTs were powering the necessary molecular forces for GC to pass over the non-adhesive substrate (Turney et al., 2020). Experimental evidence has extensively validated the clutch hypothesis during *in vivo* axon wiring (Berezin and Walmod, 2014), so this new data suggests the existence of additional regulatory levels in the mechanism of GC motility.

A classic study analyzing the *in vivo* GC morphology of retinal axons performed in the 80's described that retinal axons display long and slender GCs when navigating the optic nerve, while at the guidance decision point of the optic chiasm GCs become shorter, wider and grow multiple filopodia (Bovolenta and Mason, 1987). The study revealed that GC behaviors, and the underlying mechanisms, can differ between bulk navigation regions and guidance decision environments. This sets a model out where GCs may either waive or activate substrate adhesion mechanisms according to extracellular guidance factors or neuron-intrinsic commands (Padmanabhan and Goodhill, 2018), integrating the *a priori* antagonistic evidences previously exposed. However, further work is needed to fully understand the mechanotransduction events during *in vivo* axon navigation.

Microtubules as the Mechanistic Effectors of Growth Cone Turning

The reorganization of the GC cytoskeleton during axon steering is ultimately enabled by a tight regulation of the MT-actin interplay (Gordon-Weeks, 2004; Lowery and Vactor, 2009; Dent et al., 2011). The targeting of the actin cytoskeleton, either by downregulation of actin isoforms or by depolymerization of F-actin using Cytochalasin B, reduces the size of the growth cone, hinders filopodial dynamics and abolishes the axonal turning response (Forscher and Smith, 1988; Zheng et al., 1996; Moradi et al., 2017). Despite the requirement of F-actin for axon

steering, it has been shown that neurons can still elongate their axons after F-actin depolymerization or inhibition of myosin II (Bentley and Toroian-Raymond, 1986; Zheng et al., 1996; Bradke and Dotti, 1999; Hur et al., 2011b), indicating that F-actin filaments remodeling is essential for motility and steering but dispensable for axon extension. In contrast, MT dynamics is necessary for axon growth (Yamada et al., 1970; Bamburg et al., 1986; Mansfield and Gordon-Weeks, 1991; Tanaka et al., 1995; Yu and Baas, 1995; Rochlin et al., 1996; Tischfield et al., 2010) but the role of MTs in GC steering is yet a matter of discussion.

More than 30 years ago, pioneer studies already showed that MTs asymmetrically invade the P-domain of the GC in the direction of the turn and their reorganization is essential during GC maneuvers (Forscher and Smith, 1988; Sabry et al., 1991; Tanaka et al., 1995; Williamson et al., 1996). In addition, MTs entering the filopodia were found to be captured and stabilized by preventing shrinkage. These stabilized MTs allowed the flow of cytoplasmic organelles and increased the filopodia lifetimes, enabling directional axon outgrowth (Gordon-Weeks, 1991; Sabry et al., 1991; Geraldo et al., 2008). Ever since, different works have demonstrated that axon guidance signaling proteins influence MT dynamics at the GCs. For instance, bath incubation of Sema3A and netrin-1 in neuron cultures revealed that Sema3A treatments result in the collapse of MT networks, while netrin-1 incubation stimulates MT splaying and exploration in the GC peripheral region (Dent et al., 2004; Shao et al., 2017). Nerve growth factor (NGF) signaling in sensory neurons also redistributed the MTs in the distal part of axons (Zhou et al., 2004; Turney et al., 2016), and Wnt3a or Wnt5a treatments changed the organization and directionality of MT polymerization in the GC (Purro et al., 2008; Li et al., 2014). Micro-gradients of Brain-derived neurotrophic factor (BDNF) or Sema3A over GCs of sensory axons also biased the direction of MT growth toward the treated GC side or the opposite side, respectively (Pavez et al., 2019). In addition, genetic studies in *Caenorhabditis elegans* showed that UNC-6/Netrin signaling hampers MT accumulation in the GC and inhibits protrusion, through a molecular pathway that involves the repulsive Netrin receptor UNC-5, RHO-1/RhoA and UNC-33/CRPM (Gujar et al., 2019). Consistently with these findings, the inhibition of MT dynamics blunts GC turning in response to guidance cues. The exposure of GCs and axons to drugs that disrupt MT dynamics, such as taxol or nocodazole, reduced the GC activity and abolished the turning of GCs exposed to netrin-1 and glutamate gradients or substrate boundaries (Tanaka and Kirschner, 1995; Challacombe et al., 1997; Buck and Zheng, 2002; Suter et al., 2004). Yet, because the spatial distribution of MTs in the GC periphery is strongly influenced by actomyosin forces and F-actin dynamics, MTs have been classically relegated to simple supporters of actin-guided movements during axon navigation.

Now, mounting evidences support the idea that MTs and MAPs can also instruct axon pathfinding even when actin dynamics are not directly perturbed. Seminal studies performed 20 years-ago showed that the focal application of the MT stabilizing drug taxol to one side of the GC induces turning toward the drug source, whereas the application of the MT destabilizing drug nocodazole triggers GC turning away from the application side (Buck and Zheng, 2002). Experimental evidence also demonstrated that MT-initiated GC turning engages F-actin remodeling during the movement, since the inhibition of actin polymerization abolished the taxol-evoked attractive GC turning (Buck and Zheng, 2002). Subsequent works employing micro-scale chromophore-assisted laser inactivation (micro-CALI) have also revealed that several MAPs can trigger GC steering. Micro-CALI technique has been exploited to address the role of specific proteins in GC steering (Chang et al., 1995; Diefenbach et al., 2002), although it may have caveats, such as a rapid recovery dependent on protein diffusion or trafficking. The asymmetric inactivation of the MT-stabilizing protein MAP1B or the Adenomatous polyposis coli (APC) protein – a +TIP that stimulates MT polymerization – by micro-CALI in one side of the GC, led to the collapse of the irradiated side followed by GC turning toward the opposite direction (Mack et al., 2000; Koester et al., 2007). In contrast, the asymmetric inactivation of the MT extension-modulator CRMP2 or the MT-sliding motor Kinesin-5 in half of the GC by micro-CALI, resulted in GC turning toward the irradiated side (Higurashi et al., 2012; Nadar et al., 2012). Overall, these experiments support the idea that MT dynamics are not just required for guidance-evoked GC steering movements, but they play an instructive role in GC turning. Corroborating their instructive role in axon guidance signal transduction, evidences from Liu's laboratory have proven that the neuron-specific tubulin isotype TUBB3 – polymerized in MTs – is a direct target of netrin-1 signaling (Qu et al., 2013; Huang et al., 2015; Shao et al., 2017). Netrin-1 is a dual guidance cue that can evoke attractive and repulsive responses by binding to its high-affinity GC receptors DCC and UNC5, respectively (Alcántara et al., 2000). It was reported that the exposure of cortical neuron cultures to netrin-1 induces GC chemoattraction and stimulates the MT dynamics in the GC. Both of these netrin-1 effects required the direct interaction of its receptor DCC with the neuron-specific tubulin isotype TUBB3, integrated in the MT polymer. Indeed, the interaction of TUBB3 with DCC was greatly increased by exogenous netrin-1 addition and this interaction was dependent on MT dynamics (Qu et al., 2013). Conversely, the GC repulsion induced by netrin-1 exposure through UNC5C receptor signaling also relied on TUBB3-UNC5C binding. UNC5C directly interacts with polymerized TUBB3 *in vitro* and both partially colocalize in the GC periphery of primary neurons. The focal application of Netrin-1 was found to disengage UNC5C-TUBB3 interaction in GCs and stimulate MT polymerization in the GC region distally to the netrin-1 source, promoting the repulsive response (Shao et al., 2017). Missense mutations of *TUBB3* in humans are associated to an abnormal development of the corpus callosum, the anterior commissure, the corticospinal tracts or optic nerves in human patients (**Table 1**). Additionally, it was found that *TUBB3* mutations impaired MT dynamics and abolished both netrin-1-evoked attractive and repulsive responses of cortical axons *in vitro* (Poirier et al., 2010; Tischfield et al., 2010; Whitman et al., 2016; Huang et al., 2018; Shao et al., 2019). Although the deficits caused by *TUBB3* loss-of-function in neural circuits

TABLE 1 | Links of microtubule-associated proteins (MAPs) with axon guidance.

Roles in MT networks	MAP	Function on GC motility	Axon tract development in animal models	Guidance pathways participated	Nerve tract associated pathology in humans	Actin crosstalk
Structural	TUBB3	Interaction with DCC or UNC5 increase/decrease upon netrin-1 signaling, interfering with MT dynamics and promoting both the attractive and repulsive responses of the GC.	Disease-associated *Tubb3* mutant mice show abnormal AC, CC and cranial nerves (Tischfield et al., 2010; Latremoliere et al., 2018)	Netrin-1-DCC (Qu et al., 2013); Netrin-1-UNC5 (Shao et al., 2017)	CFEOM3. Defects in the CC, AC or corticospinal tracts. Asymmetric cortical dysplasia and gyral disorganization (Poirier et al., 2010; Tischfield et al., 2010)	–
Structural	TUBA1A	Loss-of-function hindered neurite outgrowth in cortical neurons and altered GC cytoskeleton	*Tuba1a* ko mice show abnormal development of forebrain commissures (Buscaglia et al., 2020)	–	Abnormalities of the CC and basal ganglia/internal capsule. Lissencephaly and other cortical and cerebellar dysgenesis (Romaniello et al., 2018)	–
Structural	TUBB (TUBB5)	Altered MT dynamics and MT-based transport in patient's fibroblasts	–	–	Hypoplasia or partial agenesis of the CC, and other cortical and cerebellar dysgenesis (Romaniello et al., 2018)	–
Nucleation modulator	TPX2	Localizes to neurite tips together with RanGTP to promote local MT nucleation in hippocampal neurons	–	–	–	–
Stability	MAP1B	Phospho-MAP1B stabilizes MTs at the GC periphery. Phosphorylated by GSK3β and CDK5 upon guidance signaling	*Map1b* ko mice display defective cortical and thalamocortical wiring, and CFEOM (Meixner et al., 2000; Del Río et al., 2004; Cheng et al., 2014)	Netrin-1 (Del Río et al., 2004); Draxin-DCC (Meli et al., 2015); Sema3A (Takabatake et al., 2020)	White matter deficit, hypoplasia of the CC (Walters et al., 2018)	Binds F-actin *in vitro*. Coordinates MTs and F-actin remodeling in DRG GCs (Villarroel-Campos and Gonzalez-Billault, 2014)
Stability	Tau	Hyperphosphorylated tau detaches from MTs and compromises MT stability in the GC. Phosphorylated by GSK3β, CDK5, or CaMKII upon guidance signaling	No phenotype in *tau* ko mice likely due to function overlapping with MAP1B	Sema3A (Sasaki et al., 2002); Wnt5a (Li et al., 2014; Biswas and Kalil, 2018); EphrinB1-EphB2 (Jiang et al., 2015); Sema3C (Moreno-Flores et al., 2004)	–	Crosslinks MT-F-actin *in vitro* (Elie et al., 2015). Couples MT and F-actin in GCs of cortical neurons (Biswas and Kalil, 2018)
Polymerization/ stability	CRMP2	Non-phosphorylated CRMP2 transports tubulin heterodimers to distal axons via kinesin-1, to support MT growth. Phosphorylated sequentially by CDK5 and GSK3β upon guidance signaling	*Crmp2* ko mice display abnormal development of peripheral nerves and CC (Ziak et al., 2020)	Sema3A (Goshima et al., 1995); Sema4D-plexinB1 (Ito et al., 2006): RGMa (Wang et al., 2013); EphrinA5 (Arimura et al., 2005)	–	Binds the actin regulators: cytoskeleton a2-chimaerin and Sra-1/WAVE1 complex in axons (Brown et al., 2004; Kawano et al., 2005)
Stability	DCX	Stabilizes MT in the GC periphery. Phosphorylated by CDK5 upon Sema3A signaling, resulting in MT destabilization	*Dcx/Dclk1* ko mice show widespread defects in brain axon tracts (Deuel et al., 2006; Koizumi et al., 2006)	Netrin-1 (Fu et al., 2013); Sema3A (Bott et al., 2020)	Lissencephaly and double cortex syndrome (laminar heterotopias) (Bahi-Buisson et al., 2013)	Binds the actin-binding protein Spinophilin to organize F-actin. Coordinates MTs and F-actin in GCs (Tsukada et al., 2005; Tint et al., 2009)

(Continued)

TABLE 1 | (Continued)

Roles in MT networks	MAP	Function on GC motility	Axon tract development in animal models	Guidance pathways participated	Nerve tract associated pathology in humans	Actin crosstalk
Instability	SCG10	Active (non-phosphorylated) SCG10 destabilizes MTs, stimulating MT dynamics and promoting axon outgrowth and regeneration	–	EphB (Suh, 2004); Sema4D-PlexinB1? (Oinuma et al., 2004; Li Y.-H. et al., 2009)	–	–
Severing	Spastin	Spastin isoform M1 represses BMP guidance signaling during spinal motor axon pathfinding in developing zebrafish	–	BMP (Jardin et al., 2018)	Hereditary spastic paraplegia (Roll-Mecak and Vale, 2008)	–
Severing	Fignl1	Involved in spinal motor axons wiring during zebrafish development	–	–	–	–
Polymerization inhibition	KIF21A	Decreases MT polymerization and suppresses catastrophes, modulating the GC morphology, axon growth and pathfinding	Mutant *Kif21a* mice show defects in oculomotor nerves development (Cheng et al., 2014)	Sema3F (van der Vaart et al., 2013)	CFEOM1 (Yamada et al., 2003)	Binds and regulates the localization of Kank1, an F-actin polymerization inhibitor (Kakinuma and Kiyama, 2009)
Pausing	KIF21B	Accumulates in MT plus-ends and acts as autonomous pausing factor	*Kif21b* ko mice display thinner CC (Kannan et al., 2017)	–	Agenesis of the CC and microcephaly (Asselin et al., 2020)	Associates with ELMO1, a Rac1 regulator (Morikawa et al., 2018)
Polymerization inhibition	KIF2A	Prevents MT overstabilization in the GC.	*Kif2a* ko mice show aberrant overextension of hippocampal axons (Homma et al., 2003)	–	Malformations of cortical development, including microcephaly and gyration phenotypes (Poirier et al., 2013)	–
Transport	Dynein motor complex	Retrograde transport of signaling endosomes. Antiparallel MT sliding	–	NGF (Sainath and Gallo, 2015)	Polymicrogyria and Charcot-Marie-Tooth disease type2 (Poirier et al., 2013)	–
Transport	Kinesin-5	Antiparallel MT sliding. Blocks MT invasion into the GC periphery and determines GC turning. Required for evoked-turning response	–	–	Microcephaly and chorioretinopathy (Jones et al., 2014)	–
Transport	Kinesin-1 motor complex	Axonal transport of CB1R in hippocampal neurons	*Klc1* ko mice show pathfinding defects in corticofugal axons (Saez et al., 2020)	Endocannabinoids (Saez et al., 2020)	*Kif5C*: microcephaly, gyration phenotypes and white matter dysgenesis (Poirier et al., 2013; Michels et al., 2017)	–
Transport	KIF13B	Transports the F-actin-based motor Myosin X and its cargo DCC anterogradely along axons upon guidance signaling	–	Netrin-1-DCC (Yu et al., 2020)	–	–
Transport	KIF1BP	–	*Kif1bp* ko mice show defects in the anterior commissure and sympathetic innervation, but not in CC (Hirst et al., 2017)	–	Microcephaly, peripheral neuropathy (Goldberg-Shprintzen syndrome) (Drévillon et al., 2013)	–

(Continued)

TABLE 1 | (Continued)

Roles in MT networks	MAP	Function on GC motility	Axon tract development in animal models	Guidance pathways participated	Nerve tract associated pathology in humans	Actin crosstalk
Transport	KIF1Bβ	Axonal transport of IGF1R to mediate IGF-1-induced axon growth	*Kif1b* ko mice show abnormal development of the CC (Zhao et al., 2001)	IGF1-IGF1R (Xu et al., 2018)	Charcot-Marie-Tooth disease type 2A (Zhao et al., 2001)	–
Polymerization/ scaffold	EB1, EB3	Guidance signaling instructs the asymmetric invasion of EB-labeled MT plus-ends or the MT polymerization dynamics	–	Sema4D-plexin (Laht et al., 2012, 2014); SDF1-CXCR4 *via* EB1/Drebrin module (Shan et al., 2021); BDNF, Sema3A *via* EB3/STIM1 module (Pavez et al., 2019)	–	EB3/drebrin coordinates MT-actin and regulates F-actin dynamics (Geraldo et al., 2008; Mizui et al., 2009; Mikati et al., 2013; Grintsevich and Reisler, 2014)
Stability	CLASP	Phosphorylation by Abl and GSK3β upon guidance signaling determines MT plus-end binding	–	Slit-Robo (Lee et al., 2004). PDGF (Engel et al., 2014).	–	Binds F-actin *in vitro* and regulates F-actin networks in sensory GCs (Marx et al., 2013)
Stability/ RNA transport	APC	Asymmetric accumulation of APC in the GC anticipates the steering movement. Guidance signaling modulates APC MT plus-end binding via PI3K-GSK3β activity	*Apc* ko mice show widespread white matter defects (Yokota et al., 2009)	NGF (Zhou et al., 2004; Villarin et al., 2016); Wnt3a (Purro et al., 2008)	–	Regulates mDia and IQGAP1 (Watanabe et al., 2009; Okada et al., 2010). Required for MT-dependent F-actin assembly in hippocampal GCs (Efimova et al., 2020)
Stability	APC2	Defines the guidance of retinal ganglion cell axons at the chiasm midline	–	EphrinA2 (Shintani et al., 2009); Wnt5a (Morenilla-Palao et al., 2020)	–	Regulates actin dynamics through the formin DIA in *Drosophila* (Zhou et al., 2011)
Crosslink/ arrangement	MACF1	Links MTs and F-actin. Coordinates MTs and F-actin interaction to organize the axonal cytoskeleton	Midline axon guidance in flies (Lee et al., 2007). *Macf1* ko mice show widespread white matter defects (Chen et al., 2006; Ka and Kim, 2016)	Wnt-β catenin (Chen et al., 2006)	Thin CC and AC, with lissencephaly (Dobyns et al., 2018)	Binds, stabilizes and organizes F-actin configurations (Kodama et al., 2003)
Stability/ crosslink	NAV1	Stabilizes paused MT plus-ends. Couples MTs and F-actin in the GC of hippocampal neurons	–	Netrin-1 (Martínez-López et al., 2005; Sánchez-Huertas et al., 2020)	–	Binds F-actin *in vitro,* crosslinks MT-F-actin. Recruits the Trio to MT plus-ends (van Haren et al., 2014; Sánchez-Huertas et al., 2020)
Polymerization/ nucleation modulator	XMAP215	Promotes MT entry in filopodia, regulates GC morphology and axon outgrowth in *Xenopus* neurons	–	EphrinA5 (Slater et al., 2019)	–	Co-aligns MTs and F-actin in GCs (Slater et al., 2019)
Polymerization	TACC3	Forms a complex with XMAP215. Phosphorylated by Abl. Phospho-mutants interfere with axon pathfinding	–	Slit2, EphrinA5 (Erdogan et al., 2017, 2020)	–	–
Crosslink	Gas2L1	Regulates axon outgrowth and branching	–	–	–	Stabilizes F-actin upon MT-F-actin interaction (Willige et al., 2019)
Stability/ crosslink	DAAM	Actin assembly factor involved in axon growth and guidance. Regulates GC filopodia dynamics also *via* interaction with + TIPs	–	Wnt5 (Gombos et al., 2015)	–	Crosslinks MT and F-actin *in vitro* and coordinates the GC cytoskeleton in *Drosophila* neurons (Szikora et al., 2017)
Stability/ crosslink	mDia1, mDia3	Actin assembly factor involved in axon growth and guidance. Binds and stabilizes MTs	Double *mDia* ko mice show midline crossing defects in the spinal cord (Toyoda et al., 2013)	EphrinA5, EphrinB3, Sema3A (Toyoda et al., 2013); SDF1-α (Arakawa et al., 2003)	–	Play dual roles in actin and MT dynamics (Thurston et al., 2012)
Stability/ crosslink	FMN2	Enables MT capture by F-actin bundles and focal adhesion-based traction in filopodia	Fmn2 depletion impairs midline crossing in chick spinal cord (Sahasrabudhe et al., 2016)	Wnt (Lian et al., 2016)	–	Couples MTs and F-actin in GCs (Kundu et al., 2021)

MT, microtubules; F-actin, actin fibers; GC, growth cone; +TIPS, MT plus-end interacting proteins; CFEOM, congenital fibrosis of the extraocular muscles; CC, corpus callosum; AC, anterior commissure; GC, growth cone; NGF, nerve growth factor; BDNF, brain-derived neurotrophic factor; BMP, bone morphogenetic protein; DRG, dorsal root ganglia.

development may be compensated by the remaining β-tubulin isotypes (Latremoliere et al., 2018).

Other mutations in human α-and β-tubulin-encoding genes – such as *TUBA1A, TUBB2B, TUBA8, TUBB4A, TUBB2A, TUBB* – are linked to severe brain malformations and motor-cognitive disabilities, collectively refereed as tubulinopathies. These syndromes present gross brain malformations and an abnormal development of various nerve tracts, suggesting a putative role in axon guidance (Romaniello et al., 2018). Recent analysis performed on *TUBA1A* loss-of-function mice and cultured fibroblasts from *TUBB*-associated tubulinopathy patients have revealed an impaired MT dynamics and aberrant cytoskeleton configurations in the axonal GCs (Buscaglia et al., 2020; Sferra et al., 2020). However, it remains to be uncovered whether and which guidance molecules are involved in these MT-associated axon tract malformations.

MICROTUBULE-ASSOCIATED PROTEINS IN AXON GUIDANCE

The assembly, stability and remodeling of MT networks during axon navigation mostly relies on the localization and activity of a wide range of MAPs located in the axon and GC compartments. MAPs manage many aspects of the MT cytoskeleton, including the spatial-temporal control of MT nucleation, polymerization, depolymerization, stability, pausing, bundling, severing, trafficking or interaction with other cellular structures (Goodson and Jonasson, 2018). Therefore, MAPs play a pivotal role in the transduction of attractive and repulsive guidance signaling over MT dynamics in axons and growth cones. Consistently, mutations in human MAP-coding genes have been associated to a wide spectrum of neurodevelopmental disorders linked to axon misrouting (Poirier et al., 2013; Chilton and Guthrie, 2017; Lasser et al., 2018; Romaniello et al., 2018). In this section we will summarize the intracellular pathways downstream axon guidance signaling that directly control the activity, localization or expression of MAPs to achieve GC protrusion and steering, as well as MAPs requirement for axon tract development *in vivo*. For clarity, we have classified the MAPs as: (1) MT-nucleation MAPs, (2) MT-stabilizing and polymerization-supporting MAPs, (3) MT-severing, destabilizing and polymerization-inhibitory MAPs, (4) MT-tracking motor proteins and (5) MT plus-tip interacting proteins (+TIPs).

Microtubule-Nucleation Microtubule-Associated Proteins

In the shaft of cortical axons, MTs are formed *de novo* – nucleated – locally in an acentrosomal manner, by a mechanism involving the Augmin/HAUS complex and the γ-tubulin ring complex (γTuRC) that ensures the uniform polarity of the MT network (Sánchez-Huertas et al., 2016; Cunha-Ferreira et al., 2018). Although local events of MT nucleation have not been yet reported in the axonal GCs, acentrosomal γTuRC-dependent MT nucleation has been recently observed over endosomes in the dendritic GCs of invertebrate neurons (Liang et al., 2020; Yoong et al., 2020). These evidences, in combination with the following recent findings, allow to put forward the hypothesis of axon guidance signaling influencing local MT nucleation events in the distal axon.

The γTuRC-dependent MT nucleation in eukaryotic cells undergoes spatial and temporal regulation by means of additional MAPs, such as TPX2 and its activator RanGTP, and both proteins have been found to be enriched at neuritic tips (Chen et al., 2017; Huang et al., 2020; Liu et al., 2021). MT-bound TPX2 participates in MT nucleation at elongating neurite tips in cultured hippocampal neurons (Chen et al., 2017). RanGTP is transported anterogradely along the axons through actin waves, it colocalizes with actin-based structures in the axonal GC and enables local nucleation events at neurite tips (Chen et al., 2017; Huang et al., 2020). Actin waves (also known as growth cone-like waves) are dynamic cytoskeletal structures traveling anterogradely along the axon shaft. These waves are associated to transient MT generation activity along the axons, including an increase in MT polymerization and MT-based transport (Winans et al., 2016). Therefore, it is possible that RanGTP and TPX2 are transported to the GC, jointly with other MT nucleation machinery such as γ-TuRCs, to trigger local short-lived MT nucleation events.

New results also suggest that Wnt signaling could shape axonal MT configurations via regulation of local MT nucleation mechanisms. Weiner et al. (2020) showed that in *Drosophila*, some Wnt signaling proteins, such as Fz, LRP5/6 or Axin, recruit the MT core-nucleation protein γ-Tubulin to endosomes in the dendritic branch points, enabling local MT nucleation and indicating that extracellular Wnt signaling can regulate local MT nucleation in dendrites. In addition, two other recent studies have revealed that the Wnt pathway controls axon specification in developing neurons by organizing the polarity of MT networks both in the axon (Stanganello et al., 2019) and in non-axonal neurites (Puri et al., 2021). Plus, it is known that local MT nucleation contribute the MT arrangements in these compartments (Sánchez-Huertas et al., 2016; Cunha-Ferreira et al., 2018). Overall, these results convey a putative mechanism whereby extracellular Wnt signaling might control MT architecture in axons and dendrites via spatial-temporal control of MT nucleation in developing neurons. Hence, we believe that the contribution of local MT nucleation events in distal axons to guidance cue-instructed navigation should be further investigated.

Microtubule-Stabilizing and Polymerization-Supporting Microtubule-Associated Proteins

Microtubules are heavily stabilized in the axonal shaft, whereas in the GC they are very dynamic. The stability status and polymerization rate of MTs in the axons rely on the activity of specific MAPs, such as MAP1B, tau or CRMP2, whose activities are directly regulated by axon guidance signaling pathways (**Figure 2**). MAP1B is a MT-stabilizing protein that associates with the lattice of dynamic MTs in the most distal region of the axon and in the GC. Studies of asymmetric laser inactivation in GCs together with genetic analyses revealed that the phosphorylated form of MAP1B is a direct effector

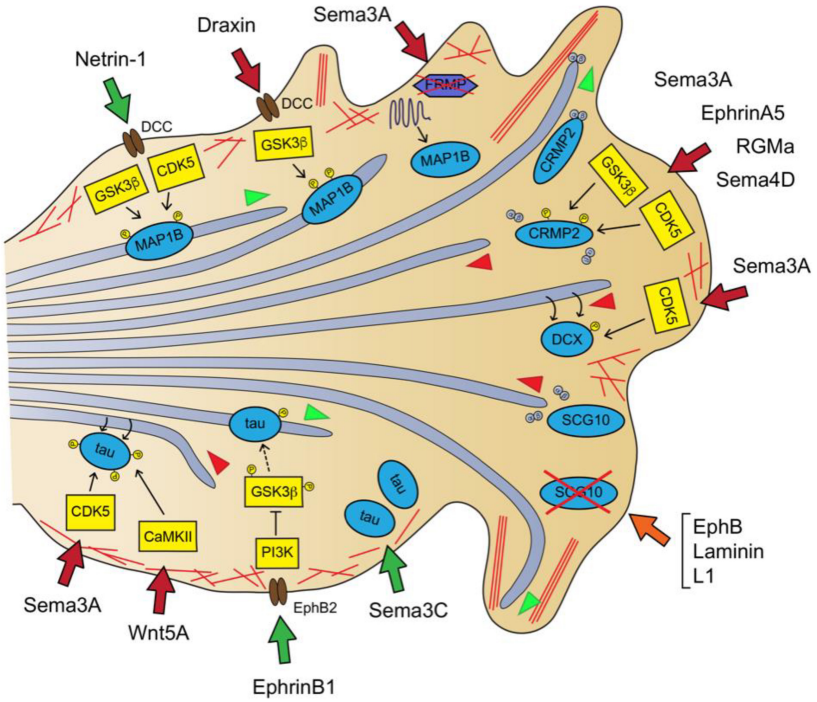

FIGURE 2 | Guidance signaling downstream pathways involved in MT dynamics in the axon and GC I: MT-stabilizing, MT-destabilizing and MT-polymerization supporters. Netrin-1-DCC signaling produces MT stabilization via MAP1B phosphorylation through GSK3 and CDK5 activity (Del Río et al., 2004). Draxin binds DCC receptor and leads to MAP1B phosphorylation via GSK3β (Meli et al., 2015). Sema3A stimulates MAP1B mRNA local translation by promoting the proteasome-dependent degradation of the repressor FRMP (Takabatake et al., 2020). Sema3A, EphrinA5, RGMa or Sema4D inhibit MT polymerization by increasing CRMP2 phosphorylation via GSK3β and CDK5 (Arimura et al., 2005; Cole et al., 2006; Ito et al., 2006; Wang et al., 2013). Sema3A promotes MT destabilization by promoting DCX-fall off the MT lattice via CDK5-dependent phosphorylation of DCX (Bott et al., 2020). The combined action of EphB, laminin and L1 leads to MT overgrowth and buckling by reducing SCG10 protein levels (Suh, 2004). Sema3C increases tau protein levels (Moreno-Flores et al., 2004). EphrinB1-EphB2 signaling reduces tau hyperphosphorylation via PI3K-dependent inhibition of GSK3 (Jiang et al., 2015). Wnt5a promotes MT redistribution by stimulating CaMKII-dependent phosphorylation of tau at Ser262 (Li et al., 2014). Sema3A transiently increases tau phosphorylation at Ser202 and Thr205 via CDK5-dependent phosphorylation (Sasaki et al., 2002). MTs are shown as light purple tubes, F-actin as red lines. MAPs are represented in blue, kinases in yellow and MAP-interacting proteins in purple. Guidance cue receptors are in brown. Guidance-evoked responses are represented in green (attraction), red (repulsion) and orange (pause) arrows. MT advance and retraction are represented with green and red arrowheads, respectively.

of axon turning because selectively stabilizes MTs at the GC periphery (Black et al., 1994; Mack et al., 2000; Bouquet et al., 2004). MAP1B phosphorylation levels are increased in cortical neurons after Netrin1 treatment via GSK3β and CDK5 kinase activity. Consistently, growing axons from MAP1B-deficient CNS explants are irresponsive to netrin-1-induced chemoattraction. MAP1B mutant mice are viable but exhibit misguided cortical, thalamocortical and hippocampal axons (**Table 1**) (Meixner et al., 2000; Del Río et al., 2004). These dramatic axon wiring defects suggest that MAP1B is involved in additional axon guidance pathways, other than netrin-1. Indeed, the repulsive axonal guidance responses evoked by Draxin and Sema3A treatments also involve MAP1B in their downstream pathways. Draxin, which is an essential guidance cue for the development of forebrain commissural tracts, interacts with the netrin receptor DCC and activates the GSK3β-MAP1B pathway in order to induce a repulsive response in cortical axons (Meli et al., 2015). On the other hand, Sema3A treatment of hippocampal neurons increases MAP1B levels in distal axons in a local translation-dependent manner (Campbell and Holt, 2001; Li C. et al., 2009). Specifically, Sema3A induces the local degradation of the translational suppressor FMRP via the ubiquitin-proteasome pathway, which results in the increase of MAP1B mRNA-coding translation in the GC (Takabatake et al., 2020). Thus, it appears that MAP1B is a downstream mediator of both attractive and repulsive guidance cues. This high degree of MAP1B tunability could be entailed by its multiple phosphorylation sites (Kawasaki et al., 2018), sensitive to CDK5 and GSK3β activity, but further work is needed to understand the molecular mechanisms whereby MAP1B promotes GC steering.

Tau is another phospho-MAP that binds the MT lattice and stabilizes the MTs in the axon shaft, playing a critical role in axon specification, growth and branching. Tau hyperphosphorylation generally correlates with impaired MT binding and axonal MT cytoskeleton disruption (Cleveland et al., 1977; Binder et al., 1985; Drubin and Kirschner, 1986; Grundke-Iqbal et al., 1986). Similar to MAP1B, Tau is a downstream target of GSK3β and CDK5 - among other kinases (Guo et al., 2017). In particular, it was found that Sema3A treatment transiently increases phospho-tau levels in the GC of chick neuron cultures via CDK5-dependent phosphorylation previously to GC collapse (Sasaki et al., 2002). Also, Wnt5a promotes the reorganization of MTs in the GC of

cortical neurons through CaMKII-dependent phosphorylation of tau within its MT-binding site (Ser262) in order to evoke a repulsive axonal response (Li et al., 2014). In opposition to this, the activation of EphB2 receptor by ephrin B1 reduces tau hyperphosphorylation through GSK3β inhibition *in vivo* in the CA3 hippocampal region of tau transgenic mice (Jiang et al., 2015). Moreover, Sema3C addition upregulates the total tau protein levels in cultured cerebellar granule neurons, preserving survival and stimulating neuritogenesis (Moreno-Flores et al., 2004). Interestingly, it was uncovered that tau promotes the co-alignment of MT and actin fibers *in vitro*, and stimulates the coordinated polymerization of both cytoskeleton networks (Elie et al., 2015). In line with this, it was recently reported that tau does not only decorates the lattice of stabilized MTs along the axon shaft but also associates to dynamic MTs aligned with actin filaments in the GC periphery of cortical neurons. Tau downregulation disrupted the MT bundling in the GC central domain, prevented MT invasion into the periphery and misoriented MT trajectories. Overall, tau loss-of-function inhibited the turning of cortical axons exposed to Wnt5a gradients (Biswas and Kalil, 2018).

The collapsin response mediator proteins (CRMPs) family are cytosolic phospho-MAPs that play important roles in the developing nervous system, including axon guidance (Nakamura et al., 2020). CRMP family name was given because its first member identified, CRMP2, was a molecular mediator of GC collapse upon stimulation with Sema3A (originally known as Collapsin) (Goshima et al., 1995). There are five human CRMPs (CRMP1-5), displaying different subcellular localization and cytoskeletal targets. Among them, CRMP2 localizes to the axon and the C-domain of the GC and controls MT polymerization/stability. Indeed, it has been observed that CRMP2 participates in axon specification, elongation, branching and guidance effect by several guidance cues (Inagaki et al., 2001; Lin et al., 2011; Higurashi et al., 2012; Yamashita and Goshima, 2012). When CRMP2 monomers are non-phosphorylated, they bind tubulin heterodimers and the complex is transported to the distal part of growing axons, by kinesin-1-dependent motor forces, to support MT polymerization and axon growth. Upon Sema3A stimulation, CRMP2 is sequentially phosphorylated at its C-terminal domain by CDK5 and GSK3β kinases, hampering its tubulin-binding properties and leading to GC collapse via MT destabilization (**Figure 2**). The Sema3A-induced CRMP2 inactivation is achieved by phosphorylation at Ser522 by CDK5, followed by GSK3β-dependent phosphorylation at Ser518, Thr514 and Thr509 (Fukata et al., 2002; Kimura et al., 2005; Cole et al., 2006). In addition to Sema3A, other repulsive guidance cues induced CRMP2 phosphorylation via GSK3 and/or Rho kinase to achieve GC collapse, these include Sema4D, RGMa and ephrinA5 (Arimura et al., 2005; Ito et al., 2006; Wang et al., 2013). Consistently, CRMP2 has been demonstrated to be essential for axon navigation *in vivo* because *CRMP2KO mice* exhibit axon guidance defects in peripheral nerves and in the corpus callosum (Ziak et al., 2020).

Mutations in the genes encoding the MAP doublecortin (DCX) account for the majority of the human cases of double cortex syndrome, which exhibits severe brain cortex malformations primarily attributable to neuronal migration and proliferation deficits (Gleeson et al., 1998; Bahi-Buisson et al., 2013). DCX is a MT-stabilizing phospho-protein abundant in the axonal GCs, which decorates the lattice of MTs invading the F-actin rich peripheral region of the GC (Moores et al., 2004; Tint et al., 2009). Interestingly, the double genetic deletion of DCX and its closest homolog protein doublecortin-like kinase1 (DCLK1) in mice led to widespread defects in axon tracts, affecting the corpus callosum, anterior commissure, subcortical fiber tracts and internal capsule. More specifically, the DCX mutant axons exhibit impaired transport, growth and are irresponsive to netrin-1-evoked chemoattraction, although the latter was suggested to stem from DCX regulatory effects on actin configurations (Deuel et al., 2006; Koizumi et al., 2006; Fu et al., 2013). This data suggests that DCX is required for guidance signaling-evoked axonal steering during nervous system development. Indeed, a recent study uncovered that DCX mediates the repulsive response of GCs upon Sema3A treatment (Bott et al., 2020). Bott et al. (2020) showed that DCX forms a complex with Nestin that enables DCX phosphorylation by CDK5/p35 downstream Sema3A signaling. They also demonstrated that DCX phosphorylation by CDK5 decreased its MT affinity and resulted in MT destabilization.

Microtubule-Destabilizing, Severing and Polymerization-Inhibitory Microtubule-Associated Proteins

In addition to MT polymerization and stability, MT depolymerization and severing are also critical mechanisms for the arrangement of MT networks. Several of these MAPs have been involved in the transduction of axon guidance signaling. SCG10 (superior cervical ganglion-10)/Stathmin-2 is a neuron-specific member of the MT-destabilizing protein family of the stathmins. Stathmins bind tubulin dimers, sequestering them from growing plus-ends and thereby, promoting MT depolymerization (Charbaut et al., 2001; Grenningloh et al., 2004). SCG10 is considered an axon survival protein, highly enriched in the GCs C-domain of developing neurons, and its levels are dynamically regulated by local degradation and KIF1B-dependent axonal transport toward the GC (Shin et al., 2012; Drerup et al., 2016). Axon extension during neuron differentiation requires SGC10 activity, since its downregulation produces MT overstabilization and looping in the GC of hippocampal neurons (Morii et al., 2006). The repulsive protein EphB typically triggers GC collapse, but in the presence of laminin and L1 leads to paused GCs, which retain their normal filopodial dynamics and actin distribution. It was found that this guidance cue combination specifically reduced SCG10 levels in GC, which stimulated the invasion of long curved MTs into the GC periphery and led to GC pause (**Figure 2**) (Suh, 2004). Additionally, SCG10 interacts with the small RhoGTPase Rnd1, and this interaction enhances SCG10 MT destabilizing activity in neurons. Rnd1 is known to mediate the GC collapse induced by Sema4D-Plexin-B1 signaling in hippocampal neurons (Oinuma et al., 2004; Li Y.-H. et al., 2009), suggesting that SCG10 may also function downstream of the Sema4D signaling pathway.

On the other hand, the MT-severing enzymes cut MT fibers into shorter fragments, creating new local MT seeds and influencing axon branching (Sharp and Ross, 2012). Spastin is a MT-severing protein required for axon morphogenesis, associated to a degenerative disease of the corticospinal axon tracts, named Hereditary spastic paraplegia (Roll-Mecak and Vale, 2008). Recently, the alternative translation of spastin mRNA transcripts has been found to influence both motor neuron axon guidance and migration downstream of bone morphogenic protein (BMP) and neuropilin-1 signaling during zebrafish development (Jardin et al., 2018). Fidgetin-like-1 (Fignl1) is another MT-severing protein enriched in the growth cone of zebrafish growing axons, whose downregulation led to pathfinding defects in spinal motor axons and impaired larvae locomotion (Fassier et al., 2018), although no specific guidance proteins controlling Fignl1 activity have been identified.

Concerning MT polymerization inhibitors, the kinesin-4 family members KIF21A and KIF21B and the immotile kinesin-13 family member KIF2A, have been linked to neurodevelopmental malformations associated with axon growth and guidance defects in human patients (**Table 1**) (Yamada et al., 2003; Poirier et al., 2013; Asselin et al., 2020). More specifically, *KIF21A* is a gene risk factor for the CFEOM1 (congenital fibrosis of the extraocular muscles type-1), a developmental oculomotor nerve disorder. CFEOM1-associated *Kif21a* mutations in mice caused aberrant axon branching, stalling and misorientation defects in oculomotor nerves (Yamada et al., 2003; Cheng et al., 2014). It was reported that KIF21A decreases MT polymerization rate and suppresses MT plus-end catastrophes. KIF21A overexpression in hippocampal neurons slendered the GC morphology, stimulated axon growth and suppressed the repulsive axonal response to Sema3F (van der Vaart et al., 2013). In turn, KIF2A has been proposed to regulate axon pruning by preventing MT overstabilization in the GC. It was found that Kif2a$^{-/-}$ mice exhibit an aberrant axonal overextension in hippocampal neurons, due to reduced MT depolymerization in the GCs (Homma et al., 2003; Maor-Nof et al., 2013).

Microtubule-Tracking Motor Proteins

As aforementioned, dynein-driven motor forces facilitate the entry of MTs into the GC periphery, influencing neurite initiation, axon outgrowth and steering (Dehmelt et al., 2006; Myers et al., 2006; Grabham et al., 2007). In support of dynein's role in guidance-evoked GC movements, dynein loss-of-function experiments using RNAi or Cilibrevin D revealed an impairment in NGF-evoked filopodia formation and in GC turning over substrate boundaries. However, both dynein-driven MT-sliding into the GC periphery or MT-based retrograde transport of signaling endosomes could contribute to these instructed axon movements (Myers et al., 2006; Sainath and Gallo, 2015). Likewise, MT-based kinesin-dependent anterograde transport is necessary for axonal extension and steering. For instance, the MT-sliding activity of kinesin-5 – also called Eg5 or kif11 – inhibits the MT invasion into the GC periphery and it is required for GC turning in response to repulsive substrate boundaries. It was found that an asymmetric accumulation in the GC of the phosphorylated form of kinesin-5 precedes turning, and its acute inactivation in one side of the GC elicits the MT invasion into the hampered side and GC turning (Nadar et al., 2008, 2012).

A recent study has pinpointed the kinesin KIF13B as the molecular motor responsible of Myo X localization to axons upon netrin-1 stimulation. Myo X is an actin-based motor protein that transports lipids and transmembrane receptors, such as DCC, to the filopodia tip during axon pathfinding. It was found that netrin-1 signaling increases Myo X-KIF13B interaction and its anterograde MT-dependent transport along the axons, in order to stimulate axon initiation and axon branching in the cortical commissural projections (Yu et al., 2020). The kinesin family member 1 binding protein (KIF1BP) is also necessary for a proper development of the anterior commissures and the sympathetic innervation of the gut (Hirst et al., 2017). Mutations in the *Kif1*β gene, associated to the Charcot-Marie-Tooth peripheral neuropathy, have been found to prevent KIF1Bβ binding to the insulin-like growth factor 1 (IGF1) receptor IGF1R, involved in sensory axon guidance. These mutations blocked the MT-dependent axonal transport of IGF1R and inhibited IGF1-evoked axon outgrowth (Scolnick et al., 2008; Xu et al., 2018).

The kinesin-1 motor complex has also been suggested to participate in the netrin-1-evoked repulsive response in invertebrate motor axons and is a phosphorylation target of GSK3β, a major transduction hub of various guidance signaling pathways (Teulière et al., 2011; Banerjee et al., 2018). Furthermore, mutations in gene encoding the subunit KIF5C of the kinesin-1 complex (encoded by the *Kif5* genes) have been linked to an abnormal development of the axon tracts of the corpus callosum and the internal capsule (**Table 1**) (Poirier et al., 2013; Michels et al., 2017). The recent analysis of a mutant mice lacking the kinesin-1 light chain KLC1 has revealed hypoplasia of the internal capsule tract, that includes corticofugal and thalamocortical axons. The innervation defects were found to be caused by an impaired kinesin-1-dependent axonal transport of the cannabinoid type-1 receptors (CB1R), and the subsequent axon unresponsiveness to endocannabinoids signaling (Saez et al., 2020).

Microtubule Plus-Tip Interacting Proteins (+TIPs)

Plus-end tracking proteins (+TIPs) regulate MT plus-end polymerization and stability, and mediate interactions between the MT ends and actin fibers, organelles and plasma membrane (van de Willige et al., 2016). Evidences obtained during the last 15 years have demonstrated that axon guidance signaling pathways directly target via regulation of +TIPs' activity and localization (**Figure 3**) (Bearce et al., 2015; Cammarata et al., 2016; Voelzmann et al., 2016).

Microtubule end-binding (EB) proteins are the most abundant +TIPs in cells. EBs (EB1, EB2, and EB3) directly associate with MT plus-ends through their N-terminal calponin homology (CH) domain and are autonomous regulators of plus-end dynamics. MT tip-tracking of EBs mainly correlates with MT polymerization episodes, since it favors a continuous polymerization and reduces the number of catastrophes. Importantly, EBs and are also scaffold-providers for other +TIPs through their C-terminal domain, and for this reason

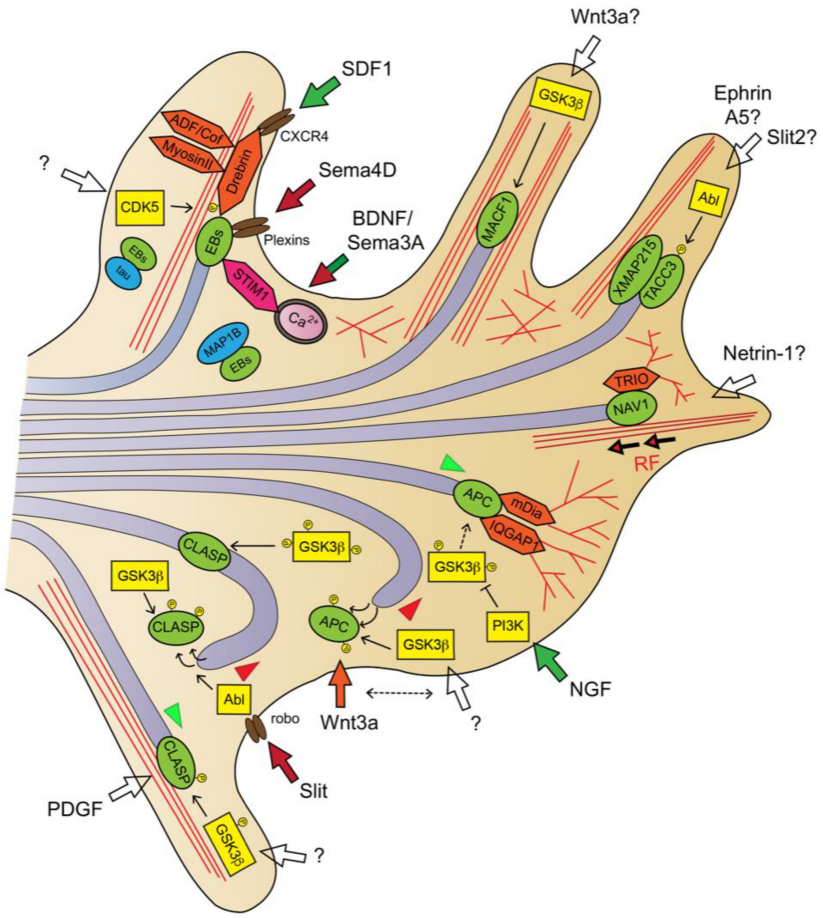

FIGURE 3 | Guidance signaling downstream pathways involved in MT dynamics in the axon and GC II: +TIPs. SDF1/CXCR4 signaling activates the EB1/Drebrin module for MT remodeling (Shan et al., 2021). Sema4D/plexin signaling inhibits EB3-labeled MT polymerization (Laht et al., 2012, 2014). BDNF and Sema3A promote asymmetric MT invasion via STIM1-EB3 interaction (Pavez et al., 2019). NGF stimulates APC-dependent MT plus-end stabilization via local inhibition of GSK3β activity (Zhou et al., 2004). Wnt3a alters MT polymerization direction by misslocating APC from the MT plus-ends (Purro et al., 2008). Slit/Robo signaling promotes MT growth arrest by dissociating CLASP from the MT plus-end via Abl-dependent CLASP phosphorylation (Lee et al., 2004). High GSK3 kinase activity (poorly phosphorylated) dissociates CLASP from plus-ends, low GSK3 activity (highly phosphorylated) misslocates CLASP from plus-ends to the MT lattice, moderate GSK3 activity allows CLASP plus-end binding, MT stabilization and growth (Hur et al., 2011a). MTs are shown as light purple tubes, F-actin as red lines. +TIPs are represented in green, kinases in yellow, actin-interacting/regulatory proteins in orange and other +TIP-interacting proteins in pink. Guidance cue receptors are in brown. Guidance-evoked responses are represented in green (attraction), red (repulsion) or orange (pause) arrows. Empty arrows were used when downstream transduction pathways are unclear or guidance cues unknown. MT advance and retraction are represented with green and red arrowheads, respectively.

EBs are considered master regulators of +TIP network. EB1 protein is ubiquitous, whereas EB3 is predominantly expressed by neurons, and both EB1 and EB3 are necessary for axon extension (Akhmanova and Steinmetz, 2015; van de Willige et al., 2016). Semaphorin4D can influence the EB3-labeled MT plus-ends polymerization dynamics in hippocampal neurons, and it was found that both EB1 and EB3 interact with the intracellular domains of the Plexin-A2, Plexin-B1, and Plexin-B3 Semaphorin family receptors (Laht et al., 2012, 2014). This data suggest that the semaphorin-plexin-EB pathway may regulate MT dynamics during axon pathfinding. When MT plus-ends enter the actin-rich P-domain of GCs, EB3 recruits the F-actin-binding protein Drebrin to couple growing MT tips to actin filaments. Hence, the EB3-Drebrin module facilitates the invasion of exploratory MTs into the GC periphery, and enables growth cone formation and neuritic elongation (Geraldo et al., 2008). It has been recently proposed that the EB1-Drebrin module at plus-ends interacts with the chemokine receptor type 4 (CXCR4) upon stromal cell-derived factor-1 (SDF-1) signaling. The chemokine SDF-1 can regulate axonal elongation and branching, and the SDF-1/CXCR4/Drebrin/EB1 pathway appears to be critical for SDF-1-induced MT cytoskeleton remodeling during neuronal motility (Pujol et al., 2005; Shan et al., 2021). Furthermore, EB3 colocalizes at the MT plus-ends within the GC filopodia with the stromal interacting molecule (STIM1), which is a calcium-sensing protein that mediates GC steering in response to various axon guidance cues (Mitchell et al., 2012; Pavez et al., 2019). New data revealed that EB3-STIM1 interaction at MT plus-ends is calcium-sensitive and STIM1 instructs the asymmetric invasion of EB3-labeled MT plus-end into the motile GC side downstream of BDNF or

Sema3A signaling in sensory neuron cultures. Moreover, *in vivo* experiments in zebrafish showed that the EB3-STIM pathway regulates the axon guidance of spinal motor neurons (Pavez et al., 2019). In addition, EB1/3 proteins can bind MAP1B and Tau, and this interaction sequesters EBs from MT plus-ends and jeopardizes MT growth (Tortosa et al., 2013; Sayas et al., 2015). Because MAP1B and tau are downstream effectors of several axon guidance pathways, their interaction with EBs could indirectly influence the MT dynamics and the assembly of the +TIP complex on account of its dependence on EB scaffold.

One of the pioneer studies that assigned + TIPs a prominent role in axon guidance refers to the cytoplasmic linker associated protein (CLASP) and the Slit-evoked repellent response (Lee et al., 2004). CLASP decorates the MT plus-ends that polymerize over F-actin bundles in the GC periphery, and its overexpression causes MT overstabilization, looping and prevents their extension beyond the transition zone (Hur et al., 2011a). Orbit/MAST, the CLASP ortholog in invertebrates, is an Abelson tyrosine kinase (Abl) target downstream of Slit/Robo signaling that mediates repulsion. These evidences served the authors to propose that focal Slit stimulation in one side of the GC provokes asymmetric activation of the Abl-CLASP pathway and MT growth arrest, entailing a GC movement away of the source of Slit (Lee et al., 2004). CLASP is recruited to MT plus-ends through EB binding, although it contains tumor overexpressed gene (TOG) domains which can serve as tubulin-binding modules (Mimori-Kiyosue et al., 2005; Al-Bassam and Chang, 2011). Indeed, it has been observed that CLASP localization in the MTs can alternate between the plus-end and the MT lattice, based on its phosphorylation by GSK3β. These MT-binding activities determine the degree of MT protrusion and subsequent axon growth in an opposing manner. A high GSK3 kinase activity promotes CLASP dissociation from MT plus-ends, leading to MT destabilization and impaired axon growth, while a moderate GSK3 activity allows CLASP plus-end binding, promoting MT stabilization and axon extension. A low GSK3 activity leads to CLASP localization to the MT lattice, producing MT overstabilization and looping in the GCs, and axon growth attenuation (Akhmanova et al., 2001; Hur et al., 2011a). Given that GSK3 kinase activity is fine-tuned by many downstream axon guidance pathways, CLASP may also act as transducing factor of other extracellular guidance cues (Hur and Zhou, 2010).

APC (Adenomatous Polyposis Coli Protein) is a critical tumor suppressor, initially reported as Wnt-signaling regulator. In the Wnt pathway, APC forms a complex with GSK3 and other proteins to target and degrade the oncoprotein β-catenin (Stamos and Weis, 2013). In addition to this function, APC is an EB-binding +TIP that stabilizes the MT plus-ends and, similar to CLASP, this activity is abolished by GSK3β-mediated phosphorylation (Nakamura et al., 2001; Zumbrunn et al., 2001). In neurons, APC is transported toward the distal region of the growing axon by kinesin-1 motor forces, and distributes asymmetrically within the GC. Indeed, the local accumulation of APC in one side of the GC anticipates the steering movement of the axon in this axial direction (Koester et al., 2007; Ruane et al., 2016). It was demonstrated that the focal stimulation of GCs with Nerve Growth Factor (NGF) produces the localized inactivation of GSK3β via PI3K activity, which enables APC-dependent stabilization of MT plus-ends in GCs and rapid axon elongation (Zhou et al., 2004). Additionally, the treatment with the GC-pausing guidance cue Wnt3a led to altered MT growth directionality in the GC by misallocating APC from the MT plus-ends at the P-domain (Purro et al., 2008). *In vivo*, despite initial contradictory results obtained in *Drosophila*, APC has been shown to play an important role in neural circuits formation. APC mutant mice exhibit gross misrouting defects in the internal capsule, posterior commissure or thalamocortical axons, and APC-deficient neurons displayed an abnormal axonal arborization and curling at the tips (Rusan et al., 2008; Yokota et al., 2009; Jin et al., 2018). Besides its MT-stabilizing role at the plus-end, APC participates in the MT-based transport of mRNAs, such as those encoding β-actin, Tubb2b or the dynein complex subunit Lis1, toward the axon. Importantly, APC association with their mRNA targets to transport them along sensory axons is triggered by exogenous stimulation with NGF (Preitner et al., 2014; Villarin et al., 2016; Baumann et al., 2020).

APC2, APC's brain specific homolog, is a MT-binding protein and contains a C-terminal region with MT tip-tracking properties. APC2 localizes to GCs of chick retinal axons and participates in retinotectal axon guidance through regulation of MT stability. *Apc2*-knockdown display an attenuated response to ephrin-A2 in retinal ganglion cells (Shintani et al., 2009; Kahn et al., 2018). Also in retinal neurons, APC2 has been identified as a direct target of the transcription factor Zic2, the main determinant of axon midline avoidance, which also regulates the guidance receptors EphB1 and Unc5c (Herrera et al., 2003, 2019b; Escalante et al., 2013; Kridsada et al., 2018; Murcia-Belmonte et al., 2019). In ipsilaterally projecting neurons, *Apc2* expression is intrinsically downregulated by Zic2 likely to facilitate Wnt5a and ephrinB2-mediated axon repulsion at the optic chiasm (Morenilla-Palao et al., 2020).

Microtubule-actin crosslinking factor 1 (MACF1), also known as actin-crosslinking factor 7 (ACF7), is a large multidomain protein of the spectraplakin family, highly expressed in the nervous system. MACF1 interacts with MT plus-ends and enables MT capture by F-actin, facilitating MT polymerization over F-actin bundles at the cellular periphery (Kodama et al., 2003; Wu et al., 2008). MACF1 can directly interact with MTs through its C-terminal Gas2-related (GAR) domain or indirectly by EB binding, and simultaneously binds F-actin through its N-terminal calponin-homology (CH) domains. In addition, MACF1 has a C-terminal AAA-ATPase domain that can exert molecular forces over the MT cytoskeleton (Moffat et al., 2017). Genetic studies in *Drosophila* showed that MACF1 homolog protein *Shot* is required for axon extension and midline guidance, and that its MT plus-tip tracking enabled by EB1-binding is necessary to maintain an organized MT network in axons (Lee et al., 2007; Alves-Silva et al., 2012). Consistently, mammalian MACF1 also regulates neuronal MTs configurations and filopodia formation, a role dependent on both MACF1 F-actin- and MT-binding domains (Sanchez-Soriano et al., 2009). MACF1 mediates Wnt/GSK3β signaling, and its loss-of-function in mice phenocopied the early developmental defects observed in $Wnt3^{-/-}$ embryos. Specifically, the conditional deletion

of MACF1 in neural progenitors produced the agenesis of the anterior commissure and an abnormal development of the thalamocortical fibers and the hippocampal commissure in neonatal mice (Chen et al., 2006; Goryunov et al., 2010). Moreover, MACF1 downregulation in cortical early postmitotic neurons interfered with the normal arrangement of MTs and F-actin networks in neurites, inhibited neuron radial migration and disrupted callosal axon innervation (Ka et al., 2014; Ka and Kim, 2016). Interestingly, heterozygous missense mutations in the MT-binding GAR domain of MACF1 have been recently identified in human individuals exhibiting axonal midline crossing phenotypes, among other defects (**Table 1**) (Dobyns et al., 2018).

Neuron navigator-1 (NAV1) belongs to the +TIP family of Navigators (NAVs), which is represented by NAV1, NAV2, and NAV3 in mammals. NAVs are large proteins, carrying N-terminal calponin-homology (CH) domains and an intriguing C-terminal ATPase domain, which have been associated to axon outgrowth (Martínez-López et al., 2005; van Haren et al., 2009; McNeill et al., 2010; Abe et al., 2014). In particular, NAV1 expression was found to be largely restricted to the developing nervous system being enriched in the neuritic tips and GCs. Hindbrain neurons lacking NAV1 do not respond to Netrin-1, which suggested a function downstream of Netrin-1 signaling (Martínez-López et al., 2005; van Haren et al., 2014). It was recently described that, similar to CLASP or MACF1, NAV1 is an EB-dependent +TIP that can directly bind actin fibers *in vitro,* and data suggest that it crosslinks MT plus-ends to the F-actin network within the GCs from mammalian cortical neurons (Sánchez-Huertas et al., 2020). In the proposed model, EB proteins recruit NAV1 to the MT tip during polymerization inside F-actin-enriched regions. Following EB-complex disassembly and MT growth arrest, NAV1 switches to an EB-independent form of association with the MT plus-end and stabilizes it, reducing the frequency of MT shrinkage. Thereafter, paused plus-ends undergo retrograde translocation coupled to F-actin retrograde flow via MT-NAV1-F-actin crosslinking (Sánchez-Huertas et al., 2020). However, NAV1 sequence does not possess a CH domain for actin binding, neither GAR nor TOG domains for direct MT interaction. Hence, the specific NAV1 domains responsible for direct F-actin binding and whether NAV1-MT interaction requires an intermediary autonomous MT-binding protein, still remain to be elucidated. NAV1 was also found to mediate the chemoattractive response of cortical axons toward a source of netrin-1 and the radial migration of pyramidal neurons during *in vivo* corticogenesis (Sánchez-Huertas et al., 2020). NAV1 mRNA and protein levels are highly enriched in developing cortical layer V, mainly populated by projection neurons innervating subcortical targets, such as the brainstem or the spinal cord (Martínez-López et al., 2005; Sorensen et al., 2015). This observation suggests that NAV1 might be required for axonal navigation by layer V projection neurons in particular, and allows to hypothesize that *ad hoc* neuron cytoskeletal machinery may transduce guidance signaling differently in specific neuron subtypes.

Recent evidences suggest that the module formed by the +TIPs XMAP215 (chTOG or CKAP5 in mammalian cells) and transforming acidic coiled-coil 3 (TACC3) protein represent an unconventional EB-independent regulatory mechanism of MT plus-end dynamics downstream axon guidance signaling. XMAP215 is a conserved processive MT polymerase that catalyzes tubulin addition into the polymer while it tracks the MT plus-ends (Gard and Kirschner, 1987; Brouhard et al., 2008). Although XMAP215 and EB1 can act synergistically to promote MT growth, XMAP215 does not require EB proteins to track MT plus-ends because it binds MTs directly through its five N-terminal TOG domains. Indeed, XMAP215 locates to the extreme MT plus-end several tens of nanometers ahead of the region bound by EB1 and remains attached to the MT plus-end even during shrinkage events (Nakamura et al., 2012; Zanic et al., 2013; Maurer et al., 2014). XMAP215 downregulation greatly increases MT catastrophe frequency throughout the neuron cell body and compromises hippocampal axon growth (van der Vaart et al., 2012). While in most cellular contexts XMAP215 downregulation decreases MT plus-end growth, in GCs it accelerates MT plus-end velocities. This increase was proposed to arise from higher MT anterograde translocation rates in the GCs, likely due to the uncoupling between MT plus-ends and the F-actin retrograde flow in the absence of XMAP215 (Lowery et al., 2013). More recently, it was reported that XMAP215 directly binds actin fibers and it is necessary for MT-F-actin alignment in the GCs. Indeed, it has been demonstrated that XMAP215 regulates MT invasion into GC filopodia, influences GC morphology and protrusion, and mediates the repulsive response to ephrinA5 (Slater et al., 2019).

TACC3, first identified as a regulator of astral and spindle MT length, has been classified as + TIP on account of its binding to MT plus-ends through its TACC domain and assigned a role in plus-end dynamics and axon outgrowth (Gergely et al., 2000; Nwagbara et al., 2014). TACC3 interacts with XMAP215 in the distal region of MT plus-ends, and they are important for each other's localization to the plus-end. Indeed, TACC3 and XMAP215 can rescue each other's downregulation phenotypes in axon elongation, and it has been suggested that TACC3 strengthens the XMAP215-TACC3 complex binding to MTs in order to drive polymerization activity (Nwagbara et al., 2014; Erdogan et al., 2017). TACC3 is a phosphorylation target of the kinase Abl, whose activity is known to be regulated by axon guidance signaling (Kannan and Giniger, 2017). A TACC3 phospho-null mutant failed to localize at MT plus-ends in GCs, leading to an increase of MT invasion into the filopodia and impaired axon pathfinding. Interestingly, the overexpression of TACC3 interfered with the responsiveness of axons from *Xenopus* neurons explants upon Slit2 and Ephrin-A5 signaling (Erdogan et al., 2017, 2020).

MICROTUBULES INSTRUCT F-ACTIN REMODELING IN THE GROWTH CONE

The interaction of MTs with actin filaments and the involvement of MAPs in this crosstalk is a matter of study since more than 40 years (Griffith and Pollard, 1978; Selden and Pollard, 1983). This body of work has established that axonal navigation responses to guidance signals demand an intense and coordinated

cytoskeleton remodeling, during which both MT and F-actin influence each other's dynamics. As aforementioned, F-actin dynamics influence MT advance and retrograde translocation in the GC periphery (Schaefer et al., 2002; Zhou et al., 2002). Even along the axonal shaft, F-actin structures contribute to the maintenance and dynamics of the MT networks (Winans et al., 2016; Qu et al., 2017). Conversely, the entry of MT plus-ends into the actin-rich cortical regions promotes changes in actin-based structures of the growth cone. Seminal works reported that drugs that inhibit MT dynamics, without appreciable depolymerization, halt the bundling and splaying movements in the peripheral GC domain. At higher concentrations, MT drugs resulted in the loss of lamellipodia and an increase in filopodial length but not filopodial number in the GCs (Tanaka et al., 1995; Gallo, 1998). MT dynamics were also found to be necessary for the maintenance of the F-actin foci that formed in GCs in response to substrate adhesions. In particular, it was found that dampening MT dynamics with drugs suppressed focal F-actin assembly upon laminin signal detection, while the washout of the drug restored these foci, indicating that extracellular signaling can influence F-actin in the GC via MTs (Grabham et al., 2003; Suter et al., 2004). More recently, live microscopy experiments on hippocampal cultures exposed to MT-targeting drugs, revealed that decreasing MT stability significantly reduced F-actin treadmilling in the GC periphery of the nascent axons. Conversely, increasing the MT stability or the MT density in axons resulted in an increase in F-actin dynamics in GCs (Zhao et al., 2017). Together, this data showed that MT dynamics influence F-actin turnover in the GC periphery and revealed the critical role of MTs in the maintenance of the actin-based lamellar and filopodial structures of GCs.

The MT-stabilizing MAPs MAP1B and Tau can simultaneously bind actin filaments and contribute to MT-actin coalignment in the GC. Additionally, MAP1B and tau can stimulate F-actin polymerization and bundling (Villarroel-Campos and Gonzalez-Billault, 2014; Elie et al., 2015; Biswas and Kalil, 2018). However, F-actin and MTs crosstalk mainly takes place at the MT plus-ends and the most suitable candidates to assemble both networks are the +TIPs (Bearce et al., 2015; Cammarata et al., 2016). A minimal engineered version of the + TIP MACF1, containing N-terminal CH domains and C-terminal EB-binding motifs – denominated TipAct – showed efficient MT plus-end tracking and binding to F-actin structures at the cell periphery. TipAct showed low F-actin binding affinity *in vitro*, but its local concentration at MT plus-ends allowed MT tips to link actin fibers. Therefore, when TipAct was added to mixed preparations of purified tubulin and actin, it enabled MTs to transport, pull and bundle actin fibers, globally arranging F-actin configurations (Preciado López et al., 2014). The +TIP CLIP170 also exhibited capacity to stimulate *in vitro* F-actin elongation in MT-actin re-constitution experiments via CLIP170 interaction with the formin mDia1. It was shown that CLIP170-mDia1 complexes are recruited to growing MT ends by EB1 and stimulate F-actin polymerization from the MT surface. The actin fibers remained attached to MTs until they spontaneously detached or were released by a MT catastrophe event (Henty-Ridilla et al., 2016). Furthermore, a recent study performed in hippocampal neurons uncovered that MT plus-ends assemble F-actin networks in the GC periphery in an APC-dependent manner (Efimova et al., 2020). APC modulates the activity of various actin regulators, such as the formin mDia or IQGAP1, which is a downstream effector of Rac1 and Cdc42 GTPases (Watanabe et al., 2009; Okada et al., 2010). In support of this data, electron microscopy analysis reported that APC targets MT plus-ends at the MT-actin interphase in the GC periphery of hippocampal neurons, and that APC is necessary for the local assembly of branched actin filaments in these GCs and also for filopodial protrusions. Importantly, encounters of dynamics APC-positive MT tips with the membranous cell cortex induced local actin-rich protrusions (Efimova et al., 2020). These experiments demonstrate that MTs are important regulators of actin configurations in the GC, either by controlling F-actin treadmilling and polymerization, or by templating F-actin organization.

Other +TIPs have also been shown to bind actin fibers *in vitro* and/or influence F-actin configurations in the GC or filopodial dynamics. CLASP directly binds F-actin *in vitro* and its downregulation alters the F-actin networks in the GC of invertebrate neurons. It was described that CLASP-depleted GCs lack a dense F-actin meshwork and contain less actin bundles, and that lamellipodial architecture relies on CLASP interaction with MTs. Interestingly, CLASP binding to both MTs and F-actin was found to be regulated by Abl-dependent phosphorylation upon serum or platelet-derived growth factor (PDGF) signaling (Marx et al., 2013; Engel et al., 2014). Growing MT plus-ends that enter F-actin-rich areas of the GC are decorated with EB1-NAV1 complexes, and NAV1 transiently crosslinks MTs to F-actin. It has been shown that NAV1 restrains filopodial dynamics and compacts the GC morphology, suggesting a role in F-actin remodeling perhaps through recruiting the RhoGEF Trio to MT plus-ends invading the GC periphery. In addition, NAV1 protein mediates the netrin-1-evoked chemoattraction over cortical axons (van Haren et al., 2014; Sánchez-Huertas et al., 2020). Similarly, the EB3-Drebrin module also contributes to MT-actin coordination and moreover, drebrin inhibits myosin II activity, reduces cofilin-induced severing of F-actin and stabilizes F-actin (Geraldo et al., 2008; Mizui et al., 2009; Mikati et al., 2013; Grintsevich and Reisler, 2014; Zhao et al., 2017). Drebrin's F-actin bundle-binding activity is controlled via CDK5 phosphorylation, and CDK5 is a molecular hub downstream various guidance signaling pathways (Gordon-Weeks, 2017). Yet, the specific guidance cues leading to Debrin's phosphorylation via CDK5 remain to be identified. In addition, the protein Growth arrest-specific 2-like 1 (Gas2L1) has a domain composition similar to MACF1 and a recent study revealed that it performs as a MT-F-actin cytolinker. The simultaneous interaction of Gas2L1 with MTs and actin fibers *in vitro* released its autoinhibition. Thus, it was proposed that MT-F-actin crosslinking via Gas2L1 in actin-rich regions promotes local F-actin stabilization and influences axon outgrowth and branching. In contrast, MT dynamics were unaffected in neurons following Gas2L1 depletion (Willige et al., 2019).

Other emerging players of MT-actin crosstalk in the GC of navigating axons are the formins, a protein family composed

by F-actin assembly factors. Formins may also display MT stabilizing and organizing activities, in some cases independently of their actin polymerization roles, to regulate axon pathfinding (Kawabata Galbraith and Kengaku, 2019). For instance, mDia1 and mDia3 appear to mediate the axonal response to ephrinA5, ephrinB3, Sema3A or SDF1-α in different neuron types, and knockout mice models demonstrate that they are required for spinal cord midline crossing (Arakawa et al., 2003; Thurston et al., 2012; Toyoda et al., 2013). In *Drosophila*, Disheveled-associated activator in morphogenesis (DAAM) is a downstream effector of Wnt5 signaling that exhibits MT-F-actin crosslinking activity during axonal development. It has been proposed that DAAM reshapes filopodia and actin structures in GCs via interaction with +TIPs at MT plus-ends (Gombos et al., 2015; Szikora et al., 2017). Another member of the formin family, FMN2, also participates in the stability of focal adhesions and the generation of traction forces in filopodia and facilitates MT capture by F-actin bundles in the GC of spinal neurons. Interestingly, chick FMN2-depleted spinal commissural neurons exhibited midline crossing defects (Sahasrabudhe et al., 2016; Kundu et al., 2021).

FUTURE DIRECTIONS

During the last years, our understanding of the molecular mechanisms and proteins involved in the cytoskeletal transduction of axon guidance signaling has greatly progressed. While the list of upstream guidance cues and receptor families has not significantly grown, novel combinatorial mechanisms involved in signal transduction and cytoskeleton-regulatory proteins recipient of guidance information are continuously emerging (Stoeckli, 2018; Zang et al., 2021). Among the latter, Microtubule-Associated Proteins (MAPs) represent a significant group. Yet, the role of numerous MAPs in axon guidance is still unexplored and the intricate mechanisms of MT-F-actin coordination in the GC remain unclear.

Despite significant advances, experimental designs performed in non-neuronal cells or limited to few cytoskeleton-regulatory proteins and guidance cues, may not reflect the full scope of cytoskeletal changes triggered by extracellular guidance signaling during axon pathfinding. As a sign of the complex regulation of physiological MT dynamics in cells, recent data has demonstrated that MAP combinations exert collective effects on MTs and MAPs must follow certain hierarchies in their MT recruitment to achieve specific functions (Niu et al., 2019; Hahn et al., 2021). Besides, in addition to stereotyped mechanisms of guidance signal transduction - including regulated guidance receptor expression, dimerization or trafficking - other molecular mechanisms underlying axon guidance decisions are being characterized (Harada et al., 2020; Klein and Pasterkamp, 2021). For instance, it was recently shown that retinal ganglion cell (RGC) axons exhibit an intrinsic pathfinding program in absence of any paracrine signaling from the surrounding tissue (Harada et al., 2020). This sort of cell-autonomous guidance mechanism could act in coordination with extrinsic guidance cues to enable divergent axonal responses to the same guidance information. Indeed, mathematical models predict that extracellular signaling may instruct axon guidance by simply controlling neuron-intrinsic stochastic transitions between GC states (Padmanabhan and Goodhill, 2018).

In summary, we believe that further experiment conceptualization approaching the molecular mechanisms of axon guidance should keep in mind that: (i) downstream guidance pathways may simultaneously target both actin and MT regulatory proteins, enabling an intricate cytoskeletal crosstalk in the GC, (ii) the expanding and diverse MAP network can exert combined effects on MT dynamics, (iii) GC-intrinsic states (stalled/dynamic) and *ad hoc* cytoskeletal machinery may influence axon behavior in specific neuron subtypes, and (iv) GCs navigate a three-dimensional environment and transduction pathways described in the literature may not perfectly match with those operating in living organisms. Furthermore, the use of transcriptomics and proteomics techniques applied to the GC fraction of specific neuron subpopulations (Poulopoulos et al., 2019), high-resolution cytoskeleton imaging (Jung et al., 2020; Katrukha et al., 2021) or 3D microfluidic assays (Spijkers et al., 2021) will expand our understanding of the steered GC locomotion mechanisms and reveal new molecular specificities in the long-range growing axons accounting for neural circuits development.

AUTHOR CONTRIBUTIONS

CS-H wrote the article and made the figures. EH edited the article. Both authors contributed to the article and approved the submitted version.

FUNDING

CS-H acknowledges the financial support of the "Severo Ochoa" Program for Centers of Excellence in R&D (SEV-2013-0317). EH laboratory was funded by the Spain's National Grant Research Program (PID2019-110535GB-100) and Prometeo Program (2020/007) from Generalitat Valenciana.

ACKNOWLEDGMENTS

We are grateful to Jens Lüders and Augusto Escalante for comments on the manuscript. We apologize to those of our colleagues whose contributions could not be acknowledged due to space limitations.

REFERENCES

Abe, T., Yamazaki, D., Murakami, S., Hiroi, M., Nitta, Y., Maeyama, Y., et al. (2014). The NAV2 homolog Sickie regulates F-actin-mediated axonal growth in *Drosophila mushroom* body neurons via the non-canonical Rac-Cofilin pathway. *Development* 141, 4716–4728. doi: 10.1242/dev.113308

Akhmanova, A., Hoogenraad, C. C., Drabek, K., Stepanova, T., Dortland, B., Verkerk, T., et al. (2001). Clasps are CLIP-115 and -170 associating proteins

involved in the regional regulation of microtubule dynamics in motile fibroblasts. *Cell* 104, 923–935. doi: 10.1016/s0092-8674(01)00288-284

Akhmanova, A., and Steinmetz, M. O. (2015). Control of microtubule organization and dynamics: two ends in the limelight. *Nat. Rev. Mol. Cell Biol.* 16, 711–726. doi: 10.1038/nrm4084

Al-Bassam, J., and Chang, F. (2011). Regulation of microtubule dynamics by TOG-domain proteins XMAP215/Dis1 and CLASP. *Trends Cell Biol.* 21, 604–614. doi: 10.1016/j.tcb.2011.06.007

Alcántara, S., Ruiz, M., De Castro, F., Soriano, E., and Sotelo, C. (2000). Netrin 1 acts as an attractive or as a repulsive cue for distinct migrating neurons during the development of the cerebellar system. *Development* 127, 1359–1372.

Alves-Silva, J., Sanchez-Soriano, N., Beaven, R., Klein, M., Parkin, J., Millard, T. H., et al. (2012). Spectraplakins promote microtubule-mediated axonal growth by functioning as structural microtubule-associated proteins and EB1-Dependent +TIPs (Tip Interacting Proteins). *J. Neurosci.* 32, 9143–9158. doi: 10.1523/JNEUROSCI.0416-12.2012

Amano, M., Chihara, K., Nakamura, N., Fukata, Y., Yano, T., Shibata, M., et al. (1998). Myosin II activation promotes neurite retraction during the action of Rho and Rho-kinase. *Genes Cells* 3, 177–188. doi: 10.1046/j.1365-2443.1998.00181.x

Arakawa, Y., Bito, H., Furuyashiki, T., Tsuji, T., Takemoto-Kimura, S., Kimura, K., et al. (2003). Control of axon elongation via an SDF-1alpha/Rho/mDia pathway in cultured cerebellar granule neurons. *J. Cell Biol.* 161, 381–391. doi: 10.1083/jcb.200210149

Arimura, N., Ménager, C., Kawano, Y., Yoshimura, T., Kawabata, S., Hattori, A., et al. (2005). Phosphorylation by Rho kinase regulates CRMP-2 activity in growth cones. *Mol. Cell. Biol.* 25, 9973–9984. doi: 10.1128/MCB.25.22.9973-9984.2005

Asselin, L., Rivera Alvarez, J., Heide, S., Bonnet, C. S., Tilly, P., Vitet, H., et al. (2020). Mutations in the KIF21B kinesin gene cause neurodevelopmental disorders through imbalanced canonical motor activity. *Nat. Commun.* 11:2441. doi: 10.1038/s41467-020-16294-16296

Bahi-Buisson, N., Souville, I., Fourniol, F. J., Toussaint, A., Moores, C. A., Houdusse, A., et al. (2013). New insights into genotype-phenotype correlations for the doublecortin-related lissencephaly spectrum. *Brain* 136, 223–244. doi: 10.1093/brain/aws323

Bamburg, J. R., Bray, D., and Chapman, K. (1986). Assembly of microtubules at the tip of growing axons. *Nature* 321, 788–790. doi: 10.1038/321788a0

Banerjee, R., Rudloff, Z., Naylor, C., Yu, M. C., and Gunawardena, S. (2018). The presenilin loop region is essential for glycogen synthase kinase 3 β (GSK3β) mediated functions on motor proteins during axonal transport. *Hum. Mol. Genet.* 27, 2986–3001. doi: 10.1093/hmg/ddy190

Bard, L., Boscher, C., Lambert, M., Mège, R.-M., Choquet, D., and Thoumine, O. (2008). A molecular clutch between the actin flow and N-cadherin adhesions drives growth cone migration. *J. Neurosci.* 28, 5879–5890. doi: 10.1523/JNEUROSCI.5331-07.2008

Basto, R., Lau, J., Vinogradova, T., Gardiol, A., Woods, C. G., Khodjakov, A., et al. (2006). Flies without centrioles. *Cell* 125, 1375–1386. doi: 10.1016/j.cell.2006.05.025

Baumann, S., Komissarov, A., Gili, M., Ruprecht, V., Wieser, S., and Maurer, S. P. (2020). A reconstituted mammalian APC-kinesin complex selectively transports defined packages of axonal mRNAs. *Sci. Adv.* 6:eaaz1588. doi: 10.1126/sciadv.aaz1588

Bearce, E. A., Erdogan, B., and Lowery, L. A. (2015). TIPsy tour guides: how microtubule plus-end tracking proteins (+TIPs) facilitate axon guidance. *Front. Cell. Neurosci.* 9:241. doi: 10.3389/fncel.2015.00241

Bentley, D., and Toroian-Raymond, A. (1986). Disoriented pathfinding by pioneer neurone growth cones deprived of filopodia by cytochalasin treatment. *Nature* 323, 712–715. doi: 10.1038/323712a0

Berezin, V., and Walmod, P. S. (eds) (2014). *Cell Adhesion Molecules: Implications in Neurological Diseases*. New York, NY: Springer, doi: 10.1007/978-1-4614-8090-7

Binder, L. I., Frankfurter, A., and Rebhun, L. I. (1985). The distribution of tau in the mammalian central nervous system. *J. Cell Biol.* 101, 1371–1378. doi: 10.1083/jcb.101.4.1371

Biswas, S., and Kalil, K. (2018). The microtubule-associated protein tau mediates the organization of microtubules and their dynamic exploration of actin-rich lamellipodia and filopodia of cortical growth cones. *J. Neurosci.* 38, 291–307. doi: 10.1523/JNEUROSCI.2281-17.2017

Black, M. M., Slaughter, T., and Fischer, I. (1994). Microtubule-associated protein 1b (MAP1b) is concentrated in the distal region of growing axons. *J. Neurosci.* 14, 857–870.

Bott, C. J., McMahon, L. P., Keil, J. M., Yap, C. C., Kwan, K. Y., and Winckler, B. (2020). Nestin selectively facilitates the phosphorylation of the lissencephaly-linked protein doublecortin (DCX) by cdk5/p35 to regulate growth cone morphology and Sema3a sensitivity in developing neurons. *J. Neurosci.* 40, 3720–3740. doi: 10.1523/JNEUROSCI.2471-19.2020

Bouquet, C., Soares, S., von Boxberg, Y., Ravaille-Veron, M., Propst, F., and Nothias, F. (2004). Microtubule-associated protein 1B controls directionality of growth cone migration and axonal branching in regeneration of adult dorsal root ganglia neurons. *J. Neurosci.* 24, 7204–7213. doi: 10.1523/JNEUROSCI.2254-04.2004

Bovolenta, P., and Mason, C. (1987). Growth cone morphology varies with position in the developing mouse visual pathway from retina to first targets. *J. Neurosci.* 7, 1447–1460.

Bradke, F., and Dotti, C. G. (1999). The role of local actin instability in axon formation. *Science* 283, 1931–1934. doi: 10.1126/science.283.5409.1931

Brouhard, G. J., Stear, J. H., Noetzel, T. L., Al-Bassam, J., Kinoshita, K., Harrison, S. C., et al. (2008). XMAP215 is a processive microtubule polymerase. *Cell* 132, 79–88. doi: 10.1016/j.cell.2007.11.043

Brown, M., Jacobs, T., Eickholt, B., Ferrari, G., Teo, M., Monfries, C., et al. (2004). Alpha2-chimaerin, cyclin-dependent Kinase 5/p35, and its target collapsin response mediator protein-2 are essential components in semaphorin 3A-induced growth-cone collapse. *J. Neurosci.* 24, 8994–9004. doi: 10.1523/JNEUROSCI.3184-04.2004

Buck, K. B., and Zheng, J. Q. (2002). Growth cone turning induced by direct local modification of microtubule dynamics. *J. Neurosci.* 22, 9358–9367.

Burnette, D. T., Ji, L., Schaefer, A. W., Medeiros, N. A., Danuser, G., and Forscher, P. (2008). Myosin II activity facilitates microtubule bundling in the neuronal growth cone neck. *Dev. Cell* 15, 163–169. doi: 10.1016/j.devcel.2008.05.016

Buscaglia, G., Aiken, J., Hoff, K. J., Northington, K. R., and Bates, E. A. (2020). Tuba1a is uniquely important for axon guidance through midline commissural structures. *bioRxiv* [preprint]. doi: 10.1101/2020.05.05.079376

Cammarata, G. M., Bearce, E. A., and Lowery, L. A. (2016). Cytoskeletal social networking in the growth cone: how +TIPs mediate microtubule-actin cross-linking to drive axon outgrowth and guidance: +TIPs mediate microtubule-actin cross-linking. *Cytoskeleton* 73, 461–476. doi: 10.1002/cm.21272

Campbell, D. S., and Holt, C. E. (2001). Chemotropic responses of retinal growth cones mediated by rapid local protein synthesis and degradation. *Neuron* 32, 1013–1026. doi: 10.1016/s0896-6273(01)00551-557

Challacombe, J. F., Snow, D. M., and Letourneau, P. C. (1997). Dynamic microtubule ends are required for growth cone turning to avoid an inhibitory guidance cue. *J. Neurosci.* 17, 3085–3095.

Chang, H. Y., Takei, K., Sydor, A. M., Born, T., Rusnak, F., and Jay, D. G. (1995). Asymmetric retraction of growth cone filopodia following focal inactivation of calcineurin. *Nature* 376, 686–690. doi: 10.1038/376686a0

Charbaut, E., Curmi, P. A., Ozon, S., Lachkar, S., Redeker, V., and Sobel, A. (2001). Stathmin family proteins display specific molecular and tubulin binding properties. *J. Biol. Chem.* 276, 16146–16154. doi: 10.1074/jbc.M010637200

Chédotal, A. (2019). Roles of axon guidance molecules in neuronal wiring in the developing spinal cord. *Nat. Rev. Neurosci.* 20, 380–396. doi: 10.1038/s41583-019-0168-167

Chedotal, A., and Richards, L. J. (2010). Wiring the brain: the biology of neuronal guidance. *Cold Spring Harb. Perspect. Biol.* 2:a001917. doi: 10.1101/cshperspect.a001917

Chen, H.-J., Lin, C.-M., Lin, C.-S., Perez-Olle, R., Leung, C. L., and Liem, R. K. H. (2006). The role of microtubule actin cross-linking factor 1 (MACF1) in the Wnt signaling pathway. *Genes Dev.* 20, 1933–1945. doi: 10.1101/gad.1411206

Chen, W.-S., Chen, Y.-J., Huang, Y.-A., Hsieh, B.-Y., Chiu, H.-C., Kao, P.-Y., et al. (2017). Ran-dependent TPX2 activation promotes acentrosomal microtubule nucleation in neurons. *Sci. Rep.* 7:42297. doi: 10.1038/srep42297

Cheng, L., Desai, J., Miranda, C. J., Duncan, J. S., Qiu, W., Nugent, A. A., et al. (2014). Human CFEOM1 mutations attenuate KIF21A autoinhibition and cause oculomotor axon stalling. *Neuron* 82, 334–349. doi: 10.1016/j.neuron.2014.02.038

Chilton, J. K., and Guthrie, S. (2017). Axons get ahead: insights into axon guidance and congenital cranial dysinnervation disorders. *Dev. Neurobiol.* 77, 861–875. doi: 10.1002/dneu.22477

Cleveland, D. W., Hwo, S. Y., and Kirschner, M. W. (1977). Purification of tau, a microtubule-associated protein that induces assembly of microtubules from purified tubulin. *J. Mol. Biol.* 116, 207–225. doi: 10.1016/0022-2836(77)90213-90213

Cole, A. R., Causeret, F., Yadirgi, G., Hastie, C. J., McLauchlan, H., McManus, E. J., et al. (2006). Distinct priming kinases contribute to differential regulation of collapsin response mediator proteins by glycogen synthase kinase-3 in vivo. *J. Biol. Chem.* 281, 16591–16598. doi: 10.1074/jbc.M513344200

Coles, C. H., and Bradke, F. (2015). Coordinating neuronal actin-microtubule dynamics. *Curr. Biol.* 25, R677–R691. doi: 10.1016/j.cub.2015.06.020

Cunha-Ferreira, I., Chazeau, A., Buijs, R. R., Stucchi, R., Will, L., Pan, X., et al. (2018). The HAUS complex is a key regulator of non-centrosomal microtubule organization during neuronal development. *Cell Rep.* 24, 791–800. doi: 10.1016/j.celrep.2018.06.093

Dehmelt, L., Nalbant, P., Steffen, W., and Halpain, S. (2006). A microtubule-based, dynein-dependent force induces local cell protrusions: implications for neurite initiation. *Brain Cell Biol.* 35, 39–56. doi: 10.1007/s11068-006-9001-9000

Del Río, J. A., González-Billault, C., Ureña, J. M., Jiménez, E. M., Barallobre, M. J., Pascual, M., et al. (2004). MAP1B is required for netrin 1 signaling in neuronal migration and axonal guidance. *Curr. Biol.* 14, 840–850. doi: 10.1016/j.cub.2004.04.046

Dent, E. W., Barnes, A. M., Tang, F., and Kalil, K. (2004). Netrin-1 and semaphorin 3A promote or inhibit cortical axon branching, respectively, by reorganization of the cytoskeleton. *J. Neurosci.* 24, 3002–3012. doi: 10.1523/JNEUROSCI.4963-03.2004

Dent, E. W., Gupton, S. L., and Gertler, F. B. (2011). The growth cone cytoskeleton in axon outgrowth and guidance. *Cold Spring Harb. Perspect. Biol.* 3:a001800. doi: 10.1101/cshperspect.a001800

Dent, E. W., and Kalil, K. (2001). Axon branching requires interactions between dynamic microtubules and actin filaments. *J. Neurosci.* 21, 9757–9769.

Desai, A., and Mitchison, T. J. (1997). Microtubule polymerization dynamics. *Annu. Rev. Cell Dev. Biol.* 13, 83–117. doi: 10.1146/annurev.cellbio.13.1.83

Deuel, T. A. S., Liu, J. S., Corbo, J. C., Yoo, S.-Y., Rorke-Adams, L. B., and Walsh, C. A. (2006). Genetic interactions between doublecortin and doublecortin-like kinase in neuronal migration and axon outgrowth. *Neuron* 49, 41–53. doi: 10.1016/j.neuron.2005.10.038

Diefenbach, T. J., Latham, V. M., Yimlamai, D., Liu, C. A., Herman, I. M., and Jay, D. G. (2002). Myosin 1c and myosin IIB serve opposing roles in lamellipodial dynamics of the neuronal growth cone. *J. Cell Biol.* 158, 1207–1217. doi: 10.1083/jcb.200202028

Dobyns, W. B., Aldinger, K. A., Ishak, G. E., Mirzaa, G. M., Timms, A. E., Grout, M. E., et al. (2018). MACF1 mutations encoding highly conserved zinc-binding residues of the GAR domain cause defects in neuronal migration and axon guidance. *Am. J. Hum. Genet.* 103, 1009–1021. doi: 10.1016/j.ajhg.2018.10.019

Drerup, C. M., Lusk, S., and Nechiporuk, A. (2016). Kif1B interacts with KBP to promote axon elongation by localizing a microtubule regulator to growth cones. *Journal of Neuroscience* 36, 7014–7026. doi: 10.1523/JNEUROSCI.0054-16.2016

Drévillon, L., Megarbane, A., Demeer, B., Matar, C., Benit, P., Briand-Suleau, A., et al. (2013). KBP-cytoskeleton interactions underlie developmental anomalies in Goldberg-Shprintzen syndrome. *Hum. Mol. Genet.* 22, 2387–2399. doi: 10.1093/hmg/ddt083

Drubin, D. G., and Kirschner, M. W. (1986). Tau protein function in living cells. *J. Cell Biol.* 103, 2739–2746. doi: 10.1083/jcb.103.6.2739

Dudanova, I., and Klein, R. (2013). Integration of guidance cues: parallel signaling and crosstalk. *Trends Neurosci.* 36, 295–304. doi: 10.1016/j.tins.2013.01.007

Efimova, N., Yang, C., Chia, J. X., Li, N., Lengner, C. J., Neufeld, K. L., et al. (2020). Branched actin networks are assembled on microtubules by adenomatous polyposis coli for targeted membrane protrusion. *J. Cell Biol.* 219:e202003091. doi: 10.1083/jcb.202003091

Elie, A., Prezel, E., Guérin, C., Denarier, E., Ramirez-Rios, S., Serre, L., et al. (2015). Tau co-organizes dynamic microtubule and actin networks. *Sci. Rep.* 5:9964. doi: 10.1038/srep09964

Engel, U., Zhan, Y., Long, J. B., Boyle, S. N., Ballif, B. A., Dorey, K., et al. (2014). Abelson phosphorylation of CLASP2 modulates its association with microtubules and actin. *Cytoskeleton* 71, 195–209. doi: 10.1002/cm.21164

Erdogan, B., Cammarata, G. M., Lee, E. J., Pratt, B. C., Francl, A. F., Rutherford, E. L., et al. (2017). The microtubule plus-end-tracking protein TACC3 promotes persistent axon outgrowth and mediates responses to axon guidance signals during development. *Neural Dev.* 12:3. doi: 10.1186/s13064-017-0080-87

Erdogan, B., St. Clair, R. M., Cammarata, G. M., Zaccaro, T., Ballif, B. A., and Lowery, L. A. (2020). Investigating the impact of the phosphorylation status of tyrosine residues within the TACC domain of TACC3 on microtubule behavior during axon growth and guidance. *Cytoskeleton* 77, 277–291. doi: 10.1002/cm.21622

Escalante, A., Murillo, B., Morenilla-Palao, C., Klar, A., and Herrera, E. (2013). Zic2-dependent axon midline avoidance controls the formation of major ipsilateral tracts in the CNS. *Neuron* 80, 1392–1406. doi: 10.1016/j.neuron.2013.10.007

Fassier, C., Fréal, A., Gasmi, L., Delphin, C., Ten Martin, D., De Gois, S., et al. (2018). Motor axon navigation relies on Fidgetin-like 1-driven microtubule plus end dynamics. *J. Cell Biol.* 217, 1719–1738. doi: 10.1083/jcb.201604108

Forscher, P., and Smith, S. J. (1988). Actions of cytochalasins on the organization of actin filaments and microtubules in a neuronal growth cone. *J. Cell Biol.* 107, 1505–1516. doi: 10.1083/jcb.107.4.1505

Fu, X., Brown, K. J., Yap, C. C., Winckler, B., Jaiswal, J. K., and Liu, J. S. (2013). Doublecortin (Dcx) family proteins regulate filamentous actin structure in developing neurons. *J. Neurosci.* 33, 709–721. doi: 10.1523/JNEUROSCI.4603-12.2013

Fukata, Y., Itoh, T. J., Kimura, T., Ménager, C., Nishimura, T., Shiromizu, T., et al. (2002). CRMP-2 binds to tubulin heterodimers to promote microtubule assembly. *Nat. Cell Biol.* 4, 583–591. doi: 10.1038/ncb825

Gallo, G. (1998). Involvement of microtubules in the regulation of neuronal growth cone morphologic remodeling. *J. Neurobiol.* 35, 121–140.

Gard, D. L., and Kirschner, M. W. (1987). A microtubule-associated protein from *Xenopus eggs* that specifically promotes assembly at the plus-end. *J. Cell Biol.* 105, 2203–2215. doi: 10.1083/jcb.105.5.2203

Geraldo, S., and Gordon-Weeks, P. R. (2009). Cytoskeletal dynamics in growth-cone steering. *J. Cell Sci.* 122, 3595–3604. doi: 10.1242/jcs.042309

Geraldo, S., Khanzada, U. K., Parsons, M., Chilton, J. K., and Gordon-Weeks, P. R. (2008). Targeting of the F-actin-binding protein drebrin by the microtubule plus-tip protein EB3 is required for neuritogenesis. *Nat. Cell Biol.* 10, 1181–1189. doi: 10.1038/ncb1778

Gergely, F., Karlsson, C., Still, I., Cowell, J., Kilmartin, J., and Raff, J. W. (2000). The TACC domain identifies a family of centrosomal proteins that can interact with microtubules. *Proc. Natl. Acad. Sci. U.S.A.* 97, 14352–14357. doi: 10.1073/pnas.97.26.14352

Gleeson, J. G., Allen, K. M., Fox, J. W., Lamperti, E. D., Berkovic, S., Scheffer, I., et al. (1998). doublecortin, a brain-specific gene mutated in human X-Linked lissencephaly and double cortex syndrome, encodes a putative signaling protein. *Cell* 92, 63–72. doi: 10.1016/S0092-8674(00)80899-80895

Gombos, R., Migh, E., Antal, O., Mukherjee, A., Jenny, A., and Mihály, J. (2015). The formin DAAM functions as molecular effector of the planar cell polarity pathway during axonal development in Drosophila. *J. Neurosci.* 35, 10154–10167. doi: 10.1523/JNEUROSCI.3708-14.2015

Gomez, T. M., and Letourneau, P. C. (2014). Actin dynamics in growth cone motility and navigation. *J. Neurochem.* 129, 221–234. doi: 10.1111/jnc.12506

Goode, B. L., and Eck, M. J. (2007). Mechanism and function of formins in the control of actin assembly. *Annu. Rev. Biochem.* 76, 593–627. doi: 10.1146/annurev.biochem.75.103004.142647

Goodson, H. V., and Jonasson, E. M. (2018). Microtubules and microtubule-associated proteins. *Cold Spring Harb. Perspect. Biol.* 10:a022608. doi: 10.1101/cshperspect.a022608

Gordon-Weeks, P. R. (1991). Evidence for microtubule capture by filopodial actin filaments in growth cones. *Neuroreport* 2, 573–576. doi: 10.1097/00001756-199110000-199110005

Gordon-Weeks, P. R. (2004). Microtubules and growth cone function. *J. Neurobiol.* 58, 70–83. doi: 10.1002/neu.10266

Gordon-Weeks, P. R. (2017). "Phosphorylation of drebrin and its role in neuritogenesis," in *Drebrin Advances in Experimental Medicine and Biology*, eds T. Shirao and Y. Sekino (Tokyo: Springer), 49–60. doi: 10.1007/978-4-431-56550-5_4

Goryunov, D., He, C.-Z., Lin, C.-S., Leung, C. L., and Liem, R. K. H. (2010). Nervous-tissue-specific elimination of microtubule-actin crosslinking factor 1a results in multiple developmental defects in the mouse brain. *Mol. Cell. Neurosci.* 44, 1–14. doi: 10.1016/j.mcn.2010.01.010

Goshima, Y., Nakamura, F., Strittmatter, P., and Strittmatter, S. M. (1995). Collapsin-induced growth cone collapse mediated by an intracellular protein related to UNC-33. *Nature* 376, 509–514. doi: 10.1038/376509a0

Grabham, P. W., Reznik, B., and Goldberg, D. J. (2003). Microtubule and Rac 1-dependent F-actin in growth cones. *J. Cell Sci.* 116, 3739–3748. doi: 10.1242/jcs.00686

Grabham, P. W., Seale, G. E., Bennecib, M., Goldberg, D. J., and Vallee, R. B. (2007). Cytoplasmic dynein and LIS1 are required for microtubule advance during growth cone remodeling and fast axonal outgrowth. *J. Neurosci.* 27, 5823–5834. doi: 10.1523/JNEUROSCI.1135-07.2007

Grenningloh, G., Soehrman, S., Bondallaz, P., Ruchti, E., and Cadas, H. (2004). Role of the microtubule destabilizing proteins SCG10 and stathmin in neuronal growth. *J. Neurobiol.* 58, 60–69. doi: 10.1002/neu.10279

Griffith, L. M., and Pollard, T. D. (1978). Evidence for actin filament-microtubule interaction mediated by microtubule-associated proteins. *J. Cell Biol.* 78, 958–965. doi: 10.1083/jcb.78.3.958

Grintsevich, E. E., and Reisler, E. (2014). Drebrin inhibits cofilin-induced severing of F-actin. *Cytoskeleton* 71, 472–483. doi: 10.1002/cm.21184

Grundke-Iqbal, I., Iqbal, K., Tung, Y. C., Quinlan, M., Wisniewski, H. M., and Binder, L. I. (1986). Abnormal phosphorylation of the microtubule-associated protein tau (tau) in Alzheimer cytoskeletal pathology. *Proc. Natl. Acad. Sci. U.S.A.* 83, 4913–4917. doi: 10.1073/pnas.83.13.4913

Guillaud, L., El-Agamy, S. E., Otsuki, M., and Terenzio, M. (2020). Anterograde axonal transport in neuronal homeostasis and disease. *Front. Mol. Neurosci.* 13:556175. doi: 10.3389/fnmol.2020.556175

Gujar, M. R., Stricker, A. M., and Lundquist, E. A. (2019). RHO-1 and the Rho GEF RHGF-1 interact with UNC-6/Netrin signaling to regulate growth cone protrusion and microtubule organization in *Caenorhabditis elegans*. *PLoS Genet.* 15:e1007960. doi: 10.1371/journal.pgen.1007960

Guo, T., Noble, W., and Hanger, D. P. (2017). Roles of tau protein in health and disease. *Acta Neuropathol.* 133, 665–704. doi: 10.1007/s00401-017-1707-1709

Hahn, I., Voelzmann, A., Parkin, J., Fülle, J. B., Slater, P. G., Lowery, L. A., et al. (2021). Tau, XMAP215/Msps and Eb1 co-operate interdependently to regulate microtubule polymerisation and bundle formation in axons. *PLoS Genet.* 17:e1009647. doi: 10.1371/journal.pgen.1009647

Hall, A., and Lalli, G. (2010). Rho and Ras GTPases in axon growth, guidance, and branching. *Cold Spring Harb. Perspect. Biol.* 2:a001818. doi: 10.1101/cshperspect.a001818

Harada, H., Charish, J., and Monnier, P. P. (2020). Emerging evidence for cell-autonomous axon guidance. *Dev. Growth Differ.* 62, 391–397. doi: 10.1111/dgd.12666

Henty-Ridilla, J. L., Rankova, A., Eskin, J. A., Kenny, K., and Goode, B. L. (2016). Accelerated actin filament polymerization from microtubule plus ends. *Science* 352, 1004–1009. doi: 10.1126/science.aaf1709

Herrera, E., Brown, L., Aruga, J., Rachel, R. A., Dolen, G., Mikoshiba, K., et al. (2003). Zic2 patterns binocular vision by specifying the uncrossed retinal projection. *Cell* 114, 545–557. doi: 10.1016/s0092-8674(03)00684-686

Herrera, E., Erskine, L., and Morenilla-Palao, C. (2019a). Guidance of retinal axons in mammals. *Semin. Cell Dev. Biol.* 85, 48–59. doi: 10.1016/j.semcdb.2017.11.027

Herrera, E., Agudo-Barriuso, M., and Murcia-Belmonte, V. (2019b). Cranial pair ii: the optic nerves. *Anat. Rec. (Hoboken)* 302, 428–445. doi: 10.1002/ar.23922

Higurashi, M., Iketani, M., Takei, K., Yamashita, N., Aoki, R., Kawahara, N., et al. (2012). Localized role of CRMP1 and CRMP2 in neurite outgrowth and growth cone steering. *Dev. Neurobiol.* 72, 1528–1540. doi: 10.1002/dneu.22017

Hirokawa, N., Niwa, S., and Tanaka, Y. (2010). Molecular motors in neurons: transport mechanisms and roles in brain function, development, and disease. *Neuron* 68, 610–638. doi: 10.1016/j.neuron.2010.09.039

Hirst, C. S., Stamp, L. A., Bergner, A. J., Hao, M. M., Tran, M. X., Morgan, J. M., et al. (2017). Kif1bp loss in mice leads to defects in the peripheral and central nervous system and perinatal death. *Sci. Rep.* 7:16676. doi: 10.1038/s41598-017-16965-16963

Homma, N., Takei, Y., Tanaka, Y., Nakata, T., Terada, S., Kikkawa, M., et al. (2003). Kinesin superfamily protein 2A (KIF2A) functions in suppression of collateral branch extension. *Cell* 114, 229–239. doi: 10.1016/s0092-8674(03)00522-521

Huang, H., Shao, Q., Qu, C., Yang, T., Dwyer, T., and Liu, G. (2015). Coordinated interaction of down syndrome cell adhesion molecule and deleted in colorectal cancer with dynamic TUBB3 mediates Netrin-1-induced axon branching. *Neuroscience* 293, 109–122. doi: 10.1016/j.neuroscience.2015.02.042

Huang, H., Yang, T., Shao, Q., Majumder, T., Mell, K., and Liu, G. (2018). Human TUBB3 mutations disrupt netrin attractive signaling. *Neuroscience* 374, 155–171. doi: 10.1016/j.neuroscience.2018.01.046

Huang, Y.-A., Hsu, C.-H., Chiu, H.-C., Hsi, P.-Y., Ho, C. T., Lo, W.-L., et al. (2020). Actin waves transport RanGTP to the neurite tip to regulate non-centrosomal microtubules in neurons. *J. Cell Sci.* 133:jcs241992. doi: 10.1242/jcs.241992

Hur, E.-M., Saijilafu, Lee, B. D., Kim, S.-J., Xu, W.-L., and Zhou, F.-Q. (2011a). GSK3 controls axon growth via CLASP-mediated regulation of growth cone microtubules. *Genes Dev.* 25, 1968–1981. doi: 10.1101/gad.17015911

Hur, E.-M., Yang, I. H., Kim, D.-H., Byun, J., Saijilafu, Xu, W.-L., et al. (2011b). Engineering neuronal growth cones to promote axon regeneration over inhibitory molecules. *Proc. Natl. Acad. Sci. U.S.A.* 108, 5057–5062. doi: 10.1073/pnas.1011258108

Hur, E.-M., and Zhou, F.-Q. (2010). GSK3 signalling in neural development. *Nat. Rev. Neurosci.* 11, 539–551. doi: 10.1038/nrn2870

Inagaki, N., Chihara, K., Arimura, N., Ménager, C., Kawano, Y., Matsuo, N., et al. (2001). CRMP-2 induces axons in cultured hippocampal neurons. *Nat. Neurosci.* 4, 781–782. doi: 10.1038/90476

Ito, Y., Oinuma, I., Katoh, H., Kaibuchi, K., and Negishi, M. (2006). Sema4D/plexin-B1 activates GSK-3β through R-Ras GAP activity, inducing growth cone collapse. *EMBO Rep.* 7, 704–709. doi: 10.1038/sj.embor.7400737

Jardin, N., Giudicelli, F., Ten Martín, D., Vitrac, A., De Gois, S., Allison, R., et al. (2018). BMP- and neuropilin 1-mediated motor axon navigation relies on spastin alternative translation. *Development* 145:dev162701. doi: 10.1242/dev.162701

Jiang, J., Wang, Z.-H., Qu, M., Gao, D., Liu, X.-P., Zhu, L.-Q., et al. (2015). Stimulation of EphB2 attenuates tau phosphorylation through PI3K/Akt-mediated inactivation of glycogen synthase kinase-3β. *Sci. Rep.* 5:11765. doi: 10.1038/srep11765

Jiang, K., Hua, S., Mohan, R., Grigoriev, I., Yau, K. W., Liu, Q., et al. (2014). Microtubule minus-end stabilization by polymerization-driven CAMSAP deposition. *Dev. Cell* 28, 295–309. doi: 10.1016/j.devcel.2014.01.001

Jin, T., Peng, G., Wu, E., Mendiratta, S., and Elul, T. (2018). N-terminal and central domains of APC function to regulate branch number, length and angle in developing optic axonal arbors in vivo. *Brain Res.* 1697, 34–44. doi: 10.1016/j.brainres.2018.05.045

Jones, G. E., Ostergaard, P., Moore, A. T., Connell, F. C., Williams, D., Quarrell, O., et al. (2014). Microcephaly with or without chorioretinopathy, lymphoedema, or mental retardation (MCLMR): review of phenotype associated with KIF11 mutations. *Eur. J. Hum. Genet.* 22, 881–887. doi: 10.1038/ejhg.2013.263

Jung, M., Kim, D., and Mun, J. Y. (2020). Direct visualization of actin filaments and actin-binding proteins in neuronal cells. *Front. Cell Dev. Biol.* 8:588556. doi: 10.3389/fcell.2020.588556

Ka, M., Jung, E.-M., Mueller, U., and Kim, W.-Y. (2014). MACF1 regulates the migration of pyramidal neurons via microtubule dynamics and GSK-3 signaling. *Dev. Biol.* 395, 4–18. doi: 10.1016/j.ydbio.2014.09.009

Ka, M., and Kim, W.-Y. (2016). Microtubule-Actin crosslinking factor 1 is required for dendritic arborization and axon outgrowth in the developing brain. *Mol. Neurobiol.* 53, 6018–6032. doi: 10.1007/s12035-015-9508-9504

Kahn, O. I., and Baas, P. W. (2016). Microtubules and growth cones: motors drive the turn. *Trends Neurosci.* 39, 433–440. doi: 10.1016/j.tins.2016.04.009

Kahn, O. I., Schätzle, P., van de Willige, D., Tas, R. P., Lindhout, F. W., Portegies, S., et al. (2018). APC2 controls dendrite development by promoting microtubule dynamics. *Nat. Commun.* 9:2773. doi: 10.1038/s41467-018-05124-5125

Kakinuma, N., and Kiyama, R. (2009). A major mutation of KIF21A associated with congenital fibrosis of the extraocular muscles type 1 (CFEOM1) enhances translocation of Kank1 to the membrane. *Biochem. Biophys. Res. Commun.* 386, 639–644. doi: 10.1016/j.bbrc.2009.06.109

Kalil, K., Li, L., and Hutchins, B. I. (2011). Signaling mechanisms in cortical axon growth, guidance, and branching. *Front. Neuroanat.* 5:62. doi: 10.3389/fnana.2011.00062

Kannan, M., Bayam, E., Wagner, C., Rinaldi, B., Kretz, P. F., Tilly, P., et al. (2017). WD40-repeat 47, a microtubule-associated protein, is essential for brain development and autophagy. *Proc. Natl. Acad. Sci. USA* 114, E9308–E9317. doi: 10.1073/pnas.1713625114

Kannan, R., and Giniger, E. (2017). New perspectives on the roles of Abl tyrosine kinase in axon patterning. *Fly* 11, 260–270. doi: 10.1080/19336934.2017.1327106

Kapitein, L. C., and Hoogenraad, C. C. (2015). Building the neuronal microtubule cytoskeleton. *Neuron* 87, 492–506. doi: 10.1016/j.neuron.2015.05.046

Katrukha, E. A., Jurriens, D., Salas Pastene, D. M., and Kapitein, L. C. (2021). Quantitative mapping of dense microtubule arrays in mammalian neurons. *eLife* 10:e67925. doi: 10.7554/eLife.67925

Kawabata Galbraith, K., and Kengaku, M. (2019). Multiple roles of the actin and microtubule-regulating formins in the developing brain. *Neurosci. Res.* 138, 59–69. doi: 10.1016/j.neures.2018.09.008

Kawano, Y., Yoshimura, T., Tsuboi, D., Kawabata, S., Kaneko-Kawano, T., Shirataki, H., et al. (2005). CRMP-2 is involved in kinesin-1-dependent transport of the Sra-1/WAVE1 complex and axon formation. *Mol. Cell. Biol.* 25, 9920–9935. doi: 10.1128/MCB.25.22.9920-9935.2005

Kawasaki, A., Okada, M., Tamada, A., Okuda, S., Nozumi, M., Ito, Y., et al. (2018). Growth cone phosphoproteomics reveals that GAP-43 phosphorylated by JNK is a marker of axon growth and regeneration. *iScience* 4, 190–203. doi: 10.1016/j.isci.2018.05.019

Kerstein, P. C., Nichol, R. H. I., and Gomez, T. M. (2015). Mechanochemical regulation of growth cone motility. *Front. Cell. Neurosci.* 9:244. doi: 10.3389/fncel.2015.00244

Kimura, T., Watanabe, H., Iwamatsu, A., and Kaibuchi, K. (2005). Tubulin and CRMP-2 complex is transported via Kinesin-1. *J. Neurochem.* 93, 1371–1382. doi: 10.1111/j.1471-4159.2005.03063.x

Klein, R., and Pasterkamp, R. J. (2021). Recent advances in inter-cellular interactions during neural circuit assembly. *Curr. Opin. Neurobiol.* 69, 25–32. doi: 10.1016/j.conb.2020.12.004

Kodama, A., Karakesisoglou, I., Wong, E., Vaezi, A., and Fuchs, E. (2003). ACF7: an essential integrator of microtubule dynamics. *Cell* 115, 343–354. doi: 10.1016/s0092-8674(03)00813-814

Koester, M. P., Müller, O., and Pollerberg, G. E. (2007). Adenomatous polyposis coli is differentially distributed in growth cones and modulates their steering. *J. Neurosci.* 27, 12590–12600. doi: 10.1523/JNEUROSCI.2250-07.2007

Koizumi, H., Tanaka, T., and Gleeson, J. G. (2006). Doublecortin-like kinase functions with doublecortin to mediate fiber tract decussation and neuronal migration. *Neuron* 49, 55–66. doi: 10.1016/j.neuron.2005.10.040

Kolodkin, A. L., and Pasterkamp, R. J. (2013). SnapShot: axon guidance II. *Cell* 153:722.e1. doi: 10.1016/j.cell.2013.04.004

Kolodkin, A. L., and Tessier-Lavigne, M. (2011). Mechanisms and molecules of neuronal wiring: a primer. *Cold Spring Harb. Perspect. Biol.* 3:a001727. doi: 10.1101/cshperspect.a001727

Kridsada, K., Niu, J., Haldipur, P., Wang, Z., Ding, L., Li, J. J., et al. (2018). Roof plate-derived radial glial-like cells support developmental growth of rapidly adapting mechanoreceptor ascending axons. *Cell Rep.* 23, 2928–2941. doi: 10.1016/j.celrep.2018.05.025

Kuhn, T. B., Meberg, P. J., Brown, M. D., Bernstein, B. W., Minamide, L. S., Jensen, J. R., et al. (2000). Regulating actin dynamics in neuronal growth cones by ADF/cofilin and rho family GTPases. *J. Neurobiol.* 44, 126–144.

Kundu, T., Dutta, P., Nagar, D., Maiti, S., and Ghose, A. (2021). Coupling of dynamic microtubules to F-actin by Fmn2 regulates chemotaxis of neuronal growth cones. *J. Cell Sci.* 134:jcs252916. doi: 10.1242/jcs.252916

Laht, P., Otsus, M., Remm, J., and Veske, A. (2014). B-plexins control microtubule dynamics and dendrite morphology of hippocampal neurons. *Exp. Cell Res.* 326, 174–184. doi: 10.1016/j.yexcr.2014.06.005

Laht, P., Pill, K., Haller, E., and Veske, A. (2012). Plexin-B3 interacts with EB-family proteins through a conserved motif. *Biochim. Biophys. Acta Gen.Subj.* 1820, 888–893. doi: 10.1016/j.bbagen.2012.02.007

Lasser, M., Tiber, J., and Lowery, L. A. (2018). The role of the microtubule cytoskeleton in neurodevelopmental disorders. *Front. Cell Neurosci.* 12:165. doi: 10.3389/fncel.2018.00165

Latremoliere, A., Cheng, L., DeLisle, M., Wu, C., Chew, S., Hutchinson, E. B., et al. (2018). Neuronal-specific TUBB3 is not required for normal neuronal function but is essential for timely axon regeneration. *Cell Rep.* 24, 1865–1879.e9. doi: 10.1016/j.celrep.2018.07.029

Lee, H., Engel, U., Rusch, J., Scherrer, S., Sheard, K., and Van Vactor, D. (2004). The microtubule plus end tracking protein Orbit/MAST/CLASP acts downstream of the tyrosine kinase abl in mediating axon guidance. *Neuron* 42, 913–926. doi: 10.1016/j.neuron.2004.05.020

Lee, S., Nahm, M., Lee, M., Kwon, M., Kim, E., Zadeh, A. D., et al. (2007). The F-actin-microtubule crosslinker shot is a platform for Krasavietz-mediated translational regulation of midline axon repulsion. *Development* 134, 1767–1777. doi: 10.1242/dev.02842

Leterrier, C., Dubey, P., and Roy, S. (2017). The nano-architecture of the axonal cytoskeleton. *Nat. Rev. Neurosci.* 18, 713–726. doi: 10.1038/nrn.2017.129

Letourneau, P. C. (1983). Differences in the organization of actin in the growth cones compared with the neurites of cultured neurons from chick embryos. *J. Cell Biol.* 97, 963–973. doi: 10.1083/jcb.97.4.963

Leyva-Díaz, E., and López-Bendito, G. (2013). In and out from the cortex: development of major forebrain connections. *Neuroscience* 254, 26–44. doi: 10.1016/j.neuroscience.2013.08.070

Li, C., Bassell, G. J., and Sasaki, Y. (2009). Fragile X mental retardation protein is involved in protein synthesis-dependent collapse of growth cones induced by semaphorin-3A. *Front. Neural Circuits* 3:11. doi: 10.3389/neuro.04.011.2009

Li, Y.-H., Ghavampur, S., Bondallaz, P., Will, L., Grenningloh, G., and Pu¨ schel, A. W. (2009). Rnd1 regulates axon extension by enhancing the microtubule destabilizing activity of SCG10. *J. Biol. Chem.* 284, 363–371. doi: 10.1074/jbc.M808126200

Li, L., Fothergill, T., Hutchins, B. I., Dent, E. W., and Kalil, K. (2014). Wnt5a evokes cortical axon outgrowth and repulsive guidance by tau mediated reorganization of dynamic microtubules. *Dev. Neurobiol.* 74, 797–817. doi: 10.1002/dneu.22102

Lian, G., Dettenhofer, M., Lu, J., Downing, M., Chenn, A., Wong, T., et al. (2016). Filamin A- and formin 2-dependent endocytosis regulates proliferation via the canonical Wnt pathway. *Development* 143, 4509–4520. doi: 10.1242/dev.139295

Liang, X., Kokes, M., Fetter, R. D., Sallee, M. D., Moore, A. W., Feldman, J. L., et al. (2020). Growth cone-localized microtubule organizing center establishes microtubule orientation in dendrites. *elife* 9:e56547. doi: 10.7554/eLife.56547

Lin, P.-C., Chan, P. M., Hall, C., and Manser, E. (2011). Collapsin Response Mediator Proteins (CRMPs) are a new class of microtubule-associated protein (MAP) that selectively interacts with assembled microtubules via a taxol-sensitive binding interaction. *J. Biol. Chem.* 286, 41466–41478. doi: 10.1074/jbc.M111.283580

Liu, G., and Dwyer, T. (2014). Microtubule dynamics in axon guidance. *Neurosci. Bull.* 30, 569–583. doi: 10.1007/s12264-014-1444-1446

Liu, P., Würtz, M., Zupa, E., Pfeffer, S., and Schiebel, E. (2021). Microtubule nucleation: the waltz between γ-tubulin ring complex and associated proteins. *Curr. Opin. Cell Biol.* 68, 124–131. doi: 10.1016/j.ceb.2020.10.004

Lowery, L., Stout, A., Faris, A. E., Ding, L., Baird, M. A., Davidson, M. W., et al. (2013). Growth cone-specific functions of XMAP215 in restricting microtubule dynamics and promoting axonal outgrowth. *Neural. Dev.* 8:22. doi: 10.1186/1749-8104-8-22

Lowery, L. A., and Vactor, D. V. (2009). The trip of the tip: understanding the growth cone machinery. *Nat. Rev. Mol. Cell Biol.* 10, 332–343. doi: 10.1038/nrm2679

Mack, T. G., Koester, M. P., and Pollerberg, G. E. (2000). The microtubule-associated protein MAP1B is involved in local stabilization of turning growth cones. *Mol. Cell. Neurosci.* 15, 51–65. doi: 10.1006/mcne.1999.0802

Mansfield, S. G., and Gordon-Weeks, P. R. (1991). Dynamic post-translational modification of tubulin in rat cerebral cortical neurons extending neurites in culture: effects of taxol. *J. Neurocytol.* 20, 654–666. doi: 10.1007/BF01187067

Maor-Nof, M., Homma, N., Raanan, C., Nof, A., Hirokawa, N., and Yaron, A. (2013). Axonal pruning is actively regulated by the microtubule-destabilizing protein kinesin superfamily protein 2A. *Cell Rep.* 3, 971–977. doi: 10.1016/j.celrep.2013.03.005

Martínez-López, M. J., Alcántara, S., Mascaró, C., Pérez-Brangulí, F., Ruiz-Lozano, P., Maes, T., et al. (2005). Mouse Neuron navigator 1, a novel microtubule-associated protein involved in neuronal migration. *Mol. Cell. Neurosci.* 28, 599–612. doi: 10.1016/j.mcn.2004.09.016

Marx, A., Godinez, W. J., Tsimashchuk, V., Bankhead, P., Rohr, K., and Engel, U. (2013). Xenopus cytoplasmic linker-associated protein 1 (XCLASP1) promotes axon elongation and advance of pioneer microtubules. *Mol. Biol. Cell* 24, 1544–1558. doi: 10.1091/mbc.E12-08-0573

Maurer, S. P., Cade, N. I., Bohner, G., Gustafsson, N., Boutant, E., and Surrey, T. (2014). EB1 accelerates two conformational transitions important for microtubule maturation and dynamics. *Curr. Biol.* 24, 372–384. doi: 10.1016/j.cub.2013.12.042

McNeill, E. M., Roos, K. P., Moechars, D., and Clagett-Dame, M. (2010). Nav2 is necessary for cranial nerve development and blood pressure regulation. *Neural Dev.* 5:6. doi: 10.1186/1749-8104-5-6

Medeiros, N. A., Burnette, D. T., and Forscher, P. (2006). Myosin II functions in actin-bundle turnover in neuronal growth cones. *Nat. Cell Biol.* 8, 215–226. doi: 10.1038/ncb1367

Meixner, A., Haverkamp, S., Wässle, H., Führer, S., Thalhammer, J., Kropf, N., et al. (2000). Map1b is required for axon guidance and is involved in the development of the central and peripheral nervous system. *J. Cell Biol.* 151, 1169–1178. doi: 10.1083/jcb.151.6.1169

Meli, R., Weisová, P., and Propst, F. (2015). Repulsive axon guidance by draxin is mediated by protein kinase B (Akt), glycogen synthase Kinase-3β (GSK-3β) and microtubule-associated protein 1B. *PLoS One* 10:e0119524. doi: 10.1371/journal.pone.0119524

Michels, S., Foss, K., Park, K., Golden-Grant, K., Saneto, R., Lopez, J., et al. (2017). Mutations of KIF5C cause a neurodevelopmental disorder of infantile-onset epilepsy, absent language, and distinctive malformations of cortical development. *Am. J. Med. Genet. A* 173, 3127–3131. doi: 10.1002/ajmg.a.38496

Mikati, M. A., Grintsevich, E. E., and Reisler, E. (2013). Drebrin-induced stabilization of actin filaments. *J. Biol. Chem.* 288, 19926–19938. doi: 10.1074/jbc.M113.472647

Miller, K. E., and Suter, D. M. (2018). An integrated cytoskeletal model of neurite outgrowth. *Front. Cell. Neurosci.* 12:447. doi: 10.3389/fncel.2018.00447

Mimori-Kiyosue, Y., Grigoriev, I., Lansbergen, G., Sasaki, H., Matsui, C., Severin, F., et al. (2005). CLASP1 and CLASP2 bind to EB1 and regulate microtubule plus-end dynamics at the cell cortex. *J. Cell Biol.* 168, 141–153. doi: 10.1083/jcb.200405094

Mitchell, C. B., Gasperini, R. J., Small, D. H., and Foa, L. (2012). STIM1 is necessary for store-operated calcium entry in turning growth cones. *J. Neurochem.* 122, 1155–1166. doi: 10.1111/j.1471-4159.2012.07840.x

Mizui, T., Kojima, N., Yamazaki, H., Katayama, M., Hanamura, K., and Shirao, T. (2009). Drebrin E is involved in the regulation of axonal growth through actin-myosin interactions. *J. Neurochem.* 109, 611–622. doi: 10.1111/j.1471-4159.2009.05993.x

Moffat, J. J., Ka, M., Jung, E.-M., Smith, A. L., and Kim, W.-Y. (2017). The role of MACF1 in nervous system development and maintenance. *Semin. Cell Dev. Biol.* 69, 9–17. doi: 10.1016/j.semcdb.2017.05.020

Moores, C. A., Perderiset, M., Francis, F., Chelly, J., Houdusse, A., and Milligan, R. A. (2004). Mechanism of microtubule stabilization by doublecortin. *Mol. Cell.* 14, 833–839. doi: 10.1016/j.molcel.2004.06.009

Moradi, M., Sivadasan, R., Saal, L., Lüningschrör, P., Dombert, B., Rathod, R. J., et al. (2017). Differential roles of α-, β-, and γ-actin in axon growth and collateral branch formation in motoneurons. *J. Cell Biol.* 216, 793–814. doi: 10.1083/jcb.201604117

Morenilla-Palao, C., López-Cascales, M. T., López-Atalaya, J. P., Baeza, D., Calvo-Díaz, L., Barco, A., et al. (2020). A Zic2-regulated switch in a noncanonical Wnt/βcatenin pathway is essential for the formation of bilateral circuits. *Sci. Adv.* 6:eaaz8797. doi: 10.1126/sciadv.aaz8797

Moreno-Flores, M. T., Martín-Aparicio, E., Martín-Bermejo, M. J., Agudo, M., McMahon, S., Ávila, J., et al. (2004). Semaphorin 3C preserves survival and induces neuritogenesis of cerebellar granule neurons in culture: Sema3C-dependent survival and neuritogenesis of cultured CGN. *J. Neurochem.* 87, 879–890. doi: 10.1046/j.1471-4159.2003.02051.x

Morii, H., Shiraishi-Yamaguchi, Y., and Mori, N. (2006). SCG10, a microtubule destabilizing factor, stimulates the neurite outgrowth by modulating microtubule dynamics in rat hippocampal primary cultured neurons. *J. Neurobiol.* 66, 1101–1114. doi: 10.1002/neu.20295

Morikawa, M., Tanaka, Y., Cho, H.-S., Yoshihara, M., and Hirokawa, N. (2018). The molecular motor KIF21B mediates synaptic plasticity and fear extinction by terminating Rac1 activation. *Cell Rep.* 23, 3864–3877. doi: 10.1016/j.celrep.2018.05.089

Moutin, M.-J., Bosc, C., Peris, L., and Andrieux, A. (2021). Tubulin post-translational modifications control neuronal development and functions. *Dev. Neurobiol.* 81, 253–272. doi: 10.1002/dneu.22774

Murcia-Belmonte, V., Coca, Y., Vegar, C., Negueruela, S., de Juan Romero, C., Valiño, A. J., et al. (2019). A retino-retinal projection guided by unc5c emerged in species with retinal waves. *Curr. Biol.* 29, 1149–1160.e4. doi: 10.1016/j.cub.2019.02.052

Myers, J. P., and Gomez, T. M. (2011). Focal adhesion kinase promotes integrin adhesion dynamics necessary for chemotropic turning of nerve growth cones. *J. Neurosci.* 31, 13585–13595. doi: 10.1523/JNEUROSCI.2381-11.2011

Myers, K. A., Tint, I., Nadar, C. V., He, Y., Black, M. M., and Baas, P. W. (2006). Antagonistic forces generated by cytoplasmic dynein and Myosin-ii during growth cone turning and axonal retraction. *Traffic* 7, 1333–1351. doi: 10.1111/j.1600-0854.2006.00476.x

Nadar, V. C., Ketschek, A., Myers, K. A., Gallo, G., and Baas, P. W. (2008). Kinesin-5 is essential for growth-cone turning. *Curr. Biol.* 18, 1972–1977. doi: 10.1016/j.cub.2008.11.021

Nadar, V. C., Lin, S., and Baas, P. W. (2012). Microtubule redistribution in growth cones elicited by focal inactivation of kinesin-5. *J. Neurosci.* 32, 5783–5794. doi: 10.1523/JNEUROSCI.0144-12.2012

Nakamura, F., Ohshima, T., and Goshima, Y. (2020). Collapsin response mediator proteins: their biological functions and pathophysiology in neuronal development and regeneration. *Front. Cell. Neurosci.* 14:188. doi: 10.3389/fncel.2020.00188

Nakamura, M., Zhou, X. Z., and Lu, K. P. (2001). Critical role for the EB1 and APC interaction in the regulation of microtubule polymerization. *Curr. Biol.* 11, 1062–1067.

Nakamura, S., Grigoriev, I., Nogi, T., Hamaji, T., Cassimeris, L., and Mimori-Kiyosue, Y. (2012). Dissecting the nanoscale distributions and functions of microtubule-end-binding proteins EB1 and ch-TOG in interphase HeLa cells. *PLoS One* 7:e51442. doi: 10.1371/journal.pone.0051442

Nguyen, M. M., McCracken, C. J., Milner, E. S., Goetschius, D. J., Weiner, A. T., Long, M. K., et al. (2014). Γ-tubulin controls neuronal microtubule polarity independently of Golgi outposts. *Mol. Biol. Cell* 25, 2039–2050. doi: 10.1091/mbc.E13-09-0515

Nguyen, M. M., Stone, M. C., and Rolls, M. M. (2011). Microtubules are organized independently of the centrosome in *Drosophila neurons*. *Neural Dev.* 6:38. doi: 10.1186/1749-8104-6-38

Niftullayev, S., and Lamarche-Vane, N. (2019). Regulators of Rho GTPases in the nervous system: molecular implication in axon guidance and neurological disorders. *IJMS* 20:1497. doi: 10.3390/ijms20061497

Niu, X., Zheng, F., and Fu, C. (2019). The concerted actions of Tip1/CLIP-170, Klp5/Kinesin-8, and Alp14/XMAP215 regulate microtubule catastrophe at the cell end. *J. Mol. Cell Biol.* 11, 956–966. doi: 10.1093/jmcb/mjz039

Nwagbara, B. U., Faris, A. E., Bearce, E. A., Erdogan, B., Ebbert, P. T., Evans, M. F., et al. (2014). TACC3 is a microtubule plus end-tracking protein that promotes axon elongation and also regulates microtubule plus end dynamics in multiple embryonic cell types. *MBoC* 25, 3350–3362. doi: 10.1091/mbc.e14-06-1121

Oinuma, I., Ishikawa, Y., Katoh, H., and Negishi, M. (2004). The Semaphorin 4D receptor Plexin-B1 is a GTPase activating protein for R-Ras. *Science* 305, 862–865. doi: 10.1126/science.1097545

Okada, K., Bartolini, F., Deaconescu, A. M., Moseley, J. B., Dogic, Z., Grigorieff, N., et al. (2010). Adenomatous polyposis coli protein nucleates actin assembly and synergizes with the formin mDia1. *J. Cell Biol.* 189, 1087–1096. doi: 10.1083/jcb.201001016

Omotade, O. F., Pollitt, S. L., and Zheng, J. Q. (2017). Actin-based growth cone motility and guidance. *Mol. Cell. Neurosci.* 84, 4–10. doi: 10.1016/j.mcn.2017.03.001

Ori-McKenney, K. M., Jan, L. Y., and Jan, Y.-N. (2012). Golgi outposts shape dendrite morphology by functioning as sites of acentrosomal microtubule nucleation in neurons. *Neuron* 76, 921–930. doi: 10.1016/j.neuron.2012.10.008

Padmanabhan, P., and Goodhill, G. J. (2018). Axon growth regulation by a bistable molecular switch. *Proc. R. Soc. B.* 285:20172618. doi: 10.1098/rspb.2017.2618

Pasterkamp, R. J., and Burk, K. (2021). Axon guidance receptors: endocytosis, trafficking and downstream signaling from endosomes. *Prog. Neurobiol.* 198:101916. doi: 10.1016/j.pneurobio.2020.101916

Pavez, M., Thompson, A. C., Arnott, H. J., Mitchell, C. B., D'Atri, I., Don, E. K., et al. (2019). STIM1 is required for remodeling of the endoplasmic reticulum and microtubule cytoskeleton in steering growth cones. *J. Neurosci.* 39, 5095–5114. doi: 10.1523/JNEUROSCI.2496-18.2019

Paz, J., and Lüders, J. (2018). Microtubule-organizing centers: towards a minimal parts list. *Trends Cell Biol.* 28, 176–187. doi: 10.1016/j.tcb.2017.10.005

Poirier, K., Lebrun, N., Broix, L., Tian, G., Saillour, Y., Boscheron, C., et al. (2013). Mutations in TUBG1, DYNC1H1, KIF5C and KIF2A cause malformations of

cortical development and microcephaly. *Nat. Genet.* 45, 639–647. doi: 10.1038/ng.2613

Poirier, K., Saillour, Y., Bahi-Buisson, N., Jaglin, X. H., Fallet-Bianco, C., Nabbout, R., et al. (2010). Mutations in the neuronal ß-tubulin subunit TUBB3 result in malformation of cortical development and neuronal migration defects. *Hum. Mol. Genet.* 19, 4462–4473. doi: 10.1093/hmg/ddq377

Poulopoulos, A., Murphy, A. J., Ozkan, A., Davis, P., Hatch, J., Kirchner, R., et al. (2019). Subcellular transcriptomes and proteomes of developing axon projections in the cerebral cortex. *Nature* 565, 356–360. doi: 10.1038/s41586-018-0847-y

Preciado López, M., Huber, F., Grigoriev, I., Steinmetz, M. O., Akhmanova, A., Koenderink, G. H., et al. (2014). Actin-microtubule coordination at growing microtubule ends. *Nat. Commun.* 5:4778. doi: 10.1038/ncomms5778

Preitner, N., Quan, J., Nowakowski, D. W., Hancock, M. L., Shi, J., Tcherkezian, J., et al. (2014). APC is an RNA-Binding protein, and its interactome provides a link to neural development and microtubule assembly. *Cell* 158, 368–382. doi: 10.1016/j.cell.2014.05.042

Pujol, F., Kitabgi, P., and Boudin, H. (2005). The chemokine SDF-1 differentially regulates axonal elongation and branching in hippocampal neurons. *J. Cell Sci.* 118, 1071–1080. doi: 10.1242/jcs.01694

Puri, D., Ponniah, K., Biswas, K., Basu, A., Dey, S., Lundquist, E. A., et al. (2021). Wnt signaling establishes the microtubule polarity in neurons through regulation of Kinesin-13. *J. Cell Biol.* 220:e202005080. doi: 10.1083/jcb.202005080

Purro, S. A., Ciani, L., Hoyos-Flight, M., Stamatakou, E., Siomou, E., and Salinas, P. C. (2008). Wnt regulates axon behavior through changes in microtubule growth directionality: a new role for adenomatous polyposis coli. *J. Neurosci.* 28, 8644–8654. doi: 10.1523/JNEUROSCI.2320-08.2008

Qu, C., Dwyer, T., Shao, Q., Yang, T., Huang, H., and Liu, G. (2013). Direct binding of TUBB3 with DCC couples netrin-1 signaling to intracellular microtubule dynamics in axon outgrowth and guidance. *J. Cell Sci.* 126, 3070–3081. doi: 10.1242/jcs.122184

Qu, X., Kumar, A., Blockus, H., Waites, C., and Bartolini, F. (2019). Activity-Dependent nucleation of dynamic microtubules at presynaptic boutons controls neurotransmission. *Curr. Biol.* 29, 4231–4240.e5. doi: 10.1016/j.cub.2019.10.049

Qu, Y., Hahn, I., Webb, S. E. D., Pearce, S. P., and Prokop, A. (2017). Periodic actin structures in neuronal axons are required to maintain microtubules. *Mol. Biol. Cell* 28, 296–308. doi: 10.1091/mbc.e16-10-0727

Rao, A. N., Patil, A., Black, M. M., Craig, E. M., Myers, K. A., Yeung, H. T., et al. (2017). Cytoplasmic dynein transports axonal microtubules in a polarity-sorting manner. *Cell Rep.* 19, 2210–2219. doi: 10.1016/j.celrep.2017.05.064

Rochlin, M. W., Wickline, K. M., and Bridgman, P. C. (1996). Microtubule stability decreases axon elongation but not axoplasm production. *J. Neurosci.* 16, 3236–3246.

Roll-Mecak, A., and Vale, R. D. (2008). Structural basis of microtubule severing by the hereditary spastic paraplegia protein spastin. *Nature* 451, 363–367. doi: 10.1038/nature06482

Romaniello, R., Arrigoni, F., Fry, A. E., Bassi, M. T., Rees, M. I., Borgatti, R., et al. (2018). Tubulin genes and malformations of cortical development. *Eur. J. Med. Genet.* 61, 744–754. doi: 10.1016/j.ejmg.2018.07.012

Roossien, D. H., Lamoureux, P., and Miller, K. E. (2014). Cytoplasmic dynein pushes the cytoskeletal meshwork forward during axonal elongation. *J. Cell Sci.* 127, 3593–3602. doi: 10.1242/jcs.152611

Ruane, P. T., Gumy, L. F., Bola, B., Anderson, B., Wozniak, M. J., Hoogenraad, C. C., et al. (2016). Tumour suppressor adenomatous polyposis coli (APC) localisation is regulated by both Kinesin-1 and Kinesin-2. *Sci. Rep.* 6:27456. doi: 10.1038/srep27456

Rusan, N. M., Akong, K., and Peifer, M. (2008). Putting the model to the test: are APC proteins essential for neuronal polarity, axon outgrowth, and axon targeting? *J. Cell Biol.* 183, 203–212. doi: 10.1083/jcb.200807079

Sabry, J. H., O'Connor, T. P., Evans, L., Toroian-Raymond, A., Kirschner, M., and Bentley, D. (1991). Microtubule behavior during guidance of pioneer neuron growth cones in situ. *J. Cell Biol.* 115, 381–395. doi: 10.1083/jcb.115.2.381

Saez, T. M. M., Fernandez Bessone, I., Rodriguez, M. S., Alloatti, M., Otero, M. G., Cromberg, L. E., et al. (2020). Kinesin-1-mediated axonal transport of CB1 receptors is required for cannabinoid-dependent axonal growth and guidance. *Development* 147:dev184069. doi: 10.1242/dev.184069

Sahasrabudhe, A., Ghate, K., Mutalik, S., Jacob, A., and Ghose, A. (2016). Formin 2 regulates the stabilization of filopodial tip adhesions in growth cones and affects neuronal outgrowth and pathfinding in vivo. *Development* 143, 449–460. doi: 10.1242/dev.130104

Sainath, R., and Gallo, G. (2015). The dynein inhibitor Ciliobrevin D inhibits the bidirectional transport of organelles along sensory axons and impairs NGF-mediated regulation of growth cones and axon branches: ciliobrevin D inhibits axon transport. *Dev. Neurobiol.* 75, 757–777. doi: 10.1002/dneu.22246

Sánchez-Huertas, C., Bonhomme, M., Falco, A., Fagotto-Kaufmann, C., van Haren, J., Jeanneteau, F., et al. (2020). The +TIP Navigator-1 is an actin-microtubule crosslinker that regulates axonal growth cone motility. *J. Cell Biol.* 219:e201905199. doi: 10.1083/jcb.201905199

Sánchez-Huertas, C., Freixo, F., Viais, R., Lacasa, C., Soriano, E., and Lüders, J. (2016). Non-centrosomal nucleation mediated by augmin organizes microtubules in post-mitotic neurons and controls axonal microtubule polarity. *Nat. Commun.* 7:12187. doi: 10.1038/ncomms12187

Sanchez-Soriano, N., Travis, M., Dajas-Bailador, F., Goncalves-Pimentel, C., Whitmarsh, A. J., and Prokop, A. (2009). Mouse ACF7 and Drosophila Short stop modulate filopodia formation and microtubule organisation during neuronal growth. *J. Cell Sci.* 122, 2534–2542. doi: 10.1242/jcs.046268

Santos, T. E., Schaffran, B., Broguière, N., Meyn, L., Zenobi-Wong, M., and Bradke, F. (2020). Axon growth of CNS neurons in three dimensions is amoeboid and independent of adhesions. *Cell Rep.* 32:107907. doi: 10.1016/j.celrep.2020.107907

Sasaki, Y., Cheng, C., Uchida, Y., Nakajima, O., Ohshima, T., Yagi, T., et al. (2002). Fyn and Cdk5 mediate Semaphorin-3A signaling, which is involved in regulation of dendrite orientation in cerebral cortex. *Neuron* 35, 907–920. doi: 10.1016/S0896-6273(02)00857-857

Sayas, C. L., Tortosa, E., Bollati, F., Ramírez-Ríos, S., Arnal, I., and Avila, J. (2015). Tau regulates the localization and function of End-binding proteins 1 and 3 in developing neuronal cells. *J. Neurochem.* 133, 653–667. doi: 10.1111/jnc.13091

Schaefer, A. W., Kabir, N., and Forscher, P. (2002). Filopodia and actin arcs guide the assembly and transport of two populations of microtubules with unique dynamic parameters in neuronal growth cones. *J. Cell Biol.* 158, 139–152. doi: 10.1083/jcb.200203038

Schaefer, A. W., Schoonderwoert, V. T. G., Ji, L., Mederios, N., Danuser, G., and Forscher, P. (2008). Coordination of actin filament and microtubule dynamics during neurite outgrowth. *Dev. Cell* 15, 146–162. doi: 10.1016/j.devcel.2008.05.003

Scolnick, J. A., Cui, K., Duggan, C. D., Xuan, S., Yuan, X.-B., Efstratiadis, A., et al. (2008). Role of IGF signaling in olfactory sensory map formation and axon guidance. *Neuron* 57, 847–857. doi: 10.1016/j.neuron.2008.01.027

Selden, S. C., and Pollard, T. D. (1983). Phosphorylation of microtubule-associated proteins regulates their interaction with actin filaments. *J. Biol. Chem.* 258, 7064–7071.

Sferra, A., Petrini, S., Bellacchio, E., Nicita, F., Scibelli, F., Dentici, M. L., et al. (2020). TUBB variants underlying different phenotypes result in altered vesicle trafficking and microtubule dynamics. *Int. J. Mol. Sci.* 21:E1385. doi: 10.3390/ijms21041385

Shakir, M. A., Jiang, K., Struckhoff, E. C., Demarco, R. S., Patel, F. B., Soto, M. C., et al. (2008). The Arp2/3 activators WAVE and WASP have distinct genetic interactions with Rac GTPases in *Caenorhabditis elegans* axon guidance. *Genetics* 179, 1957–1971. doi: 10.1534/genetics.108.088963

Shan, Y., Farmer, S. M., and Wray, S. (2021). Drebrin regulates cytoskeleton dynamics in migrating neurons through interaction with CXCR4. *Proc. Natl. Acad. Sci. U. S. A.* 118:e2009493118. doi: 10.1073/pnas.2009493118

Shao, Q., Yang, T., Huang, H., Alarmanazi, F., and Liu, G. (2017). Uncoupling of UNC5C with polymerized TUBB3 in microtubules mediates Netrin-1 repulsion. *J. Neurosci.* 37, 5620–5633. doi: 10.1523/JNEUROSCI.2617-16.2017

Shao, Q., Yang, T., Huang, H., Majumder, T., Khot, B. A., Khouzani, M. M., et al. (2019). Disease-associated mutations in human TUBB3 disturb netrin repulsive signaling. *PLoS One* 14:e0218811. doi: 10.1371/journal.pone.0218811

Sharp, D. J., and Ross, J. L. (2012). Microtubule-severing enzymes at the cutting edge. *J. Cell Sci.* 125(Pt 11), 2561–2569. doi: 10.1242/jcs.101139

Shekarabi, M., Moore, S. W., Tritsch, N. X., Morris, S. J., Bouchard, J.-F., and Kennedy, T. E. (2005). Deleted in colorectal cancer binding netrin-1 mediates cell substrate adhesion and recruits Cdc42, Rac1, Pak1, and N-WASP into

an intracellular signaling complex that promotes growth cone expansion. *J. Neurosci.* 25, 3132–3141. doi: 10.1523/JNEUROSCI.1920-04.2005

Shimada, T., Toriyama, M., Uemura, K., Kamiguchi, H., Sugiura, T., Watanabe, N., et al. (2008). Shootin1 interacts with actin retrograde flow and L1-CAM to promote axon outgrowth. *J. Cell Biol.* 181, 817–829. doi: 10.1083/jcb.200712138

Shin, J. E., Miller, B. R., Babetto, E., Cho, Y., Sasaki, Y., Qayum, S., et al. (2012). SCG10 is a JNK target in the axonal degeneration pathway. *Proc. Natl. Acad. Sci. U. S. A.* 109, E3696–E3705. doi: 10.1073/pnas.1216204109

Shintani, T., Ihara, M., Tani, S., Sakuraba, J., Sakuta, H., and Noda, M. (2009). APC2 plays an essential role in axonal projections through the regulation of microtubule stability. *J. Neurosci.* 29, 11628–11640. doi: 10.1523/JNEUROSCI.2394-09.2009

Short, C. A., Onesto, M. M., Rempel, S. K., Catlett, T. S., and Gomez, T. M. (2021). Familiar growth factors have diverse roles in neural network assembly. *Curr. Opin. Neurobiol.* 66, 233–239. doi: 10.1016/j.conb.2020.12.016

Slater, P. G., Cammarata, G. M., Samuelson, A. G., Magee, A., Hu, Y., and Lowery, L. A. (2019). XMAP215 promotes microtubule-F-actin interactions to regulate growth cone microtubules during axon guidance in Xenopus laevis. *J. Cell Sci.* 132:jcs224311. doi: 10.1242/jcs.224311

Sorensen, S. A., Bernard, A., Menon, V., Royall, J. J., Glattfelder, K. J., Desta, T., et al. (2015). Correlated gene expression and target specificity demonstrate excitatory projection neuron diversity. *Cereb. Cortex* 25, 433–449. doi: 10.1093/cercor/bht243

Spijkers, X. M., Pasteuning-Vuhman, S., Dorleijn, J. C., Vulto, P., Wevers, N. R., and Pasterkamp, R. J. (2021). A directional 3D neurite outgrowth model for studying motor axon biology and disease. *Sci. Rep.* 11:2080. doi: 10.1038/s41598-021-81335-z

Stamos, J. L., and Weis, W. I. (2013). The β-catenin destruction complex. *Cold Spring Harb. Perspect. Biol.* 5:a007898. doi: 10.1101/cshperspect.a007898

Stanganello, E., Zahavi, E. E., Burute, M., Smits, J., Jordens, I., Maurice, M. M., et al. (2019). Wnt signaling directs neuronal polarity and axonal growth. *iScience* 13, 318–327. doi: 10.1016/j.isci.2019.02.029

Stiess, M., Maghelli, N., Kapitein, L. C., Gomis-Rüth, S., Wilsch-Bräuninger, M., Hoogenraad, C. C., et al. (2010). Axon extension occurs independently of centrosomal microtubule nucleation. *Science* 327, 704–707. doi: 10.1126/science.1182179

Stoeckli, E. T. (2018). Understanding axon guidance: are we nearly there yet? *Development* 145:dev151415. doi: 10.1242/dev.151415

Strasser, G. A., Rahim, N. A., VanderWaal, K. E., Gertler, F. B., and Lanier, L. M. (2004). Arp2/3 is a negative regulator of growth cone translocation. *Neuron* 43, 81–94. doi: 10.1016/j.neuron.2004.05.015

Suh, L. H. (2004). L1/Laminin modulation of growth cone response to EphB triggers growth pauses and regulates the microtubule destabilizing protein SCG10. *J. Neurosci.* 24, 1976–1986. doi: 10.1523/JNEUROSCI.1670-03.2004

Suter, D. M., Errante, L. D., Belotserkovsky, V., and Forscher, P. (1998). The Ig superfamily cell adhesion molecule, apCAM, mediates growth cone steering by substrate-cytoskeletal coupling. *J. Cell Biol.* 141, 227–240. doi: 10.1083/jcb.141.1.227

Suter, D. M., Schaefer, A. W., and Forscher, P. (2004). Microtubule dynamics are necessary for SRC family kinase-dependent growth cone steering. *Curr. Biol.* 14, 1194–1199. doi: 10.1016/j.cub.2004.06.049

Szikora, S., Földi, I., Tóth, K., Migh, E., Vig, A., Bugyi, B., et al. (2017). The formin DAAM is required for coordination of the actin and microtubule cytoskeleton in axonal growth cones. *J. Cell Sci.* 130, 2506–2519. doi: 10.1242/jcs.203455

Takabatake, M., Goshima, Y., and Sasaki, Y. (2020). Semaphorin-3A promotes degradation of fragile X mental retardation protein in growth cones via the ubiquitin-proteasome pathway. *Front. Neural Circuits* 14:5. doi: 10.3389/fncir.2020.00005

Tanaka, E., Ho, T., and Kirschner, M. W. (1995). The role of microtubule dynamics in growth cone motility and axonal growth. *J. Cell Biol.* 128, 139–155. doi: 10.1083/jcb.128.1.139

Tanaka, E., and Kirschner, M. W. (1995). The role of microtubules in growth cone turning at substrate boundaries. *J. Cell Biol.* 128, 127–137. doi: 10.1083/jcb.128.1.127

Teulière, J., Gally, C., Garriga, G., Labouesse, M., and Georges-Labouesse, E. (2011). MIG-15 and ERM-1 promote growth cone directional migration in parallel to UNC-116 and WVE-1. *Development* 138, 4475–4485. doi: 10.1242/dev.061952

Thurston, S. F., Kulacz, W. A., Shaikh, S., Lee, J. M., and Copeland, J. W. (2012). The ability to induce microtubule acetylation is a general feature of formin proteins. *PLoS One* 7:e48041. doi: 10.1371/journal.pone.0048041

Tint, I., Jean, D., Baas, P. W., and Black, M. M. (2009). Doublecortin associates with microtubules preferentially in regions of the axon displaying actin-rich protrusive structures. *J. Neurosci.* 29, 10995–11010. doi: 10.1523/JNEUROSCI.3399-09.2009

Tischfield, M. A., Baris, H. N., Wu, C., Rudolph, G., Van Maldergem, L., He, W., et al. (2010). Human TUBB3 mutations perturb microtubule dynamics, kinesin interactions, and axon guidance. *Cell* 140, 74–87. doi: 10.1016/j.cell.2009.12.011

Toriyama, M., Kozawa, S., Sakumura, Y., and Inagaki, N. (2013). Conversion of a signal into forces for axon outgrowth through Pak1-mediated shootin1 phosphorylation. *Curr. Biol.* 23, 529–534. doi: 10.1016/j.cub.2013.02.017

Tortosa, E., Galjart, N., Avila, J., and Sayas, C. L. (2013). MAP1B regulates microtubule dynamics by sequestering EB1/3 in the cytosol of developing neuronal cells. *EMBO J.* 32, 1293–1306. doi: 10.1038/emboj.2013.76

Toyoda, Y., Shinohara, R., Thumkeo, D., Kamijo, H., Nishimaru, H., Hioki, H., et al. (2013). EphA4-dependent axon retraction and midline localization of Ephrin-B3 are disrupted in the spinal cord of mice lacking mDia1 and mDia3 in combination. *Genes Cells* 18, 873–885. doi: 10.1111/gtc.12081

Tran, P. T., Walker, R. A., and Salmon, E. D. (1997). A metastable intermediate state of microtubule dynamic instability that differs significantly between plus and minus ends. *J. Cell Biol.* 138, 105–117. doi: 10.1083/jcb.138.1.105

Tsukada, M., Prokscha, A., Ungewickell, E., and Eichele, G. (2005). Doublecortin association with actin filaments is regulated by neurabin II. *J. Biol. Chem.* 280, 11361–11368. doi: 10.1074/jbc.M405525200

Turney, S. G., Ahmed, M., Chandrasekar, I., Wysolmerski, R. B., Goeckeler, Z. M., Rioux, R. M., et al. (2016). Nerve growth factor stimulates axon outgrowth through negative regulation of growth cone actomyosin restraint of microtubule advance. *Mol. Biol. Cell* 27, 500–517. doi: 10.1091/mbc.E15-09-0636

Turney, S. G., Chandrasekar, I., Ahmed, M., Rioux, R. M., Whitesides, G. M., and Bridgman, P. C. (2020). Variation and selection in axon navigation through microtubule-dependent stepwise growth cone advance. *bioRxiv* [Prperint]. doi: 10.1101/2020.01.29.925602

van Beuningen, S. F. B., Will, L., Harterink, M., Chazeau, A., van Battum, E. Y., Frias, C. P., et al. (2015). TRIM46 controls neuronal polarity and axon specification by driving the formation of parallel microtubule arrays. *Neuron* 88, 1208–1226. doi: 10.1016/j.neuron.2015.11.012

van de Willige, D., Hoogenraad, C. C., and Akhmanova, A. (2016). Microtubule plus-end tracking proteins in neuronal development. *Cell Mol. Life Sci.* 73, 2053–2077. doi: 10.1007/s00018-016-2168-2163

van der Vaart, B., Franker, M. A. M., Kuijpers, M., Hua, S., Bouchet, B. P., Jiang, K., et al. (2012). Microtubule plus-end tracking proteins SLAIN1/2 and ch-TOG promote axonal development. *J. Neurosci.* 32, 14722a–14728a. doi: 10.1523/JNEUROSCI.1240-12.2012

van der Vaart, B., van Riel, W. E., Doodhi, H., Kevenaar, J. T., Katrukha, E. A., Gumy, L., et al. (2013). CFEOM1-associated kinesin KIF21A is a cortical microtubule growth inhibitor. *Dev. Cell* 27, 145–160. doi: 10.1016/j.devcel.2013.09.010

van Haren, J., Boudeau, J., Schmidt, S., Basu, S., Liu, Z., Lammers, D., et al. (2014). Dynamic microtubules catalyze formation of Navigator-TRIO complexes to regulate neurite extension. *Curr. Biol.* 24, 1778–1785. doi: 10.1016/j.cub.2014.06.037

van Haren, J., Draegestein, K., Keijzer, N., Abrahams, J. P., Grosveld, F., Peeters, P. J., et al. (2009). Mammalian Navigators are microtubule plus-end tracking proteins that can reorganize the cytoskeleton to induce neurite-like extensions. *Cell Motil. Cytoskeleton* 66, 824–838. doi: 10.1002/cm.20370

Villarin, J. M., McCurdy, E. P., Martínez, J. C., and Hengst, U. (2016). Local synthesis of dynein cofactors matches retrograde transport to acutely changing demands. *Nat. Commun.* 7:13865. doi: 10.1038/ncomms13865

Villarroel-Campos, D., and Gonzalez-Billault, C. (2014). The MAP1B case: an old MAP that is new again: novel roles for MAP1B. *Dev. Neurobio* 74, 953–971. doi: 10.1002/dneu.22178

Vitriol, E. A., and Zheng, J. Q. (2012). Growth cone travel in space and time: the cellular ensemble of cytoskeleton, adhesion, and membrane. *Neuron* 73, 1068–1081. doi: 10.1016/j.neuron.2012.03.005

Voelzmann, A., Hahn, I., Pearce, S. P., Sánchez-Soriano, N., and Prokop, A. (2016). A conceptual view at microtubule plus end dynamics in neuronal axons. *Brain Res. Bull.* 126, 226–237. doi: 10.1016/j.brainresbull.2016.08.006

Walker, R. A., Inoué, S., and Salmon, E. D. (1989). Asymmetric behavior of severed microtubule ends after ultraviolet-microbeam irradiation of individual microtubules in vitro. *J. Cell Biol.* 108, 931–937. doi: 10.1083/jcb.108.3.931

Walters, G. B., Gustafsson, O., Sveinbjornsson, G., Eiriksdottir, V. K., Agustsdottir, A. B., Jonsdottir, G. A., et al. (2018). MAP1B mutations cause intellectual disability and extensive white matter deficit. *Nat. Commun.* 9:3456. doi: 10.1038/s41467-018-05595-5596

Wang, T., Wu, X., Yin, C., Klebe, D., Zhang, J. H., and Qin, X. (2013). CRMP-2 is involved in axon growth inhibition induced by RGMa in vitro and in vivo. *Mol. Neurobiol.* 47, 903–913. doi: 10.1007/s12035-012-8385-3

Watanabe, T., Noritake, J., Kakeno, M., Matsui, T., Harada, T., Wang, S., et al. (2009). Phosphorylation of CLASP2 by GSK-3β regulates its interaction with IQGAP1, EB1 and microtubules. *J. Cell Sci.* 122, 2969–2979. doi: 10.1242/jcs.046649

Weiner, A. T., Seebold, D. Y., Torres-Gutierrez, P., Folker, C., Swope, R. D., Kothe, G. O., et al. (2020). Endosomal Wnt signaling proteins control microtubule nucleation in dendrites. *PLoS Biol.* 18:e3000647. doi: 10.1371/journal.pbio.3000647

Whitman, M. C., Andrews, C., Chan, W.-M., Tischfield, M. A., Stasheff, S. F., Brancati, F., et al. (2016). Two unique TUBB3 mutations cause both CFEOM3 and malformations of cortical development. *Am. J. Med. Genet. A* 170A, 297–305. doi: 10.1002/ajmg.a.37362

Wiese, C., and Zheng, Y. (2000). A new function for the gamma-tubulin ring complex as a microtubule minus-end cap. *Nat. Cell Biol.* 2, 358–364. doi: 10.1038/35014051

Wilkes, O. R., and Moore, A. W. (2020). Distinct microtubule organizing center mechanisms combine to generate neuron polarity and arbor complexity. *Front. Cell Neurosci.* 14:594199. doi: 10.3389/fncel.2020.594199

Williamson, T., Gordon-Weeks, P. R., Schachner, M., and Taylor, J. (1996). Microtubule reorganization is obligatory for growth cone turning. *Proc. Natl. Acad. Sci. U. S. A.* 93, 15221–15226. doi: 10.1073/pnas.93.26.15221

Willige, D., Hummel, J. J., Alkemade, C., Kahn, O. I., Au, F. K., Qi, R. Z., et al. (2019). Cytolinker Gas2L1 regulates axon morphology through microtubule-modulated actin stabilization. *EMBO Rep.* 20:e47732. doi: 10.15252/embr.201947732

Winans, A. M., Collins, S. R., and Meyer, T. (2016). Waves of actin and microtubule polymerization drive microtubule-based transport and neurite growth before single axon formation. *eLife* 5:e12387. doi: 10.7554/eLife.12387

Woo, S., and Gomez, T. M. (2006). Rac1 and RhoA promote neurite outgrowth through formation and stabilization of growth cone point contacts. *J. Neurosci.* 26, 1418–1428. doi: 10.1523/JNEUROSCI.4209-05.2006

Wu, X., Kodama, A., and Fuchs, E. (2008). ACF7 regulates cytoskeletal-focal adhesion dynamics and migration and has ATPase activity. *Cell* 135, 137–148. doi: 10.1016/j.cell.2008.07.045

Xu, F., Takahashi, H., Tanaka, Y., Ichinose, S., Niwa, S., Wicklund, M. P., et al. (2018). KIF1Bβ mutations detected in hereditary neuropathy impair IGF1R transport and axon growth. *J. Cell Biol.* 217, 3480–3496. doi: 10.1083/jcb.201801085

Yam, P. T., and Charron, F. (2013). Signaling mechanisms of non-conventional axon guidance cues: the Shh, BMP and Wnt morphogens. *Curr. Opin. Neurobiol.* 23, 965–973. doi: 10.1016/j.conb.2013.09.002

Yamada, K., Andrews, C., Chan, W.-M., McKeown, C. A., Magli, A., de Berardinis, T., et al. (2003). Heterozygous mutations of the kinesin KIF21A in congenital fibrosis of the extraocular muscles type 1 (CFEOM1). *Nat. Genet.* 35, 318–321. doi: 10.1038/ng1261

Yamada, K. M., Spooner, B. S., and Wessells, N. K. (1970). Axon growth: roles of microfilaments and microtubules. *Proc. Natl. Acad. Sci. U. S. A.* 66, 1206–1212. doi: 10.1073/pnas.66.4.1206

Yamashita, N., and Goshima, Y. (2012). Collapsin response mediator proteins regulate neuronal development and plasticity by switching their phosphorylation status. *Mol. Neurobiol.* 45, 234–246. doi: 10.1007/s12035-012-8242-8244

Yokota, Y., Kim, W.-Y., Chen, Y., Wang, X., Stanco, A., Komuro, Y., et al. (2009). The adenomatous polyposis coli protein is an essential regulator of radial glial polarity and construction of the cerebral cortex. *Neuron* 61, 42–56. doi: 10.1016/j.neuron.2008.10.053

Yoong, L.-F., Lim, H.-K., Tran, H., Lackner, S., Zheng, Z., Hong, P., et al. (2020). Atypical myosin tunes dendrite arbor subdivision. *Neuron* 106, 452–467.e8. doi: 10.1016/j.neuron.2020.02.002

Yu, H.-L., Peng, Y., Zhao, Y., Lan, Y.-S., Wang, B., Zhao, L., et al. (2020). Myosin X interaction with KIF13B, a crucial pathway for netrin-1-induced axonal development. *J. Neurosci.* 40, 9169–9185. doi: 10.1523/JNEUROSCI.0929-20.2020

Yu, W., and Baas, P. W. (1995). The growth of the axon is not dependent upon net microtubule assembly at its distal tip. *J. Neurosci.* 15, 6827–6833.

Zang, Y., Chaudhari, K., and Bashaw, G. J. (2021). New insights into the molecular mechanisms of axon guidance receptor regulation and signaling. *Curr. Top. Dev. Biol.* 142, 147–196. doi: 10.1016/bs.ctdb.2020.11.008

Zanic, M., Widlund, P. O., Hyman, A. A., and Howard, J. (2013). Synergy between XMAP215 and EB1 increases microtubule growth rates to physiological levels. *Nat. Cell Biol.* 15, 688–693. doi: 10.1038/ncb2744

Zhang, R., Alushin, G. M., Brown, A., and Nogales, E. (2015). Mechanistic origin of microtubule dynamic instability and its modulation by EB proteins. *Cell* 162, 849–859. doi: 10.1016/j.cell.2015.07.012

Zhao, B., Meka, D. P., Scharrenberg, R., König, T., Schwanke, B., Kobler, O., et al. (2017). Microtubules modulate F-actin dynamics during neuronal polarization. *Sci. Rep.* 7:9583. doi: 10.1038/s41598-017-09832-9838

Zhao, C., Takita, J., Tanaka, Y., Setou, M., Nakagawa, T., Takeda, S., et al. (2001). Charcot-Marie-Tooth disease type 2A caused by mutation in a microtubule motor KIF1Bbeta. *Cell* 105, 587–597. doi: 10.1016/s0092-8674(01)00363-364

Zheng, J. Q., Wan, J. J., and Poo, M. M. (1996). Essential role of filopodia in chemotropic turning of nerve growth cone induced by a glutamate gradient. *J. Neurosci.* 16, 1140–1149.

Zhou, F.-Q., Waterman-Storer, C. M., and Cohan, C. S. (2002). Focal loss of actin bundles causes microtubule redistribution and growth cone turning. *J. Cell Biol.* 157, 839–849. doi: 10.1083/jcb.200112014

Zhou, F.-Q., Zhou, J., Dedhar, S., Wu, Y.-H., and Snider, W. D. (2004). NGF-induced axon growth is mediated by localized inactivation of GSK-3beta and functions of the microtubule plus end binding protein APC. *Neuron* 42, 897–912. doi: 10.1016/j.neuron.2004.05.011

Zhou, M.-N., Kunttas-Tatli, E., Zimmerman, S., Zhouzheng, F., and McCartney, B. M. (2011). Cortical localization of APC2 plays a role in actin organization but not in Wnt signaling in *Drosophila*. *J. Cell Sci.* 124, 1589–1600. doi: 10.1242/jcs.073916

Zhou, Y., Falenta, K., and Lalli, G. (2014). Endocannabinoid signalling in neuronal migration. *Int. J. Biochem. Cell Biol.* 47, 104–108. doi: 10.1016/j.biocel.2013.12.007

Ziak, J., Weissova, R., Jeøábková, K., Janikova, M., Maimon, R., Petrasek, T., et al. (2020). CRMP 2 mediates Sema3F-dependent axon pruning and dendritic spine remodeling. *EMBO Rep.* 21:e48512. doi: 10.15252/embr.201948512

Zumbrunn, J., Kinoshita, K., Hyman, A. A., and Näthke, I. S. (2001). Binding of the adenomatous polyposis coli protein to microtubules increases microtubule stability and is regulated by GSK3 beta phosphorylation. *Curr. Biol.* 11, 44–49. doi: 10.1016/s0960-9822(01)00002-1

Conflict of Interest: The authors declare that the research was conducted in the absence of any commercial or financial relationships that could be construed as a potential conflict of interest.

Publisher's Note: All claims expressed in this article are solely those of the authors and do not necessarily represent those of their affiliated organizations, or those of the publisher, the editors and the reviewers. Any product that may be evaluated in this article, or claim that may be made by its manufacturer, is not guaranteed or endorsed by the publisher.

Copyright © 2021 Sánchez-Huertas and Herrera. This is an open-access article distributed under the terms of the Creative Commons Attribution License (CC BY). The use, distribution or reproduction in other forums is permitted, provided the original author(s) and the copyright owner(s) are credited and that the original publication in this journal is cited, in accordance with accepted academic practice. No use, distribution or reproduction is permitted which does not comply with these terms.

frontiers in Molecular Neuroscience

ORIGINAL RESEARCH
published: 09 December 2021
doi: 10.3389/fnmol.2021.790466

FLRT3 Marks Direction-Selective Retinal Ganglion Cells That Project to the Medial Terminal Nucleus

Tobias Ruff[1,2†], Christian Peters[1†], Akihiro Matsumoto[3], Stephan J. Ihle[2], Pilar Alcalá Morales[1], Louise Gaitanos[1], Keisuke Yonehara[3], Daniel del Toro[1,4] and Rüdiger Klein[1]**

[1] Department of Molecules, Signaling, and Development, Max Planck Institute of Neurobiology, Martinsried, Germany, [2] Laboratory of Biosensors and Bioelectronics, ETH Zürich, Zurich, Switzerland, [3] Department of Biomedicine, Nordic-EMBL Partnership for Molecular Medicine, Danish Research Institute of Translational Neuroscience – DANDRITE, Aarhus University, Aarhus, Denmark, [4] Department of Biological Sciences, Faculty of Medicine, Institute of Neurosciences, IDIBAPS, CIBERNED, University of Barcelona, Barcelona, Spain

OPEN ACCESS

Edited by:
Joaquim Egea,
Biomedical Research Institute of Lleida, Spain

Reviewed by:
Ulrike Grünert,
The University of Sydney, Australia
Rebecca M. Sappington,
Wake Forest School of Medicine, United States

***Correspondence:**
Daniel del Toro
danieldeltoro@ub.edu
Rüdiger Klein
rklein@neuro.mpg.de

† These authors have contributed equally to this work

Specialty section:
This article was submitted to Neuroplasticity and Development, a section of the journal Frontiers in Molecular Neuroscience

Received: 06 October 2021
Accepted: 19 November 2021
Published: 09 December 2021

Citation:
Ruff T, Peters C, Matsumoto A, Ihle SJ, Morales PA, Gaitanos L, Yonehara K, del Toro D and Klein R (2021) FLRT3 Marks Direction-Selective Retinal Ganglion Cells That Project to the Medial Terminal Nucleus. Front. Mol. Neurosci. 14:790466. doi: 10.3389/fnmol.2021.790466

The mammalian retina extracts a multitude of diverse features from the visual scene such as color, contrast, and direction of motion. These features are transmitted separately to the brain by more than 40 different retinal ganglion cell (RGC) subtypes. However, so far only a few genetic markers exist to fully characterize the different RGC subtypes. Here, we present a novel genetic Flrt3-CreERT2 knock-in mouse that labels a small subpopulation of RGCs. Using single-cell injection of fluorescent dyes in Flrt3 positive RGCs, we distinguished four morphological RGC subtypes. Anterograde tracings using a fluorescent Cre-dependent Adeno-associated virus (AAV) revealed that a subgroup of Flrt3 positive RGCs specifically project to the medial terminal nucleus (MTN), which is part of the accessory optic system (AOS) and is essential in driving reflex eye movements for retinal image stabilization. Functional characterization using *ex vivo* patch-clamp recordings showed that the MTN-projecting Flrt3 RGCs preferentially respond to downward motion in an ON-fashion. These neurons distribute in a regular pattern and most of them are bistratified at the level of the ON and OFF bands of cholinergic starburst amacrine cells where they express the known ON-OFF direction-selective RGC marker CART. Together, our results indicate that MTN-projecting Flrt3 RGCs represent a new functionally homogeneous AOS projecting direction-selective RGC subpopulation.

Keywords: FLRT3, RGC, MTN, ON direction selective, downward movement

INTRODUCTION

Retinal ganglion cells (RGCs) transmit visual information captured by the eyes to different regions in the brain. Distinct RGC subtypes respond with different activity patterns to the same set of visual stimuli (Baden et al., 2016). The feature selectivity of each RGC subtype is established by the various patterns of connections with different types of amacrine and bipolar cells in the inner plexiform layer (IPL). One such feature is the selective activity in response to motion stimuli into a certain

direction (Vaney et al., 2012). The detection of motion direction in the visual system is essential to drive the optokinetic reflex to stabilize the retinal image in response to the slow head or eye movements (Yoshida et al., 2001; Yonehara et al., 2016). In the brain, these stabilization signals are processed by different nuclei of the accessory optic system (AOS): the medial and lateral terminal nuclei (MTN and LTN), and the optic tract and the dorsal terminal nucleus (NOT/DTN) (Yonehara et al., 2009). It has been shown that three types of ON and one type of ON-OFF direction-selective RGC that project to the AOS are tuned to either upward (ON), downward (ON), or forward (ON, ON-OFF) direction (Dhande et al., 2013). To fully understand how each channel contributes to the smooth adaptive eye movements of the optokinetic reflex, it is essential to gain specific genetic access to each of the four input channels. Generally, all four types of AOS projecting RGCs are genetically accessible using the Hoxd10 mouse line (Dhande et al., 2013). So far only the SPIG1 and the Pcdh9-Cre line were shown to each specifically label one type, the dorsal (ON), or ventral (ON) selective RGCs (Yonehara et al., 2009; Lilley et al., 2019). However, we still lack specific genetic access to each of the remaining two AOS projecting RGCs.

Previous work from our lab using the fibronectin leucine rich-repeat transmembrane (Flrt) protein, showed that these cell adhesion molecules lead to cortex folding and altered distribution of pyramidal neurons during cortical development (Seiradake et al., 2014) in the mouse (del Toro et al., 2017). We observed that Flrt3 is expressed in early postnatal stages (Seiradake et al., 2014), and in the adult retina (Visser et al., 2015), and thought it could thus be interesting to evaluate it as a genetic marker. Here, using a novel, inducible CreERT2 knock-in line inserted into the *Flrt3* locus on chromosome 2 and a combination of morphological, molecular, and electrophysiological characterizations, we identified four morphologically distinct RGC types. Anterograde tracings revealed that one Flrt3-positive RGC subtype specifically projects to the medial terminal nucleus (MTN) of the AOS. Functional characterizations of the MTN-projecting Flrt3-subtype revealed that they are ON-RGCs and respond preferentially to downward moving stimuli. Interestingly, most MTN-projecting Flrt3-RGCs are bistratified in the ON and OFF-ChAT band, which has not been described before. Thus, our results indicate the presence of an additional fifth AOS projecting direction-selective RGC subtype.

MATERIALS AND METHODS

Mouse Lines

The following mouse lines used in this work have been previously described and were back-crossed to C57BL/6J mice: FLRT1^{LacZ} (EUCOMM), Flrt2^{LacZ} (EUCOMM), Flrt3^{LacZ} (Egea et al., 2008), Ai9$^{lsl-tdTomato}$ [B6.Cg-Gt(ROSA)26Sor$^{TM9(CAG-tdTomato)Hze}$/J] (Madisen et al., 2010).

Briefly, the Flrt3$^{Cre/ERT2}$ knock-in line used in this study was generated by homologous recombination in embryonic stem (ES) cells using a replacement-type targeting vector. The targeting construct for Flrt3 was generated by inserting a sequence containing part of the 5′UTR of the exon III, the CreERT2 sequence, an SV40 polyadenylation signal and a loxP-flanked neo cassette into a vector containing 3.8 kb and 6 kb homology arms surrounding exon III of the Flrt3 gene and the thymidine kinase (TK) cassette. The sequence flanking the insertion site in the 5′UTR is 5′ TAACAGAAGCTACCTGCTATAAT 3′. The sequence flanking the insertion site in the 3′UTR is 5′ TGAGAGAAGCAATGTACTGTACATTT 3′.

Embryonic stem cell cultures, electroporation, and selection were carried out according to standard protocols. Screening and homologous recombination on both arms of the constructs was assessed by Southern blot in the targeted ES cells. Germline transmission was achieved with at least two independent ES cell clones. Mice were maintained in a C57BL/6J background. They will be deposited in the Mutant Mouse Resource and Research Centers (MMRRC) for distribution. Animals were kept and used according to the regulations of the Regierung von Oberbayern.

The FLRT3-CreERT2 line was crossed to the R26-tdTomato (Ai9) line [B6.Cg-Gt(ROSA)26Sortm9(CAG-tdTomato)Hze/J] (Madisen et al., 2010).

4-Hydroxytamoxifen Administration

4-hydroxytamoxifen (Sigma, ref: H-7904) solution was prepared according to the manufacturer's protocol (Chevalier et al., 2014). To induce Cre expression in the Flrt3-CreERT2 line, adult mice (>P60) of both sexes were injected intraperitoneally with 60 μg/g 4-Hydroxytamoxifen.

Retina Histology

For retina whole-mount preparation, eyes were first enucleated and a small hole was made in the dorsal side to maintain correct orientation after dissection. Next, the cornea and lens were removed by cutting along the ora serrata and the retina cleaned of any residues from the vitreous. Finally, the retina was detached from the eyecup and transferred onto a cell culture insert (Millipore, Cat. no. PICMORG50). To allow a flat mount of the retina, 4 incisions were made. The deepest incision marked the dorsal side. Retinas were fixed on the membrane for at least 30 min in 4% paraformaldehyde (PFA).

Brain Histology

For analysis of retinofugal projections, the animals were deeply anesthetized with an overdose of Ketamine (medistar)/Xylazine (Bernburg) (1.6%/0.08%). Mice were transcardially perfused for 10 min at a speed of 1 ml/min with ice-cold PBS followed by 10 min of ice-cold 4% PFA (10% stock solution, Electron Microscopy Sciences, 15712) in PBS. Brains were post-fixed in 4% PFA for 24–48 h and subsequently stored in PBS (0.02% Sodium azide). Brains were cut at 100 μm slices using a vibratome (Leica). Retinas were dissected after transcardial perfusion.

Immunohistochemistry

For immunostainings, retinas were fixed in 4% PFA and transferred to a permeabilizing and blocking solution containing

0.3% Triton X-100, 5% donkey serum, 0.2% bovine serum albumin, 0.2% lysine, and 0.2% glycine for at least 24 h. After three washes in PBS, retinas were incubated with one of the following primary antibodies (all antibodies were used at a dilution of 1:100, unless otherwise stated): guinea pig anti-RBPMS (ABN1376, Millipore, United States); rabbit anti-Calbindin-D-28k 1:200 (702411, Thermo Fisher Scientific, United States); rabbit anti-CART 1:300 (14547S, Cell Signaling Technology, United States); rabbit anti-ChAT (AB-N34AP, ATS, United States); rabbit anti-Parvalbumin (PV27, Swant, Switzerland); rabbit anti-Satb1 (ab70004 abcam); mouse anti-SMI32 (801701, BioLegend, United States); mouse anti-Brn3c (sc-81980, Santa Cruz Biotechnology, United States). The tissue was incubated for 1–3 days with the primary antibodies (in 0.3% Triton X-100, 2% bovine serum albumin, 0.02% sodium azide in PBS). After 3 washes in PBS, the secondary antibody (in 0.3% Triton X-100, 3% donkey serum in PBS) was added for at least 1 day.

X-Gal Staining

For X-Gal staining, the retina was dissected from the eye and fixed for 30 min in an X-Gal fixative solution (0.2% Glutaraldehyde, 1% PFA in PBS, 5 mM EGTA, and 2 mM $MgCl_2$ and 0.02% NP40). Brains were fixed for 1–3 h. Retinas and brain regions were stained for beta-galactosidase activity by incubating them for 5–10 h in a 1 mg/ml X-gal solution containing 5 mM $K_4Fe(CN)_6$ and 5 mM K3Fe(CN)6. Retinas were postfixed for 10 min in 4% PFA.

Single Retinal Ganglion Cell Injections

For single-cell reconstructions, retinas of FLRT3-CreERT2 × R26-tdTomato (Ai9) mice were dissected from the eye and mildly fixed in 4% PFA for 15 min. FLRT3+ neurons were identified by Tomato expression and injected with 4% Lucifer yellow dissolved in ACSF using a sharp electrode. Sharp electrodes were pulled from borosilicate glass capillaries to a final resistance of 200 Ω (Science Products GP150F-8P) and mounted on a motorized patch-clamp manipulator. The dye was expelled using a positive current of 1–2 nA at 100 ms pulses for about 2 min (90% duty cycle).

Intravitreal Virus Injections

Mice were anesthetized intraperitoneally with a mixture of fentanyl [0.05 mg/kg, SIGMA-ALDRICH Chemie GmbH (800021)], midazolam [5 mg/kg, SIGMA-ALDRICH Chemie GmbH (800021)], and medetomidine [5 mg/kg, TCI Deutschland GmbH (800142)]. On the day of surgery, and on two subsequent days, carprofen [5 mg/kg, Zoetis (Rimadyl)] was also administered as an additional analgesic. Surgical instruments were heat-sterilized and washed with ethanol. The 7000 series Neuros Hamilton syringe with a 32G blunt needle was rinsed several times with distilled H_2O, then ethanol, and again with distilled H_2O. The animal was then fixated in a stereotaxic setup (Kopf instruments) and the eye that was injected second was kept damp with eye drops (Oculotect, Novartis). Briefly, the surgery was performed by cautiously protruding the eye from the eye socket and punctured at the ora serrata using a 30-gauge needle. Next, 1 μl of the adeno-associated virus (AAV) (rAAV2/CAG-GFP, rAAV2/Flex-GFP, rAAV2/Flex-tdTomato) was injected using a Hamilton syringe controlled by a micromanipulator (M3301R, WPI) and inserted into this opening at an oblique angle to avoid damaging the lens. After injection, the syringe was left in place for 4 min to allow the virus to disperse. After removing the Hamilton syringe, the eye was covered with eye cream (Isopto-Max, Novartis) and the procedure was repeated with the other eye. After 3 weeks, 2 μl of Cholera Toxin Subunit B conjugated with Alexa Fluor 647 (CTB647, C34778, Invitrogen, United States) (1%) was injected using a similar procedure. For histological analysis the animals were sacrificed as described previously in "brain histology" and perfused using 4% PFA 24 h later. The brain and retina were postfixed in 4% PFA for 24 and 1 h, respectively.

Stereotaxic Surgeries

Mice were anesthetized using isoflurane (Cp-pharma, 1.5–2%) and placed in a stereotaxic setup (Kopf Instruments). Body temperature was maintained using a heating pad at 37°C, and an analgesic was injected subcutaneously (5 mg/kg, Rimadyl, Zoetis). Viruses (pAAV-FLEX-tdTomato (Addgene), rAAV5-hsyn-EYFP (UNC GTC vector core, United States)), or CTB (cholera toxin subunit B, Invitrogen) were injected into the MTN (AP −2.65, ML ± 0.95, DV −5) using glass pipettes (#708707, BLAUBRAND intraMARK).

Electrophysiology

Mice were dark-adapted overnight and sacrificed by cervical dislocation. The retinas were dissected immediately after and transferred to oxygenated (95% O_2 and 5% CO_2) Ames solution at room temperature (∼22°C). The retina was placed onto an Anodisc filter membrane (Whatman, WHA68096022) with the ganglion cell layer facing upward and transferred into the recording chamber. The ventral part of the retina was marked for orientation. Flrt3-tomato neurons were visualized under brief fluorescent illumination using a microscope equipped with IR–DIC optics (Olympus BX51). All electrophysiological recordings were performed with constant superfusion of carbogenated Ames solution at 30–32°C. Whole-cell-current-clamp or cell-attached recordings were performed with a MultiClamp 700B amplifier and a Digidata 1550 digitizer (Molecular Devices). For current-clamp recordings, a patch pipette with a resistance of 4–6 MΩ was filled with an intracellular recording solution (130 mM potassium gluconate, 10 mM KCl, 2 mM $MgCl_2$, 10 mM HEPES, 2 mM Na-ATP, 0.2 mM Na_2GTP, 0.2% neurobiotin, pH7.35, and 290 mOsm). For cell-attached recordings, the patch pipette was filled with Ames solution.

Blue light stimuli were presented using a DLP projector (DLP® LightCrafter 4500) through a 4× objective. Direction selectivity was analyzed by presenting a moving grid (bar width = 285 μm, speed = 570 μm/s, time = 2 s) in eight different directions. Only a few neurons were unresponsive to visual stimuli and thus discarded. Responses to stationary centered flashing dots of increasing size [(50–1,200 μm), time = 2 s] were recorded.

For firing adaptation calculation, we used the formula $[1 - (T_{last}/T_{initial})]$, where T_{last} is the time interval between the last two action potentials and $T_{initial}$ is the time interval between the first two action potentials. Consequently, a value of 0 represents no change in spike frequency, while higher values represent a decay in the spiking rate of a neuron.

Cell Distribution Analysis

For cell distribution analysis, cells of interest were manually marked using the cell counter plugin from Fiji. To evaluate the cell distribution regularity, density recovery profiles (DRP) were calculated using a custom made python script. To calculate the density recovery profile, the amount of cells (N) within different radii (r) of each cell was counted and divided by the area (A) covered between radius r and $r + \partial r$. The DRP was then calculated as density $p(r) = N(r + \partial r)/(A(r + \partial r)$. We defined the regularity index as the mean nearest neighbor distance divided by the standard error of the mean.

Cell Morphology Analysis and Classification

For cell morphology analysis, each cell was traced in a semi-automatic fashion using the Fiji plugin Simple Neurite tracer. To extract morphology features (such as stratification depth, number of branching points, and total neurite length) a custom-made python script was used based on the NeuroM toolkit from the Blue Brain Project[1].

Inner Plexiform Straightening to Enable Stratification Analysis

For stratification analysis, z-stacks of retinal sections (vibratome cut cross sections orthogonal to the retinal cell layers) were imaged using a Leica SP8 microscope. A custom-made python script was used to straighten the curved retina sections. The script used the DAPI staining of the ganglion cell layer and inner nuclear layer to define the boundaries of the inner plexiform layer. Afterward, the sections were straightened using the bilinearly blended Coons patch using the previously established boundaries of the inner plexiform layer (Farin and Hansford, 1999). Retinal sections in which straightening failed were discarded from the analysis.

Data Analysis

Data and statistical analyses were performed using GraphPad Prism v5, Python 3.6, and Clampfit (Molecular Devices, United States). Significance levels were analyzed using a two-tailed unpaired Student's *t*-test when comparing two groups (**Figure 3C**), or one-way ANOVA test with Tukey's *post hoc* test when comparing multiple groups (**Figures 5D,E**), where *P*-values represent $^{*}p < 0.05$; $^{**}p < 0.01$; $^{***}p < 0.001$. All data are represented as the mean ± SEM. All sample sizes and definitions are provided in the figure legends. The python scripts used in this study are available upon request.

[1]https://neurom.readthedocs.io/en/stable/

RESULTS

Flrt3 Is Expressed in a Subpopulation of Retinal Ganglion Cells

In previous work, we observed Flrt3 expression in the early postnatal retina (Seiradake et al., 2014). Additionally, all three members of the Flrt family of cell-adhesion molecules (Flrt1, 2, and 3) were found to be expressed in the adult retina (Visser et al., 2015). Using our Flrt1^{LacZ}, Flrt2^{lacZ}, and Flrt3^{lacZ} reporter mouse lines, we confirmed that all three Flrts are expressed in a subpopulation of neurons in the ganglion cell layer (GCL) (**Supplementary Figures 1A–F** and data not shown). Since Flrt3 showed a sparser expression pattern in the GCL than Flrt1 and 2, we decided to focus on characterizing the Flrt3 population (**Supplementary Figures 1A,B**). To gain genetic access to the Flrt3-RGCs, we generated a tamoxifen-inducible Flrt3-CreERT2 knock-in line (**Figure 1A**). By crossing the Flrt3-CreERT2 line to a tdTomato reporter line, we confirmed that Flrt3-Cre expression matched Flrt3^{LacZ} expression in the brain (**Supplementary Figures 2A–C**). Immunostainings using the pan RGC marker RBPMS [RNA-binding protein (Rodriguez et al., 2014)] showed that 22.7% of all Flrt3+ neurons in the GCL were RGCs, while 77.3% were amacrine cells (**Figures 1B,C**). Conversely, Flrt3-RGCs represented a sparse population of about 4.6% of all RGCs. Retinal sections (vibratome cut sections orthogonal to the retinal cell layers) of the Flrt3-CreERT2-Tomato line showed that Flrt3 was not only expressed in the GCL but also in the inner nuclear layer (INL) (**Figure 1D** and **Supplementary Figure 1F**). Flrt3+ amacrine cells, RGCs, and possibly also bipolar cells of the INL and GCL contribute to the stratification pattern observed within the IPL. The peak stratification is located between the two ON and OFF ChAT bands (Voigt, 1986) (**Figure 1D**). Moreover, the Flrt3-CreERT2 line also labels a population of horizontal cells in the OPL (data not shown).

A relatively homogeneous distribution and small fraction of Flrt3-RGCs suggested that only a limited number of functionally specific RGCs types were labeled (**Figures 1E,F**). To examine if Flrt3-RGCs represented an anatomically homogeneous subpopulation with a regular spacing, we analyzed their spatial arrangement based on density recovery profiles (DRP) (**Supplementary Figure 2D**) (Rodieck, 1991). We found that Flrt3-RGCs were distributed across the whole retina, with a peak density in the ventral regions (**Figure 1E**). However, DRP analysis showed random distribution in both Flrt3-RGCs (**Figure 1F**) and Flrt3-amacrine cells (**Supplementary Figure 2E**). In summary, these results suggest that Flrt3 labels more than one functional RGC and amacrine subpopulation.

Morphological Characterization Indicates at Least Four Flrt3-RGC Subpopulations

The depth of dendritic stratification in the IPL is a good feature to classify functional RGC subpopulations (Seung and Sümbül, 2014). Thus, we used the Flrt3-CreERT2-Tomato line to label the morphology of Flrt3^{+} RGCs and amacrine cells by

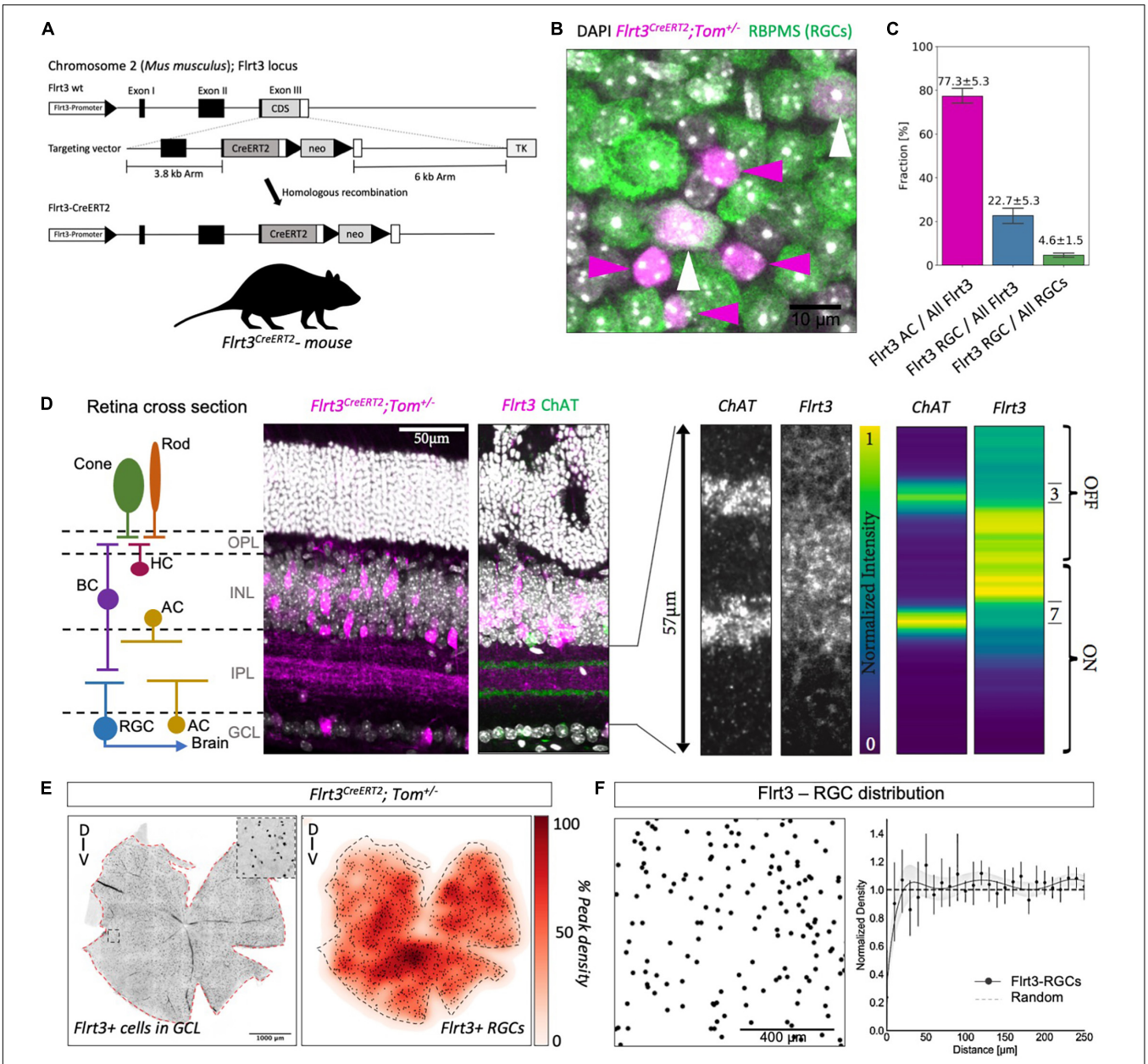

FIGURE 1 | Flrt3 neuronal distribution in the mouse retina. **(A)** Scheme of the Flrt3-CreERT2 mouse. **(B)** Immunostaining showing Flrt3+ cells in magenta (tomato), RGCs in green (RBPMS), and the nucleus in white (DAPI). The white arrows indicate FLRT3-RGCs and the magenta arrows FLRT3-amacrine cells. **(C)** Plot showing the fractions of Flrt3-amacrine (AC) and FLRT3-RGCs in the Flrt3-CreERT2 mouse. Two complete retinas were counted and another three representative regions of interest (ROIs) of another two retinas were included in the quantification. **(D)** Retina sections of *Flrt3-CreERT2;Tom*$^{\pm}$ mouse showing Flrt3 cells in purple and ChAT bands in green. The left panel shows the anatomical structure and cell types of a typical retinal section. The right panel shows a zoom of the IPL region and normalized intensity of ChAT and Flrt3 signals. AC, amacrine cells; BC, bipolar cells; HC, horizontal cells; RGC, retinal ganglion cell; OPL, outer plexiform layer; INL, inner nuclear layer; IPL, inner plexiform layer; GCL, ganglion cell layer. **(E)** Representative retina density profile (%) of *Flrt3-CreERT2;Tom*$^{\pm}$ mice. The left panel shows the distribution of Flrt3+ cells in the ganglion cell layer. The right panel shows the density of Flrt3+ RGCs identified from the left panel. N = 2 retinas from 2 mice **(F)** Random distribution of Flrt3-RGCs. Left panel: Flrt3-RGC distribution in a ROI of a retina region. Each dot represents a Flrt3+ RGC. Right panel: Density recovery profile of Flrt3+ RGC showing a random distribution. Graph shows Mean value ± SEM. Line represents a 7th order fit of the mean values. Shaded area is the 99% confidence interval. N = 4 retinas from 2 mice.

electrophoretic injection of fluorescent dyes in random locations of the retina (Lucifer yellow and Alexa 488, **Figures 2A,D,E**). We divided the IPL into five layers (S1–S5) and used this to assign the dendritic distribution of the individual labeled cells (**Figure 2B**). We found that Flrt3-RGCs consist of 4 subtypes: 53% of all Flrt3-RGCs were bistratified in the ON and OFF layers S2 and S4, 37% stratified in the ON layers (2 subtypes) S4 or S5, and a small fraction (∼10%) stratified only in the OFF layer S1 (**Figure 2C**).

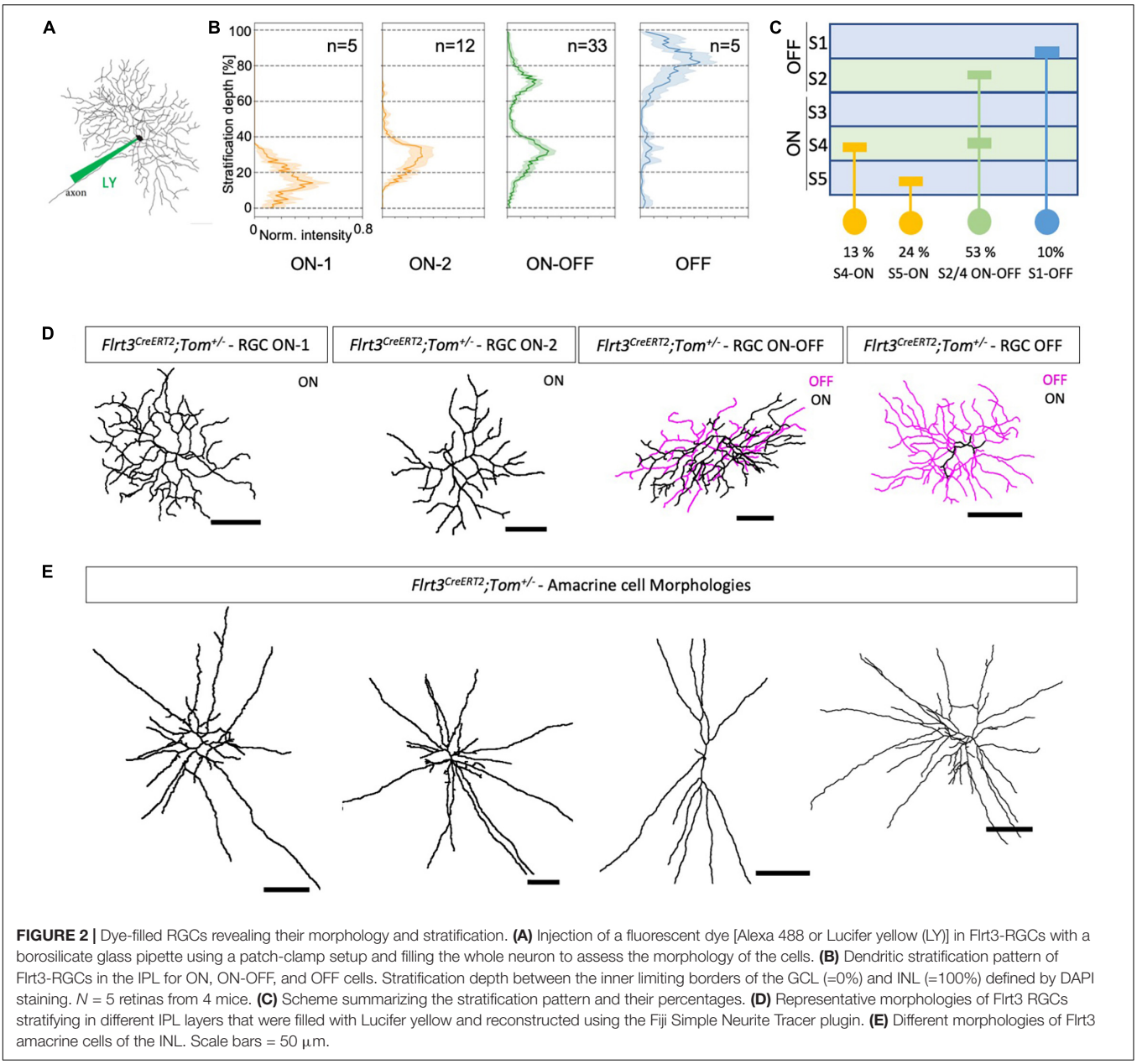

FIGURE 2 | Dye-filled RGCs revealing their morphology and stratification. **(A)** Injection of a fluorescent dye [Alexa 488 or Lucifer yellow (LY)] in Flrt3-RGCs with a borosilicate glass pipette using a patch-clamp setup and filling the whole neuron to assess the morphology of the cells. **(B)** Dendritic stratification pattern of Flrt3-RGCs in the IPL for ON, ON-OFF, and OFF cells. Stratification depth between the inner limiting borders of the GCL (=0%) and INL (=100%) defined by DAPI staining. *N* = 5 retinas from 4 mice. **(C)** Scheme summarizing the stratification pattern and their percentages. **(D)** Representative morphologies of Flrt3 RGCs stratifying in different IPL layers that were filled with Lucifer yellow and reconstructed using the Fiji Simple Neurite Tracer plugin. **(E)** Different morphologies of Flrt3 amacrine cells of the INL. Scale bars = 50 μm.

To further characterize the Flrt3-RGC subpopulations, we performed immunostainings against known RGC markers. The strongest co-labeling of Flrt3+ RGCs (RBPMS+) was found with Calbindin (28 ± 2.7%), followed by Parvalbumin (19 ± 3.6%), and then the ON-OFF direction selective ganglion cell marker CART (22 ± 4.8) (**Supplementary Figures 3A–F**, mean ± SEM). Overall, none of the markers labeled all Flrt3+ RGCs, suggesting that Flrt3 labels a new combination of RGC subtypes. Importantly, it has been shown in mice that parvalbumin and calbindin label at least eight and ten (PV1–PV8), respectively, morphologically different RGC types differing in their stratification pattern and dendritic field size (Kim and Jeon, 2006; Gu et al., 2016). CART positive RGCs are known to label the four ON-OFF direction selective ganglion cells (ooDSGC) that can be distinguished using combinatorial staining of Cadherin 6, MMP17, and Collagen 25a1 (Kay et al., 2011).

Electrophysiological Characterization Revealed Three Major Response Patterns

To physiologically characterize Flrt3-RGCs, we performed patch clamp recordings from Flrt3-Tom mice, showing different movie patterns (e.g., moving bars, stripes, or dots) directly onto the retina to monitor light-evoked firing activities (**Figure 3A**). In an initial evaluation, we analyzed the firing properties of Flrt3-RGCs by injecting current pulses with different intensities in whole-cell current-clamp mode. We recorded 21 Flrt3-negative and 16

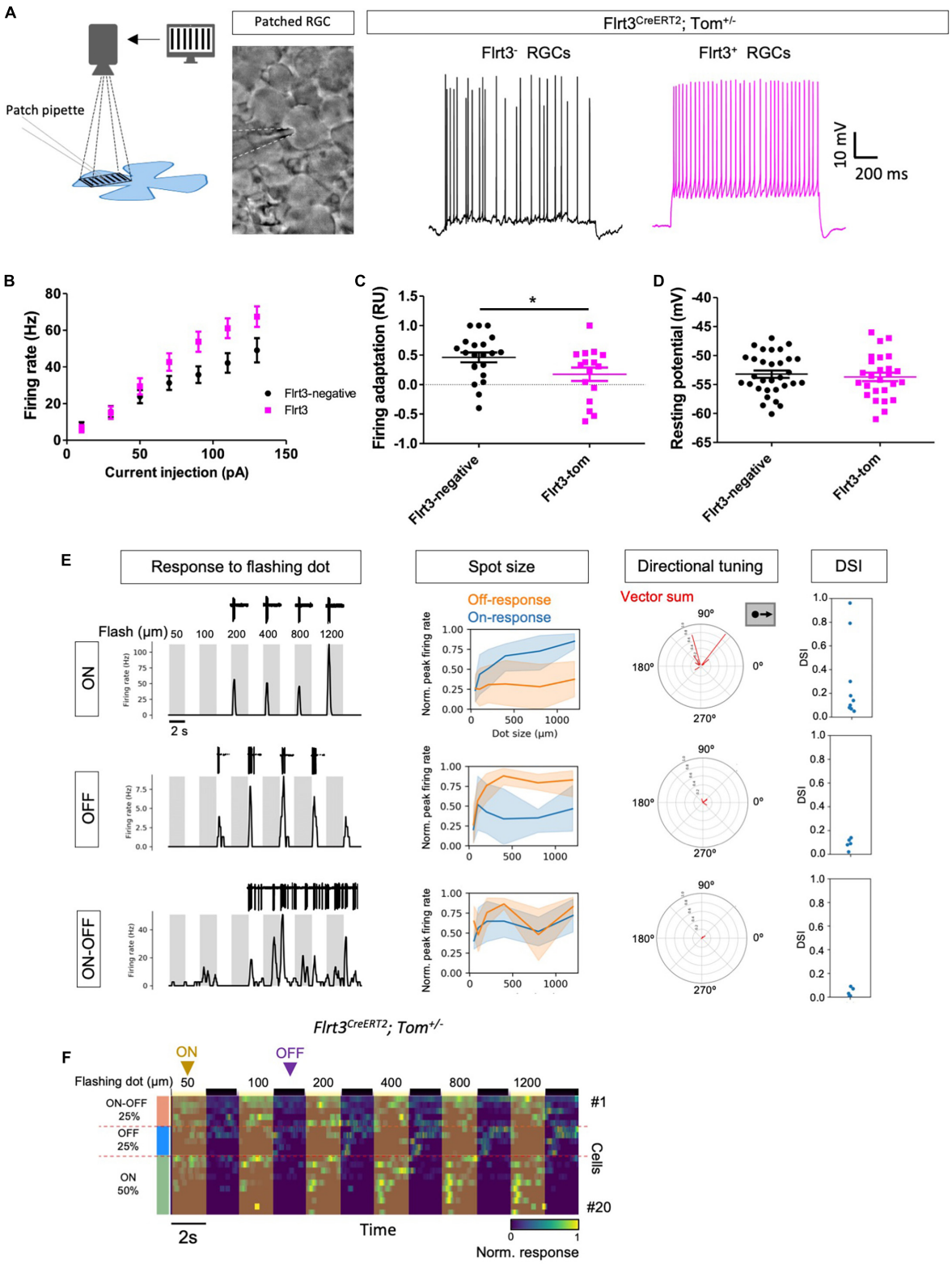

FIGURE 3 | Flrt3-Tom-RGCs are mainly ON neurons. **(A)** The left panel shows a schematic of the experiment in which an RGC is patch-clamped while different movie patterns are shown with a projector. The right panel shows representative whole-cell current-clamp recordings displaying firing after a step of current injection in Flrt3^{+} and Flrt3^{-} RGCs. **(B)** Plot showing the firing rate (Hz) after increasing current steps. **(C)** Firing adaptation from the recordings in **(A)**. A value for firing adaptation closer to 1 represents cells with a higher adapting firing, while a value closer to 0 is more regular (see section "Materials and Methods"). *N* = 16–21 cells

(Continued)

FIGURE 3 | from 2 retinas and 2 animals. Two-tailed unpaired *t*-test. $^*P < 0.05$. **(D)** Resting potential (mV) in Flrt3$^+$ and Flrt3$^-$ RGCs. **(E)** The first column of data shows representative responses (ON, OFF, and ON-OFF) in cell-attached mode to a flashing dot of increasing sizes with ON (gray) and OFF (white) over the center of each cell; the top of the plots show representative recordings in cell-attached mode. The second column shows the firing rate after the flashing spot stimulus. The third and fourth columns show the directional tuning and direction selectivity index (DSI), respectively, after the moving dot stimulus. The results show the responses to dots moving across the center of the RGCs in different directions. Polar plots represent the number of spikes fired for bars moving in each of the eight directions. **(F)** Heatmap plot showing the firing rate of 20 Flrt3-Tom-RGCs during the flashing dot stimulus. The yellow and black lines on top represent the dot flashing ON and OFF, respectively. Flrt3-Tom-RGCs are 50% ON, 25% OFF, and 25% ON-OFF. *N* = 20 cells from 6 animals. Neurons of unknown identity were discarded (*N* = 4 cells, data not shown).

Flrt3-positive RGCs from random retina regions. Interestingly, Flrt3-RGCs showed a higher firing rate than those of Flrt3-negative RGCs (**Figures 3A,B**). Moreover, when comparing the temporal features of firing patterns, Flrt3-RGCs showed non-adaptive and regular firing patterns (Flrt3-negative 0.46 ± 0.08, Flrt3-Tom 0.18 ± 0.11, *t*-test $^*p < 0.05$) (**Figure 3C**). The membrane potential of Flrt3 and Flrt3-negative RGCs did not show any significant differences (Flrt3-negative −53.21 ± 0.63, Flrt3-Tom −53.69 ± 0.74) (**Figure 3D**).

To evaluate the visual responses of Flrt3-RGCs, we performed cell-attached recordings to analyze the light-evoked firing activity in response to a set of different movie patterns: static flashing spot with different sizes (50–1,200 μm), and moving bars (**Figures 3E,F**). The responses to static flash stimulus revealed that Flrt3-RGCs included ON (50%), OFF (25%), and ON-OFF (25%) cells. A subset of ON cells showed direction selectivity to upward movements (2 out of 10 cells) (**Figure 3E**). Within our sample size no OFF and ON-OFF cells showed any direction selectivity (**Figure 3E**).

Flrt3-RGCs Project to Nuclei in the Accessory Optic System

Retinal ganglion cells project to one of more than 50 different target regions in the mouse brain (Martersteck et al., 2017), and the projection patterns vary depending on RGC subtypes (Lawrence and Studholme, 2014). To analyze the projection pattern of Flrt3-RGCs, we performed intravitreal virus injections using a Cre-dependent GFP expressing AAV to specifically label the projection targets of Flrt3 RGCs, and compared it to the overall projection pattern of all RGCs using CTB647 (**Figures 4A–C**). The expression pattern showed non-specific innervation of the superior colliculus and LGN (**Figures 4D,E**). No Flrt3-RGCs axons were found in the intergeniculate leaflet (IGL) or the suprachiasmatic nucleus (SCN) (**Figures 4E,F**). Interestingly, Flrt3 RGCs projected to the medial terminal nucleus (MTN) and nucleus of the optic tract (NOT) (**Figures 4G,H**) which are part of the AOS and are known to be essential in driving the optokinetic reflex.

Medial Terminal Nucleus Projecting FLRT3 Retinal Ganglion Cells Are ON-DSGC

Based on the finding that Flrt3-RGCs project to the MTN of the AOS, we hypothesized that Flrt3-RGCs contain a subpopulation of direction selective ganglion cells (DSGC) encoding one of the four cardinal axes. To specifically label only Flrt3-RGCs projecting to the MTN, we injected a retrograde Cre-dependent AAV-Tomato into the MTN of Flrt3-CreERT2 mice (**Figure 5A**). After 3 weeks of viral expression, we were able to identify MTN-projecting Flrt3-RGCs in the retina (**Figure 5B**). Density recovery profile analyzes revealed a regular distribution of MTN projecting Flrt3-RGCs, indicating a homogenous subpopulation (**Figure 5C**). Indeed, the regularity index (RI) (see section "Materials and Methods") and mean nearest neighbor distance (NND) showed higher values for MTN-projecting Flrt3-RGCs (RI = 2.08 ± 0.07; NND = 111.4 ± 5.29) than for total Flrt3-RGCs (RI = 1.7 ± 0.17; NND = 54.04 ± 6.44) and Flrt3-amacrine cells (RI = 1.92 ± 0.04; NND = 31.57 ± 2.22) (**Figures 5D,E**), suggesting that MTN projecting Flrt3-RGCs consist of a single RGC subtype.

The majority of MTN-projecting Flrt3-RGCs bistratified in the S4 ON and S2 OFF layer (∼74%) of the inner plexiform layer (IPL) and overlapped with the two outer bands of Calbindin (**Figure 5F**). The remaining MTN-projecting Flrt3-RGCs mono-stratified in the S4 layer and overlapped with the inner most band of Calbindin (**Figure 5I**). Immunostainings showed that most MTN-projecting Flrt3-RGCs are positive for the ON-OFF DSGC marker CART (89 ± 11%, *n* = 69 cells) and Calbindin (97 ± 2%, *n* = 98 cells) (**Figures 5G,H**), which have been shown to label at least 10 morphologically distinguishable RGC types (Gu et al., 2016). Interestingly, among Calbindin-containing RGCs, Gu et al. (2016) reported that calretinin-containing RGCs include only 1 type ("CB3" type) that is bistratified in the S2/S4 layers of the IPL, similar to what we show with our MTN-projecting Flrt3-RGCs (Gu et al., 2016). Approximately 56 ± 5% (*n* = 49 cells) co-labeled for the calcium-binding protein parvalbumin (**Figures 5G,H**), which has been shown to label 8 morphologically distinct RGC types (PV1-8), and only the PV3 subtype shows the same bistratification pattern as most of the MTN-projecting Flrt3-RGCs (Yi et al., 2012). These data indicate that the known CB3 and PV3 RGCs are possible candidates for the cell types of MTN-projecting Flrt3-RGCs.

Although the majority of MTN-projecting Flrt3-RGCs had bistratified dendrites in the ON and OFF layers, the light-evoked firing activity monitored by cell-attached recordings revealed that MTN-projecting Flrt3-RGCs are physiologically ON cells, responding to luminance increments of static flashes (50–1,200 μm) (**Figure 6A**). Interestingly, almost all MTN-projecting Flrt3-RGCs (14 out of 15) were direction selective cells, and preferentially responded to an upward-moving grating (**Figures 6B,C,E**), corresponding to ventrally moving objects in the living animal (**Figure 6D**). Together, these results indicate that MTN-projecting Flrt3 RGCs represent a homogeneous AOS projecting direction-selective RGC subpopulation.

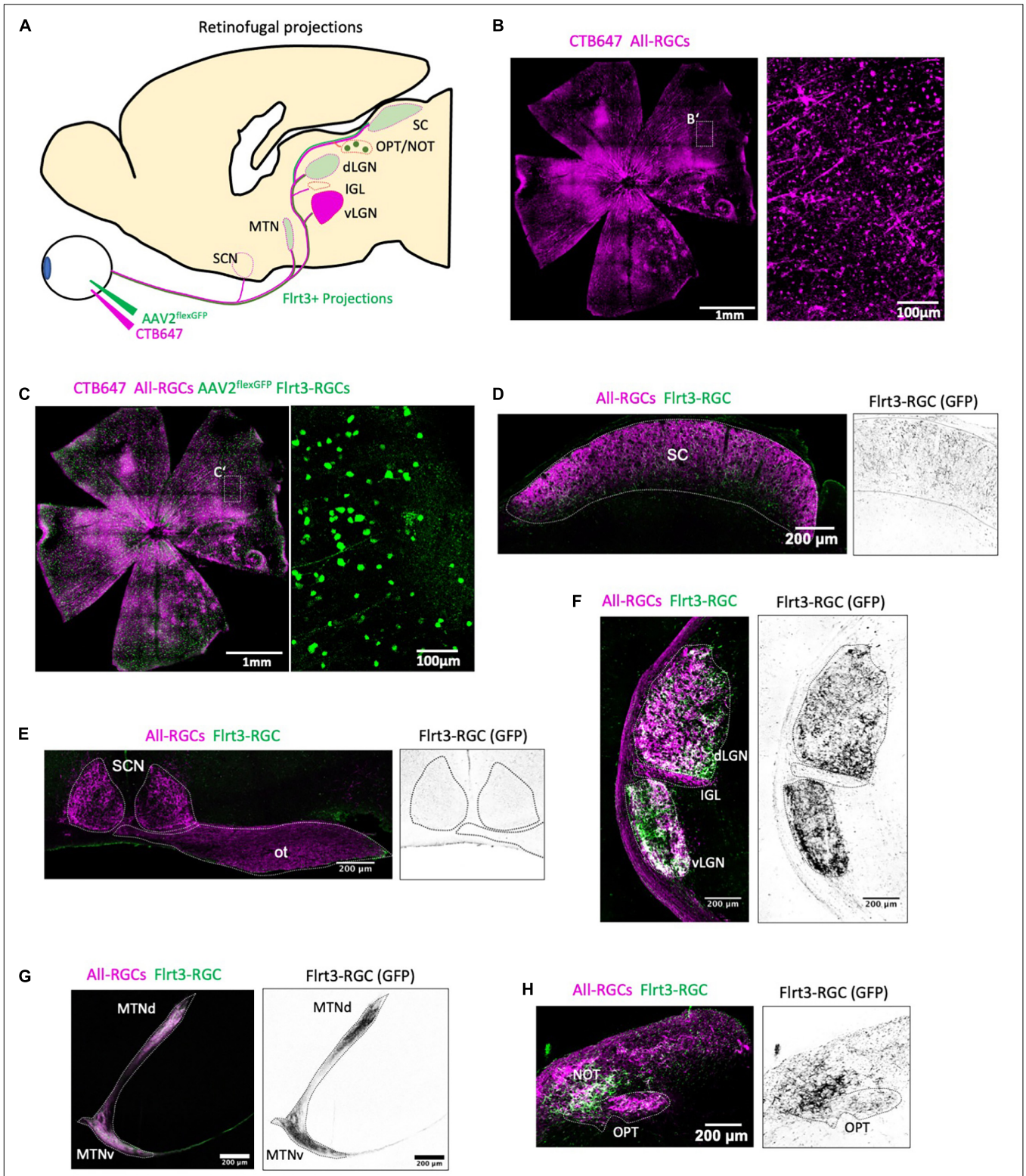

FIGURE 4 | Flrt3-RGCs projections in the mouse brain. **(A)** Scheme showing intravitreal injection of CTB647 and the cre-dependent AAV2-flex-GFP virus in Flrt3-CreERT2 mice. Representative images from one animal. **(B,C)** Representative whole mount retinas showing CTB647 labeled RGCs (magenta) and GFP expressing RGCs (green). **(B)** Shows an overlay of CTB647 and GFP. The right panel shows a zoom from each of **(B',C')**, respectively. **(D–H)** Specific projections of Flrt3 RGCs (green) and all RGC (magenta) axons in the **(D)** superior colliculus (SC), **(E)** SCN and optic tract (ot), **(F)** dLGN, IGL and vLGN, **(G)** MTN, **(H)** NOT and OPT.

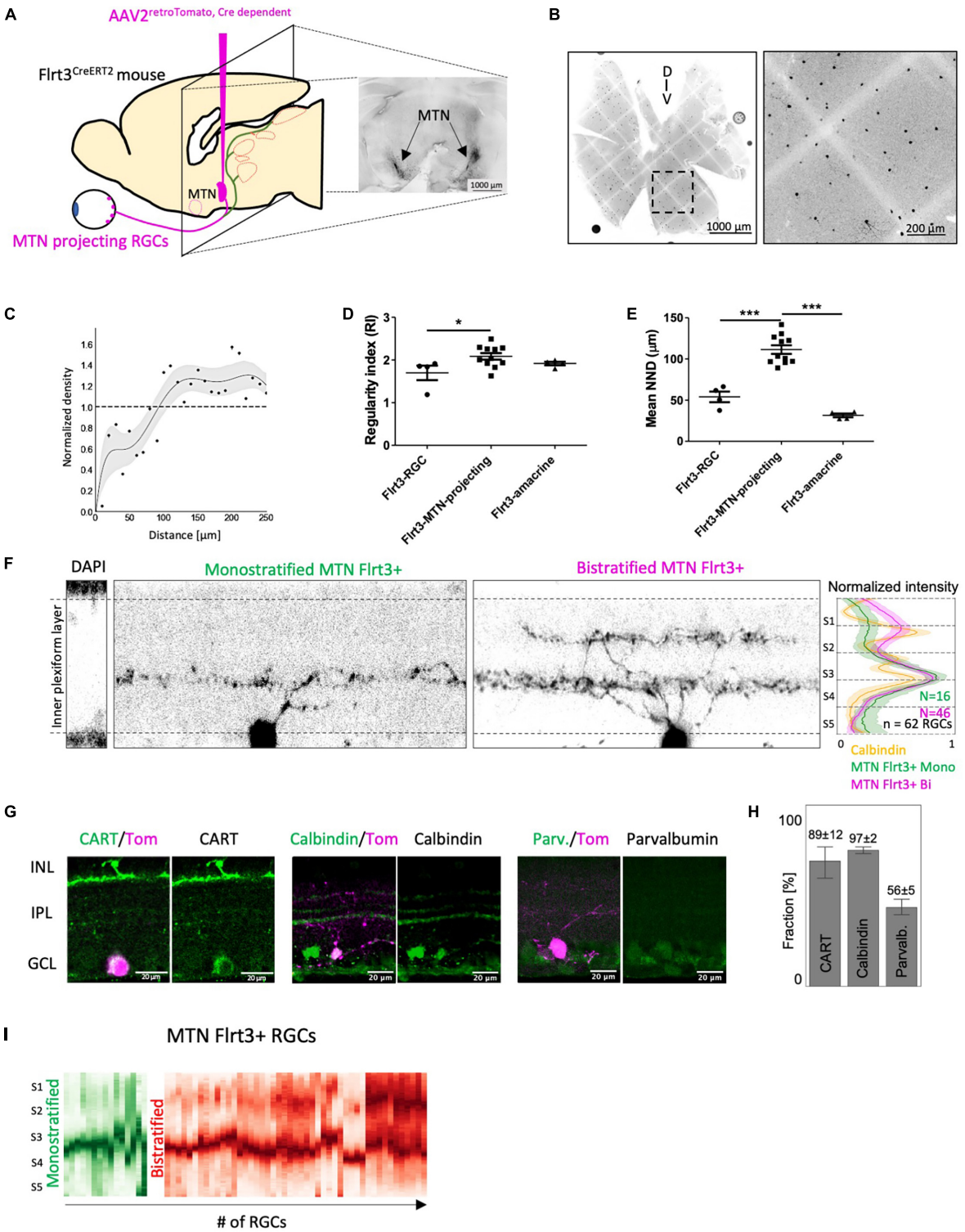

FIGURE 5 | MTN-projecting Flrt3-RGCs are a homogeneous downward ON-DSGC subpopulation. **(A)** Stereotaxic injection of AAV2$^{retro-cre-Tomato}$ in the MTN of Flrt3-CreERT2 mice to identify Flrt3-RGCs projecting to the MTN. The image on the right shows a representative MTN-injection site after 3 weeks of viral expression. $N = 4$ mice. **(B)** Whole mount retina showing the distribution of MTN-projecting Flrt3-RGCs. **(C)** Normalized density profile of MTN-projecting Flrt3-RGCs. $N = 50$ ROIs from 11 retinas and 8 animals. **(D)** Regularity index plot for Flrt3-RGC, Flrt3-MTN-projecting-RGC and Flrt3-amacrine cells. $N = 4$–11 ROI from different retinas of 3–4 mice (as shown in **(B)**. One-way ANOVA Tukey's Multiple Comparison Test, $^{*}P < 0.05$. **(E)** Average nearest neighbor distance (µm), calculated from same ROIs as in **(D)**. One-way ANOVA Tukey's Multiple Comparison Test, $^{***}P < 0.001$. **(F)** Orthogonal section through the IPL to visualize the stratification pattern of

(Continued)

FIGURE 5 | MTN-projecting Flrt3-RGCs. The right panel shows the average normalized stratification pattern of Calbindin (orange), mono- (green, *n* = 16 cells from 3 animals, 26%) and bistratified MTN-projecting Flrt3-RGCs (magenta, *n* = 46 cells from 3 animals, 74%). **(G)** Immunostaining for CART, Calbindin and Parvalbumin in a retinal sections of MTN injected mice from **(A)**. Tomato signal (magenta) shows MTN-projecting Flrt3-RGCs. **(H)** Fraction (%) of MTN-projecting Flrt3-RGCs positive for CART, Calbindin and Parvalbumin. *N* = 60–66 ROIs for each marker from 3 retinas. **(I)** Normalized stratification patterns of mono- (green) and bistratified (red) MTN-Flrt3-RGCs in the inner plexiform layer, from **(F)**. *N* = 46 cells from 3 animals.

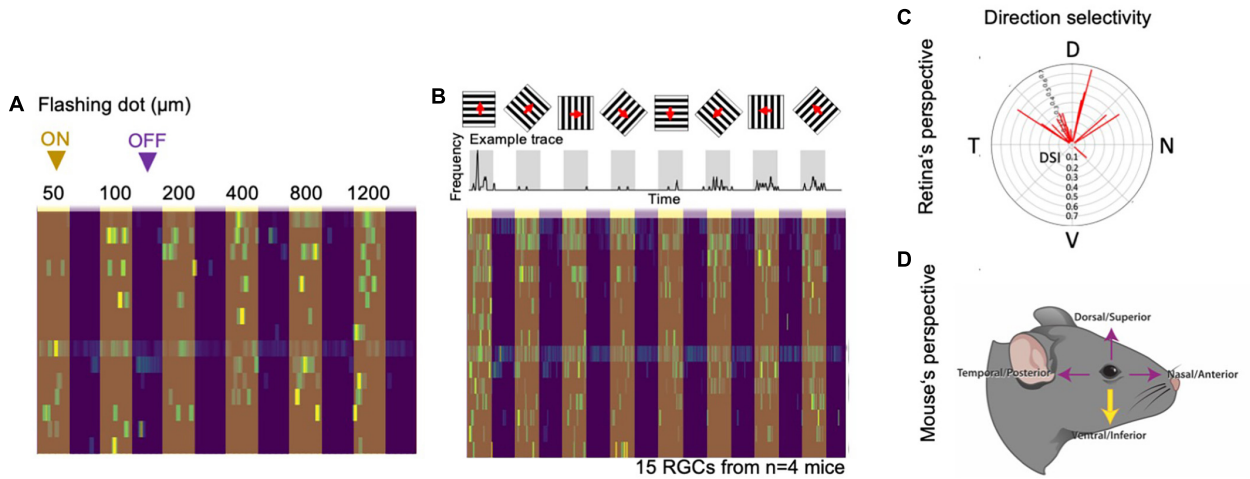

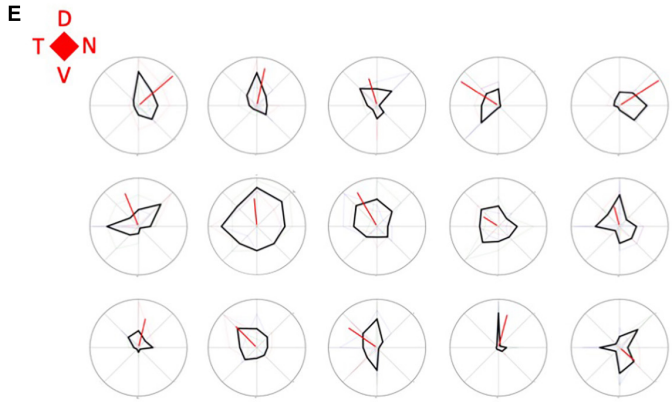

FIGURE 6 | MTN-projecting Flrt3-RGCs are a homogeneous downward ON-DSGC subpopulation. **(A)** Heatmap plot showing the frequency of firing in cell-attached MTN-projecting Flrt3-RGCs while showing a flashing dot with different diameters (50–1,200 µm). **(B)** Top: Scheme representing the recordings of MTN-projecting Flrt3-RGCs firing rate while displaying a moving grid in eight different directions. The frequency plot shows the average frequency of firing. Bottom: The heatmap plot shows the individual frequencies for each neuron patched for each moving grid displayed. *N* = 15 RGCs from 4 animals. **(C)** Polar plot showing the direction selectivity of the RGCs recorded from the retina's perspective. *N* = 15 RGCs from 4 animals. **(D)** Cartoon showing the mouse's perspective of the moving object. **(E)** Direction selectivity plots of fifteen different MTN-Flrt3-RGCs. *N* = 15 cells from 4 animals.

DISCUSSION

In this work, we generated a new Flrt3-CreERT2 knock-in mouse line to genetically target and characterize Flrt3 positive RGCs in the mouse retina. We found that Flrt3-RGCs represent a small subpopulation of ∼4.6% of all RGCs. Based on their stratification patterns, Flrt3-RGCs can be subdivided into four morphologically and three functionally distinct subtypes. Electrophysiological recordings showed that Flrt3-RGCs have more non-adaptive and higher firing rates than Frt3-negative RGCs. Fifty percent of Flrt3-RGCs are ON-responding cells when they are stimulated with a static flashing light. Retinofugal projection and electrophysiological analyses revealed that the functional ON subtype of the Flrt3 population projects to the MTN. Histologically, MTN-projecting Flrt3-RGCs bistratify in the IPL and express the ooDSGC marker CART (∼89%) and Calbindin (∼97%). Further analysis showed that MTN-projecting Flrt3-RGCs are direction selective cells, preferring downward direction.

Prior research on MTN-projecting direction-selective RGCs (Dhande et al., 2013) revealed that the Hoxd10-EGFP mouse line includes three ON subtypes, each of which encodes upward, downward or forward motion, and one ON-OFF type encode forward movements. So far, the Fstl4^{TM1Mno} (here referred

to as SPIG1) mouse line is the only mouse model that specifically labels the upward direction-selective ON-mono-stratifying MTN-RGCs. For the remaining 3 subtypes, no genetic marker exists (Yonehara et al., 2009; Dhande et al., 2013). In contrast to our MTN-projecting Flrt3-RGCs, downward selective cells in Hoxd10 mice show an ON mono-stratifying pattern in the IPL. Interestingly, Dhande et al. described a small (11%) population of RGCs in the Hoxd10 line that co-localized with the ON-OFF DSGC marker CART. However, the cell type was not further characterized. Another genetic line, Pcdh9-Cre, also labels MTN projecting ON RGCs. Like the MTN projecting Flrt3+ cells, the Pcdh9-Cre line labels 2 subtypes that either stratify mostly in the ON S4 layer, or show weaker stratifications in the S2 OFF layer. Both subtypes, however, respond to upward moving stimuli. In contrast to the MTN projecting Flrt3+ RGCs, the Pcdh9 ON-DS cells show a transient OFF response to the trailing edge of the moving stimulus (Lilley et al., 2019). Overall, this data suggests that Flrt3-RGCs could represent the CART positive RGCs of the Hoxd10 mouse line and thus describe a new and as yet uncharacterized MTN-projecting RGC population.

The co-stratification of MTN projecting Flrt3-RGCs within the same layer of the ON and OFF starburst amacrine (SAC) dendrites suggests that their direction selectivity toward downward moving objects is mediated by modulating GABAergic and cholinergic input from SACs (Mauss et al., 2017). However, we found a discrepancy between the stratification pattern and physiological response properties. Although MTN-Flrt3-RGCs showed a bi-stratifying ON-OFF morphology within the IPL, they lacked any functional OFF response. The small OFF responses seen despite the ON-OFF dendritic bistratification could be caused by the offset of OFF excitatory inputs by inhibitory inputs or presynaptic inhibition of OFF bipolar cells (Jacoby, 2015; Nath and Schwartz, 2016). Indeed, the same discrepancy between dendritic bi-stratification and ON dominant responses has been revealed in orientation selective RGCs (Nath and Schwartz, 2016), suppressed-by-contrast RGCs (Jacoby, 2015) and MTN/SC projecting ON DSGCs (Gauvain and Murphy, 2015), in which OFF dendrites did not receive any excitatory inputs. The absent OFF response could also be explained by the shorter dendritic ramification in the OFF layer in comparison with the longer projection into the ON layer (**Figure 5F**; Nath and Schwartz, 2016).

CONCLUSION

Based on the light responses of RGCs and basic anatomical criteria, we found a new genetic marker to identify a novel FLRT3$^+$ cell-type in the mouse retina, corresponding to an ON downward-selective MTN-projecting RGC. Like the Hoxd10 mouse, which identified an additional ON-OFF RGC that projects to the NOT of the AOS, our findings add a homogeneously distributed ON RGC-type that projects to the MTN of the AOS. Interestingly, this MTN-projecting FLRT3$^+$ cell-type is positive for CART, a marker for ON-OFF RGCs. Moreover, this RGC-type bistratified in the ON and OFF layer, but the electrophysiological recordings showed that they fire only when the light is ON, probably because the stratification pattern is larger in the ON layer compared to the OFF layer of the IPL.

In conclusion, the current work shows that almost all MTN-projecting Flrt3 cells are: (1) bistratified, (2) ON-dominant response, and (3) direction selective RGCs. Finally, using intersectional genetics, our Flrt3 line in combination with the Parvalbumin, Calbindin or CART transgenic mouse lines could provide functional access to these RGCs, which would enable us to study the function of the downward selective Flrt3-RGCs *in vivo*.

AUTHOR'S NOTE

The retinal ganglion cells (RGCs) in the retina are the only cells that transmit visual information into the brain. Until now, more than 40 different RGC types have been identified which respond in a very specific way to the same visual stimuli. However, only a small fraction of these can be studied using specific genetic markers. We found that Flrt3 labels a new RGC subpopulation that projects to the medial terminal nucleus (MTN) which is essential to drive reflexive eye movements for retinal image stabilization. Flrt3 labels MTN projecting RGCs that preferentially respond to downward moving objects by increasing their firing rate (ON-response). Thus, Flrt3 provides the first genetic tool for studying downward motion selective RGCs projecting to MTN.

DATA AVAILABILITY STATEMENT

The original contributions presented in the study are included in the article/**Supplementary Material**, further inquiries can be directed to the corresponding author/s.

ETHICS STATEMENT

The animal study was reviewed and approved by the Regierung von Oberbayern under the license 55.2-2532.Vet_02-20-10.

AUTHOR CONTRIBUTIONS

RK, DT, and TR initiated and conceived the project. CP performed electrophysiological recordings and intracranial injections. AM helped with electrophysiological recordings supervised by KY. TR performed all remaining experiments. PM and LG performed ES cell gene targeting. SI wrote the python analysis script to straighten the curved retina sections for stratification analysis. TR and CP wrote the manuscript with support from all other authors. LG checked the English grammar of the manuscript. All authors contributed to the article and approved the submitted version.

FUNDING

This research was partially funded by a Boehringer Ingelheim Fonds Ph.D. fellowship (TR), Max Planck Society (RK), VELUX

FONDEN Postdoctoral Ophthalmology Research Fellowship (AM), and Lundbeck Foundation (KY). DT is supported by the Ramón y Cajal program (RYC-2017-23486/RTI2018-095580-A-I00).

ACKNOWLEDGMENTS

We thank the MPIN transgenic service unit for their technical assistance, Jana Lindner for her help with embryonic stem cell work, Cecilia González for graphic design assistance, and Joel Bauer for help with intravitreal injections.

SUPPLEMENTARY MATERIAL

The Supplementary Material for this article can be found online at: https://www.frontiersin.org/articles/10.3389/fnmol.2021.790466/full#supplementary-material

Supplementary Figure 1 | Flrt2 and 3^{LacZ} lines express Flrts in a subpopulation of neurons in the ganglion cell layer. **(A)** Representative retina from Flrt3-LacZ animals. The immunostaining in the right panel shows Flrt3 cells (light blue, Xgal) and RGCs (green, RBPMS). White asterisks indicate Flrt3+ RGCs. Scale bar = 25 μm. **(B)** Top: percentage of $Flrt3^+$ RGCs and amacrine cells in the ganglion cell layer. Bottom: percentage of $Flrt3^+$ cells among RGCs. Scale bar = 25 μm. **(C,D)** Same figures as **(A,B)**, but with Flrt2-LacZ mice. White asterisks indicate Flrt2+ RGCs. **(E,F)** Retina sections from Flrt2-LacZ and Flrt3-LacZ mice, respectively, with Xgal staining at different developmental time points.

Supplementary Figure 2 | Flrt3-CreERT2 expression matches $Flrt3^{LacZ}$ expression in the brain. **(A)** Coronal brain slices of Flrt3-CreERT2; $Tom^{\pm}$ mice, from anterior to posterior. **(B)** Zoomed in view of different regions from **(A)** (dashed boxes). **(C)** Comparison between Flrt3-Tom and Flrt3/LacZ mice. **(D)** Algorithm showing how the DRP values were calculated. Rectangular regions of the retina were selected to create an autocorrelogram. Annuli around the center of the autocorrelogram were drawn to calculate the binned density from the center to the periphery and represented as the density recovery profile. **(E)** Random distribution of Flrt3-amacrine cells. Left panel: Flrt3-amacrine cell distribution in a ROI. Each dot represents a Flrt3+ amacrine cell. Right panel: Density recovery profile of Flrt3+ amacrine cells showing a random distribution. Graph shows mean value ± SEM. Line represents a 7th order fit of the mean values. Shaded area is the 99% confidence interval. *N* = 14 ROIs from 4 retinas and 2 mice.

s **Supplementary Figure 3 |** Immunostainings showing some overlap with other known RGC markers. **(A–F)** Staining for various known markers: Safb1, SMI32, Calbindin, Bm3c, Parvalbumin, and CART (blue) in Flrt3-RGCs (Tom, magenta) and RBPMS (green). The blue arrowhead shows an example of RGC that co-localizes with Flrt3 and the different markers. **(G)** Quantification of the percentage of Flrt3-RGCs expressing the markers shown in **(A–F)**. Mean value ± SEM.

REFERENCES

Baden, T., Berens, P., Franke, K., Roman-Roson, M., Bethge, M., and Euler, T. (2016). The functional diversity of mouse retinal ganglion cells. *Nature* 529, 345–351.

Chevalier, C., Nicolas, J.-F., and Petit, A.-C. (2014). Preparation and delivery of 4-hydroxy-tamoxifen for clonal and polyclonal labeling of cells of the surface ectoderm, skin, and hair follicle. *Methods Mol. Biol.* 1195, 239–245. doi: 10.1007/7651_2013_63

del Toro, D., Ruff, T., Cederfjäll, E., Villalba, A., Seyit-Bremer, G., Borrell, V., et al. (2017). Regulation of cerebral cortex folding by controlling neuronal migration via FLRT adhesion molecules. *Cell* 169, 621–635.e16. doi: 10.1016/j.cell.2017.04.012

Dhande, O. S., Estevez, M. E., Quattrochi, L. E., El-Danaf, R. N., Nguyen, P. L., Berson, D. M., et al. (2013). Genetic dissection of retinal inputs to brainstem nuclei controlling image stabilization. *J. Neurosci.* 33, 17797–17813. doi: 10.1523/JNEUROSCI.2778-13.2013

Egea, J., Erlacher, C., Montanez, E., Burtscher, I., Yamagishi, S., Heß, M., et al. (2008). Genetic ablation of FLRT3 reveals a novel morphogenetic function for the anterior visceral endoderm in suppressing mesoderm differentiation. *Genes Dev.* 22, 3349–3362. doi: 10.1101/gad.486708

Farin, G., and Hansford, D. (1999). Discrete Coons patches. *Comput. Aided Geom. Des.* 16, 691–700.

Gauvain, G., and Murphy, G. J. (2015). Projection-specific characteristics of retinal input to the brain. *J. Neurosci.* 35, 6575–6583. doi: 10.1523/JNEUROSCI.4298-14.2015

Gu, Y. N., Lee, E. S., and Jeon, C. J. (2016). Types and density of calbindin D28k-immunoreactive ganglion cells in mouse retina. *Exp. Eye Res.* 145, 327–336. doi: 10.1016/j.exer.2016.02.001

Jacoby, J. G. S. (2015). An amacrine cell circuit for signaling steady illumination in the retina. *Physiol. Behav.* 13, 2663–2670. doi: 10.1016/j.celrep.2015.11.062

Kay, J. N., De la Huerta, I., Kim, I.-J., Zhang, Y., Yamagata, M., Chu, M. W., et al. (2011). Retinal ganglion cells with distinct directional preferences differ in molecular identity, structure, and central projections. *J. Neurosci.* 31:753. doi: 10.1523/JNEUROSCI.0907-11.2011

Kim, T. J., and Jeon, C. J. (2006). Morphological classification of parvalbumin-containing retinal ganglion cells in mouse: single-cell injection after immunocytochemistry. *Investig. Ophthalmol. Vis. Sci.* 47, 2757–2764.

Lawrence, P. M., and Studholme, K. M. (2014). Retinofugal projections in the mouse. *J. Comp. Neurol.* 3753, 3733–3753. doi: 10.1002/cne.23635

Lilley, B. N., Sabbah, S., Hunyara, J. L., Gribble, K. D., Al-Khindi, T., Xiong, J., et al. (2019). Genetic access to neurons in the accessory optic system reveals a role for Sema6A in midbrain circuitry mediating motion perception. *J. Comp. Neurol.* 527, 282–296. doi: 10.1002/cne.24507

Madisen, L., Zwingman, T. A., Sunkin, S. M., Oh, S. W., Zariwala, H. A., Gu, H., et al. (2010). A robust and high-throughput Cre reporting and characterization system for the whole mouse brain. *Nat. Neurosci.* 13, 133–140. doi: 10.1038/nn.2467

Martersteck, E. M., Hirokawa, K. E., Evarts, M., Bernard, A., Duan, X., Li, Y., et al. (2017). Diverse central projection patterns of retinal ganglion cells. *Cell Rep.* 18, 2058–2072.

Mauss, A. S., Vlasits, A., Borst, A., and Feller, M. (2017). Visual circuits for direction selectivity. *Annu. Rev. Neurosci.* 40, 211–230. doi: 10.1146/annurev-neuro-072116-031335

Nath, A., and Schwartz, G. W. (2016). Cardinal orientation selectivity is represented by two distinct ganglion cell types in mouse retina. *J. Neurosci.* 36, 3208–3221. doi: 10.1523/JNEUROSCI.4554-15.2016

Rodieck, R. W. (1991). The density recovery profile: a method for the analysis of points in the plane applicable to retinal studies. *Vis. Neurosci.* 6, 95–111. doi: 10.1017/s095252380001049x

Rodriguez, A. R., de Sevilla Müller, L. P., and Brecha, N. C. (2014). The RNA binding protein RBPMS is a selective marker of ganglion cells in the mammalian retina. *J. Comp. Neurol.* 522, 1411–1443. doi: 10.1002/cne.23521

Seiradake, E., delToro, D., Nagel, D., Cop, F., Härtl, R., Ruff, T., et al. (2014). flrt structure: balancing repulsion and cell adhesion in cortical and vascular development. *Neuron* 84, 370–385. doi: 10.1016/j.neuron.2014.10.008

Seung, H. S., and Sümbül, U. (2014). Neuronal cell types and connectivity: lessons from the retina. *Neuron* 83, 1262–1272.

Vaney, D. I., Sivyer, B., and Taylor, W. R. (2012). Direction selectivity in the retina: symmetry and asymmetry in structure and function. *Nat. Rev. Neurosci.* 13, 194–208. doi: 10.1038/nrn3165

Visser, J. J., Cheng, Y., Perry, S. C., Chastain, A. B., Parsa, B., Masri, S. S., et al. (2015). An extracellular biochemical screen reveals that FLRTs and Unc5s mediate neuronal subtype recognition in the retina. *Elife* 4:e08149. doi: 10.7554/eLife.08149

Voigt, T. (1986). Cholinergic amacrine cells in the rat retina. *J. Comp. Neurol.* 248, 19–35.

Yi, C.-W., Yu, S.-H., Lee, E.-S., Lee, J.-G., and Jeon, C.-J. (2012). Types of parvalbumin-containing retinotectal ganglion cells in mouse. *Acta Histochem. Cytochem.* 45, 201–210. doi: 10.1267/ahc.11061

Yonehara, K., Fiscella, M., Drinnenberg, A., Esposti, F., Trenholm, S., Krol, J., et al. (2016). Congenital nystagmus gene FRMD7 is necessary for establishing a neuronal circuit asymmetry for direction selectivity. *Neuron* 89, 177–193. doi: 10.1016/j.neuron.2015.11.032

Yonehara, K., Ishikane, H., Sakuta, H., Shintani, T., Nakamura-Yonehara, K., Kamiji, N. L., et al. (2009). Identification of retinal ganglion cells and their projections involved in central transmission of information about upward and downward image motion. *PLoS One* 4:e4320. doi: 10.1371/journal.pone.0004320

Yoshida, K., Watanabe, D., Ishikane, H., Tachibana, M., Pastan, I., and Nakanishi, S. (2001). A key role of starburst amacrine cells in originating retinal directional selectivity and optokinetic eye movement. *Neuron* 30, 771–780. doi: 10.1016/s0896-6273(01)00316-6

Conflict of Interest: The authors declare that the research was conducted in the absence of any commercial or financial relationships that could be construed as a potential conflict of interest.

Publisher's Note: All claims expressed in this article are solely those of the authors and do not necessarily represent those of their affiliated organizations, or those of the publisher, the editors and the reviewers. Any product that may be evaluated in this article, or claim that may be made by its manufacturer, is not guaranteed or endorsed by the publisher.

Copyright © 2021 Ruff, Peters, Matsumoto, Ihle, Morales, Gaitanos, Yonehara, del Toro and Klein. This is an open-access article distributed under the terms of the Creative Commons Attribution License (CC BY). The use, distribution or reproduction in other forums is permitted, provided the original author(s) and the copyright owner(s) are credited and that the original publication in this journal is cited, in accordance with accepted academic practice. No use, distribution or reproduction is permitted which does not comply with these terms.

frontiers in Molecular Neuroscience

REVIEW
published: 15 December 2021
doi: 10.3389/fnmol.2021.767965

Structural and Functional Aspects of the Neurodevelopmental Gene *NR2F1*: From Animal Models to Human Pathology

Chiara Tocco†, Michele Bertacchi† and Michèle Studer*

Université Côte d'Azur, CNRS, Inserm, iBV, Nice, France

OPEN ACCESS

Edited by:
Inmaculada Segura, Ludwig Maximilian University of Munich, Germany

Reviewed by:
Graeme Preston, Mayo Clinic, United States
Joseph D. Dougherty, Washington University in St. Louis, United States

***Correspondence:**
Michèle Studer
Michele.studer@unice.fr

†These authors have contributed equally to this work

Specialty section:
This article was submitted to Brain Disease Mechanisms, a section of the journal Frontiers in Molecular Neuroscience

Received: *31 August 2021*
Accepted: *25 October 2021*
Published: *15 December 2021*

Citation:
Tocco C, Bertacchi M and Studer M (2021) Structural and Functional Aspects of the Neurodevelopmental Gene NR2F1: From Animal Models to Human Pathology. Front. Mol. Neurosci. 14:767965. doi: 10.3389/fnmol.2021.767965

The assembly and maturation of the mammalian brain result from an intricate cascade of highly coordinated developmental events, such as cell proliferation, migration, and differentiation. Any impairment of this delicate multi-factorial process can lead to complex neurodevelopmental diseases, sharing common pathogenic mechanisms and molecular pathways resulting in multiple clinical signs. A recently described monogenic neurodevelopmental syndrome named Bosch-Boonstra-Schaaf Optic Atrophy Syndrome (BBSOAS) is caused by *NR2F1* haploinsufficiency. The *NR2F1* gene, coding for a transcriptional regulator belonging to the steroid/thyroid hormone receptor superfamily, is known to play key roles in several brain developmental processes, from proliferation and differentiation of neural progenitors to migration and identity acquisition of neocortical neurons. In a clinical context, the disruption of these cellular processes could underlie the pathogenesis of several symptoms affecting BBSOAS patients, such as intellectual disability, visual impairment, epilepsy, and autistic traits. In this review, we will introduce NR2F1 protein structure, molecular functioning, and expression profile in the developing mouse brain. Then, we will focus on Nr2f1 several functions during cortical development, from neocortical area and cell-type specification to maturation of network activity, hippocampal development governing learning behaviors, assembly of the visual system, and finally establishment of cortico-spinal descending tracts regulating motor execution. Whenever possible, we will link experimental findings in animal or cellular models to corresponding features of the human pathology. Finally, we will highlight some of the unresolved questions on the diverse functions played by Nr2f1 during brain development, in order to propose future research directions. All in all, we believe that understanding BBSOAS mechanisms will contribute to further unveiling pathophysiological mechanisms shared by several neurodevelopmental disorders and eventually lead to effective treatments.

Keywords: BBSOAS, neurodevelopmental disease, *NR2F1*, mouse models, cortical development

INTRODUCTION

Neurodevelopmental disorders (NDDs) are a highly heterogeneous class of mainly genetic pathological conditions, often due to defects of early mechanisms of brain development, such as cell proliferation, migration and differentiation, as well as activity and connectivity. Such an early origin represents a great challenge for scientists aiming at investigating physiological and pathological mechanisms underlying nervous system development. While historically *in vivo* mouse and *in vitro* two-dimensional (2D) cell culture models have been the favorite experimental approaches to study NDDs, new techniques such as three-dimensional (3D) organoids carrying patient-specific mutations have been recently developed and are now extensively coupled with more traditional methods.

The high heterogeneity of NDDs is reported at both genetic and clinical levels, with several causative genes and variable genotype-dependent severity of multiple clinical signs (Cristino et al., 2014; Hormozdiari et al., 2015; Parenti et al., 2020). However, despite such heterogeneity, NDD patients carrying distinct mutations often present a comorbidity of multiple symptoms [e.g., intellectual disability (ID), autism spectrum disorder (ASD), and epilepsy; van Bokhoven, 2011; Du et al., 2018; Parenti et al., 2020], suggesting the existence of common molecular pathways ultimately converging on similar clinical features. Recent insights in support of this hypothesis showed that several NDD-causative genes are involved in protein homeostasis, such as the mTOR pathway (Kelleher and Bear, 2008; Sahin and Sur, 2015; Borrie et al., 2017; Parenti et al., 2020), transcriptional and epigenetic regulation (Ronan et al., 2013; Parenti et al., 2020), and synaptic signaling and plasticity (Bourgeron, 2015; Südhof, 2018; Parenti et al., 2020). Hence, studying the molecular mechanisms of a specific syndrome might also help to shed light on NDDs in general, eventually leading to faster diagnosis and better treatments for patients.

Among NDDs, a recently described genetic condition called Bosch-Boonstra-Schaff Optic Atrophy Syndrome (BBSOAS) has been first reported in 2014 (Bosch et al., 2014). Till now, about 100 patients have been diagnosed (Rech et al., 2020), but more cases are regularly identified worldwide, indicating that the prevalence of this new syndrome is still, most probably, underestimated. BBSOAS symptoms are very heterogeneous and combine, among others, intellectual deficits, global developmental delay, epilepsy, motor dysfunctions and autistic traits, often associated with optic nerve atrophy and cerebral visual impairment. The combination of clear cognitive and visual disorders makes this syndrome quite unique and distinct from other NDDs.

BBSOAS is caused by *NR2F1* haploinsufficiency, implying that all patients so far identified carry a non-functional *NR2F1* allele, either due to deletion or missense point mutations that compromise its expression levels and/or its molecular activity. Although reported mainly as *de novo* mutations, a few BBSOAS inherited variants have been recently described (Rech et al., 2020; Jurkute et al., 2021). The BBSOAS causative gene -*NR2F1*- and its homolog *NR2F2* code for transcriptional regulators belonging to the superfamily of steroid/thyroid hormone receptors. Both factors are considered as orphan nuclear receptors, since their physiological ligands have not been identified yet (Wang et al., 1989, 1991; Qiu et al., 1995; Pereira et al., 2000). Their protein structure resembles that of other members of the family, with two highly conserved domains: a zinc-finger DNA binding domain (DBD) able to recognize target DNA sequences (direct repeats spaced by one nucleotide, called DR1), and a putative ligand binding domain (LBD), necessary for dimerization and binding of cofactors (Tsai and Tsai, 1997). Variable degrees of symptom severity have been reported among BBSOAS patients with distinct point mutations, suggesting the existence of a genotype-phenotype correlation. In particular, BBSOAS patients carrying *loss-of-function* mutations in the DBD display more severe clinical features compared to patients with variants in other regions of the protein (Rech et al., 2020). As NR2F1 binds the DNA in the form of dimers, this genotype-phenotype correlation could be due to a dominant negative effect of a mutated NR2F1 protein over a normally functional one during dimerization.

Thanks to the high degree of homology between human *NR2F1* and mouse *Nr2f1* orthologs, several mouse models have been employed to mimic BBSOAS pathogenesis and investigate the underlying neurodevelopmental processes. In this review, we will introduce the structure and molecular function of *Nr2f1* as a key transcriptional regulator orchestrating mouse brain development, able to both activate or repress the expression of target genes depending on the cellular context. We will then introduce a summary of the roles played by Nr2f1 in distinct developmental contexts: regulation of cortical neuron differentiation and establishment of area identity; modulation of intrinsic electric neural properties during corticogenesis; control of interneuron generation, hippocampal formation, sensorimotor system establishment and, finally, assembly of peripheral and central visual systems. Furthermore, we will relate some of the Nr2f1 functions, described in animal models, to corresponding symptoms reported in BBSOAS patients. Finally, we will discuss recently developed methodological approaches that could be employed to further unravel NR2F1 roles in both physiological and pathological brain development.

Nr2f1 MOLECULAR STRUCTURE AND TRANSCRIPTIONAL REGULATION MECHANISMS

Since 1999, a unified nomenclature system has renamed *COUP-TF* as "*NR2F*" for *Nuclear Receptor Subfamily 2 Group F* of the steroid/thyroid hormone superfamily of nuclear receptors (Auwerx et al., 1999). Prior to that, these factors were known as *COUP-TF*s, for "*Chicken Ovalbumin Upstream Promoter Transcriptional Factors*", reflecting their first reported role in regulating the chicken ovalbumin gene expression through direct binding to its promoter region (Pastorcic et al., 1986; Sagami et al., 1986). They are also defined as "orphan" receptors, since the identity of their physiological ligands is still elusive. Two major homologs of *Nr2f*s have been identified in vertebrates: *COUP-TFI*/*NR2F1* and *COUP-TFII*/*NR2F2* (Wang et al., 1989;

Qiu et al., 1995). Their molecular structure resembles that of other nuclear receptors of the same family, encompassing two highly conserved domains: the DNA binding domain (DBD; consisting of two conserved Zinc-finger motifs), and the ligand-binding domain (LBD; **Figures 1A,B**). Based on their highly conserved sequence (Pastorcic et al., 1986), orthologs in mice, rats, *Xenopus*, chicken, hamster, *Drosophila*, *C. elegans*, zebrafish, and sea urchin have also been cloned and functionally characterized (reviewed in Alfano and Studer, 2013). The homology between human and mouse *NR2F* genes is very high (ranging from 95% to 100% amino acid sequence homology, depending on the protein regions; Qiu et al., 1995; Alfano and Studer, 2013), suggesting that their functions and targets might be conserved in both species. Another functionally relevant region is the C-terminal activation domain (named AF-2), whose active conformational state allows the binding of cofactors to the LBD and ultimately controls the transcriptional regulation of target genes (Germain et al., 2006). This active conformation state is generally reached *via* interactions with specific ligands, as for example the binding of retinoic acid (RA) and activation of the AF-2 domain of Retinoid X Receptor-α (RXRα; Bourguet et al., 1995; Egea et al., 2000; Germain et al., 2006). In the specific case of NR2F2, crystallographic studies have shown that the LBD is normally present in an auto-inhibited conformation, due to the binding between the AF-2 and cofactor binding sites, and that this auto-repressed state can be reverted with high concentration of RA (Kruse et al., 2008). Due to the high homology between NR2F1 and NR2F2, it is reasonable to speculate that a similar mechanism is also valid for NR2F1, but this has not been tested yet. Furthermore, RA-mediated activation of NR2F2 is itself still under debate, as: (i) the concentration of RA used in the study were above physiological levels and (ii) NR2F members might follow different mechanisms of activation, included being intrinsically active and able to regulate target genes regardless of the presence of any ligand, as previously shown for other members of the family (Wang et al., 2003). In addition, since NR2F2 affinity for RA is quite low, it is conceivable that other unidentified endogenous ligands do exist and activate NR2F nuclear receptors more efficiently.

Differently from the highly conserved AF-2 domain, the N-terminus activation domain (AF-1), necessary for co-factor recruitment, shows a lower degree of homology between NR2F members and other orthologs. This could imply that NR2F factors bind to similar cis-responding elements on the DNA, but then greatly differ in their molecular interactions with co-factors, an important aspect for acquiring cellular- and time-specific functions.

As transcriptional regulators, NR2F/Nr2f factors can both promote or inhibit gene expression through several distinct molecular and cellular mechanisms (Cooney et al., 1992; Leng et al., 1996; Alfano and Studer, 2013). For instance, repression can be elicited through direct binding of the target gene regulatory sequence together with Silencing Mediator for Retinoid or Thyroid-hormone receptors (SMRT) or Nuclear receptor Co-Repressor (N-CoR) co-factors (Hwung et al., 1988; Cooney et al., 1992; Montemayor et al., 2010; **Figure 1C**), or *via* indirect mechanisms by sequestering important proteins for the transcriptional machinery (Evans and Mangelsdorf, 2014; **Figure 1D**). As positive regulators, Nr2fs have been found to act either by directly binding the regulatory sequence of their target genes (**Figure 1E**), or as co-factors of other transcription factors (such as Sp1) in the context of chromatin complexes (Leng et al., 1996; Pipaón et al., 1999; **Figure 1F**).

In some instances, Nr2fs are reported to recruit chromatin remodeling co-activators (e.g., *CREB Binding Protein -CBP-* and *Steroid Receptor Coactivator-1 -SRC1-*) and induce H3K9 acetylation, finally resulting in an open chromatin state which facilitates gene expression (Montemayor et al., 2010). Additionally, Nr2f1 can also help recruit DNA methyltransferases and actively assist chromatin demethylation (Gallais et al., 2007). However, an opposite mechanism has also been reported. For instance, in dormant cancerous cells (Sosa et al., 2014) or virally Ad12-infected human cells (Smirnov et al., 2000), *Nr2f1* mainly acts as a global chromatin repressor. This dual, contrasting Nr2f function might be accomplished *via* a ligand-activated conformational change, a common mechanism of action for nuclear receptors (Cooney et al., 2001; Weikum et al., 2018), or by interaction with distinct co-factors depending on the cellular context.

In summary, NR2F/Nr2f factors can either function as activators or repressors of target genes found in a chromatin permissive state in a time- and region-specific manner or alternatively, as chromatin remodellers themselves, by either facilitating or repressing acetylation or methylation, possibly depending on their conformation. However, more studies are needed to further comprehend their mechanistic function during the regulation of target gene expression.

ONE GENE TO RULE THEM ALL: *Nr2f1*-DEPENDENT REGULATION OF CELL PROLIFERATION, DIFFERENTIATION, AND MIGRATION

Due to a highly dynamic pattern of expression, the ability to interact with distinct sets of co-factors and the capacity to differentially regulate several target genes dissecting the cellular functions of transcription factors has always represented a challenging task. *Nr2f1* makes no exception as it plays multi-faceted, sometimes contrasting, roles during several developmental processes. As an example, *Nr2f1* can either positively or negatively regulate cell proliferation, differentiation, and migration, depending on the developmental time or co-expression of key co-factors. Despite this high level of complexity, several studies have started to unravel *Nr2f1* complex functions, especially in the context of neural progenitors and their progeny. At the cell-intrinsic level, *Nr2f1* can: (a) regulate cell cycle dynamics, in turn affecting the balance between neuronal progenitor proliferation and differentiation (Faedo et al., 2008; Bertacchi et al., 2020); (b) influence neuronal migration (Adam et al., 2000; Alfano et al., 2011; Touzot et al., 2016; Parisot et al., 2017), axonal elongation, and arborization (Qiu et al., 1997; Zhou et al., 1999; Armentano et al., 2006); (c) control identity and temporal competency of neuronal

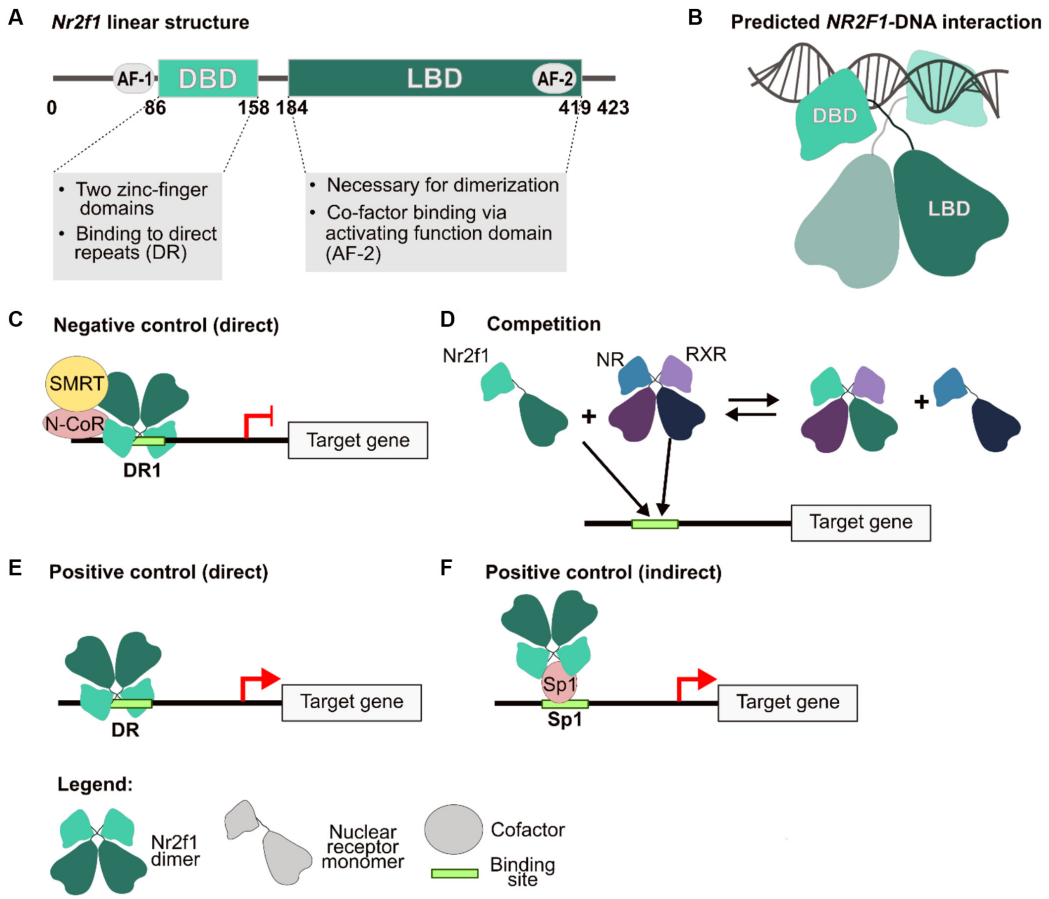

FIGURE 1 | NR2F1 structure and molecular mechanisms of gene expression regulation. **(A)** Human NR2F1 linear structure showing conserved protein domains. The activation function (AF) 1 and 2, the DNA-binding domain (DBD) and ligand-binding domain (LBD) are depicted as circles and boxes, respectively. **(B)** Schematic model of an NR2F1 dimer, based upon predictive homology obtained by using NR2F2 structure as a template (96% aminoacidic sequence homology with NR2F1; Kruse et al., 2008). In the scheme, the LBD mediates the dimerization, whereas the DBD, consisting of two highly conserved zinc finger domains, are implicated in the interaction with the double DNA helix. Between the two domains, an undefined region depicted as a loose string, which does not contain secondary structures, has not been resolved to date. **(C–F)** Different regulatory mechanisms carried out by Nr2f1. The nuclear receptor can act both as a direct inhibitor **(C)**, as a competitor by binding to the regulatory sequence of target genes, and/or by sequestering other nuclear receptors as heterodimers **(D)**, or as an activator, either directly **(E)** or indirectly **(F)**, by interacting with other factors, such as Sp1, to induce transcription. AF-1/2, activation function domain 1 and 2; DBD, DNA-binding domain; DR1, direct repeat sites (spaced by one nucleotide); N-CoR, nuclear receptor co-repressor; NR, nuclear receptor; RXR, retinoic X receptor; SMRT, silencing mediator of retinoic acid and thyroid hormone receptor; Sp1, transcription factor specificity protein 1. Modified from Tang et al. (2015) and Bertacchi et al. (2019b).

progenitor cells (Faedo et al., 2008; Naka et al., 2008; Okano and Temple, 2009); and (d) establish area-specific identity in progenitors and neurons (Zhou et al., 2001; Armentano et al., 2007; Tomassy et al., 2010; Alfano et al., 2014; Harb et al., 2016). In the following sections, we will summarize *Nr2f1* roles in these fundamental cellular processes, and the corresponding pathophysiological consequences that could result from *NR2F1* mutations in BBSOAS patients.

Nr2f1 SHAPES NEOCORTICAL MORPHOLOGY BY REGIONAL-SPECIFIC MODULATION OF NEUROGENESIS

The formation of the neocortex, the most highly evolved part of the mammalian brain, starts early during embryogenesis when neural progenitors (NPs) expand by proliferating, and then differentiate into all distinct neuronal subpopulations of the adult brain. In the forming mouse neocortex, early NPs called apical radial glia (aRG) cells, produce cortical neurons in a direct or indirect way, *via* intermediate progenitors (IPs; **Figure 2**). Then, newly generated neurons migrate to the cortical plate (CP), creating layers of radially organized neuronal classes that extend their axons to form brain circuits. In recent years, additional subtypes of self-renewing RG cells have been described in the developing human cortex, including basal radial glia (bRG; Hansen et al., 2010; Nonaka-Kinoshita et al., 2013; Pilz et al., 2013; Pollen et al., 2015). Notably, bRG cells are responsible for the abundant production of upper layer neurons in humans and other primates (Pollen et al., 2015; Nowakowski et al., 2016), and ultimately concur to

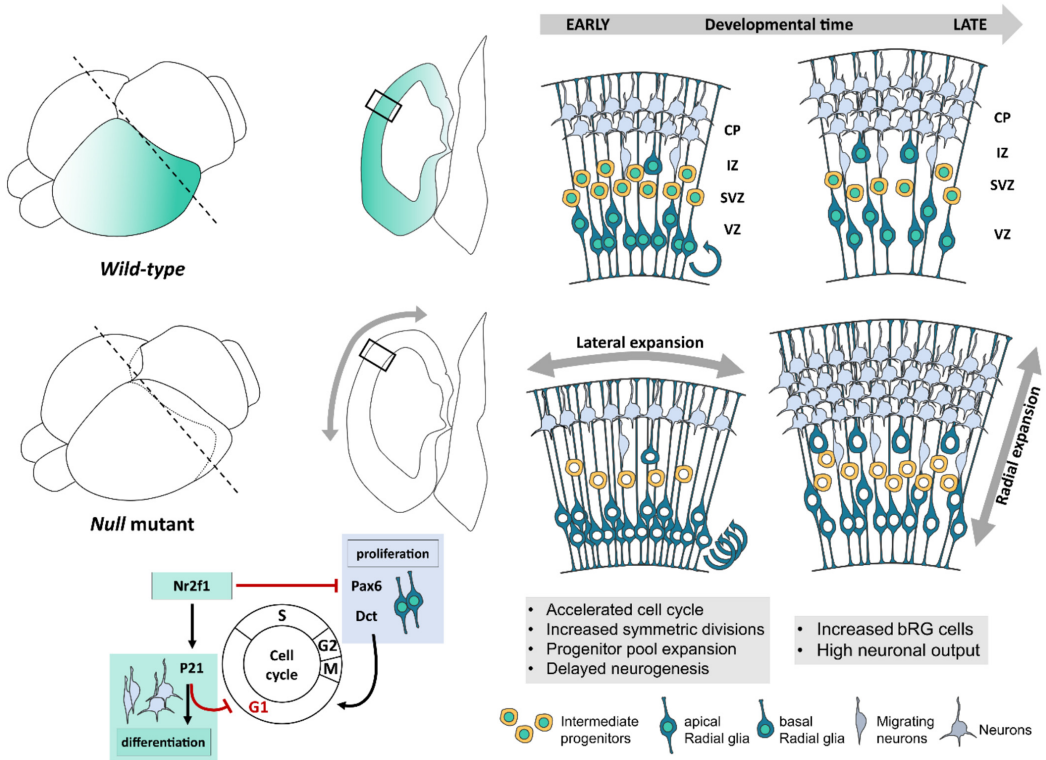

FIGURE 2 | *Nr2f1*-mediated control of cellular and morphological dynamics during early corticogenesis. Schematic illustration of *Nr2f1* antero-low to postero-high expression gradient (blue color code, brain scheme on the left) and latero-high to medial-low gradient (transversal sections on the right) in the developing neocortex. *Nr2f1* expression in neural progenitors (NPs) spans from the ventricular zone (VZ) in apical radial glia cells (aRGs) to sub-ventricular zone (SVZ) in intermediate progenitors (IPs) and basal RGs (bRGs). RGs produce neurons directly or indirectly, *via* IPs, newly generated neurons migrating towards the intermediate zone (IZ) and then forming distinct layers in the cortical plate (CP). Upon *Nr2f1* loss (*null* mutants), the posterior NP pool expands leading to an occipital enlargement, reminiscent of megalencephaly. The NP pool expansion is caused by cell cycle acceleration (round arrows), increased symmetrical divisions and self-renewal, and delayed neurogenesis causing an early decrease of IPs and of migrating and differentiating neurons in IZ and CP. At later stages, IPs, bRGs and neurons are produced at a high rate, leading to the formation of a thicker posterior CP in mutant embryos compared to *wild type*. The morphological consequences of *Nr2f1* loss are an early lateral expansion followed by late radial expansion (gray arrows) of cortical hemispheres. At the molecular level, *Nr2f1* orchestrates NP cell cycle progression and neural differentiation by repressing Pax6 and Dct and thus cell cycling progression, while activating P21-mediated cell cycle exit to promote terminal neural differentiation. aRG, apical radial glia; bRG, basal radial glia; CP, cortical plate; IZ, intermediate zone; SVZ, sub-ventricular zone; VZ, ventricular zone.

the expansion of the cortical surface and the formation of neocortical convolutions. The gyrification, i.e., the folding of the cortical surface that generates convolutions (gyri) separated by spaces (sulci), provides an increased surface of the neuronal tissue to fit the intracranial space. Despite the significance of gyrencephaly and its link with brain size still being debated (Kelava et al., 2013; Zilles et al., 2013), evidence from several studies shows a strong correlation between cortical morphology and gyrification defects, and the onset of neurodevelopmental diseases (Casanova et al., 2004; Lin et al., 2007; Wolosin et al., 2009; Zhang et al., 2010; Lebed et al., 2013; Juric-Sekhar and Hevner, 2019).

Interestingly, some BBSOAS patients show specific neocortical malformations, such as macrocephaly and ventricular enlargement/asymmetry (Chen et al., 2016; Kaiwar et al., 2017), suggesting that impairments in the basic mechanism of NP self-renewal and neurogenesis could be associated with *NR2F1* haploinsufficiency. The recent characterization of the cortical morphology by Magnetic Resonance Imaging (MRI) in six novel patients has unraveled aberrant convolutions in the form of polymicrogyria-like brain malformations, or dysgyria, in the temporo-parieto-occipital (TPO) cortex, a brain territory heavily involved in several high-level neurological functions (Bertacchi et al., 2020). These cortical defects hint at a new and distinct role for the human *NR2F1* gene in controlling gyrification. The presence of cortical malformations in BBSOAS patients links the *NR2F1* gene to the heterogeneous group of neurodevelopmental diseases, called malformations of cortical development (MCD), in which structural brain anomalies and abnormal gyrification are associated with syndromic features, such as mild to moderate ID, infantile spasms and impaired oromotor skills (Jansen and Andermann, 2005; Manzini and Walsh, 2011; Barkovich et al., 2012; Guerrini and Dobyns, 2014; Parrini et al., 2016; Juric-Sekhar and Hevner, 2019). Notably, folding defects observed in BBSOAS patients affect the supramarginal and angular gyri, regions known to be involved in various aspects of language and emotional responses, memory retrieval, attention, and number processing (Stoeckel

et al., 2009; Seghier, 2013; Oberhuber et al., 2016), suggesting that such malformations could be linked to the reported cognitive deficits.

In humans as in mice, the balance between self-renewal (proliferation) and neurogenesis (neuronal differentiation) of cortical NP cells needs to be tightly regulated, and their radial migration as well as laminar organization regionally controlled, in order to properly shape the mature cerebral cortex (Florio and Huttner, 2014; Villalba et al., 2021). An imbalance between self-renewal and neurogenesis impairs the production of the number and type of neurons during corticogenesis; as an example, excessive early neurogenesis will deplete the progenitor pool and result in a microcephalic brain with fewer neurons, whereas disproportionate proliferation might delay neurogenesis and produce a macrencephalic brain. Several determinant genes are involved in this process, including *Nr2f1*.

The use of an *Nr2f1* constitutive (*null*) mutant mouse as a BBSOAS model showed that *Nr2f1* can finely regulate the self-renewal/differentiation balance of specific neocortical progenitor classes. Differently from other NDD mouse models, this control turned to be regionalized, in accordance with *Nr2f1* antero-posterior graded expression displaying highest levels in the occipital cortex in mice (Liu et al., 2000; Zhou et al., 2001; Armentano et al., 2006; Tomassy et al., 2010), and in humans (Alzu'Bi et al., 2017; Bertacchi et al., 2020; Foglio et al., 2021). In the caudal cortex, *Nr2f1* promotes asymmetric divisions by driving NP differentiation (Faedo et al., 2008; Bertacchi et al., 2020); hence, *Nr2f1* loss resulted in delayed neurogenesis and amplification of both apical and basal RG cells, ultimately leading to expanded occipital hemispheres (Bertacchi et al., 2020; **Figure 2**). Furthermore, bRGs, which are normally scarcely represented in murine brains (Reillo et al., 2011; Wang et al., 2011), are abnormally enlarged in *Nr2f1* mutant brains (**Figure 2**). An increase of the progenitor pool is also in line with a slight increase of the overall neocortical volume measured by MRI in adult *heterozygous (HET)* mice (Chen et al., 2020) and consistent with expanded/elongated occipital convolutions observed in two BBSOAS patients (Bertacchi et al., 2020). At the molecular level, *Paired box protein-6* (*Pax6*) could be partially responsible for the caudal increase of progenitors and neurons (Faedo et al., 2008; Bertacchi et al., 2020), being directly regulated by *Nr2f1* (Tang et al., 2010). *Nr2f1* mutants showed sustained levels of Pax6 in RG cells, in particular caudally, where Pax6 is normally expressed at low levels (Bertacchi et al., 2020), and known to modulate bRG amplification (Wong et al., 2015). Similarly to *Nr2f1*, mouse *Pax6* is a master regulator of NP cell cycle, differentiation rate and, more in general, neocortical development and area mapping (Bishop et al., 2000, 2002; Estivill-Torrus et al., 2002; Englund et al., 2005; Asami et al., 2011). Consistently, mutations in the human *PAX6* gene are also associated with MCDs and polymicrogyria-like malformations (Mitchell et al., 2003; Spalice et al., 2009).

Together with *Nr2f1* and *Pax6*, other key master genes of neocortical development, such as *Empty spiracle homeobox-2* (*Emx2*), *Specificity Protein-8* (*Sp8*) and *Forkhead box protein G1* (*Foxg1*), operate a similar control of cell cycle progression, NP proliferation, neurogenesis and neuronal maturation (Bishop et al., 2000; Martynoga et al., 2005; Samson et al., 2005; Dehay and Kennedy, 2007; Zembrzycki et al., 2007; Georgala et al., 2011; Mi et al., 2013; Borello et al., 2014; Borrell and Calegari, 2014), even though only a few of them act in a regionalized manner. Hence, *Nr2f1* could belong to a wider gene network orchestrating cortical development along the antero-posterior (A-P), dorso-ventral (D-V), and latero-medial (L-M) cortical axes (Alfano and Studer, 2013; Bertacchi et al., 2019b; Cadwell et al., 2019). A dose-dependent combinatorial code of these and other genes could prompt NPs to acquire different neurogenic potentials depending on their spatial coordinates, ultimately operating an area-specific control of the number and type of neurons locally produced in distinct cortical regions (Bertacchi et al., 2019b).

However, while mouse models greatly advance our knowledge on *Nr2f1*-dependent control of NP physiology, it is useful to remember that, contrary to humans and primates, the mouse brain has a smooth surface without any convolution (namely "lissencephalic") and contains a very small population of bRG cells; hence, murine models are not optimal to challenge *Nr2f1* and similar genes in bRG-dependent processes of cortical convolution and gyrus morphology. Further experiments in gyrencephalic experimental models, such as the ferret or the marmoset (Kelava et al., 2013), will be necessary to assess *Nr2f1* contribution to gyrencephaly and better correlate experimental data to BBSOAS clinical observations.

Nr2f1 REGIONALLY CONTROLS CELL CYCLE DYNAMICS OF NEOCORTICAL PROGENITORS

One of the mechanisms underlying the balance between NP proliferation and neurogenesis is the tight control of cell cycle progression, either in terms of checkpoint regulation or duration of the distinct phases (Dehay and Kennedy, 2007; Borrell and Calegari, 2014). These steps are coordinated by genes directly involved in cell cycle dynamics but also by transcription factors acting upstream of cell-cycle genes.

A recent study shows that *Nr2f1* directly controls cell cycle length, particularly in the caudal cortex by acting as a break. Indeed, *Nr2f1*-loss results in G1-phase shortening and overall cell cycle acceleration, finally leading to progenitor pool amplification and possibly impacting cortical area size (Bertacchi et al., 2020; **Figure 2**). The extension of cortical areas and the size of their neuronal pool had been previously shown to be affected by cell cycle duration and rate of NP cell cycle re-entry (Lukaszewicz et al., 2005). In fact, enlarged brain size can be recreated by artificially accelerating cell cycle progression (Nonaka-Kinoshita et al., 2013). NPs with shorter cell cycle duration, due to a significantly shorter G1-phase, have been demonstrated to be "younger" and to favor self-renewal over neurogenesis (Calegari et al., 2005; Lange et al., 2009; Arai et al., 2011). Hence, the accelerated cell cycle in *Nr2f1* mutants, associated with delayed neurogenesis, suggests that loss of *Nr2f1* brings back the biological clock

of NPs and that Nr2f1 acts as a temporal regulator of corticogenesis, as previously suggested (Naka et al., 2008). This is partially mediated by the cyclin-dependent kinase inhibitor P21 (Bertacchi et al., 2020), which triggers cell cycle exit and differentiation in NPs (Siegenthaler and Miller, 2005; Buttitta and Edgar, 2007; Heldring et al., 2013; **Figure 2**). However, the role of *Nr2f1* in the G1-to-S phase transition and thus in cell cycle regulation is strictly tissue specific. Indeed, while mouse *Nr2f1* promotes cell cycle exit also in medial and caudal ganglionic eminences (Lodato et al., 2011; Touzot et al., 2016), as in the neocortex, it instead promotes cell cycle progression in other brain regions, such as the hippocampus (Parisot et al., 2017). Hence, further studies will be necessary to establish how tissue-specific co-factors contribute to redirecting *Nr2f1* function towards either activating or inhibiting cell cycle progression.

Nr2f1-MEDIATED REGULATION OF NEURONAL MIGRATION IN SEVERAL CELL TYPES

In addition to defective NP cell cycle progression, abnormal migration of newly differentiated neurons can further impact cortical morphology and layer organization of the nascent cortical plate, converging to cause specific features of NDDs. As an example, altered neuronal migration can impair cortical layering, resulting in ectopic nodular heterotopia (clusters of neurons stuck in ectopic position; Guerrini and Parrini, 2010; Guerrini and Dobyns, 2014; Watrin et al., 2015). Such morphological defects often correlate with ID and possibly concur to trigger epileptic traits (Aghakhani et al., 2005). *Nr2f1* has been proved to control neuronal migration first in cell cultures (Adam et al., 2000), and then in both embryonic (Alfano et al., 2011; Lodato et al., 2011; Parisot et al., 2017) and postnatal stages of brain development (Bovetti et al., 2013; Flore et al., 2016; Bonzano et al., 2018). In migrating neurons, *Nr2f1* transcriptionally controls the expression of the *Rho family GTPase-2* (*Rnd2*) known to act on actin cytoskeleton organization (Azzarelli et al., 2015). Upon *Nr2f1* loss, *Rnd2* levels are highly increased, impairing the bipolar-to-multipolar state transition of late-born migrating cortical neurons and thus affecting their laminar localization (Alfano et al., 2011; Bertacchi et al., 2019b). Moreover, *Nr2f1* loss leads to reduced dendritic arborization and axonal defects of cortical upper layer neurons (Alfano et al., 2011). Together, these morphological defects might explain the thinning of the corpus callosum described in mutant mice (Armentano et al., 2006; Alfano et al., 2011) and reported in BBSOAS patients (Bosch et al., 2014; Chen et al., 2016; Rech et al., 2020). Impaired differentiation and/or migration of other projection neurons most probably impact the formation of further brain commissures and long-range tracts, as previously described (Armentano et al., 2006). Consistently with *Nr2f1* role in controlling migration, some *NR2F1*-haploinsufficient patients have signs of periventricular neuronal heterotopia in their posterior cortex (Guerrini et al., 2009; Bertacchi et al., 2020). However, a direct causative link between *NR2F1* deletion/mutation and heterotopia formation is still missing to date.

THE BLUEPRINT OF NEOCORTICAL ORGANIZATION: *Nr2f1* GRADED EXPRESSION AND ITS IMPLICATION IN AREALIZATION

Besides being produced in the right number and at the correct developmental time, cortical neurons also need to adopt a specific identity along all cortical axes. The mechanisms which pattern the neocortex into distinct functional areas along its tangential surface are termed "arealization", and imply a specialization of the generic six-layered structure to acquire distinct cytoarchitectures and peculiar abundance of several neuronal classes, reflecting individual area-specific functionality and wiring (O'Leary and Nakagawa, 2002; O'Leary and Sahara, 2008; Tomassy et al., 2010). As an example, the subpopulation of layer V corticofugal neurons, that send output information to subcerebral structures, such as the spinal cord and pontine nuclei, is broader in the adult primary motor area (M1) than in the primary somatosensory area (S1). Conversely, layer IV granular neurons, that receive sensory inputs from the thalamus, show the exact opposite trend. How cortical layers develop this regional diversity has been the subject of decades of research. Although the process is not yet completely elucidated, it appears to occur in two major steps: (i) the definition of an early protomap through the combinatorial graded expression of patterning genes, followed by (ii) an activity-dependent refinement of cortical area functionality (Cadwell et al., 2019).

The characteristic *Nr2f1* graded expression in the cortical primordium and its maintenance in primary sensory areas advocate for its implication in early and late events of arealization (Zhou et al., 1999; Liu et al., 2000). In the mouse, *Nr2f1* expression starts at mouse embryonic (E) age 9.0–9.5 in the neuroectoderm, when the anterior neural plate starts to close (Qiu et al., 1994; Armentano et al., 2006). Then, its graded expression expands in several regions of the telencephalon, such as the cerebral cortex, hippocampus, thalamus, ganglionic eminences, and preoptic area (Armentano et al., 2006). In neocortical progenitors, its expression is higher in caudo-lateral and lower in rostro-medial regions, a gradient that is maintained in postmitotic cells and postnatally when areas are well-defined (Liu et al., 2000; Zhou et al., 2001; Armentano et al., 2007; **Figure 3A**).

Initial spatial coordinates are set up by morphogens, such as *Fibroblast Growth Factors* (*FGFs*), *Sonic Hedgehog* (*SHH*), *Retinoic acid* (RA), and *Bone Morphogenetic Proteins* (*BMPs*). These molecules are produced by signaling centers (O'Leary and Nakagawa, 2002; Shimogori et al., 2004; Samson et al., 2005; Shimogori and Grove, 2005) and are important for the establishment of proper coordinates along the A-P and D-V axes (Fukuchi-Shimogori and Grove, 2001; Grove and Fukuchi-Shimogori, 2003; Sur and Rubenstein, 2005; Sansom and Livesey, 2009; Greig et al., 2013) by acting in a dose-,

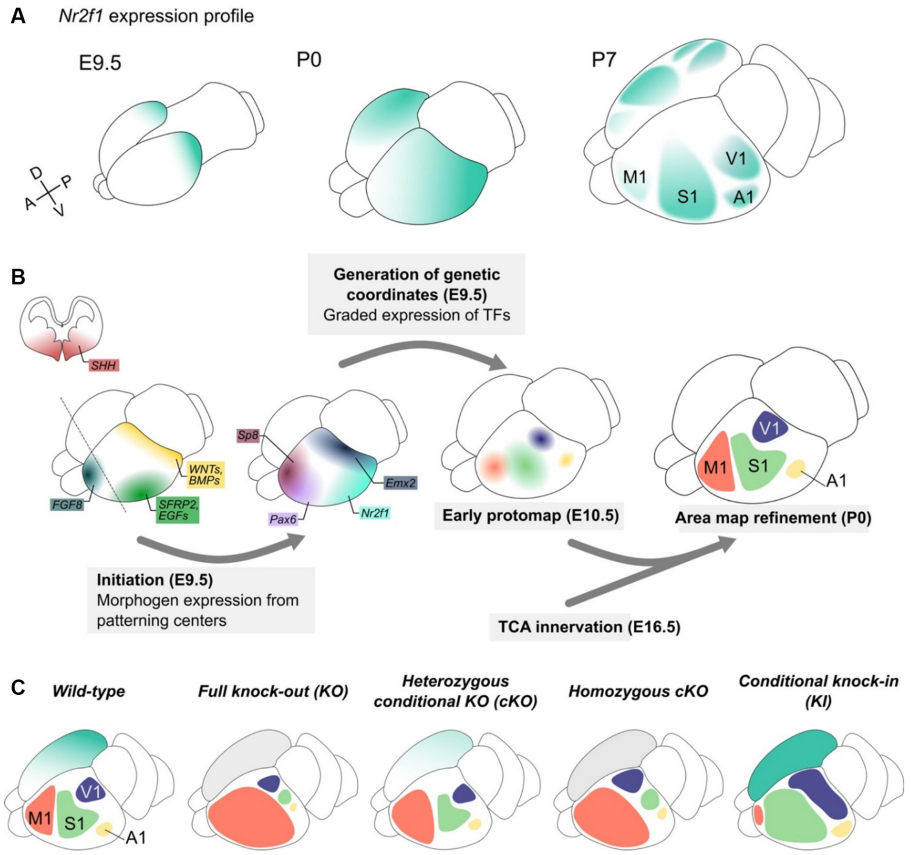

FIGURE 3 | *Nr2f1* graded expression drives cortical arealization during embryonic development. **(A)** *Nr2f1* graded expression (blue color code) in the telencephalon starts at embryonic day (E) 9.5 posteriorly and then spreads forming a diffuse gradient from high postero-lateral to low antero-medial levels in the post-natal (P) 0 cortex. From the onset of area refinement (here represented at P7), *Nr2f1* high expression is maintained in the primary sensory areas (S1, V1 and A1), but almost absent from secondary sensory areas and from the frontal motor area (M1). **(B)** Graphic representing the different steps of the arealization process. Starting from E8.0, several morphogens (*SHH, WNTs, BMPs, SFRP2, EGFs, and FGF8* among others) are secreted from distinctly located patterning centers and diffuse along gradients in the developing neocortex, in turns driving the graded expression of transcription factors (TFs) in cortical progenitor cells. The strong caudal expression of *Emx2* and *Nr2f1* promotes the specification of sensory areas, while rostral high expression of *Pax6* and *Sp8* drives the specification of motor identity. This "protomap" is then refined with the arrival of thalamic axons (TCA innervation) conveying external sensory information. **(C)** Schematic of M1 (pink), S1 (green), V1 (purple) and A1 (yellow) areas in *wild-type* brains and in different mouse models of *Nr2f1* downregulation (constitutive knock-out -*KO*- and conditional one -*cKO*-) and upregulation (knock-in -*KI*-). The right hemisphere depicts *Nr2f1* expression, while the left one schematizes the position and size of distinct areas upon genetic manipulation. To note, changes in size and extension of the functional areas are not associated with significant changes in overall cortex volume, with the only exception of caudal megalencephaly in *null* animals (see **Figure 2**). A1, primary auditory area; M1, primary motor area; S1, primary somatosensory area; V1, primary visual area.

context- and time-dependent manner (**Figure 3B**-initiation). Their main effectors are area patterning genes such as *Pax6, Sp8*, and *Emx2* among others, and *Nr2f1* itself (Grove and Fukuchi-Shimogori, 2003; O'Leary and Sahara, 2008; Alfano and Studer, 2013; **Figure 3B**-generation of genetic coordinates). Their combinatorial expression in neocortical progenitors provides precise spatial coordinates and regulates cell differentiation, area identity, neuronal maturation and network connectivity and function. Among early morphogens, *FGF8* plays a major role in the arealization process, by inducing rostrally-determining genes and repressing *Nr2f1* and other caudal genes (Garel et al., 2003; Samson et al., 2005; Storm et al., 2006; Toyoda et al., 2010). *Vice versa*, *Nr2f1* inhibits FGF signaling (but not *FGF8* expression) and antagonizes the expression of the major FGF8-activated gene, *Sp8* (Sahara et al., 2007; Faedo et al., 2008; Borello et al., 2014). However, expression gradients of area patterning genes in progenitors and early differentiating neurons only provide a pre-identity signature to the different proto-areas, with still no clear-cut boundaries and functions (Greig et al., 2013). Only a later activity-dependent refinement, conveyed by thalamocortical axonal afferences (TCA), leads to fully-shaped cortical areas with a clear distinction between primary and secondary functional areas (**Figure 3B**-TCA innervation).

Nr2f1 SPECIFIES THE IDENTITY OF POSTERIOR SENSORY AREAS

A key role for *Nr2f1* in area mapping was first reported in a constitutive *Nr2f*1 k*nock-out* (named *KO* or *null*) mouse line,

which displayed reduced expression of sensory cortical markers and enlarged expression of motor markers, with no clear cortical area subdivision (Zhou et al., 2001). In addition, TCAs failed to innervate layer IV in *null* animals, causing the premature death of these neurons and thus raising the possibility that impaired area division could just be an indirect consequence of the lack of thalamic inputs (Zhou et al., 2001). However, due to severe feeding problems, most *null* animals died perinatally (Qiu et al., 1997), hindering the study of cortical arealization at postnatal stages.

The use of cortico-specific *Nr2f1 conditional KO (cKO)* mouse lines, in which *Nr2f1* expression was abolished either in cortical progenitor cells at E10.5 (Armentano et al., 2007) or specifically in postmitotic neurons at E11.5–E12 (Alfano et al., 2014) prevented any influence from the thalamus, as well as perinatal mortality, and thus allowed to elucidate the cortex-specific *Nr2f1* role during arealization. Although the neocortex of *Nr2f1 KO* mutants was first described as a uniform "area-less" cortex (Zhou et al., 2001; O'Leary and Sahara, 2008), the analysis of both *cKO* mutants revealed that all sensory areas were still present, but greatly reduced in size (Armentano et al., 2007). While leaving the overall cortical surface unaffected, the cortex-specific ablation of *Nr2f1* influenced the size and location of the main functional areas, as demonstrated by several regionalized molecular markers and improper thalamo-cortical topography. For instance, primary somatosensory (S1), visual and auditory areas were all caudally misplaced and their size drastically reduced in mutants, in favor of an enlarged frontal motor (M1) area (Armentano et al., 2007). Because of the similar expression patterns observed between normal M1 and mutant S1, the area was therefore named "motorized S1" (mS1; Armentano et al., 2007; Tomassy et al., 2010). Although shifted, the relative position of adjacent areas was maintained upon loss of *Nr2f1*, as proven by the existence of a miniaturized S1 barrel field retaining normal genetic identity and TCA connectivity (Armentano et al., 2007; **Figure 3C**).

The cortical area defects observed in *Nr2f1* mutant brains (Armentano et al., 2007) are very severe compared to those resulting from the *loss-of-function* of other area patterning genes expressed solely in progenitors (Bishop et al., 2000, 2002; Mallamaci et al., 2000; Hamasaki et al., 2004; Manuel et al., 2007; Sahara et al., 2007; Zembrzycki et al., 2007, 2013; Tran et al., 2009). Furthermore, other genes belonging to the FGF pathway (i.e., FGF8 and Sp8) act in strong connection with *Nr2f1* and partially influence area patterning (O'Leary et al., 2007; Faedo et al., 2008, 2010; Borello et al., 2014). It is thus conceivable that FGF signaling and *Nr2f1* might act together as upstream regulators of a cascade of molecular events governing area patterning, whereas other genes such as *Pax6* and *Emx2* would act either as secondary downstream effectors or in parallel pathways and have a weaker effect on arealization. Finally, several chromatin regulators, such as the methyl-transferase *Setd2* (Xu et al., 2021), the transcription co-regulator *Cited2* (Fame et al., 2016; Wagner and MacDonald, 2021) and the epigenetic co-factor *LIM Domain Only-4* (*Lmo4*; Harb et al., 2016), have been reported to influence area identity refinement. Considering *Nr2f1* ability to recruit epigenetic factors (Montemayor et al., 2010), it might be interesting to investigate whether these or similar chromatin regulators act in association with or under the control of *Nr2f1* in the late arealization process.

In summary, the use of cortical conditional *KO (cKO)* models, compared to full *KO*s, has demonstrated that early area map impairments arise despite normal *Nr2f1* expression in thalamic neurons, pointing to an *Nr2f1* cell-intrinsic neocortical control of area identity (Armentano et al., 2007). Further experiments will be necessary to establish whether any area shift in *HET* animals, more similar to BBSOAS patients, has specific consequences on cortical function. Furthermore, whether *NR2F1* haploinsufficiency has consequences on human arealization, which could correlate with ID, is still an open question. Since a similar neocortical *NR2F1* gradient has been reported in human brains (Zhou et al., 2001; Armentano et al., 2007; Alzu'Bi et al., 2017; Molnár et al., 2019; Foglio et al., 2021), an evolutionarily conserved role for human *NR2F1* in area patterning is conceivable (Clowry et al., 2018).

POST-MITOTIC *Nr2f1* EXPRESSION IS NECESSARY AND SUFFICIENT FOR NEOCORTICAL AREALIZATION

Initially established in progenitors, *Nr2f1* graded expression is maintained by post-mitotic neurons radially migrating into the cortical plate. *Nr2f1* inactivation solely in cortical post-mitotic cells reproduces the severe area defect obtained upon loss in progenitor cells, indicating that *Nr2f1* expression only in progenitors is not sufficient to maintain proper neuronal specification (Alfano et al., 2014; Bertacchi et al., 2019b). Conversely, *Nr2f1* overexpression in post-mitotic cells in a constitutive *Nr2f1 KO* model rescues sensory identity, laminar specification and topographic thalamocortical connectivity in S1 (Alfano et al., 2014). Hence, *Nr2f1* post-mitotic expression is necessary and sufficient to specify sensory (caudal) area identity in the developing neocortex. Similar mechanisms for the consolidation of neocortical arealization have started to emerge for other post-mitotic genes, such as *LIM homeobox-2* (*Lhx2*; Zembrzycki et al., 2015), *Pre-B-Cell Leukaemia Homeobox-1* (*Pbx1*; Golonzhka et al., 2015), *Basic Helix-Loop-Helix Protein-5* (*Bhlhb5*; Joshi et al., 2008), *T-Box Brain Transcription Factor-1* (*Tbr1*; Bedogni et al., 2010) and *COUP-TF interacting protein-1* (*Ctip1*; Greig et al., 2016). This indicates that genes expressed in young post-mitotic neurons play a fundamental role in neuronal and area specification, independently from progenitor identity (Fishell and Hanashima, 2008; Joshi et al., 2008; Bedogni et al., 2010; Greig et al., 2013).

The expression in both progenitors and neurons is a peculiar characteristic of *Nr2f1*, as other area patterning genes are expressed only in apical progenitors (*Pax6, Emx2*), or transiently in intermediate progenitors (*Tbr2, Ap2y*) or exclusively in post-mitotic cells (*Tbr1, Lhx2, Pbx1*). The preserved *Nr2f1* expression gradient in both cycling and differentiating cells could explain the strong effect on the area size and position observed

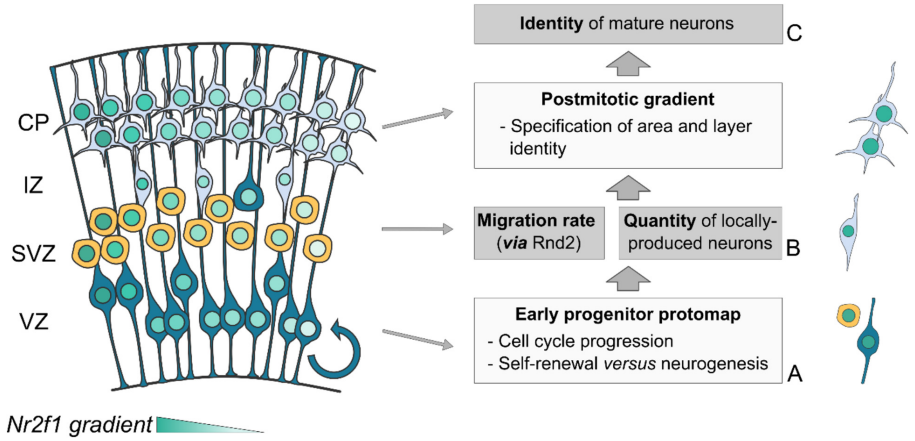

FIGURE 4 | Triple *Nr2f1*-mediated control of neocortical mapping. The *Nr2f1* gradient in the developing neocortex (blue color code) is key for a regional-specific control of three fundamental processes of corticogenesis: cell proliferation **(A)**, cell migration **(B)** and neuronal identity acquisition **(C)**. **(A)** In progenitor cells, *Nr2f1* regulates cell cycle progression and the balance between self-renewal and differentiation (neurogenesis), ultimately controlling the number of newborn neurons locally produced along neocortical axes. **(B)** In newborn neurons, *Nr2f1* controls the rate and efficiency of radial migration , *via* the regulation of *Rnd2* expression. **(C)** Post-mitotically, *Nr2f1* leads the establishment and consolidation of mature neuron identity. Being expressed in both progenitors and neurons allows *Nr2f1* to connect all these distinct cellular processes, ultimately controlling the position and size of neocortical areas. CP, cortical plate; IZ, intermediate zone; SVZ, sub-ventricular zone; VZ, ventricular zone.

in mutants, compared to that of other patterning genes. In this scenario, *Nr2f1* post-mitotic expression further reinforces areal identity specification initially imparted in progenitors (Alfano et al., 2014).

In summary, *Nr2f1* plays multiple roles during corticogenesis, mainly depending on the cellular context and developmental time (**Figure 4**). In cycling neural progenitors, it regulates cell cycle speed and balance between self-renewal and neurogenesis in a region-specific manner, ultimately determining how many neurons are produced (Faedo et al., 2008; Bertacchi et al., 2020). Notably, young neurons exiting the cell cycle radially migrate to the CP, and such migration rate is also regionally controlled by *Nr2f1* by directly regulating *Rnd2* expression (Alfano et al., 2011). Finally, *Nr2f1* influence over area identity is not limited to the establishment of an early progenitor protomap (Armentano et al., 2007; O'Leary et al., 2007; O'Leary and Sahara, 2008), but is most prominently accomplished *via* its post-mitotic role in the specification and consolidation of area and layer identity (Alfano et al., 2014). Being expressed in a gradient in both progenitors and neurons, *Nr2f1* can link different processes, ultimately orchestrating the number and type of neurons produced in a region-specific manner.

THALAMIC *Nr2f1* EXPRESSION ORCHESTRATES ACTIVITY-DEPENDENT REFINEMENT OF CORTICAL AREAS

After the arealization process initiates prenatally, a further refinement is controlled postnatally, when TCAs start innervating the neocortex. In fact, the establishment of thalamocortical connectivity, responsible for relaying sensory input to their respective cortical targets, concours in refining boundaries between neocortical functional areas (Rubenstein and Rakic, 1999; Sur and Rubenstein, 2005; Rakic et al., 2009; Alfano and Studer, 2013). *Nr2f1* expression in sensory thalamic progenitors and neurons peaks at mid-gestation (Armentano et al., 2006; Zembrzycki et al., 2013), but is maintained at perinatal stages only in the lateral geniculate and ventro-posterior nuclei of the dorsal thalamus (Armentano et al., 2006).

The use of cortical *cKO* models showed that thalamo-cortical axons correctly reached the subplate at E16.5–E18.5, but that only a few succeeded in innervating the CP, while the majority were aberrantly wired. Additionally, cortico-thalamic projections were affected too. In normal conditions, projections from M1, S1 and V1 principally innervate the ventrolateral (VL), the ventroposterior (VP), and the dorsolateral genuculate (dLGN) nuclei of the thalamus, respectively. However, in cortical *cKO* brains, projections from both M1 and mS1 target the VL nucleus, with caudally displaced S1 projections connecting with the dLGN and very few projections reaching the VP (Armentano et al., 2007). Conversely, the use of thalamic *cKO* models showed that the genetic manipulation of sensory thalamic nuclei was sufficient to affect the organization of primary and secondary sensory areas in the neocortex (Chou et al., 2013; Vue et al., 2013; Antón-Bolaños et al., 2018). Accordingly, the selective inactivation of *Nr2f1* in the dLGN influences the organization of primary *versus* high-order (secondary) visual cortical regions, with V1 resulting virtually absent, in favor of enlarged higher-order areas (Chou et al., 2013).

In summary, the use of tissue-specific conditional mouse models has pointed to a dual role of *Nr2f1* during area mapping and formation: (i) cell-intrinsic specification of a proto-sensory neocortical map (*via* cortical intrinsic genetic programs and in

tight link with FGF signaling); and (ii) non-cell-autonomous refinement of primary and secondary cortical maps through TCA inputs to their topographic cortical targets.

Nr2f1 REGULATES CELL INTRINSIC ELECTROPHYSIOLOGICAL PROPERTIES DURING NEOCORTICAL MATURATION

Along with acquiring a precise cytoarchitectural organization, the mammalian neocortex is also characterized by the onset of spontaneous activity, an essential feature in specifying the composition and organization of neural circuits within and between functional areas (Jabaudon, 2017; Simi and Studer, 2018). The formation of an efficient network relies on several processes, including cell-intrinsic mechanisms regulating cell excitability of cortical pyramidal neurons, non-cell-intrinsic and activity-dependent fine-tuning *via* TCA innervation, as well as the correct balance between excitatory and inhibitory neuronal populations in mature circuits. Before a sensory-driven activity is conveyed to the cerebral cortex by TCAs, the developing cortex is already genetically primed to establish patterns of local spontaneous activity, characterized by large groups of synchronously firing neurons, and contributing to the generation of local neuronal circuits (Kirischuk et al., 2017; Andreae and Burrone, 2018; Antón-Bolaños et al., 2018; Luhmann and Khazipov, 2018). Cell-intrinsic regulation of excitability in neocortical neurons influences the formation of a functional somatotopic map, ultimately preparing cortical areas and circuits for upcoming sensory inputs (Antón-Bolaños et al., 2019). Simultaneously, spontaneous neuronal activity arises in the embryonic thalamus and is then conveyed to the immature cortex. As early patterns of spontaneous activity play a key role in setting the nascent cortical network organization, their alteration during cortical development leads to cortical circuit dysfunction (Kirkby et al., 2013; Li et al., 2013).

The impact of *Nr2f1* loss on neocortical arealization and neuronal differentiation raised the possibility that they could correlate with altered spontaneous activity. Other transcriptional determinants of cortical specification, such as *matrix metallopeptidase-9* (*MMP-9*) and *leucine-rich glioma inactivated-1* (*LGI-1*) factors (Boillot et al., 2016; Murase et al., 2016), have been shown to impinge on spontaneous activity. As another example, the transcription factor *Tbr1*, known to regulate cortical layer identity, also influences the intrinsic excitability of neocortical neurons (Fazel Darbandi et al., 2018). However, whether *Tbr1* similarly regulates spontaneous network activity even during early developmental stages remains to be addressed.

Recent data have shown that loss of *Nr2f1* from cortical progenitors affects spontaneous network activity, synchronization *in vitro*, as well as intrinsic bioelectric properties of cortical pyramidal neurons *in vivo* (Del Pino et al., 2020). For instance, *Nr2f1* mutant neurons were characterized by increased resting membrane potential, reduced rheobase and sag current, hinting at increased intrinsic excitability (**Figure 5**). Expression profile analysis revealed that *Nr2f1* transcriptionally regulates a plethora of layer V-expressed ion channels, including the *hyperpolarization-activated cation channel-1* (*HCN1*), a well-known regulator of rhythmic oscillatory activity, ultimately controlling neuronal excitability (Huang et al., 2009; Bonzanni et al., 2018; Marini et al., 2018). Notably, *Nr2f1* can directly bind to *HCN1* regulatory regions *via* several consensus sequences (Del Pino et al., 2020). As a result, both *HCN1* transcript and protein levels are specifically downregulated in layer V neurons upon *Nr2f1* cortical ablation. Interestingly, genetic or pharmacological disruption of HCN channels activity results in dysfunctional somatosensory-motor coordination in mice, such as reduced forelimb reaching accuracy and atypical movements during a single-pellet skill reaching task (Boychuk et al., 2017). These behavioral deficits resemble those displayed in cortical *Nr2f1 cKO* mice (Tomassy et al., 2010) and remind motor-coordination deficits of *NR2F1* haploinsufficient patients (Bosch et al., 2014; Chen et al., 2016; Rech et al., 2020). Nevertheless, although HCN1 is a potential direct effector of *Nr2f1* in inducing an intrinsic electrophysiological phenotype, other ion channels may contribute to the impairment of network activity and intrinsic excitability upon *Nr2f1* loss. The electric impairment is also accompanied by structural and morphological modifications, in line with previous studies (Tien and Kerschensteiner, 2018). Cortical pyramidal neurons showed reduced complexity of their basal arborization, alongside with a defective axon initial segment (AIS; Del Pino et al., 2020), a specialized region localized between the somatic and axonal compartments, responsible for the initiation of action potentials (Leterrier, 2018). However, since *Nr2f1* also regulates the expression of cytoskeletal genes (Armentano et al., 2006; Alfano et al., 2011), the effect of *Nr2f1* loss on pyramidal neuron morphology and on the AIS size could also depend on direct modulation of cytoskeletal proteins, rather than being an indirect effect of altered excitability. A similar mechanism has been demonstrated for another key determinant of corticogenesis, *autism susceptibility candidate-2* (*AUTS2*; Hori et al., 2014). These studies revealed impairments in bioelectric properties of cortical neuronal populations and/or network activity upon loss of transcriptional regulators, illustrating that genetic determinants implicated in NDDs often link neuronal specification to cellular excitability (Huang and Hsueh, 2015; Rodríguez-Tornos et al., 2016; Khandelwal et al., 2021; Runge et al., 2021). In summary, *Nr2f1* might influence cell excitability, either *via* the regulation of ion channels, or *via* the control of cytoskeletal components shaping neuronal structural features. Altered excitability and/or morphology of layer V neurons in BBSOAS patients might be the cause of pathological features, such as ID, epileptic traits, but also poor motor coordination of fine skilled movements.

AN INTRINSIC ROLE OF *Nr2f1* IN INTERNEURON SPECIFICATION, MIGRATION, AND FUNCTION

To maintain a proper balance of cortical network activity, different types of inhibitory interneurons will modulate the

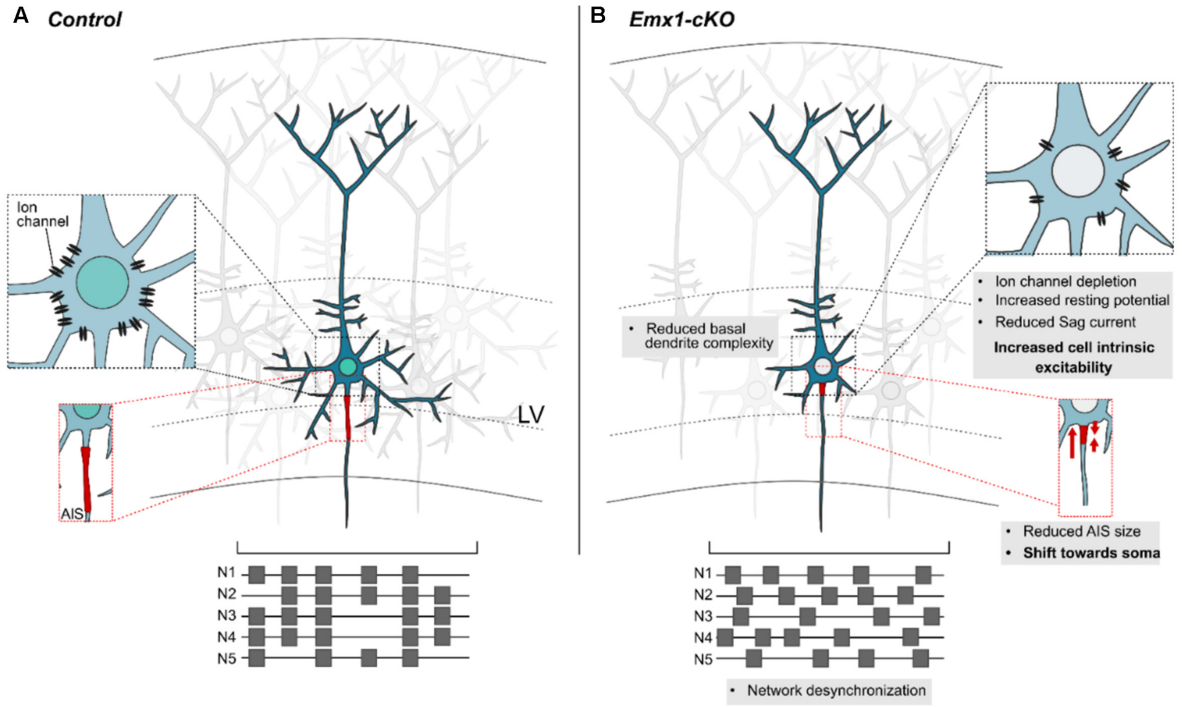

FIGURE 5 | *Nr2f1* controls the bioelectric and cytostructural nature of layer V cortical neurons. **(A)** Schematic representation of a layer V pyramidal neuron in a physiological context. A specific asset of ion channels is displayed on the cell membrane (magnification in the black dashed box) and determines cell electrophysiological properties (i.e., resting membrane potential, sag current, etc.) and proper network synchronization. The firing pattern of five neurons -N1 to N5- is schematized in the lower scheme, in the form of gray squares (representing firing events) distributed along lines (indicating measurement time during recording). Structural features of dendrite complexity and axon initial segment (AIS; magnified in the red dashed box) are also influenced by the cellular bioelectric state. **(B)** Summary of the main defects observed upon loss of *Nr2f1*. Several ion channels are downregulated in mutant neurons (inset in the black dashed box), resulting in increased intrinsic excitability. Furthermore, distinct neurons lose their ability to efficiently fire action potentials in a synchronized way (lower scheme), suggesting that the overall network synchronization is affected. At the morphological level, the complexity of the basal dendrites is drastically diminished upon *Nr2f1* loss, and the AIS is reduced in size and misplaced closer to the soma (magnified in the red dashed box). Modified from Del Pino et al. (2020). LV, layer V.

activity of excitatory pyramidal neurons. Cortical GABAergic interneurons are generated in the ventral telencephalon and sequentially migrate into the dorsal telencephalon to integrate the forming local circuitry. In the ventral telencephalon, *Nr2f1* is first expressed in progenitors in a broad and graded pattern spanning the caudal, medial and lateral ganglionic eminences (CGE, MGE, and LGE). Then, it becomes gradually restricted to the CGE, before being maintained by distinct subpopulations of CGE-derived GABAergic interneurons, such as Vasoactive Intestinal Peptide (VIP) and Calretinin (CR)-expressing interneurons (Flames et al., 2007; Lodato et al., 2011; Touzot et al., 2016). As in rodents, both human *NR2F1* and *NR2F2* are also expressed in embryonic progenitors and migrating interneurons (Reinchisi et al., 2012; Varga et al., 2015; Alzu'Bi et al., 2017), and their expression is maintained in some mature cortical interneuron subtypes, with a preference for CGE-derived interneurons.

The use of a specific conditional *KO* mouse model showed that the loss of *Nr2f1* expression in interneuron precursors affected the balance between MGE- and CGE-derived populations, without altering the overall interneuron number. Specifically, late-born CGE-derived VIP+ and CR+ interneurons were decreased in number and aberrantly migrated towards the forming neocortex. Conversely, the number of early-born MGE-derived Parvalbumin (PV)-expressing interneurons increased, possibly due to augmented proliferation in the MGE (Lodato et al., 2011; Touzot et al., 2016). As a result of the enlarged PV+ inhibitory population, interneuron-specific *cKO* animals appear to be more resistant to seizure induction (Lodato et al., 2011). However, this does not recapitulate the human syndrome, since BBSOAS patients are often affected by epileptic seizures (Chen et al., 2016; Rech et al., 2020). A possible explanation is that in patients, *NR2F1* is simultaneously lost from both dorsal and ventral telencephalon, equally affecting the function of excitatory neurons and inhibitory interneurons and leading to an imbalance in the overall brain activity. Instead, in the interneuron-specific *cKO* animals, only interneurons are affected by *Nr2f1* loss, while the function of pyramidal neurons is not directly altered, hence resulting in a more resilient network state.

Impaired excitation/inhibition (E/I) balance upon loss of *Nr2f1* has been supported by a recent study employing the first "patient-specific" *Nr2f1* mutant mouse model, carrying in heterozygosity the *Nr2f1* point mutation R112K (Zhang et al.,

2020). Mutants are characterized by reduced expression of dorsal telencephalic markers and a concomitant increase of ventral ones. This translates, at later stages of development, into a decrease of cortical excitatory pyramidal neurons and an increase of inhibitory interneurons, thus perturbing the overall E/I balance. At the electrophysiological level, this imbalance leads to a frequency reduction of miniaturized excitatory postsynaptic currents and an increase in inhibitory ones. E/I imbalance has been reported as a possible cause for both epilepsy and ASD (Powell, 2013), two pathological features frequently reported in BBSOAS patients. Whether this is the case for patients carrying variants different from the one tested in this study, remains to be assessed. So far, the use of this novel mouse model carrying a human-specific mutation succeeded in correlating E/I imbalance with ASD-like behavior deficits, such as reduced sociability, excessive grooming, repetitive and anxiety-like behaviors (Zhang et al., 2020), but whether such E/I imbalance also underlies BBSOAS-related epilepsy has yet to be directly tested.

BEYOND THE NEOCORTEX: *Nr2f1* REGULATES THE ANATOMICAL AND FUNCTIONAL DEVELOPMENT OF THE HIPPOCAMPUS

All the previously described *Nr2f1*-dependent processes orchestrating neocortical development and network maturation could be directly connected to ID reported in BBSOAS patients (Rech et al., 2020). However, the hippocampus (HP), a key cortical structure regulating cognitive processes such as learning and memory (Broadbent et al., 2004; Kumaran and Maguire, 2005; Hannula et al., 2013) also resulted affected in BBSOAS patients. Due to the central role of the HP in controlling key cognitive skills, even small developmental defects can have a dramatic impact on behavioral performances (Mátéffyová et al., 2006; Ramos, 2008; Wan et al., 2021; Zhao et al., 2021). While the dorsal hippocampal pole is more involved in spatial navigation (Moser et al., 1995), the ventral one controls non-spatial learning and emotional behaviors (Kheirbek et al., 2013; Wang et al., 2013). Interestingly, some BBSOAS patients show hippocampal morphological defects, such as dysmorphic HP or hippocampal malrotation (Cardoso et al., 2009; Chen et al., 2016), suggesting that specific cognitive abnormalities reported in these patients could derive from HP developmental impairments. Cortex-specific conditional mouse models (*cKOs*) and constitutive *HET* animals have helped dissect the *Nr2f1* role in HP morphogenesis and function (Flore et al., 2016; Parisot et al., 2017; Chen et al., 2020), as well as in HP-controlled adult behavior (Tomassy et al., 2010; Flore et al., 2016; Contesse et al., 2019). Loss of *Nr2f1* in the cortex at early stages leads to severe shrinkage of the intermediate and dorsal but not ventral regions of the HP, as well as impaired connectivity of topographic inputs from the entorhinal cortex (Flore et al., 2016). This ultimately results in selective impairment of spatial learning and memory, whereas emotional behavior and visual cue navigation remain intact (Flore et al., 2016). The impact of *Nr2f1* loss on HP development depends on both NP proliferation and neuronal migration during embryonic and early postnatal development (Parisot et al., 2017; Bertacchi et al., 2019b). Differently from the neocortex, *Nr2f1* acts as a pro-mitotic factor during hippocampal and dentate gyrus (DG) development and positively regulates NP migration along the primary, secondary, and tertiary DG matrices (Parisot et al., 2017). Interestingly, several genes are differentially expressed in gradients along the D-V HP axis (Leonardo et al., 2006; Lein et al., 2007; O'Reilly et al., 2015; Lee et al., 2017), but *Nr2f1* is one of the few genes which regionalized expression is directly linked to hippocampal development and behavioral function. The existence of a link between *Nr2f1* graded expression and hippocampal regionalization reminds the one described in the neocortex (Zhou et al., 2001; Armentano et al., 2007; Alfano et al., 2014), indicating that gradient gene expression might be a general mechanism for proper structural brain development.

A recent study used an *Nr2f1 HET* mouse model to better recapitulate the haploinsufficiency condition of BBSOAS patients (Chen et al., 2020). Electrophysiological investigation in hippocampal slices revealed impairment of two major cellular processes involved in learning and memory: long-term potentiation and long-term depression (Chen et al., 2020), suggesting that altered hippocampal synaptic plasticity may contribute to BBSOAS cognitive impairments. Although *HET* mutants confirmed decreased hippocampal volume, such defect was not as severe as in homozygous *cKO* mutants. Furthermore, normal spatial memory but specific deficits in fear memory were described (Chen et al., 2020). The contrasting results obtained in cortical *cKO* and *HET* animals might be attributed to the different genetic nature and entity of the *loss-of-function* mouse model. For instance, in *cKO* mice, loss of both *Nr2f1* alleles is limited to the cortex, and leads to severe but spatially restricted anatomical defects, accompanied by specific behavioral abnormalities. *Vice versa*, the constitutive *HETs* lack just one allele, but the loss affects the entire organism. This might explain the downsized morphological defects (since approximately 50% of the *Nr2f1* protein pool is produced and functional in *HETs*) as well as the more complex behavioral phenotype (due to the disruption of other brain structures involved in the regulation of learning, memory, and emotional behavior in *HET* animals). Further studies will be necessary to dissect the exact contribution of hippocampal deficits on BBSOAS ID and to distinguish it from malformations due to other cortical or subcortical regions.

Nr2f1-DEPENDENT DEVELOPMENT OF THE SENSORIMOTOR SYSTEM

The progressive development and refinement of proto-areas and functional areas, implies that distinct cortical regions wire to other cortical and/or subcortical structures to orchestrate complex behaviors, such as planning, control, and execution of voluntary movements. The circuit regulating voluntary movements was first described as the cerebro-cerebellar pathway (Brodal, 2010). However, several recent studies have shown how other brain regions, such as the pontine nuclei and

the ventrolateral nuclei of the thalamus (VL), also retain an active role in the regulation of distinct voluntary movements (Schwarz and Thier, 1999; Bosch-Bouju et al., 2013; Guo et al., 2021). This network connects the cerebral neocortex to the cerebellum *via* the pontine nuclei and *vice versa* the cerebellum to the neocortex through the VL nucleus of the thalamus. In humans, up to 90% of the neocortical layer V projections are estimated to target the pontine nuclei, a percentage that is even higher in rodents, where almost the whole layer V population is projecting towards these structures. Similarly, up to 90% of pontine mossy cells are sending their axons to the cerebellum. Once the information reaches the cerebellum, it is further elaborated and a feedback output is sent back to the neocortex, through the VL (Schwarz and Thier, 1999; Bosch-Bouju et al., 2013). In both the neocortex and the cerebellum, neuronal populations involved in the regulation of voluntary movements are arranged in topographically organized maps, with different body parts being represented in largely continuous maps in the somatosensory cortex (Woolsey and Van der Loos, 1970; Welker, 1971; Chapin and Lin, 1984; Fabri and Burton, 1991), and discontinuous, fractured maps in the cerebellum (Bower et al., 1981; Bower and Kassel, 1990; Bower, 2011). The intercalated regions of this network receive and integrate signals from different structures, thus helping to coordinate and seamlessly execute fine motor behaviors (Badura et al., 2013; Mottolese et al., 2013). Cortical descending tracts, such as the cortico-spinal tract then convey the motor command to the spinal cord.

BBSOAS patients often present motor abnormalities, such as delayed motor development, poor motor planning and coordination, as well as stereotyped repetitive movements (Rech et al., 2020). A detailed patient report hypothesized that some of these motor impairments might be traced back to defects of the voluntary movement network (Bojanek et al., 2020). In addition, defects in both reaction time and movement accuracy could specifically arise from abnormal functioning of the cerebro-ponto-cerebellar pathway (Bojanek et al., 2020). Studies on the motor functions of a bigger BBSOAS cohort would help to further characterize the voluntary movement network affected by *NR2F1* haploinsufficiency.

Previous reports in mice have helped describe the development of cortical descending tracts and started unraveling the specific assets of molecular players, including axon guidance cues, signaling molecules, cell adhesion proteins as well as transcription factors necessary for the assembly of the voluntary movement circuitry in general, and the development of the corticospinal tract in particular (Welniarz et al., 2017). *Nr2f1* mutants have been proved efficient models for recapitulating some motor impairments that may underlie BBSOAS-like motor deficits. The impairment observed upon loss of *Nr2f1* function in the tangential (area) organization of the forming neocortex is also accompanied by radial (laminar) changes in the structure of neocortical layers, which ultimately results in abnormal connectivity between the cortex and its subcortical targets (Armentano et al., 2007; Tomassy et al., 2010; Greig et al., 2013; Alfano et al., 2014). In physiological conditions, subcortical projection neurons from M1 and S1 follow slightly different paths: while M1 axons mainly reach the spinal cord and constitute only a small fraction of the pontine nuclei innervation, S1 axons almost exclusively target the pontine nuclei (**Figure 6A**). However, following the disruption of cortical area specification caused by *Nr2f1* inactivation (Zhou et al., 2001; Armentano et al., 2007; Alfano et al., 2014), these proportions change with both S1 and M1 populations equally projecting to the pontine nuclei. Only a depleted population of axons coming from the motor-like sensory cortex ("mS1") will reach the spinal cord in mutants (**Figure 6B**; Tomassy et al., 2010). This defective connectivity has, most probably, a deleterious effect on motor execution and behavior. *Nr2f1 cKO* animals are characterized by abnormal dexterity and voluntary movement execution, in terms of reduced forelimb reaching accuracy and atypical movements during a single-pellet reaching task, as well as hyperactive features (Tomassy et al., 2010; Contesse et al., 2019). These observations support the *cKO* mice as a reliable animal model for further understanding the impaired development and/or defective circuits at the origin of the voluntary movement execution and hyperactive behavior. Further, a recent study assessing the role of pontine nuclei in voluntary movements supports their direct involvement in the timing and accuracy of movements rather than its initiation. Specifically, upon optogenetic disruption of the pontine nuclei activity, the animals retained the ability to initiate the reaching phase of the single-pellet task but showed either reduced precision of the grasping phase or a general delay in the complete execution of the task (Guo et al., 2021). Since the defects showed by *Nr2f1* cortical *cKO* mice resemble those presented in this work, with an almost intact reaching phase but inaccurate grasping (Tomassy et al., 2010), it is tempting to speculate that gradient cortical *Nr2f1* expression could impart topographic information to descending tracts during development by influencing their connectivity to subcortical structures, such as the pontine nuclei and the spinal cord. This would imply that *Nr2f1* can link key processes of corticogenesis, such as area identity, layer formation and tract connectivity, allowing the correct development of voluntary motor networks.

MORE THAN MEETS THE EYE: *Nr2f1* ORCHESTRATES VISUAL SYSTEM DEVELOPMENT FROM PERIPHERAL RETINAL TO CENTRAL THALAMIC AND NEOCORTICAL AREAS

BBSOAS patients were first identified for their unique combination of cerebral and visual impairments, suggesting that besides cortical development, NR2F1 might also influence the establishment of the visual system. Several clinical reports describe that a major clinical feature of BBSOAS patients is the profound impairment of visual performances (Bosch et al., 2014; Chen et al., 2016; Kaiwar et al., 2017; Rech et al., 2020; Starosta et al., 2020; Zou et al., 2020), due to optic nerve atrophy and/or optic nerve hypoplasia, decreased visual acuity and cerebral visual impairment, defined as impaired analysis

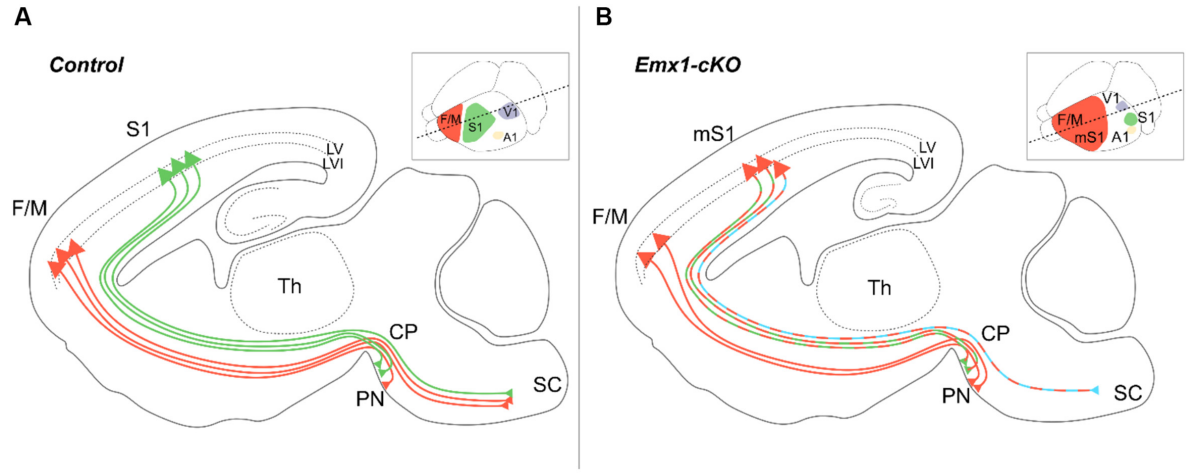

FIGURE 6 | Layer V pyramidal neuron subtype specification is under the control of *Nr2f1* cortical expression. In *wild-type* mice **(A)**, subcortical projecting neurons of layer V target distinct brain regions depending on their area localization. Layer V neurons from the fronto-motor areas (F/M, orange) mainly project to the spinal cord (SC) with very few axons targeting the pontine nuclei (PN), whereas layer V neurons from S1 (green) mainly target the pontine nuclei with fewer projections towards the SC. In conditional cortical-specific *Nr2f1* mutants (*Emx1-cKO*) **(B)**, F/M axons are incorrectly wired and stop at the level of the cerebral peduncle (CP), resulting in a depletion of corticospinal connections upon *Nr2f1* loss. Layer V axons from the motorized S1 (mS1) still project to the PN (green/orange dashed lines), but not to the SC, which is instead aberrantly innervated by layer VI mS1 neurons (blue/orange dashed line). A1, primary auditory area; CP, cerebral peduncle; F/M, fronto-motor area; LV, layer V; LVI, layer VI; mS1, motorized primary somatosensory area; PN, pontine nucleus; S1, primary somatosensory area; SC, spinal cord; V1, primary visual area.

and interpretation of visual stimuli (Bosch et al., 2016). While recent reports are detailing the ophthalmological features of visually impaired BBSOAS children (Zou et al., 2020; Jurkute et al., 2021), mouse models offer again the unique opportunity to further understand the role of *Nr2f1* in vision, from the developmental and the functional points of view. Previous *Nr2f1* conditional mouse models failed in reproducing key patient eye defects, such as malformed optic discs and optic atrophy (Tang et al., 2010), but constitutive models, better mimicking patients' haploinsufficiency, efficiently recapitulate a plethora of BBSOAS-like symptoms (Bertacchi et al., 2019a). From the peripheral-most relay points of the visual system, i.e., the retina and the optic nerve, to more central brain structures deputed to the analysis of visual stimuli, such as the visual thalamus and cortices, we summarize in this section how *Nr2f1/NR2F1* graded expression in distinct relay-points of the developing visual system impacts the function of mouse and human vision (**Figure 7A**).

IMPAIRED RETINOGENESIS AND NON-PROGRESSIVE DECREASE OF RGC DENSITY UPON *Nr2f1* LOSS

Optic nerve atrophy (ONA) and/or optic nerve hypoplasia (ONH), often reported in BBSOAS patients (Rech et al., 2020), are characterized by a reduced optic nerve (ON) exiting the retina, together with thinning of retinal layers, retinal ganglion cell (RGC) and retinal nerve fiber layers (RNFL), where RGCs and their axons reside, respectively (Jurkute et al., 2021). *NR2F1* is dynamically expressed in different retinal cell types of the human eye, including RGCs (Bertacchi et al., 2019a), which form the ON by elongating their axons from the retina to the brain. The high degree of conservation of *Nr2f1* expression between the human and rodent visual pathway (Alfano et al., 2014; Bertacchi et al., 2019b) allowed the use of the mouse as a model system to study BBSOAS-related visual impairments. Starting from the peripheral-most structure of the visual system, the retina, *Nr2f1* shows a dynamic expression along a dorsal-low to ventral-high gradient, whereas its homolog *Nr2f2* displays an opposite gradient (Tang et al., 2010, 2015). This dorso-ventral (D-V) *Nr2f1* gradient has specific consequences on neural development: D-V specification of regional retinal identities is compromised in the absence of both *Nr2f* genes, with Pax6 expression being abnormally enhanced at the expense of key genes imparting a ventral identity to the mouse eye, such as *Ventral anterior homeobox-1* and *-2* (*Vax1* and *Vax2*, respectively; Barbieri et al., 1999; Mui et al., 2005; Tang et al., 2010; **Figure 7B**). Later in development, *Nr2f1* and *Nr2f2* convey the D-V regional information to direct the expression of Opsins, a family of light-sensitive proteins localized in photoreceptors (Satoh et al., 2009). The presence of *Nr2f* D-V gradients also suggests that these genes might be involved in the appropriate formation of the retinotopic projection map of RGC axons, the only long-range projections from the retina to the brain. Even if further experiments will be necessary to tackle this question, recent data about axonal misrouting in *Nr2f1*-deficient mice point in this direction (Jurkute et al., 2021). Besides axonal guidance, the number of RGCs in the retina was also affected in mutants, since a stable decrease in RGC density was

reported in adult *HET* mice (Jurkute et al., 2021). This defect originates early in development and possibly involves RGC apoptosis around birth (Bertacchi et al., 2019a). Notably, the RGC decrease found in the mouse model fits well with the finding of ONA and ONH in patients, displaying a decreased amount of RGC fibers in the ON and showing non-progressive, stable reduction of RGC and RNFL thickness. Overall, these observations suggest an early developmental cause for the axonal depletion within the ON (Bosch et al., 2014; Chen et al., 2016; Jurkute et al., 2021).

Finally, little is known whether *Nr2f1* can influence the development and distribution of other retinal cell types. Given that *Nr2f1* expression is maintained in the ganglion cell and inner nuclear layers and, at lower levels, in the outer nuclear layer of the adult mouse retina (Inoue et al., 2010; Bertacchi et al., 2019a; Jurkute et al., 2021), it is reasonable to hypothesize a role for Nr2f1/NR2F1 in the maintenance and functionality of mature retinal cells. High *Nr2f1* expression was also detected in both mouse and human retinal pigment epithelial (RPE) cells (Jurkute et al., 2021); it is tempting to speculate that *Nr2f1* could then influence photoreceptor function indirectly *via* RPE-mediated mechanisms.

Nr2f1 PLACES THE OPTIC DISC BOUNDARY BY REGULATING NEURAL RETINA AND OPTIC STALK GENES

Early studies unraveled an *Nr2f*-modulated network of genes expressed in the neural retina and optic stalks, such as *Pax6*, *Pax2*, *Otx2* and *melanocyte inducing transcription factor* (*Mitf*), necessary for eye development and for placing the optic disc region between the neural retina and the optic stalk (**Figure 7B**; Schwarz et al., 2000; Tang et al., 2010; Pattabiraman et al., 2014). The optic disc, specified by the combinatorial expression of transcription factors, is in turn fundamental for producing signaling molecules for RGC axonal guidance (Deiner et al., 1997). While neither *Nr2f1* nor *Nr2f2* single *KO* mice seemed to develop major optic disc abnormalities, double *KO* mice (characterized by the combined inactivation of both homologs) showed severe coloboma, microphthalmia, and misplacement of the eye border resulting in a proximal shift of the optic disc (Tang et al., 2010). The compensatory effect of both homologs (*Nr2f1* and *Nr2f2*) during mouse eye development was quite surprising since BBSOAS patients show ocular impairments with high penetrance, already upon loss of one single copy of *NR2F1*. The discrepancy was probably due to the mouse model initially used to dissect the role of *Nr2f1* in eye development, a conditional mutant in which *Nr2f1* expression was selectively abolished in retinal tissue (Furukawa et al., 1997; Swindell et al., 2006; Tang et al., 2010). The use of an *Nr2f1* constitutive mutant instead, characterized by a reduction in *Nr2f1* dosage in the entire organism and from the earliest stages of development, allowed a better reproduction of BBSOAS-like conditions, and helped demonstrate how this genetic network is disrupted by the loss of *Nr2f1* alone (Bertacchi et al., 2019a). In fact, the sole absence of *Nr2f1* is sufficient to cause a shift of the border between the neural retina and the optic stalk, which in turn has heavy consequences on the expression of optic disc molecular determinants, such as Netrin1, and on the RGC projections exiting the eyeball (Jurkute et al., 2021; **Figure 7B**). However, compared to *KO* mutants, *Nr2f1 HET* animals have more subtle defects, that are partially recovered during late embryonic development (Bertacchi et al., 2019a). This is in striking contrast to BBSOAS patients, that continue to show various eye malformations, such as excavated and pale optic discs from childhood to adulthood. Understanding the origin for these species-specific differences will require further studies.

ASTROGLIOSIS AND HYPOMYELINATION CONVERGE TO OPTIC NERVE ATROPHY IN A *Nr2f1*-DEFICIENT MODEL

Besides showing atrophy, the ON of the mouse BBSOAS model revealed low levels of myelination (Bertacchi et al., 2019a), caused by a delay in oligodendrocyte precursor proliferation and differentiation (**Figure 7C**). In normal physiological conditions, mouse oligodendrocytes are generated in the pre-optic area, then enter the ON guided by local signaling molecules, proliferate *in loco* and finally differentiate in the first post-natal month into mature oligodendrocytes, wrapping RGC axons to allow optimal signal conductivity (Tsai and Miller, 2002; Stolt et al., 2004; Ono et al., 2017). These processes are impaired in *HET* mice and almost absent in *KOs*, suggesting a key role for *Nr2f1* in the maturation of oligodendrocytes and in the myelination process, consistently with a previous report (Yamaguchi et al., 2004). Hypomyelination could in turn exacerbate the loss of ON axonal fibers by affecting RGC survival (Teixeira et al., 2016). It would be interesting to investigate whether this is a common mechanism happening in other structures, for example in the neocortical white matter, since MRI scans have revealed impaired myelination in some BBSOAS patients (Chen et al., 2016; Rech et al., 2020). In parallel to hypomyelination, the atrophic ON in mutant mice is further impacted by inflammatory processes reactivating dormant astrocytes (Bertacchi et al., 2019a), as observed by both morphological changes and expression of inflammatory markers such as *SRY-box transcription factor-2 (Sox2)* (**Figure 7C**; Bani-Yaghoub et al., 2006; Hernandez et al., 2008; Zhang et al., 2013; Pekny et al., 2014). Hence, *Nr2f1* represents the core of a genetic network regulating the astrocytic inflammatory process and neuron-astroglia cell fate decision in other brain regions, such as the adult mouse hippocampal neurogenic niche (Bonzano et al., 2018). Further studies will be necessary to unravel the temporal order and possible causative relationships between these distinct processes—oligodendrocyte hypomyelination, astrocyte inflammation, and RGC survival—that by influencing each other could exacerbate the *Nr2f1*-dependent phenotype.

Likely due to both inflammation and ON hypomyelination, electrophysiological recordings disclosed a significant delay in the conduction velocity of visual stimuli along

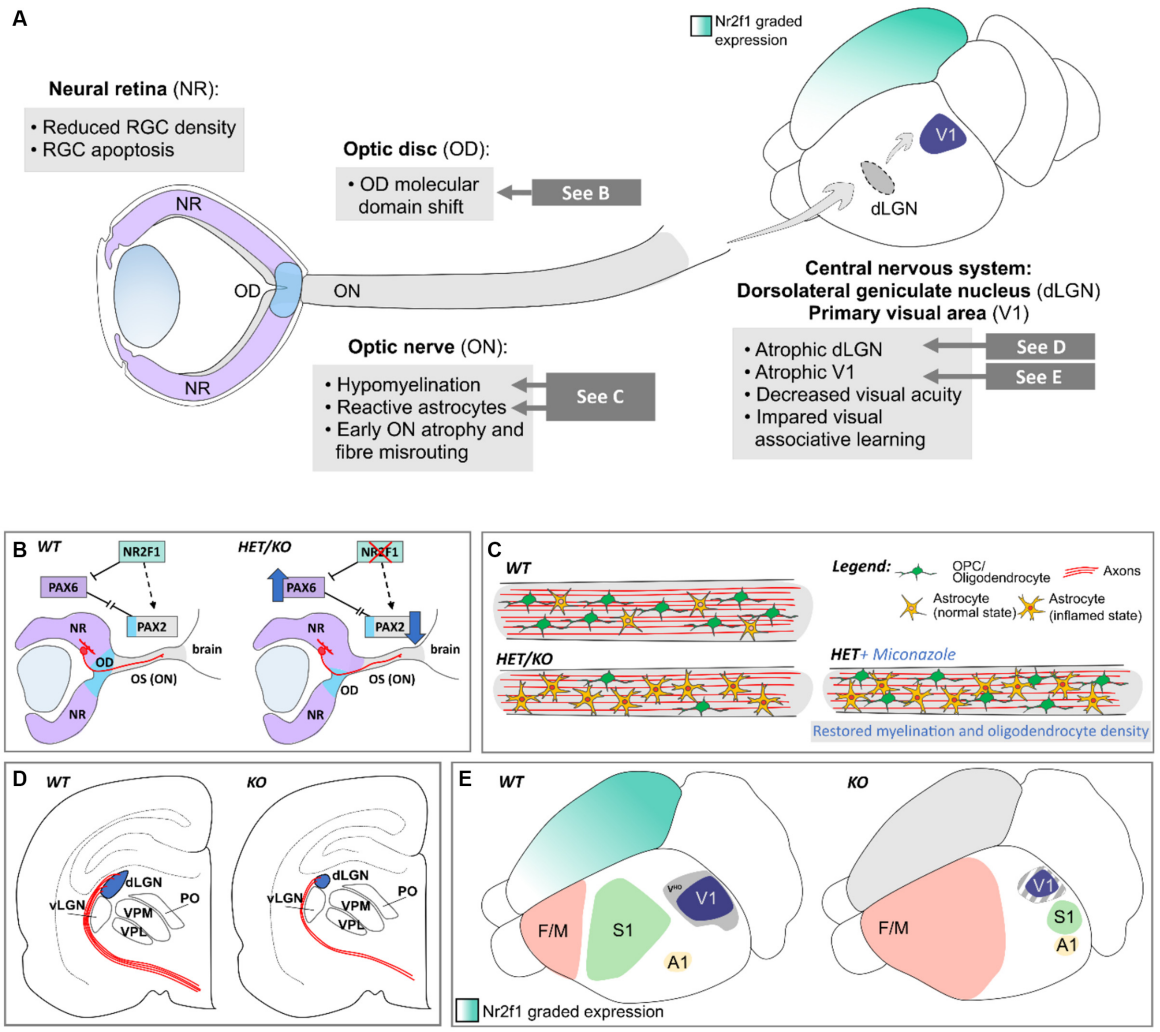

FIGURE 7 | *Nr2f1*-dependent development of the peripheral and central visual system in mouse. **(A)** Overview of the phenotypes observed in several structures of the mouse visual system upon *Nr2f1* loss, comprising the neural retina (NR), the optic disc (OD), the optic nerve (ON), and distinct central structures, such as the dorsolateral geniculate nucleus (dLGN) and the primary visual area (V1). **(B)** *Nr2f1* loss causes a molecular shift of the Pax6+ NR domain towards the Pax2+ optic stalk (OS)/ON domain, resulting in aberrant positioning of the OD border and axonal misguidance of retinal ganglion cell (RGC) axons exiting the developing eyeball. **(C)** *Nr2f1* haploinsufficient (*HET*) or depleted (*KO*) mice show decreased size of the ON compared to wild-type (*WT*) animals, resembling ON atrophy reported in BBSOAS patients. Upon *Nr2f1* loss, a population of Sox2+ astrocytes with inflamed morphology outnumbers oligodendrocyte progenitors (OPCs), resulting in ON inflammation and hypomyelination. While the myelination defect can be rescued by Miconazole treatment, the high proportion of reactive astrocytes and consequent gliosis and the general ON atrophy are not reverted by pro-myelinating chemical drugs. **(D)** Reduced axonal innervation and connectivity (in red) from the NR to the atrophic dLGN (in blue) in *Nr2f1*-deficient mice. **(E)** Atrophic V1 (blue) and impaired maturation of secondary associative visual cortices (visual high order cortex -V^{HO}-; gray) due to arealization defects upon *Nr2f1* loss. A1, primary auditory area; dLGN, dorsolateral geniculate nucleus; F/M, frontal/motor area; NR, neural retina; OD, optic disc; ON, optic nerve; OPC, oligodendrocyte precursor cell; OS, optic stalk; S1, primary somatosensory area; V1, primary visual area; V^{HO}, high-order visual associative secondary areas; vLGN, ventrolateral geniculate nucleus.

the ONs of mutant animals (Bertacchi et al., 2019a). Interestingly, myelination could be artificially boosted *in vivo* by early treatments of specific chemical drugs, in both physiological conditions and pathological models (Harlow et al., 2015; Najm et al., 2015; Porcu et al., 2015; Eleuteri et al., 2017; Su et al., 2018). Early post-natal injection of Miconazole, a chemical drug promoting oligodendrocyte differentiation, efficiently rescued the hypomyelination phenotype of *Nr2f1* haploinsufficient mice (**Figure 7C**; Bertacchi et al., 2019a), opening promising therapeutic avenues for BBSOAS visually-impaired patients and, more in general, supporting the feasibility of employing mouse models for therapeutic drug screening. However, Miconazole treatment rescued myelination but had no effect on astrogliosis, indicating that the two pathological events are independent in BBSOAS-like optic neuropathy and that additional treatments should be tested to revert the ON inflammatory state.

Nr2f1 INFLUENCES COMPLEX VISUAL ASSOCIATIVE BEHAVIORS BY CONTROLLING THALAMIC AND NEOCORTICAL DEVELOPMENT

Abnormal perception, elaboration, and interpretation of visual stimuli occurring in patients with cerebral visual impairments (affecting around 70% of BBSOAS patients; Bosch et al., 2016; Bertacchi et al., 2019a; Rech et al., 2020) suggests an impairment of higher-order visual centers (such as primary and associative visual cortices) besides peripheral structures, such as the retina and the ON (Philip and Dutton, 2014). Even in this context, mouse models offer the unique opportunity to investigate the impact of *Nr2f1* loss on the establishment of central thalamic and neocortical structures and to characterize the electrophysiological and behavioral consequences. Mouse *Nr2f1* is dynamically expressed in the thalamus, with high levels in the dorso-lateral geniculate nucleus (dLGN) receiving ON fibers (Qiu et al., 1994; Armentano et al., 2006; Alzu'Bi et al., 2017). Upon *Nr2f1* loss, the thalamic nuclei are affected in their size and connections, in turn impinging on the maturation of primary and secondary visual areas (**Figures 7D,E**; Zhou et al., 2001; Armentano et al., 2007; Chou et al., 2013). Interestingly, other key visual developmental factors, such as *Sox2*, can converge to similar thalamic phenotypes, when lost or mutated, by affecting the size and connection of the dLGN in a similar way (Mercurio et al., 2021). This suggests that *Nr2f1* might belong to a complex genetic network that is fundamental for the correct establishment of thalamic nuclei and their wiring to both cortex and retina. Electrophysiological recordings of visually evoked potentials in the dLGN of *Nr2f1 HET* mice revealed delayed transmission of visual stimuli and decreased visual acuity compared to *wild-type* littermates, consistently with low visual acuity (Bosch et al., 2014; Chen et al., 2016; Rech et al., 2020) and non-degenerative vision loss in BBSOAS patients (Jurkute et al., 2021).

Finally, the cerebral visual impairment described in patients could depend on the aberrant elaboration of visual stimuli in higher-order associative cortices (Malkowicz et al., 2006; Philip and Dutton, 2014; Bosch et al., 2016). As mentioned above, *Nr2f1* expression in thalamic and cortical structures is essential for the activity-dependent refinement of the secondary visual cortex in mouse (**Figure 7E**; Chou et al., 2013), implying that *Nr2f1* could control the maturation of higher-order associative cortices. Hence, the establishment of visual associative behavior was evaluated in *Nr2f1 HET* and control mice *via* a light-dependent operant conditioning task, in which a reward was obtained only when a visual stimulus (a small light bulb) was present and switched on. While control animals learned to associate the dim visual stimulus with the operant task, mutant animals failed to do so, somehow recapitulating an associative deficit in the interpretation of visual stimuli (Bertacchi et al., 2019a). However, *Nr2f1*-deficient mice were still able to learn and execute complex tasks (Flore et al., 2016; Bertacchi et al., 2019a), suggesting a specific impairment in the perception and elaboration of visual stimuli in high-order cortices rather than a generalized defect during the learning process. The visual impairments at the cortical level due to reduced *Nr2f1* dosage could contribute to one of the main features of ID reported in BBSOAS children.

CONCLUSIONS AND FUTURE DIRECTIONS

Because of their highly interactive nature and their involvement in several simultaneous processes, early expressed transcriptional regulators have always constituted a difficult subject when approached to dissect their molecular mechanisms of action. The nuclear receptor *Nr2f1* makes no exception, as it regulates several cellular programs, sometimes bearing opposite effects in different regions and even at different developmental stages. A possible explanation for such functional differences could reside in the tissue- and time-specific availability of distinct assets of co-factors, through which *Nr2f1* enforces transcriptional regulation of target genes. So far, very few molecular interactors have been reported and, in most cases, it is still difficult to understand whether single or both *Nr2fs* are part of the same regulatory network. Moreover, most studies on *Nr2f* molecular interaction and transcriptional regulation were carried out *in vitro*, where the availability of Nr2f proteins and of their presumptive interacting factors is not closely mimicking physiological conditions (Cooney et al., 1992; Kliewer et al., 1992; Tran et al., 1992). To complement these studies, genome-wide expression analysis of *Nr2f1*-expressing cell populations isolated from distinct brain regions and at different developmental stages is required. This would help to more precisely characterize *Nr2f1*-regulated transcriptional mechanisms and to identify novel targets, in a time- and region-specific manner. Furthermore, mass spectrometry on similar samples would give insights into the identity of elusive co-factors involved in the various regulatory machineries in discrete developmental contexts and brain areas. The use of more physiological systems, such as living human cells, could also improve our understanding of *NR2F1* molecular functioning.

Taking advantage of the high evolutionary conservation of Nr2f proteins among different species, several models have been used in the past to investigate their function *in vivo*. In *D. melanogaster*, for example, the *Nr2f* ortholog seven up (*SVP*) is a key factor for cell identity acquisition in both the central nervous system and the developing eye (Begemann et al., 1995; Kanai et al., 2005; Benito-Sipos et al., 2011). Similarly, the *C. elegans* ortholog UNC55 acts in cell fate determination, enabling the differentiation of two discrete populations of motor neurons (Walthall and Plunkett, 1995; Mimi Zhou and Walthall, 1998; Petersen et al., 2011). Finally, in *X. laevis, xCOUP-TFA* and *B* direct the antero-posterior patterning of the central nervous system (Van Der Wees et al., 1996; Tanibe et al., 2012).

To date, the most employed animal model is by far the mouse, and several different mutant lines have been generated in the attempt to dissect the wide-ranging function of *Nr2f1* during brain development (**Table 1**). Due to the *Nr2f1* pleiotropic nature, the analysis performed in different models occasionally produced contradictory results. We discussed, for example, how a retina-specific conditional *Nr2f1 cKO* model is

TABLE 1 | List of available Nr2f1 mouse models and main related studies.

		Mouse model	Reference(s)	Nr2f1-dependent function(s) and phenotype(s)	Putative corresponding BBSOAS feature(s)
Visual system		***double cKO*** *(Nr2f1 and Nr2f2 floxed) with Rax-Cre*	Tang et al. (2010)	Optic nerve development, optic disc specification and severe coloboma.	Optic disc and optic nerve abnormalities.
		Null mouse *(exon 3 HET and KO)*	Bertacchi et al. (2019a)	RGC apoptosis; optic nerve atrophy, astrogliosis and hypomyelination; affected visual associative learning.	Optic atrophy and cerebral visual impairment.
			Jurkute et al. (2021)	Conduction velocity of visual stimuli; visual acuity in adult mice; RGC density.	Decreased visual acuity, thinning of retinal ganglion cell and nerve fiber layers.
Hippocampal formation	Development	***cKO*** *(Nr2f1 floxed) with Emx1-Cre*	Flore et al. (2016)	Functional organization of the hippocampal septo-temporal longitudinal axis; spatial learning and memory.	Hippocampal malformations.
		(Nr2f1 floxed) with Emx1-Cre or Nex-Cre	Parisot et al. (2017)	Cxcr4-dependent hippocampal development and morphogenesis.	Intellectual disability (common) and hippocampal malrotation (sporadic).
		(Nr2f1 floxed) with Emx1-Cre	Contesse et al. (2019)	Hyperactivity and anxiolytic-like behaviors.	ADHD (common) but also anxiety (rare).
		Null mouse *(exons 1-2 HET)*	Chen et al. (2020)	Hippocampal synaptic plasticity; hearing defects; neonatal hypotonia.	Intellectual disability and unusual long-term memory, neonatal hypotonia and (sporadic) hearing defects.
	Adult	***cKO*** *(Nr2f1 floxed) with Glast-CreERT2 or Ascl1-CreERT2*	Bonzano et al. (2018)	Neuron-astroglia fate decision during adult dentate gyrus neurogenesis.	UNKNOWN
Neocortex	Arealization	***Null mouse*** *(exons 1-2 KO)*	Zhou et al. (2001)	Early regionalization of the neocortex.	UNKNOWN
		(exons 1-2 KO)	Faedo et al. (2008)	Altered signaling pathways in early cortical patterning and neurogenesis.	UNKNOWN
		(exon 3 HET and KO)	Bertacchi et al. (2020)	Progenitor pool amplification by delayed neurogenesis and accelerated cell cycle, caudal cortical expansion.	Malformations of parietal and occipital cortex (dysgyria and elongated occipital convolutions).
		cKO *(Nr2f1 floxed) with Emx1-Cre*	Armentano et al. (2007)	Area specification in neocortical progenitors.	UNKNOWN
		(Nr2f1 floxed) with Emx1-Cre or Nex-Cre ***cKI*** *CAGGS-lox-stop-lox-hCOUP-TFI with Nex-Cre*	Alfano et al. (2014)	Post-mitotic control of area specification.	UNKNOWN
	Electric properties	***cKO*** *(Nr2f1 floxed) with Emx1-Cre*	Del Pino et al. (2020)	Dendrite structure, ion channel expression and electrophysiological intrinsic properties of pyramidal neurons.	Epileptic features.

(Continued)

TABLE 1 | Continued

		Mouse model	Reference(s)	Nr2f1-dependent phenotype(s)	Putative corresponding BBSOAS feature(s)
Neocortex	Connectivity	***Null mouse*** *(exons 1-2 KO)*	Zhou et al. (1999)[#]	Guidance of thalamo-cortical axons and differentiation of subplate neurons.	UNKNOWN
		(exon 3 KO)	Armentano et al. (2006)	Formation of forebrain commissural projections	Hypomorphic corpus callosum.
		cKO *(Nr2f1 floxed) with Emx1-Cre*	Alfano et al. (2011)	Rnd2-dependent radial migration and morphology of upper layer callosal neurons.	Hypomorphic corpus callosum.
	Olfactory bulbs	***cKO*** *(Nr2f1 flox) with Dlx5/6-Cre or Emx1-Cre*	Bovetti et al. (2013)	Activity-dependent tyrosine hydroxylase (TH) expression in adult dopaminergic olfactory bulb interneurons.	UNKNOWN
		double cKO *(Nr2f1 and Nr2f2 flox) with hGFAP-Cre*	Zhou et al. (2015)	Migration and survival of olfactory bulb granule cells.	UNKNOWN
	Ventral pallium	***cKO*** *(Nr2f1 flox) with Dlx5/6-Cre*	Lodato et al. (2011)	Abnormal specification of cortical interneuron subtypes; altered cortical inhibitory circuitry.	Altered brain electrical activity.
			Touzot et al. (2016)	Control of cortical interneuron migratory streams.	Altered brain electrical activity.
	Others	***Null mouse*** *(exons 1-2 KO)*	Qiu et al. (1997)[#]	Defective glossopharyngeal nerve formation; impaired milk suckling and swallowing; perinatal death.	Early feeding problems; oro-motor dysfunction.
		(exons 1-2 KO)	Yamaguchi et al. (2004)[#]	Delayed oligodendrocyte differentiation and abnormal myelin formation.	White matter loss (rare).
		NR2F1-R112K HET mouse	Zhang et al. (2020)	Excitatory/inhibitory neuron imbalance; behavioral social deficits.	Epileptic and autistic-like features.
		cKO *(Nr2f1 floxed) with Emx1-Cre;* ***cKI*** *CAGGS-lox-stop-lox-hCOUP-TFI with Emx1-Cre*	Feng et al. (2021)	Entorhinal cortex specification and regulation of cell adhesion.	UNKNOWN

[#] *In these studies, both WT and HET were used as controls. cKI, conditional knock-in; cKO, conditional knock-out.*

not efficiently reproducing the BBSOAS-like eye development deficits (Tang et al., 2010), as it is instead reported in *Nr2f1 HET* mutants (Bertacchi et al., 2019a). In the latter, the loss of function is not limited to a specific compartment but affects the entire developing organism from very early stages, as in human patients (Bertacchi et al., 2019a). Similarly, a ventral telencephalon *Nr2f*1 c*KO*, which specifically affects the generation of interneurons, did not induce a cortical E/I imbalance, in contrast to the appearance of epileptic episodes in BBSOAS patients and electric dysfunctions observed in a mouse model carrying a human-like mutation in heterozygosity (Lodato et al., 2011; Touzot et al., 2016; Zhang et al., 2020).

Although not being appropriate for studying the BBSOA Syndrome as a whole, conditional *KO* models are valuable tools to dissect the molecular contribution of *Nr2f1* in distinct brain regions and/or different developmental windows. So far, studies employing *cKO* models helped dissecting the involvement of *Nr2f1* during: (i) neocortical arealization, discriminating between early and late functions in progenitor cells and postmitotic neurons (Armentano et al., 2007; Alfano et al., 2014); (ii) generation of specific classes of interneurons from distinct regions of the ganglionic eminences (Lodato et al., 2011; Touzot et al., 2016); (iii) optic disc and retina formation (Tang et al., 2010); and (iv) formation of higher-order cortical visual areas (Chou et al., 2013), among others.

To further dissect the role of Nr2f1 in specific sub-domains during development, it would be interesting to employ *Nr2f1* neocortical layer-specific *cKO*. This would allow the investigation of cell-intrinsic functions of *Nr2f1* in cell maturation and differentiation in different subpopulations, without affecting the early arealization and lamination processes *in toto*. To this purpose, several layer-specific *Cre* mouse lines could be used to assess *Nr2f1* loss either in layer V (Gong et al., 2007; Taniguchi et al., 2011) or layer IV (Liao and Xu, 2008; Abraira et al., 2017). This would allow to evaluate whether the functional (Del Pino et al., 2020) and/or morphological defects (Hou et al., 2019; Del Pino et al., 2020) observed upon removal of *Nr2f1* from the entire pool of cortical progenitor cells are in fact the result of cell-intrinsic mechanisms, or rather a secondary effect of aberrant area and layer formation.

Vice versa, constitutive *HET* mice better recapitulate the complexity and the broad spectrum of developmental defects found in BBSOAS patients. In addition to the use of *HET* models, *constitutive KO* animals (*null*) have been used to further stress the developmental processes and efficiently identify underlying alterations. However, this condition is never observed in human patients, possibly due to foetal or perinatal death. Despite being very accurate in reproducing the symptoms observed in haploinsufficient patients, the *HET* model is still not representative of the entire patient cohort, in which various types of mutations have been identified (spanning from point missense mutations to whole-gene deletions), often corresponding to different degrees of symptom severity. Moreover, genotype-phenotype correlation assessment in human patients shows that whole-gene deletions do not usually lead to the most severe symptoms, hence the *HET* mutant phenotype could be too mild to fully recapitulate the whole BBSOAS spectrum.

A recently developed mouse model, carrying a single copy of a patient-specific mutation (Zhang et al., 2020), seems to be a promising approach, in terms of accuracy and reliability in comparing animal models to BBSOAS patients. It becomes imperative to generate more patient-specific mouse lines and to compare them at the molecular and functional levels, aiming for a better characterization of the genotype-phenotype correlation. However, these models come with their own limitations. For instance, the lissencephalic mouse brain is not suitable for studies on cortical gyrification defects, and the limited pool of murine basal RG cells makes it impossible to study the effects of *Nr2f1* loss on this key population of progenitors. Further, some aspects of cell physiology and biology vary substantially among different species, hence requiring a more human-like model. For this reason, it is necessary to move into *in vitro* human systems, such as 3D brain organoids. The use of brain organoids, coupled with advanced tools of genome editing, such as CRISPR-Cas9, could answer those questions that cannot be investigated in mice. On the other side, being an artificial *in vitro* system, brain organoids come with their own caveats and limitations, such as the lack of cytoarchitecturally-defined layers and areas, and a time-restricted window of investigation, due to their relatively short viability compared to living organisms. In this sense, the combination of *in vivo* animal models and *in vitro* human organoids, each providing its own technical and biological advantages, could be a winning strategy.

In parallel to the studies on animal models, clinical research is advancing our knowledge of BBSOAS features, expanding the list of symptoms as new patients are identified. To date, some aspects of BBSOAS patients are yet to be characterized, and very little is known about their pathological causes. For example, cortical morphology defects have been observed *via* MRI analysis on a small cohort of patients (Bertacchi et al., 2020), and animal models are shown to partially recapitulate such malformations. However, further investigations are required to understand whether this is a shared feature in other patients and evaluate the overall prevalence of these morphological alterations among the whole BBSOAS cohort. Moreover, BBSOAS patients were described to suffer from complex IV deficiency of the mitochondrial respiratory chain (Martín-Hernández et al., 2018), but the overall prevalence of mitochondrial deficits in BBSOAS patients is unknown to date. If present in other patients, it would be interesting to understand whether mitochondrial defects lead to ON atrophy, further impacting RGC physiology (Bertacchi et al., 2019a). Additional investigation using *in vitro* models, such as 2D and 3D cultures of neuronal progenitors, could help elucidate the role of *Nr2f1* in regulating the physiological mechanisms of mitochondrial function, while *in vivo* animal models could help challenge the influence of *Nr2f1* on the general energetic balance of the organism, as a whole.

Overall, the use of experimental models to characterize human diseases, BBSOAS included, is a bidirectional approach. On one hand, human clinical data steer the direction of experimental studies: new patients are identified and reported, new symptoms emerge, and the underlying mechanisms can be investigated in different experimental models. Considering how each model has its both advantages and disadvantages,

only their combination will allow a comprehensive and reliable characterization of the pathology. On the other hand, information obtained in experimental models can direct future clinical explorations and be eventually used by clinicians to reveal novel BBSOAS features linked to *NR2F1* haploinsufficiency. Thus, close interactions between *Nr2f1* studies in animal models and clinical assessment of BBSOAS patients constitute the best approach for advancing our understanding of BBSOAS pathophysiology. Finally, as distinct NDDs have been shown to share common pathological features, a better characterization of BBSOAS causative mechanisms will also benefit the understanding of other NDDs, leading to improved diagnosis and development of personalized therapies for a diversified plethora of patients.

AUTHOR CONTRIBUTIONS

CT and MB contributed equally to the writing and figures of this review. MS revised the text and figures. All authors contributed to the article and approved the submitted version.

FUNDING

This work was funded by the Fondation Recherche Médicale; Equipe FRM 2020 (#EQU202003010222) and by the Fondation Jérôme Lejeune (#1872) to MS; by a PhD contract from Région PACA/Inserm and FRM 4th year PhD to CT.

REFERENCES

Abraira, V. E., Kuehn, E. D., Chirila, A. M., Springel, M. W., Toliver, A. A., Zimmerman, A. L., et al. (2017). The cellular and synaptic architecture of the mechanosensory dorsal horn. *Cell* 168, 295–310.e19. doi: 10.1016/j.cell.2016.12.010

Adam, F., Sourisseau, T., Métivier, R., Le Page, Y., Desbois, C., Michel, D., et al. (2000). COUP-TFI (chicken ovalbumin upstream promoter-transcription factor I) regulates cell migration and axogenesis in differentiating P19 embryonal carcinoma cells. *Mol. Endocrinol.* 14, 1918–1933. doi: 10.1210/mend.14.12.0562

Aghakhani, Y., Kinay, D., Gotman, J., Soualmi, L., Andermann, F., Olivier, A., et al. (2005). The role of periventricular nodular heterotopia in epileptogenesis. *Brain* 128, 641–651. doi: 10.1093/brain/awh388

Alfano, C., and Studer, M. (2013). Neocortical arealization: evolution, mechanisms and open questions. *Dev. Neurobiol.* 73, 411–447. doi: 10.1002/dneu.22067

Alfano, C., Magrinelli, E., Harb, K., Hevner, R. F., and Studer, M. (2014). Postmitotic control of sensory area specification during neocortical development. *Nat. Commun.* 5:5632. doi: 10.1038/ncomms6632

Alfano, C., Viola, L., Heng, J. I. T., Pirozzi, M., Clarkson, M., Flore, G., et al. (2011). COUP-TFI promotes radial migration and proper morphology of callosal projection neurons by repressing Rnd2 expression. *Development* 138, 4685–4697. doi: 10.1242/dev.068031

Alzu'Bi, A., Lindsay, S. J., Harkin, L. F., McIntyre, J., Lisgo, S. N., and Clowry, G. J. (2017). The transcription factors COUP-TFI and COUP-TFII have distinct roles in arealisation and GABAergic interneuron specification in the early human fetal telencephalon. *Cereb. Cortex* 27, 4971–4987. doi: 10.1093/cercor/bhx185

Andreae, L. C., and Burrone, J. (2018). The role of spontaneous neurotransmission in synapse and circuit development. *J. Neurosci. Res.* 96, 354–359. doi: 10.1002/jnr.24154

Antón-Bolaños, N., Espinosa, A., and López-Bendito, G. (2018). Developmental interactions between thalamus and cortex: a true love reciprocal story. *Curr. Opin. Neurobiol.* 52, 33–41. doi: 10.1016/j.psj.2021.101491

Antón-Bolaños, N., Sempere-Ferràndez, A., Guillamón-Vivancos, T., Martini, F. J., Pérez-Saiz, L., Gezelius, H., et al. (2019). Prenatal activity from thalamic neurons governs the emergence of functional cortical maps in mice. *Science* 364, 987–990. doi: 10.1126/science.aav7617

Arai, Y., Pulvers, J. N., Haffner, C., Schilling, B., Nüsslein, I., Calegari, F., et al. (2011). Neural stem and progenitor cells shorten S-phase on commitment to neuron production. *Nat. Commun.* 2, 1–12. doi: 10.1038/ncomms1155

Armentano, M., Chou, S.-J. J., Srubek Tomassy, G., Leingärtner, A., O'Leary, D. D. M., Studer, M., et al. (2007). COUP-TFI regulates the balance of cortical patterning between frontal/motor and sensory areas. *Nat. Neurosci.* 10, 1277–1286. doi: 10.1038/nn1958

Armentano, M., Filosa, A., Andolfi, G., and Studer, M. (2006). COUP-TFI is required for the formation of commissural projections in the forebrain by regulating axonal growth. *Development* 133, 4151–4162. doi: 10.1242/dev.02600

Asami, M., Pilz, G. A., Ninkovic, J., Godinho, L., Schroeder, T., Huttner, W. B., et al. (2011). The role of Pax6 in regulating the orientation and mode of cell division of progenitors in the mouse cerebral cortex. *Development* 138, 5067–5078. doi: 10.1242/dev.074591

Auwerx, J., Baulieu, E., Beato, M., Becker-Andre, M., Burbach, P. H., Camerino, G., et al. (1999). A unified nomenclature system for the nuclear receptor superfamily. *Cell* 97, 161–163. doi: 10.1016/s0092-8674(00)80726-6

Azzarelli, R., Guillemot, F., and Pacary, E. (2015). Function and regulation of Rnd proteins in cortical projection neuron migration. *Front. Neurosci.* 9:19. doi: 10.3389/fnins.2015.00019

Badura, A., Schonewille, M., Voges, K., Galliano, E., Renier, N., Gao, Z., et al. (2013). Climbing fiber input shapes reciprocity of purkinje cell firing. *Neuron* 78, 700–713. doi: 10.1016/j.neuron.2013.03.018

Bani-Yaghoub, M., Tremblay, R. G., Lei, J. X., Zhang, D., Zurakowski, B., Sandhu, J. K., et al. (2006). Role of sox2 in the development of the mouse neocortex. *Dev. Biol.* 295, 52–66. doi: 10.1016/j.ydbio.2006.03.007

Barbieri, A. M., Lupo, G., Bulfone, A., Andreazzoli, M., Mariani, M., Fougerousse, F., et al. (1999). A homeobox gene, vax2, controls the patterning of the eye dorsoventral axis. *Proc. Natl. Acad. Sci. U S A* 96, 10729–10734. doi: 10.1073/pnas.96.19.10729

Barkovich, A. J., Guerrini, R., Kuzniecky, R. I., Jackson, G. D., and Dobyns, W. B. (2012). A developmental and genetic classification for malformations of cortical development: update 2012. *Brain* 135, 1348–1369. doi: 10.1093/brain/aws019

Bedogni, F., Hodge, R. D., Elsen, G. E., Nelson, B. R., Daza, R. A. M., Beyer, R. P., et al. (2010). Tbr1 regulates regional and laminar identity of postmitotic neurons in developing neocortex. *Proc. Natl. Acad. Sci. U S A* 107, 13129–13134. doi: 10.1073/pnas.1002285107

Begemann, G., Michon, A.-M., v.d. Voorn, L., Wepf, R. A., and Mlodzik, M. (1995). The Drosophila orphan nuclear receptor seven-up requires the Ras pathway for its function in photoreceptor determination. *Development* 121, 225–235. Available online at: https://www.researchgate.net/publication/15330732_The_Drosophila_orphan_nuclear_receptor_Seven-up__requires_the__Ras_pathway_for_its_function_in_photoreceptor_determination. Accessed May 14, 2021.

Benito-Sipos, J., Ulvklo, C., Gabilondo, H., Baumgardt, M., Angel, A., Torroja, L., et al. (2011). Seven up acts as a temporal factor during two different stages of neuroblast 5-6 development. *Development* 138, 5311–5320. doi: 10.1242/dev.070946

Bertacchi, M., Gruart, A., Kaimakis, P., Allet, C., Serra, L., Giacobini, P., et al. (2019a). Mouse Nr2f1 haploinsufficiency unveils new pathological mechanisms of a human optic atrophy syndrome. *EMBO Mol. Med.* 11:e10291. doi: 10.15252/emmm.201910291

Bertacchi, M., Parisot, J., and Studer, M. (2019b). The pleiotropic transcriptional regulator COUP-TFI plays multiple roles in neural development and disease. *Brain Res.* 1705, 75–94. doi: 10.1016/j.brainres.2018.04.024

Bertacchi, M., Romano, A. L., Loubat, A., Mau-them, F. T., Willems, M., Faivre, L., et al. (2020). Altered regional progenitor dynamics in the neocortex of a BBSOA disease mouse model. *EMBO J.* 39:e104163. doi: 10.15252/embj.2019104163

Bishop, K. M., Goudreau, G., and O'Leary, D. D. M. (2000). Regulation of area identity in the mammalian neocortex by Emx2 and Pax6. *Science* 288, 344–349. doi: 10.1126/science.288.5464.344

Bishop, K. M., Rubenstein, J. L. R., and O'Leary, D. D. M. (2002). Distinct actions of Emx1, Emx2 and Pax6 in regulating the specification of areas in the developing neocortex. *J. Neurosci.* 22, 7627–7638. doi: 10.1523/JNEUROSCI.22-17-07627.2002

Boillot, M., Lee, C. Y., Allene, C., Leguern, E., Baulac, S., and Rouach, N. (2016). LGI1 acts presynaptically to regulate excitatory synaptic transmission during early postnatal development. *Sci. Rep.* 6:21769. doi: 10.1038/srep21769

Bojanek, E. K., Mosconi, M. W., Guter, S., Betancur, C., Macmillan, C., and Cook, E. H. (2020). Clinical and neurocognitive issues associated with Bosch-Boonstra-Schaaf optic atrophy syndrome: a case study. *Am. J. Med. Genet. Part A* 182, 213–218. doi: 10.1002/ajmg.a.61409

Bonzanni, M., DiFrancesco, J. C., Milanesi, R., Campostrini, G., Castellotti, B., Bucchi, A., et al. (2018). A novel *de novo* HCN1 loss-of-function mutation in genetic generalized epilepsy causing increased neuronal excitability. *Neurobiol. Dis.* 118, 55–63. doi: 10.1016/j.nbd.2018.06.012

Bonzano, S., Crisci, I., Podlesny-Drabiniok, A., Rolando, C., Krezel, W., Studer, M., et al. (2018). Neuron-astroglia cell fate decision in the adult mouse hippocampal neurogenic niche is cell-intrinsically controlled by COUP-TFI *in vivo*. *Cell Rep.* 24, 329–341. doi: 10.1016/j.celrep.2018.06.044

Borello, U., Madhavan, M., Vilinsky, I., Faedo, A., Pierani, A., Rubenstein, J., et al. (2014). Sp8 and COUP-TF1 reciprocally regulate patterning and fgf signaling in cortical progenitors. *Cereb. Cortex* 24, 1409–1421. doi: 10.1093/cercor/bhs412

Borrell, V., and Calegari, F. (2014). Mechanisms of brain evolution: regulation of neural progenitor cell diversity and cell cycle length. *Neurosci. Res.* 86, 14–24. doi: 10.1016/j.neures.2014.04.004

Borrie, S. C., Brems, H., Legius, E., and Bagni, C. (2017). Cognitive dysfunctions in intellectual disabilities: the contributions of the Ras-MAPK and PI3K-AKT-mTOR pathways. *Annu. Rev. Genomics Hum. Genet.* 18, 115–142. doi: 10.1146/annurev-genom-091416-035332

Bosch, D. G., Boonstra, F. N., de Leeuw, N., Pfundt, R., Nillesen, W. M., de Ligt, J., et al. (2016). Novel genetic causes for cerebral visual impairment. *Eur. J. Hum. Genet.* 24, 660–665. doi: 10.1038/ejhg.2015.186

Bosch, D. G. M., Boonstra, F. N., Gonzaga-Jauregui, C., Xu, M., de Ligt, J., Jhangiani, S., et al. (2014). NR2F1 mutations cause optic atrophy with intellectual disability. *Am. J. Hum. Genet.* 94, 303–309. doi: 10.1016/j.ajhg.2014.01.002

Bosch-Bouju, C., Hyland, B. I., and Parr-Brownlie, L. C. (2013). Motor thalamus integration of cortical, cerebellar and basal ganglia information: implications for normal and parkinsonian conditions. *Front. Comput. Neurosci.* 7:163. doi: 10.3389/fncom.2013.00163

Bourgeron, T. (2015). From the genetic architecture to synaptic plasticity in autism spectrum disorder. *Nat. Rev. Neurosci.* 16, 551–563. doi: 10.1038/nrn3992

Bourguet, W., Ruff, M., Chambon, P., Gronemeyer, H., and Moras, D. (1995). Crystal structure of the ligand-binding domain of the human nuclear receptor RXR-α. *Nature* 375, 377–382. doi: 10.1038/375377a0

Bovetti, S., Bonzano, S., Garzotto, D., Giannelli, S. G., Iannielli, A., Armentano, M., et al. (2013). COUP-TFI controls activity-dependent tyrosine hydroxylase expression in adult dopaminergic olfactory bulb interneurons. *Development* 140, 4850–4859. doi: 10.1242/dev.089961

Bower, J. M. (2011). Functional implications of tactile projection patterns to the lateral hemispheres of the cerebellum of the albino rat: the legacy of wally welker. *Ann. N Y Acad. Sci.* 1225, 130–141. doi: 10.1111/j.1749-6632.2011.06020.x

Bower, J. M., and Kassel, J. (1990). Variability in tactile projection patterns to cerebellar folia crus IIa of the norway rat. *J. Comp. Neurol.* 302, 768–778. doi: 10.1002/cne.903020409

Bower, J. M., Beermann, D. H., Gibson, J. M., Shambes, G. M., and Welker, W. (1981). Principles of organization of a cerebro-cerebellar circuit: micromapping the projections from cerebral (SI) to cerebellar (Granule Cell Layer) tactile areas of rats. *Brain Behav. Evol.* 18, 1–18. doi: 10.1159/000121772

Boychuk, J. A., Farrell, J. S., Palmer, L. A., Singleton, A. C., Pittman, Q. J., and Teskey, G. C. (2017). HCN channels segregate stimulation-evoked movement responses in neocortex and allow for coordinated forelimb movements in rodents. *J. Physiol.* 595, 247–263. doi: 10.1113/JP273068

Broadbent, N. J., Squire, L. R., and Clark, R. E. (2004). Spatial memory, recognition memory and the hippocampus. *Proc. Natl. Acad. Sci. U S A* 101, 14515–14520. doi: 10.1073/pnas.0406344101

Brodal, P. (2010). *The Central Nervous System: Structure and function*, 4th edition. USA: Oxford University Press.

Buttitta, L. A., and Edgar, B. A. (2007). Mechanisms controlling cell cycle exit upon terminal differentiation. *Curr. Opin. Cell Biol.* 19, 697–704. doi: 10.1016/j.ceb.2007.10.004

Cadwell, C. R., Bhaduri, A., Mostajo-Radji, M. A., Keefe, M. G., and Nowakowski, T. J. (2019). Development and arealization of the cerebral cortex. *Neuron* 103, 980–1004. doi: 10.1016/j.ceb.2007.10.004

Calegari, F., Haubensak, W., Haffher, C., and Huttner, W. B. (2005). Selective lengthening of the cell cycle in the neurogenic subpopulation of neural progenitor cells during mouse brain development. *J. Neurosci.* 25, 6533–6538. doi: 10.1523/JNEUROSCI.0778-05.2005

Cardoso, C., Boys, A., Parrini, E., Mignon-Ravix, C., McMahon, J. M., Khantane, S., et al. (2009). Periventricular heterotopia, mental retardation and epilepsy associated with 5q14.3–q15 deletion. *Neurology* 72, 784–792. doi: 10.1212/01.wnl.0000336339.08878.2d

Casanova, M. F., Araque, J., Giedd, J., and Rumsey, J. M. (2004). Reduced brain size and gyrification in the brains of dyslexic patients. *J. Child Neurol.* 19, 275–281. doi: 10.1177/088307380401900407

Chapin, J. K., and Lin, C. -S. (1984). Mapping the body representation in the SI cortex of anesthetized and awake rats. *J. Comp. Neurol.* 229, 199–213. doi: 10.1002/cne.902290206

Chen, C. A., Bosch, D. G. M. M., Cho, M. T., Rosenfeld, J. A., Shinawi, M., Lewis, R. A., et al. (2016). The expanding clinical phenotype of Bosch-Boonstra-Schaaf optic atrophy syndrome: 20 new cases and possible genotype-phenotype correlations. *Genet. Med.* 18, 1143–1150. doi: 10.1038/gim.2016.18

Chen, C.-A. A., Wang, W., Pedersen, S. E., Raman, A., Seymour, M. L., Ruiz, F. R., et al. (2020). Nr2f1 heterozygous knockout mice recapitulate neurological phenotypes of Bosch-Boonstra-Schaaf optic atrophy syndrome and show impaired hippocampal synaptic plasticity. *Hum. Mol. Genet.* 29, 705–715. doi: 10.1093/hmg/ddz233

Chou, S.-J., Babot, Z., Leingärtner, A., Studer, M., Nakagawa, Y., and O'Leary, D. D. M. (2013). Geniculocortical input drives genetic distinctions between primary and higher-order visual areas. *Science* 340, 1239–1242. doi: 10.1126/science.1232806

Clowry, G. J., Alzu'bi, A., Harkin, L. F., Sarma, S., Kerwin, J., and Lindsay, S. J. (2018). Charting the protomap of the human telencephalon. *Semin. Cell Dev. Biol.* 76, 3–14. doi: 10.1016/j.semcdb.2017.08.033

Contesse, T., Ayrault, M., Mantegazza, M., Studer, M., and Deschaux, O. (2019). Hyperactive and anxiolytic-like behaviors result from loss of COUP-TFI/Nr2f1 in the mouse cortex. *Genes Brain Behav.* 18:e12556. doi: 10.1111/gbb.12556

Cooney, A. J., Lee, C. T., Lin, S. C., Tsai, S. Y., and Tsai, M. J. (2001). Physiological function of the orphans GCNF and COUP-TF. *Trends Endocrinol. Metab.* 12, 247–251. doi: 10.1016/s1043-2760(01)00424-6

Cooney, A. J., Tsai, S. Y., O'Malley, B. W., and Tsai, M. J. (1992). Chicken ovalbumin upstream promoter transcription factor (COUP-TF) dimers bind to different GGTCA response elements, allowing COUP-TF to repress hormonal induction of the vitamin D3, thyroid hormone and retinoic acid receptors. *Mol. Cell. Biol.* 12, 4153–4163. doi: 10.1128/mcb.12.9.4153-4163.1992

Cristino, A. S., Williams, S. M., Hawi, Z., An, J. Y., Bellgrove, M. A., Schwartz, C. E., et al. (2014). Neurodevelopmental and neuropsychiatric disorders represent an interconnected molecular system. *Mol. Psychiatry* 19, 294–301. doi: 10.1038/mp.2013.16

Dehay, C., and Kennedy, H. (2007). Cell-cycle control and cortical development. *Nat. Rev. Neurosci.* 8, 438–450. doi: 10.1038/nrn2097

Deiner, M. S., Kennedy, T. E., Fazeli, A., Serafini, T., Tessier-Lavigne, M., and Sretavan, D. W. (1997). Netrin-1 and DCC mediate axon guidance locally at the optic disc: loss of function leads to optic nerve hypoplasia. *Neuron* 19, 575–589. doi: 10.1016/s0896-6273(00)80373-6

Del Pino, I., Tocco, C., Magrinelli, E., Marcantoni, A., Ferraguto, C., Tomagra, G., et al. (2020). COUP-TFI/Nr2f1 orchestrates intrinsic neuronal activity during development of the somatosensory cortex. *Cereb. Cortex* 30, 5667–5685. doi: 10.1093/cercor/bhaa137

Du, X., Gao, X., Liu, X., Shen, L., Wang, K., Fan, Y., et al. (2018). Genetic diagnostic evaluation of trio-based whole exome sequencing among children with diagnosed or suspected autism spectrum disorder. *Front. Genet.* 9:594. doi: 10.3389/fgene.2018.00594

Egea, P. F., Mitschler, A., Rochel, N., Ruff, M., Chambon, P., and Moras, D. (2000). Crystal structure of the human RXRα ligand-binding domain bound to its natural ligand: 9-cis retinoic acid. *EMBO J.* 19, 2592–2601. doi: 10.1093/emboj/19.11.2592

Eleuteri, C., Olla, S., Veroni, C., Umeton, R., Mechelli, R., Romano, S., et al. (2017). A staged screening of registered drugs highlights remyelinating drug candidates for clinical trials. *Sci. Rep.* 7:45780. doi: 10.1038/srep 45780

Englund, C., Fink, A., Lau, C., Pham, D., Daza, R. A. M., Bulfone, A., et al. (2005). Pax6, Tbr2 and Tbr1 are expressed sequentially by radial glia, intermediate progenitor cells and postmitotic neurons in developing neocortex. *J. Neurosci.* 25, 247–251. doi: 10.1523/JNEUROSCI.2899-04.2005

Estivill-Torrus, G., Pearson, H., van Heyningen, V., Price, D. J., and Rashbass, P. (2002). Pax6 is required to regulate the cell cycle and the rate of progression from symmetrical to asymmetrical division in mammalian cortical progenitors. *Development* 129, 455–466. doi: 10.1242/dev.129.2.455

Evans, R. M., and Mangelsdorf, D. J. (2014). Nuclear receptors, RXR and the big bang. *Cell* 157, 255–266. doi: 10.1016/j.cell.2014.03.012

Fabri, M., and Burton, H. (1991). Ipsilateral cortical connections of primary somatic sensory cortex in rats. *J. Comp. Neurol.* 311, 405–424. doi: 10.1002/cne.903110310

Faedo, A., Borello, U., and Rubenstein, J. L. R. (2010). Repression of Fgf signaling by sprouty1–2 regulates cortical patterning in two distinct regions and times. *J. Neurosci.* 30, 4015–4023. doi: 10.1523/JNEUROSCI.0307-10.2010

Faedo, A., Tomassy, G. S., Ruan, Y., Teichmann, H., Krauss, S., Pleasure, S. J., et al. (2008). COUP-TFI coordinates cortical patterning, neurogenesis and laminar fate and modulates MAPK/ERK, AKT and β-catenin signaling. *Cereb. Cortex* 18, 2117–2131. doi: 10.1093/cercor/bhm238

Fame, R. M., Macdonald, J. L., Dunwoodie, S. L., Takahashi, E., and Macklis, J. D. (2016). Cited2 regulates neocortical layer II/III generation and somatosensory callosal projection neuron development and connectivity. *J. Neurosci.* 36, 6403–6419. doi: 10.1523/JNEUROSCI.4067-15.2016

Fazel Darbandi, S., Robinson Schwartz, S. E., Q29, Q., Catta-Preta, R., Pai, E. L.-L. L., Mandell, J. D., et al. (2018). Neonatal Tbr1 dosage controls cortical layer 6 connectivity. *Neuron* 100, 831–845.e7. doi: 10.1016/j.neuron.2018.09.027

Feng, J., Hsu, W.-H., Patterson, D., Tseng, C.-S., Hsing, H.-W., Zhuang, Z.-H., et al. (2021). COUP-TFI specifies the medial entorhinal cortex identity and induces differential cell adhesion to determine the integrity of its boundary with neocortex. *Sci. Adv.* 7:eabf6808. doi: 10.1126/sciadv.abf6808

Fishell, G., and Hanashima, C. (2008). Pyramidal neurons grow up and change their mind. *Neuron* 57, 333–338. doi: 10.1016/j.neuron.2008.01.018

Flames, N., Pla, R., Gelman, D. M., Rubenstein, J. L. R., Puelles, L., and Marín, O. (2007). Delineation of multiple subpallial progenitor domains by the combinatorial expression of transcriptional codes. *J. Neurosci.* 27, 9682–9695. doi: 10.1523/JNEUROSCI.2750-07.2007

Flore, G., Di Ruberto, G., Parisot, J., Sannino, S., Russo, F., Illingworth, E. A., et al. (2016). Gradient COUP-TFI expression is required for functional organization of the hippocampal septo-temporal longitudinal axis. *Cereb. Cortex* 27, 1629–1643. doi: 10.1093/cercor/bhv336

Florio, M., and Huttner, W. B. (2014). Neural progenitors, neurogenesis and the evolution of the neocortex. *Development* 141, 2182–2194. doi: 10.1242/dev.090571

Foglio, B., Rossini, L., Garbelli, R., Regondi, M. C., Mercurio, S., Bertacchi, M., et al. (2021). Dynamic expression of NR2F1 and SOX2 in developing and adult human cortex: comparison with cortical malformations. *Brain Struct. Funct.* 226, 1303–1322. doi: 10.1007/s00429-021-02242-7

Fukuchi-Shimogori, T., and Grove, E. A. (2001). Neocortex patterning by the secreted signaling molecute FGF8. *Science* 294, 1071–1074. doi: 10.1126/science.1064252

Furukawa, T., Kozak, C. A., and Cepko, C. L. (1997). rax, a novel paired-type homeobox gene, shows expression in the anterior neural fold and developing retina. *Proc. Natl. Acad. Sci. U S A* 94, 3088–3093. doi: 10.1073/pnas.94.7.3088

Gallais, R., Demay, F., Barath, P., Finot, L., Jurkowska, R., Le Guével, R., et al. (2007). Deoxyribonucleic acid methyl transferases 3a and 3b associate with the nuclear orphan receptor COUP-TFI during gene activation. *Mol. Endocrinol.* 21, 2085–2098. doi: 10.1210/me.2006-0490

Garel, S., Huffman, K. J., and Rubenstein, J. L. R. (2003). Molecular regionalization of the neocortex is disrupted in Fgf8 hypomorphic mutants. *Development* 130, 1903–1914. doi: 10.1242/dev.00416

Georgala, P. A., Manuel, M., and Price, D. J. (2011). The generation of superficial cortical layers is regulated by levels of the transcription factor Pax6. *Cereb. Cortex* 21, 81–94. doi: 10.1093/cercor/bhq061

Germain, P., Staels, B., Dacquet, C., Spedding, M., and Laudet, V. (2006). Overview of nomenclature of nuclear receptors. *Pharmacol. Rev.* 58, 685–704. doi: 10.1124/pr.58.4.2

Golonzhka, O., Nord, A., Tang, P. L. F., Lindtner, S., Ypsilanti, A. R., Ferretti, E., et al. (2015). Pbx regulates patterning of the cerebral cortex in progenitors and postmitotic neurons. *Neuron* 88, 1192–1207. doi: 10.1016/j.neuron.2015.10.045

Gong, S., Doughty, M., Harbaugh, C. R., Cummins, A., Hatten, M. E., Heintz, N., et al. (2007). Targeting Cre recombinase to specific neuron populations with bacterial artificial chromosome constructs. *J. Neurosci.* 27, 9817–9823. doi: 10.1523/JNEUROSCI.2707-07.2007

Greig, L. C., Woodworth, M. B., Galazo, M. J., Padmanabhan, H., and Macklis, J. D. (2013). Molecular logic of neocortical projection neuron specification, development and diversity. *Nat. Rev. Neurosci.* 14, 755–769. doi: 10.1038/nrn3586

Greig, L. C., Woodworth, M. B., Greppi, C., and Macklis, J. D. (2016). Ctip1 controls acquisition of sensory area identity and establishment of sensory input fields in the developing neocortex. *Neuron* 90, 261–277. doi: 10.1016/j.neuron.2016.03.008

Grove, E. A., and Fukuchi-Shimogori, T. (2003). Generating the cerebral cortical area map. *Annu. Rev. Neurosci.* 26, 355–380. doi: 10.1146/annurev.neuro.26.041002.131137

Guerrini, R., and Dobyns, W. B. (2014). Malformations of cortical development: clinical features and genetic causes. *Lancet Neurol.* 13, 710–726. doi: 10.1016/S1474-4422(14)70040-7

Guerrini, R., and Parrini, E. (2010). Neuronal migration disorders. *Neurobiol. Dis.* 38, 154–166. doi: 10.1016/j.nbd.2009.02.008

Guerrini, R., Cardoso, C., Boys, A., Parrini, E., Mignon-Ravix, C., McMahon, J. M., et al. (2009). Periventricular heterotopia, mental retardation and epilepsy associated with 5q14.3–q15 deletion. *Neurology* 72, 784–792. doi: 10.1212/01.wnl.0000336339.08878.2d

Guo, J.-Z., Sauerbrei, B. A., Cohen, J. D., Mischiati, M., Graves, A. R., Pisanello, F., et al. (2021). Disrupting cortico-cerebellar communication impairs dexterity. *eLife* 10:e65906. doi: 10.7554/eLife.65906

Hamasaki, T., Leingärtner, A., Ringstedt, T., and O'Leary, D. D. M. (2004). EMX2 regulates sizes and positioning of the primary sensory and motor areas in neocortex by direct specification of cortical progenitors. *Neuron* 43, 359–372. doi: 10.1016/j.neuron.2004.07.016

Hannula, D. E., Libby, L. A., Yonelinas, A. P., and Ranganath, C. (2013). Medial temporal lobe contributions to cued retrieval of items and contexts. *Neuropsychologia* 51, 2322–2332. doi: 10.1016/j.neuropsychologia.2013.02.011

Hansen, D. V., Lui, J. H., Parker, P. R. L., and Kriegstein, A. R. (2010). Neurogenic radial glia in the outer subventricular zone of human neocortex. *Nature* 464, 554–561. doi: 10.1038/nature08845

Harb, K., Magrinelli, E., Nicolas, C. S., Lukianets, N., Frangeul, L., Pietri, M., et al. (2016). Area-specific development of distinct projection neuron subclasses is regulated by postnatal epigenetic modifications. *eLife* 5:e09531. doi: 10.7554/eLife.09531

Harlow, D. E., Honce, J. M., and Miravalle, A. A. (2015). Remyelination therapy in multiple sclerosis. *Front. Neurol.* 6:257. doi: 10.3389/fneur.2015.00257

Heldring, N., Joseph, B., Hermanson, O., and Kioussi, C. (2013). Pitx2 expression promotes p21 expression and cell cycle exit in neural stem cells. *CNS Neurol. Disord. Drug Targets* 11, 884–892. doi: 10.2174/1871527311201070884

Hernandez, M. R., Miao, H., and Lukas, T. (2008). Astrocytes in glaucomatous optic neuropathy. *Prog. Brain Res.* 173, 353–373. doi: 10.1016/S0079-6123(08)01125-4

Hori, K., Nagai, T., Shan, W., Sakamoto, A., Taya, S., Hashimoto, R., et al. (2014). Cytoskeletal regulation by AUTS2 in neuronal migration

and neuritogenesis. *Cell Rep.* 9, 2166–2179. doi: 10.1016/j.celrep.2014.11.045

Hormozdiari, F., Penn, O., Borenstein, E., and Eichler, E. E. (2015). The discovery of integrated gene networks for autism and related disorders. *Genome Res.* 25, 142–154. doi: 10.1101/gr.178855.114

Hou, P. S., Miyoshi, G., and Hanashima, C. (2019). Sensory cortex wiring requires preselection of short- and long-range projection neurons through an Egr-Foxg1-COUP-TFI network. *Nat. Commun.* 10:3581. doi: 10.1038/s41467-019-11043-w

Huang, T. N., and Hsueh, Y. P. (2015). Brain-specific transcriptional regulator T-brain-1 controls brain wiring and neuronal activity in autism spectrum disorders. *Front. Neurosci.* 9:406. doi: 10.3389/fnins.2015.00406

Huang, Z., Kawase-Koga, Y., Zhang, S., Visvader, J., Toth, M., Walsh, C. A., et al. (2009). Transcription factor Lmo4 defines the shape of functional areas in developing cortices and regulates sensorimotor control. *Dev. Biol.* 327, 132–142. doi: 10.1016/j.ydbio.2008.12.003

Hwung, Y. P., Wang, L. H., Tsai, S. Y., and Tsai, M. J. (1988). Differential binding of the chicken ovalbumin upstream promoter (COUP) transcription factor to two different promoters. *J. Biol. Chem.* 263, 13470–13474.

Inoue, M., Iida, A., Satoh, S., Kodama, T., and Watanabe, S. (2010). COUP-TFI and -TFII nuclear receptors are expressed in amacrine cells and play roles in regulating the differentiation of retinal progenitor cells. *Exp. Eye Res.* 90, 49–56. doi: 10.1016/j.exer.2009.09.009

Jabaudon, D. (2017). Fate and freedom in developing neocortical circuits. *Nat. Commun.* 8:16042. doi: 10.1038/ncomms16042

Jansen, A., and Andermann, E. (2005). Genetics of the polymicrogyria syndromes. *J. Med. Genet.* 42, 369–378. doi: 10.1136/jmg.2004.023952

Joshi, P. S., Molyneaux, B. J., Feng, L., Xie, X., Macklis, J. D., and Gan, L. (2008). Bhlhb5 regulates the postmitotic acquisition of area identities in layers II-V of the developing neocortex. *Neuron* 60, 258–272. doi: 10.1016/j.neuron.2008.08.006

Juric-Sekhar, G., and Hevner, R. F. (2019). Malformations of cerebral cortex development: molecules and mechanisms. *Annu. Rev. Pathol.* 14, 293–318. doi: 10.1146/annurev-pathmechdis-012418-012927

Jurkute, N., Bertacchi, M., Arno, G., Tocco, C., Kim, U. S., Kruszewski, A. M., et al. (2021). Pathogenic NR2F1 variants cause a developmental ocular phenotype recapitulated in a mutant mouse model. *Brain Commun.* 3:fcab162. doi: 10.1093/braincomms/fcab162

Kaiwar, C., Zimmermann, M. T., Ferber, M. J., Niu, Z., Urrutia, R. A., Klee, E. W., et al. (2017). Novel NR2F1 variants likely disrupt DNA binding: molecular modeling in two cases, review of published cases, genotype-phenotype correlation and phenotypic expansion of the Bosch-Boonstra-Schaaf optic atrophy syndrome. *Cold Spring Harb. Mol. Case Stud.* 3:a002162. doi: 10.1101/mcs.a002162

Kanai, M. I., Okabe, M., and Hiromi, Y. (2005). Seven-up controls switching of transcription factors that specify temporal identities of *Drosophila* neuroblasts. *Dev. Cell* 8, 203–213. doi: 10.1016/j.devcel.2004.12.014

Kelava, I., Lewitus, E., and Huttner, W. B. (2013). The secondary loss of gyrencephaly as an example of evolutionary phenotypical reversal. *Front. Neuroanat.* 7:16. doi: 10.3389/fnana.2013.00016

Kelleher, R. J., and Bear, M. F. (2008). The autistic neuron: troubled translation. *Cell* 135, 401–406. doi: 10.1016/j.cell.2008.10.017

Khandelwal, N., Cavalier, S., Rybalchenko, V., Kulkarni, A., Anderson, A. G., Konopka, G., et al. (2021). FOXP1 negatively regulates intrinsic excitability in D2 striatal projection neurons by promoting inwardly rectifying and leak potassium currents. *Mol. Psychiatry* 26, 1761–1774. doi: 10.1038/s41380-020-00995-x

Kheirbek, M. A., Drew, L. J., Burghardt, N. S., Costantini, D. O., Tannenholz, L., Ahmari, S. E., et al. (2013). Differential control of learning and anxiety along the dorsoventral axis of the dentate gyrus. *Neuron* 77, 955–968. doi: 10.1016/j.neuron.2012.12.038

Kirischuk, S., Sinning, A., Blanquie, O., Yang, J. W., Luhmann, H. J., and Kilb, W. (2017). Modulation of neocortical development by early neuronal activity: physiology and pathophysiology. *Front. Cell. Neurosci.* 11:379. doi: 10.3389/fncel.2017.00379

Kirkby, L. A., Sack, G. S., Firl, A., and Feller, M. B. (2013). A role for correlated spontaneous activity in the assembly of neural circuits. *Neuron* 80, 1129–1144. doi: 10.1016/j.neuron.2013.10.030

Kliewer, S. A., Umesono, K., Heyman, R. A., Mangelsdorf, D. J., Dyck, J. A., and Evans, R. M. (1992). Retinoid X receptor-COUP-TF interactions modulate retinoic acid signaling. *Proc. Natl. Acad. Sci. U S A* 89, 1448–1452. doi: 10.1073/pnas.89.4.1448

Kruse, S. W., Suino-Powell, K., Zhou, X. E., Kretschman, J. E., Reynolds, R., Vonrhein, C., et al. (2008). Identification of COUP-TFII orphan nuclear receptor as a retinoic acid-activated receptor. *PLoS Biol.* 6:e227. doi: 10.1371/journal.pbio.0060227

Kumaran, D., and Maguire, E. A. (2005). The human hippocampus: cognitive maps or relational memory. *J. Neurosci.* 25, 7254–7259. doi: 10.1523/JNEUROSCI.1103-05.2005

Lange, C., Huttner, W. B., and Calegari, F. (2009). Cdk4/CyclinD1 overexpression in neural stem cells shortens G1, delays neurogenesis and promotes the generation and expansion of basal progenitors. *Cell Stem Cell* 5, 320–331. doi: 10.1016/j.stem.2009.05.026

Lebed, E., Jacova, C., Wang, L., and Beg, M. F. (2013). Novel surface-smoothing based local gyrification index. *IEEE Trans. Med. Imaging* 32, 660–669. doi: 10.1109/TMI.2012.2230640

Lee, A. R., Kim, J. H., Cho, E., Kim, M., and Park, M. (2017). Dorsal and ventral hippocampus differentiate in functional pathways and differentially associate with neurological disease-related genes during postnatal development. *Front. Mol. Neurosci.* 10:331. doi: 10.3389/fnmol.2017.00331

Lein, E. S., Hawrylycz, M. J., Ao, N., Ayres, M., Bensinger, A., Bernard, A., et al. (2007). Genome-wide atlas of gene expression in the adult mouse brain. *Nature* 445, 168–176. doi: 10.1038/nature05453

Leng, X., Cooney, A. J., Tsai, S. Y., and Tsai, M. J. (1996). Molecular mechanisms of COUP-TF-mediated transcriptional repression: evidence for transrepression and active repression. *Mol. Cell. Biol.* 16, 2332–2340. doi: 10.1128/MCB.16.5.2332

Leonardo, E. D., Richardson-Jones, J. W., Sibille, E., Kottman, A., and Hen, R. (2006). Molecular heterogeneity along the dorsal-ventral axis of the murine hippocampal CA1 field: a microarray analysis of gene expression. *Neuroscience* 137, 177–186. doi: 10.1016/j.neuroscience.2005.08.082

Leterrier, C. (2018). The axon initial segment: an updated viewpoint. *J. Neurosci.* 38, 2135–2145. doi: 10.1016/j.neuroscience.2005.08.082

Li, H., Fertuzinhos, S., Mohns, E., Hnasko, T. S., Verhage, M., Edwards, R., et al. (2013). Laminar and columnar development of barrel cortex relies on thalamocortical neurotransmission. *Neuron* 79, 970–986. doi: 10.1016/j.neuron.2013.06.043

Liao, G. Y., and Xu, B. (2008). Cre recombinase-mediated gene deletion in layer 4 of murine sensory cortical areas. *Genesis* 46, 289–293. doi: 10.1002/dvg.20393

Lin, J. J., Salamon, N., Lee, A. D., Dutton, R. A., Geaga, J. A., Hayashi, K. M., et al. (2007). Reduced neocortical thickness and complexity mapped in mesial temporal lobe epilepsy with hippocampal sclerosis. *Cereb. Cortex* 17, 2007–2018. doi: 10.1093/cercor/bhl109

Liu, Q., Dwyer, N. D., and O'Leary, D. D. M. (2000). Differential expression of COUP-TFI, CHL1 and two novel genes in developing neocortex identified by differential display PCR. *J. Neurosci.* 20, 7682–7690. doi: 10.1523/JNEUROSCI.20-20-07682.2000

Lodato, S., Tomassy, G. S., De Leonibus, E., Uzcategui, Y. G., Andolfi, G., Armentano, M., et al. (2011). Loss of COUP-TFI alters the balance between caudal ganglionic eminence- and medial ganglionic eminence-derived cortical interneurons and results in resistance to epilepsy. *J. Neurosci.* 31, 4650–4662. doi: 10.1523/JNEUROSCI.6580-10.2011

Luhmann, H. J., and Khazipov, R. (2018). Neuronal activity patterns in the developing barrel cortex. *Neuroscience* 368, 4650–4662. doi: 10.1016/j.neuroscience.2017.05.025

Lukaszewicz, A., Savatier, P., Cortay, V., Giroud, P., Huissoud, C., Berland, M., et al. (2005). G1 phase regulation, area-specific cell cycle control and cytoarchitectonics in the primate cortex. *Neuron* 47, 353–364. doi: 10.1016/j.neuron.2005.06.032

Mátéffyová, A., Otáhal, J., Tsenov, G., Mareš, P., and Kubová, H. (2006). Intrahippocampal injection of endothelin-1 in immature rats results in neuronal death, development of epilepsy and behavioral abnormalities later in life. *Eur. J. Neurosci.* 24, 351–360. doi: 10.1111/j.1460-9568.2006.04910.x

Malkowicz, D., Myers, G., and Leisman, G. (2006). Rehabilitation of cortical visual impairment in children. *Int. J. Neurosci.* 116, 1015–1033. doi: 10.1080/00207450600553505

Mallamaci, A., Muzio, L., Chan, C. H., Parnavelas, J., and Boncinelli, E. (2000). Area identity shifts in the early cerebral cortex of Emx2(-/-) mutant mice. *Nat. Neurosci.* 3, 679–686. doi: 10.1038/76630

Manuel, M., Georgala, P. A., Carr, C. B., Chanas, S., Kleinjan, D. A., Martynoga, B., et al. (2007). Controlled overexpression of Pax6 *in vivo* negatively auto-regulates the Pax6 locus, causing cell-autonomous defects of late cortical progenitor proliferation with little effect on cortical arealization. *Development* 134, 545–555. doi: 10.1242/dev.02764

Manzini, M. C., and Walsh, C. A. (2011). What disorders of cortical development tell us about the cortex: one plus one does not always make two. *Curr. Opin. Genet. Dev.* 21, 333–339. doi: 10.1016/j.gde.2011.01.006

Marini, C., Porro, A., Rastetter, A., Dalle, C., Rivolta, I., Bauer, D., et al. (2018). HCN1 mutation spectrum: from neonatal epileptic encephalopathy to benign generalized epilepsy and beyond. *Brain* 41, 3160–3178. doi: 10.1093/brain/awy263

Martín-Hernández, E., Rodríguez-García, M. E., Chen, C.-A., Cotrina-Vinagre, F. J., Carnicero-Rodríguez, P., Bellusci, M., et al. (2018). Mitochondrial involvement in a Bosch-Boonstra-Schaaf optic atrophy syndrome patient with a novel *de novo* NR2F1 gene mutation. *J. Hum. Genet.* 63, 525–528. doi: 10.1001/jamanetworkopen.2021.31012

Martynoga, B., Morrison, H., Price, D. J., and Mason, J. O. (2005). Foxg1 is required for specification of ventral telencephalon and region-specific regulation of dorsal telencephalic precursor proliferation and apoptosis. *Dev. Biol.* 283, 113–127. doi: 10.1016/j.ydbio.2005.04.005

Mercurio, S., Alberti, C., Serra, L., Meneghini, S., Berico, P., Bertolini, J., et al. (2021). An early Sox2-dependent gene expression programme required for hippocampal dentate gyrus development. *Open Biol.* 11:200339. doi: 10.1098/rsob.200339

Mi, D., Carr, C. B., Georgala, P. A., Huang, Y. T., Manuel, M. N., Jeanes, E., et al. (2013). Pax6 exerts regional control of cortical progenitor proliferation *via* direct repression of Cdk6 and hypophosphorylation of pRb. *Neuron* 78, 269–284. doi: 10.1016/j.neuron.2013.02.012

Mimi Zhou, H., and Walthall, W. W. (1998). UNC-55, an orphan nuclear hormone receptor, orchestrates synaptic specificity among two classes of motor neurons in Caenorhabditis elegans. *J. Neurosci.* 18, 10438–10444. doi: 10.1523/JNEUROSCI.18-24-10438.1998

Mitchell, T. N., Free, S. L., Williamson, K. A., Stevens, J. M., Churchill, A. J., Hanson, I. M., et al. (2003). Polymicrogyria and absence of pineal gland due toPAX6 mutation. *Ann. Neurol.* 53, 658–663. doi: 10.1002/ana.10576

Molnár, Z., Clowry, G. J., Šestan, N., Alzu'bi, A., Bakken, T., Hevner, R. F., et al. (2019). New insights into the development of the human cerebral cortex. *J. Anat.* 235, 432–451. doi: 10.1111/joa.13055

Montemayor, C., Montemayor, O. A., Ridgeway, A., Lin, F., Wheeler, D. A., Pletcher, S. D., et al. (2010). Genome-wide analysis of binding sites and direct target genes of the orphan nuclear receptor NR2F1/COUP-TFI. *PLoS One* 5:e8910. doi: 10.1371/journal.pone.0008910

Moser, M. B., Moser, E. I., Forrest, E., Andersen, P., and Morris, R. G. M. (1995). Spatial learning with a minislab in the dorsal hippocampus. *Proc. Natl. Acad. Sci. U S A* 92, 9697–9701. doi: 10.1073/pnas.92.21.9697

Mottolese, C., Richard, N., Harquel, S., Szathmari, A., Sirigu, A., and Desmurget, M. (2013). Mapping motor representations in the human cerebellum. *Brain* 136, 330–342. doi: 10.1093/brain/aws186

Mui, S. H., Kim, J. W., Lemke, G., and Bertuzzi, S. (2005). Vax genes ventralize the embryonic eye. *Genes Dev.* 19, 1249–1259. doi: 10.1101/gad.1276605

Murase, S., Lantz, C. L., Kim, E., Gupta, N., Higgins, R., Stopfer, M., et al. (2016). Matrix metalloproteinase-9 regulates neuronal circuit development and excitability. *Mol. Neurobiol.* 53, 3477–3493. doi: 10.1007/s12035-015-9295-y

Najm, F. J., Madhavan, M., Zaremba, A., Shick, E., Karl, R. T., Factor, D. C., et al. (2015). Drug-based modulation of endogenous stem cells promotes functional remyelination *in vivo*. *Nature* 522, 216–220. doi: 10.1038/nature14335

Naka, H., Nakamura, S., Shimazaki, T., and Okano, H. (2008). Requirement for COUP-TFI and II in the temporal specification of neural stem cells in CNS development. *Nat. Neurosci.* 11, 1014–1023. doi: 10.1038/nn.2168

Nonaka-Kinoshita, M., Reillo, I., Artegiani, B., Ángeles Martínez-Martínez, M., Nelson, M., Borrell, V., et al. (2013). Regulation of cerebral cortex size and folding by expansion of basal progenitors. *EMBO J.* 32, 1817–1828. doi: 10.1038/emboj.2013.96

Nowakowski, T. J., Pollen, A. A., Sandoval-Espinosa, C., and Kriegstein, A. R. (2016). Transformation of the radial glia scaffold demarcates two stages of human cerebral cortex development. *Neuron* 91, 1219–1227. doi: 10.1016/j.neuron.2016.09.005

O'Leary, D. D. M., Chou, S. J., and Sahara, S. (2007). Area patterning of the mammalian cortex. *Neuron* 56, 252–269. doi: 10.1055/a-1678-3381

O'Leary, D. D. M., and Nakagawa, Y. (2002). Patterning centers, regulatory genes and extrinsic mechanisms controlling arealization of the neocortex. *Curr. Opin. Neurobiol.* 12, 14–25. doi: 10.1055/a-1678-3381

O'Leary, D. D. M., and Sahara, S. (2008). Genetic regulation of arealization of the neocortex. *Curr. Opin. Neurobiol.* 18, 90–100. doi: 10.1055/a-1678-3381

O'Reilly, K. C., Flatberg, A., Islam, S., Olsen, L. C., Kruge, I. U., and Witter, M. P. (2015). Identification of dorsal-ventral hippocampal differentiation in neonatal rats. *Brain Struct. Funct.* 220, 2873–2893. doi: 10.1055/a-1678-3381

Oberhuber, M., Hope, T. M. H., Seghier, M. L., Parker Jones, O., Prejawa, S., Green, D. W., et al. (2016). Four functionally distinct regions in the left supramarginal gyrus support word processing. *Cereb. Cortex* 26, 4212–4226. doi: 10.1093/cercor/bhw251

Okano, H., and Temple, S. (2009). Cell types to order: temporal specification of CNS stem cells. *Curr. Opin. Neurobiol.* 19, 112–119. doi: 10.1016/j.conb.2009.04.003

Ono, K., Yoshii, K., Tominaga, H., Gotoh, H., Nomura, T., Takebayashi, H., et al. (2017). Oligodendrocyte precursor cells in the mouse optic nerve originate in the preoptic area. *Brain Struct. Funct.* 222, 2441–2448. doi: 10.1007/s00429-017-1394-2

Parenti, I., Rabaneda, L. G., Schoen, H., and Novarino, G. (2020). Neurodevelopmental disorders: from genetics to functional pathways. *Trends Neurosci.* 43, 608–621. doi: 10.1016/j.tins.2020.05.004

Parisot, J., Flore, G., Bertacchi, M., and Studer, M. (2017). COUP-TFI mitotically regulates production and migration of dentate granule cells and modulates hippocampal Cxcr4 expression. *Development* 144, 2045–2058. doi: 10.1242/dev.139949

Parrini, E., Conti, V., Dobyns, W. B., and Guerrini, R. (2016). Genetic basis of brain malformations. *Mol. Syndromol.* 7, 220–233. doi: 10.1159/000448639

Pastorcic, M., Wang, H., Elbrecht, A., Tsai, S. Y., Tsai, M. J., and O'Malley, B. W. (1986). Control of transcription initiation *in vitro* requires binding of a transcription factor to the distal promoter of the ovalbumin gene. *Mol. Cell. Biol.* 6, 2784–2791. doi: 10.1128/mcb.6.8.2784-2791.1986

Pattabiraman, K., Golonzhka, O., Lindtner, S., Nord, A. S., Taher, L., Hoch, R., et al. (2014). Transcriptional regulation of enhancers active in protodomains of the developing cerebral cortex. *Neuron* 82, 989–1003. doi: 10.1016/J.Neuron.2014.04.014

Pekny, M., Wilhelmsson, U., and Pekna, M. (2014). The dual role of astrocyte activation and reactive gliosis. *Neurosci. Lett.* 565, 30–38. doi: 10.1016/j.neulet.2013.12.071

Pereira, F. A., Tsai, M. J., and Tsai, S. Y. (2000). COUP-TF orphan nuclear receptors in development and differentiation. *Cell. Mol. Life Sci.* 57, 1388–1398. doi: 10.1007/PL00000624

Petersen, S. C., Watson, J. D., Richmond, J. E., Sarov, M., Walthall, W. W., and Miller, D. M. (2011). A transcriptional program promotes remodeling of GABAergic synapses in Caenorhabditis elegans. *J. Neurosci.* 31, 15362–15375. doi: 10.1523/JNEUROSCI.3181-11.2011

Philip, S. S., and Dutton, G. N. (2014). Identifying and characterising cerebral visual impairment in children: a review. *Clin. Exp. Optom.* 97, 196–208. doi: 10.1111/cxo.12155

Pilz, G. A., Shitamukai, A., Reillo, I., Pacary, E., Schwausch, J., Stahl, R., et al. (2013). Amplification of progenitors in the mammalian telencephalon includes a new radial glial cell type. *Nat. Commun.* 4:2125. doi: 10.1038/ncomms3125

Pipaón, C., Tsai, S. Y., and Tsai, M. J. (1999). COUP-TF upregulates NGFI-A gene expression through an Sp1 binding site. *Mol. Cell. Biol.* 19, 2734–2745. doi: 10.3389/fpsyg.2021.732865

Pollen, A. A., Nowakowski, T. J., Chen, J., Retallack, H., Sandoval-Espinosa, C., Nicholas, C. R., et al. (2015). Molecular identity of human outer radial

glia during cortical development. *Cell* 163, 55–67. doi: 10.1016/j.cell.2015.09.004

Porcu, G., Serone, E., De Nardis, V., Di Giandomenico, D., Lucisano, G., Scardapane, M., et al. (2015). Clobetasol and halcinonide act as smoothened agonists to promote myelin gene expression and RxRγ receptor activation. *PLoS One* 10:e0144550. doi: 10.1371/journal.pone.0144550

Powell, E. M. (2013). Interneuron development and epilepsy: early genetic defects cause long-term consequences in seizures and susceptibility. *Epilepsy Curr.* 13, 172–176. doi: 10.5698/1535-7597-13.4.172

Qiu, Y., Cooney, A. J., Kuratani, S., DeMayo, F. J., Tsai, S. Y., and Tsai, M. J. (1994). Spatiotemporal expression patterns of chicken ovalbumin upstream promoter-transcription factors in the developing mouse central nervous system: evidence for a role in segmental patterning of the diencephalon. *Proc. Natl. Acad. Sci. U S A* 91, 4451–4455. doi: 10.1073/pnas.91.10.4451

Qiu, Y., Krishnan, V., Zeng, Z., Gilbert, D. J., Copeland, N. G., Gibson, L., et al. (1995). Isolation, characterization and chromosomal localization of mouse and human COUP-TF I and II Genes. *Genomics* 29, 240–246. doi: 10.1006/geno.1995.1237

Qiu, Y., Pereira, F. A., DeMayo, F. J., Lydon, J. P., Tsai, S. Y., and Tsai, M. J. (1997). Null mutation of mCOUP-TFI results in defects in morphogenesis of the glossopharyngeal ganglion, axonal projection and arborization. *Genes Dev.* 11, 1925–1937. doi: 10.1101/gad.11.15.1925

Rakic, P., Ayoub, A. E., Breunig, J. J., and Dominguez, M. H. (2009). Decision by division: making cortical maps. *Trends Neurosci.* 32, 291–301. doi: 10.1016/j.tins.2009.01.007

Ramos, J. M. J. (2008). Hippocampal damage impairs long-term spatial memory in rats: Comparison between electrolytic and neurotoxic lesions. *Physiol. Behav.* 93, 1078–1085. doi: 10.1016/j.physbeh.2008.01.004

Rech, M. E., McCarthy, J. M., Chen, C. A., Edmond, J. C., Shah, V. S., Bosch, D. G. M., et al. (2020). Phenotypic expansion of Bosch-Boonstra-Schaaf optic atrophy syndrome and further evidence for genotype-phenotype correlations. *Am. J. Med. Genet. Part A* 182, 1426–1437. doi: 10.1002/ajmg.a.61580

Reillo, I., De Juan Romero, C., García-Cabezas, M. Á., and Borrell, V. (2011). A Role for intermediate radial glia in the tangential expansion of the mammalian cerebral cortex. *Cereb. Cortex* 21, 1674–1694. doi: 10.1093/cercor/bhq238

Reinchisi, G., Ijichi, K., Glidden, N., Jakovcevski, I., and Zecevic, N. (2012). COUP-TFII expressing interneurons in human fetal forebrain. *Cereb. Cortex* 22, 2820–2830. doi: 10.1093/cercor/bhr359

Rodríguez-Tornos, F. M., Briz, C. G., Weiss, L. A., Sebastián-Serrano, A., Ares, S., Navarrete, M., et al. (2016). Cux1 enables interhemispheric connections of layer II/III neurons by regulating Kv1-dependent firing. *Neuron* 89, 494–506. doi: 10.1016/j.neuron.2015.12.020

Ronan, J. L., Wu, W., and Crabtree, G. R. (2013). From neural development to cognition: unexpected roles for chromatin. *Nat. Rev. Genet.* 14, 347–359. doi: 10.1038/nrg3413

Rubenstein, J. L. R., and Rakic, P. (1999). Genetic control of cortical development. *Cereb. Cortex* 9, 521–523. doi: 10.1093/cercor/9.6.521

Runge, K., Mathieu, R., Bugeon, S., Lafi, S., Beurrier, C., Sahu, S., et al. (2021). Disruption of NEUROD2 causes a neurodevelopmental syndrome with autistic features *via* cell-autonomous defects in forebrain glutamatergic neurons. *Mol. Psychiatry* doi: 10.1038/s41380-021-01234-7. [Online ahead of print].

Südhof, T. C. (2018). Towards an understanding of synapse formation. *Neuron* 100, 276–293. doi: 10.1016/j.neuron.2018.09.040 [Online ahead of Print].

Sagami, I., Tsai, S. Y., Wang, H., Tsai, M. J., and O'Malley, B. W. (1986). Identification of two factors required for transcription of the ovalbumin gene. *Mol. Cell. Biol.* 6, 4259–4267. doi: 10.1128/mcb.6.12.4259-4267.1986

Sahara, S., Kawakami, Y., Belmonte, J. C. I., and O'Leary, D. D. M. (2007). Sp8 exhibits reciprocal induction with Fgf8 but has an opposing effect on anterior-posterior cortical area patterning. *Neural Dev.* 2:10. doi: 10.1186/1749-8104-2-10

Sahin, M., and Sur, M. (2015). Genes, circuits and precision therapies for autism and related neurodevelopmental disorders. *Science* 350:aab3897. doi: 10.1126/science.aab3897

Samson, S. N., Hébert, J. M., Thammongkol, U., Smith, J., Nisbet, G., Surani, M. A., et al. (2005). Genomic characterisation of a Fgf-regulated gradient-based neocortical protomap. *Development* 132, 3947–3961. doi: 10.1242/dev.01968

Sansom, S. N., and Livesey, F. J. (2009). Gradients in the brain: the control of the development of form and function in the cerebral cortex. *Cold Spring Harb. Perspect. Biol.* 1:a002519. doi: 10.1101/cshperspect.a002519

Satoh, S., Tang, K., Iida, A., Inoue, M., Kodama, T., Tsai, S. Y., et al. (2009). The spatial patterning of mouse cone opsin expression is regulated by bone morphogenetic protein signaling through downstream effector COUP-TF nuclear receptors. *J. Neurosci.* 29, 12401–12411. doi: 10.1523/JNEUROSCI.0951-09.2009

Schwarz, M., Cecconi, F., Bernier, G., Andrejewski, N., Kammandel, B., Wagner, M., et al. (2000). Spatial specification of mammalian eye territories by reciprocal transcriptional repression of Pax2 and Pax6. *Development* 127, 4325–4334. doi: 10.1242/dev.127.20.4325

Schwarz, C., and Thier, P. (1999). Binding of signals relevant for action: towards a hypothesis of the functional role of the pontine nuclei. *Trends Neurosci.* 22, 443–451. doi: 10.1016/s0166-2236(99)01446-0

Seghier, M. L. (2013). The angular gyrus: multiple functions and multiple subdivisions. *Neuroscientist* 19, 43–61. doi: 10.1177/1073858412440596

Shimogori, T., Banuchi, V., Ng, H. Y., Strauss, J. B., and Grove, E. A. (2004). Embryonic signaling centers expressing BMP, WNT and FGF proteins interact to pattern the cerebral cortex. *Development* 131, 5639–5647. doi: 10.1242/dev.01428

Shimogori, T., and Grove, E. A. (2005). Fibroblast growth factor 8 regulates neocortical guidance of area-specific thalamic innervation. *J. Neurosci.* 25, 6550–6560. doi: 10.1523/JNEUROSCI.0453-05.2005

Siegenthaler, J. A., and Miller, M. W. (2005). Transforming growth factor β1 promotes cell cycle exit through the cyclin-dependent kinase inhibitor p21 in the developing cerebral cortex. *J. Neurosci.* 25, 8627–8636. doi: 10.1523/JNEUROSCI.1876-05.2005

Simi, A., and Studer, M. (2018). Developmental genetic programs and activity-dependent mechanisms instruct neocortical area mapping. *Curr. Opin. Neurobiol.* 53, 96–102. doi: 10.1016/j.conb.2018.06.007

Smirnov, D. A., Hou, S., and Ricciardi, R. P. (2000). Association of histone deacetylase with COUP-TF in tumorigenic Ad12- transformed cells and its potential role in shut-off of MHC class I transcription. *Virology* 268, 319–328. doi: 10.1006/viro.1999.0181

Sosa, M. S., Bragado, P., and Aguirre-Ghiso, J. A. (2014). Mechanisms of disseminated cancer cell dormancy: an awakening field. *Nat. Rev. Cancer* 14, 611–622. doi: 10.1038/nrc3793

Spalice, A., Parisi, P., Nicita, F., Pizzardi, G., Del Balzo, F., and Iannetti, P. (2009). Neuronal migration disorders: clinical, neuroradiologic and genetics aspects. *Acta Paediatr.* 98, 421–433. doi: 10.1111/j.1651-2227.2008.01160.x

Starosta, R. T., Tarnowski, J., Vairo, F. P. E., Raymond, K., Preston, G., and Morava, E. (2020). Bosch-Boonstra-Schaaf optic atrophy syndrome (BBSOAS) initially diagnosed as ALG6-CDG: functional evidence for benignity of the ALG6 c.391T>C (p.Tyr131His) variant and further expanding the BBSOAS phenotype. *Eur. J. Med. Genet.* 63:103941. doi: 10.1016/j.ejmg.2020.103941

Stoeckel, C., Gough, P. M., Watkins, K. E., and Devlin, J. T. (2009). Supramarginal gyrus involvement in visual word recognition. *Cortex* 45, 1091–1096. doi: 10.1016/j.cortex.2008.12.004

Stolt, C. C., Lommes, P., Friedrich, R. P., and Wegner, M. (2004). Transcription factors Sox8 and Sox10 perform non-equivalent roles during oligodendrocyte development despite functional redundancy. *Development* 131, 2349–2358. doi: 10.1242/dev.01114

Storm, E. E., Garel, S., Borello, U., Hebert, J. M., Martinez, S., McConnel, S. K., et al. (2006). Dose-dependent functions fo Fgf8 in regulating telencephalic patterning centers. *Development* 133, 1831–1844. doi: 10.1242/dev.02324

Su, X., Tang, W., Luan, Z., Yang, Y., Wang, Z., Zhang, Y., et al. (2018). Protective effect of miconazole on rat myelin sheaths following premature infant cerebral white matter injury. *Exp. Ther. Med.* 15, 2443–2449. doi: 10.3892/etm.2018.5717

Sur, M., and Rubenstein, J. L. R. (2005). Patterning and plasticity of the cerebral cortex. *Science* 310, 805–810. doi: 10.1126/science.1112070

Swindell, E. C., Bailey, T. J., Loosli, F., Liu, C., Amaya-Manzanares, F., Mahon, K. A., et al. (2006). Rx-Cre, a tool for inactivation of gene expression in the developing retina. *Genesis* 44, 361–363. doi: 10.1002/dvg.20225

Tang, K., Tsai, S. Y., and Tsai, M. J. (2015). COUP-TFs and eye development. *Biochim. Biophys. Acta* 1849, 201–209. doi: 10.1016/j.bbagrm.2014.05.022

Tang, K., Xie, X., Park, J. I., Jamrich, M., Tsai, S., and Tsai, M. J. (2010). COUP-TFs regulate eye development by controlling factors essential for optic vesicle morphogenesis. *Development* 137, 725–734. doi: 10.1242/dev.040568

Tanibe, M., Ishiura, S. I., Asashima, M., and Michiue, T. (2012). xCOUP-TF-B regulates xCyp26 transcription and modulates retinoic acid signaling for anterior neural patterning in *Xenopus*. *Int. J. Dev. Biol.* 56, 239–244. doi: 10.1387/ijdb.113482mt

Taniguchi, H., He, M., Wu, P., Kim, S., Paik, R., Sugino, K., et al. (2011). A resource of Cre driver lines for genetic targeting of GABAergic neurons in cerebral cortex. *Neuron* 71, 995–1013. doi: 10.1016/j.neuron.2011.07.026

Teixeira, L. B. C., Ver Hoeve, J. N., Mayer, J. A., Dubielzig, R. R., Smith, C. M., Radcliff, A. B., et al. (2016). Modeling the chronic loss of optic nerve axons and the effects on the retinal nerve fiber layer structure in primary disorder of myelin. *Invest. Ophthalmol. Vis. Sci.* 57, 4859–4868. doi: 10.1167/iovs.16-19871

Tien, N., and Kerschensteiner, D. (2018). Homeostatic plasticity in neural development. *Neural Dev.* 13:9. doi: 10.1186/s13064-018-0105-x

Tomassy, G. S., De Leonibus, E., Jabaudon, D., Lodato, S., Alfano, C., Mele, A., et al. (2010). Area-specific temporal control of corticospinal motor neuron differentiation by COUP-TFI. *Proc. Natl. Acad. Sci. U S A* 107, 3576–3581. doi: 10.1073/pnas.0911792107

Touzot, A., Ruiz-Reig, N., Vitalis, T., and Studer, M. (2016). Molecular control of two novel migratory paths for CGE-derived interneurons in the developing mouse brain. *Development* 143, 1753–1765. doi: 10.1242/dev.131102

Toyoda, R., Assimacopoulos, S., Wilcoxon, J., Taylor, A., Feldman, P., Suzuki-Hirano, A., et al. (2010). FGF8 acts as a classic diffusible morphogen to pattern the neocortex. *Development* 137, 3439–3448. doi: 10.1242/dev.055392

Tran, C. T., Radyushkin, K., Tonchev, A. B., Piñon, M. C., Ashery-Padan, R., Molnár, Z., et al. (2009). Selective cortical layering abnormalities and behavioral deficits in cortex-specific Pax6 knock-out mice. *J. Neurosci.* 29, 8335–8349. doi: 10.1523/JNEUROSCI.5669-08.2009

Tran, P., Zhang, X. K., Salbert, G., Hermann, T., Lehmann, J. M., and Pfahl, M. (1992). COUP orphan receptors are negative regulators of retinoic acid response pathways. *Mol. Cell. Biol.* 12, 4666–4676. doi: 10.1128/mcb.12.10.4666-4676.1992

Tsai, H. H., and Miller, R. H. (2002). Glial cell migration directed by axon guidance cues. *Trends Neurosci.* 25, 173–175. doi: 10.1016/s0166-2236(00)02096-8

Tsai, S. Y., and Tsai, M.-J. (1997). Chick Ovalbumin Upstream Promoter-Transcription Factors (COUP-TFs): coming of age. *Endocr. Rev.* 18, 229–240. doi: 10.1210/edrv.18.2.0294

van Bokhoven, H. (2011). Genetic and epigenetic networks in intellectual disabilities. *Annu. Rev. Genet.* 45, 81–104. doi: 10.1146/annurev-genet-110410-132512

Van Der Wees, J., Matharu, P. J., De Roos, K., Destrée, O. H. J., Godsave, S. F., Durston, A. J., et al. (1996). Developmental expression and differential regulation by retinoic acid of xenopus COUP-TF-A and COUP-TF-B. *Mech. Dev.* 54, 173–184. doi: 10.1016/0925-4773(95)00471-8

Varga, C., Tamas, G., Barzo, P., Olah, S., and Somogyi, P. (2015). Molecular and electrophysiological characterization of GABAergic interneurons expressing the transcription factor COUP-TFII in the adult human temporal cortex. *Cereb. Cortex* 25, 4430–4449. doi: 10.1093/cercor/bhv045

Villalba, A., Götz, M., and Borrell, V. (2021). The regulation of cortical neurogenesis. *Curr. Top. Dev. Biol.* 142, 1–66. doi: 10.1016/bs.ctdb.2020.10.003

Vue, T. Y., Lee, M., Tan, Y. E., Werkhoven, Z., Wang, L., and Nakagawa, Y. (2013). Thalamic control of neocortical area formation in mice. *J. Neurosci.* 33, 8442–8453. doi: 10.1523/JNEUROSCI.5786-12.2013

Wagner, N. R., and MacDonald, J. L. (2021). Atypical neocortical development in the cited2 conditional knockout leads to behavioral deficits associated with neurodevelopmental disorders. *Neuroscience* 455, 65–78. doi: 10.1016/j.neuroscience.2020.12.009

Walthall, W. W., and Plunkett, J. A. (1995). Genetic transformation of the synaptic pattern of a motoneuron class in caenorhabditis elegans. *J. Neurosci.* 15, 1035–1043. doi: 10.1523/JNEUROSCI.15-02-01035.1995

Wan, J., Shen, C. M., Wang, Y., Wu, Q. Z., Wang, Y. L., Liu, Q., et al. (2021). Repeated exposure to propofol in the neonatal period impairs hippocampal synaptic plasticity and the recognition function of rats in adulthood. *Brain Res. Bull.* 169, 63–72. doi: 10.1016/j.brainresbull.2021.01.007

Wang, Z., Benoit, G., Liu, J., Prasad, S., Aarnisalo, P., Liu, X., et al. (2003). Structure and function of Nurr1 identifies a class of ligand-independent nuclear receptors. *Nature* 423, 555–560. doi: 10.1038/nature01645

Wang, M. E., Fraize, N. P., Yin, L., Yuan, R. K., Petsagourakis, D., Wann, E. G., et al. (2013). Differential roles of the dorsal and ventral hippocampus in predator odor contextual fear conditioning. *Hippocampus* 23, 451–466. doi: 10.1002/hipo.22105

Wang, L. H., Ing, N. H., Tsai, S. Y., O'Malley, B. W., and Tsai, M. J. (1991). The COUP-TFs compose a family of functionally related transcription factors. *Gene Expr.* 1, 207–216.

Wang, L. H., Tsai, S. Y., Cook, R. G., Beattie, W. G., Tsai, M. J., and O'Malley, B. W. (1989). COUP transcription factor is a member of the steroid receptor superfamily. *Nature* 340, 163–166. doi: 10.1038/340163a0

Wang, X., Tsai, J. W., Lamonica, B., and Kriegstein, A. R. (2011). A new subtype of progenitor cell in the mouse embryonic neocortex. *Nat. Neurosci.* 14, 555–561. doi: 10.1038/nn.2807

Watrin, F., Manent, J.-B., Cardoso, C., and Represa, A. (2015). Causes and consequences of gray matter heterotopia. *CNS Neurosci. Ther.* 21, 112–122. doi: 10.1111/cns.12322

Weikum, E. R., Liu, X., and Ortlund, E. A. (2018). The nuclear receptor superfamily: a structural perspective. *Protein Sci.* 27, 1876–1892. doi: 10.1002/pro.3496

Welker, C. (1971). Microelectrode delineation of fine grain somatotopic organization of SmI cerebral neocortex in albino rat. *Brain Res.* 26, 259–275. doi: 10.1016/S0006-8993(71)80004-5

Welniarz, Q., Dusart, I., and Roze, E. (2017). The corticospinal tract: Evolution, development and human disorders. *Dev. Neurobiol.* 77, 810–829. doi: 10.1002/dneu.22455

Wolosin, S. M., Richardson, M. E., Hennessey, J. G., Denckla, M. B., and Mostofsky, S. H. (2009). Abnormal cerebral cortex structure in children with ADHD. *Hum. Brain Mapp.* 30, 175–184. doi: 10.1002/hbm.20496

Wong, F. K., Fei, J. F., Mora-Bermúdez, F., Taverna, E., Haffner, C., Fu, J., et al. (2015). Sustained pax6 expression generates primate-like basal radial glia in developing mouse neocortex. *PLoS Biol.* 13:e1002217. doi: 10.1371/journal.pbio.1002217

Woolsey, T. A., and Van der Loos, H. (1970). The structural organization of layer IV in the somatosensory region (S I) of mouse cerebral cortex. *Brain Res.* 17, 205–242. doi: 10.1016/0006-8993(70)90079-X

Xu, L., Zheng, Y., Li, X., Wang, A., Huo, D., Li, Q., et al. (2021). Abnormal neocortex arealization and sotos-like syndrome-associated behavior in setd2 mutant mice. *Sci. Adv.* 7:eaba1180. doi: 10.1126/sciadv.aba1180

Yamaguchi, H., Zhou, C., Lin, S. C., Durand, B., Tsai, S. Y., and Tsai, M. J. (2004). The nuclear orphan receptor COUP-TFI is important for differentiation of oligodendrocytes. *Dev. Biol.* 266, 238–251. doi: 10.1016/j.ydbio.2003.10.038

Zembrzycki, A., Chou, S. J., Ashery-Padan, R., Stoykova, A., and O'Leary, D. D. M. (2013). Sensory cortex limits cortical maps and drives top-down plasticity in thalamocortical circuits. *Nat. Neurosci.* 16, 1060–1067. doi: 10.1038/nn.3454

Zembrzycki, A., Griesel, G., Stoykova, A., and Mansouri, A. (2007). Genetic interplay between the transcription factors Sp8 and Emx2 in the patterning of the forebrain. *Neural Dev.* 2:8. doi: 10.1186/1749-8104-2-8

Zembrzycki, A., Perez-Garcia, C. G., Wang, C. F., Chou, S. J., and O'Leary, D. D. M. (2015). Postmitotic regulation of sensory area patterning in the mammalian neocortex by Lhx2. *Proc. Natl. Acad. Sci. U S A* 112, 6736–6741. doi: 10.1073/pnas.1424440112

Zhang, S., Li, W., Wang, W., Zhang, S. S., Huang, P., and Zhang, C. (2013). Expression and activation of STAT3 in the astrocytes of optic nerve in a rat model of transient intraocular hypertension. *PLoS One* 8:e55683. doi: 10.1371/journal.pone.0055683

Zhang, K., Yu, F., Zhu, J., Han, S., Chen, J., Wu, X., et al. (2020). Imbalance of excitatory/inhibitory neuron differentiation in neurodevelopmental disorders

with an NR2F1 point mutation. *Cell Rep.* 31:107521. doi: 10.1016/j.celrep.2020.03.085

Zhang, Y., Zhou, Y., Yu, C., Lin, L., Li, C., and Jiang, T. (2010). Reduced cortical folding in mental retardation. *Am. J. Neuroradiol.* 31, 1063–1067. doi: 10.3174/ajnr.A1984

Zhao, A., Fang, F., Li, B., Chen, Y., Qiu, Y., Wu, Y., et al. (2021). Visual abnormalities associate with hidpocampus in mild cognitive impairment and early Alzheimer's disease. *Front. Aging Neurosci.* 12:597491. doi: 10.3389/fnagi.2020.597491

Zhou, X., Liu, F., Tian, M., Xu, Z., Liang, Q., Wang, C., et al. (2015). Transcription factors COUP-TFI and COUP-TFII are required for the production of granule cells in the mouse olfactory bulb. *Development* 142, 1593–1605. doi: 10.1242/dev.115279

Zhou, C., Qiu, Y., Pereira, F. A., Crair, M. C., Tsai, S. Y., and Tsai, M. J. (1999). The nuclear orphan receptor COUP-TFI is required for differentiation of subplate neurons and guidance of thalamocortical axons. *Neuron* 24, 847–859. doi: 10.1016/s0896-6273(00)81032-6

Zhou, C., Tsai, S. Y., and Tsai, M. J. (2001). COUP-TFI: an intrinsic factor for early regionalization of the neocortex. *Genes Dev.* 15, 2054–2059. doi: 10.1101/gad.913601

Zilles, K., Palomero-Gallagher, N., and Amunts, K. (2013). Development of cortical folding during evolution and ontogeny. *Trends Neurosci.* 36, 275–284. doi: 10.1016/j.tins.2013.01.006

Zou, W., Cheng, L., Lu, S., and Wu, Z. (2020). A *de novo* nonsense mutation in the N-terminal of ligand-binding domain of NR2F1 gene provoked a milder phenotype of BBSOAS. *Ophthalmic Genet.* 41, 88–89. doi: 10.1080/13816810.2020.1719520

Conflict of Interest: The authors declare that the research was conducted in the absence of any commercial or financial relationships that could be construed as a potential conflict of interest.

Publisher's Note: All claims expressed in this article are solely those of the authors and do not necessarily represent those of their affiliated organizations, or those of the publisher, the editors and the reviewers. Any product that may be evaluated in this article, or claim that may be made by its manufacturer, is not guaranteed or endorsed by the publisher.

Copyright © 2021 Tocco, Bertacchi and Studer. This is an open-access article distributed under the terms of the Creative Commons Attribution License (CC BY). The use, distribution or reproduction in other forums is permitted, provided the original author(s) and the copyright owner(s) are credited and that the original publication in this journal is cited, in accordance with accepted academic practice. No use, distribution or reproduction is permitted which does not comply with these terms.

frontiers in Molecular Neuroscience

REVIEW
published: 17 December 2021
doi: 10.3389/fnmol.2021.793004

GLP-1 Suppresses Feeding Behaviors and Modulates Neuronal Electrophysiological Properties in Multiple Brain Regions

Xin-Yi Chen[1,2], Lei Chen[3], Wu Yang[1] and An-Mu Xie[2]**

[1] Department of International Medicine, Affiliated Hospital of Qingdao University, Qingdao, China, [2] Department of Neurology, Affiliated Hospital of Qingdao University, Qingdao, China, [3] Department of Physiology and Pathophysiology, School of Basic Medicine, Qingdao University, Qingdao, China

The glucagon-like peptide-1 (GLP-1) plays important roles in the regulation of food intake and energy metabolism. Peripheral or central GLP-1 suppresses food intake and reduces body weight. The electrophysiological properties of neurons in the mammalian central nervous system reflect the neuronal excitability and the functional organization of the brain. Recent studies focus on elucidating GLP-1-induced suppression of feeding behaviors and modulation of neuronal electrophysiological properties in several brain regions. Here, we summarize that activation of GLP-1 receptor (GLP-1R) suppresses food intake and induces postsynaptic depolarization of membrane potential and/or presynaptic modulation of glutamatergic or GABAergic neurotransmission in brain nuclei located within the medulla oblongata, pons, mesencephalon, diencephalon, and telencephalon. This review may provide a background to guide future research about the cellular mechanisms of GLP-1-induced feeding inhibition.

Keywords: GLP-1, electrophysiological property, feeding behavior, spontaneous firing activity, synaptic transmission

OPEN ACCESS

Edited by:
Inmaculada Segura, Ludwig Maximilian University of Munich, Germany

Reviewed by:
Jong-Woo Sohn, Korea Advanced Institute of Science and Technology, South Korea
Stefan Trapp, University College London, United Kingdom

Correspondence:
Wu Yang
yangwu788@163.com
An-Mu Xie
xieanmu@163.com

Specialty section:
This article was submitted to Molecular Signalling and Pathways, a section of the journal Frontiers in Molecular Neuroscience

Received: *11 October 2021*
Accepted: *29 November 2021*
Published: *17 December 2021*

Citation:
Chen X-Y, Chen L, Yang W and Xie A-M (2021) GLP-1 Suppresses Feeding Behaviors and Modulates Neuronal Electrophysiological Properties in Multiple Brain Regions. Front. Mol. Neurosci. 14:793004. doi: 10.3389/fnmol.2021.793004

INTRODUCTION

The pre-proglucagon (Gcg) gene product peptides include glucagon-like peptide 1 (GLP-1), GLP-2, oxyntomodulin (OXM), intervening peptide 1 (IP1), and glicentin. The GLP-1-producing preproglucagon (PPG) neurons located in the nucleus tractus solitarius (NTS) and the intermediate reticular nucleus of the medulla oblongata are the major source of endogenous GLP-1 in the central nervous system, which project widely throughout the central nervous system especially the autonomic control areas (Merchenthaler et al., 1999; Barrera et al., 2011; Llewellyn-Smith et al., 2011; Holt et al., 2019; Muller et al., 2019). Ablation of the PPG neurons in the NTS largely reduces the level of GLP-1 in the hypothalamus, brainstem, and spinal cord (Holt et al., 2019). In addition to the central source, peripheral GLP-1 is released from enteroendocrine L-cells in intestinal mucosa (Eissele et al., 1992) which plays an important role in regulating glucose homeostasis (Edwards et al., 1999; Williams, 2009). Furthermore, a small population of PPG neurons has been identified within the olfactory bulb with only local projection (Thiebaud et al., 2016). Central GLP-1 binds to GLP-1 receptor (GLP-1R) to exert many important effects including modulation of energy balance, cardiovascular system, learning and memory, rewarding effect of food, and thermogenesis (Trapp and Cork, 2015). GLP-1R belongs to G protein-coupled receptors with predominate $G\alpha_s$ coupling, leading to activation of adenylate cyclase and in turn increased levels of cAMP (Mayo et al., 2003).

GLP-1R expressing cells are widely expressed in mouse and non-human primate brain (Cork et al., 2015; Heppner et al., 2015). Recent immunocytochemistry revealed the distribution and subcellular localization of GLP-1R in rat brain (Farkas et al., 2021).

GLP-1 is involved in the regulation of food intake and energy metabolism. Both human clinical trials and animal experiments demonstrated that peripheral or central GLP-1 and GLP-1 analogs suppress food intake and reduce body weight (Turton et al., 1996; Hayes et al., 2008, 2011; Dossat et al., 2011; Heppner and Perez-Tilve, 2015). A recent study revealed that central and peripheral GLP-1 inhibits feeding behaviors through independent gut-brain circuits (Brierley et al., 2021). Activation of GLP-1R in a variety of brain regions, including the hypothalamus (Schick et al., 2003), mesolimbic system (Dossat et al., 2011; Alhadeff et al., 2012; Dickson et al., 2012), and hindbrain (Hayes et al., 2011; Alhadeff et al., 2014), reduces food intake. Drugs targeting GLP-1R have been used as weight loss and anti-diabetic glucose-lowering therapies (Heppner and Perez-Tilve, 2015).

The brain is the most intricate network structure which facilitates a concerted communication between single neurons, different neuronal populations, and remote brain (Gupta et al., 2020). Neurons are the basic structural and functional units in the central nervous system. The electrophysiological properties of neurons such as the spontaneous firing activities and the synaptic neurotransmission in the mammalian central nervous system reflect the neuronal excitability and the functional organization of the brain (Llinás, 1989, 2014). To date, measuring the electrophysiological features of neurons remains one of the most valuable methods to study the functional phenomena of the nervous system. The specific deficits of the electrophysiological properties contribute to some brain diseases (Bernard and Shevell, 2008; Klassen et al., 2011; Tai et al., 2014). Therefore, manipulation of the electrophysiological properties including the spontaneous firing activity of central neurons may play roles in the manifestation of some neurological disorders. For example, the electrophysiological characteristics of dopaminergic neurons in the substantia nigra pars compacta change before the appearance of motor symptoms in parkinsonian mice (Qi et al., 2017), while excitatory stimulation of dopaminergic neurons may improve the survival of the neurons (Michel et al., 2013). Many studies have demonstrated that GLP-1 suppresses feeding behaviors and modulates the spontaneous firing activities and/or glutamatergic or GABAergic neurotransmission in multiple brain regions. This review highlights the activation of GLP-1R-induced suppression of feeding as well as the modulation of neuronal electrophysiological properties of several brain regions in medulla oblongata, pons, mesencephalon, diencephalon, and telencephalon.

MEDULLA OBLONGATA AND PONS

The medullar oblongata in rodents and monkeys expresses a high level of GLP-1R (Merchenthaler et al., 1999; Cork et al., 2015; Heppner et al., 2015; Farkas et al., 2021). In human brain tissue of autopsies, GLP-1R is also expressed in the medullar oblongata including the area postrema, the dorsal motor nucleus of the vagus, and the NTS (Farr et al., 2016). GLP-1 modulates feeding behaviors in the medullar oblongata. Recently, Gaykema et al. (2017) reported that selectively chemogenetic stimulation of caudal medulla pre-proglucagon-producing neurons reduces food intake in both fed and fasted states and suppresses glucose production. Patch-clamp electrophysiological recordings in brain slices further demonstrated that chemogenetic activation selectively depolarizes neuronal membrane potential and increases the firing frequency of labeled medulla pre-proglucagon-producing neurons without affecting unlabeled neurons.

The NTS is the main source of endogenous GLP-1 within the brain (Barrera et al., 2011; Holt et al., 2019). Application of the stable GLP-1R analog exendin-4 into the medial subnucleus of the NTS (mNTS) reduces high-fat diet intake (Alhadeff and Grill, 2014; **Table 1**). However, electrophysiological studies revealed that GLP-1 or exendin-4 does not change the spontaneous firing activity as well as the synaptic transmission suggesting lack of functional GLP-1R in PPG neurons (Hisadome et al., 2010). Consistent with the electrophysiological results, the morphological study showed a weak/faint expression of GLP-1R in the NTS. It is reported that astrocytes in NTS are components of the GLP-1 signaling system which is involved in food intake control (Reiner et al., 2016). Intracerebroventricular application of GLP-1R agonist binds to GLP-1R on both neurons and astrocytes in the NTS. Activation of GLP-1R induces an increase in intracellular Ca^{2+} in 40% of NTS astrocytes, while selective inhibition of astrocyte function in NTS abolishes exendin-4-induced inhibition of food intake (Reiner et al., 2016). Therefore, complex mechanisms in both neurons and astrocytes may be involved in GLP-1-induced modulation of food intake in the NTS.

The parabrachial nucleus (PBN) in the pons is associated with the regulation of feeding behaviors. The PBN receives direct GLP-1 projections from NTS neurons (Richard et al., 2014). Stimulation of GLP-1R with exendin-4 in the PBN reduces food intake and therefore decreases body weight in rats. Electrophysiological evidence further revealed that application of exendin-4 results in a remarkable increase in the spontaneous firing rate of the PBN neurons (Richard et al., 2014; **Figure 1A**). Using the methods of immuno-electron microscopy, Farkas et al. (2021) recently revealed a very widespread distribution of GLP-1R fibers in rat brain suggesting the possible presynaptic effects of GLP-1R in the central nervous system. As the external part of the lateral parabrachial nucleus (LPBN) expresses the highest density of GLP-1R immunoreactive fibers (Farkas et al., 2021), further electrophysiological studies are needed to study the possible presynaptic modulation of the electrophysiological activities of the PBN neurons.

MESENCEPHALON

The ventral tegmental area (VTA) is a possible brain region for GLP-1-induced suppression of food intake. Functional study

TABLE 1 | Activation of GLP-1R suppresses feeding behaviors and modulates neuronal electrophysiological properties in several brain nuclei.

Brain regions	Neurons	Associated effects in feeding behaviors		Electrophysiological effects of activating GLP-1R	GLP-1R agonists	References
		Activation of GLP-1R	Ablation of GLP-1R			
mNTS	PPG neurons	Reduction of high-fat diet intake	N/A	No change in firing activity and synaptic transmission	Exendin-4 GLP-1	Hisadome et al., 2010; Alhadeff and Grill, 2014
PBN	Unidentified neurons	Reduction of food intake and body weight	N/A	Increase in firing rate	Exendin-4	Richard et al., 2014
VTA	DAergic VTA-to-NAc projection neurons	Suppression of high-fat food intake	N/A	Increase of sEPSCs frequency Inhibition of mEPSCs	Exendin-4	Mietlicki-Baase et al., 2013; Wang et al., 2015
ARC	POMC neurons	N/A	N/A	Depolarization and increase in firing rate *via* TRPC5 channels Increase of EPSCs frequency	Liraglutide	Secher et al., 2014; He et al., 2019
	NPY/AgRP neurons	N/A	N/A	Hyperpolarization *via* enhanced $GABA_A$ receptor-mediated neurotransmission	Liraglutide	Secher et al., 2014; He et al., 2019
	Kisspeptin (Kiss1)-expressing neurons	N/A	N/A	Depolarization and increase in firing rate	Liraglutide	Heppner et al., 2017
PVN	Unidentified neurons	Reduction of food intake	Increase of food intake and induction of obesity	Hyperpolarization *via* enhancement of inhibitory postsynaptic transmission Depolarization or inward current accompanied by an increase in membrane conductance	Exendin-4 GLP-1	Larsen et al., 1997; McMahon and Wellman, 1998; Acuna-Goycolea and van den Pol, 2004; Cork et al., 2015
	CRH neurons	N/A	N/A	Enhancement of EPSC amplitude		Liu et al., 2017
LH	Orexinergic neurons	N/A	N/A	Depolarization and increase in firing rate postsynaptically *via* sodium-dependent non-specific cationic conductance Enhancement of both glutamatergic and GABAergic neurotransmission presynaptically	Exendin-4	Acuna-Goycolea and van den Pol, 2004
PVT	Unidentified neurons	Reduction of food intake Decrease of food-seeking and food-motivated behaviors	N/A	Decrease in firing rate probably *via* suppression of glutamatergic synaptic transmission	Exendin-4	Ong et al., 2017
NAc	MSNs	Suppression of food intake	N/A	Reduction of evoked action potential postsynaptically Increase of mEPSCs frequency presynaptically	Exendin-4	Dossat et al., 2011; Mietlicki-Baase et al., 2014
BNST	Unidentified neurons	Food suppression during the dark phase	N/A	Inward current and depolarization accompanied by an increase in membrane conductance Increase or decrease in firing rate Hyperpolarization probably *via* opening of potassium channels	GLP-1	Cork et al., 2015 Williams et al., 2018
HC	CA1 neurons	Reduction of food intake and body weight	Increase of food motivated behaviors Depolarization in most hippocampal neurons, and hyperpolarization in a few neurons	Increase and then decrease in firing activity	Active fragment of GLP-1, GLP-1 (7-36) amide GLP-1 Cork et al., 2015; Gullo et al., 2017	Oka et al., 1999; Hsu et al., 2015, 2018
OB	MCs	N/A	N/A	Increase of the excitability probably *via* inhibition of voltage-dependent potassium channel	GLP-1 Exendin-4	Thiebaud et al., 2016; Schwartz et al., 2021

ARC, arcuate nucleus; BNST, bed nucleus of the stria terminalis; CRH, corticotropin-releasing hormone; EPSCs, excitatory postsynaptic currents; HC, hippocampus; LH, lateral hypothalamus; MCs, mitral cells; mEPSCs, miniature excitatory postsynaptic currents; mNTS, medial subnucleus of the nucleus tractus solitaries; MSNs, medium spiny neurons; N/A, not applicable; NAc, nucleus accumbens; NPY/AgRP, Neuropeptide Y/Agouti gene related peptide; OB, olfactory bulb; PBN, parabrachial nucleus; POMC, proopiomelanocortin; PVN, paraventricular nucleus; PVT, paraventricular thalamic nucleus; VTA, ventral tegmental area.

revealed that application of GLP-1R antagonist into the VTA attenuates peripheral application of exendin-4-induced anorectic effects (Mietlicki-Baase et al., 2013). Electrophysiological recordings revealed that exendin-4 increases the frequency of spontaneous excitatory postsynaptic currents (sEPSCs) of VTA dopaminergic neurons suggesting the possible presynaptic

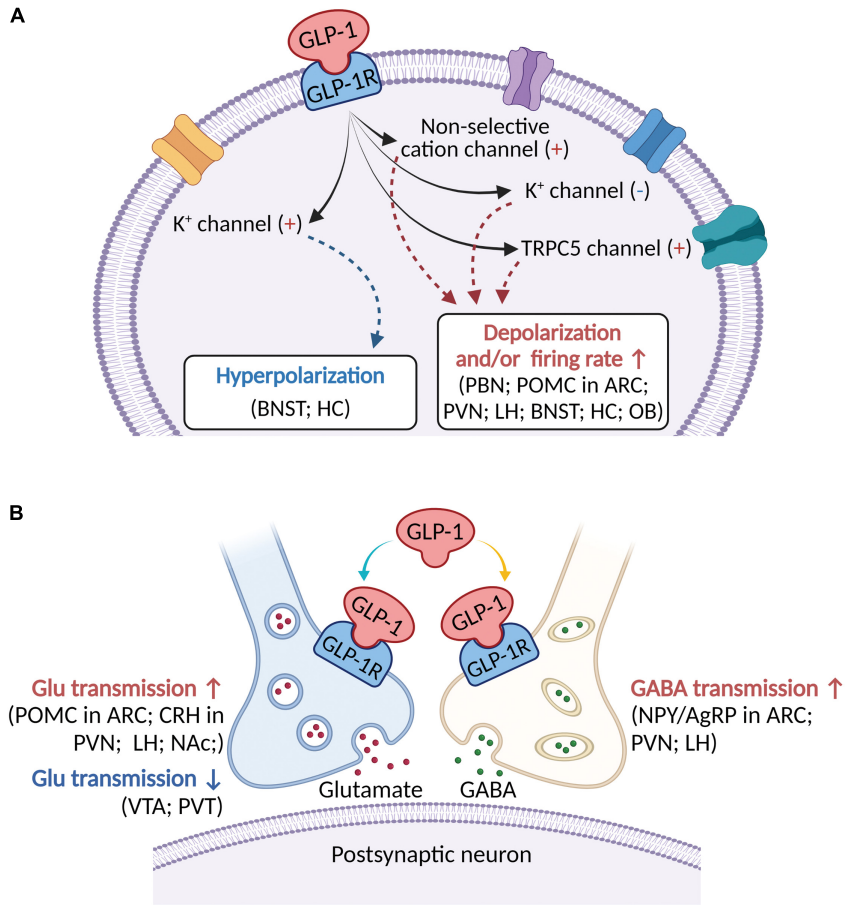

FIGURE 1 | A schematic diagram describing the major electrophysiological effects of activating GLP-1R in brain areas involved in modulation of feeding behaviors. **(A)** GLP-1 (including its agonists) binds to postsynaptic GLP-1R to depolarize membrane potential and/or increase firing rate in most brain regions, but hyperpolarize membrane potential in a few brain areas. Several ionic mechanisms, including non-selective cation channel, K^+ channel, and TRPC5 channel, may be involved in activation of GLP-1R-induced depolarization or hyperpolarization. **(B)** In addition to postsynaptic receptors, GLP-1 acts on presynaptic GLP-1R to modulate both glutamatergic and GABAergic neurotransmission. ARC, arcuate nucleus; BNST, bed nucleus of the stria terminalis; Glu, glutamate; CRH, corticotropin-releasing hormone; HC, hippocampus; LH, lateral hypothalamus; NAc, nucleus accumbens; NPY/AgRP, Neuropeptide Y/Agouti gene-related peptide; OB, olfactory bulb; PBN, parabrachial nucleus; POMC, proopiomelanocortin; PVN, paraventricular nucleus; PVT, paraventricular thalamic nucleus; VTA, ventral tegmental area.

modulation of GLP-1R on glutamatergic terminals. Behavioral study also demonstrated that modulating AMPA/kainite, but not NMDA, receptor-mediated glutamatergic neurotransmission within VTA is involved in GLP-1-induced intake-suppressive effects (Mietlicki-Baase et al., 2013). In addition, intra-VTA application of exendin-4 suppresses high-fat food intake, which is consistent with the results of chemogenetic activation of endogenously released GLP-1 nerve terminals in the VTA (Wang et al., 2015). In contrast to the enhancement of spontaneous excitatory postsynaptic transmission (Mietlicki-Baase et al., 2013), using retrograde labeling of VTA to nucleus accumbens (NAc) medial shell projecting neurons, *in vitro* patch-clamp recordings showed that exendin-4 selectively inhibits the miniature excitatory postsynaptic currents (mEPSCs) within the dopaminergic VTA-to-NAc projection neurons (Wang et al., 2015; **Figure 1B**) suggesting the presynaptic inhibition of glutamatergic neurotransmission. As NAc is also an important brain region associated with GLP-1-induced feeding suppression, further electrophysiological studies are necessary to explore the contribution of glutamatergic neurotransmission to endogenously released GLP-1-induced suppression of high-fat food intake in the VTA.

DIENCEPHALON

The arcuate nucleus (ARC) of the hypothalamus plays a particularly important role in the central regulation of food intake (Bouret et al., 2004). Two distinct types of neurons within the ARC, proopiomelanocortin (POMC) and Neuropeptide Y (NPY)/Agouti gene-related peptide (AgRP) neurons, play important roles in energy balance and glucose homeostasis (Gautron et al., 2015; Caron et al., 2018). Activation of both the NPY/AgRP neurons and POMC neurons coordinates the activity of the paraventricular nucleus (PVN), promoting stimulation or inhibition of feeding, respectively. It is well known that

the anti-diabetic drug, long-acting GLP-1R agonist, liraglutide reduces body weight. The highest level of GLP-1R expressing cells, detected by transgene expression (Cork et al., 2015), *in situ* hybridization (Merchenthaler et al., 1999; Heppner et al., 2015), and immunocytochemistry (Farkas et al., 2021), is present in the ARC. *In vitro* patch-clamp electrophysiological recordings revealed that modulating the electrophysiological properties of both POMC and cocaine- and amphetamine-regulated transcript (CART) neurons (POMC/CART neurons) and NPY/AgRP neurons are the possible mechanism of liraglutide-induced weight loss (Secher et al., 2014). Peripheral application of fluorescently labeled liraglutide binds GLP-1R within the ARC (Secher et al., 2014). Liraglutide depolarizes membrane potential and increases the spontaneous action potentials directly through postsynaptic GLP-1R in the ARC neurons expressing POMC (Secher et al., 2014; He et al., 2019). In peripheral pancreatic β cells, GLP-1 depolarizes membrane potential through activation of Na^+-permeable TRPM4 and TRPM5 channels (Shigeto et al., 2015). Similarly, TRPC5 channels are involved in liraglutide-induced postsynaptic excitation of arcuate neurons (He et al., 2019). In addition to perikarya and dendrites expression, high level of GLP-1R was also observed in axons of ARC neurons (Farkas et al., 2021). Consistently, electrophysiological recordings showed that liraglutide increases the EPSCs frequency of POMC neurons suggesting the modulation of presynaptic excitatory synaptic transmission (He et al., 2019).

GABA released by the NPY/AgRP neurons is very important to the control of food intake probably *via* inhibiting the anorectic effects of the POMC neurons. Further electrophysiological study showed that, opposite to the effects on arcuate POMC neurons, GLP-1 hyperpolarizes arcuate NPY neurons indirectly *via* increased $GABA_A$ receptor-mediated neurotransmission of local GABAergic interneurons (Secher et al., 2014; He et al., 2019). The Kisspeptin (Kiss1)-expressing neurons located in the ARC are responsible for gonadotropin-releasing hormone (GnRH)/luteinizing hormone (LH) release (Li et al., 2009; Han et al., 2015). The Kiss1 neurons may be a key integrator of metabolic status with GnRH/LH release. Liraglutide increases the action potential firing and causes a direct membrane depolarization of ARC Kiss1 cells in brain slices (Heppner et al., 2017).

Morphological studies demonstrated a particularly high density of GLP-1R expression in the PVN of mice (Cork et al., 2015), rats (Merchenthaler et al., 1999; Farkas et al., 2021), and primates (Heppner et al., 2015). Early study showed that exendin-4 induces diverse responses including depolarization, hyperpolarization, and no response in paraventricular hypothalamic neurons. The GLP-1-induced hyperpolarization of PVN neurons may be induced by an enhancement of inhibitory postsynaptic transmission (Acuna-Goycolea and van den Pol, 2004). Consistent with exendin-4-induced depolarization, Cork et al. (2015) also revealed that bath application of GLP-1 induces an inward current which is accompanied by an increase in membrane conductance. Activation of GLP-1R with exendin-4 enhances the amplitude but not the frequency of AMPA receptor-mediated EPSCs in PVN corticotropin-releasing hormone (CRH) neurons and thus promotes the excitability of CRH neurons postsynaptically (Liu et al., 2017). Functional studies revealed that activation of GLP-1R in the PVN reduces food intake (Larsen et al., 1997; McMahon and Wellman, 1998). Consistently, postnatal depletion of GLP-1R in the PVN increases food intake and induces obesity (Liu et al., 2017).

Different neural circuits have been proposed to maintain energy homeostasis. Both central GLP-1 and orexin pathways play an important role in neural integration of satiation and food reward. GLP-1 projections from NTS to NAc and VTA promote satiation and reduce food reward, while orexinergic projection from lateral hypothalamus to NTS suppresses satiation and increases food reward (Dossat et al., 2011). Early study revealed a direct modulation of GLP-1R on the electrophysiological activities of orexinergic neurons in the lateral hypothalamus. Application of exendin-4 depolarizes the membrane potential and increases the spontaneous discharge rate of orexinergic neurons in the lateral hypothalamus (Acuna-Goycolea and van den Pol, 2004). The GLP-1-induced excitation of orexinergic neurons is a directly postsynaptic effect that may be mediated by sodium-dependent non-specific cationic conductances. In addition, activation of GLP-1R enhances both glutamatergic and GABAergic neurotransmission presynaptically in orexinergic neurons. However, exendin-4 does not change the membrane potential as well as the firing rate of melanin-concentrating hormone (MCH) neurons in the lateral hypothalamus (Acuna-Goycolea and van den Pol, 2004). The GLP-1R activation-induced both postsynaptic and presynaptic modulation of orexinergic neurons may suggest some complex integration of satiation and food reward.

The paraventricular thalamic nucleus (PVT) neurons receive GLP-1 innervation from NTS and express GLP-1R (Cork et al., 2015; Farkas et al., 2021). PVT is involved in energy balance and reward control. Behavioral tests showed that intra-PVT application of exendin-4 reduces food intake and decreases food-seeking and food-motivated behaviors (Ong et al., 2017). Further electrophysiological recordings revealed that exendin-4 inhibits the spontaneous action potential firing in PVN neurons projecting to NAc core. Suppression of glutamatergic synaptic transmission may be associated with the reduced excitability of GLP-1R activation (Ong et al., 2017).

TELENCEPHALON

Moderate density of GLP-1R is expressed in both the cell bodies and fibers of the NAc shell and core (Cork et al., 2015; Heppner et al., 2015; Farkas et al., 2021). Activation of GLP-1R in NAc core induces suppression of food intake (Dossat et al., 2011; Mietlicki-Baase et al., 2014). Current-clamp recordings illustrated that exendin-4 induces a small reduction in evoked action potential from medium spiny neurons (MSNs) suggesting slightly postsynaptic effects. In addition to perikarya expression, GLP-1R is also expressed on the processes of NAc (Farkas et al., 2021) suggesting some possibly presynaptic modulation of the NAc activity. Indeed, further electrophysiological studies demonstrated that exendin-4 predominantly activates presynaptic GLP-1R in

NAc to increase the frequency of AMPA/kainate receptor-mediated mEPSCs. Therefore, the enhancement of glutamatergic AMPA/Kainate signaling is probably involved in GLP-1-induced inhibition of food intake (Mietlicki-Baase et al., 2014). In addition to modulating food intake, recent publication revealed that NAc is also a possible molecular target for GLP-1-induced addiction behaviors (Hernandez and Schmidt, 2019; Hernandez et al., 2019). Intra-NAc application of exendin-4 increases the spontaneous firing rate of MSNs in cocaine-experienced rats and reduces cocaine-seeking behavior in rats (Hernandez et al., 2019).

Morphological studies revealed that the neurons in the bed nucleus of the stria terminalis (BNST) express a high level of GLP-1R (Cork et al., 2015; Heppner et al., 2015; Farkas et al., 2021). Application of GLP-1 elicits an inward current and depolarization accompanied by an increase in membrane conductance (Cork et al., 2015). Recently, under the model of cell-attached patch-clamp recordings, Williams et al. (2018) reported that GLP-1 induces either an increase or a decrease of spontaneous firing rate in GLP-1R expressing BNST neurons. Further whole-cell patch-clamp recordings revealed that GLP-1 induces either a depolarizing or hyperpolarizing response, while dopamine evokes response in a reciprocal fashion to that of GLP-1. The GLP-1-induced hyperpolarization is accompanied by an increase in membrane conductance suggesting the opening of potassium channels (Williams et al., 2018). In addition, functional study demonstrated that local injection of GLP-1 into the BNST induces food suppression during the dark phase (Williams et al., 2018).

Inconsistent distribution patterns of GLP-1R in the hippocampus have been reported by different morphological studies (Cork et al., 2015; Jensen et al., 2018; Farkas et al., 2021). For example, a relatively high level of GLP-1R-immunoreactivity was observed in mouse hippocampus (Jensen et al., 2018) while a low level of GLP-1R-immunoreactivity was revealed in rat hippocampus (Farkas et al., 2021), which may suggest some species difference of the GLP-1R expression in the hippocampus. However, functional studies did detect the effects of GLP-1R in the hippocampus. Early *in vivo* electrophysiological recordings showed that juxtacellular application of the active fragment of GLP-1, GLP-1 (7–36) amide induces an increase and then a decrease of firing activity in the hippocampal CA1 neurons. Modulation of non-NMDA glutamate receptor-mediated synaptic transmission is involved in GLP-1-induced effects (Oka et al., 1999). Bath application of GLP-1 induces a depolarization in most hippocampal neurons and a hyperpolarization in a few neurons (Cork et al., 2015). In addition, *in vitro* electrophysiological recordings further demonstrated that exendin-4 elicits an early fast excitatory response dose-dependently (Gullo et al., 2017). Consistent with the electrophysiological recordings, behavioral studies showed that activation of GLP-1R in the ventral hippocampal CA1 regions reduces food intake and body weight, while targeted ventral CA1 GLP-1R knockdown increases food-motivated behaviors (Hsu et al., 2015, 2018). In addition to modulating feeding behaviors, GLP-1 promotes the proliferation of progenitor cells and increases immature neurons in the hippocampus and in turn reverses memory impairment (Lennox et al., 2014). Activation of GLP-1R with liraglutide improves cognition decline of db/db mice *via* increasing neuronal survival in the CA1, CA3, and DG regions of hippocampus (Zhang et al., 2021).

The olfactory bulb is the basic brain region responsible for olfactory information. The deep short axon cells (dSACs) in the granule cell layer (GCL) of olfactory bulb, named PPG neurons, could synthesize and release GLP-1 and in turn modulate the activity of the first-order neurons, mitral cells (MCs) which are the primary projection neurons of the olfactory bulb (Thiebaud et al., 2016). Positive expression of GLP-1R is detected in the GCL of olfactory bulb (Cork et al., 2015). Patch-clamp recordings revealed that bath application of GLP-1 or exendin-4 increases the spontaneous firing frequency and decreases the excitation threshold for MC firing in olfactory bulb. Decreasing the conductance of voltage-dependent potassium channels, Kv1.3, is the possible ionic mechanism of GLP-1-induced enhancement of MC excitability (Thiebaud et al., 2016). Recently, further studies revealed that optogenetic activation of PPG neurons in the GCL generates biphasic inhibition-excitation response in MCs. However, a single pulse light stimulation of PPG neurons produces only glutamatergic EPSCs, but not IPSCs, in granule cells. The stimulation of PPG neurons-induced glutamatergic EPSCs is much faster than that of GABAergic IPSCs in MCs. Under the condition of blocking GABAergic neurotransmission, light stimulation of PPG neurons results in an increase in the excitation of MCs suggesting the involvement of PPG neurons in shaping the MC firing patterns (Thiebaud et al., 2019). It is known that, in addition to olfactory physiology, MC activity is also associated with feeding and nutritional status (Fadool et al., 2011; Aimé et al., 2014; Thiebaud et al., 2014; Riera et al., 2017). The olfactory acuity is regulated by the metabolic state and therefore the olfactory system is a driver of feeding behavior. Enhancement of neuronal excitability of the major output neurons of the olfactory bulb *via* blocking voltage-dependent potassium channel reduces body weight in obese mice (Schwartz et al., 2021). Previous study suggested that chronic administration of fat in the diet impairs the spontaneous firing rate of MCs (Fadool et al., 2011), and reduces the amplitude of electro-olfactogram (EOG). Furthermore, the volume of olfactory bulb is significantly smaller in individuals with obesity and negatively correlated with body mass index (BMI) (Poessel et al., 2020). Therefore, the GLP-1-induced excitation of MCs, probably *via* inhibition of voltage-dependent potassium channel conductance and enhancement of glutamatergic neurotransmission, could lead to changed excitability of higher olfactory cortical as well as hypothalamic regions to change metabolic states.

CONCLUSION

Being a peptide involved in the regulation of food intake and energy metabolism, GLP-1 has been demonstrated to suppress food intake and reduce body weight. In this review, we provide a description of recent advances of GLP-1-induced

inhibition of feeding behaviors and modulation of neuronal electrophysiological activities in multiple brain nuclei located within the medulla oblongata, pons, mesencephalon, diencephalon, and telencephalon (**Table 1**). Activation of GLP-1R suppresses food intake and induces postsynaptic depolarization of membrane potential (**Figure 1A**) and/or presynaptic modulation of glutamatergic or GABAergic neurotransmission (**Figure 1B**). Several ionic mechanisms such as non-selective cation channel, voltage-dependent potassium channel, and TRPC5 channel may be associated with activation of GLP-1R-induced electrophysiological effects (**Figure 1A**). This review may provide a rationale about the cellular mechanisms of GLP-1-induced suppression of feeding behaviors.

AUTHOR CONTRIBUTIONS

X-YC wrote the original draft. LC revised the manuscript. WY and A-MX contributed to the conception, design, and revision of the manuscript. All authors contributed to the article and approved the submitted version.

FUNDING

This work was supported by grants from the National Natural Science Foundation of China (81971192, 81571225, and 31671076).

REFERENCES

Acuna-Goycolea, C., and van den Pol, A. (2004). Glucagon-Like Peptide 1 Excites Hypocretin/Orexin Neurons by Direct and Indirect Mechanisms: Implications for Viscera-Mediated Arousal. *J. Neurosci.* 24, 8141–8152. doi: 10.1523/JNEUROSCI.1607-04.2004

Aimé, P., Palouzier-Paulignan, B., Salem, R., Koborssy, D. A., Garcia, S., Duchamp, C., et al. (2014). Romestaing C, Julliard AK. Modulation of olfactory sensitivity and glucose-sensing by the feeding state in obese Zucker rats. *Front. Behav. Neurosci.* 8:326. doi: 10.3389/fnbeh.2014.00326

Alhadeff, A. L., Baird, J. P., Swick, J. C., Hayes, M. R., and Grill, H. J. (2014). Glucagon-like peptide-1 receptor signaling in the lateral parabrachial nucleus contributes to the control of food intake and motivation to feed. *Neuropsychopharmacology* 39, 2233–2243. doi: 10.1038/npp.2014.74

Alhadeff, A. L., and Grill, H. J. (2014). Hindbrain nucleus tractus solitarius glucagon-like peptide-1 receptor signaling reduces appetitive and motivational aspects of feeding. *Am. J. Physiol. Regul. Integr. Comp. Physiol.* 307, R465–R470. doi: 10.1152/ajpregu.00179.2014

Alhadeff, A. L., Rupprecht, L. E., and Hayes, M. R. (2012). GLP-1 neurons in the nucleus of the solitary tract project directly to the ventral tegmental area and nucleus accumbens to control for food intake. *Endocrinology* 153, 647–658. doi: 10.1210/en.2011-1443

Barrera, J. G., Jones, K. R., Herman, J. P., D'Alessio, D. A., Woods, S. C., and Seeley, R. J. (2011). Hyperphagia and increased fat accumulation in two models of chronic CNS glucagon-like peptide-1 loss of function. *J. Neurosci.* 31, 3904–3913. doi: 10.1523/JNEUROSCI.2212-10.2011

Bernard, G., and Shevell, M. I (2008). Channelopathies: A Review. *Pediatr. Neurol.* 38, 73–85. doi: 10.1016/j.pediatrneurol.2007.09.007

Bouret, S. G., Draper, S. J., and Simerly, R. B. (2004). Formation of Projection Pathways from the Arcuate Nucleus of the Hypothalamus to Hypothalamic Regions Implicated in the Neural Control of Feeding Behavior in Mice. *J. Neurosci.* 24, 2797–2805. doi: 10.1523/JNEUROSCI.5369-03.2004

Brierley, D. I., Holt, M. K., Singh, A., de Araujo, A., McDougle, M., Vergara, M., et al. (2021). Central and peripheral GLP-1 systems independently suppress eating. *Nat. Metab.* 3, 258–273. doi: 10.1038/s42255-021-00344-4

Caron, A., Dungan, L. H. M., Castorena, C. M., Fujikawa, T., Lee, S., Lord, C. C., et al. (2018). POMC neurons expressing leptin receptors coordinate metabolic responses to fasting via suppression of leptin levels. *eLife* 7:e33710. doi: 10.7554/eLife.33710

Cork, S. C., Richards, J. E., Holt, M. K., Gribble, F. M., Reimann, F., and Trapp, S. (2015). Distribution and characterisation of Glucagon-like peptide-1 receptor expressing cells in the mouse brain. *Mol. Metab.* 4, 718–731. doi: 10.1016/j.molmet.2015.07.008

Dickson, S. L., Shirazi, R. H., Hansson, C., Bergquist, F., Nissbrandt, H., and Skibicka, K. P. (2012). The glucagon-like peptide 1 (GLP-1) analogue, exendin-4, decreases the rewarding value of food: a new role for mesolimbic GLP-1 receptors. *J. Neurosci.* 32, 4812–4820. doi: 10.1523/JNEUROSCI.6326-11.2012

Dossat, A. M., Lilly, N., Kay, K., and Williams, D. L. (2011). Glucagon-Like Peptide 1 Receptors in Nucleus Accumbens Affect Food Intake. *J. Neurosci.* 31, 14453–14457. doi: 10.1523/JNEUROSCI.3262-11.2011

Edwards, C. M., Todd, J. F., Mahmoudi, M., Wang, Z., Wang, R. M., Ghatei, M. A., et al. (1999). Glucagon-like peptide 1 has a physiological role in the control of postprandial glucose in humans: studies with the antagonist exendin 9-39. *Diabetes* 48, 86–93. doi: 10.2337/diabetes.48.1.86

Eissele, R., Göke, R., Willemer, S., Harthus, H. P., Vermeer, H., Arnold, R., et al. (1992). Glucagon-like peptide-1 cells in the gastrointestinal tract and pancreas of rat, pig and man. *Eur. J. Clin. Invest.* 22, 283–291. doi: 10.1111/j.1365-2362.1992.tb01464.x

Fadool, D. A., Tucker, K., and Pedarzani, P. (2011). Mitral Cells of the Olfactory Bulb Perform Metabolic Sensing and Are Disrupted by Obesity at the Level of the Kv1.3 Ion Channel. *PLoS One* 6:e24921. doi: 10.1371/journal.pone.0024921

Farkas, E., Szilvásy-Szabó, A., Ruska, Y., Sinkó, R., Rasch, M. G., Egebjerg, T., et al. (2021). Distribution and ultrastructural localization of the glucagon-like peptide-1 receptor (GLP-1R) in the rat brain. *Brain Struct. Funct.* 226, 225–245. doi: 10.1007/s00429-020-02189-1

Farr, O. M., Sofopoulos, M., Tsoukas, M. A., Dincer, F., Thakkar, B., Sahin-Efe, A., et al. (2016). GLP-1 receptors exist in the parietal cortex, hypothalamus and medulla of human brains and the GLP-1 analogue liraglutide alters brain activity related to highly desirable food cues in individuals with diabetes: a crossover, randomised, placebo-controlled trial. *Diabetologia* 59, 954–965. doi: 10.1007/s00125-016-3874-y

Gautron, L., Elmquist, J. K., and Williams, K. W. (2015). Neural control of energy balance: translating circuits to therapies. *Cell* 161, 133–145. doi: 10.1016/j.cell.2015.02.023

Gaykema, R. P., Newmyer, B. A., Ottolini, M., Raje, V., Warthen, D. M., Lambeth, P. S., et al. (2017). Activation of murine pre-proglucagon–producing neurons reduces food intake and body weight. *J. Clin. Invest.* 127, 1031–1045. doi: 10.1172/JCI8133

Gullo, F., Ceriani, M., D'Aloia, A., Wanke, E., Constanti, A., Costa, B., et al. (2017). Plant Polyphenols and Exendin-4 Prevent Hyperactivity and TNF-α Release in LPS-Treated *In vitro* Neuron/Astrocyte/Microglial Networks. *Front. Neurosci.* 11:500. doi: 10.3389/fnins.2017.00500

Gupta, P., Balasubramaniam, N., Chang, H. Y., Tseng, F. G., and Santra, T. S. (2020). A Single-Neuron: Current Trends and Future Prospects. *Cells* 9:1528. doi: 10.3390/cells9061528

Han, S. Y., McLennan, T., Czieselsky, K., and Herbison, A. E. (2015). Selective optogenetic activation of arcuate kisspeptin neurons generates pulsatile luteinizing hormone secretion. *Proc. Natl. Acad. Sci. U S A.* 112, 13109–13114. doi: 10.1073/pnas.1512243112

Hayes, M. R., Leichner, T. M., Zhao, S., Lee, G. S., Chowansky, A., Zimmer, D., et al. (2011). Intracellular signals mediating the food intake-suppressive effects of hindbrain glucagon-like peptide-1 receptor activation. *Cell Metab.* 13, 320–330. doi: 10.1016/j.cmet.2016.02.010

Hayes, M. R., Skibicka, K. P., and Grill, H. J. (2008). Caudal brainstem processing is sufficient for behavioral, sympathetic, and parasympathetic responses driven by peripheral and hindbrain glucagon-like-peptide-1 receptor stimulation. *Endocrinology* 149, 4059–4068. doi: 10.1210/en.2007-1743

He, Z., Gao, Y., Lieu, L., Afrin, S., Cao, J., Michael, N. J., et al. (2019). Direct and indirect effects of liraglutide on hypothalamic POMC and NPY/AgRP

neurons – Implications for energy balance and glucose control. *Mol. Metab.* 28, 120–134. doi: 10.1016/j.molmet.2019.07.008

Heppner, K. M., Baquero, A. F., Bennett, C. M., Lindsley, S. R., Kirigiti, M. A., Bennett, B., et al. (2017). GLP-1R Signaling Directly Activates Arcuate Nucleus Kisspeptin Action in Brain Slices but Does not Rescue Luteinizing Hormone Inhibition in Ovariectomized Mice During Negative Energy Balance. *eNeuro* 4, e198–e116. doi: 10.1523/ENEURO.0198-16.2016

Heppner, K. M., Kirigiti, M., Secher, A., Paulsen, S. J., Buckingham, R., and Pyke, C., et al. (2015). Expression and distribution of glucagon-like peptide1 receptor mRNA, protein and binding in the male nonhuman primate (Macaca mulatta) brain. *Endocrinology* 156, 255–267. doi: 10.1210/en.2014-1675

Heppner, K. M., and Perez-Tilve, D. (2015). GLP-1 based therapeutics: simultaneously combating T2DM and obesity. *Front. Neurosci.* 9:92. doi: 10.3389/fnins.2015.00092

Hernandez, N. S., O'Donovan, B., Ortinski, P. I., and Schmidt, H. D. (2019). Activation of glucagon-like peptide-1 receptors in the nucleus accumbens attenuates cocaine seeking in rats. *Addict. Biol.* 24, 170–181. doi: 10.1111/adb.12583

Hernandez, N. S., and Schmidt, H. D. (2019). Central GLP-1 Receptors: Novel Molecular Targets for Cocaine Use Disorder. *Physiol. Behav.* 206, 93–105. doi: 10.1016/j.physbeh.2019.03.026

Hisadome, K., Reimann, F., Gribble, F. M., and Trapp, S. (2010). Leptin Directly Depolarizes Preproglucagon Neurons in the Nucleus Tractus Solitarius: Electrical Properties of Glucagon-Like Peptide 1 Neurons. *Diabetes* 59, 1890–1898. doi: 10.2337/db10-0128

Holt, M. K., Richards, J. E., Cook, D. R., Brierley, D. I., Williams, D. L., Reimann, F., et al. (2019). Preproglucagon Neurons in the Nucleus of the Solitary Tract Are the Main Source of Brain GLP-1, Mediate Stress-Induced Hypophagia, and Limit Unusually Large Intakes of Food. *Diabetes* 68, 21–33. doi: 10.2337/db18-0729

Hsu, T. M., Hahn, J. D., Konanur, V. R., Lam, A., and Kanoski, S. E. (2015). Hippocampal GLP-1 receptors influence food intake, meal size, and effort-based responding for food through volume transmission. *Neuropsychopharmacology* 40, 327–337. doi: 10.1038/npp.2014.175

Hsu, T. M., Noble, E. E., Liu, C. M., Cortella, A. M., Konanur, V. R., Suarez, A. N., et al. (2018). A hippocampus to prefrontal cortex neural pathway inhibits food motivation through glucagon-like peptide-1 signaling. *Mol. Psychiatry* 23, 1555–1565. doi: 10.1038/mp.2017.91

Jensen, C. B., Pyke, C., Rasch, M. G., Dahl, A. B., Knudsen, L. B., and Secher, A. (2018). Characterization of the glucagonlike peptide-1 receptor in male mouse brain using a novel antibody and *in situ* hybridization. *Endocrinology* 159, 665–675. en.2017-00812 doi: 10.1210/

Klassen, T., Davis, C., Goldman, A., Burgess, D., Chen, T., Wheeler, D., et al. (2011). Exome sequencing of ion channel genes reveals complex profiles confounding personal risk assessment in epilepsy. *Cell* 145, 1036–1048. doi: 10.1016/j.cell.2011.05.025

Larsen, P. J., Tang-Christensen, M., and Jessop, D. S. (1997). Central administration of glucagon-like peptide-1 activates hypothalamic neuroendocrine neurons in the rat. *Endocrinology* 138, 4445–4455. doi: 10.1210/endo.138.10.5270

Lennox, R., Flatt, P. R., and Gault, V. A. (2014). Lixisenatide improves recognition memory and exerts neuroprotective actions in high-fat fed mice. *Peptides* 61, 38–47. doi: 10.1016/j.peptides.2014.08.014

Li, X. F., Kinsey-Jones, J. S., Cheng, Y., Knox, A. M., Lin, Y., Petrou, N. A., et al. (2009). Kisspeptin signalling in the hypothalamic arcuate nucleus regulates GnRH pulse generator frequency in the rat. *PLoS One* 4:e8334. doi: 10.1371/journal.pone.0008334

Liu, J., Conde, K., Zhang, P., Lilascharoen, V., Xu, Z., Lim, B. K., et al. (2017). Enhanced AMPA receptor trafficking mediates the anorexigenic effect of endogenous glucagon like peptide-1 in the paraventricular hypothalamus. *Neuron* 96, 897–909. doi: 10.1016/j.neuron.2017.09.042

Llewellyn-Smith, I. J., Reimann, F., Gribble, F. M., and Trapp, S. (2011). Preproglucagon neurons project widely to autonomic control areas in the mouse brain. *Neuroscience* 180, 111–121. doi: 10.1016/j.neuroscience.2011.02.023

Llinás, R. R. (1989). The intrinsic electrophysiological properties of mammalian neurons: insights into central nervous system function. *Science* 242, 1654–1664. doi: 10.1126/science.3059497

Llinás, R. R. (2014). Intrinsic electrical properties of mammalian neurons and CNS function: a historical perspective. *Front. Cell Neurosci.* 8:320. doi: 10.3389/fncel.2014.00320

Mayo, K. E., Miller, L. J., Bataille, D., Dalle, S., Goke, B., Thorens, B., et al. (2003). International Union of Pharmacology. XXXV. The glucagon receptor family. *Pharm. Rev.* 55, 167–194. doi: 10.1124/pr.55.1.6

McMahon, L. R., and Wellman, P. J. (1998). PVN infusion of GLP-1-(7-36) amide suppresses feeding but does not induce aversion or alter locomotion in rats. *Am. J. Physiol.* 274, R23–R29. gu.1998.274.1.r23 doi: 10.1152/ajpre

Merchenthaler, I., Lane, M., and Shughrue, P. (1999). Distribution of pre-pro-glucagon and glucagon-like peptide-1 receptor messenger RNAs in the rat central nervous system. *J. Comp. Neurol.* 403, 261–280. doi: 10.1002/(SICI)1096-9861(19990111)403:23.0.CO

Michel, P. P., Toulorge, D., Guerreiro, S., and Hirsch, E. C. (2013). Specific needs of dopamine neurons for stimulation in order to survive: implication for Parkinson disease. *FASEB. J.* 27, 3414–3423. doi: 10.1096/fj.12-220418

Mietlicki-Baase, E. G., Ortinski, P. I., Reiner, D. J., Sinon, C. G., McCutcheon, J. E., Pierce, R. C., et al. (2014). Glucagon-like peptide-1 receptor activation in the nucleus accumbens core suppresses feeding by increasing glutamatergic AMPA/kainate signaling. *J. Neurosci.* 34, 6985–6992. doi: 10.1523/JNEUROSCI.0115-14.2014

Mietlicki-Baase, E. G., Ortinski, P. I., Rupprecht, L. E., Olivos, D. R., Alhadeff, A. L., Pierce, R. C., et al. (2013). The food intake-suppressive effects of glucagon-like peptide-1 receptor signaling in the ventral tegmental area are mediated by AMPA/kainate receptors. *Am. J. Physiol. Endocrinol. Metab.* 305, E1367–E1374. doi: 10.1152/ajpendo.00413.2013

Muller, T. D., Finan, B., Bloom, S. R., D'Alessio, D., Drucker, D. J., Flatt, P. R., et al. (2019). Glucagon-like peptide 1 (GLP-1). *Mol. Metab.* 30, 72–130. t.2019.09.010 doi: 10.1016/j.molme

Oka, J. I., Goto, N., and Kameyama, T. (1999). Glucagon-like peptide-1 modulates neuronal activity in the rat's hippocampus. *Neuroreport* 10, 1643–1646. doi: 10.1097/00001756-199906030-00004

Ong, Z. Y., Liu, J. J., Pang, Z. P., and Grill, H. J. (2017). Paraventricular Thalamic Control of Food Intake and Reward: Role of Glucagon-Like Peptide-1 Receptor Signaling. *Neuropsychopharmacology* 42, 2387–2397. doi: 10.1038/npp.2017.150

Poessel, M., Breuer, N., Joshi, A., Pampel, A., Villringer, A., Hummel, T., et al. (2020). Reduced Olfactory Bulb Volume in Obesity and Its Relation to Metabolic Health Status. *Front. Hum. Neurosci.* 14:586998. doi: 10.3389/fnhum.2020.586998

Qi, C., Varga, S., Oh, S. J., Lee, C. J., and Lee, D. (2017). Optogenetic rescue of locomotor dysfunction and dopaminergic degeneration caused by alpha-synuclein and EKO genes. *Exp. Neurobiol.* 26, 97–103. doi: 10.5607/en.2017.26.2.97

Reiner, D. J., Mietlicki-Baase, E. G., McGrath, L. E., Zimmer, D. J., Bence, K. K., Sousa, G. L., et al. (2016). Astrocytes regulate GLP-1 receptor-mediated effects on energy balance. *J. Neurosci.* 36, 3531–3540. doi: 10.1523/JNEUROSCI.3579-15.2016

Richard, J. E., Farkas, I., Anesten, F., Anderberg, R. H., Dickson, S. L., Gribble, F. M., et al. (2014). GLP-1 Receptor Stimulation of the Lateral Parabrachial Nucleus Reduces Food Intake: Neuroanatomical, Electrophysiological, and Behavioral Evidence. *Endocrinology* 155, 4356–4367. doi: 10.1210/en.2014-1248

Riera, C. E., Tsaousidou, E., Halloran, J., Follett, P., Hahn, O., Pereira, M. M. A., et al. (2017). The sense of smell impacts metabolic health and obesity. *Cell Metab.* 26, 198–211. doi: 10.1016/j.cmet.2017.06.015

Schick, R. R., Zimmermann, J. P., vorm Walde, T., and Schusdziarra, V. (2003). Peptides that regulate food intake: glucagon-like peptide 1-(7-36) amide acts at lateral and medial hypothalamic sites to suppress feeding in rats. *Am. J. Physiol. Regul. Integr. Comp. Physiol.* 284, R1427–R1435. doi: 10.1152/ajpregu.00479.2002

Schwartz, A. B., Kapur, A., Huang, Z., Anangi, R., Spear, J. M., Stagg, S., et al. (2021). Olfactory bulb targeted QD bioconjugate and Kv1.3 blocking peptide improve metabolic health in obese male mice. *J. Neurochem.* 157, 1876–1896. doi: 10.1111/jnc.15200

Secher, A., Jelsing, J., Baquero, A. F., Hecksher-Sørensen, J., Cowley, M. A., Dalbøge, L. S., et al. (2014). The arcuate nucleus mediates GLP-1 receptor agonist liraglutide-dependent weight loss. *J. Clin. Invest.* 124, 4473–4488. doi: 10.1172/JCI75276

Shigeto, M., Ramracheya, R., Tarasov, A. I., Cha, C. Y., Chibalina, M. V., Hastoy, B., et al. (2015). GLP-1 stimulates insulin secretion by PKC-dependent TRPM4 and TRPM5 activation. *J. Clin. Invest.* 125, 4714–4728. doi: 10.1172/JCI81975

Tai, C., Abe, Y., Westenbroek, R. E., Scheuer, T., and Catterall, W. A. (2014). Impaired excitability of somatostatin- and parvalbumin-expressing cortical interneurons in a mouse model of Dravet syndrome. *Proc. Natl. Acad. Sci. U S A*. 111, E3139–E3148. doi: 10.1073/pnas.1411131111

Thiebaud, N., Gribble, F., Reimann, F., Trapp, S., and Fadool, D. A. (2019). A unique olfactory bulb microcircuit driven by neurons expressing the precursor to glucagon-like peptide 1. *Sci. Rep.* 9:15542. doi: 10.1038/s41598-019-5880-9

Thiebaud, N., Johnson, M. C., Butler, J. L., Bell, G. A., Ferguson, K. L., Fadool, A. R., et al. (2014). Hyperlipidemic diet causes loss of olfactory sensory neurons, reduces olfactory discrimination, and disrupts odor-reversal learning. *J. Neurosci.* 34, 6970–6984. doi: 10.1523/JNEUROSCI.3366-13.2014

Thiebaud, N., Llewellyn-Smith, I. J., Gribble, F., Reimann, F., Trapp, S., and Fadool, D. A. (2016). The incretin hormone glucagon—like peptide 1 increases mitral cell excitability by decreasing conductance of a voltage—dependent potassium channel. *J. Physiol.* 594, 2607–2628. doi: 10.1113/JP272322

Trapp, S., and Cork, S. C. (2015). PPG neurons of the lower brain stem and their role in brain GLP-1 receptor activation. *Am. J. Physiol. Regul. Integr. Comp. Physiol.* 309, R795–R804. doi: 10.1152/ajpregu.00333.2015

Turton, M. D., O'Shea, D., Gunn, I., Beak, S. A., Edwards, C. M., Meeran, K., et al. (1996). A role for glucagon-like peptide-1 in the central regulation of feeding. *Nature* 379, 69–72. doi: 10.1038/379069a0

Wang, X. F., Liu, J. J., Xia, J., Liu, J., Mirabella, V., and Pang, Z. P. (2015). Endogenous Glucagon-like peptide-1 suppresses high-fat food intake by reducing synaptic drive onto mesolimbic dopamine neurons. *Cell Rep.* 12, 726–733. doi: 10.1016/j.celrep.2015.06.062

Williams, D. L. (2009). Minireview: finding the sweet spot: peripheral versus central glucagon-like peptide 1 action in feeding and glucose homeostasis. *Endocrinology* 150, 2997–3001. doi: 10.1210/en.2009-0220

Williams, D. L., Lilly, N. A., Edwards, I. J., Yao, P., Richards, J. E., and Trapp, S. (2018). GLP-1 action in the mouse bed nucleus of the stria terminalis. *Neuropharmacology* 131, 83–95. doi: 10.1016/j.neuropharm.2017.12.007

Zhang, H., Chu, Y., Zheng, H., Wang, J., Song, B., and Sun, Y. (2021). Liraglutide improved the cognitive function of diabetic mice via the receptor of advanced glycation end products down-regulation. *Aging* 13, 525–536. doi: 10.18632/aging.202162

Conflict of Interest: The authors declare that the research was conducted in the absence of any commercial or financial relationships that could be construed as a potential conflict of interest.

Publisher's Note: All claims expressed in this article are solely those of the authors and do not necessarily represent those of their affiliated organizations, or those of the publisher, the editors and the reviewers. Any product that may be evaluated in this article, or claim that may be made by its manufacturer, is not guaranteed or endorsed by the publisher.

Copyright © 2021 Chen, Chen, Yang and Xie. This is an open-access article distributed under the terms of the Creative Commons Attribution License (CC BY). The use, distribution or reproduction in other forums is permitted, provided the original author(s) and the copyright owner(s) are credited and that the original publication in this journal is cited, in accordance with accepted academic practice. No use, distribution or reproduction is permitted which does not comply with these terms.

frontiers in Molecular Neuroscience

MINI REVIEW
published: 08 March 2022
doi: 10.3389/fnmol.2022.829365

Biosensors for Studying Neuronal Proteostasis

*Irina Dudanova**

Molecular Neurodegeneration Group, Max Planck Institute of Neurobiology, Martinsried, Germany

Cellular health depends on the integrity and functionality of the proteome. Each cell is equipped with a protein quality control machinery that maintains protein homeostasis (proteostasis) by helping proteins adopt and keep their native structure, and ensuring the degradation of damaged proteins. Postmitotic cells such as neurons are especially vulnerable to disturbances of proteostasis. Defects of protein quality control occur in aging and have been linked to several disorders, including neurodegenerative diseases. However, the exact nature and time course of such disturbances in the context of brain diseases remain poorly understood. Sensors that allow visualization and quantitative analysis of proteostasis capacity in neurons are essential for gaining a better understanding of disease mechanisms and for testing potential therapies. Here, I provide an overview of available biosensors for assessing the functionality of the neuronal proteostasis network, point out the advantages and limitations of different sensors, and outline their potential for biological discoveries and translational applications.

Keywords: proteostasis, protein quality control, protein folding, neuron, biosensor, protein misfolding diseases

OPEN ACCESS

Edited by:
Inmaculada Segura, Ludwig Maximilian University of Munich, Germany

Reviewed by:
Arun Upadhyay, Northwestern University, United States
Thorsten Hoppe, Universität zu Köln, Germany

***Correspondence:**
Irina Dudanova
idudanova@neuro.mpg.de

Specialty section:
This article was submitted to Molecular Signalling and Pathways, a section of the journal Frontiers in Molecular Neuroscience

Received: *05 December 2021*
Accepted: *31 January 2022*
Published: *08 March 2022*

Citation:
Dudanova I (2022) Biosensors for Studying Neuronal Proteostasis. Front. Mol. Neurosci. 15:829365. doi: 10.3389/fnmol.2022.829365

INTRODUCTION

To maintain cellular health, proteins have to be synthesized in required amounts, correctly folded and assembled into complexes, and turned over at appropriate rates. Cells possess an elaborate protein quality control machinery for accomplishing these tasks and guarding protein homeostasis (proteostasis; Labbadia and Morimoto, 2015; Hipp et al., 2019). This machinery, referred to as the proteostasis network, includes protein synthesis components, molecular chaperones, the ubiquitin-proteasome system (UPS) as well as the autophagy-lysosomal system (**Figure 1**). Chaperones guide proteins on their folding pathways, keep them in the proper conformation, and ensure the timely removal of excess or damaged proteins by degradation systems (Shiber and Ravid, 2014; Balchin et al., 2016). Monomeric proteins are degraded by the UPS upon their unfolding, while large multimeric complexes are cleared through the autophagy-lysosomal pathway (Dikic, 2017).

Mutations, mRNA processing defects, translation errors, and various types of external stress can lead to protein misfolding, imposing a burden on the proteostasis network (Hipp et al., 2019). Misfolded species are normally recognized by chaperones and either refolded or targeted for degradation. However, if not efficiently cleared, misfolded proteins might accumulate and form aggregates (**Figure 1**), with potentially harmful consequences for the cells. Indeed, protein aggregates are a common feature of protein misfolding diseases, including neurodegenerative disorders such as Alzheimer's, Parkinson's, or Huntington's disease. As proteostasis capacity undergoes an age-related decline, aging represents a common risk factor for these

diseases (Douglas and Dillin, 2010; Brehme et al., 2014; Vilchez et al., 2014; Hipp et al., 2019). Moreover, mutations in components of the proteostasis network are often associated with neurodegeneration (Labbadia and Morimoto, 2015).

The composition and function of the proteostasis network, as well as susceptibility to its disturbances, varies between tissues and cell types (Guisbert et al., 2013; Labbadia and Morimoto, 2015). Neurons are particularly vulnerable to protein misfolding for several reasons. As postmitotic cells, they are unable to rejuvenate and redistribute damaged protein species through cell divisions, or clear them as efficiently as has been shown for neural stem cells (Vilchez et al., 2012; Bufalino et al., 2013; Moore et al., 2015; Leeman et al., 2018). In addition, neurons are exceptionally long-lived and have to endure proteotoxic insults that accumulate during the whole life span. Interestingly, at least some types of neurons also fail to efficiently activate the heat shock response (Marcuccilli et al., 1996; Batulan et al., 2003), a canonical stress response that leads to upregulation of chaperones and alleviates proteotoxic stress (Morimoto, 2011). Finally, proteostasis capacity can vary considerably between neuronal cell types, depending on their repertoire of proteostasis network components and regulators (Tagawa et al., 2007; Tsvetkov et al., 2013).

The proteostasis system is amenable to pharmacological manipulation, and interventions that enhance the cellular proteostasis capacity hold great promise for the treatment of neurodegeneration (Balch et al., 2008; Labbadia and Morimoto, 2015; Baranczak and Kelly, 2016; Hommen et al., 2021). For example, treatment with the small molecule arimoclomol, which improves proteostasis by potentiating the heat-shock response and inducing expression of several chaperones, ameliorated disease signs in mouse models of several neurodegenerative proteinopathies (Kieran et al., 2004; Malik et al., 2013; Ahmed et al., 2021), and also produced promising results in amyotrophic lateral sclerosis patients (Benatar et al., 2018). A prerequisite for the development of such therapeutic strategies for different neurodegenerative conditions is a thorough understanding of the changes in neuronal proteostasis in healthy aging and during the course of the disease. In addition, the success of potential proteostasis-targeting interventions has to be monitored with a robust readout. To this end, there is a need for proteostasis biosensors that can measure the functionality of neuronal protein quality control *in vivo*. Several such sensors have been developed and used in different model organisms. In the following sections, I will review the major classes of proteostasis sensors, their advantages and limitations, and their applications in neurons.

PROTEOSTASIS BIOSENSORS

Biosensors are tools that specifically detect certain biomolecules and provide information on their concentration, localization, and/or function. Biosensors have proven extremely useful in biomedical research by allowing visualization and quantification of dynamic processes in living cells (Velasco-Garcia, 2009; Greenwald et al., 2018). In the field of neurosciences, specialized sensors have been developed e.g., for interrogating synaptic function, monitoring intracellular trafficking, and detecting activation of various signaling cascades (Choquet et al., 2021; Laviv and Yasuda, 2021). Most commonly, such sensors rely on fluorescence, but some use other readouts such as luminescence.

Proteostasis sensors are used to monitor the functional state of the protein quality control system in living cells and whole organisms. Their major current and future applications include mechanistic studies of proteostasis pathways in health and disease, development of proteostasis-modifying drugs, as well as diagnostics and treatment monitoring of protein misfolding disorders.

Various reporters exist for the proteostasis network on the whole, as well as for some of its parts. Here, I will focus on general proteostasis sensors that report primarily on the folding capacity of cells, with a particular emphasis on the tools suitable for investigating neuronal proteostasis in animal models. These sensors typically either detect endogenous proteins in an unfolded state or are themselves chaperone clients whose unfolded state triggers changes in their fluorescence, cellular distribution and/or function. In addition to folding sensors, specialized tools have been developed for probing the UPS system and autophagy (reviewed in Lindsten et al., 2003; Matilainen et al., 2016; Klionsky et al., 2021). Finally, sensors for monitoring certain chaperones and canonical stress responses such as the heat shock response or the unfolded protein response of the endoplasmic reticulum are also available (e.g., Batulan et al., 2003; Morley and Morimoto, 2004; van Oosten-Hawle et al., 2013; Kijima et al., 2018; Pereira et al., 2018; Miles and van Oosten-Hawle, 2020; Shen et al., 2021), but will not be discussed in detail here.

TYPES OF PROTEOSTASIS SENSORS

General proteostasis sensors can be divided into three major groups: small molecule sensors, genetically encoded sensors based on endogenous proteins, and genetically encoded sensors based on ectopic proteins (**Table 1**).

Small Molecule Sensors

Small molecule sensors are represented by fluorogenic small molecules that become fluorescent upon binding to free thiol groups of cysteine residues in unfolded proteins. Free cysteines not engaged in disulfide bonds are usually buried within the three-dimensional structure of native proteins but are exposed in unfolded ones. These sensors, therefore, allow estimating the pool of unfolded proteins in a cell. An example of such a sensor is tetraphenylethene maleimide (TPE-MI, **Figure 2A**). In addition to immunofluorescence and flow cytometry applications, TPE-MI is well suited for proteomics approaches, as its binding leads to a change in cysteine residue-containing peptides, and allows identifying the proteins that are unfolded under certain conditions (Chen et al., 2017). The drawbacks of TPE-MI are its low water solubility and absorption peak in the ultraviolet range. Its optimized derivative, TPE-NMI, is more hydrophilic and shows a red-shifted spectrum, making it better suited for commonly used lasers (Zhang et al., 2019). Importantly, the TPE-MI and TPE-NMI sensors have been verified in neuron-like Neuro2A cells, as well as in iPSC-derived

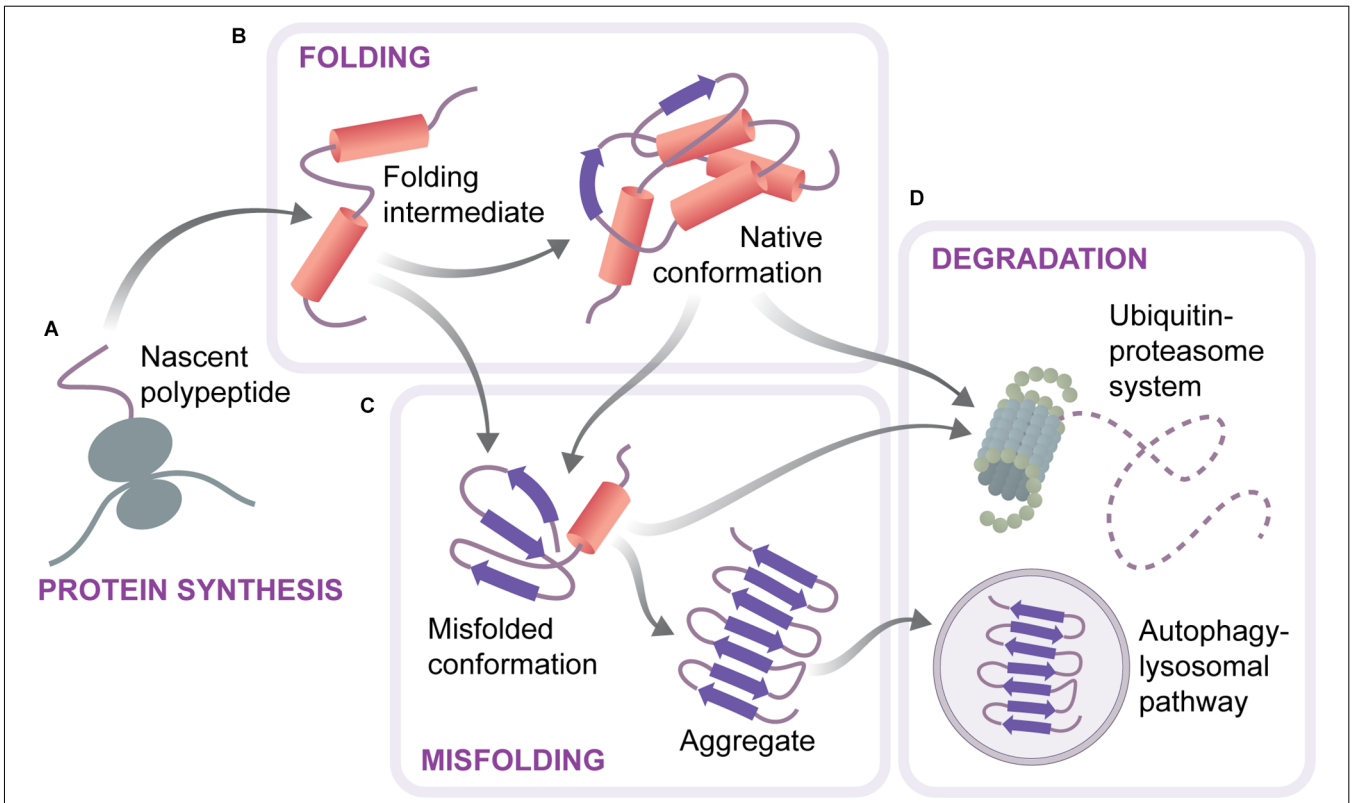

FIGURE 1 | Scheme of the proteostasis system. Proteins are synthesized on ribosomes as unfolded polypeptides **(A)**. They reach their native conformation through a folding process that is assisted by chaperones and can include several folding intermediates **(B)**. Proteins can also adopt alternative, misfolded conformations, which are prone to aggregation and lead to the formation of amyloid-like aggregates **(C)**. Aberrant or excessive proteins are removed by two cellular degradation systems, the ubiquitine-proteasome system and autophagy **(D)**.

primitive neural precursor cells, in both cases revealing reduced folding capacity in the presence of mutant Huntingtin prior to the formation of visible aggregates (Chen et al., 2017; Zhang et al., 2019). An interesting recent addition to the suite of maleimide sensors is NTPAN-MI, described as a "molecular chameleon" (Owyong et al., 2020). Due to its polarity-sensitive emission profile, it can visualize the subcellular changes in polarity that occur in the local environment of unfolded proteins. As different subcellular compartments display inherent differences in polarity and its dynamics upon proteotoxic stress, NTPAN-MI can provide a refined spatial map of proteostasis disbalance in a cell. This would be particularly interesting to investigate in morphologically complex cells like neurons.

One of the limitations of maleimides is their reduced stability in certain pH conditions (Koniev and Wagner, 2015). This shortcoming was addressed by the development of another thiol-reactive small molecule, the BODIPY-based probe VB1Cl, which is stable in a broad pH range (Mu et al., 2021).

Small molecule sensors do not impose an additional burden on the protein quality control system, are easy to use, and allow precise temporal control of the experiments, as they are membrane-permeable and can be bath-applied to cultured cells. Moreover, they provide a direct measure of the state of the cellular proteome due to their binding to endogenous unfolded proteins. Assays using these sensors are easily scalable and ideal for large screens, e.g., for testing proteostasis-correcting molecules in iPSC-derived neurons. However, small molecule sensors cannot be specifically targeted to certain tissues or cell types, and are not suitable for long-term studies over the lifetime of an organism. While well established in cell culture settings, they have not yet been tested in animal models. Further potential improvements in these sensors include the development of molecules with fluorescence in different parts of the spectrum, for easier combination with other available fluorescent tools and imaging techniques.

Genetically Encoded Sensors

Genetically encoded reporters are ideal for longitudinal observation of disease progression in model organisms. Pioneered by the lab of Richard Morimoto (Morley et al., 2002; Gidalevitz et al., 2006), such sensors are usually comprised of conformationally unstable client proteins that require chaperone assistance for maintaining their native conformation. In proteotoxic stress conditions when the cellular folding capacity is consumed by other clients, the sensors misfold and aggregate. The occurrence and extent of misfolding, which can be detected by different readouts, serve as an indication of proteostasis impairment.

TABLE 1 | Available proteostasis sensors.

Sensor type	Main advantages (+) and limitations (–)	Examples of sensors	Readout(s) of proteostasis impairments	Model systems the sensor has been used in	References
Small molecules	(+) Precise temporal control of application, no burden on the protein quality control system, ideal for large screens	TPE-MI, TPE-NMI	Turn-on fluorescence	Cell lines, iPSC-derived neural precursors	Chen et al. (2017) and Zhang et al. (2019)
	(–) No cell type specificity, not suitable for long-term *in vivo* studies	NTPAN-MI	Turn-on fluorescence with polarity-sensitive spectrum	Cell lines	Owyong et al. (2020)
		VB1CI	Turn-on fluorescence	Cell lines	Mu et al. (2021)
Endogenous proteins	(+) Suitable for long-term *in vivo* studies (–) Burden on the protein quality control system, potential loss-of-function effects	Paramyosin(ts), dynamin(ts), perlecan(ts), unc-45(ts), ras(ts), gas-1(ts), acetylcholine receptor(ts)	Different readouts depending on the specific protein, e.g., at cellular level: mislocalization of the sensor, altered protease sensitivity; at organismal level: embryonic lethality/ development arrest, movement impairment, egg-laying defect	*C. elegans*	Gidalevitz et al. (2006) and Ben-Zvi et al. (2009)
Ectopic proteins	(+) Suitable for long-term *in vivo* studies, no loss-of-function effects	Fluc-EGFP	Decrease in bioluminescence, formation of Fluc-EGFP foci	Cell lines, primary neurons, *C. elegans*, transgenic mice	Gupta et al. (2011) and Blumenstock et al. (2021)
	(–) Burden on the protein quality control system	AgHalo	Turn-on fluorescence	Cell lines	Liu et al. (2017), Fares et al. (2018), and Liu et al. (2018)
		Retroaldolase	Formation of fluorescent aggregates	Cell lines	Liu et al. (2015)
		Barnase FRET sensor	FRET	Cell lines	Wood et al. (2018)

Genetically Encoded Sensors Based on Endogenous Proteins

A set of studies in *Caenorhabditis elegans (C. elegans)* models made use of conformationally destabilized endogenous proteins to detect global imbalance in protein quality control (Gidalevitz et al., 2006; Ben-Zvi et al., 2009; van Oosten-Hawle et al., 2013; Miles and van Oosten-Hawle, 2020). These endogenous proteins contain temperature-sensitive (ts) point mutations known to cause specific phenotypes at restrictive (elevated), but not permissive (control) temperatures. In proteotoxic conditions due to aging or co-expression of aggregating proteins, misfolding of the destabilized ts proteins occurs already at permissive temperature, leading to the exposure of their specific mutant phenotypes. A whole panel of ts sensors have been generated based on proteins enriched in different tissues, including muscle, neuronal, intestinal, and hypodermal cells. Among the neuronal sensors are ts versions of dynamin (**Figure 2B**), ras, gas-1, and acetylcholine receptor. Depending on the type of ts-protein, various readouts can be used to analyze its loss of function at the organismal level, such as movement coordination, paralysis, and lethality, as well as the sensitivity of the worms to different stress conditions. At the cellular level, the misfolded destabilized proteins mislocalize, form aggregate-like structures, and show altered sensitivity to proteolysis, indicating a disturbance in the cellular folding environment (Gidalevitz et al., 2006; Ben-Zvi et al., 2009).

Destabilized endogenous proteins have enabled several seminal discoveries on proteostasis in *C. elegans* models (Gidalevitz et al., 2006; Ben-Zvi et al., 2009; van Oosten-Hawle et al., 2013). The advantage of these sensors is their biological relevance within the cells under study. However, mutated endogenous proteins also have notable shortcomings when used as proteostasis sensors, as tissue-specific phenotypes of different proteins are difficult to compare. Another major concern is the potential loss-of-function effects resulting from the misfolding and aggregation of endogenous proteins. Several unrelated destabilized proteins can be used to ensure that the findings are not only valid for one specific client and likely do not result from its loss-of-function (Gidalevitz et al., 2006; Ben-Zvi et al., 2009), however, such studies would not be feasible in more complex organisms.

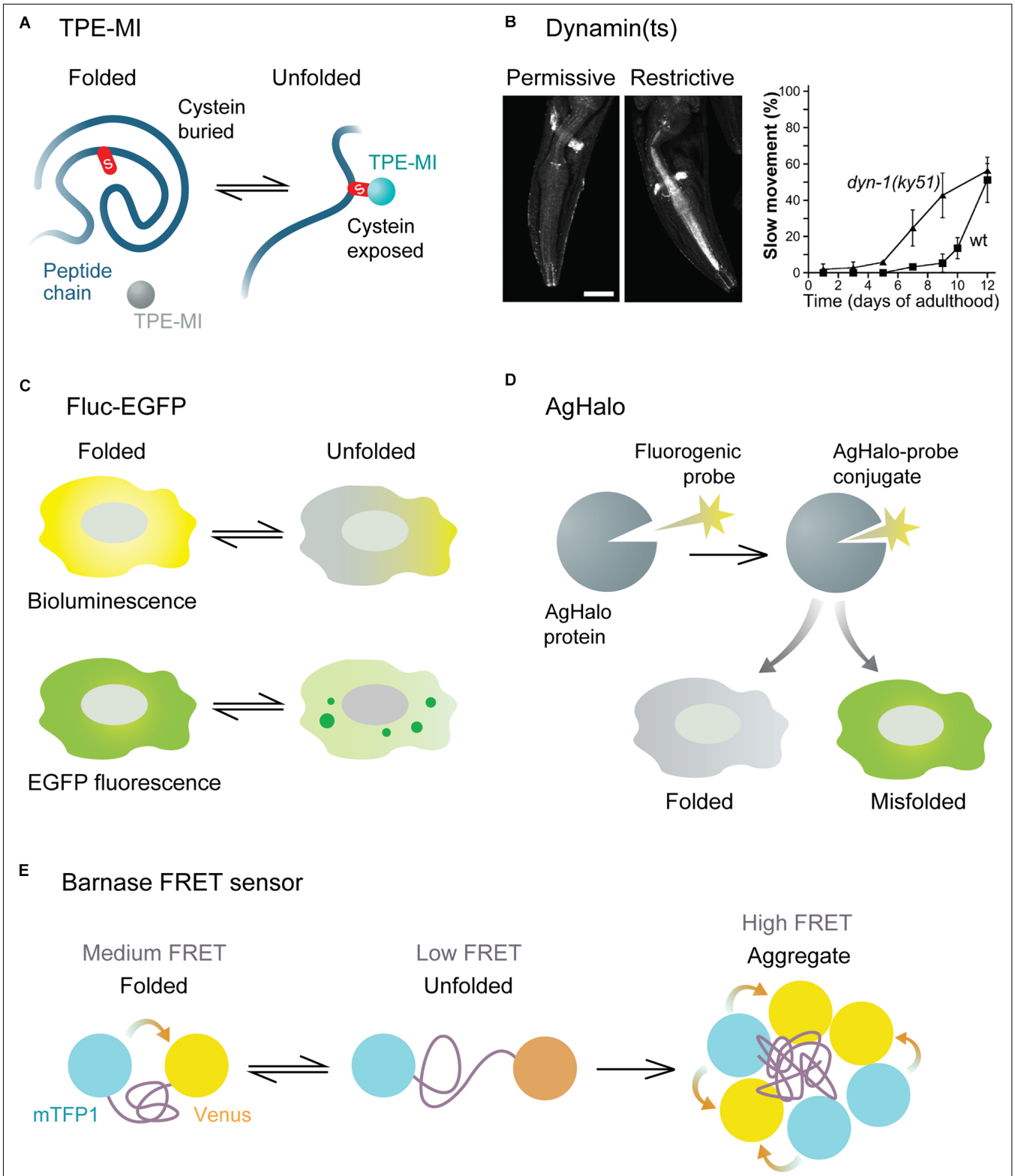

FIGURE 2 | Functional principles of various proteostasis sensors. **(A)** TPE-MI small molecule sensor becomes fluorescent upon binding to free cysteine residues of unfolded proteins. **(B)** Dynamin temperature sensitive (ts) mutant mislocalizes (left) and causes movement defects (right) in conditions of impaired proteostasis. Images are adapted with permission from Ben-Zvi et al. (2009). **(C)** Fluc-EGFP sensor displays reduced luciferase activity and forms fluorescent foci when not folded correctly. **(D)** AgHalo sensor forms a conjugate with a small molecule probe, which emits fluorescence when the sensor is misfolded. **(E)** Barnase sensor displays different levels of FRET in folded, unfolded, and aggregated states.

Genetically Encoded Sensors Based on Ectopic Proteins

Sensors based on ectopically expressed proteins lack an endogenous function, are therefore more inert, and cause less interference with cellular physiology. Such bioorthogonal sensors include different versions of luciferase, an enzyme that catalyzes a light-emitting bioluminescence reaction (Rokney et al., 2009; Winkler et al., 2010; Gupta et al., 2011; Donnelly et al., 2014; Frottin et al., 2019). In conditions of impaired proteostasis, these proteins form aggregates, visible as fluorescent foci if the sensor is fused to a fluorescent protein. In addition, luciferase offers a second way of analyzing folding efficiency, as it displays reduced enzymatic activity when not folded properly. This can be detected by measuring bioluminescence emitted in a luciferase assay, providing a reliable quantitative readout with a large dynamic range. One of such sensors made up of the luciferase from the firefly *Photinus pyralis* fused to an enhanced green fluorescent protein (Fluc-EGFP, **Figure 2C**), is available as a series of progressively destabilized mutants (Gupta et al., 2011), which broaden the spectrum of proteostasis capacity states that can be probed. As the pool of Fluc-EGFP is not entirely folded in mammalian cells at baseline conditions, the state of improved proteostasis, e.g., as a result of activated stress responses, can also be detected by an increase in luciferase activity. The functionality of this sensor has been proven not only in cell lines and in *C. elegans*, but also in primary murine neurons. Moreover, a transgenic mouse with Fluc-EGFP expression in the nervous system has been generated, which gives a unique opportunity to investigate *in vivo* proteostasis changes in normal aging and in mouse disease models (Blumenstock et al., 2021). Thus, the sensor revealed proteostasis impairments in a tauopathy model at an early stage, preceding neuronal cell death and behavioral symptoms. At the single-cell level, a clear reaction of the sensor was observed in tau-expressing cells even in the absence of tau neurofibrillary tangles. These findings point to proteostasis alterations as an early hallmark of neurodegeneration *in vivo*. Of note, while the bioluminescence readout showed very high sensitivity in cell lines, it proved less sensitive in bulk brain tissue of proteinopathy model mice (Gupta et al., 2011; Blumenstock et al., 2021), possibly due to the heterogeneity of neuronal cell types that differ in their reactions to misfolding. This underlines the importance of single-cell sensor readouts in order to capture the complexity of cell types *in vivo*.

Some sensors are designed to interact with a fluorogenic small molecule probe, forming a sensor-probe conjugate. One of such reporters is AgHalo, an unstable, aggregation-prone variant of the HaloTag protein (Los et al., 2008; Liu et al., 2017). The conjugate of AgHalo with its small molecule ligand is non-fluorescent in the folded state but shows a strong increase in fluorescence in a misfolded or aggregated state (**Figure 2D**). With an improved version of the fluorogenic probe, this reporter was shown to be highly sensitive even to early stages of protein misfolding under mild proteotoxic stress (Fares et al., 2018). In addition, possible applications of the AgHalo sensor are broadened by the availability of multicolor probes. Thus, a combination of probes can be used to simultaneously label the folded and misfolded sensor pools within the same cell and observe their dynamics in real time (Liu et al., 2018). Another sensor that works in complex with a fluorogenic small molecule is the *de novo* designed enzyme retroaldolase with destabilizing mutations. In this case, the small molecule probe becomes fluorescent upon binding to the sensor, and proteostasis disturbance is detected by a redistribution of fluorescence in a cell from diffuse to granular (Liu et al., 2015). Small molecule-regulated sensors enable precise temporal measurements of proteostasis capacity alterations, including pulse-chase approaches, as the contribution of newly synthesized sensor to the readout is excluded after the unbound probe has been washed out. The limitation of these sensors is that longitudinal studies in living organisms would require repeated delivery of the fluorogenic probe. Up to date, this type of sensor has only been used in bacteria and in mammalian cell lines.

A further group of genetic sensors takes advantage of fluorescence resonance energy transfer (FRET) between a pair of fluorophores fused to the N- and C-termini of an unstable protein to visualize the folding efficiency. One such sensor comprises the prokaryotic protein barnase attached to a cyan (mTFP1) and yellow (Venus) FRET pair (Wood et al., 2018). The FRET signal is low in the unfolded state of the sensor, medium in the folded state, and high in the aggregated state (**Figure 2E**). With the help of mathematical modeling, the proteostasis capacity can be quantified based on the proportion of cells in different FRET intensity states measured by flow cytometry. Like Fluc-EGFP, the barnase sensor is able to detect not only impairments but also improvements in folding efficiency. In addition, a range of progressively destabilized barnase mutants are also available (Wood et al., 2018). An important advantage of this sensor is that it provides a precise quantitative measure of the cellular folding capacity under different experimental conditions. However, it should be noted that the quantitative FRET readout of the sensor, which makes use of flow cytometry, would be challenging *in vivo*, as it requires isolation and dissociation of the cells of interest. The less quantitative evaluation of visible sensor aggregates remains feasible also in a living organism. Another FRET-based sensor consists of the mutated phosphoglycerate kinase (PGK) protein with a green/red fluorophore pair (Ebbinghaus et al., 2010). It was developed for monitoring protein folding in cells upon brief temperature jumps but has not yet been validated in the context of disease-related proteostasis impairments. In general, FRET-dependent sensors have so far only been tested in non-neuronal cell lines, and the utility of these sensors in neurons remains to be explored. When using transient transfection to express sensors based on ectopic proteins, it should be kept in mind that the poor control of the sensor expression levels might lead to a high variability of the results.

All genetically encoded sensors have the important advantage that they can be targeted to specific cell populations by using different promoters. This opens the unique possibility to dissect the relations between proteostasis of different tissues of an organism (van Oosten-Hawle et al., 2013) and potentially of different cell types within a tissue. Such applications are

particularly relevant in a complex organ like the brain, containing a great variety of neuronal and glial cell types.

On the other hand, a common consideration for all genetically encoded sensors is that conformationally unstable proteins might themselves to some extent trigger stress responses and enhance adverse phenotypes in proteinopathy models (Gidalevitz et al., 2006; Gupta et al., 2011). Therefore, care should be taken when using destabilized proteins as sensors, and their expression should be kept low to avoid occupying a large fraction of the proteostasis machinery with the sensor itself. To ameliorate this limitation, inducible genetic strategies would be preferable, as they allow tighter temporal control of expression and minimize undesired stress responses and chronic adaptations of the protein quality control system. However, such strategies are more complex and require the expression of multiple constructs, limiting their use in animal models.

DISCUSSION AND FUTURE DIRECTIONS

The available toolbox of proteostasis biosensors has been quickly expanding during the last decade. For small molecule sensors, major recent improvements include increased sensitivity, stability, and spectral properties. Genetically encoded sensors have become more biologically inert, and their readouts more quantitative. It should be kept in mind that different sensors, albeit intended to report on the global state of the proteostasis system rather than its specific branches, might be biased towards certain parts of the protein quality control machinery or certain client proteins, and might not be representative of the state of the entire proteome. The comparability of different sensors has not been systematically explored and remains to be clarified in future experiments. A combination of sensors is therefore desirable for a more comprehensive assessment of a condition under study.

Cellular compartments and organelles such as the nucleus, mitochondria, and endoplasmic reticulum have evolved distinct proteostasis pathways, and recent studies have highlighted the impact of these organelle-specific mechanisms on cellular proteostasis (Walter and Ron, 2011; Kirstein et al., 2015; Miller et al., 2015; Frakes and Dillin, 2017; Shpilka and Haynes, 2018; Frottin et al., 2019; Moehle et al., 2019). Some of the existing proteostasis sensors have already been targeted to different cellular compartments (Winkler et al., 2010; Frottin et al., 2019; Blumenstock et al., 2021; Melo et al., 2021; Raeburn et al., 2021). A set of spectrally distinct, compartment-specific sensors that could be combined with each other would be a helpful resource for elucidating intra-compartmental crosstalk.

While proteostasis sensors have proven very useful in cell culture and *C. elegans* models, investigating neuronal proteostasis in higher organisms has for a long time remained a challenge. The generation of proteostasis reporter mice (Blumenstock et al., 2021) opens exciting new avenues for fundamental insights into *in vivo* mechanisms of protein misfolding. Thus, transgenic Fluc-EGFP mice will allow longitudinal investigations of the dynamics of proteostasis impairments during disease progression at the single-cell level with modern imaging methods such as *in vivo* two-photon microscopy. In addition, thanks to the recent advances in microfluidics, single-cell RNA-sequencing, and proteomic methods, linking the *in vivo* folding efficiency of single neurons to their molecular profiles is now within reach. Comparison of the proteostasis capacity of different cell types might enable important discoveries about neuronal vulnerability to disease.

In addition to elucidating the basic mechanisms of aging and disease, proteostasis sensors hold great promise for more translational applications, particularly as biomarkers of protein misfolding disorders including neurodegeneration. Proteostasis disturbances are among the earliest hallmarks of these diseases, therefore proteostasis biosensors could be used for early diagnostics or even prophylactic screening to identify individuals at risk. Longitudinal monitoring of proteostasis alterations in biosamples from patients could furthermore provide an efficacy measure for therapeutic interventions. The use of proteostasis sensors in mammalian models is an important milestone for these exciting future clinical applications.

AUTHOR CONTRIBUTIONS

ID conceived and wrote the manuscript.

FUNDING

I acknowledge funding from the European Research Council (grant FP7 GA ERC-2012-SyG_318987-ToPAG) and from the Max Planck Society for the Advancement of Science.

ACKNOWLEDGMENTS

I thank Julia Kuhl for excellent assistance with the illustrations.

REFERENCES

Ahmed, M., Spicer, C., Harley, J., Petersen, N., Taylor, P., Jensen, T., et al. (2021). Amplifying the heat shock response ameliorates pathology in mouse and human models of ALS and FTD *Res. Square* [Preprint]. doi: 10.21203/rs.3.rs-152813/v1

Balch, W. E., Morimoto, R. I., Dillin, A., and Kelly, J. W. (2008). Adapting proteostasis for disease intervention. *Science* 319, 916–919. doi: 10.1126/science.1141448

Balchin, D., Hayer-Hartl, M., and Hartl, F. U. (2016). *In vivo* aspects of protein folding and quality control. *Science* 353:aac4354. doi: 10.1126/science.aac4354

Baranczak, A., and Kelly, J. W. (2016). A current pharmacologic agent versus the promise of next generation therapeutics to ameliorate protein misfolding and/or aggregation diseases. *Curr. Opin. Chem. Biol.* 32, 10–21. doi: 10.1016/j.cbpa.2016.01.009

Batulan, Z., Shinder, G. A., Minotti, S., He, B. P., Doroudchi, M. M., Nalbantoglu, J., et al. (2003). High threshold for induction of the stress response in motor neurons is associated with failure to activate HSF1. *J. Neurosci.* 23, 5789–5798. doi: 10.1523/JNEUROSCI.23-13-05789.2003

Benatar, M., Wuu, J., Andersen, P. M., Atassi, N., David, W., Cudkowicz, M., et al. (2018). Randomized, double-blind, placebo-controlled trial of arimoclomol in rapidly progressive SOD1 ALS. *Neurology* 90, e565–e574. doi: 10.1212/WNL.0000000000004960

Ben-Zvi, A., Miller, E. A., and Morimoto, R. I. (2009). Collapse of proteostasis represents an early molecular event in *Caenorhabditis elegans* aging. *Proc. Natl. Acad. Sci. U S A* 106, 14914–14919. doi: 10.1073/pnas.0902882106

Blumenstock, S., Schulz-Trieglaff, E. K., Voelkl, K., Bolender, A. L., Lapios, P., Lindner, J., et al. (2021). Fluc-EGFP reporter mice reveal differential alterations of neuronal proteostasis in aging and disease. *EMBO J.* 40:e107260. doi: 10.15252/embj.2020107260

Brehme, M., Voisine, C., Rolland, T., Wachi, S., Soper, J. H., Zhu, Y., et al. (2014). A chaperome subnetwork safeguards proteostasis in aging and neurodegenerative disease. *Cell Rep.* 9, 1135–1150. doi: 10.1016/j.celrep.2014.09.042

Bufalino, M. R., DeVeale, B., and van der Kooy, D. (2013). The asymmetric segregation of damaged proteins is stem cell-type dependent. *J. Cell Biol.* 201, 523–530. doi: 10.1083/jcb.201207052

Chen, M. Z., Moily, N. S., Bridgford, J. L., Wood, R. J., Radwan, M., Smith, T. A., et al. (2017). A thiol probe for measuring unfolded protein load and proteostasis in cells. *Nat. Commun.* 8:474. doi: 10.1038/s41467-017-00203-5

Choquet, D., Sainlos, M., and Sibarita, J. B. (2021). Advanced imaging and labelling methods to decipher brain cell organization and function. *Nat. Rev. Neurosci.* 22, 237–255. doi: 10.1038/s41583-021-00441-z

Dikic, I. (2017). Proteasomal and autophagic degradation systems. *Annu. Rev. Biochem.* 86, 193–224. doi: 10.1146/annurev-biochem-061516-044908

Donnelly, N., Passerini, V., Durrbaum, M., Stingele, S., and Storchova, Z. (2014). HSF1 deficiency and impaired HSP90-dependent protein folding are hallmarks of aneuploid human cells. *EMBO J.* 33, 2374–2387. doi: 10.15252/embj.201488648

Douglas, P. M., and Dillin, A. (2010). Protein homeostasis and aging in neurodegeneration. *J. Cell Biol.* 190, 719–729. doi: 10.1083/jcb.201005144

Ebbinghaus, S., Dhar, A., McDonald, J. D., and Gruebele, M. (2010). Protein folding stability and dynamics imaged in a living cell. *Nat. Methods* 7, 319–323. doi: 10.1038/nmeth.1435

Fares, M., Li, Y., Liu, Y., Miao, K., Gao, Z., Zhai, Y., et al. (2018). A molecular rotor-based halo-tag ligand enables a fluorogenic proteome stress sensor to detect protein misfolding in mildly stressed proteome. *Bioconjug. Chem.* 29, 215–224. doi: 10.1021/acs.bioconjchem.7b00763

Frakes, A. E., and Dillin, A. (2017). The UPR(ER): sensor and coordinator of organismal homeostasis. *Mol. Cell* 66, 761–771. doi: 10.1016/j.molcel.2017.05.031

Frottin, F., Schueder, F., Tiwary, S., Gupta, R., Korner, R., Schlichthaerle, T., et al. (2019). The nucleolus functions as a phase-separated protein quality control compartment. *Science* 365, 342–347. doi: 10.1126/science.aaw9157

Gidalevitz, T., Ben-Zvi, A., Ho, K. H., Brignull, H. R., and Morimoto, R. I. (2006). Progressive disruption of cellular protein folding in models of polyglutamine diseases. *Science* 311, 1471–1474. doi: 10.1126/science.1124514

Greenwald, E. C., Mehta, S., and Zhang, J. (2018). Genetically encoded fluorescent biosensors illuminate the spatiotemporal regulation of signaling networks. *Chem. Rev.* 118, 11707–11794. doi: 10.1021/acs.chemrev.8b00333

Guisbert, E., Czyz, D. M., Richter, K., McMullen, P. D., and Morimoto, R. I. (2013). Identification of a tissue-selective heat shock response regulatory network. *PLoS Genet.* 9:e1003466. doi: 10.1371/journal.pgen.1003466

Gupta, R., Kasturi, P., Bracher, A., Loew, C., Zheng, M., Villella, A., et al. (2011). Firefly luciferase mutants as sensors of proteome stress. *Nat. Methods* 8, 879–884. doi: 10.1038/nmeth.1697

Hipp, M. S., Kasturi, P., and Hartl, F. U. (2019). The proteostasis network and its decline in ageing. *Nat. Rev. Mol. Cell Biol.* 20, 421–435. doi: 10.1038/s41580-019-0101-y

Hommen, F., Bilican, S., and Vilchez, D. (2021). Protein clearance strategies for disease intervention. *J. Neural Transm. (Vienna)* doi: 10.1007/s00702-021-02431-y. [Online ahead of print].

Kieran, D., Kalmar, B., Dick, J. R., Riddoch-Contreras, J., Burnstock, G., and Greensmith, L. (2004). Treatment with arimoclomol, a coinducer of heat shock proteins, delays disease progression in ALS mice. *Nat. Med.* 10, 402–405. doi: 10.1038/nm1021

Kijima, T., Eguchi, T., Neckers, L., and Prince, T. L. (2018). Monitoring of the heat shock response with a real-time luciferase reporter. *Methods Mol. Biol.* 1709, 35–45. doi: 10.1007/978-1-4939-7477-1_3

Kirstein, J., Morito, D., Kakihana, T., Sugihara, M., Minnen, A., Hipp, M. S., et al. (2015). Proteotoxic stress and ageing triggers the loss of redox homeostasis across cellular compartments. *EMBO J.* 34, 2334–2349. doi: 10.15252/embj.201591711

Klionsky, D. J., Abdel-Aziz, A. K., Abdelfatah, S., Abdellatif, M., Abdoli, A., Abel, S., et al. (2021). Guidelines for the use and interpretation of assays for monitoring autophagy (4th edition)[1]. *Autophagy* 17, 1–382. doi: 10.1080/15548627.2020.1797280

Koniev, O., and Wagner, A. (2015). Developments and recent advancements in the field of endogenous amino acid selective bond forming reactions for bioconjugation. *Chem. Soc. Rev.* 44, 5495–5551. doi: 10.1039/c5cs00048c

Labbadia, J., and Morimoto, R. I. (2015). The biology of proteostasis in aging and disease. *Annu. Rev. Biochem.* 84, 435–464. doi: 10.1146/annurev-biochem-060614-033955

Laviv, T., and Yasuda, R. (2021). Imaging neuronal protein signaling dynamics *in vivo*. *Curr. Opin. Neurobiol.* 69, 68–75. doi: 10.1016/j.conb.2021.02.002

Leeman, D. S., Hebestreit, K., Ruetz, T., Webb, A. E., McKay, A., Pollina, E. A., et al. (2018). Lysosome activation clears aggregates and enhances quiescent neural stem cell activation during aging. *Science* 359, 1277–1283. doi: 10.1126/science.aag3048

Lindsten, K., Menendez-Benito, V., Masucci, M. G., and Dantuma, N. P. (2003). A transgenic mouse model of the ubiquitin/proteasome system. *Nat. Biotechnol.* 21, 897–902. doi: 10.1038/nbt851

Liu, Y., Fares, M., Dunham, N. P., Gao, Z., Miao, K., Jiang, X., et al. (2017). AgHalo: a facile fluorogenic sensor to detect drug-induced proteome stress. *Angew. Chem. Int. Ed. Engl.* 56, 8672–8676. doi: 10.1002/anie.201702417

Liu, Y., Miao, K., Li, Y., Fares, M., Chen, S., and Zhang, X. (2018). A haloTag-based multicolor fluorogenic sensor visualizes and quantifies proteome stress in live cells using solvatochromic and molecular rotor-based fluorophores. *Biochemistry* 57, 4663–4674. doi: 10.1021/acs.biochem.8b00135

Liu, Y., Zhang, X., Chen, W., Tan, Y. L., and Kelly, J. W. (2015). Fluorescence turn-on folding sensor to monitor proteome stress in live cells. *J. Am. Chem. Soc.* 137, 11303–11311. doi: 10.1021/jacs.5b04366

Los, G. V., Encell, L. P., McDougall, M. G., Hartzell, D. D., Karassina, N., Zimprich, C., et al. (2008). HaloTag: a novel protein labeling technology for cell imaging and protein analysis. *ACS Chem. Biol.* 3, 373–382. doi: 10.1021/cb800025k

Malik, B., Nirmalananthan, N., Gray, A. L., La Spada, A. R., Hanna, M. G., and Greensmith, L. (2013). Co-induction of the heat shock response ameliorates disease progression in a mouse model of human spinal and bulbar muscular atrophy: implications for therapy. *Brain* 136, 926–943. doi: 10.1093/brain/aws343

Marcuccilli, C. J., Mathur, S. K., Morimoto, R. I., and Miller, R. J. (1996). Regulatory differences in the stress response of hippocampal neurons and glial cells after heat shock. *J. Neurosci.* 16, 478–485. doi: 10.1523/JNEUROSCI.16-02-00478.1996

Matilainen, O., Jha, S., and Holmberg, C. I. (2016). Fluorescent tools for *in vivo* studies on the ubiquitin-proteasome system. *Methods Mol. Biol.* 1449, 215–222. doi: 10.1007/978-1-4939-3756-1_12

Melo, E. P., Farace, I., Konno, T., Awadelkareem, M. A., Skov, L. R., Sancho, T. P., et al. (2021). Stress-induced protein disaggregation in the Endoplasmic Reticulum catalysed by BiP. *bioRxiv* [Preprint]. doi: 10.1101/2021.05.09.442953

Miles, J., and van Oosten-Hawle, P. (2020). Tissue-specific RNAi tools to identify components for systemic stress signaling. *J. Vis. Exp.* doi: 10.3791/61357

Miller, S. B., Ho, C. T., Winkler, J., Khokhrina, M., Neuner, A., Mohamed, M. Y., et al. (2015). Compartment-specific aggregases direct distinct nuclear and cytoplasmic aggregate deposition. *EMBO J.* 34, 778–797. doi: 10.15252/embj.201489524

Moehle, E. A., Shen, K., and Dillin, A. (2019). Mitochondrial proteostasis in the context of cellular and organismal health and aging. *J. Biol. Chem.* 294, 5396–5407. doi: 10.1074/jbc.TM117.000893

Moore, D. L., Pilz, G. A., Arauzo-Bravo, M. J., Barral, Y., and Jessberger, S. (2015). A mechanism for the segregation of age in mammalian neural stem cells. *Science* 349, 1334–1338. doi: 10.1126/science.aac9868

Morimoto, R. I. (2011). The heat shock response: systems biology of proteotoxic stress in aging and disease. *Cold Spring Harb. Symp. Quant. Biol.* 76, 91–99. doi: 10.1101/sqb.2012.76.010637

Morley, J. F., Brignull, H. R., Weyers, J. J., and Morimoto, R. I. (2002). The threshold for polyglutamine-expansion protein aggregation and cellular

toxicity is dynamic and influenced by aging in *Caenorhabditis elegans*. *Proc. Natl. Acad. Sci. U S A* 99, 10417–10422. doi: 10.1073/pnas.152161099

Morley, J. F., and Morimoto, R. I. (2004). Regulation of longevity in *Caenorhabditis elegans* by heat shock factor and molecular chaperones. *Mol. Biol. Cell* 15, 657–664. doi: 10.1091/mbc.e03-07-0532

Mu, H., Miki, K., Kubo, T., Otsuka, K., and Ohe, K. (2021). Substituted meso-vinyl-BODIPY as thiol-selective fluorogenic probes for sensing unfolded proteins in the endoplasmic reticulum. *Chem. Commun. (Camb)* 57, 1818–1821. doi: 10.1039/d0cc08160d

Owyong, T. C., Subedi, P., Deng, J., Hinde, E., Paxman, J. J., White, J. M., et al. (2020). A molecular chameleon for mapping subcellular polarity in an unfolded proteome environment. *Angew. Chem. Int. Ed. Engl.* 59, 10129–10135. doi: 10.1002/anie.201914263

Pereira, M., Tome, D., Domingues, A. S., Varanda, A. S., Paulo, C., Santos, M. A. S., et al. (2018). A fluorescence-based sensor assay that monitors general protein aggregation in human cells. *Biotechnol. J.* 13:e1700676. doi: 10.1002/biot.201700676

Raeburn, C. B., Ormsby, A., Moily, N. S., Cox, D., Ebbinghaus, S., Dickson, A., et al. (2021). A biosensor to gauge protein homeostasis resilience differences in the nucleus compared to cytosol of mammalian cells. *bioRxiv* [Preprint]. doi: 10.1101/2021.04.19.440383

Rokney, A., Shagan, M., Kessel, M., Smith, Y., Rosenshine, I., and Oppenheim, A. B. (2009). E. coli transports aggregated proteins to the poles by a specific and energy-dependent process. *J. Mol. Biol.* 392, 589–601. doi: 10.1016/j.jmb.2009.07.009

Shen, D., Bai, Y., and Liu, Y. (2021). Chemical biology toolbox to visualize protein aggregation in live cells. *Chembiochem* doi: 10.1002/cbic.202100443. [Online ahead of print].

Shiber, A., and Ravid, T. (2014). Chaperoning proteins for destruction: diverse roles of Hsp70 chaperones and their co-chaperones in targeting misfolded proteins to the proteasome. *Biomolecules* 4, 704–724. doi: 10.3390/biom4030704

Shpilka, T., and Haynes, C. M. (2018). The mitochondrial UPR: mechanisms, physiological functions and implications in ageing. *Nat. Rev. Mol. Cell Biol.* 19, 109–120. doi: 10.1038/nrm.2017.110

Tagawa, K., Marubuchi, S., Qi, M. L., Enokido, Y., Tamura, T., Inagaki, R., et al. (2007). The induction levels of heat shock protein 70 differentiate the vulnerabilities to mutant huntingtin among neuronal subtypes. *J. Neurosci.* 27, 868–880. doi: 10.1523/JNEUROSCI.4522-06.2007

Tsvetkov, A. S., Arrasate, M., Barmada, S., Ando, D. M., Sharma, P., Shaby, B. A., et al. (2013). Proteostasis of polyglutamine varies among neurons and predicts neurodegeneration. *Nat. Chem. Biol.* 9, 586–592. doi: 10.1038/nchembio.1308

van Oosten-Hawle, P., Porter, R. S., and Morimoto, R. I. (2013). Regulation of organismal proteostasis by transcellular chaperone signaling. *Cell* 153, 1366–1378. doi: 10.1016/j.cell.2013.05.015

Velasco-Garcia, M. N. (2009). Optical biosensors for probing at the cellular level: a review of recent progress and future prospects. *Semin. Cell Dev. Biol.* 20, 27–33. doi: 10.1016/j.semcdb.2009.01.013

Vilchez, D., Boyer, L., Morantte, I., Lutz, M., Merkwirth, C., Joyce, D., et al. (2012). Increased proteasome activity in human embryonic stem cells is regulated by PSMD11. *Nature* 489, 304–308. doi: 10.1038/nature11468

Vilchez, D., Saez, I., and Dillin, A. (2014). The role of protein clearance mechanisms in organismal ageing and age-related diseases. *Nat. Commun.* 5:5659. doi: 10.1038/ncomms6659

Walter, P., and Ron, D. (2011). The unfolded protein response: from stress pathway to homeostatic regulation. *Science* 334, 1081–1086. doi: 10.1126/science.1209038

Winkler, J., Seybert, A., Konig, L., Pruggnaller, S., Haselmann, U., Sourjik, V., et al. (2010). Quantitative and spatio-temporal features of protein aggregation in Escherichia coli and consequences on protein quality control and cellular ageing. *EMBO J.* 29, 910–923. doi: 10.1038/emboj.2009.412

Wood, R. J., Ormsby, A. R., Radwan, M., Cox, D., Sharma, A., Vopel, T., et al. (2018). A biosensor-based framework to measure latent proteostasis capacity. *Nat. Commun.* 9:287. doi: 10.1038/s41467-017-02562-5

Zhang, S., Liu, M., Tan, L. Y. F., Hong, Q., Pow, Z. L., Owyong, T. C., et al. (2019). A maleimide-functionalized tetraphenylethene for measuring and imaging unfolded proteins in cells. *Chem. Asian J.* 14, 904–909. doi: 10.1002/asia.201900150

Conflict of Interest: The author declares that the research was conducted in the absence of any commercial or financial relationships that could be construed as a potential conflict of interest.

The handling editor IS declared a shared affiliation with one of the authors ID at time of review.

Publisher's Note: All claims expressed in this article are solely those of the authors and do not necessarily represent those of their affiliated organizations, or those of the publisher, the editors and the reviewers. Any product that may be evaluated in this article, or claim that may be made by its manufacturer, is not guaranteed or endorsed by the publisher.

Copyright © 2022 Dudanova. This is an open-access article distributed under the terms of the Creative Commons Attribution License (CC BY). The use, distribution or reproduction in other forums is permitted, provided the original author(s) and the copyright owner(s) are credited and that the original publication in this journal is cited, in accordance with accepted academic practice. No use, distribution or reproduction is permitted which does not comply with these terms.

frontiers | Frontiers in Molecular Neuroscience

ORIGINAL RESEARCH
published: 08 April 2022
doi: 10.3389/fnmol.2022.873658

Sevoflurane-Induced Apoptosis in the Mouse Cerebral Cortex Follows Similar Characteristics of Physiological Apoptosis

*Qi Wang†, Yuan Li†, Hong Tan and Yingwei Wang**

Department of Anesthesiology, Huashan Hospital, Fudan University, Shanghai, China

OPEN ACCESS

Edited by:
Inmaculada Segura, Ludwig Maximilian University of Munich, Germany

Reviewed by:
Rustem Khazipov, Institut National de la Santé et de la Recherche Médicale (INSERM), France
Hui Zheng, Chinese Academy of Medical Sciences and Peking Union Medical College, China

***Correspondence:**
Yingwei Wang
wangyw@fudan.edu.cn

† These authors have contributed equally to this work and share first authorship

Specialty section:
This article was submitted to Molecular Signalling and Pathways, a section of the journal Frontiers in Molecular Neuroscience

Received: *11 February 2022*
Accepted: *17 March 2022*
Published: *08 April 2022*

Citation:
Wang Q, Li Y, Tan H and Wang Y (2022) Sevoflurane-Induced Apoptosis in the Mouse Cerebral Cortex Follows Similar Characteristics of Physiological Apoptosis. Front. Mol. Neurosci. 15:873658. doi: 10.3389/fnmol.2022.873658

General anesthetics are capable of inducing neuronal apoptosis during the rapid synaptogenesis of immature mammalian brains. In this vulnerable time window, physiological apoptosis also occurs to eliminate excess and inappropriately integrated neurons. We previously showed that physiological and ketamine-induced apoptosis in mouse primary somatosensory cortex (S1) followed similar developmental patterns. However, since sevoflurane is more widely used in pediatric anesthesia, and targets mainly on different receptors, as compared with ketamine, it is important to determine whether sevoflurane-induced apoptosis also follows similar developmental patterns as physiological apoptosis or not. Mice at postnatal days 5 (P5) and P9 were anesthetized with 1.5% sevoflurane for 4 h, and the apoptotic neurons in S1 were quantitated by immunohistochemistry. The results showed that sevoflurane raised the levels of apoptosis in S1 without interfering with the developmental patterns of physiological apoptosis. The cells more vulnerable to both physiological and sevoflurane-induced apoptosis shifted from layer V pyramidal neurons at P5 to layers II–IV GABAergic neurons by P9. The magnitude of both sevoflurane-induced and physiological apoptosis was more attenuated at P9 than P5. To determine whether the Akt-FoxO1-PUMA pathway contributes to the developmental decrease in magnitude of both physiological and sevoflurane-induced apoptosis, Western blot was used to measure the levels of related proteins in S1 of P5 and P9 mice. We observed higher levels of antiapoptotic phosphorylated Akt (p-Akt) and phosphorylated FoxO1 (p-FoxO1), and lower levels of the downstream proapoptotic factor PUMA in control and anesthetized mice at P9 than P5. In addition, the Akt-FoxO1-PUMA pathway may also be responsible for sevoflurane-induced apoptosis. Together, these results suggest that magnitude, lamination pattern and cell-type specificity to sevoflurane-induced apoptosis are age-dependent and follow physiological apoptosis pattern. Moreover, The Akt-FoxO1-PUMA pathway may mediate the developmental decreases in magnitude of both physiological and sevoflurane-induced apoptosis in neonatal mouse S1.

Keywords: sevoflurane, neonates, neuronal apoptosis, Akt, FoxO1, PUMA

INTRODUCTION

An increasing number of children receive general anesthesia during surgery or examination, and the potential effect of general anesthetics on brain development has aroused widespread concern. Many laboratory studies have demonstrated that general anesthetics can adversely affect the development of the central nervous system in rodents and non-human primates by inducing neuronal apoptosis and affecting synaptic development and plasticity, and even induce permanent cognitive decline (Jevtovic-Todorovic et al., 2003; Kahraman et al., 2008; Brambrink et al., 2012; Raper et al., 2015; Bosnjak et al., 2016; Vutskits and Xie, 2016; Jevtovic-Todorovic, 2018). Clinical studies also suggest that repeated exposure to general anesthesia in infants negatively impacts their learning, cognition, language, and motor ability (McCann et al., 2019; Aksenov et al., 2020). Therefore, it is important to explore the potential influence of general anesthetics on the brain development and determine the possible underlying mechanisms.

Studies have shown that nearly all general anesthetics used in clinical practice have neurotoxic effects on the developing brain and can cause neuronal apoptosis. In the developing cerebral cortex, the vulnerable time window for anesthetic-induced apoptosis coincides with the developmental period of synaptogenesis, which in rodents is the first 2 weeks postnatally (Ikonomidou et al., 1999; Wang et al., 2017; Lee et al., 2021). During the period of synaptogenesis, physiological apoptosis occurs to eliminate excess and inappropriately integrated cells (Southwell et al., 2012; Nikolić et al., 2013). In our previous study, we found that ketamine can increase neuronal apoptosis in the mouse primary somatosensory cortex (S1), and ketamine-induced apoptosis follows the characteristics of physiological apoptosis; the apoptotic neurons were mainly distributed in layer V at postnatal day (P) 5, and the majority were pyramidal neurons, whereas at P9, the apoptosis mainly targeted GABAergic interneurons in layers II-IV (Wang et al., 2017). However, whether other kinds of general anesthetics, in addition to ketamine, also increase apoptosis in neonatal mouse S1 following developmental patterns similar to those of physiological apoptosis, has scarcely been reported.

Sevoflurane is a commonly used inhaled pediatric anesthetic in the clinic. Unlike ketamine which inhibits excitatory glutamate-mediated synaptic transmission through NMDA receptor blockade, sevoflurane mainly exerts modulatory effects on $GABA_A$ receptors and enhances $GABA_A$ receptor-mediated inhibitory synaptic transmission (Rudolph and Antkowiak, 2004; Hemmings et al., 2005). Besides, it has been demonstrated that sevoflurane also exerts positive effects on K^+ channels, such as voltage-gated (Kv) channels and the background/leak or tandem 2-pore (K2P) families (Li et al., 2018). Previous studies in neonatal animal models have indicated that sevoflurane inhalation could induce widespread neuronal apoptosis and even subsequent cognitive impairment (Tao et al., 2014; Wei et al., 2019; Shen et al., 2021). However, there is insufficient information for the comparison of the developmental characteristics between physiological and sevoflurane-induced apoptosis in S1. Similarity in the time course and vulnerable cell populations between physiological and anesthetic-induced apoptosis may suggest common underlying mechanisms. The transcription factor family FoxO (forkhead box, O class), including FoxO1, FoxO3a, FoxO4, and FoxO6, is involved in diverse cellular processes, including apoptosis, cell proliferation, DNA repair, cell cycle, and metabolism (Tzivion et al., 2011). FoxO1 is widely expressed in the developing brain, and impacts neuronal apoptosis, growth, and maturation (Brunet et al., 1999; de la Torre-Ubieta et al., 2010; Xing et al., 2018; Semenza et al., 2021). The activity of FoxO1 is mainly regulated by the PI3K/Akt pathway. PI3K phosphorylates Akt to phosphorylated Akt (p-Akt), and the latter is responsible for inducing phosphorylation of FoxO1, reducing the transcriptional activity of the latter by promoting its subcellular redistribution from the nucleus to the cytoplasm (Hughes et al., 2011; Maiese, 2015; Dong et al., 2018). Activated nuclear FoxO1 controls the expression of numerous downstream genes, which in turn impact multiple cellular processes including apoptosis. PUMA (p53 upregulated modulator of apoptosis) mRNA is among the downstream targets of activated FoxO1 (Hughes et al., 2011). As a Bcl-2 family member, PUMA promotes apoptosis in a p53-dependent and -independent manner in response to a wide variety of stimuli (Yu and Zhang, 2008). However, whether the Akt-FoxO1-PUMA pathway is developmentally involved in regulating both physiological and anesthetic-induced neuronal apoptosis in the neonatal brain is insufficiently documented.

Therefore, in the present study, we investigated the developmental characteristics of sevoflurane-induced apoptosis in S1 of neonatal mouse and explored whether the Akt-FoxO1-PUMA signaling pathway plays a role in regulating the magnitude of both physiological and sevoflurane-induced neuronal apoptosis.

MATERIALS AND METHODS

Experimental Animals

C57BL/6 mice of postnatal days 5 and 9 (P5 and P9, respectively) were used. In a subset of experiments, GAD67-GFP knock-in mice [also known as $Gad1^{TM1.1Tama}$; GAD67-GFP (delta neo)], in which enhanced GFP was targeted to the *Gad67* locus that encodes GAD67, were used to investigate the apoptosis of GABAergic neurons (Tamamaki et al., 2003). All the mice were reared on a 12-h light/dark cycle in temperature- and humidity-controlled rooms. To reduce suffering of the animals, we used the minimum number of mice required for statistical accuracy. The procedures adhered to the National Institutes of Health Guide for the Care and Use of Laboratory Animals and were approved by the Ethical Committee for Animal Research of Fudan University.

Anesthesia

Littermates were randomly assigned to the control and anesthesia groups. The anesthesia group underwent a 4-h exposure to 1.5% sevoflurane in 30% oxygen and 70% room air, and the control group inhaled the carrier gas. Initial experiments did not reveal any sex-based differences in neuroapoptosis, and both female and

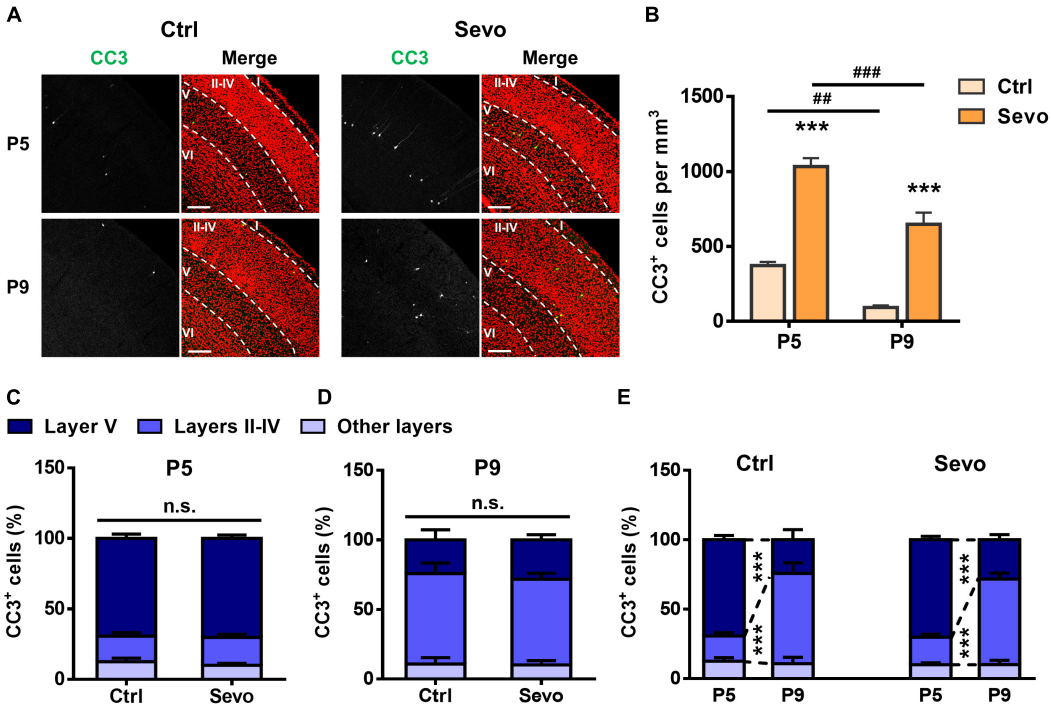

FIGURE 1 | During development, sevoflurane-induced apoptosis follows a lamination pattern similar to that of physiological apoptosis. **(A)** Representative confocal images of coronal primary somatosensory cortex (S1) sections immunolabelled for cleaved caspase-3 (CC3; green) and co-stained for nuclei with TOPRO (red) to visualize cortical lamination. Age and treatment conditions are as indicated. Cortical layers are indicated by Roman numerals, and borders between cortical layers marked using dotted lines. The scale bar is 200 μm. **(B)** Quantitation of the number of $CC3^+$ cells per mm^3 in the S1. Age and treatment conditions are as indicated. *, sevoflurane group compared to control group of the same age; #, P5 compared to P9 of each treatment condition; ***, $P < 0.001$; ##, $P < 0.01$; ###, $P < 0.001$, using two-way analysis of variance (ANOVA) followed by Bonferroni *post hoc* tests. **(C,D)** Distribution of the proportion of $CC3^+$ cells in different cortical layers at P5 **(C)** and P9 **(D).** In each age group, the percentage of $CC3^+$ cells in layers II–IV, layer V, or other layers (layer I and layer VI) in the sevoflurane group is not significantly different from that of the control group; $P > 0.05$ by two-way ANOVA followed by Bonferroni *post hoc* tests. **(E)** Replot of the data presented in panels **(C,D)** for the control and sevoflurane groups, showing developmental changes in the apoptosis pattern. ***, $P < 0.001$ by two-way ANOVA followed by Bonferroni *post hoc* tests. Three mice were used per condition, and 10 brain slices from each mouse were quantitated. Data are shown as the mean ± standard error of mean.

male littermates were used. A gas analyzer (RGM 5250; Datex-Ohmeda, Louisville, CO, United States) was used to monitor the concentrations of sevoflurane, oxygen, and carbon dioxide. Throughout the experiment, animals were kept in padded acrylic containers equipped with incubators, at a temperature of 37°C.

Immunohistochemistry, Image Acquisition, and Analysis

Immunohistochemistry and image acquisition were completed with a modification of the procedure described in our previous studies (Wang et al., 2017). Mice pups were deeply anesthetized with 0.7% sodium pentobarbital 6 h after anesthesia initiation and perfused with 0.9% saline followed by 4% paraformaldehyde in phosphate-buffered saline. We subsequently removed the brains, post-fixed them in 4% paraformaldehyde/phosphate buffer solution for 4-6 h at 4°C, and then equilibrated them in 30% sucrose. A cryostat (Leica CM1950, Wetzlar, Germany) was used to cut coronal sections (30 μm) containing the S1. Every 5th section was immunostained and incubated in a blocking solution containing 5% bovine serum albumin and 0.5% Triton X-100 for 2 h at 37°C. Subsequently, the sections were incubated overnight at 4°C in primary rabbit monoclonal antibody against cleaved caspase-3 (CC3, 9661 L, 1:400; Cell Signaling Technology, Beverly, MA, United States) in 0.3% bovine serum albumin. Sections were washed in phosphate-buffered saline for three times. We then incubated them with Alexa Fluor-conjugated (488 or 568 nm) secondary antibodies at a 1:500 dilution (Thermo Fisher Scientific, Waltham, MA, United States) for 2 h at 37°C. The nuclei were labeled for 30 min at 37°C with TO-PRO-3 (TOPRO, T3605, 1:10,000; Thermo Fisher Scientific).

A Pascal confocal microscope (Zeiss, Jena, Germany) with a 10 × Fluor objective (N.A. = 0.5) or a NiE-A1 plus confocal microscope (Nikon, Tokyo, Japan) with a 10 × Fluor objective (N.A. = 0.45), both with a Z-step of 5 μm, were used to quantify the number of $CC3^+$ cells. A Nikon NiE-A1 plus a confocal microscope with a 40 × Plan Fluor oil-immersion objective (N.A. = 1.3) was used at a Z-step of 0.6 μm to estimate the amount of co-localization between $CC3^+$ cells and GAD67-GFP. ImageProPlus software (Media-Cybernetics, Rockville, MD, United States) was used to analyze the images by researchers blinded to the experimental conditions. If CC3-stained cells were above the threshold size and displayed a detectable cellular outline, they were considered as $CC3^+$. Further, we used TOPRO

to measure the image area and identify cortical lamination. To investigate the co-localization of $CC3^+$ and GAD67-GFP, all Z-stack layers were checked to ensure colocalization. We imaged and examined approximately 40 $CC3^+$ cells per pup. Ten image frames were examined per pup in all investigations. Brain slices from each group were co-processed in all the steps involved in immunostaining, imaging, and data analysis.

Arterial Blood Gas Measurements

We measured arterial blood gas in the P5 pups at 2- or 4-h following sevoflurane anesthesia. A heparinized 32-gauge hypodermic needle was used to obtain arterial blood from the left ventricle by transcardiac aspiration. A portable clinical analyzer (ABL800FLEX, Radiometer, Copenhagen, Denmark) was used to measure the pH, partial pressure of carbon dioxide, partial pressure of oxygen, oxygen saturation, and HCO_3^- concentration immediately after the arterial blood was obtained.

Western Blotting

We used intraperitoneal injection of sodium pentobarbital to deeply anesthetize the mice 6 h following sevoflurane or carrier gas inhalation. They were then decapitated, and the regions encompassing the bilateral S1 were removed and stored in liquid nitrogen. We homogenized the tissues in ice-cold radioimmunoprecipitation-assay lysis buffer (Beyotime Biotechnology, Shanghai, China) supplemented with 0.1 mM phenylmethylsulfonyl fluoride protease inhibitors and phosphatase inhibitors. Next, the tissues were lysed on ice for 30 min and centrifuged at 4°C for 10 min to extract total S1 proteins. The samples were then heated at 95°C for 10 min in loading buffer. Subsequently, we filled the 10% sodium dodecyl sulfate-polyacrylamide gel electrophoresis chambers with equal amounts of protein. Samples were separated and transferred to polyvinylidene difluoride membranes by electrophoresis. The membranes were blocked with 5% non-fat milk for 2 h at room temperature and incubated at 4°C with a primary antibody [FoxO1, 1:1000 dilution, CST#2880; Phospho-FoxO1, 1:1000 dilution, CST#84192; Puma (E2P7G), 1:1000 dilution, CST#98672; Akt, 1:1000 dilution, CST#9272; Phospho-Akt (Ser473), 1:1000 dilution, CST#4060] or β-actin (1:500 dilution, Boster#BM3873, Wuhan, China) overnight. The membranes were washed 3 × with tris-buffered saline with Tween 20 and incubated within horseradish peroxidase-conjugated secondary anti-rabbit IgG (1:2000 dilution; Abcam#ab6721, Cambridge, MA, United States) for 2 h at room temperature. The bands were visualized using enhanced chemiluminescence (Thermo Fisher China, Shanghai, China). ImageJ software (National Institutes of Health, Bethesda, MD, United States) was used to perform the densitometry analysis.

Statistical Analysis

Statistical analyses were performed using Graph Pad Prism 6 (Graph Pad Software, La Jolla, CA, United States). One-way analysis of variance (ANOVA, comparing three or more conditions) followed by Dunnett's test (all conditions compared to the control) and two-way ANOVA (for comparing two independent variables) were used for assessing statistical significance, followed by Bonferroni's or Tukey's multiple comparisons test, as specified in the figure legends. Data are shown as mean ± standard error of the mean. $P < 0.05$ was considered statistically significant, and all the conditions statistically different from controls were reported.

RESULTS

Similar Changes in the Magnitude and Laminar Pattern of Sevoflurane-Induced and Physiological Neuronal Apoptosis in S1 During Development

Our previous work demonstrated that ketamine-induced neuronal apoptosis in the mouse S1 follows a developmental pattern similar to that of physiological apoptosis, peaking during P5-P7, and shifting from primarily layer V pyramidal neurons at P5 to mostly layers II-IV GABAergic interneurons at P9 (Wang et al., 2017). To explore whether sevoflurane could induce apoptosis in S1 with similar characteristics, P5 and P9 mice were anesthetized by inhalation of 1.5% sevoflurane for 4 h (Sevo), and the control littermates inhaled the carrier gas (30% O_2 + 70% air) (Ctrl). Cleaved caspase-3 (CC3) plays a central role in the occurrence of apoptosis and is generally considered a marker of apoptosis (Amente et al., 2011). Therefore, we measured the number of $CC3^+$ cells in the mouse S1. We found that sevoflurane could significantly increase neuronal apoptosis in S1 of P5 and P9 mice (P5, Ctrl: 373.33 ± 23.18/mm^3, Sevo: 1033.33 ± 55.43/mm^3, $P < 0.001$; P9, Ctrl: 93.33 ± 14.51/mm^3, Sevo: 648.33 ± 77.20/mm^3, $P < 0.001$; **Figures 1A,B**) and the extent of apoptosis in both Ctrl and Sevo groups significantly decreased from P5 to P9 (Ctrl, P5: 373.33 ± 23.18/mm^3, P9: 93.33 ± 14.51/mm^3, $P < 0.01$; Sevo, P5: 1033.33 ± 55.43/mm^3, P9: 648.33 ± 77.20/mm^3, $P < 0.001$; **Figures 1A,B**).

To further explore whether sevoflurane induced apoptosis following a similar age-dependent laminar pattern as that of physiological apoptosis, the proportion of $CC3^+$ cells in different cortical layers were quantitated. The results showed that, in each group, the $CC3^+$ cells were mainly distributed in layer V at P5 (Ctrl: 69.34 ± 3.03%, Sevo: 70.19 ± 2.45%, $P > 0.05$; **Figures 1A,C**), while they were mostly localized in layers II-IV at P9 (Ctrl: 65.08 ± 7.53%, Sevo: 61.58 ± 4.30%, $P > 0.05$; **Figures 1A,D**). The proportion of $CC3^+$ apoptotic cells in different S1 layers was plotted from P5 to P9 to better compare the developmental changes in the laminar pattern of apoptosis. Regardless of anesthetization, a significant shift of $CC3^+$ cells from layer V to layers II-IV was noted going from P5 to P9 (**Figure 1E**). For both ages and conditions, $CC3^+$ cells in layers I and VI accounted for only a small proportion, and the percentage did not change with age or treatment condition (**Figure 1**).

To determine whether sevoflurane-induced neuronal apoptosis was caused by hypoxia or hypercapnia, arterial blood gas analysis was performed in mice 2 and 4 h following sevoflurane anesthesia. The results showed that 1.5% sevoflurane anesthesia did not affect levels of pH, pressure of carbon dioxide ($PaCO_2$), partial pressure of oxygen (PaO_2), HCO_3^-, or oxygen

TABLE 1 | Arterial blood-gas analysis of postnatal-day-5 (P5) mice following 1.5% sevoflurane.

Parameter	Ctrl		Sevo	
	2 h	4 h	2 h	4 h
pH	7.53 ± 0.02	7.60 ± 0.02	7.49 ± 0.05	7.47 ± 0.03
$PaCO_2$ (mmHg)	26.58 ± 3.98	22.48 ± 2.48	36.38 ± 4.32	32.50 ± 4.47
PaO_2 (mmHg)	109.50 ± 23.99	127.25 ± 20.13	100.25 ± 16.96	115.00 ± 15.32
HCO_3^- (mM)	23.75 ± 0.66	22.63 ± 0.81	22.83 ± 1.01	22.28 ± 1.58
SaO_2 (%)	97.25 ± 1.56	99.00 ± 0.47	96.43 ± 1.95	97.40 ± 1.60

The parameters measured and conditions are as indicated. Measurements were taken at 2 h and 4 h following anesthesia. Four to ten mice were used per condition. No significant differences were detected between the control and anesthesia conditions for any parameter. P > 0.05, one-way analysis of variance (ANOVA), followed by Dunnett's multiple comparisons test.

saturation (SaO_2) in P5 mice (**Table 1**). The results indicated that the mouse pups could maintain normal respiration and oxygenation during anesthesia and ruled out the influence of hypoxia or hypercapnia on neuronal apoptosis.

The Vulnerability of GABAergic Neurons to Apoptosis Changes During Development

The above results showed that physiological and sevoflurane-induced apoptosis in S1 exhibited similar age-dependent changes in magnitude and laminar pattern. Next, we explored whether the cell-type vulnerability to sevoflurane-induced apoptosis also changed developmentally as observed in physiological apoptosis. GAD67-GFP transgenic mouse littermates inhaled sevoflurane (1.5%, 4 h) and carrier gas (30% O_2 + 70% air), respectively. The results showed that at P5, GAD67-GFP$^+$ interneurons accounted for less than one-third of the CC3$^+$ apoptotic neurons in S1 (Ctrl: 21.25% ± 2.65%, Sevo: 22.27% ± 3.15%; **Figures 2A,C**), and there was no significant difference between the control and sevoflurane groups ($P > 0.05$; **Figures 2A,C**). Most of the apoptotic neurons had typical pyramidal neuron morphology, with triangular cell bodies and long apical dendrites (**Figure 2A**). However, by P9, the majority of the apoptotic neurons were GAD67-GFP$^+$ interneurons in both control and sevoflurane groups (Ctrl: 74.54 ± 1.81%, Sevo: 73.32 ± 1.61%, $P > 0.05$; **Figures 2B,C**).

These results indicated that the cell type susceptible to both physiological and sevoflurane-induced apoptosis in S1 shifted from mostly pyramidal neurons at P5 to GABAergic interneurons at P9. Sevoflurane augmented neuronal apoptosis in S1 without affecting the developmental switch in the cell-type specificity of physiological apoptosis.

The Akt-FoxO1-PUMA Pathway Is Developmentally Affected by Sevoflurane

The developmental similarity of sevoflurane-induced apoptosis and physiological apoptosis in time-course, laminar pattern, and cell-type specificity implied the possibility of common proapoptotic mechanisms. The PI3K/Akt-FoxO1 signaling pathway plays an essential role in regulating cell apoptosis by modulating the expression of the downstream target PUMA (Hughes et al., 2011). Akt, phosphorylated by PI3K (p-Akt), inactivates FoxO1 by inducing its phosphorylation, leading to low expression of the proapoptotic factor PUMA. Since sevoflurane significantly increased the number of apoptotic cells in S1 at both P5 and P9, and the magnitude of either physiological or sevoflurane-induced apoptosis significantly decreased at P9 compared to P5 (**Figures 1A,B**), we next explored whether the Akt-FoxO1-PUMA pathway participated in sevoflurane-induced apoptosis or the developmental reduction of apoptosis. We showed that, compared with control littermates, in the S1 of sevoflurane-anesthetized mice, the levels of both p-Akt and phosphorylated FoxO1 (p-FoxO1) significantly decreased at P5 (Ctrl vs Sevo: p-Akt, 1.00 ± 0.01 vs 0.27 ± 0.02, $P < 0.001$; p-FoxO1, 1.00 ± 0.01 vs 0.30 ± 0.01, $P < 0.001$) and P9 (Ctrl vs Sevo: p-Akt, 1.17 ± 0.01 vs 0.71 ± 0.01, $P < 0.001$; p-FoxO1, 1.89 ± 0.09 vs 0.69 ± 0.01, $P < 0.001$) (**Figures 3A–D**). Accordingly, the level of the proapoptotic downstream product PUMA was significantly greater in sevoflurane-anesthetized mice than in control littermates at both P5 (Ctrl vs Sevo, 1.00 ± 0.02 vs 6.48 ± 0.06, $P < 0.001$) and P9 (Ctrl vs Sevo, 0.59 ± 0.02 vs 4.30 ± 0.05, $P < 0.001$) (**Figures 3E,F**). The reduction of p-Akt and p-FoxO1, along with an increase in the PUMA levels, suggests that the Akt-FoxO1-PUMA pathway might mediate sevoflurane-induced apoptosis in S1 of P5 and P9 pups. To determine whether this pathway is also involved in regulating the reduction of either physiological or sevoflurane-induced apoptosis from P5 to P9, we subsequently assayed the developmental changes in levels of p-Akt, p-FoxO1, and PUMA. We showed that in both control and sevoflurane groups, the level of p-Akt (P5 vs P9: Ctrl, 1.00 ± 0.01 vs 1.17 ± 0.01, $P < 0.001$; Sevo, 0.27 ± 0.02 vs 0.71 ± 0.01, $P < 0.001$) and p-FoxO1 (P5 vs P9: Ctrl, 1.00 ± 0.01 vs 1.89 ± 0.09, $P < 0.001$; Sevo, 0.30 ± 0.01 vs 0.69 ± 0.01, $P < 0.001$) in the S1 was significantly higher at P9 than at P5 (**Figures 3A–D**), whereas the level of PUMA significantly declined from P5 to P9 (P5 vs P9: Ctrl, 1.00 ± 0.02 vs 0.59 ± 0.02, $P < 0.001$; Sevo, 6.48 ± 0.06 vs 4.30 ± 0.05, $P < 0.001$) (**Figures 3E,F**). These results indicate that the Akt–FoxO1–PUMA signaling pathway may play a role in the developmental reduction of both physiological and sevoflurane-induced apoptosis.

DISCUSSION

It is well documented that nearly all commonly used general anesthetics are able to cause widespread apoptotic neurodegeneration in various newborn animal species (Jevtovic-Todorovic et al., 2013; Lin et al., 2014; Lee et al., 2017). The window of vulnerability to apoptosis induced by general anesthetics coincides with the brain growth spurt period, which occurs during the first 2 postnatal weeks in rodents (Dobbing and Sands, 1979). Physiological apoptosis also occurs during this period, and is essential for the establishment of the normal central

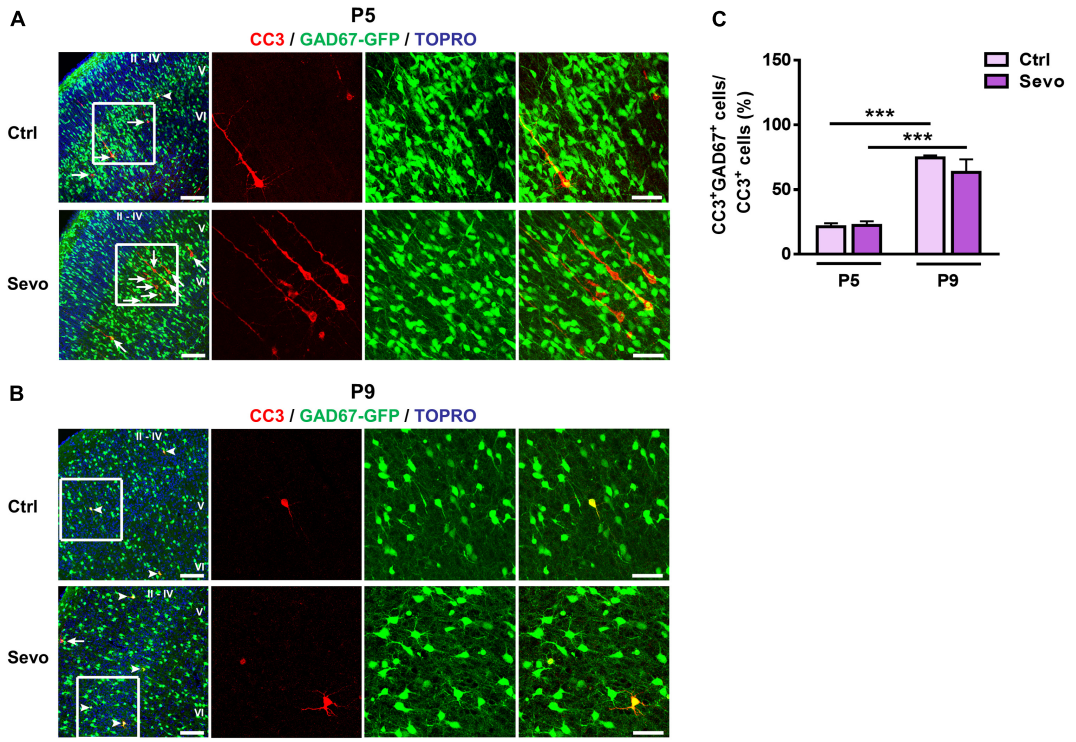

FIGURE 2 | Vulnerability of GABAergic neurons to sevoflurane-induced apoptosis is age-dependent. **(A,B)** Representative confocal images of S1 sections labeled for cleaved caspase-3 (CC3, red), GAD67-GFP (green), and TOPRO (blue) at P5 **(A)** and P9 **(B)**. The cortical layers are indicated by Roman numerals. Conditions are as indicated. White arrowheads indicate $CC3^+$ cells co-localized with GAD67-GFP, while the white arrows indicate those that are not co-localized. The scale bar is 100 μm. Zoomed images of boxed regions are presented to the right of each panel with scale bars = 50 μm. **(C)** Proportion of $CC3^+$ cells co-labeled with GAD67-GFP in all cortical layers. Three to four mice were used for each condition. ***, $P < 0.001$, using two-way analysis of variance followed by Bonferroni *post hoc* tests. Data are shown as the mean ± standard error of the mean.

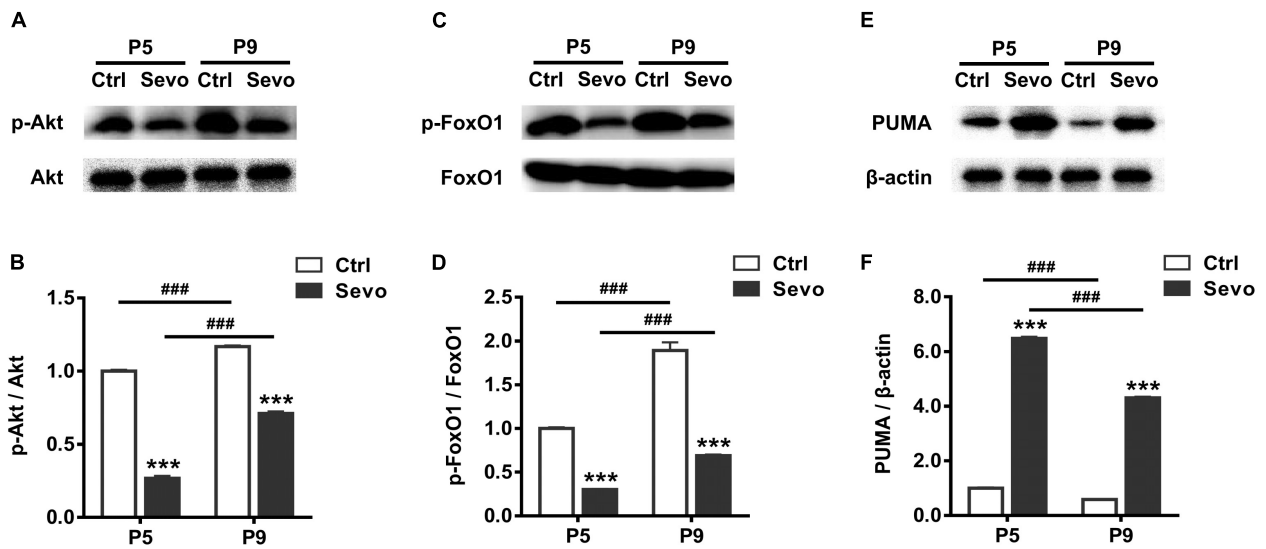

FIGURE 3 | Developmental changes in the Akt–FoxO1–PUMA pathway in regulating physiological and sevoflurane-induced apoptosis. Immunoblots and quantitation of phosphorylated Akt **(A,B)**, phosphorylated FoxO1 **(C,D)**, and PUMA **(E,F)** from the S1 region of control and sevoflurane-anesthetized mice at P5 and P9, respectively. *, sevoflurane group compared to control group of the same age; #, P5 compared to P9 in each treatment condition; ***, $P < 0.001$; ###, $P < 0.001$, using two-way analysis of variance followed by Tukey's multiple comparisons test. Four mice were used per condition. Data are shown as the mean ± standard error of the mean.

nervous system structure (Kuida et al., 1996). The hypernomic neuronal apoptosis induced by general anesthetics may disrupt brain development and subsequently cause neurocognitive impairment (Creeley, 2016).

Since physiological apoptosis also occurs during the period when brain was vulnerable to anesthetic-induced apoptosis, it is important to explore whether anesthetic-induced apoptosis targets the same or different populations in comparison with those targeted by physiological apoptosis. Our previous work compared the characteristics of ketamine-induced apoptosis in the mouse S1 with those of physiological apoptosis (Wang et al., 2017). We showed that ketamine-induced and physiological apoptosis shared similar developmental patterns, peaking during P5–P7, becoming insignificant by P12, and shifting from primarily layer V pyramidal neurons at P5 to mostly layers II-IV GABAergic interneurons by P9 (Wang et al., 2017). Ketamine mediates its effects mainly by blocking N-methyl-D-aspartate receptors (Ikonomidou et al., 1999), and we wondered whether anesthetic agents acting primarily on $GABA_A$ receptors have similar characteristics regarding the induction of apoptosis in neonatal mouse S1. Thus, herein, the developmental characteristics of sevoflurane-induced apoptosis in the S1 were explored and compared with those of physiological apoptosis. We found that a 4-h 1.5% sevoflurane anesthesia significantly augmented neuronal apoptosis in the S1, and, consistent with the developmental changes in magnitude of physiological apoptosis, sevoflurane-induced apoptosis was more prominent at P5 than at P9 (**Figure 1**). Moreover, the cell types vulnerable to sevoflurane-induced apoptosis at P5 included mainly pyramidal neurons in layer V, whereas at P9, mainly GABAergic interneurons in layers II-IV were involved (**Figures 1**, **2**). Although sevoflurane and ketamine act mainly on different targets, they induce apoptosis in the neonatal mouse S1 similarly to physiological apoptosis in terms of developmental time-course, lamination, and cell-type specificity (Wang et al., 2017), which is the major innovation point of the current study.

Referring to sevoflurane-induced neuronal apoptosis, an immediately arising question is whether isoflurane has comparable effects as sevoflurane on inducing neuronal apoptosis during postnatal development. Isoflurane is also a commonly used volatile anesthetic in clinical and has frequently been reported to induce widespread apoptotic neurodegeneration when administered to neonatal animals. Despite the similar effects on enhancing $GABA_A$ receptor function and activating certain types of K^+ channels, isoflurane has been reported to induced a significantly greater amount of apoptotic neurons in different brain regions than an equipotent exposure of sevoflurane (Liang et al., 2010; Zhao et al., 2020). Isoflurane induced neuronal apoptosis in neonatal brain mainly by activation the mitochondrial pathway, while sevoflurane is more prone to causing endoplasmic reticulum (ER) stress-induced apoptosis (Zhao et al., 2020). In terms of the vulnerable cell population targeted by isoflurane, more detailed observation have been reported on neonatal non-human primates (NHPs). Exposure of P6 rhesus macaques to isoflurane significantly increased apoptosis of neurons and oligodendrocyte (Brambrink et al., 2010; Noguchi et al., 2017). Oligodendrocyte apoptosis was uniformly distributed throughout the white matter whereas neuroapoptosis occurred mainly in the cortex, caudate, putamen and thalamus (Noguchi et al., 2017). In the temporal cortex of the isoflurane-exposed rhesus macaques brain the laminar pattern and cell-type specificity are also evident, with GABAergic interneurons in layer II and pyramidal neurons in layer IV being the most severely affected (Brambrink et al., 2010). However, whether and how the laminar pattern and cell-type specificity of isoflurane-induced apoptosis changed during development are waiting for exploration. In addition to general anesthetics, ethanol has also been involved in inducing widespread neuronal apoptosis when exposed to neonates in age- and dose-dependent manners (Olney et al., 2002a,b; Lebedeva et al., 2017; Britton and Miller, 2018). Previous studies investigating the age-dependent apoptosis induced by ethanol in the cerebral cortex reported switch in laminar pattern from layer V at P4-P7 to layer II/III at P10-P13, which is similar with our observation on ketamine- and sevoflurane-induced apoptosis (Lebedeva et al., 2017; Britton and Miller, 2018). However, these studies did not assay whether the apoptotic neurons were pyramidal or GABAergic.

Previous studies exploring developmental changes in cell numbers in the cerebral cortex reported most significant changes in cortical layers II-IV during P5-P10, but they did not assay whether the apoptotic layer II-V neurons were pyramidal or GABAergic, nor did they quantify whether the number of apoptotic cells in different layers changed during development (Ferrer et al., 1992; Ikonomidou et al., 1999). Consistent with our observation, Blanquie et al. showed that the developmental apoptosis of cortical neurons peaked at P5-P6, most of which were GAD67-negative, glutamatergic neurons in layer V of S1 (Blanquie et al., 2017b). However, they did not show whether the cell-type specificity changed with development. Wong et al. reported that most pyramidal neurons undergo apoptosis between P2 and P5 in the mouse cortex, while the period of apoptotic neurodegeneration for cortical interneurons is slightly later compared to pyramidal neurons, with most apoptosis occurring between P5 and P10 (Wong et al., 2018).

In our previous and the current studies, a shift in the lamination pattern of apoptotic cells from mostly layer V pyramidal neurons at P5 to mostly layers II-IV GABAergic interneurons at P9 could be observed in physiological, ketamine- and sevoflurane-induced apoptosis in S1. The similarity does not negate potential adverse effects of anesthesia-induced apoptosis on neural circuit formation and function, however, it may suggest potentially similar underlying mechanisms. What physiological mechanism or process could underlie this developmental change? Since neurons migrated into the cortical plate in an inside-out manner that earlier generated neurons occupy the deeper layers and later generated neurons migrate to form the upper layers of the cortex, neurons in the upper layers are generally less mature than those in the deeper layers (Kriegstein and Noctor, 2004; Wonders and Anderson, 2006). Consistent with the inside-out developmental pattern, it has been shown that the earlier born medial ganglionic eminence (MGE)-derived GABAergic neurons mostly populate deep layers (V-VI) whereas later born MGE cells mostly populate superficial layers (II-IV) (Bartolini et al., 2013). The apoptosis pattern we observed

is consistent with developmental trajectory, in that deep layer neurons are more vulnerable at earlier ages. In terms of the developmental changes in cell-type specificity of apoptosis, recent experiments showed that, rather than extrinsic competition-based mechanisms, GABAergic interneurons went through apoptosis drived by an intrinsic timer when they reach a specific maturation stage (Song et al., 2012; Southwell et al., 2012). The cell age 11-18 days interneurons are more vulnerable to apoptosis (Southwell et al., 2012). We surmise that the similar intrinsic program may also exist to drive the apoptosis of pyramidal neurons. Then, why general anesthetics can increase neuronal apoptosis following similar laminar pattern and cell-type specificity?

During the early postnatal period, neural activity, both in the form of spontaneous electrical activity and sensory stimulation, is critical to neuronal survival (Blanquie et al., 2017a). Inhibition of neural activity mainly through blocking NMDA receptor and/or enhancing $GABA_A$ receptor functions plays a critical role in general anesthetic-induced neuronal apoptosis (Jevtovic-Todorovic et al., 2013). However, this could not be sufficient to explain the age-dependent changes in laminar pattern and cell-type specificity of ketamine- and sevoflurane-induced apoptosis in S1. Previous study investigated the effect of isoflurane on late- and adult-generated neurons in dentate gyrus (DG) and olfactory bulb of newborn, juvenile, and adult mice, and found vulnerability to isoflurane-induced apoptosis was cell age-specific, rather than organism age-specific (Hofacer et al., 2013). Neurons with cellular age 13-15 days were most vulnerable to anesthetic-induced apoptosis, although the cell types were not distinguished (Hofacer et al., 2013). Interestingly, the most vulnerable cell ages exactly overlaps between anesthetic-induced neuronal apoptosis and physiological apoptosis of GABAergic neurons. We surmise that an intrinsic program may regulate neuronal apoptosis during the rapid synaptogenesis of immature brains, and anesthetics (especially ketamine and sevoflurane) may augment the developmental apoptosis by lowering the threshold of the intrinsic program of apoptosis.

The other innovation point of our study is that we found the Akt-FoxO1-PUMA signaling pathway may participate in mediating sevoflurane-induced apoptosis. The PI3K-Akt signaling pathway is extremely important in mediating survival signals in multiple cell types, including neurons (Brunet et al., 2001). P-Akt exerts an anti-apoptotic effect by phosphorylating numerous downstream targets. Previous studies reported that the inactivation of the PI3K-Akt-GSK3β and PI3K-Akt-mTOR pathways were involved in general-anesthetic-induced neurotoxicity (Xing et al., 2020; Zhang et al., 2021; Zhu et al., 2021). Our results add to the existing knowledge by showing that the Akt-FoxO1-PUMA pathway participates in mediating sevoflurane-induced neuronal apoptosis in S1 of neonatal mice. FoxO transcription proteins play crucial roles in a broad range of cellular functions (Accili and Arden, 2004), and are considered important factors regulating memory formation and cognitive functions (Manolopoulos et al., 2010; Fang et al., 2019). FoxO1, a representative member with abundant expression, has been demonstrated to be involved in apoptosis induction, reactive oxygen species suppression, neural progenitor cell proliferation, and more (Santo and Paik, 2018; Semenza et al., 2021). The PI3K/Akt pathway is one of the prime regulators of FoxO1 activity. P-Akt by PI3K subsequently phosphorylates FoxO1, resulting in its nuclear exclusion and cytoplasmic sequestration. Thus, an increase in p-FoxO1 adversely regulates the expression of target genes (Brunet et al., 1999). PUMA is one of the numerous FoxO1 downstream targets whose expression is related to triggering apoptosis by activating the proapoptotic family member Bax (Hughes et al., 2011; Kon et al., 2019). Accordingly, we demonstrated that the level of p-Akt and its immediately downstream target p-FoxO1 was significantly attenuated following sevoflurane anesthesia, which is responsible for the striking elevation of PUMA expression we observed in S1 at P5 and P9 (**Figure 3**). The increase in PUMA levels may contribute to the greater number of $CC3^+$ apoptotic neurons observed in S1 of sevoflurane-anesthetized mouse pups. Moreover, our results demonstrated that the Akt-FoxO1-PUMA pathway could also be involved in mediating the developmental reduction of both physiological and sevoflurane-induced apoptosis in the S1. Supporting the fact that $CC3^+$ apoptotic neurons significantly decreased from P5 to P9 in both control and sevoflurane-anesthetized pups (**Figure 1**), we observed a significant increase in p-Akt and p-FoxO1 levels, and consequently, a notable attenuation in the downstream PUMA levels in S1 of both groups from P5 to P9 (**Figure 3**). The developmental reduction in levels of the proapoptotic PUMA is assumed to be responsible for the age-dependent decrease of both physiological and sevoflurane-induced apoptosis. Together, these results provide evidence for the roles of the Akt-FoxO1-PUMA signaling pathway in mediating sevoflurane-induced apoptosis, as well as the reduction of physiological and sevoflurane-induced apoptosis in S1 following the postnatal development.

Some limitations still exist in our study: Firstly, we used a relatively lower concentration of sevoflurane (1.5%) to minimize the adverse effects on cardiopulmonary physiology and mortality. This may underestimate the effect of sevoflurane on neurodegeneration. Moreover, despite the developmental changes in lamination pattern of ketamine-induced apoptosis in S1 are not affected by drug concentrations, whether that would be the case in sevoflurane-induced apoptosis still needs to explore. Secondly, it has been well-documented that PUMA can mediate cell death in an p53-dependent and -independent manner (Yu and Zhang, 2008), and consistent with the increase in neuronal apoptosis induced by sevoflurane, we observed the significantly higer levels of PUMA expression in S1. However, the direct evidence of PUMA takes part in mediating sevoflurane-induced apoptosis is lacking. Thirdly, as discussed above, the laminar pattern and cell-type specificity of both physiological and sevoflurane-induced apoptosis may mediated by similar intrinsic programs, which should be deeply explored by further *in vivo* and *in vitro* experiments.

In conclusion, our results demonstrate that sevoflurane-induced neuronal apoptosis in the neonatal mouse S1 follows patterns similar to those of physiological apoptosis in terms of the time-course, lamination, and cell-type specificity. Moreover, the Akt-FoxO1-PUMA signaling pathway probably participates in mediating apoptosis induced by sevoflurane and contributes

to the developmental reduction of both physiological and sevoflurane-induced apoptosis in S1.

DATA AVAILABILITY STATEMENT

The original contributions presented in the study are included in the article/supplementary material, further inquiries can be directed to the corresponding author.

ETHICS STATEMENT

The animal study was reviewed and approved by the Ethical Committee for Animal Research of Fudan University.

AUTHOR CONTRIBUTIONS

QW and YW contributed to conception and design of the study. QW and YL organized the database. QW, YL, and HT performed the statistical analysis. QW, YL, and YW wrote the manuscript. All authors contributed to manuscript revision, read, and approved the submitted version.

FUNDING

This work was supported by the National Natural Science Foundation, People's Republic of China (grant no. 81730031 to YW), the Foundation of Shanghai Municipal Key Clinical Specialty (grant no. shslczdzk06901 to YW), and the Scientific Research Projects supported by Huashan Hospital, Fudan University (grant no. 2021QD027 to QW).

ACKNOWLEDGMENTS

We thank Xiang Yu (Peking University, China) for the GAD67-GFP transgenic mice. We thank the entire staff of the Department of Anesthesiology, Huashan Hospital, Fudan University, for useful discussions.

REFERENCES

Accili, D., and Arden, K. C. (2004). FoxOs at the crossroads of cellular metabolism, differentiation, and transformation. *Cell* 117, 421–426. doi: 10.1016/s0092-8674(04)00452-0

Aksenov, D. P., Venkatasubramanian, P. N., Miller, M. J., Dixon, C. J., Li, L., and Wyrwicz, A. M. (2020). Effects of neonatal isoflurane anesthesia exposure on learning-specific and sensory systems in adults. *Sci. Rep.* 10, 1–3. doi: 10.1038/s41598-020-70818-0

Amente, S., Zhang, J., Lavadera, M. L., Lania, L., Avvedimento, E. V., and Majello, B. (2011). Myc and PI3K/AKT signaling cooperatively repress FOXO3a-dependent PUMA and GADD45a gene expression. *Nucleic Acids Res.* 39, 9498–9507. doi: 10.1093/nar/gkr638

Bartolini, G., Ciceri, G., and Marin, O. (2013). Integration of GABAergic interneurons into cortical cell assemblies: lessons from embryos and adults. *Neuron* 79, 849–864. doi: 10.1016/j.neuron.2013.08.014

Blanquie, O., Kilb, W., Sinning, A., and Luhmann, H. J. (2017a). Homeostatic interplay between electrical activity and neuronal apoptosis in the developing neocortex. *Neuroscience* 358, 190–200. doi: 10.1016/j.neuroscience.2017.06.030

Blanquie, O., Yang, J. W., Kilb, W., Sharopov, S., Sinning, A., and Luhmann, H. J. (2017b). Electrical activity controls area-specific expression of neuronal apoptosis in the mouse developing cerebral cortex. *Elife* 6:e27696.

Bosnjak, Z. J., Logan, S., Liu, Y., and Bai, X. (2016). Recent insights into molecular mechanisms of propofol-induced developmental neurotoxicity: implications for the protective strategies. *Anesth. Analg.* 123, 1286–1296.

Brambrink, A. M., Evers, A. S., Avidan, M. S., Farber, N. B., Smith, D. J., Martin, L. D., et al. (2012). Ketamine-induced neuroapoptosis in the fetal and neonatal rhesus macaque brain. *Anesthesiology* 116, 372–384.

Brambrink, A. M., Evers, A. S., Avidan, M. S., Farber, N. B., Smith, D. J., Zhang, X., et al. (2010). Isoflurane-induced neuroapoptosis in the neonatal rhesus macaque brain. *Anesthesiology* 112, 834–841. doi: 10.1097/aln.0b013e3181d049cd

Britton, S. M., and Miller, M. W. (2018). Neuronal loss in the developing cerebral cortex of normal and bax-deficient mice: effects of ethanol exposure. *Neuroscience* 369, 278–291. doi: 10.1016/j.neuroscience.2017.11.013

Brunet, A., Bonni, A., Zigmond, M. J., Lin, M. Z., Juo, P., Hu, L. S., et al. (1999). Akt promotes cell survival by phosphorylating and inhibiting a Forkhead transcription factor. *Cell* 96, 857–868. doi: 10.1016/s0092-8674(00)80595-4

Brunet, A., Datta, S. R., and Greenberg, M. E. (2001). Transcription-dependent and -independent control of neuronal survival by the PI3K-Akt signaling pathway. *Curr. Opin. Neurobiol.* 11, 297–305. doi: 10.1016/s0959-4388(00)00211-7

Creeley, C. E. (2016). From drug-induced developmental neuroapoptosis to pediatric anesthetic neurotoxicity-where are we now? *Brain Sci.* 6:32. doi: 10.3390/brainsci6030032

de la Torre-Ubieta, L., Gaudillière, B., Yang, Y., Ikeuchi, Y., Yamada, T., DiBacco, S., et al. (2010). A FOXO-Pak1 transcriptional pathway controls neuronal polarity. *Genes Dev.* 24, 799–813. doi: 10.1101/gad.1880510

Dobbing, J., and Sands, J. (1979). Comparative aspects of the brain growth spurt. *Early Hum. Dev.* 3, 79–83. doi: 10.1016/0378-3782(79)90022-7

Dong, P., Zhang, X., Zhao, J., Li, D., Li, L., and Yang, B. (2018). Anti-microRNA-132 causes sevoflurane-induced neuronal apoptosis via the PI3K/AKT/FOXO3a pathway. *Int. J. Mol. Med.* 42, 3238–3246. doi: 10.3892/ijmm.2018.3895

Fang, E. F., Hou, Y., Palikaras, K., Adriaanse, B. A., Kerr, J. S., Yang, B., et al. (2019). Mitophagy inhibits amyloid-beta and tau pathology and reverses cognitive deficits in models of Alzheimer's disease. *Nat. Neurosci.* 22, 401–412. doi: 10.1038/s41593-018-0332-9

Ferrer, I., Soriano, E., del Rio, J. A., Alcantara, S., and Auladell, C. (1992). Cell death and removal in the cerebral cortex during development. *Prog. Neurobiol.* 39, 1–43. doi: 10.1016/0301-0082(92)90029-e

Hemmings, H. C. Jr., Akabas, M. H., Goldstein, P. A., Trudell, J. R., Orser, B. A., and Harrison, N. L. (2005). Emerging molecular mechanisms of general anesthetic action. *Trends Pharmacol. Sci.* 26, 503–510. doi: 10.1016/j.tips.2005.08.006

Hofacer, R. D., Deng, M., Ward, C. G., Joseph, B., Hughes, E. A., Jiang, C., et al. (2013). Cell age-specific vulnerability of neurons to anesthetic toxicity. *Ann. Neurol.* 73, 695–704. doi: 10.1002/ana.23892

Hughes, K. J., Meares, G. P., Hansen, P. A., and Corbett, J. A. (2011). FoxO1 and SIRT1 regulate beta-cell responses to nitric oxide. *J. Biol. Chem.* 286, 8338–8348. doi: 10.1074/jbc.M110.204768

Ikonomidou, C., Bosch, F., Miksa, M., Bittigau, P., Vöckler, J., Dikranian, K., et al. (1999). Blockade of NMDA receptors and apoptotic neurodegeneration in the developing brain. *Science* 283, 70–74. doi: 10.1126/science.283.5398.70

Jevtovic-Todorovic, V. (2018). Exposure of developing brain to general anesthesia: what is the animal evidence? *Anesthesiology* 128, 832–839. doi: 10.1097/ALN.0000000000002047

Jevtovic-Todorovic, V., Absalom, A. R., Blomgren, K., Brambrink, A., Crosby, G., Culley, D. J., et al. (2013). Anaesthetic neurotoxicity and neuroplasticity: an expert group report and statement based on the BJA Salzburg Seminar. *Br. J. Anaesth.* 111, 143–151. doi: 10.1093/bja/aet177

Jevtovic-Todorovic, V., Hartman, R. E., Izumi, Y., Benshoff, N. D., Dikranian, K., Zorumski, C. F., et al. (2003). Early exposure to common anesthetic agents causes widespread neurodegeneration in the developing rat brain and persistent learning deficits. *J. Neurosci.* 23, 876–882.

Kahraman, S., Zup, S. L., McCarthy, M. M., and Fiskum, G. (2008). GABAergic mechanism of propofol toxicity in immature neurons. *J. Neurosurg. Anesthesiol.* 20, 233–240. doi: 10.1097/ANA.0b013e31817ec34d

Kon, N., Wang, D., and Gu, W. (2019). Loss of SET reveals both the p53-dependent and the p53-independent functions in vivo. *Cell Death Dis.* 10:237.

Kriegstein, A. R., and Noctor, S. C. (2004). Patterns of neuronal migration in the embryonic cortex. *Trends Neurosci.* 27, 392–399.

Kuida, K., Zheng, T. S., Na, S., Kuan, C. Y., Yang, D., Karasuyama, H., et al. (1996). Decreased apoptosis in the brain and premature lethality in CPP32-deficient mice. *Nature* 384, 368–372. doi: 10.1038/384368a0

Lebedeva, J., Zakharov, A., Ogievetsky, E., Minlebaeva, A., Kurbanov, R., Gerasimova, E., et al. (2017). Inhibition of cortical activity and apoptosis caused by ethanol in neonatal rats in Vivo. *Cereb Cortex.* 27, 1068–1082. doi: 10.1093/cercor/bhv293

Lee, J. R., Joseph, B., Hofacer, R. D., Upton, B., Lee, S. Y., Ewing, L., et al. (2021). Effect of dexmedetomidine on sevoflurane-induced neurodegeneration in neonatal rats. *Br. J. Anaesth.* 126, 1009–1021. doi: 10.1016/j.bja.2021.01.033

Lee, J. R., Lin, E. P., Hofacer, R. D., Upton, B., Lee, S. Y., Ewing, L., et al. (2017). Alternative technique or mitigating strategy for sevoflurane-induced neurodegeneration: a randomized controlled dose-escalation study of dexmedetomidine in neonatal rats. *Br. J. Anaesth.* 119, 492–505. doi: 10.1093/bja/aex219

Li, Y., Xu, J., Xu, Y., Zhao, X. Y., Liu, Y., Wang, J., et al. (2018). Regulatory effect of general anesthetics on activity of potassium channels. *Neurosci. Bull.* 34, 887–900. doi: 10.1007/s12264-018-0239-1

Liang, G., Ward, C., Peng, J., Zhao, Y., Huang, B., and Wei, H. (2010). Isoflurane causes greater neurodegeneration than an equivalent exposure of sevoflurane in the developing brain of neonatal mice. *Anesthesiology* 112, 1325–1334. doi: 10.1097/ALN.0b013e3181d94da5

Lin, E. P., Soriano, S. G., and Loepke, A. W. (2014). Anesthetic neurotoxicity. *Anesthesiol. Clin.* 32, 133–155.

Maiese, K. (2015). O proteins in the nervous system. *Anal. Cell. Pathol.* 2015:569392.

Manolopoulos, K. N., Klotz, L. O., Korsten, P., Bornstein, S. R., and Barthel, A. (2010). Linking Alzheimer's disease to insulin resistance: the FoxO response to oxidative stress. *Mol. Psychiatry* 15, 1046–1052. doi: 10.1038/mp.2010.17

McCann, M. E., de Graaff, J. C., Dorris, L., Disma, N., Withington, D., Bell, G., et al. (2019). Neurodevelopmental outcome at 5 years of age after general anaesthesia or awake-regional anaesthesia in infancy (GAS): an international, multicentre, randomised, controlled equivalence trial. *Lancet* 393, 664–677.

Nikolić, M., Gardner, H. A., and Tucker, K. L. (2013). Postnatal neuronal apoptosis in the cerebral cortex: physiological and pathophysiological mechanisms. *Neuroscience* 254, 369–378. doi: 10.1016/j.neuroscience.2013.09.035

Noguchi, K. K., Johnson, S. A., Dissen, G. A., Martin, L. D., Manzella, F. M., Schenning, K. J., et al. (2017). Isoflurane exposure for three hours triggers apoptotic cell death in neonatal macaque brain. *Br. J. Anaesth.* 119, 524–531. doi: 10.1093/bja/aex123

Olney, J. W., Tenkova, T., Dikranian, K., Muglia, L. J., Jermakowicz, W. J., D'Sa, C., et al. (2002a). Ethanol-induced caspase-3 activation in the in vivo developing mouse brain. *Neurobiol. Dis.* 9, 205–219. doi: 10.1006/nbdi.2001.0475

Olney, J. W., Tenkova, T., Dikranian, K., Qin, Y. Q., Labruyere, J., and Ikonomidou, C. (2002b). Ethanol-induced apoptotic neurodegeneration in the developing C57BL/6 mouse brain. *Brain Res. Dev. Brain Res.* 133, 115–126. doi: 10.1016/s0165-3806(02)00279-1

Raper, J., Alvarado, M. C., Murphy, K. L., and Baxter, M. G. (2015). Multiple anesthetic exposure in infant monkeys alters emotional reactivity to an acute stressor. *Anesthesiology* 123, 1084–1092. doi: 10.1097/ALN.0000000000000851

Rudolph, U., and Antkowiak, B. (2004). Molecular and neuronal substrates for general anaesthetics. *Nat. Rev. Neurosci.* 5, 709–720. doi: 10.1038/nrn1496

Santo, E. E., and Paik, J. (2018). FOXO in neural cells and diseases of the nervous system. *Curr. Top. Dev. Biol.* 127, 105–118. doi: 10.1016/bs.ctdb.2017.10.002

Semenza, E. R., Harraz, M. M., Abramson, E., Malla, A. P., Vasavda, C., Gadalla, M. M., et al. (2021). D-cysteine is an endogenous regulator of neural progenitor cell dynamics in the mammalian brain. *Proc. Natl Acad. Sci. USA* 118:e2110610118. doi: 10.1073/pnas.2110610118

Shen, Y., Zhou, T., Liu, X., Liu, Y., Li, Y., Zeng, D., et al. (2021). Sevoflurane-induced miR-211-5p promotes neuronal apoptosis by inhibiting Efemp2. *ASN Neuro.* 13:36. doi: 10.1177/17590914211035036

Song, J., Christian, K. M., Ming, G. L., and Song, H. (2012). Life or death: developing cortical interneurons make their own decision. *EMBO J.* 31, 4373–4374. doi: 10.1038/emboj.2012.290

Southwell, D. G., Paredes, M. F., Galvao, R. P., Jones, D. L., Froemke, R. C., Sebe, J. Y., et al. (2012). Intrinsically determined cell death of developing cortical interneurons. *Nature* 491, 109–113. doi: 10.1038/nature11523

Tamamaki, N., Yanagawa, Y., Tomioka, R., Miyazaki, J., Obata, K., and Kaneko, T. (2003). Green fluorescent protein expression and colocalization with calretinin, parvalbumin, and somatostatin in the GAD67-GFP knock-in mouse. *J. Comp. Neurol.* 467, 60–79. doi: 10.1002/cne.10905

Tao, G., Zhang, J., Zhang, L., Dong, Y., Yu, B., Crosby, G., et al. (2014). Sevoflurane induces tau phosphorylation and glycogen synthase kinase 3beta activation in young mice. *Anesthesiology* 121, 510–527. doi: 10.1097/ALN.0000000000000278

Tzivion, G., Dobson, M., and Ramakrishnan, G. (2011). FoxO transcription factors: Regulation by AKT and 14-3-3 proteins. *Biochim. Biophys. Acta* 1813, 1938–1945. doi: 10.1016/j.bbamcr.2011.06.002

Vutskits, L., and Xie, Z. (2016). Lasting impact of general anaesthesia on the brain: mechanisms and relevance. *Nat. Rev. Neurosci.* 17, 705–717.

Wang, Q., Shen, F. Y., Zou, R., Zheng, J. J., Yu, X., and Wang, Y. W. (2017). Ketamine-induced apoptosis in the mouse cerebral cortex follows similar characteristic of physiological apoptosis and can be regulated by neuronal activity. *Mol. Brain* 10, 1–15. doi: 10.1186/s13041-017-0302-2

Wei, K., Chen, P., Shen, F. Y., Zhang, Y., Liu, Y. H., Wang, Z. R., et al. (2019). Defining the vulnerability window of anesthesia-induced neuroapoptosis in developing dentate gyrus granule cells: A transgenic approach utilizing POMC-EGFP mice. *Neuroscience* 415, 59–69. doi: 10.1016/j.neuroscience.2019.07.009

Wonders, C. P., and Anderson, S. A. (2006). The origin and specification of cortical interneurons. *Nat. Rev. Neurosci.* 7, 687–696. doi: 10.1038/nrn1954

Wong, F. K., Bercsenyi, K., Sreenivasan, V., Portales, A., Fernandez-Otero, M., and Marin, O. (2018). Pyramidal cell regulation of interneuron survival sculpts cortical networks. *Nature* 557, 668–673. doi: 10.1038/s41586-018-0139-6

Xing, N., Xing, F., Li, Y., Li, P., Zhang, J., Wang, D., et al. (2020). Dexmedetomidine improves propofol-induced neuronal injury in rat hippocampus with the involvement of miR-34a and the PI3K/Akt signaling pathway. *Life Sci.* 247:117359. doi: 10.1016/j.lfs.2020.117359

Xing, Y. Q., Li, A., Yang, Y., Li, X. X., Zhang, L. N., and Guo, H. C. (2018). The regulation of FOXO1 and its role in disease progression. *Life Sci.* 193, 124–131. doi: 10.1016/j.lfs.2017.11.030

Yu, J., and Zhang, L. (2008). PUMA, a potent killer with or without p53. *Oncogene* 27, S71–S83. doi: 10.1038/onc.2009.45

Zhang, Z., Liu, W., Shen, M., Ma, X., Li, R., Jin, X., et al. (2021). Protective effect of GM1 attenuates hippocampus and cortex apoptosis after ketamine exposure in neonatal rat via PI3K/AKT/GSK3beta pathway. *Mol. Neurobiol.* 58, 3471–3483. doi: 10.1007/s12035-021-02346-5

Zhao, S., Fan, Z., Hu, J., Zhu, Y., Lin, C., Shen, T., et al. (2020). The differential effects of isoflurane and sevoflurane on neonatal mice. *Sci. Rep.* 10:19345. doi: 10.1038/s41598-020-76147-6

Zhu, S., Wang, Z., Yu, J., Yin, L., and Zhu, A. (2021). Atractylenolide III alleviates isoflurane-induced injury in rat hippocampal neurons by activating the PI3K/Akt/mTOR pathway. *J. Food Biochem.* 45:e13892. doi: 10.1111/jfbc.13892

Conflict of Interest: The authors declare that the research was conducted in the absence of any commercial or financial relationships that could be construed as a potential conflict of interest.

Publisher's Note: All claims expressed in this article are solely those of the authors and do not necessarily represent those of their affiliated organizations, or those of the publisher, the editors and the reviewers. Any product that may be evaluated in this article, or claim that may be made by its manufacturer, is not guaranteed or endorsed by the publisher.

Copyright © 2022 Wang, Li, Tan and Wang. This is an open-access article distributed under the terms of the Creative Commons Attribution License (CC BY). The use, distribution or reproduction in other forums is permitted, provided the original author(s) and the copyright owner(s) are credited and that the original publication in this journal is cited, in accordance with accepted academic practice. No use, distribution or reproduction is permitted which does not comply with these terms.

frontiers | Frontiers in Molecular Neuroscience

ORIGINAL RESEARCH
published: 09 August 2022
doi: 10.3389/fnmol.2022.868583

Behavioral and Molecular Responses to Exogenous Cannabinoids During Pentylenetetrazol-Induced Convulsions in Male and Female Rats

*Antonella Zirotti Rosenberg[1], Maxs Méndez-Ruette[2], Mario Gorziglia[3], Benjamín Alzerreca[3], Javiera Cabello[3], Sofía Kaufmann[3], Lukas Rambousek[4], Andrés Iturriaga Jofré[5], Ursula Wyneken[3,6] and Carlos A. Lafourcade[7]**

[1]Escuela de Biotecnología, Facultad de Ciencias, Universidad Mayor, Santiago, Chile, [2]Centro de investigación e innovación Biomédica (CiiB), Laboratorio de Neurociencias, Universidad de Los Andes, Santiago, Chile, [3]Facultad de Medicina, Universidad de Los Andes, Santiago, Chile, [4]Institute of Experimental Immunology, University of Zurich, Zurich, Switzerland, [5]Facultad de Ciencia, Universidad de Santiago de Chile, Santiago, Chile, [6]IMPACT, Center of Interventional Medicine for Precision and Advanced Cellular Therapy, Santiago, Chile, [7]Department of Biological Sciences, Xi'an Jiaotong-Liverpool University (XJTLU), Suzhou, China

OPEN ACCESS

Edited by:
Inmaculada Segura,
Ludwig Maximilian University of Munich, Germany

Reviewed by:
Giuditta Gambino,
University of Palermo, Italy
Robert B. Laprairie,
University of Saskatchewan, Canada

***Correspondence:**
Carlos A. Lafourcade
clafourcade@gmail.com

Specialty section:
This article was submitted to Brain Disease Mechanisms, a section of the journal Frontiers in Molecular Neuroscience

Received: 02 Februray 2022
Accepted: 13 May 2022
Published: 09 August 2022

Citation:
Zirotti Rosenberg A, Méndez-Ruette M, Gorziglia M, Alzerreca B, Cabello J, Kaufmann S, Rambousek L, Iturriaga Jofré A, Wyneken U and Lafourcade CA (2022) Behavioral and Molecular Responses to Exogenous Cannabinoids During Pentylenetetrazol-Induced Convulsions in Male and Female Rats. Front. Mol. Neurosci. 15:868583. doi: 10.3389/fnmol.2022.868583

Epilepsy is a disabling, chronic brain disease, affecting ∼1% of the World's population, characterized by recurrent seizures (sudden, uncontrolled brain activity), which may manifest with motor symptoms (e.g., convulsions) or non-motor symptoms. Temporal lobe epilepsies (TLE) compromising the hippocampus are the most common form of focal epilepsies. Resistance in ∼1/3 of epileptic patients to the first line of treatment, i.e., antiepileptic drugs (AEDs), has been an important motivation to seek alternative treatments. Among these, the plant *Cannabis sativa* (commonly known as marihuana) or compounds extracted from it (cannabinoids) have gained widespread popularity. Moreover, sex differences have been proposed in epilepsy syndromes and in cannabinoid action. In the hippocampus, cannabinoids interact with the CB1R receptor whose membrane levels are regulated by β-Arrestin2, a protein that promotes its endocytosis and causes its downregulation. In this article, we evaluate the modulatory role of WIN 55,212-2 (WIN), a synthetic exogenous cannabinoid on behavioral convulsions and on the levels of CB1R and β-Arrestin2 in female and male adolescent rats after a single injection of the proconvulsant pentylenetetrazol (PTZ). As epilepsies can have a considerable impact on synaptic proteins that regulate neuronal toxicity, plasticity, and cognition, we also measured the levels of key proteins markers of excitatory synapses, in order to examine whether exogenous cannabinoids may prevent such pathologic changes after acute seizures. We found that the exogenous administration of WIN prevented convulsions of medium severity in females and males and increased the levels of phosphorylated CaMKII in the hippocampus. Furthermore, we observed a higher degree of colocalization between CB1R and β-Arrestin2 in the granule cell layer.

Keywords: cannabinoids, seizures, epilepsy, beta arrestin-2, hippocampus, dentate gyrus

INTRODUCTION

Epilepsy is a brain disorder caused by excessive neuronal activity, that may involve both (i.e., generalized) or only one (i.e., focal) hemisphere. Focal epilepsies usually involve the uncontrolled hyperexcitability of the hippocampal formation, a vulnerable region prone to developing seizures (Tatum, 2012; Chatzikonstantinou, 2014). If antiepileptic drugs (AEDs) do not improve the condition of patients (∼30% of cases), resective surgery is the only remaining option, though this alternative presents its own challenges. Not all patients are surgical candidates, ∼1/3 of patients will not be seizure free after the procedure, and comorbidities, including memory decline, may arise (Wiebe and Jette, 2012). Patients with drug-resistant epilepsies may be therefore drawn to try alternative treatments, including the smoking or consumption of the plant Cannabis sativa (commonly known as marihuana) or compounds derived from it, sometimes based on information obtained from the press or the internet (Kerr et al., 2019). Most preclinical epilepsy research has been focused on the two main cannabinoids found in the plant, Δ^9-tetrahydrocannabinol and cannabidiol (THC and CBD, respectively), and on synthetic agonists of cannabinoid receptors 1 and 2 (CB1R and CB2R, respectively). In the brain, exogenous and endogenous cannabinoids exert much of their action through activation of presynaptic CB1R, a seven transmembrane G-protein coupled receptor (GPCR) that is present in most cell types, resulting in decreased neurotransmitter release through a Gi/o signaling pathway (Benarroch, 2014). CB2R is found at low levels in the CNS, though recent reports show that it is inducible in some pathologies (including epilepsy; Ji et al., 2021) and may modulate plasticity (Chen et al., 2017; Kendall and Yudowski, 2017). In the hippocampus, the majority of CB1R expression occurs in gamma-aminobutyric acid (GABA)-releasing neurons, mostly on the axon terminals of cholecystokinin containing interneurons (Katona et al., 1999; Marsicano and Lutz, 1999; Nyíri et al., 2005; Földy et al., 2006). Despite lower expression levels of this receptor in glutamatergic cells of the hippocampus (Katona et al., 2006; Kawamura et al., 2006), its activation results in a higher G protein coupled signaling efficiency (Steindel et al., 2013; Busquets-Garcia et al., 2018) compared to that of interneurons. CB1R also activates β-arrestin 1 (βarr1) and 2 (βarr2) after ligand-induced phosphorylation of the receptor by GPCR kinases, a process that is independent of G-protein signaling. βarr2 initiates the endocytosis of CB1R by binding to clathrin and causing an overall desensitization of the CB1R-mediated response, thus decreasing the response to endo- or exo cannabinoids (Nogueras-Ortiz and Yudowski, 2016).

Most studies and anecdotical reports have concluded that plant-derived or synthetic exogenous cannabinoids are generally anti-convulsive (Devinsky et al., 2014; Rosenberg et al., 2015, 2017; Kerr et al., 2019), though pro-convulsive effects have also been observed for CB1R agonists, such as THC (Malyshevskaya et al., 2017), WIN (Perescis et al., 2020), or arachidonyl-2'-chloroethylamide, ACEA (Vilela et al., 2013; for recent reviews see Smolyakova et al., 2020; Kaczor et al., 2022). Little is known about whether sex differences may exist in the therapeutic action of exogenous cannabinoids in the context of epilepsy, though behavioral changes (e.g., appetite, pain) due to cannabinoid actions do show sex differences in humans and animals (Cooper and Craft, 2018). This may be an important area of research, as sex differences have been reported as well on epilepsy types, their underlying mechanisms, and associated comorbidities (Christian et al., 2020). In this study, we hypothesized that activation of CB1Rs by exogenous cannabinoids leads to a reduction in the intensity of acutely-induced seizures that is more pronounced in females compared to males, due to lower βArr2 expression levels.

Furthermore, it is not known whether exogenous cannabinoids can mitigate the impact that chronic or acute seizures have on the levels of synaptic proteins that are important mediators of excitation, cognition, and/or neurotoxicity (e.g., postsynaptic density protein 95, PSD-95; GluA2 subunit of α-amino-3-hydroxy-5-methyl-4-isoxazolepropionic acid receptors, AMPAR; Ca^{2+}/calmodulin-dependent protein kinase II, CaMKII) (Bronstein et al., 1990; Dong and Rosenberg, 2004; Ying et al., 2004; Needs et al., 2019; Lee and Kim, 2020). We therefore investigated whether similar changes could manifest early on, i.e., after an acute dose of PTZ, considered a "gold standard" in the evaluation of AEDs (Bialer and White, 2010), and whether underlying sex differences may be present.

Last, as WIN 55,212-2 (WIN from now on) is a CB1R and CB2R agonist (Felder et al., 1995), we used (±)-WIN 55,212, a racemic mixture consisting of WIN combined with the neutral CB2 antagonist, (−)-WIN 55,212-3, as a first approximation to evaluate the impact that activating CB1R while antagonizing CB2R could have in our acute model of PTZ-induced seizures.

MATERIALS AND METHODS

Animals. Adolescent female and male Sprague–Dawley rats (45–55 days old) were used, as this is one of the periods where the prevalence of epilepsy and years of life lost peaks (Beghi et al., 2019). All procedures involving animals were in accordance with the Bioethics Committee of the Universidad de los Andes (Las Condes, Chile).

Drugs. Pentylenetetrazol, PTZ (#P6500, Sigma-Aldrich, USA), 1-(2,4-dichlorophenyl)-5-(4-iodophenyl)-4-methyl-N-1-piperidinyl-1H-pyrazole-3-carboxamide (AM251, a CB1R antagonist), [(3R)-2,3-dihydro-5-methyl-3-(4-morpholinylmethyl) pyrrolo [1,2,3-de]-1,4-benzoxazin-6-yl]-1-naphthalenyl-methanone, monomethanesulfonate ((+)-WIN 55,212-2 (mesylate), WIN in the present article), [2,3-dihydro-5-methyl-3-(4-morpholinylmethyl)pyrrolo [1,2,3-de]-1,4-benzoxazin-6-yl]-1-naphthalenyl-methanone, methanesulfonate(±)-WIN 55,212 (mesylate; WINr in the present article), and N-(Piperidin-1-yl)-5-(4-iodophenyl)-1-(2,4-dichlorophenyl)-4-methyl-1H-pyrazole-3-carboxamide (AM251 in the present article), were obtained from Cayman chemical, USA (#71670, #10009023, and #10736, respectively).

Injection Protocol. The experimental design is shown in **Supplementary Figure 1A**. Drugs (or vehicles, i.e., DMSO or 0.9% NaCl) were injected i.p. WIN dose used was 1 mg/kg, a dose previously shown to be neuroprotective and anticonvulsive in juvenile rats (Rudenko et al., 2012) while PTZ was 50 mg/kg.

One hour after the last injection animals were either euthanized for Western blot analysis or perfused for immunohistochemistry.

Euthanasia. Rats were euthanized by rapid decapitation (Holson, 1992; van Rijn et al., 2011).

Seizure Activity. The four groups of animals were: C, WIN, PTZ, and WIN+PTZ, either male (n = 4, 4, 7, 4, respectively); or female (n = 9, 10, 17, 12) were video recorded simultaneously for 1 h after a single PTZ (or corresponding vehicle) injection. Offline behavioral analysis by a blind observer was done for the initial 25 min, as this is when maximal effects were observed. The time of onset, duration, and severity of seizures were described according to a modified Racine scale for rats (Lüttjohann et al., 2009). This scale evaluates intensity stages, going from 1 (lowest severity, e.g., motionless stare) to 6 (highest severity, e.g., strong convulsions).

Cellular Fractioning. The separation of proteins from crude membrane extracts and cytosol was accomplished as previously detailed (Carlin et al., 1980; Wyneken et al., 2001). Briefly, brains were quickly removed after decapitation, the hippocampi extracted, flash-frozen in liquid nitrogen, and stored at −80°C until the day of homogenization. The latter was performed in icecold homogenization buffer; 0.32 M sucrose, 5 mM Tris-HCl, 0.5 mM EGTA pH 7.4, along with protease (cOmplete™ Protease Inhibitor Cocktail #11697498001, Sigma-Aldrich, USA) and phosphatase inhibitors (Phosphatase Inhibitor Cocktail B1500, Bimake, USA), using a Teflon homogenizer. A P1 pellet was obtained after an initial 10 min centrifugation at 1,000 g. The resultant supernatant (supernatant A) was kept in ice while the pellet was resuspended in homogenization buffer and centrifuged at 700 g for 10 min. The resultant pellet (cellular debris) was discarded, and the supernatant added to supernatant A, and this mix was centrifuged at 12,000 g for 20 min. This supernatant was stored as the "cytoplasm" fraction and the pellet was resuspended in radioimmunoprecipitation assay (RIPA) buffer with protease inhibitors (the "membrane" fraction). Protein concentration was determined by the bicinchoninic acid (BCA) method of protein quantification using bovine serum albumin (BSA) as the standard. Sample absorbance was read in a Tecan Infinite M1000 PRO microplate reader (Tecan, Switzerland).

Western blots were performed using standard methodology as previously described (Lafourcade et al., 2020). Primary antibodies used were anti CB1, 1:1,000 (Ab23703, Abcam, UK), anti βArr2, 1:500 (Ab31294, Abcam), anti phospho T286phosphorylated calcium/calmodulin-dependent protein kinase II (p-CaMKII), 1:2,000 (Ab32678, Abcam), anti postsynaptic density protein 95 (PSD95) 1:1,000 (#610496, BD Biosciences, USA), anti α-amino-3-hydroxy-5-methyl-4-isoxazolepropionic acid, AMPA, subunit GluA2 (GluA2), 1:1,000 (Sc-517265, Santa Cruz Biotechnology, USA), anti calcium/calmodulin-dependent protein kinase II (total CaMKII) (Sc-5306, Santa Cruz Biotechnology), antiGolgi matrix protein 130 (GM130), 1:1,000 (#610823, BD Biosciences, USA), anti βIII-Tubulin, 1:2,500 (G7121, Promega, USA), anti N-cadherin, 1:1,000 (#33-3900, Invitrogen). Secondary antibodies were obtained from Li-cor, USA (#926-80010, #926-80011) and Invitrogen, USA (#81-1620).

Perfusion. Animals were anesthetized by an i.p. injection of ketamine (100 mg/kg) and xylazine (30 mg/kg). A standard protocol of intracardial perfusion was performed (Gage et al., 2012), first with ∼200 ml of phosphate-buffered saline (PBS, pH = 7.4), followed by ∼400 ml of paraformaldehyde 4% (PFA) to fix brain tissue. Perfusion was done at a steady rate of ∼20 ml/minute using a Masterflex Pump, model 7518 (Masterflex® Bioprocessin, USA).

Immunofluorescence. After perfusion animals were decapitated, brains removed, and post-fixed in PFA overnight (ON) followed by sucrose 30% in PBS until decantation. Brains were embedded in optimal cutting temperature compound (OCT) and sectioned (30 μm coronal sections) using a cryostat (Microm HM 525, Thermo Fisher Scientific). Sections were washed in PBS and permeabilized with Triton-X 0.2%: PBS for 30 min. Tissue was then incubated in a blocking solution containing 5% BSA and 5% horse serum in PBS for 45 min. Primary antibodies used were GluA2, 1:800 (sc-517265, Santa Cruz Biotechnology), CB1R, 1:900 (ab23703, Abcam), βArr2, 1:400 (ab31294, Abcam), and Cleaved-Cas3 (CAS3), 1:600 (9661, Cell Signaling); diluted in antibody solution (1% BSA and 1% horse serum in PBS), and incubated overnight at 4°C with agitation. Brain sections were then washed with Tween 0.2% in PBS three times (20 min each time), followed by incubation witha secondary antibody for 90 min. After three washes with PBS, sections were mounted using mounting media with DAPI and analyzed by confocal microscopy (Leica Sp8). For each condition/treatment, a group of at least five different sections were examined in the hippocampal region at Bregma -3.6 to -4.5 mm (Kruger et al., 1995; Cambridge University Press). Images were edited by Adobe Photoshop (CC 2014, California, USA) to normalize intra and inter sample background across all different channels. The average fluorescence intensities of four randomly placed sample areas (2,500 μm^2) in the granule cell layer or the hilus was used to calculate nominal (e.g., CB1R+) or colocalization (e.g., CB1R + βArr2) values. The area of reactivity of each antibody were normalized to the size of the sampled area.

Statistics. Two-tailed t-tests and ANOVA and outlier analysis tests were conducted in GraphPad Prism version 6, GraphPad Software, San Diego, California USA. MANOVA tests were performed in R Core Team (2020). R: A language and environment for statistical computing. R Foundation for Statistical Computing, Vienna, Austria.

RESULTS

First, we evaluated the effect of a single injection of WIN 55,212-2 (WIN from now on) on grooming and locomotion. Female and male rats injected with WIN showed no differences in the time spent grooming (**Supplementary Figures 1B,C**), ambulating (**Supplementary Figures 1D,E**), or motionless (**Supplementary Figures 1F,G**; **Supplementary Table 1**). To examine the effect of exogenous cannabinoids on acute convulsions we first injected female or male rats with either a vehicle (i.e., DMSO) or with WIN, and an hour later with either a vehicle (i.e., NaCl 0.9%) or Pentylenetetrazole (PTZ; **Supplementary Figure 1A**). We then compared the time of convulsions using a modified

Racine scale at each stage of severity (Lüttjohann et al., 2009; **Figures 1A–J**; **Supplementary Table 1**). Animals not injected with PTZ (control group, C, and WIN group) were recorded but not included in the analysis, as they did not display convulsions. We found a significant increase in the duration females spent at stage 1 (e.g., behavioral arrest) in animals injected with WIN + PTZ (**Figure 1A**), and a significant decrease in the time females and males spent in stage 4 (clonic seizures, sitting, **Figures 1C,H**, respectively). A MANOVA test that included males and females confirmed a significant effect for treatment and sex at stage 4 (**Supplementary Table 1**). The time spent at stage 2 (e.g., facial jerking) is not shown as few animals showed this behavior. No significant differences were found for stages 3 (e.g., neck jerks, **Figure 1B**, females and **Figure 1G**, males), 5 (convulsions while lying down, **Figure 1D**, females and **Figure 1I**, males) or 6 (e.g severe convulsions, including jumping, **Figure 1E**, females and **Figure 1J**, males). The WIN-mediated significant reduction of time spent on stage 4 convulsions (**Figure 1C**, females and **Figure 1H**, males) was abolished in females (**Supplementary Figure 1H**) and males (**Supplementary Figure 1I**; **Supplementary Table 1**) when the CB1R antagonist AM251 was injected 30 min before WIN, indicating that the anticonvulsive effect of the latter was mediated by CB1R. In our hands hormonal changes did not have a strong effect on acute PTZ-induced convulsions in the presence or absence of WIN, as we did not find significant differences between the time spent at higher stages of seizure severity (i.e., stages 4, 5, and 6) when considering the estrous cycle period in females (**Supplementary Figure 1J**, **Supplementary Table 1**).

We calculated the number of times animals reached stage 4 in the first 500 s of recording, as this was the time when generally most crises were recorded (**Supplementary Figures 2A–F**). Females injected with PTZ showed a significant increase in the number of times they reached stage 4 compared to those injected with WIN + PTZ (**Figure 1F**). No differences between these groups were observed in males (**Figure 1J**). No differences were observed when considering other time periods (i.e., from 500 to 1,000 s, or from 1,000 to 1,500 s (**Supplementary Table 1**). No significant differences were observed in the latency to reach each intensity stage (**Figures 2A–E**, females and **Figures 2F–J**, males; **Supplementary Table 2**).

Since sex differences have been observed in the binding levels of βArr2 to the corticotropin-releasing factor (CRF) receptor during the stress response (Bangasser et al., 2010), we wondered if similar mechanisms could be found in our model. To answer this question, we performed Western blots from whole hippocampal tissue. To distinguish between membrane-bound (e.g., CB1R) or cytoplasmic (e.g., βArr2) proteins (Srivastava et al., 2015), we performed a differential centrifugation protocol after the homogenization of the samples (see "Materials and Methods" Section). After establishing that our centrifugation method yielded samples enriched in membrane-bound proteins (see **Supplementary Methods**, **Supplementary Figures 3A–C**), we compared the levels of CB1R between males and females in the membrane fraction. We did not obtain significant differences in hippocampal levels of CB1R in males compared to females (**Supplementary Figures 3D,E**; **Supplementary Table 3**), though a tendency toward higher levels of CB1R in males can be observed, which is consistent with previous results (Ferraro et al., 2020). No significant differences were found in the cytoplasmic levels of βArr2 between males and females either (**Supplementary Figures 3F,G**; **Supplementary Table 3**).

Next, we examined the impact of PTZ injection in the presence or absence of WIN on hippocampal levels of membrane-bound CB1R and GluA2, an AMPAR subunit that is important for neuronal synaptic plasticity and memory processes (Hara et al., 2012). We did not observe significant changes in the levels of these two proteins, either in samples obtained from females (**Figures 3A–C**) or males (**Figures 3D–F**; **Supplementary Table 3**).

Similarly, we evaluated whether the levels of cytoplasmic proteins relevant for CB1R action (e.g., βArr2) and synaptic efficiency (i.e., GluA2, PSD95, and CaMKII) were altered after an acute exposure to PTZ, previously injected with WIN or vehicle (**Figure 4**). No differences were found in the levels of CB1R or GluA2 in our "cytoplasmic" fraction between groups, either in females (**Figures 4A–C**; **Supplementary Table 4**) or males (**Figures 4I–K**; **Supplementary Table 4**). We also measured the expression levels of βArr2 and PSD95, and did not observe differences in their expression levels, either in females (**Figures 4A,D,E**) or males (**Figures 4I,L,M**; **Supplementary Table 4**). We did observe a significant increase in the levels of phosphorylated CaMKIIα in the WIN group compared to the control and PTZ groups, and also between the WIN + PTZ group and the PTZ group in females (**Figures 4A,F**), but not in males (**Figures 4I,N**; **Supplementary Table 4**). No significant differences were obtained between groups in females or males when comparing the levels of *p*-CaMKIIβ (**Figures 4A,G,I,O**, respectively) or total CaMKII (**Figures 4A,H,I,P**, respectively; **Supplementary Table 4**).

As regional changes in βArr2 and CB1R could be missed when studying the whole hippocampus, we analyzed whether putative differences in the expression levels of βArr2 and CB1R that were not visible by Western blot could be revealed by local examination of the hippocampal dentate gyrus of female rats (representative figures, **Figures 5A,B**; **Supplementary Table 5**). This region was chosen as it is crucial in the control of excitability arising from other brain areas (e.g., entorhinal cortex), though seizures may be generated regardless of external inputs (Krook-Magnuson, 2017). In the hilus of the dentate gyrus excitatory mossy cells express CB1R (Krook-Magnuson et al., 2015; Sugaya et al., 2016; Jensen et al., 2021). Thus, in order to differentiate glutamatergic mossy cells from GABAergic interneurons in this region, we used GluA2 as a marker of mossy cells (Leranth et al., 1996). We did not find differences between our experimental groups in the expression levels of CB1R or βArr2 regardless of cell type (**Figures 5C,D** respectively), or when considering CB1R or βArr2 expression in hilar mossy cells (i.e., g, gluA2+ neurons; **Figures 5E,F**, respectively), a result that is consistent with our whole hippocampal Western blots (**Figures 3**, **4**). However, CB1R and βArr2 colocalization in the hilus (in GluA2+ regions) increased in the WIN + PTZ group when compared to PTZ (**Figure 5G**). Since neuronal loss has been observed in hippocampal tissue obtained from mesial temporal lobe patients

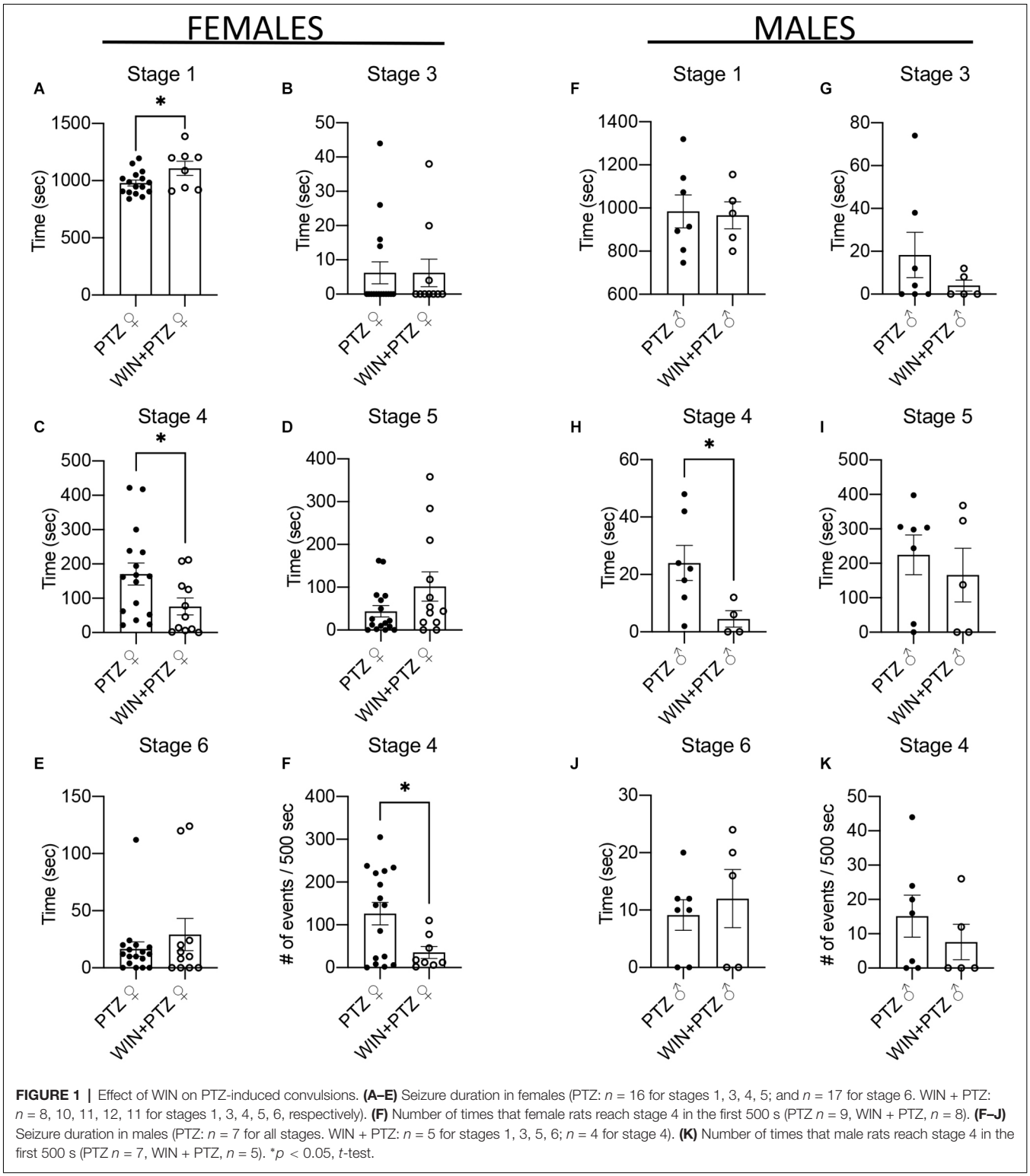

FIGURE 1 | Effect of WIN on PTZ-induced convulsions. **(A–E)** Seizure duration in females (PTZ: $n = 16$ for stages 1, 3, 4, 5; and $n = 17$ for stage 6. WIN + PTZ: $n = 8, 10, 11, 12, 11$ for stages 1, 3, 4, 5, 6, respectively). **(F)** Number of times that female rats reach stage 4 in the first 500 s (PTZ $n = 9$, WIN + PTZ, $n = 8$). **(F–J)** Seizure duration in males (PTZ: $n = 7$ for all stages. WIN + PTZ: $n = 5$ for stages 1, 3, 5, 6; $n = 4$ for stage 4). **(K)** Number of times that male rats reach stage 4 in the first 500 s (PTZ $n = 7$, WIN + PTZ, $n = 5$). $^*p < 0.05$, *t*-test.

and from chronic PTZ kindling models of epilepsy (Yardimoglu et al., 2007; Kitaura et al., 2018), we measured the levels of cleaved caspase-3 (CAS3), a marker of cells that are dying (Crowley and Waterhouse, 2016), in hippocampal slices from our experimental groups. We did not observe significant differences in the levels of CAS3 for any of the groups studied (**Figure 5H**). In the granule cell layer, GluA2 is a marker of mature granule cells (Hagihara et al., 2011), and colocalization of GluA2 with CB1R or βArr2 did not show differences between groups (**Figures 5I,J**, respectively). However, colocalization of CB1R with βArr2 in

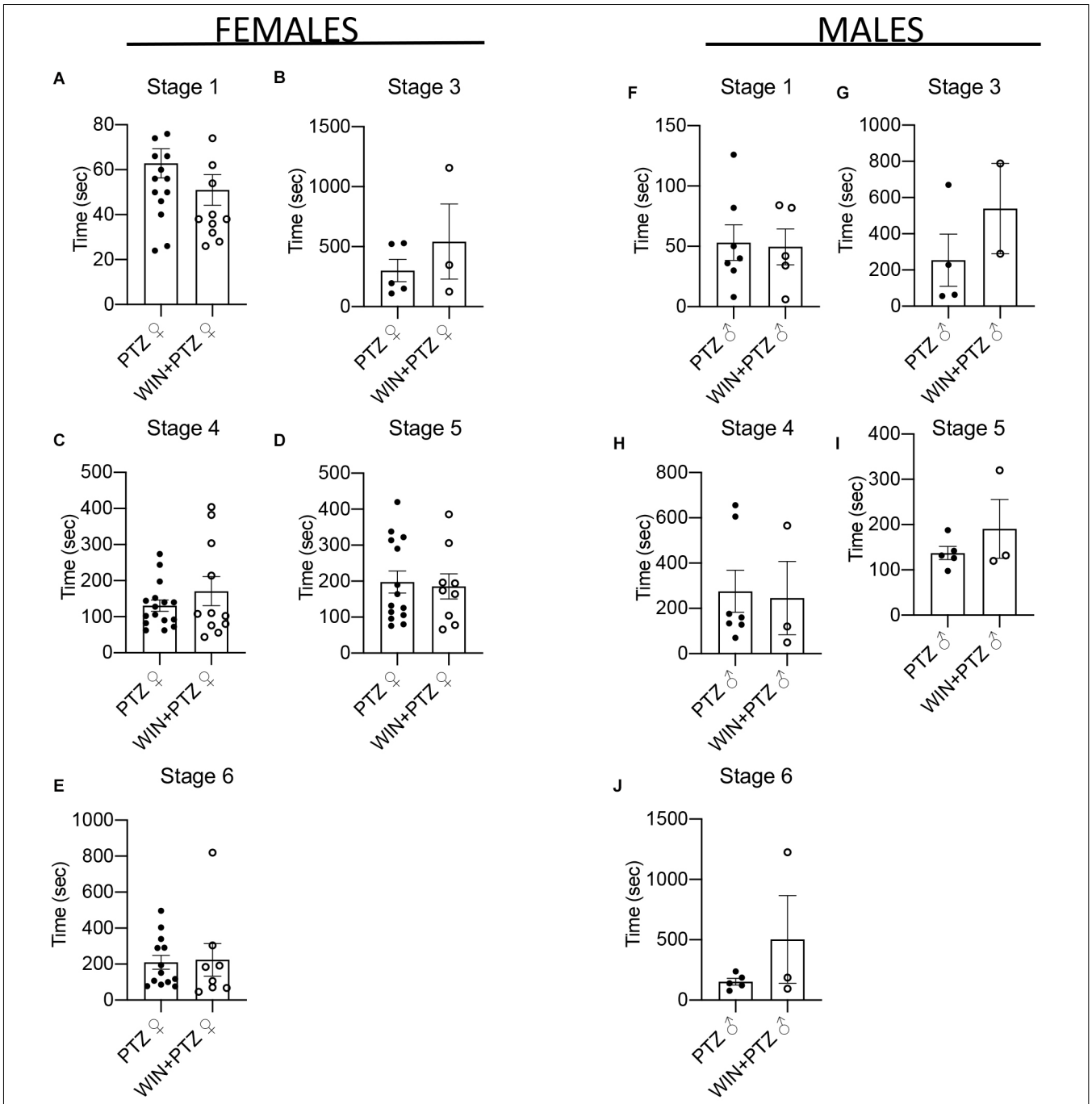

FIGURE 2 | Latency to epileptic crisis at stages of increasing severity. **(A–E)** Latency in females (PTZ: *n* = 16 for stages 1 and 4, *n* = 5 for stage 3, *n* = 14 for stage 5, *n* = 13 for stage 6. WIN + PTZ: *n* = 12, 11, 9, and 8 for stages 1, 4, 5, 6, respectively, *n* = 3 for stage 3). **(F–J)** Latency to epileptic crisis at stages of increasing severity in males (PTZ: *n* = 7 stages 1 and 4; *n* = 4 for stage 3, *n* = 5 for stages 5 and 6. WIN + PTZ: *n* = 5 for stage 1, *n* = 2 for stage 3, *n* = 3 for stages 4, 5, and 6).

GluA2+ cells was increased in the WIN + PTZ group compared to the other conditions (**Figure 5K**). No differences in cellular apoptosis were found between groups in the granule cell layer (**Figure 5L**).

Finally, we examined the putative anticonvulsant effect of WIN55212 (WIN_r), a racemic mixture of WIN 55,212-2 (WIN, the (+) isomer) and WIN 55,212-3 (the (-) isomer; **Supplementary Figure 4**; **Supplementary Table 6**). WIN 55,212-3 is considered an inactive enantiomer of WIN 55,212-2 due to the differences in potency between these two drugs (Savinainen et al., 2005). As WIN 55,212-3 is also a neutral antagonist of CB2R (Savinainen et al., 2005), we intended to investigate whether antagonizing CB2R, a receptor that has been implicated in epilepsy (Ji et al., 2021), could influence the anticonvulsive

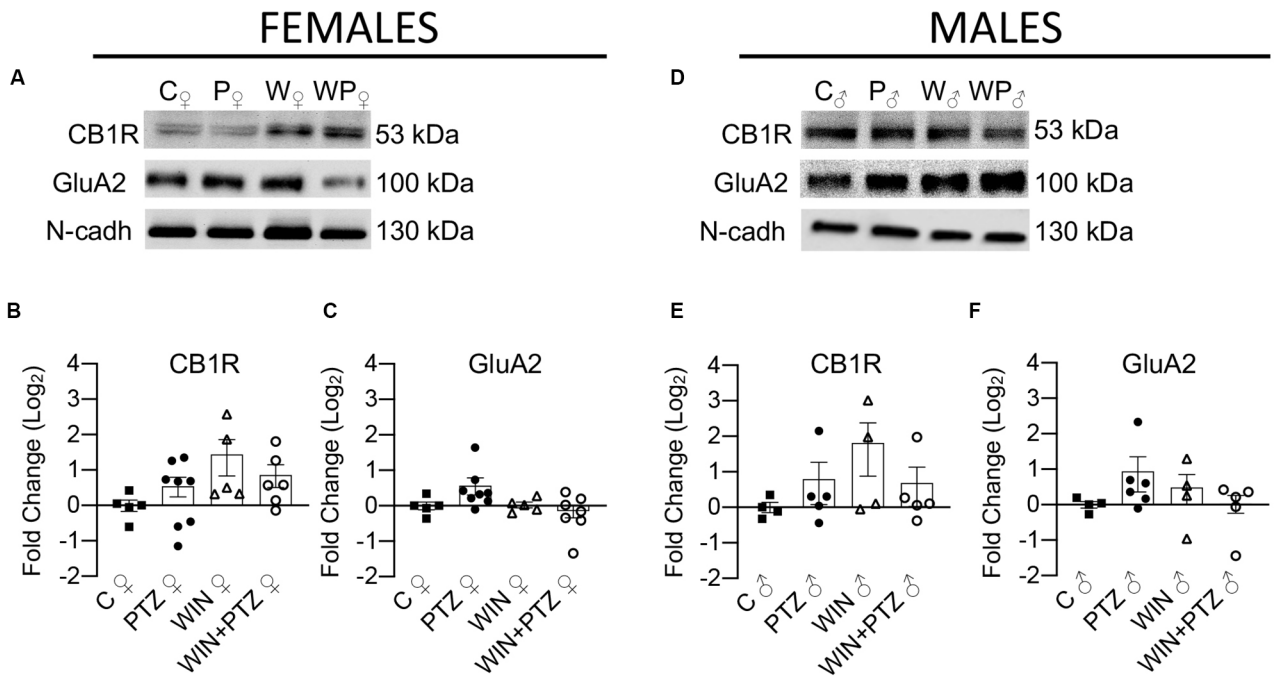

FIGURE 3 | Expression levels of membrane-bound CB1R and AMPAR subunit GluA2 in females and males. **(A)** Representative Western blots of membrane-bound CB1R and GluA2, in females and **(D)** males. **(B)** Quantification of membrane-bound CB1R levels in females (C, *n* = 5; PTZ, *n* = 8; WIN, *n* = 5; WIN + PTZ, *n* = 6). **(C)** Quantification of membrane-bound GluA2 levels in females (C, *n* = 5; PTZ, *n* = 8; WIN, *n* = 5; WIN + PTZ, *n* = 7). **(E)** Quantification of membrane-bound CB1R levels in males (C, *n* = 4; PTZ, *n* = 5; WIN, *n* = 4; WIN + PTZ, *n* = 5). **(F)** Quantification of membrane-bound GluA2 levels in males (C, *n* = 4; PTZ, *n* = 6; WIN, *n* = 4; WIN + PTZ, *n* = 5). N-cadherin was used as protein loading control for all gels.

effect of WIN. Using the same protocol as previously mentioned, our results show only slight differences between the outcome of both treatments. This time WIN_r had anticonvulsive properties only on females, in stage 1 (**Supplementary Figure 4A**) and stage 5 (**Supplementary Figure 4D**) of the modified Racine scale. We did not observe a significant difference in any other stage. We performed a similar calculation as with **Figure 1** and counted the number of times animals reached stage 5 in the first 500 s of recording (**Supplementary Figures 6A–F**). Females injected with PTZ showed a significant increase in the number of times they reached stage 5 compared to those injected with WIN + PTZ (**Supplementary Figure 4F**). No differences were observed in males (**Supplementary Figure 4L**).

No differences were observed in females or males when considering other time periods (i.e., from 500 to 1,000 s, or from 1,000 to 1,500 s (**Supplementary Table 6**).

No significant differences were found in the latency to reach the first convulsion for any stage of severity, in either females or males (**Supplementary Figures 5A–H**; **Supplementary Table 7**).

DISCUSSION

Our results show that treatment with WIN is effective in reducing medium-stage convulsion times (i.e., stage 4) in females and males injected with WIN previous to PTZ, while higher stages (i.e., 5 and 6) were not affected. We also observed a slight but significant increase in the time spent on stage 1 (e.g., motionless stare) in females injected with WIN followed by PTZ, which may compensate for the reduction in stage 4 seizures.

Possible Antiepileptic Action of CB1R Agonists

Overall, this could be suggestive of cannabinoid agonists being an appropriate anticonvulsive therapy for patients expressing specific subtypes of epilepsy (e.g., complex-partial or focal onset impaired awareness epilepsy is associated with lower stages of the Racine scale, while higher stages represent generalized seizures; Englot and Blumenfeld, 2009; Van Erum et al., 2019) or cannabinoids being effective only in convulsions of a certain intensity, perhaps bearing some resemblance to what has been described for AED (Manford, 2017). Further experiments are needed to examine whether the interaction of WIN with AEDs that may be effective in treating seizures of higher severity could result in better anticonvulsive action. Discrepancies in the literature regarding the anticonvulsive properties of CB1R agonists may be due to differences in the experimental designs used. Moreover, a better comprehension of underlying molecular mechanisms is also necessary to reconcile results that show WIN having a proconvulsive (Vilela et al., 2013) or mixed (Wendt et al., 2011) action in preclinical models. In this regard, exploring the putative direct or indirect interactions between exogenous or endogenous CB1R agonists and receptors from other systems (e.g., transient receptor potential vanilloid 1,

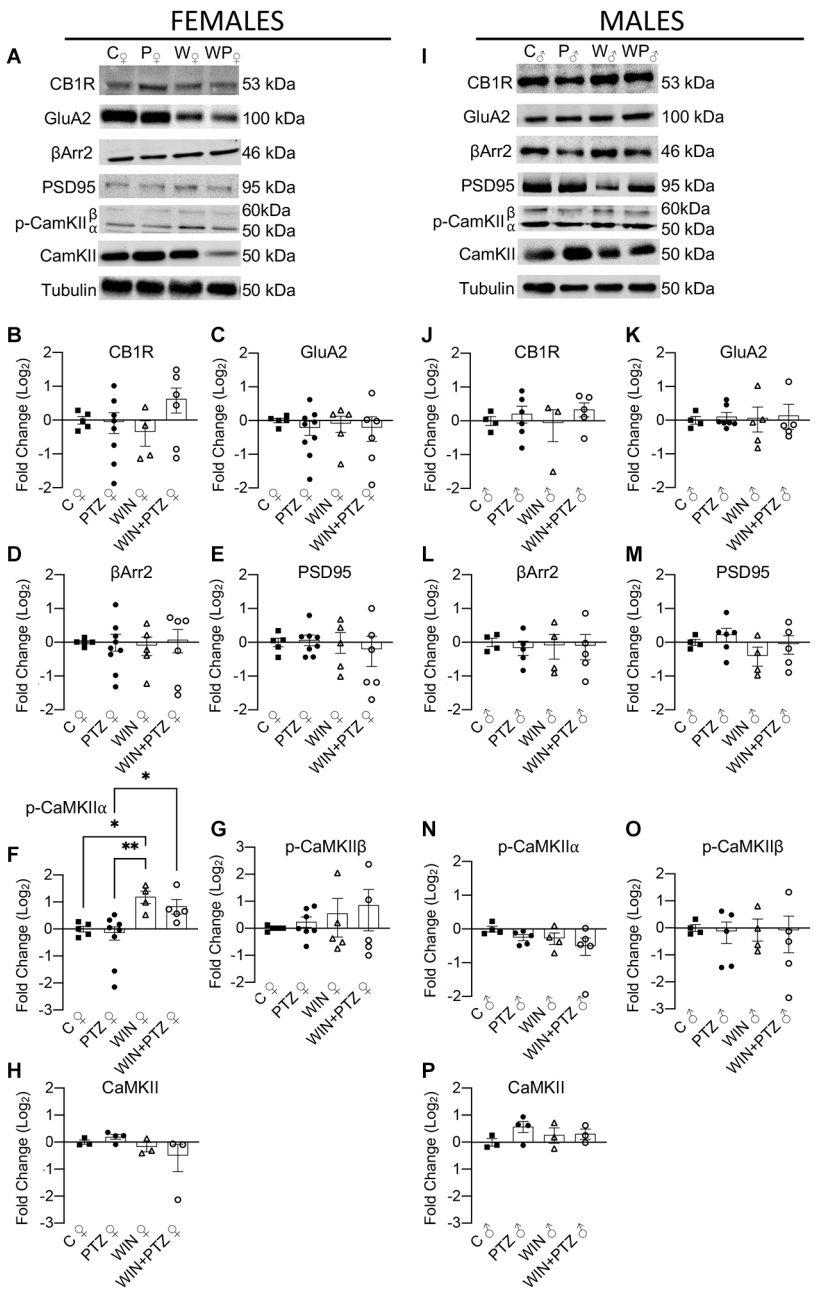

FIGURE 4 | Expression levels of proteins obtained from a fraction enriched in cytoplasmic proteins/proteins bound to small organelles. **(A)** Representative Western blots of CB1R, GluA2R, βArr2, PSD95, p-CaMKII and total CaMKII in females and **(I)** males. **(B–H)** Quantification of **(A)** (Females. CB1R: C, $n = 5$; PTZ, $n = 8$; WIN, $n = 4$; WIN + PTZ, $n = 6$; GluA2: C, $n = 5$; PTZ, $n = 9$; WIN, $n = 5$; WIN + PTZ, $n = 6$; βArr2: C, $n = 5$; PTZ, $n = 9$; WIN, $n = 5$; WIN + PTZ, $n = 6$; PSD95: C, $n = 5$; PTZ, $n = 8$; WIN, $n = 5$; WIN + PTZ, $n = 6$, *p*-CaMKIIα: C, $n = 5$; PTZ, $n = 8$; WIN, $n = 4$; WIN + PTZ, $n = 5$; *p*-CaMKIIβ: C, $n = 5$; PTZ, $n = 7$; WIN, $n = 5$; WIN + PTZ, $n = 5$; total CaMKII: C, $n = 3$; PTZ, $n = 4$; WIN, $n = 3$; WIN + PTZ, $n = 3$). **(J–P)** Quantification of **(D)** (Males. CB1R: C, $n = 4$; PTZ, $n = 6$; WIN, $n = 3$; WIN + PTZ, $n = 5$; GluA2: C, $n = 4$; PTZ, $n = 7$; WIN, $n = 5$; WIN + PTZ, $n = 5$; βArr2: C, $n = 4$; PTZ, $n = 5$; WIN, $n = 4$; WIN + PTZ, $n = 5$; PSD95: C, $n = 4$; PTZ, $n = 6$; WIN, $n = 4$; WIN + PTZ, $n = 5$, *p*-CaMKIIα: C, $n = 4$; PTZ, $n = 5$; WIN, $n = 4$; WIN + PTZ, $n = 5$; *p*-CaMKIIβ: C, $n = 4$; PTZ, $n = 5$; WIN, $n = 4$; WIN + PTZ, $n = 5$; total CaMKII: C, $n = 3$; PTZ, $n = 4$; WIN, $n = 3$; WIN + PTZ, $n = 3$). Tubulin was used as protein loading control for all gels. $^{*}p < 0.05$ and $^{**}p < 0.01$, one-way ANOVA with Tukey's multiple comparisons *post hoc*.

serotonin receptors, etc) may help explain the reasons behind the aforementioned discrepancies (Manna and Umathe, 2012; Carletti et al., 2016; Colangeli et al., 2019). Similarly, it would be interesting to evaluate in our model the impact of other compounds that have been previously shown to be successful in clinical or/and preclinical studies, like CBD (alone or combined

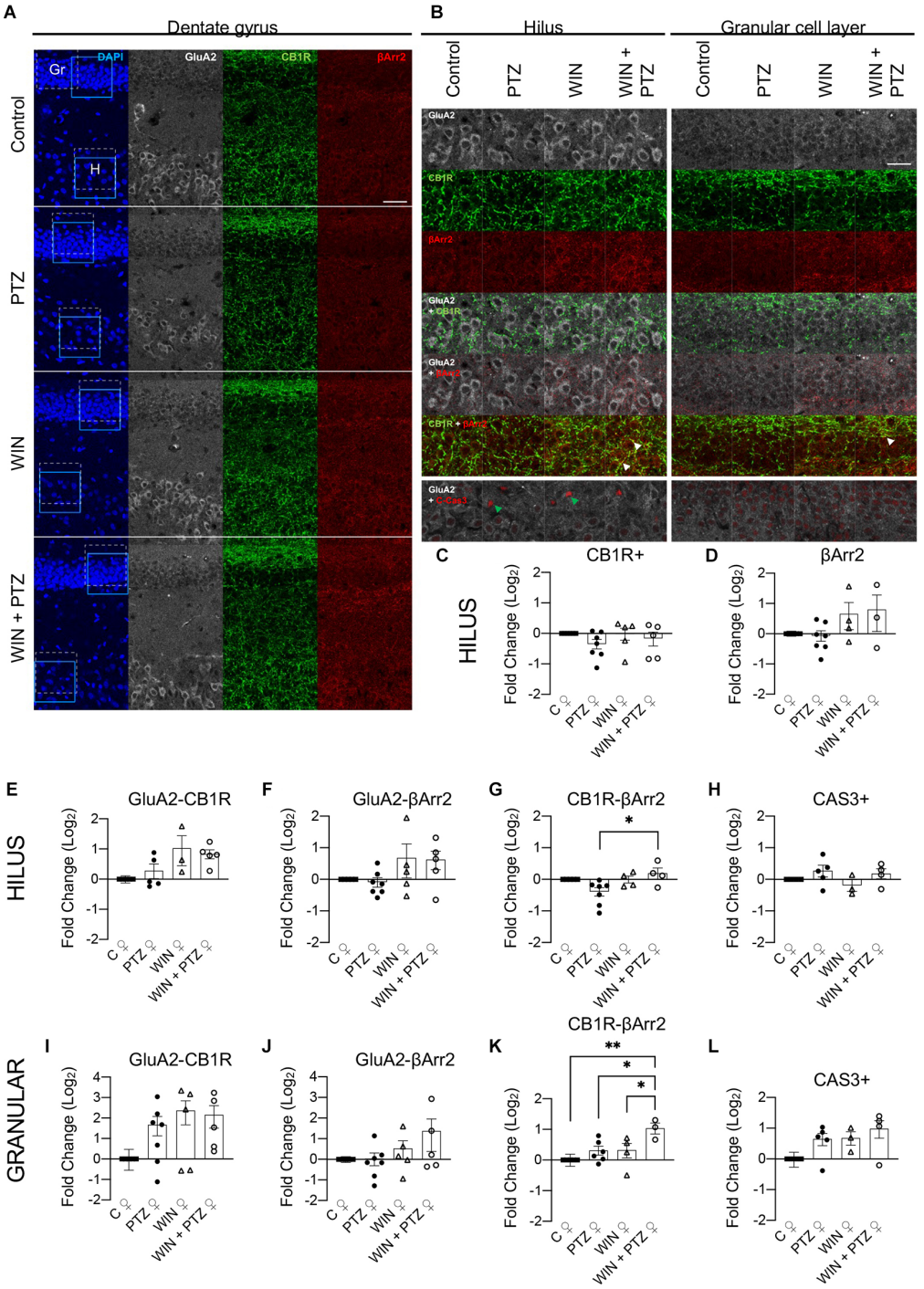

FIGURE 5 | Hilar and granule cell layer immunohistochemistry in female rats. **(A)** Representative immunofluorescent images of the dentate gyrus showing the granule cell layer (Gr) and the hilus (H) for each experimental group. Dashed square: areas used for colocalization analysis. Calibration bar: 40 μm. **(B)** Representative images used for analysis [amplified view of dashed square region from **(A)**]. Calibration bar: 25 μm. **(C–L)** quantification of **(B)**. **(C)** CB1R + (C, $n = 6$; PTZ, $n = 7$; WIN, $n = 5$; WIN + PTZ, $n = 5$) and **(D)** βArr2+ (C, $n = 5$; PTZ, $n = 7$; WIN, $n = 4$; WIN + PTZ, $n = 3$) area in the hilus. **(E)** GluA2-CB1R (C, $n = 5$; PTZ, $n = 5$; WIN, $n = 3$; WIN + PTZ, $n = 5$), **(F)** GluA2-βArr2 (C, $n = 5$; PTZ, $n = 7$; WIN, $n = 5$; WIN + PTZ, $n = 5$) and **(G)** CB1R-βArr2 (C, $n = 5$; PTZ, $n = 7$; WIN, $n = 4$; WIN + PTZ, $n = 4$) colocalization in hilus. **(H)** CAS3+ neurons (C, $n = 4$; PTZ, $n = 5$; WIN, $n = 3$; WIN + PTZ, $n = 4$) in hilus. **(I)** GluA2-CB1R (C, $n = 5$; PTZ, $n = 7$; WIN, $n = 5$; WIN + PTZ, $n = 5$), **(J)** GluA2-βArr2 (C, $n = 5$; PTZ, $n = 7$; WIN, $n = 5$; WIN + PTZ, $n = 5$), and **(K)** CB1R-βArr2 (C, $n = 5$; PTZ, $n = 6$; WIN, $n = 4$; WIN + PTZ, $n = 3$) colocalization in the granular cell layer. **(L)** CAS3+ neurons (C, $n = 4$; PTZ, $n = 5$; WIN, $n = 3$; WIN + PTZ, $n = 4$) in granular cell layer. White arrows: examples of strong colocalization between CB1R and βArr2. Green arrows: example of CAS3+ cells. $^{*}p < 0.05$ and $^{**}p < 0.01$, one-way ANOVA with Tukey's multiple comparisons *post hoc*.

with WIN). Promising results have been obtained with CBD in preclinical and clinical trials to treat genetic-based epilepsies, like Lennox-Gastaut Syndrome (LGS) and Dravet Syndrome (DS). This has led the Food and Drug Administration (FDA) to approve the use of Epidiolex, a drug based on purified CBD, to treat these two types of epilepsy (Silvestro et al., 2019). Similarly, positive modulators of CB1R have shown antiseizure properties in models of absence seizures (Roebuck et al., 2021; McElroy et al., 2022). It remains to be tested whether these compounds may interact with WIN to improve its anticonvulsive properties.

A limitation of our model is that we are focused on acute seizures, which may be viewed as a first step in the evaluation of CB1R agonists as anticonvulsants in females. Future experiments need to address whether regular administration of a CB1R agonist may be of use in models of epileptogenesis. This would require careful analysis of appropriate dosages and types of CB1R agonists, as adolescents exposed to synthetic cannabinoids (e.g., Spice/K2) present a higher incidence of seizures compared to those that are only exposed to cannabis (Havenon et al., 2011; Anderson et al., 2019).

WIN-Induced Changes in Signaling Systems and Synaptic Proteins

Taking into consideration the similarities in our behavioral data between males and females, we analyzed whether their molecular strategies (i.e., changes in the expression levels of CB1R and the associated protein βArr2) in response to an acute PTZ treatment in the presence or absence of WIN were similar as well. Our results show there were no differences between our experimental groups in either females or males on hippocampal levels of membrane-bound CB1R or cytoplasmic βArr2, though the lack of changes in synaptic protein levels in our model may be due to insufficient time for those modifications to be discernible. Interestingly, the selective increase in p-CaMKII (α subunit) levels in the WIN + PTZ group in females (and not in males) compared to the PTZ one, and in WIN injected animals compared to PTZ-injected animals and control animals suggests that WIN may be triggering a synaptic remodeling (Lemieux et al., 2012). This may include remodeling of the cannabinoid signaling system involved in the reduction of seizure severity. Considering that mice that lack the α subunit (i.e., null mutants) of this enzyme show increased susceptibility to epileptic seizures (Butler et al., 1995), the increase in p-CaMKIIα we observe could be interpreted as a mechanism to control hyperexcitability through induction of plastic changes in glutamatergic synapses that should be further explored (Robison, 2014). It needs to be established whether WIN-induced plasticity in the PTZ group reduces seizures after a second or third PTZ challenge.

Since changes in the levels of CB1R or βArr2 may not be widespread, but rather localized to certain hippocampal regions, we analyzed the levels of these proteins in the dentate gyrus by immunohistochemistry.

The increase in the colocalization levels of CB1R with βArr2 firstly confirms that the aforementioned synaptic remodeling is on course. Moreover, the increased colocalization in regions that are GluA2+ suggests that the activity of CB1R in mossy cells is reduced in the presence of WIN due to a higher interaction of CB1R with βArr2. This could result in mossy cells having higher levels of activity (e.g., due to reduced inhibition by cannabinoids), a result that may seem counterintuitive under the "irritable" mossy cell hypothesis (i.e., mossy cells exert a net excitatory effect over granule cells), but not under the "dormant" hypothesis (i.e., mossy cells inhibit granule cells through activation of interneurons; Jinde et al., 2013). In that line, a recent publication supports the idea that an increase in mossy cell activity in chronic epileptic mice reduces the possibility of electrographic seizures from becoming behavioral ones (Bui et al., 2018).

Possible Contribution of CB2R

Last, and given the discrepancies observed when examining the anticonvulsive effects of CB2R agonists and antagonists, we wondered whether the racemic mixture of (+) WIN 55,212-2 and (-) WIN 55,212-3 (WINr), could regulate convulsions differently than (+) WIN 55,212-2 alone. WIN 55,212-3 is a CB2 neutral antagonist/inverse agonist (Govaerts et al., 2004; Savinainen et al., 2005) capable of inhibiting the action of potent and specific CB2R inverse agonists (albeit at higher concentrations; Savinainen et al., 2005; Saroz et al., 2019). Our results with WIN_r were only slightly dissimilar to those obtained with WIN, implying that CB2R modulation could be a factor to consider when developing anticonvulsive drugs based on CB1R agonism. More research would be needed to examine the level of CB2R antagonism in the brain by our injection of WINr, as this study is limited by the low number of publications that have used this compound previously. Although it is necessary to expand these results using other available CB2R antagonists, our findings are partially consistent with the beneficial effects obtained by inhibiting CB2R (with a specific antagonist) in male rats (Rizzo et al., 2014).

CONCLUSION

Taken together, our results suggest that, under an acute PTZ-induced seizure model, the cannabinoid agonist WIN has a significant effect on medium-stage seizure severity. This is associated with a specific increase in the phosphorylation of CaMKIIα, a central enzyme involved in the control of synaptic plasticity and neuronal excitability, and with an increase in the colocalization of CB1R with βarr2 in the granule cell layer of the dentate gyrus, showing that WIN is triggering plastic changes in the hippocampal region that is essential in the control of seizure activity.

DATA AVAILABILITY STATEMENT

The raw data supporting the conclusions of this article will be made available by the authors, without undue reservation.

ETHICS STATEMENT

The animal study was reviewed and approved by Comité Ético Científico Universidad de los Andes.

AUTHOR CONTRIBUTIONS

AZR, MM-R, MG, BA, JC, SK, and CL carried out the experiments. CL and UW conceived the experiments and wrote the manuscript. AZR, MM-R, CL, AIJ, and UW contributed to the interpretation of results. AZR, CL, and MM-R designed the figures. CL, AZR, MM-R, and AIJ, analyzed the data. LR, UW, and CL contributed to the implementation of the research. All authors gave critical feedback and LR, UW, and CL revised the final manuscript. All authors contributed to the article and approved the submitted version.

SUPPLEMENTARY MATERIAL

The Supplementary Material for this article can be found online at: https://www.frontiersin.org/articles/10.3389/fnmol.2022.868583/full#supplementary-material.

REFERENCES

Anderson, S. A. R., Oprescu, A. M., Calello, D. P., Monte, A., Dayan, P. S., Hurd, Y. L., et al. (2019). Neuropsychiatric sequelae in adolescents with acute synthetic cannabinoid toxicity. *Pediatrics* 144:e20182690. doi: 10.1542/peds.2018-2690

Bangasser, D. A., Curtis, A., Reyes, B. A. S., Bethea, T. T., Parastatidis, I., Ischiropoulos, H., et al. (2010). Sex differences in corticotropin-releasing factor receptor signaling and trafficking: potential role in female vulnerability to stress-related psychopathology. *Mol. Psychiatry* 15, 896–904. doi: 10.1038/mp.2010.66

Beghi, E., Giussani, G., Abd-Allah, F., Abdela, J., Abdelalim, A., Abraha, H. N., et al. (2019). Global, regional and national burden of epilepsy, 1990–2016: a systematic analysis for the Global Burden of Disease Study 2016. *Lancet Neurol.* 18, 357–375. doi: 10.1016/S1474-4422(18)30454-X

Benarroch, E. E. (2014). Synaptic effects of cannabinoids: complexity, behavioral effects and potential clinical implications. *Neurology* 83, 1958–1967. doi: 10.1212/WNL.0000000000001013

Bialer, M., and White, H. S. (2010). Key factors in the discovery and development of new antiepileptic drugs. *Nat. Rev. Drug Discov.* 9, 68–82. doi: 10.1038/nrd2997

Bronstein, J. M., Farber, D. B., Micevych, P. E., Lasher, R., and Wasterlain, C. G. (1990). Kindling induced changes in calmodulin kinase II immunoreactivity. *Brain Res.* 524, 49–53. doi: 10.1016/0006-8993(90)90490-3

Bui, A. D., Nguyen, T. M., Limouse, C., Kim, H. K., Szabo, G. G., Felong, S., et al. (2018). Dentate gyrus mossy cells control spontaneous convulsive seizures and spatial memory. *Science* 359, 787–790. doi: 10.1126/science.aan4074

Busquets-Garcia, A., Bains, J., and Marsicano, G. (2018). CB 1 receptor signaling in the brain: extracting specificity from ubiquity. *Neuropsychopharmacology* 43, 4–20. doi: 10.1038/npp.2017.206

Butler, L. S., Silva, A. J., Abeliovich, A., Watanabe, Y., Tonegawa, S., and McNamara, J. O. (1995). Limbic epilepsy in transgenic mice carrying a Ca^{2+}/calmodulin-dependent kinase II α-subunit mutation. *Proc. Natl. Acad. Sci. U S A* 92, 6852–6855. doi: 10.1073/pnas.92.15.6852

Carletti, F., Gambino, G., Rizzo, V., Ferraro, G., and Sardo, P. (2016). Involvement of TRPV1 channels in the activity of the cannabinoid WIN 55,212-2 in an acute rat model of temporal lobe epilepsy. *Epilepsy Res.* 122, 56–65. doi: 10.1016/j.eplepsyres.2016.02.005

Carlin, R. K., Grab, D. J., Cohen, R. S., and Siekevitz, P. (1980). Isolation and characterization of postsynaptic densities from various brain regions: enrichment of different types of postsynaptic densities. *J. Cell Biol.* 86, 831–845. doi: 10.1083/jcb.86.3.831

Chatzikonstantinou, A. (2014). Epilepsy and the hippocampus. *Hippocampus Clin. Neurosci.* 34, 121–142. doi: 10.1159/000356435

Chen, D. J., Gao, M., Gao, F. F., Su, Q. X., and Wu, J. (2017). Brain cannabinoid receptor 2: expression, function and modulation. *Acta Pharmacol. Sin.* 38, 312–316. doi: 10.1038/aps.2016.149

Christian, C. A., Reddy, D. S., Maguire, J., and Forcelli, P. A. (2020). Sex differences in the epilepsies and associated comorbidities: implications for use and development of pharmacotherapies. *Pharmacol. Rev.* 72, 767–800. doi: 10.1124/pr.119.017392

Colangeli, R., Di Maio, R., Pierucci, M., Deidda, G., Casarrubea, M., and Di Giovanni, G. (2019). Synergistic action of CB 1 and 5-HT 2B receptors in preventing pilocarpine-induced status epilepticus in rats. *Neurobiol. Dis.* 125, 135–145. doi: 10.1016/j.nbd.2019.01.026

Cooper, Z. D., and Craft, R. M. (2018). Sex-dependent effects of cannabis and cannabinoids: a translational perspective. *Neuropsychopharmacology* 43, 34–51. doi: 10.1038/npp.2017.140

Crowley, L. C., and Waterhouse, N. J. (2016). Detecting cleaved caspase-3 in apoptotic cells by flow cytometry. *Cold Spring Harb. Protoc.* 2016, 958–962. doi: 10.1101/pdb.prot087312

Devinsky, O., Cilio, M. R., Cross, H., Fernandez-Ruiz, J., French, J., Hill, C., et al. (2014). Cannabidiol: pharmacology and potential therapeutic role in epilepsy and other neuropsychiatric disorders. *Epilepsia* 55, 791–802. doi: 10.1111/epi.12631

Dong, Y., and Rosenberg, H. C. (2004). Brief seizure activity alters Ca^{2+}/calmodulin dependent protein kinase II dephosphorylation and subcellular distribution in rat brain for several hours. *Neurosci. Lett.* 357, 95–98. doi: 10.1016/j.neulet.2003.11.069

Englot, D. J., and Blumenfeld, H. (2009). *Consciousness and Epilepsy: Why Are Complex-Partial Seizures Complex?* Amsterdam, Netherlands: Elsevier. doi: 10.1016/S0079-6123(09)17711-7

Felder, C. C., Joyce, K. E., Briley, E. M., Mansouri, J., Mackie, K., Blond, O., et al. (1995). Comparison of the pharmacology and signal transduction of the human cannabinoid CB1 and CB2 receptors. *Mol. Pharmacol.* 48, 443–450.

Ferraro, A., Wig, P., Boscarino, J., and Reich, C. G. (2020). Sex differences in endocannabinoid modulation of rat CA1 dendritic neurotransmission. *Neurobiol. Stress* 13:100283. doi: 10.1016/j.ynstr.2020.100283

Földy, C., Neu, A., Jones, M. V., and Soltesz, I. (2006). Presynaptic, activity-dependent modulation of cannabinoid type 1 receptor-mediated inhibition of GABA release. *J. Neurosci.* 26, 1465–1469. doi: 10.1523/JNEUROSCI.4587-05.2006

Gage, G. J., Kipke, D. R., and Shain, W. (2012). Whole animal perfusion fixation for rodents. *J. Vis. Exp.* e3564. doi: 10.3791/3564

Govaerts, S. J., Hermans, E., and Lambert, D. M. (2004). Comparison of cannabinoid ligands affinities and efficacies in murine tissues and in transfected cells expressing human recombinant cannabinoid receptors. *Eur. J. Pharm. Sci.* 23, 233–243. doi: 10.1016/j.ejps.2004.07.013

Hagihara, H., Ohira, K., Toyama, K., and Miyakawa, T. (2011). Expression of the AMPA receptor subunits GluR1 and GluR2 is associated with granule cell maturation in the dentate gyrus. *Front. Neurosci.* 5:100. doi: 10.3389/fnins.2011.00100

Hara, Y., Punsoni, M., Yuk, F., Sehwan Park, C., Janssen, W. G. M., Rapp, P. R., et al. (2012). Synaptic distributions of GluA2 and PKMζ in the monkey dentate gyrus and their relationships with aging and memory. *J. Neurosci.* 32, 7336–7344. doi: 10.1523/JNEUROSCI.0605-12.2012

Havenon, A. d., Chin, B., Thomas, K. C., and Afra, P. (2011). The Secret "Spice": an undetectable toxic cause of seizure. *Neurohospitalist* 1, 182–186. doi: 10.1177/1941874411417977

Holson, R. R. (1992). Euthanasia by decapitation: evidence that this technique produces prompt, painless unconsciousness in laboratory rodents. *Neurotoxicol. Teratol.* 14, 253–257. doi: 10.1016/0892-0362(92)90004-t

Jensen, K. R., Berthoux, C., Nasrallah, K., and Castillo, P. E. (2021). Multiple cannabinoid signaling cascades powerfully suppress recurrent excitation in the hippocampus. *Proc. Natl. Acad. Sci. U S A* 118:e2017590118. doi: 10.1073/pnas.2017590118

Ji, X., Zeng, Y., and Wu, J. (2021). The CB2 receptor as a novel therapeutic target for epilepsy treatment. *Int. J. Mol. Sci.* 22:8961. doi: 10.3390/ijms22168961

Jinde, S., Zsiros, V., and Nakazawa, K. (2013). Hilar mossy cell circuitry controlling dentate granule cell excitability. *Front. Neural Circuits* 7:14. doi: 10.3389/fncir.2013.00014

Kaczor, E. E., Greene, K., Zacharia, J., Tormoehlen, L., Neavyn, M., and Carriero, S. (2022). The potential proconvulsant effects of cannabis: a scoping review. *J. Med. Toxicol.* doi: 10.1007/s13181-022-00886-3[Online ahead of print]

Katona, I., Sperlágh, B., Sík, A., Käfalvi, A., Vizi, E. S., Mackie, K., et al. (1999). Presynaptically located CB1 cannabinoid receptors regulate GABA release from axon terminals of specific hippocampal interneurons. *J. Neurosci.* 19, 4544–4558. doi: 10.1523/JNEUROSCI.19-11-04544.1999

Katona, I., Urbán, G. M., Wallace, M., Ledent, C., Jung, K. M., Piomelli, D., et al. (2006). Molecular composition of the endocannabinoid system at glutamatergic synapses. *J. Neurosci.* 26, 5628–5637. doi: 10.1523/JNEUROSCI.0309-06.2006

Kawamura, Y., Fukaya, M., Maejima, T., Yoshida, T., Miura, E., Watanabe, M., et al. (2006). The CB1 cannabinoid receptor is the major cannabinoid receptor at excitatory presynaptic sites in the hippocampus and cerebellum. *J. Neurosci.* 26, 2991–3001. doi: 10.1523/JNEUROSCI.4872-05.2006

Kendall, D. A., and Yudowski, G. A. (2017). Cannabinoid receptors in the central nervous system: their signaling and roles in disease. *Front. Cell. Neurosci.* 10:294. doi: 10.3389/fncel.2016.00294

Kerr, A., Walston, V., Wong, V. S. S., Kellogg, M., and Ernst, L. (2019). Marijuana use among patients with epilepsy at a tertiary care center. *Epilepsy Behav.* 97, 144–148. doi: 10.1016/j.yebeh.2019.05.037

Kitaura, H., Shirozu, H., Masuda, H., Fukuda, M., Fujii, Y., and Kakita, A. (2018). Pathophysiological characteristics associated with epileptogenesis in human hippocampal sclerosis. *EBioMedicine* 29, 38–46. doi: 10.1016/j.ebiom.2018.02.013

Krook-Magnuson, E. (2017). The gate and the source? The dentate gyrus takes central stage in temporal lobe epilepsy. *Epilepsy Curr.* 17, 48–49. doi: 10.5698/1535-7511-17.1.48

Krook-Magnuson, E., Armstrong, C., Bui, A., Lew, S., Oijala, M., and Soltesz, I. (2015). *in vivo* evaluation of the dentate gate theory in epilepsy. *J. Physiol.* 593, 2379–2388. doi: 10.1113/JP270056

Kruger, L., Saporta, S., and Swanson, L. W.. (1995). *Photographic Atlas of the Rat Brain: The Cell and Fiber Architecture Illustrated in Three Planes with Stereotaxic Coordinates*. New York, NY: Cambridge University Press.

Lafourcade, C. A., Fernández, A., Ramírez, J. P., Corvalán, K., Carrasco, M. Á., Iturriaga, A., et al. (2020). A role for mir-26a in stress: a potential sEV biomarker and modulator of excitatory neurotransmission. *Cells* 9:1364. doi: 10.3390/cells9061364

Lee, D. S., and Kim, J. E. (2020). PDI-mediated reduction of disulfide bond on PSD95 increases spontaneous seizure activity by regulating NR2A-PSD95 interaction in epileptic rats independent of S-nitrosylation. *Int. J. Mol. Sci.* 21:2094. doi: 10.3390/ijms21062094

Lemieux, M., Labrecque, S., Tardif, C., Labrie-Dion, É., LeBel, É., and De Koninck, P. (2012). Translocation of CaMKII to dendritic microtubules supports the plasticity of local synapses. *J. Cell Biol.* 198, 1055–1073. doi: 10.1083/jcb.201202058

Leranth, C., Szeidemann, Z., Hsu, M., and Buzsáki, G. (1996). AMPA receptors in the rat and primate hippocampus: a possible absence of GluR2/3 subunits in most interneurons. *Neuroscience* 70, 631–652. doi: 10.1016/s0306-4522(96)83003-x

Lüttjohann, A., Fabene, P. F., and van Luijtelaar, G. (2009). A revised Racine's scale for PTZ-induced seizures in rats. *Physiol. Behav.* 98, 579–586. doi: 10.1016/j.physbeh.2009.09.005

Malyshevskaya, O., Aritake, K., Kaushik, M. K., Uchiyama, N., Cherasse, Y., Kikura-Hanajiri, R., et al. (2017). Natural (Δ9-THC) and synthetic (JWH-018) cannabinoids induce seizures by acting through the cannabinoid CB1 receptor. *Sci. Rep.* 7:10516. doi: 10.1038/s41598-017-10447-2

Manford, M. (2017). Recent advances in epilepsy. *J. Neurol.* 264, 1811–1824. doi: 10.1007/s00415-017-8394-2

Manna, S. S. S., and Umathe, S. N. (2012). Involvement of transient receptor potential vanilloid type 1 channels in the pro-convulsant effect of anandamide in pentylenetetrazole-induced seizures. *Epilepsy Res.* 100, 113–124. doi: 10.1016/j.eplepsyres.2012.02.003

Marsicano, G., and Lutz, B. (1999). Expression of the cannabinoid receptor CB1 in distinct neuronal subpopulations in the adult mouse forebrain. *Eur. J. Neurosci.* 11, 4213–4225. doi: 10.1046/j.1460-9568.1999.00847.x

McElroy, D. L., Roebuck, A. J., Greba, Q., Garai, S., Brandt, A. L., Yilmaz, O., et al. (2022). The type 1 cannabinoid receptor positive allosteric modulators GAT591 and GAT593 reduce spike-and-wave discharges in Genetic Absence Epilepsy Rats from Strasbourg. *IBRO Neurosci. Rep.* 12, 121–130. doi: 10.1016/j.ibneur.2022.01.006

Needs, H. I., Henley, B. S., Cavallo, D., Gurung, S., Modebadze, T., Woodhall, G., et al. (2019). Changes in excitatory and inhibitory receptor expression and network activity during induction and establishment of epilepsy in the rat Reduced Intensity Status Epilepticus (RISE) model. *Neuropharmacology* 158:107728. doi: 10.1016/j.neuropharm.2019.107728

Nogueras-Ortiz, C., and Yudowski, G. A. (2016). The multiple waves of cannabinoid 1 receptor signaling. *Mol. Pharmacol.* 90, 620–626. doi: 10.1124/mol.116.104539

Nyíri, G., Cserép, C., Szabadits, E., Mackie, K., and Freund, T. F. (2005). CB1 cannabinoid receptors are enriched in the perisynaptic annulus and on preterminal segments of hippocampal GABAergic axons. *Neuroscience* 136, 811–822. doi: 10.1016/j.neuroscience.2005.01.026

Perescis, M. F. J., Flipsen, N. A. R., van Luijtelaar, G., and van Rijn, C. M. (2020). Altered SWD stopping mechanism in WAG/Rij rats subchronically treated with the cannabinoid agonist R(+)WIN55,212-2. *Epilepsy Behav.* 102:106722. doi: 10.1016/j.yebeh.2019.106722

Rizzo, V., Carletti, F., Gambino, G., Schiera, G., Cannizzaro, C., Ferraro, G., et al. (2014). Role of CB2 receptors and cGMP pathway on the cannabinoid-dependent antiepileptic effects in an *in vivo* model of partial epilepsy. *Epilepsy Res.* 108, 1711–1718. doi: 10.1016/j.eplepsyres.2014.10.001

Robison, A. J. (2014). Emerging role of CaMKII in neuropsychiatric disease. *Trends Neurosci.* 37, 653–662. doi: 10.1016/j.tins.2014.07.001

Roebuck, A. J., Greba, Q., Smolyakova, A. M., Alaverdashvili, M., Marks, W. N., Garai, S., et al. (2021). Positive allosteric modulation of type 1 cannabinoid receptors reduces spike-and-wave discharges in Genetic Absence Epilepsy Rats from Strasbourg. *Neuropharmacology* 190:108553. doi: 10.1016/j.neuropharm.2021.108553

Rosenberg, E. C., Patra, P. H., and Whalley, B. J. (2017). Therapeutic effects of cannabinoids in animal models of seizures, epilepsy, epileptogenesis and epilepsy-related neuroprotection. *Epilepsy Behav.* 70, 319–327. doi: 10.1016/j.yebeh.2016.11.006

Rosenberg, E. C., Tsien, R. W., Whalley, B. J., and Devinsky, O. (2015). Cannabinoids and epilepsy. *Neurotherapeutics* 12, 747–768. doi: 10.1007/s13311-015-0375-5

Rudenko, V., Rafiuddin, A., Leheste, J. R., and Friedman, L. K. (2012). Inverse relationship of cannabimimetic (R+)WIN 55,212 on behavior and seizure threshold during the juvenile period. *Pharmacol. Biochem. Behav.* 100, 474–484. doi: 10.1016/j.pbb.2011.10.005

Saroz, Y., Kho, D. T., Glass, M., Graham, E. S., and Grimsey, N. L. (2019). Cannabinoid receptor 2 (CB2) signals via G-alpha-s and induces IL-6 and IL-10 cytokine secretion in human primary leukocytes. *ACS Pharmacol. Transl. Sci.* 2, 414–428. doi: 10.1021/acsptsci.9b00049

Savinainen, J. R., Kokkola, T., Salo, O. M. H., Poso, A., Järvinen, T., and Laitinen, J. T. (2005). Identification of WIN55212-3 as a competitive neutral antagonist of the human cannabinoid CB 2 receptor. *Br. J. Pharmacol.* 145, 636–645. doi: 10.1038/sj.bjp.0706230

Silvestro, S., Mammana, S., Cavalli, E., Bramanti, P., and Mazzon, E. (2019). Use of cannabidiol in the treatment of epilepsy: efficacy and security in clinical trials. *Molecules* 24:1459. doi: 10.3390/molecules24081459

Smolyakova, A. M., Zagzoog, A., Brandt, A. L., Black, T., Mohamed, K., and Laprairie, R. B. (2020). The endocannabinoid system and synthetic cannabinoids in preclinical models of seizure and epilepsy. *J. Clin. Neurophysiol.* 37, 15–27. doi: 10.1097/WNP.0000000000000633

Srivastava, A., Gupta, B., Gupta, C., and Shukla, A. K. (2015). Emerging functional divergence of β-arrestin isoforms in GPCR function. *Trends Endocrinol. Metab.* 26, 628–642. doi: 10.1016/j.tem.2015.09.001

Steindel, F., Lerner, R., Häring, M., Ruehle, S., Marsicano, G., Lutz, B., et al. (2013). Neuron-type specific cannabinoid-mediated G protein signalling in mouse hippocampus. *J. Neurochem.* 124, 795–807. doi: 10.1111/jnc.12137

Sugaya, Y., Yamazaki, M., Uchigashima, M., Kobayashi, K., Watanabe, M., Sakimura, K., et al. (2016). Crucial roles of the endocannabinoid 2-arachidonoylglycerol in the suppression of epileptic seizures. *Cell Rep.* 16, 1405–1415. doi: 10.1016/j.celrep.2016.06.083

Tatum, W. O. (2012). Mesial temporal lobe epilepsy. *J. Clin. Neurophysiol.* 29, 356–365. doi: 10.1097/WNP.0b013e31826b3ab7

Van Erum, J., Van Dam, D., and De Deyn, P. P. (2019). PTZ-induced seizures in mice require a revised Racine scale. *Epilepsy Behav.* 95, 51–55. doi: 10.1016/j.yebeh.2019.02.029

van Rijn, C. M., Krijnen, H., Menting-Hermeling, S., and Coenen, A. M. L. (2011). Decapitation in rats: latency to unconsciousness and the "wave of death". *PLoS One* 6:e16514. doi: 10.1371/journal.pone.0016514

Vilela, L. R., Medeiros, D. C., Rezende, G. H. S., de Oliveira, A. C. P., Moraes, M. F. D., and Moreira, F. A. (2013). Effects of cannabinoids and endocannabinoid hydrolysis inhibition on pentylenetetrazole-induced seizure and electroencephalographic activity in rats. *Epilepsy Res.* 104, 195–202. doi: 10.1016/j.eplepsyres.2012.11.006

Wendt, H., Soerensen, J., Wotjak, C. T., and Potschka, H. (2011). Targeting the endocannabinoid system in the amygdala kindling model of temporal lobe epilepsy in mice. *Epilepsia* 52, e62–e65. doi: 10.1111/j.1528-1167.2011.03079.x

Wiebe, S., and Jette, N. (2012). Pharmacoresistance and the role of surgery in difficult to treat epilepsy. *Nat. Rev. Neurol.* 8, 669–677. doi: 10.1038/nrneurol.2012.181

Wyneken, U., Smalla, K. H., Marengo, J. J., Soto, D., De la Cerda, A., Tischmeyer, W., et al. (2001). Kainate-induced seizures alter protein composition and N-methyl-D-aspartate receptor function of rat forebrain postsynaptic densities. *Neuroscience* 102, 65–74. doi: 10.1016/s0306-4522(00)00469-3

Yardimoglu, M., Ilbay, G., Kokturk, S., Onar, F. D., Sahin, D., Alkan, F., et al. (2007). Light and electron microscopic examinations in the hippocampus of the rat brain following PTZ-induced epileptic seizures. *J. Appl. Biol. Sci.* 1, 97–106. Available online at: https://www.jabsonline.org/index.php/jabs/article/view/38.

Ying, Z., Bingaman, W., and Najm, I. M. (2004). Increased numbers of coassembled PSD-95 to NMDA-receptor subunits NR2B and NR1 in human epileptic cortical dysplasia. *Epilepsia* 45, 314–321. doi: 10.1111/j.0013-9580.2004.37703.x

Conflict of Interest: The authors declare that the research was conducted in the absence of any commercial or financial relationships that could be construed as a potential conflict of interest.

Publisher's Note: All claims expressed in this article are solely those of the authors and do not necessarily represent those of their affiliated organizations, or those of the publisher, the editors and the reviewers. Any product that may be evaluated in this article, or claim that may be made by its manufacturer, is not guaranteed or endorsed by the publisher.

Copyright © 2022 Zirotti Rosenberg, Méndez-Ruette, Gorziglia, Alzerreca, Cabello, Kaufmann, Rambousek, Iturriaga Jofré, Wyneken and Lafourcade. his is an open-access article distributed under the terms of the Creative Commons Attribution License (CC BY). The use, distribution or reproduction in other forums is permitted, provided the original author(s) and the copyright owner(s) are credited and that the original publication in this journal is cited, in accordance with accepted academic practice. No use, distribution or reproduction is permitted which does not comply with these terms.

Advantages of publishing in Frontiers

OPEN ACCESS
Articles are free to read for greatest visibility and readership

FAST PUBLICATION
Around 90 days from submission to decision

HIGH QUALITY PEER-REVIEW
Rigorous, collaborative, and constructive peer-review

TRANSPARENT PEER-REVIEW
Editors and reviewers acknowledged by name on published articles

Frontiers
Avenue du Tribunal-Fédéral 34
1005 Lausanne | Switzerland

Visit us: www.frontiersin.org
Contact us: frontiersin.org/about/contact

REPRODUCIBILITY OF RESEARCH
Support open data and methods to enhance research reproducibility

DIGITAL PUBLISHING
Articles designed for optimal readership across devices

FOLLOW US
@frontiersin

IMPACT METRICS
Advanced article metrics track visibility across digital media

EXTENSIVE PROMOTION
Marketing and promotion of impactful research

LOOP RESEARCH NETWORK
Our network increases your article's readership